ttp://jgu.garmian.edu.krd https://doi.org/10.24271/garmian.321

Foliar Application of Bread Yeast and Organic Fertilizer to Improve Yield Quantity and Quality of Thompson Seedless Grape (*Vitis vinifera* L.)

Shabaq M. Nafea Al-Hawezy[1*] Chnar A. Ibrahim[1]

[1]Horticulture Department, Faculty of Agriculture/ University of Salahaddin, Kurdistan Region, Iraq

[*]Corresponding author. Email: shabaq.hawezy@su.edu.krd

Abstract

Study was conducted using Thompson seedless grapevines 11 years old, trained as arbors (espalier) training in a vineyard at Erbil Directorate of Agriculture Researches / Kurdistan Region / Iraq during the growing season of 2015 to investigate the possible effects of foliar application of natural bread yeast (bio-fertilizer) and liquid organic fertilizer (B&S Pot-min) on yield quantity and quality. Results indicated that the concentration of 12 g.l-1 of bread yeast, liquid organic fertilizer at 4 ml.l-1 and interaction between them affected on yield and physical characteristics of clusters, berries and chemical properties of berries significantly over other concentrations and interactions. The number of clusters/vine, cluster weight, yield increased by application of bread yeast, and there were significant differences between treatments comparing to control. Applications of bread yeast and organic fertilizer significantly improve physical characteristics of berries comparing to control. Bread yeast application caused significant increase in total soluble solid (TSS), decreased titratable acidity (TA), with highest value of TSS/TA ratio compared with control.

Keywords: Bread yeast, organic fertilizer, grapevine, Thompson seedless, Yield.

1. Introduction

Grape (*Vitis vinifera* L.) belongs to the Vitaceae family; it is one of the most essential commercial fruit crops of temperate to tropical regions (Gowda et al., 2008). Due to its high nutritive value, multipurpose use (Table grape, raisin, wine, juice and can) returns becoming more popular (Ghosh et al., 2008). Thompson seedless grapevines are planted throughout the world and are used to produce dried fruits (raisins), and for the fresh market (table grapes), because of a good taste of berries and juice that acceptable for consumers, and it is considered to be the best seedless variety for raisin (Alsaidi, 2014). Nowadays, it is doubtless that new fertilization techniques have been developed in different vineyards located in newly reclaimed areas, where, organic fertilization (in composting phase) of various grapevines has called the attention of researchers as a positive alternative to minimize the intensive amounts of mineral N (Kassem and Marzouk, 2002). Moreover, the necessity to use humic acid together with organic fertilizer for improving vine growth, nutritional status and berry quality, was supported by many experimental results (Zhu, 2000; Guo et al;. 2000; Ali et al., 2006; Eman *et al*, 2008). Organic and bio-fertilizations are very safe for consumers, due to the fact that their application leads to reduce the accumulation of nitrate and nitrite residues in the edible tissues (Montasser et al, 2003; Farag, 2006).

Fawzi et al. (2014) clarified that Influence of spraying bread yeast on growth, yield, leaf chemical composition and fruit quality of "superior" 12 years old Grapevines (*Vitis vinifera* L.) bread yeast at 0.1% and 0.2% four times during growing season (i.e. at the beginning of growth, first bloom, after fruit set and 3 weeks later). It is obvious from the obtained data that bread yeast significantly increasing, of clusters/vine, yield, cluster weight, cluster length, number of berries/cluster, berry weight and TSS compared with control. Results from Al-Atrushy and Birjely (2015) showed that organic fertilizers caused a remarkable stimulation on growth characters, yield as well as berries quality parameters compared to control. Total acidity percentage in the juice has also tended to reduce with using organic manure.
The main goal of the present study was to produce healthy fruits without the use of chemical fertilizers as well as protect our environment from pollution and to investigate the possible effects of foliar application of natural bread yeast (bio-fertilizer) and organic fertilizer (B&S Pot-min) on yield quantity and quality of Thompson seedless grapevines.

2. Materials and Methods

This study was carried out in a vineyard at Erbil Directorate of Agriculture Researches / Kurdistan Region / Iraq during 2015 growing season to investigate the possible effects of foliar application of (bio-fertilizer) natural bread yeast (*Saccharomyces cerevisiae*) at 0, 4, 8 and 12 $g.l^{-1}$ (Commercial baking yeast was dissolved in warm water (38°C) followed by adding sugar at ratio 1:1 and kept overnight before spraying for activation and reproduction of yeast (Hegab et al.,1997).) and liquid organic fertilizer (B&S Pot-min) at 0, 2 and 4 $ml.l^{-1}$ on yield quantity and quality of 11 years old grapevine cultivar (*Vitis vinifera* L.) cv. Thompson seedless. It was trained as arbors (espalier) training, planted at 2 x 4 m apart and pruned at the second week of February to leave 72 eyes/vine (6 fruiting canes with 10 eyes plus 6 renewal spurs with 2 eyes) under drip irrigation. The Physical and chemical analysis of the vineyard soil listed in table 1, soil samples were analyzed according to (Wilde *et al.*, 1985).

Table 1 Physical and chemical analysis of the vineyard soil*

Sample Depth(cm)	N mg.l^{-1}	P mg.l^{-1}	K mg.l^{-1}	Organic Matter %	pH (pH-meter)	EC (ds/m)	Type of soil
0-30	56	1.08	358	2.2	7.96	1.15	Silty clay loam
30-60	91	0.099	165	1.3	8.01	0.280	Loamy
60-90	63	0.22	177	1.2	7.93	0.300	Silty loam

*****The data were analyzed at Erbil director of agriculture researches

Bread yeast and liquid organic fertilizer in addition of control (only water) and their interactions were sprayed as foliar application at three times within twenty-one days intervals, starting from 7 days after fruit setting (19/5/2015), the first spraying was on 26/5/2015, the second on 15/6/2015 during fruit development and the third spraying was on 5/7/2015 after the veraison stage. Tween-20 at a rate of 0.1% was used with each spray solution as wetting agent. All treatments were replicated four times means that 48 vines. Chemical composition of organic liquid fertilizer showed in table 2 and 3 respectively.

Horticulture practices except the addition of bread yeast and organic fertilizer were used as usual. Effect of bread yeast and organic fertilizer were evaluated in terms of the change in number of cluster per vine, cluster weight, yield per vine, cluster length and diameter (Representative random samples of 5 clusters/ vine were harvested at maturity when TSS reached about 16 – 17 % according to (Tourky et al., 1995)) as well as number of berries per cluster, berry length, diameter, weight and size of 100 berries as Total Soluble Solid (TSS), Titratable Acidity (TA) and TSS/TA ratio (Tehranifar et al., 2010).

Table 2 Chemical composition of used Bread yeast (*Saccharomyces cerevisiae*).

Composition of minerals mg.g^{-1}		Amino acids mg.kg^{-1}	
N	20.23	Lysine	5.800
P	21.26	Histidine	7.600
K	47.20	Phenyl alanine	19.900
Mg	2.160	Methionine	4.200
Fe	0.036	Cystine	21.600
Zn	0.210	Glycine	7.810
Cu	0.015	Glutamic	21.600
Si	7.800	Aspartic	16.900
Another compounds			
Glyceriizine	3.093 %	Glucose	3.841 %
Sucrose	1.570 %	GA	0.620

Table 3 Chemical composition of used organic liquid fertilizer (B&S Pot-min)*

Content	Percentage %
Organic Carbon	30
Organic Nitrogen	0.5
Potassium Oxide	3.1
Total Nitrogen	0.5
Organic matter	48
	mg/kg
Copper	25.35
Nickel	14.27
Zinc	25.53
pH	4.8

Results were analyzed statistically according to Factorial Randomized Complete Block Design (RCBD), and analysis of variance and Duncan's multiple range tests at 5% levels were used to differentiate means using SAS program.

3. Results

3.1. Yield and physical characteristics of clusters

Data presented in Table 4 revealed that number of clusters/vine, cluster weight, yield increased by application of bread yeast, there were significant differences between treatments comparing to control. Bread yeast treatment at concentration 8 g.l^{-1} resulted in greatest increase in number of cluster/vine (52.25), while highest number of clusters weight, yield, cluster length and diameter were obtained by concentration of bread yeast at12 g.l^{-1} (173.85 g, 8.79 kg ,25.50 cm and 13.52 cm), respectively.

In addition, data declared that organic fertilizer affected on physical characteristic of cluster and yield /vine comparing to control. Increasing concentration of organic fertilizer significantly increased yield and cluster length. Whereas spraying organic fertilizer had no effect on cluster diameter.

The results from Table 4 also denoted that interaction of both factors significantly affected on physical characteristics of clusters and yield. It had significant difference between treatments. Maximum increase of number of clusters was obtained by interaction of 8 g.l^{-1} bread yeast and 4 ml.l^{-1} organic fertilizer (58.75) while, minimum level of it was obtained by control treatment (40.00). Maximum increase of yield was obtained by interaction of 12g.l^{-1} bread yeast and 4ml.l^{-1} organic fertilizer (9.25kg) while, minimum level of it was obtained by control treatment (5.61kg). Highest level of cluster length was recorded with interaction between concentration of 12g.l^{-1} bread yeast and 2ml.l^{-1} organic fertilizer (27.43cm), while maximum cluster diameter was obtunded by interaction between concentration of 12g.l^{-1} bread yeast and 4ml.l^{-1} organic fertilizer (14.88cm).

Table 4 Effect of bread yeast, organic fertilizer and their interactions on yield and physical characteristics of clusters "Thompson seedless" grapevines*

Treatments			**Parameters**				
			No.clusters/vine	**Cluster weight (g)**	**Yield (kg/vine)**	**Cluster length (cm.)**	**Cluster diameter (cm)**
Bread Yeast ($g.l^{-1}$)		**0**	44.25 d	141.54 d	6.54 d	22.56 b	11.86 b
		4	48.08 c	146.56 c	7.04 c	23.41 b	13.09 ab
		8	52.25 a	166.6 b	8.61 b	23.15 b	13.52 a
		12	50.67 b	173.85 a	8.79 a	25.50 a	14.48 a
Organic fertilizer ($ml.l^{-1}$)		**o**	46.44 c	159.53 a	7.43 c	22.83 b	12.77 a
		2	48.06 b	157.63 b	7.79 b	24.38 a	13.19 a
		4	51.94 a	154.29 c	8.01 a	23.75 a	13.75 a
Bread Yeast 0	**Organic fertilizer**	**0**	40.00 k	140.14 k	5.61 l	21.42 e	10.48 c
		2	46.75 h	145.16 i	7.60 h	23.36 b-d	11.76 bc
		4	46.00 i	139.32 l	6.41 k	22.90 c-e	13.35 a-c
Bread Yeast 4	**Organic fertilizer**	**0**	44.25 j	151.84 f	6.72 i	23.26 b-d	13.32 a-c
		2	47.00 g	142.22 j	6.70 j	22.67 c-e	12.52 a-c
		4	53.00 c	145.60 h	7.72 g	24.29 bc	13.44 a-c
Bread Yeast 8	**Organic fertilizer**	**0**	46.75 h	186.37 a	8.65 d	22.34 de	13.32 a-c
		2	51.25 d	166.21 d	8.50 e	24.06 b-d	13.59 ab
		4	58.75 a	147.41 g	8.68 c	23.06 b-e	13.65 ab
Bread Yeast 12	**Organic fertilizer**	**0**	54.75 b	159.79 e	8.75 b	24.30 bc	13.98 ab
		2	47.25 f	176.94 c	8.36 f	27.43 a	14.88 a
		4	50.00 e	184.81 b	9.25 a	24.76 b	14.57 ab

*Values within followed by the same letter in each column for each factor and interactions are not significantly different according to Duncan's Multiple Range Test at 5% level of probability.

3.2. Physical characteristics of berries

As seen in Table 5 application of bread yeast significantly increased number of berries comparing to control. Highest number of berries, berry length and diameter, and weight and size of 100 berries was occurred by 12 g.l^{-1} bread yeast (142.10, 1.47cm, 1.14cm, 121.10g and 119.42cm^3) where, these values of characteristics were recorded with control treatment (120.64, 1.25cm, 1.03cm, 109.40g and 105.60cm^3).

Data presented in Table 5 revealed that application of organic fertilizer exhibited significant increase inphysical characteristics of berries. In this concern, highest increase of number of berries, berry diameter was occurred by 4 $ml.l^{-1}$ organic fertilizer (134.10 and 1.11cm), while lowest values were obtain in control (129.77 and 1.07cm), respectively. The results alsoshowed that organic fertilizer had non-significant effect between treatments comparing to control Table 5.

The results from Table 5 denoted that interaction of both factors significantly increased number of berries per cluster, cluster length and diameter. Maximum increase was obtained by interaction of $12g.l^{-1}$ bread yeast and $4ml.l^{-1}$ organic fertilizer (150.70, 1.58cm and 1.23cm), the interaction between $8g.l^{-1}$ bread yeast and 0ml.$^{l-}$organic fertilizer indicate the significant increase of weight and size of 100 berries (137.1g and $134.66cm^3$), while, minimum level of them were obtained by control treatment (115.20, 1.11cm, 0.90cm, 104.47g and $99.01cm^3$).

Table 5 Effect of bread yeast on physical characteristics of berries of "Thompson seedless" grapevines*****

Treatments			**Parameters**				
			No. berries/cluster	**Berry length (cm)**	**Berry diameter (cm)**	**Weight.100 berries (g)**	**Size.100 berries (cm^3)**
Bread Yeast ($g.l^{-1}$)		0	120.64 d	1.25 c	1.03 c	109.40 b	105.60 b
		4	132.52 c	1.36 b	1.12 ab	108.82 b	106.72 b
		8	134.87 b	1.39 b	1.08 b	122.05 a	119.91 a
		12	142.10 a	1.47 a	1.14 a	121.10 a	119.42 a
Organic fertilizer ($ml.l^{-1)}$)		o	129.77 c	1.34 b	1.07 b	117.53 a	111.58 a
		2	133.73 b	1.40 a	1.10 ab	115.57 a	113.11 a
		4	134.10 a	1.36 ab	1.11 a	112.93 a	111.04 a
Bread Yeast 0	**Organic fertilizer**	0	115.20 l	1.11 d	0.90 d	104.47 d	99.01 g
		2	121.98 k	1.28 c	1.06 bc	114.33 b-d	110.81 b-f
		4	124.75 j	1.37 b	1.12 b	109.41 cd	106.98 e-g
Bread Yeast 4	**Organic fertilizer**	0	137.18 d	1.45 b	1.14 b	109.13 cd	106.87 e-g
		2	132.03 h	1.43 b	1.13 b	105.83 d	103.68 gf
		4	128.35 i	1.22 c	1.09 bc	111.51 b-d	109.60 c-g
Bread Yeast 8	**Organic fertilizer**	0	133.80 e	1.42 b	1.15 b	137.19 a	134.66 a
		2	138.20 c	1.45 b	1.07 bc	119.46 bc	117.24 b-e
		4	132.60 g	1.29 c	1.03 c	109.51 cd	107.82 d-g
Bread Yeast 12	**Organic fertilizer**	0	132.90 f	1.39 b	1.09 bc	119.34 bc	117.793 b-d
		2	142.70 b	1.45 b	1.12 b	122.67 b	120.7 b
		4	150.70 a	1.58 a	1.23 a	121.30 bc	119.75 bc

*Values within followed by the same letter in each column for each factor and interactions are not significantly different according to Duncan's Multiple Range Test at 5% level of probability.

3.3. Chemical characteristics of berries

From the given data in Table 6 it clearly revealed that bread yeast application rays at 4, 8 and 12g.l^{-1} caused significant increase in total soluble solid (TSS), decreased titratable acidity (TA), with highest value of TSS/TA ratio compared with control, (24.00% and 44.02) was obtained by concentration 12g.l^{-1}, while the same concentration of bread yeast significantly reduced titratable acidity (0.55), where lowest values were recorded with control (21.14% and 31.25) with the highest value of acidity (0.68).

Table 6 illustrates the significant effect of organic fertilizer on the parameter of chemical characteristics of berries which increased total soluble solid and decreased titratable acidity with highest value of TSS/TA ratio compared with control. The results in Table 6 also denote that significant differences were detected between interactions of bread yeast with organic fertilizer. Interaction of concentrations 12g.l^{-1} bread yeast with control recorded the highest value in these parameters (24.90%, 44.26 and 1.06) with lowest value of acidity (0.53) and the lowest value resulted from control (19.70%, 29.47 and 1.03) respectively.

Table 6 Effect of bread yeast, organic fertilizer and their interactions on chemical characteristics (TSS; Total Soluble Solis, TA; Titratable Acidity and TSS/TA ratio)) of berries of "Thompson seedless" grapevines

Treatments			Parameters		
			TSS (%)	**TA (g/100ml.juice)**	**TSS/TA ratio**
Bread Yeast ($g.l^{-1}$)		0	21.14 d	0.68 a	31.25 d
		4	23.10 c	0.62 b	37.79 c
		8	23.99 b	0.58 c	41.27 b
		12	24.00 a	0.55 d	44.02 a
Organic fertilizer ($ml.l^{-1}$)		o	22.56 c	0.59 c	38.24 b
		2	22.89 b	0.62 a	37.14 c
		4	23.72 a	0.60 b	40.36 a
Bread Yeast 0	**Organic fertilizer**	0	19.70 l	0.60 f	32.83 j
		2	20.85 k	0.71 b	29.47 l
		4	22.88 h	0.73 a	31.44 k
Bread Yeast 4	**Organic fertilizer**	0	22.28 j	0.65 c	34.26 i
		2	22.28 i	0.62 e	36.26 h
		4	24.74 b	0.58 g	42.86 e
Bread Yeast 8	**Organic fertilizer**	0	23.38 f	0.56 h	41.62 f
		2	24.50 c	0.63 d	39.21 g
		4	24.09 d	0.56 i	42.98 d
Bread Yeast 12	**Organic fertilizer**	0	24.90 a	0.56 h	44.26 a
		2	23.93 e	0.55 j	43.64 c
		4	23.17 g	0.53 k	44.17 b

*Values within followed by the same letter in each column for each factor and interactions are not significantly different according to Duncan's Multiple Range Test at 5% level of probability.

4. Discussion

4.1. Yield and physical characteristics of clusters

Increasing number of clusters resulting in bread yeast application may be due to bread yeast containment of Cytokinin the high content of vitamin B5 and minerals. Yeast composition might be play a considerable role in orientation and translocation of metabolites from leaves in to the productive organs and in the synthesis of protein, and nucleic acid (Natio et al, 1981). Warring and Philips (1973) stated that bread yeast is rich in tryptophan which consider precursor of IAA which stimulate cell division and elongation. Similar results to the present study was found by Mahmoud (1996) on Roomy Red Grapevines and by Akl et al., (1997) and Ahmed-Kamelia et al., (2000) on Ruby Seedless Grapevines. Results also are nearly similar to those reported by Amen et al., (2000a) on King Ruby and Gaser et al., (2006) on Flame seedless who found that bread yeast applications significantly increased the yield/vine.

The positive effect of organic fertilizer on increasing clusters number per vine may due to the role of elements in physiological processes and their effect in the accumulation of carbohydrate in the berries Delas (1981). Nitrogen organic fertilizer activates photosynthesis processes through increasing the leaf area, which leads to increasing food supply to the clusters and, in turn, decreasing abortion of those clusters which increased the production of metabolites resulted in cluster weight, number of berries per cluster, berry volume and yield (Dhillon and Aulakh 1972; Ahlawat and Yamdagni 1988; Beniwal et al., 1992 and Koblet and Candolfi-Vasconcelos, 1995). El-Shenawy and Fayed (2005) concluded that adding humic acid with organic fertilizer increased yield of Crimson Seedless grapevine significantly than organic fertilizer alone. These results are in accordance with those found by (Bhangoo et al., 1988) on Thompson seedless.

The significant increase of number of clusters and cluster weight with regard on yield/vine, it is obvious that the applied bread yeast combined with organic fertilizer resulted in significant increase in the yield/vine. This may due to the beneficial effect of both bio and nitrogen organic fertilizer together on the absorption and efficiency of plant nutrients. The obtained results are in accordance with those of EL-Boray et al., (2004).

4.2. Physical characteristics of berries

The enhancement effect of bread yeast on physical characteristics of berries of Thompson seedless might be because of yeast richness in protein and its B vitamin group content (thiamin, riboflavin and pyridoxines), and yeast are also prolific producers of vitamins, amino acid, hormones and other growth regulating substances (Harrison, 1968). Moreover, bread yeast contains tryptophan which consider precursor of IAA, so it increases size of fruit (Moor, 1979). Concerning the effect of bread yeast concentrations it was clearly observed that with increasing concentrations used significantly increased physical characteristics of berries (No. of berries/cluster, weight of 100 berry, length and diameter of berries and Juice density. These effects of bread yeast might play a role in the synthesis of protein and nucleic acids which enhances cell division and enlargement leading to number, weight, length, diameter of berry increases. Findings in this study are on line with those found by Natio et al., (1981) and Akle et al., (1997). Increasing the number of berries per cluster by using nitrogen organic fertilizer (as foliar spraying) may due to its positive effect on cell division and elongation which lead to improve growth; berry set and cluster number per vine, which reflected on improvement of the yield per vine (Ribereau-Gayon and Paynoud, 1978; Champagnol, 1978). The promoting effect of organic fertilization on fruit quality was mainly attributed to their essential role in enhancing organic foods especially total carbohydrates and plant pigments which is reflected on advancing fruit maturity (Nijjar, 1985). The positive effect of organic fertilizer treatments on berry weight, size and diameter may be attributed to the increase of organic matter content and improvement of the structure and physical properties of the soil (Gamal, 1992). The effect of organic fertilizer concentrations on physical characteristics of berries was clearly observed. The positive effects of interaction of bread yeast and organic fertilizer on berry dimensions could be due to increasing uptake of various nutrients, active photosynthesis process, cell division and cell enlargement by the physical mutants of yeast which considered as a source of IAA and cytokinins hormones.

4.3. Chemical characteristics of berries

IncreasingTSS% may due to hydrolysis of starch into sugars as it is completed, no further increase in TSS could be detected and subsequently a decline in this parameter predictable since sugars along with other organic acids are primary substrates used for respiration (Gerasopoulos and Drogoudi, 2005). Moreover, the positive effects of bread yeast application on berry chemical properties i.e. TSS%, TSS/Acid ratio and the negative effects on acidity % in the grape juice could be attributed to the enhancement effects of photosynthesis processes and increasing promoter hormones as cytokinins (Moor, 1979), it is well known that these hormones induce a considerable amount of sugar contents and consequently caused an increase in TSS%, TSS/acid ratio and a decrease in acidity % in the grape juice. Results in this study are in agreement with those found by Gaser et al., (2006) Besides, Gouble et al., (2005) recorded that the increase in TSS during fruit development is normally linked to changes in fruit color and ethylene production. Fawzi and Eman (2004) found that spraying bread yeast significantly increased TSS and TSS/acid ratio and reduced the total acidity in berry juice of Flame Seedless Grapevines. The above findings agreed with those reported by (Mansour et al., 2011 and Ayman, 2011). Yeo et al., (2000) found that bread yeast contains trehalose- 6-phosphate synthase which is a key enzyme for trehalose biosynthesis. Trehalose affects sugar metabolism as well as osmoprotection against several environmental stresses. These results are in line with that obtained by Barnett et al., (1990) and Mady (2009). The improvement in quality of berries due to spraying bread yeast was supported by Makhij'a et al., (1990) on “Perlette” Grapes on TSS, acidity and TSS/TA ratio.

References

Al-Atrushy, S.M.M. 2012. Effect of foliar application of humic acid and bread yeast on some vegetative growth characteristics, yield and quality of Grape (*Vitis vinifera* L.) cv. Rash-Mew under non irrigated condition. *Journal of University of Duhok*, 15 (1). p.36-43.

Ahlawat, V. P. and Yamdagni, R. (1988). Effects of Various Levels of Nitrogen and Potassium Application on Growth Yield and Petiole Composition on Grapes cv. Perlette. Progressive Horticulture 20 (3-4), 190-196.

Ahmed-Kamelia, I. A.; Mostafa, F. M. A. and El-Bolock, A. A. (2000). Effect of yeast application of bud burst, physical and chemical characteristics of grape berries in king ruby. Cultivar during growth stages. L-effect of applied yeast on bud burst, yield components and winter pruning wood weight. *Assiut .J. Agric. Sci., 31(4): 193-205.*

Akl, A. M.; Ahmed, F. F.; E-Morsy, F. M. and Ragab, M. A. (1997).The beneficial effects of biofertilizers on red roomy grapevines (*Vitis vinifera* L.) the effect on berry set, yield and quality of berries. *Annals of agric, sci., moshtohor.*, 35(1): 497-502.

Ali , M.A., El-Gendy, S.S and El- Shal, S.A. (2006). The role of humic acid in reducing mineral fertilizer rates applied in vineyards. *Journal of Agriculture Sciences*. Mansoura University. 21(11).p202-224.

Al-Saidi, I. H. 2000. Grape Production. 1st Edi, Mosul University Press, Dar-Alkutub for printing & publishing. Mosul. Iraq.

Ayman A. H. (2011). Effects of spraying some chemical compounds on fruit set and fruit characteristics of ' Le Conte ' pear cultivar. *J. Hort. Sci. & Ornamen. Plants*, 3(1): 55-64.

Barnett, J.A., Payne, R.W. and Yarrow, D. 1990. Yeast Characteristics and Identification, 2nd Ed. Press, Cambridge Univ., London, UK. p.999-1012.

Beniwal, S. B.; Gupta, O. P. and Ahlawat, V. P. (1992). Effect of foliar application of urea and potassium sulphate on physicochemical attributes of grapes (Vitis vinifera L.) cv. Perlette. *Haryana J. Hort. Sci*. 21(4): 161-165.

Bhangoo , M.S., Sudanagunta, V.R. and Pertrucet, V.E. (1988). Application of poultry manure influence on Thompson seedless grape production and soil properties. *Hortsscience.* 23 (6). P. 1010-1012.

Champagnol, F. (1978). Fertilization optimal de la vigine. Progress Agricole et Viticole 15 & 16: 423-440.

Delas, J. (1981). Les oligo- elements ey la Vigne, Vititechnique 45: 4-6.

Dhillon. B. S. and Aulakh, B. S. (1972). Foliar Fertilization on AnabShahi grapes. Punjab Agric. Univ. J. Res. 9:71 pp.

EL-Komy, H. M. and Wahab, A. M. A. (1998). Effect of simultaneous inoculation of Azospirillum fixation of two legumen using the N-isotope diluation technique (IDT) and the different method (DM). *Acta Microbiologica. Polonica*, 47(3): 283-296.

El-Shenawy, F.E. and Fayed, T.A. 2005. Evaluation of the conventional to organic and bio-fertilizers on Crimson Seedless Grapevine in comparison with chemical fertilization 2-Yield and fruit quality. *Egypt Journal of Applied Sciences.* 20 (1). p.212-225.

Eman, A.A., Saleh, M.M.S. and Mostafa, E.A.M. (2008). Minimizing the quantity of mineral nitrogen fertilizers on grapevine by using humic acid, organic and bio- fertilizers, *Res.J. of Agric. And Biol.Sci.* 4 (1). P. 46-50.

Fawzi, M.I.F., Haggag, L.F., Shahin, M.F.M., Merwad, M.A. and Genaidy, E.A.E. (2014). Influence of spraying urea, born, and active dry yeast on growth, yield, leaf chemical composition and fruit quality of "Superior" Grapevines (*Vitis vinifera* L.) grown in sandy soil conditions. *Middle East Journal of Applied Sciences.* 4 (3). p.740-747.

Ferguson, J.J., Aving, W.T., Allen, L.H. and Koch, K.E. 1995. Growth of CO_2 enriched sour orange seedlings treated with Gibberellic acid and cytokinins. *Proc. Florida-State Hort. Soc.* 99. p.37-39.

Gamal, A. A. (1992). Effect of soil conditioners on soil properties and plant yield. M.Sc. Thesis, Fac. Agric. AL-Azhar Univ., Egypt.

Gerasopoulos, D. and Drogoudi, P. D. (2005). Summer- pruning and preharvest calcium chloride sprays affect storability and low temperature breakdown incidence in kiwifruit. *Post-Harvest Biol. Techno.* 36: 303-308.

Ghosh, S.N., Tarai, R. and Pal, P.P. 2008. Performance of eight grape cultivars in laterite soil of west bengal. Proceedings of the International symposium on grape production and processing. *Acta Hort*. (785). p.73-77.

Gouble, B.; Bureau, S.; Grotte, M.; Reich, M.; Reling, P. and Audergon, J. M. (2005). Apricot postharvest ability in relation to ethylene production: Influence of picking time and cultivar. *Acta Horticulture*, 682, 127-134.

Gowda, V.N., Keshava, S.A. and Shyamalamma, S. 2008. Growth, yield and quality of Bangalore Blue grapes as influenced by foliar applied poly feed and multi-K. Proceedings of the International Symposium on Grape Production and Processing. *Acta Hort.* (785). p.207-211.

Harrison, J. S. (1968). Characteristics of food yeast. Proce. Biochem. Acad. Press. New York and London. 8. P. 59-62.

Kassem, H.A. and. Marzouk, H.A. 2002. Effect Of Organic And/Or mineral nitrogen fertilization on the nutritional status, yield and fruit quality of Flame seedless grapevines grown in calcareous soils. *Res. Agric. &. Biol. Sci.* 4 (1). p.46-50.

Koblet, W., Candolfi- Vasconcelos, C (1995). Development of the canopy and grape quality Abs. And Weinbau 131 (18): 468-470.

Kolble, H., Neineke, H.S. and Zhang, W.L. 1995. Differences in organic and mineral fertilization on potato tuber yield and chemical composition compared to model calculation. *Agribiol. Res.* 48 (1). p.63-73.

Mady, M. A. (2009). Effect of foliar application with yeast extract and zinc on fruit setting and yield of faba bean (Vicia faba L.). J. Biol. Chem. Environ. Sci. 4(2): 109-127.

Mahmoud, Y.A. (1996). Studies on histophysiological effects of hydrogen cyanamide (dormex) and yeast application on bud fertility vegetative growth and yield of "roumired" grape cultivars ph. D. Thesis. Fac. Agric. Assiut univ. Egypt.

Mohammed, S. M. and Abdulqader S. M. (2007). Effect of foliar application of Nitrogen and Magnesium on Grapevine cv. Taifi under non- irrigated condition. *Journal of University of Duhok*., 10 (2): 70- 74.

Montasser, A.S., El-shahat, N., Ghobreial., G.F. and El- wadoud, M.Z. (2003). Residual effect of nitrogen fertilizer on leaves and fruits of Thompson seedless grapes. *J. Environ. Sci.* 6 (2) . p. 465-484.

Moor, T.C. (1979). Biochemistry and physiology of plant hormones. Pub. By Springer-Verlag., New York, USA.

Natio , K.; Nagama, S.; Furye, K. and Suzuki, H. (1981). Effect of benzyl adenine on RNA and protein synthesis in intact bean leaves at various stages of agein. Plant Physiol., 52: 342-348.

Nijjar, G. S. (1985). Nutrition of fruit trees. Published by Mrs Usha Raj umar for Kalyani, India, New Delhi, pp: 10-52.

Saleh, M. M. S.; El-Ashry, S. and Gomaa, A. M. (2006). Performance of Thompson Seedless Grapevine (Vitis vinifera L.) as Influenced by Organic Fertilizer, Humic Acid and Biofertilizers under Sandy Soil Conditions. *Res. J. Agric. & Biol. Sci*., 2(6): 467-471.

Tehranifar, A; M. Zarei; B. Esfandiyari and Z. Nemati (2010). Physicochemical properties and antioxidant activities of pomegranate fruit (Punica granatum) of different cultivars grown in Iran. *Hort. Environ. Biotech.,* 51(6): 573-579.

Tourky, M.N., El-Shahat, S.S. and Rizk, M. H. (1995). Effect of Dormex on fruit set, quality and storage life of Thompson seedless grapes (Banati grapes). J. *Agric. Sci*., Mansoura Univ., Egypt. 20(12): 5139-5151.

Warring, P. E.; Phillips, I. D. G. (1973). The control of growth and differentiation in plants. E L B S ed., Pub by Pergamon Press Ltd. VK.

Yeo, E.; HawkBin, K.; SangEun, H.; JoonTak, L.; JinChang, V.; MyungOk, B.; Yeo, E. T.; Kwon, H. B.; Han, S. E.; Lee, J. T.; Ryu, J. C. and Byun, M. O. (2000). Genetic engineering of drought resistant potato plants by introduction of the trehalose-6-phosphate synthase (TPSI) gene from Saccharomyces cerevisiae. *Mol. Cells* 10(3): 260-268.

ttp://jgu.garmian.edu.krd https://doi.org/10.24271/garmian.322

Using Immunofluorescent Cell Marker Quantification as an Identification Method for M1 and M2 Macrophage Phenotypes

Hassan M. Rostam[1*]

[1]Division of Immunology, School of Life Sciences, University of Nottingham, University Park, Nottingham, UK

[*] Current address: Department of Biology, College of Education, University of Garmian, Kalar, Al-Sulaimaniyah, Kurdistan Region, Iraq

Email: hassan.rostam@garmian.edu.krd

Abstract

Macrophages as antigen presenting cell (APC) play a vital role in orchestrating immune responses against foreign materials. The activation status of macrophages could be determined by tracking the expression of various cell markers that can be a signal for their immune activity behaviour following cellular stimulation either towards healing or inflammation. Previously numerous immunofluorescent cell markers have been used for distinguishing between pro-inflammatory macrophage phenotype (M1) and anti-inflammatory macrophage phenotype (M2) qualitatively, although most of those fluorescent cell markers express in both phenotypes. We have developed a new strategy to identify M1 and M2 phenotype quantitatively by using immunofluorescent cell markers. This approach enables the identification of different macrophage functional phenotypes quantitatively, and their degree of polarisation. Macrophages were polarised to M1 and M2 phenotypes by GM-CSF+IFN-γ and M-CSF+IL-4, respectively. Control cells were un-polarised (naïve) macrophages or monocytes were considered as macrophage progeny. For assessing cell polarisation all cell types were stained for nucleus. Also, their surface markers were stained with calprotectin for M1 cells and mannose receptor (MR) for M2 cells, followed by fluorescent microscopy examination. Cell images were analysed using CellProfiler software in order to measure the fluorescent signal intensity of the cell markers, and create a specific profile for each cell type. These profiles formed the

basis for M1 and M2 phenotype identification. By using such fluorescent signal parameters we were able to identify M1 and M2 phenotypes effectively and distinguish them from naïve macrophages and monocytes.

***Keywords*:** Macrophages; M1and M2 phenotypes; CellProfiller; macrophage identification.

1. Introduction

Macrophages as a constituent of the innate immunity and as APC, play a crucial role in defence against foreign pathogen invaders as well as in human body haemostasis. They contribute to phagocytosing dead cells and microbes, recruiting immune cells to the micro-environment, presenting antigens and providing essential activation signals for T cells (Goerdt & Orfanos, 1999, Martinez & Gordon, 2014, Kratky *et al.*, 2011).

Various macrophage subsets have been identified, each subset with distinct functional characteristics (Sutterwala *et al.*, 1997). For example, M1 (classically activated) macrophages with pro-inflammatory and anti-tumour functions (Sutterwala *et al.*, 1997) secrete large amount of pro-inflammatory interleukin 12 (IL-12) and (IL-23) (Mantovani *et al.*, 2004). M1 phenotype is induced by interferon gamma (IFN-γ) secreted mainly from T helper 1 (T_H1) cells, natural killer (NK) cells or $CD8^+$ cytotoxic T cells (CTLs) in the presence of bacterial cell wall components such as lipopolysaccharide (LPS) (Mosser & Edwards, 2008). However, M2 (alternatively activated) macrophages with anti-inflammatory and pro-wound healing activities (Sutterwala *et al.*, 1997), secrete high levels of cytokine IL-10 (Fleming & Mosser, 2011). They can be induced by cytokines IL-4 and/or IL-13, secreted mainly by T_H2 cells (Mosser & Edwards, 2008) or mast cells (Bradding *et al.*, 1992).

In vitro, M1 phenotype can be polarised from monocytes by IFN-γ (Garcia *et al.*, 2014) and LPS (Mills *et al.*, 2000). In addition, granulocyte macrophage colony-stimulating factor (GM-CSF) has been used as a macrophage priming signal (Hamilton, 2002, 2008) which enhance the pro-inflammatory properties of polarised cells (Verreck *et al.*, 2004, Garcia *et al.*, 2014). By contrast, monocyte can be polarised toward M2 phenotype by adding IL-4 (Garcia *et al.*, 2014). M2 macrophage anti-inflammatory function can be enhanced with macrophage colony-stimulating factor (M-CSF) (Verreck *et al.*, 2004, Garcia *et al.*, 2014).

Cluster of Differentiation 68 (CD68) marker expresses in macrophages intracellularly and this marker is often used for macrophage identification (Sindrilaru *et al.*, 2011). In order to follow up macrophages activation status, a panel of: cell markers, secreted cytokines, transcription factors or metabolites are employed. For instance, production of high leveles of pro-inflammatory cytokines such as IL-1β, IL-6, tumour necrosis factor alpha (TNF-α) (Hofkens *et al.*, 2011, Hao *et al.*, 2012) IL-12 and IL-23 (Mantovani *et al.*, 2004) are considered as main characteristics of M1 macrophages subset. Furthermore, M1 macrophages have been shown to perform high level expressions of calprotectin (27E10 antigen) (Bartneck *et al.*, 2010), nitric oxide synthase 2 (NOS2) (Edin *et al.*, 2012), chemokine (C-C motif) receptor 7 (CCR7) (Agrawal, 2012), and CCR2 (Willenborg *et al.*, 2012). On other hand, M2 macrophages are identified by the secretion of high amounts of IL-10 cytokine (Mantovani, 2006), and transforming growth factor β (TGF-β) (Hao *et al.*, 2012). Moreover, M2 phenotype express high levels of mannose receptor (MR, CD206) (Agrawal, 2012;, Mantovani, 2006) , the scavenger receptor CD163 (Edin *et al.*, 2012) (Mantovani, 2006), and IL-1 receptor antagonist (IL-1RA) (Baitsch *et al.*, 2011).

With regard to gene expression and transcription factor phosphorylation, human M1 macrophages are identified by the expression of high levels of IL23a (IL23p19) and prostaglandin-endoperoxide synthase 2 (Ptgs2 or Cox2) gene, and phosphorylation of signal transducer and activator of transcription 1 (STAT1) and/or STAT3. In contrast, the main characteristics of human M2 macrophages, is the expression of high levels of chitinase 3-like 2 (Chi3l2 or Ykl39) and Kruppel-like factor 4 (Klf4) gene and phosphorylation of STAT6 (Murray & Wynn, 2011).

M1 and M2 macrophage activation results in murine that can be identified by distinct cell marker profile, while there is some overlap in the cell marker expression between both phenotype activation (status in human macrophages. For instance, Arginase-1 (Arg-1), known as murine M2 marker, has been expressed in both M1 and M2 macrophage phenotypes in human (El Kasmi *et al.*, 2008). In addition, M2 markers, chemokine (C-C motif) ligand 18 (CCL18) and MR can also be expressed on monocytes stimulated with LPS and GM-CSF or IFN-γ, respectively (Porcheray *et al.*, 2005). Accordingly, it seems that there are quantitative divergences in cell marker expression between human M1 and M2 macrophage phenotypes, rather than qualitative differences (Davis *et al.*, 2013).

The complexity of characterisation in M1/M2 human macrophages by surface cell markers has encouraged investigation in an alternative approach that would be less resource-intensive and simpler.

Studies that have reported morphological differences between macrophage phenotypes (Porcheray *et al.*, 2005, Chinetti-Gbaguidi *et al.*, 2011, Leitinger & Schulman, 2013, Pelegrin & Surprenant, 2009, Lee *et al.*, 2013, McWhorter *et al.*, 2013, Vereyken *et al.*, 2011, Rostam *et al.*, 2017) has been categorised for Image based Machine Learning for identification of macrophage subsets (Rostam *et al.*, 2017). This new approach has led us to hypothesise that cell surface marker signal intensity could be quantified and used as an indicator of activation status in macrophages.

The aim of the present study was to quantify the cell surface markers signal intensity, calprotectin (M1 cell marker) and MR (M2 cell marker) in M1 and M2 macrophage subtypes respectively. Data were collected and used to build a threshold to identify different macrophages status. Monocytes were stimulated *in vitro* for 6 days with M1 (GM-CSF+IFN-ᵧ) or M2 (M-CSF+IL-4)-inducing cytokines.

2. Materials and Methods

2.1 Monocyte isolation and culture

Buffy coats were obtained from the National Blood Service following Ethics committee approval (National Blood Services, Sheffield, UK; 2009/D055). Peripheral blood mononuclear cells (PBMCs) were obtained from buffy coats by Histopaque-

1077 (Sigma-Aldrich) density gradient centrifugation. Monocytes were isolated from PBMCs using the MACS magnetic cell separation system (positive selection with CD14 MicroBeads and LS columns, Miltenyi Biotec) (Rostam *et al.*, 2017, Rostam *et al.*, 2016). This method routinely yielded 95% pure monocytes as determined by flow cytometric analysis of CD14 expression.

Purified monocytes were suspended in RPMI-1640 medium supplemented with 10% FBS, 2 mM L-glutamine and 100 U/ml penicillin and 100 µg/ml streptomycin (all from Sigma-Aldrich) (henceforth referred to as "complete RPMI medium") with the cell density of 1 x 10^6 cells/ml. 1 ml of the suspension (=1 x 10^6 monocytes) was seeded on round coverslip 12mm in each well of 24 tissue culture well plate, then incubated at 37˚C, 5% CO_2 in a humidified incubator for six days.

2.2 Immunofluorescent staining

On day 6 all adherent cells on round coverslips were fixed in 4% paraformaldehyde (EMS Diasum) in phosphate buffer saline (PBS), then blocked with 3% (w/v) bovine serum albumin (BSA) (Sigma-Aldrich) and 1% (w/v) Glycine (Fisher Scientific) in PBS. Subsequently, another blocking step was done using 5% (w/v) goat serum (Sigma) in PBS. Adherent cells were stained with 2 µg/ml anti-human calprotectin mouse IgG1 Ab (Thermo Scientific), and with 1 µg/ml rabbit CD206 (MR) anti human primary Ab (Abcam) followed by 1 h incubation at room temperature. After washing with PBS, cells were stained with 8 µg/ml Rhodamin-x goat anti-mouse IgG (H+L) secondary Ab (Invitrogen), and 8 µg/ml Alexa flour-488 goat anti-rabbit IgG(H+L) secondary antibody (Invitrogen) for another hour at room temperature. Then nuclei were stained with 250 ng/ml DAPI (4',6-Diamidino-2-Phenylindole) (Invitrogen). Slides were covered with FluorSave™ anti-fade medium (Calbiochem) and mounted with Fluoromount™ (Sigma-Aldrich). Arrays were imaged using an automated fluorescence microscope (IMSTAR) and by using CellProfiler cell image analysis software (http://www.cellprofiler.org/) the number of positively MR and calprotectin-stained cells from surfaces were identifiedDetermining M1 and M2 phenotype identification criteria using fluorescence microscopy

Cells of different activation states were produced using cytokine addition monocytes seeded on normal glass slides: for polarisation to M1 a mixture of 20 ng/ml IFN-γ (R&D Systems) and 50 ng/ml GM-CSF (Miltenyi Biotec) was added to a total volume of 1ml; for M2 differentiation 20 ng/ml of IL-4 (Miltenyi Biotec) and 50 ng/ml M-CSF (Miltenyi Biotec) were added to the well volume of 1 ml. The cells were incubated at 37ºC, 5% CO_2 in a humidified incubator for 6 days. On day 3 of incubation, 500 µl of the medium was replaced with fresh complete RPMI medium containing the same concentration and mix of cytokines that were used for cell stimulation at the beginning of culture. After six day of incubation M1 and M2 macrophages were stained with calprotectin (M1 marker) and MR (M2 marker). Images of both phenotypes were taken with an automated fluorescent microscope. Automated image analysis software (CellProfiler) was used to measure and record the maximum fluorophore intensity per image for nine different images. This was repeated for two different samples for the same biological donor and the average values of calprotectin in M2 and MR in M1 were calculated. These values were used as threshold intensity values of calprotectin and MR in order to categorise cells not exposed to cytokines, with each cell exhibiting fluorescence intensity above these calprotectin and MR thresholds categorised as M1 and M2 respectively**.**

2.3 Polymer Surfaces Synthesis

Polymer surface were synthesized using methods previously described (Anderson *et al.*, 2004, Hook *et al.*, 2012). Briefly, Each polymerisation solution was composed of monomer (50%, v/v) in dimethylformamide with photoinitiator 2,2-dimethoxy-2-phenyl acetophenone (1%, w/v). Polymers were purchased from Aldrich, Scientific Polymers and Polysciences and coated onto epoxy-coated slides (Xenopore) dip-coated with poly(2-hydroxyethyl methacrylate) pHEMA (4% w/v, Sigma) in ethanol (95% v/v in water). Coated surfaces were sterilised by exposure to UV light for 15 minutes. The hits materials were scaled up as polymer coupons formed by pipetting polymerization solution (6µL) onto a pHEMA coated slide and irradiating for 10 mins at O_2 < 1300 ppm with a long wavelength UV source. Once formed, volatile components were removed from the polymers at <50 mTorr for 7 days. Polymers were characterized by water contact angle measurements and time-of-flight secondary ion mass spectrometry as previously described (Taylor *et al.*, 2007, Urquhart *et al.*, 2007).

3. Results

3.1 Determining macrophage pro or anti-inflammatory phenotype using fluorescent microscopy

Surface marker expression is widely used to assess macrophage phenotype and it is readily applied to high throughput assessment of cells adhered to glass slide using automated microscopy and high content image analysis (Murray *et al.*, 2014, Xue *et al.*, 2014). We chose to undertake a high throughput glass slide microarray screen using fluorescent microscopy to assess the proportion of pro-inflammatory M1 macrophages using expression levels of calprotectin and anti-inflammatory M2 phenotypes using mannose receptor (MR), or CD206 expression (Rostam *et al.*, 2016). To assess the performance of macrophage polarisation under the impact of different polymers we first measured the expression of these markers in populations of cytokine polarised M1 or M2 macrophages cultured on glass slides for reference. Fluorescence images of a minimum of 100 cells in 9 fields of view were analysed for each cytokine polarisation and in two different experiments for the same biological donor prepared on the same day. The maximum calprotectin fluorescent pixel intensity for each cell was used to represent its fluorescence expression and the average value was calculated for each cytokine polarisation to represent the mean cellular expression for M2 polarised cells, termed *M2-expression*. The same procedure was followed for the MR fluorescence to obtain a mean cellular fluorescence expression for M1 polarised cells, or *M1-expression*. These mean cell threshold fluorescence values for calprotectin and MR expression for individual cytokine polarised M1 or M2 cells were used to categorise the phenotype of the individual macrophage cells on polymer surfaces as either M2 or M1 when they exceed these average levels of fluorescence expression. This is all about methodology not results, either this part is cut down or moved to materials and methods.

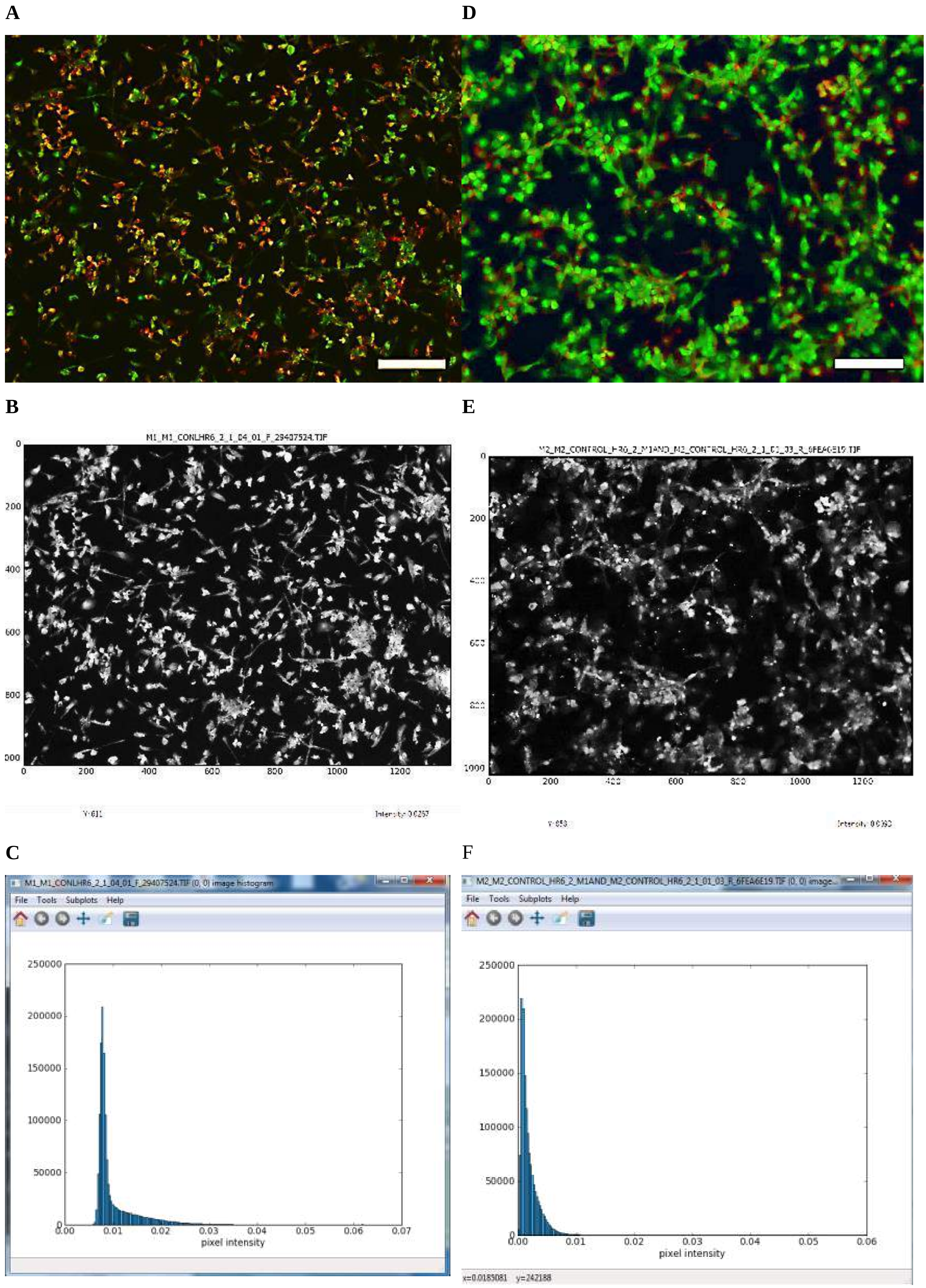

Figure 1: M1(A-C) and M2(D-F) threshold controls. (A) M1 phenotype polarised with IFN-γ + GM-CSF and

incubated for six days **(B,C)** Mean of maximum intensity of MR in M1 measured by CellProfiler per image **(D)** M2 phenotype polarised wit M-CSF+IL-4 and incubated for six days **(E,F)** Mean of maximum intensity of MR in M1 per image **(C,F)** X axis (pixel intensity), y axis (pixels). *n*= 2 sample for each phenotype, 9 images for each sample (mean of =2X9) . **(A,C)** Fluorescent images of cells stained for calprotectin (27E10 antigen, red), and mannose receptor (MR, green). Scale bar = 200 µm.

Using this procedure the cell populations polarised by cytokines to M1 and M2 that found to have a cell number ratio of M2/M1=0.3 and 4.0 respectively, illustrating good categorisation of these reference samples by the method (Figure 1). For macrophages on polymer arrays, cell populations with cell number M2/M1 ratios below or above those found in these reference populations were considered to represent polymers inducing predominantly either M1 or M2 differentiation respectively (Figure 2).

A

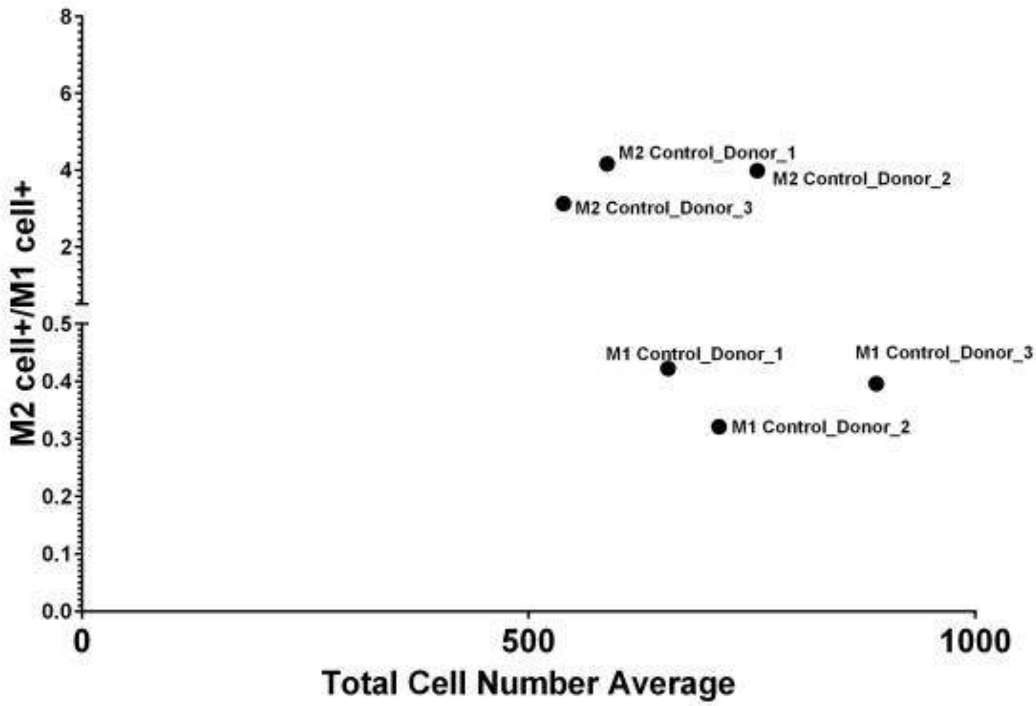

B

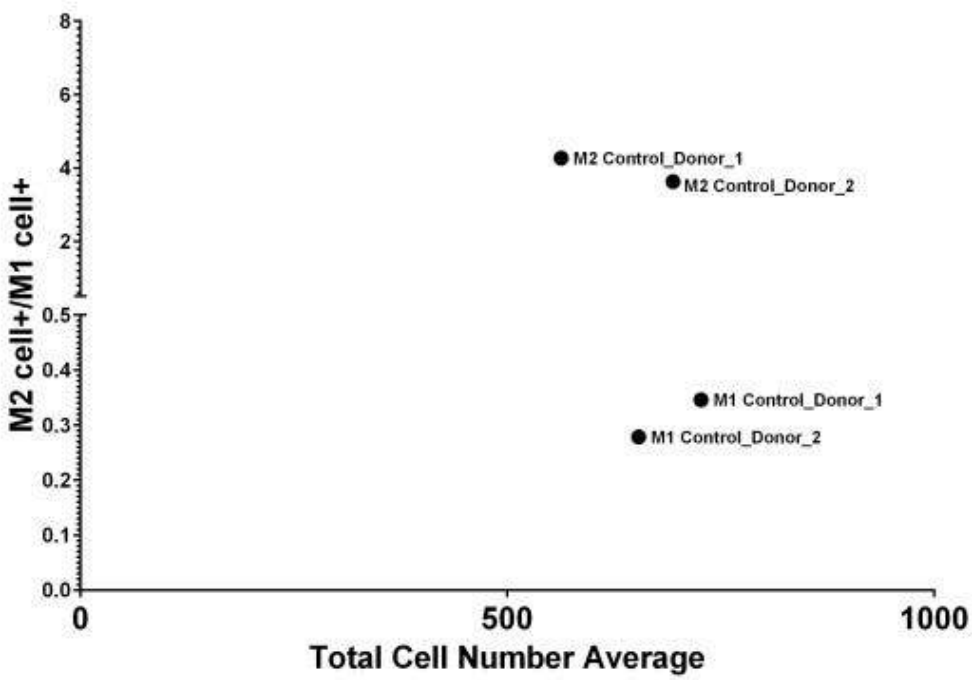

Figure 2: Determining macrophage pro or anti-inflammatory phenotype using fluorescence microscopy (**A,B)** Scatter plot for number of M2 /M1polarised cells with cytokines on glass slide, X-axis average total cell number of the adherent cells ,Y-axis is number of cells expressed MR^+(M2- phenotype)/ number of cell expressed calprotectin (M1- phenotype)on glass slide . *n*=3(D, homo-polymer arrays experiment) and 2 (E, co-polymer arrays experiment) of different samples (M1 and M2) for each sample with 2 replicates.

3.2 Macrophage polarisation

Using fluorescence microscopy the number of MR^+ and calprotectin$^+$ cells was quantified for each homo-polymer using the M1 and M2 identification criteria developed on cytokine differentiated naïve macrophages. Homo-polymer number (decyl methacrylate) was the most effective at polarising the cells towards the M2 phenotype, with 2.9 times more cells expressing MR (68±28 cells) compared to calprotectin (24±21cells) as seen in Figure 2. A high degree of cell attachment (88±23 cells) was also observed on this homo-polymer. Other materials polarising cells towards the M2 phenotype included homo-polymer numbers (hexyl acrylate) with ratios of MR^+ to calprotectin$^+$ cells of 2.6 The homo-polymers(hydroxypropyl acrylate) were the most effective at polarising cells towards the M1 phenotype whilst still supporting the attachment of more than 50 cells , with 3 times more calprotectin$^+$ cells than MR^+ cells **(Figure 3)**.

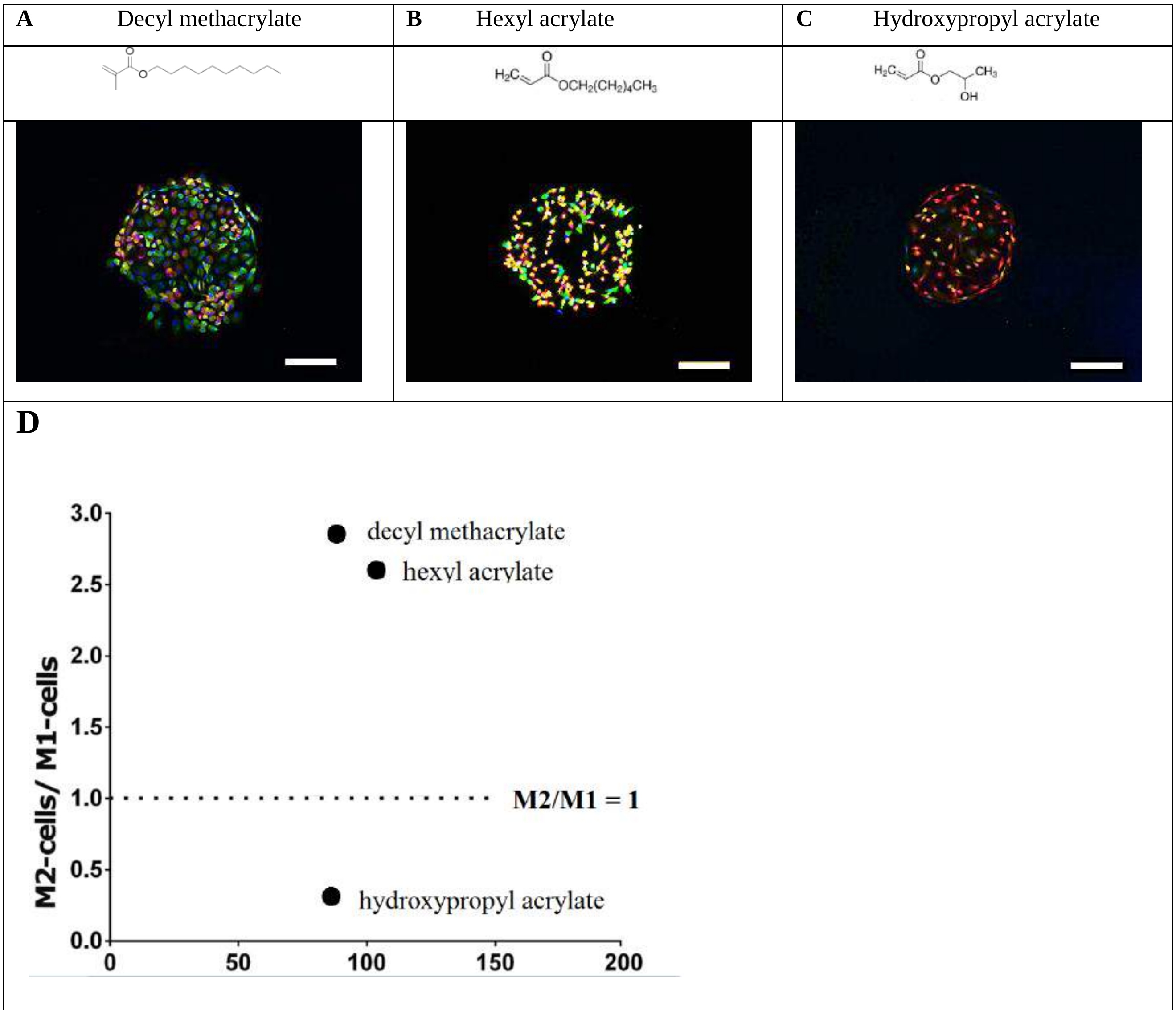

Figure 3: Effect of homo-polymers on macrophage polarisation and cell adherence. (**A**) Effective homo-polymers; (decyl methacrylate); (**B**) (Hexyl acrylate); and **(C)** 98.(hydroxypropyl acrylate) with their chemical structure, Fluorescent images of cells stained for calprotectin (27E10 antigen, red), and mannose receptor (MR, green) and nucleus (DAPI blue) on most effective homo-polymers, Scale bar = 200 µm.(**D**) Scatter plot for **number of** M2 cell/M1 cell on homo-polymers, x-axis average total cell number on homo-polymer ,Y-axis is number of cells expressed MR^+(M2-like phenotype)/ number of cell expressed calprotectin (M1-like phenotype)on homoplolymer. Dotted line is cells with M2-like cells (MR^+ cells)/M2-like cells ($Calprotectin^+$ cells) =1. Data below SNR threshold (mean/SD≥2) were excluded, *n*=3 of different donors each donor with average of three replicates.

4. Discussion

In this work, for first time MR and calprotectin has been quantified in M1 and M2 macrophage subsets, and used as threshold for M1 and M2 identification.

M2 macrophages expressing high amount of MR can be induced *in vitro* by IL-4 and IL-13 (De Paoli *et al.*, 2014). MR in macrophages observed to operate control of innate immunity and it is also believed to be involved in regulating antigen presentation and lymphocytes trafficking to lymph nodes. In addition, MR as a scavenger receptor has preference for collagens and for glycosylated proteins (Hagert *et al.*, 2018). However, M2 macrophages may express low amount of calprotectin (Hsu *et al.*, 2009) which has been considered as M1 cell marker (Bartneck *et al.*, 2010, Rostam *et al.*, 2017, Rostam *et al.*, 2016).

M1 macrophages which can be stimulated by Lipopolysaccharide (LPS) and interferon-γ (IFN-γ) (Huang *et al.*, 2017) can be characterised by expression of a high level of calprotectin (Bartneck *et al.*, 2010, Rostam *et al.*, 2017, Rostam *et al.*, 2016) which could induce pro-inflammatory cytokine production properties of the macrophages. However, calprotectin may express in monocytes and M2 macrophages (Xia *et al.*, 2018).

From visual inspection of cell surface marker expression of macrophages, immediate differences in their respective signals has been noticed, these differences has been quantified by CellProfiller software which can detect signal intensity of each cell markers and their distributions across the cell surface (Rostam *et al.*, 2017). The mean of maximum expression of calprotectin in M2 phenotype cells can be used as a save threshold for M1 phenotypes. In addition, M2 can be identified when the mean of MR signals of any cell exceeded the mean of maximum MR intensity signals of M1 phenotypes. Later, this way of cell identification successfully has been used to identify the macrophage polarisation to word M1 and M2 under the impact of surface chemistry modulation (Rostam *et al.*, 2016).

Biomaterial surface chemistry has previously been shown to modulate macrophage adhesion and function (Rostam *et al.*, 2015). In this study a high throughput screening strategy has been used to collect image data from incubated cells, the M1 and M2 phenotypes controls, and from macrophages seeded on different homo-polymers. This new approach used to investigate the effect of different homo-polymers surface chemistries on human monocyte differentiation. By using the method M1 and M2 biased homo-polymers has been identified depending on data analysis by the new method effectively.

Conclusion

Using immunofluorescent cell marker quantification, as a new effective identification method for M1 and M2 macrophage phenotypes in mixed macrophage population could pave the way for further investigations in this area. This method is capable of achieving high degrees of accuracies, in contrary to macrophage phenotype heterogeneity that can affect the cell marker signal expression. However, presented data provide strong indications for ability of this method to perform M1 and M2 subtype identification with less resource intensive and fast way of identification, still it is be too early to suggest this approach as an alternative for conventional cell phenotyping in wide scale cell identification.

References

Agrawal, H. (2012). *Open Journal of Regenerative Medicine* 01, 51-59.
Anderson, D. G., Levenberg, S. & Langer, R. (2004). *Nature Biotechnology* 22, 863-866.
Baitsch, D., Bock, H. H., Engel, T., Telgmann, R., Muller-Tidow, C., Varga, G., Bot, M., Herz, J., Robenek, H., von Eckardstein, A. & Nofer, J. R. (2011). *Arteriosclerosis, thrombosis, and vascular biology* 31, 1160-1168.
Bartneck, M., Schulte, V. A., Paul, N. E., Diez, M., Lensen, M. C. & Zwadlo-Klarwasser, G. (2010). *Acta biomaterialia* 6, 3864-3872.
Bradding, P., Feather, I. H., Howarth, P. H., Mueller, R., Roberts, J. A., Britten, K., Bews, J. P., Hunt, T. C., Okayama, Y., Heusser, C. H. & et al. (1992). *The Journal of experimental medicine* 176, 1381-1386.
Chinetti-Gbaguidi, G., Baron, M., Bouhlel, M. A., Vanhoutte, J., Copin, C., Sebti, Y., Derudas, B., Mayi, T., Bories, G., Tailleux, A., Haulon, S., Zawadzki, C., Jude, B. & Staels, B. (2011). *Circ Res* 108, 985-995.
Davis, M. J., Tsang, T. M., Qiu, Y., Dayrit, J. K., Freij, J. B., Huffnagle, G. B. & Olszewski, M. A. (2013). *mBio* 4, e00264-00213.
De Paoli, F., Staels, B. & Chinetti-Gbaguidi, G. (2014). *Circulation Journal* advpub.

Edin, S., Wikberg, M. L., Dahlin, A. M., Rutegard, J., Oberg, A., Oldenborg, P. A. & Palmqvist, R. (2012). *Plos One* 7, e47045.
El Kasmi, K. C., Qualls, J. E., Pesce, J. T., Smith, A. M., Thompson, R. W., Henao-Tamayo, M., Basaraba, R. J., Konig, T., Schleicher, U., Koo, M. S., Kaplan, G., Fitzgerald, K. A., Tuomanen, E. I., Orme, I. M., Kanneganti, T. D., Bogdan, C., Wynn, T. A. & Murray, P. J. (2008). *Nature immunology* 9, 1399-1406.
Fleming, B. D. & Mosser, D. M. (2011). *Eur J Immunol* 41, 2498-2502.
Garcia, S., Krausz, S., Ambarus, C. A., Fernandez, B. M., Hartkamp, L. M., van Es, I. E., Hamann, J., Baeten, D. L., Tak, P. P. & Reedquist, K. A. (2014). *Plos One* 9.
Goerdt, S. & Orfanos, C. E. (1999). *Immunity* 10, 137-142.
Hagert, C., Sareila, O., Kelkka, T., Jalkanen, S. & Holmdahl, R. (2018). *Frontiers in immunology* 9, 114.
Hamilton, J. A. (2002). *Trends in immunology* 23, 403-408.
Hamilton, J. A. (2008). *Nat Rev Immunol* 8, 533-544.
Hao, N. B., Lu, M. H., Fan, Y. H., Cao, Y. L., Zhang, Z. R. & Yang, S. M. (2012). *Clinical & developmental immunology* 2012, 948098.
Hofkens, W., Storm, G., van den Berg, W. & van Lent, P. (2011). *Ann Rheum Dis* 70, A40-A40.
Hook, A. L., Chang, C. Y., Yang, J., Scurr, D. J., Langer, R., Anderson, D. G., Atkinson, S., Williams, P., Davies, M. C. & Alexander, M. R. (2012). *Jove-J Vis Exp*.
Hsu, K., Champaiboon, C., Guenther, B. D., Sorenson, B. S., Khammanivong, A., Ross, K. F., Geczy, C. L. & Herzberg, M. C. (2009). *Anti-inflammatory & anti-allergy agents in medicinal chemistry* 8, 290-305.
Huang, R., Wang, X., Zhou, Y. & Xiao, Y. (2017). *Bone research* 5, 17019.
Kratky, W., Sousa, C. R. E., Oxenius, A. & Sporria, R. (2011). *Proc Natl Acad Sci U S A* 108, 17414-17419.
Lee, H. S., Stachelek, S. J., Tomczyk, N., Finley, M. J., Composto, R. J. & Eckmann, D. M. (2013). *J Biomed Mater Res A* 101, 203-212.
Leitinger, N. & Schulman, I. G. (2013). *Arterioscl Throm Vas* 33, 1120-1126.
Mantovani, A. (2006). *Blood* 108, 408-409.
Mantovani, A., Sica, A., Sozzani, S., Allavena, P., Vecchi, A. & Locati, M. (2004). *Trends in immunology* 25, 677-686.
Martinez, F. O. & Gordon, S. (2014). *F1000prime reports* 6, 13.
McWhorter, F. Y., Wang, T. T., Nguyen, P., Chung, T. & Liu, W. F. (2013). *P Natl Acad Sci USA* 110, 17253-17258.
Mills, C. D., Kincaid, K., Alt, J. M., Heilman, M. J. & Hill, A. M. (2000). *J Immunol* 164, 6166-6173.
Mosser, D. M. & Edwards, J. P. (2008). *Nat Rev Immunol* 8, 958-969.
Murray, P. J., Allen, J. E., Biswas, S. K., Fisher, E. A., Gilroy, D. W., Goerdt, S., Gordon, S., Hamilton, J. A., Ivashkiv, L. B., Lawrence, T., Locati, M., Mantovani, A., Martinez, F. O., Mege, J. L., Mosser, D. M., Natoli, G., Saeij,

J. P., Schultze, J. L., Shirey, K. A., Sica, A., Suttles, J., Udalova, I., van Ginderachter, J. A., Vogel, S. N. & Wynn, T. A. (2014). *Immunity* 41, 14-20.
Murray, P. J. & Wynn, T. A. (2011). *Nat Rev Immunol* 11, 723-737.
Pelegrin, P. & Surprenant, A. (2009). *The EMBO journal* 28, 2114-2127.
Porcheray, F., Viaud, S., Rimaniol, A. C., Leone, C., Samah, B., Dereuddre-Bosquet, N., Dormont, D. & Gras, G. (2005). *Clinical and experimental immunology* 142, 481-489.
Rostam, H. M., Reynolds, P. M., Alexander, M. R., Gadegaard, N. & Ghaemmaghami, A. M. (2017). *Scientific reports* 7, 3521.
Rostam, H. M., Singh, S., Salazar, F., Magennis, P., Hook, A., Singh, T., Vrana, N. E., Alexander, M. R. & Ghaemmaghami, A. M. (2016). *Immunobiology* 221, 1237-1246.
Rostam, H. M., Singh, S., Vrana, N. E., Alexander, M. R. & Ghaemmaghami, A. M. (2015). *Biomaterials science* 3, 424-441.
Sindrilaru, A., Peters, T., Wieschalka, S., Baican, C., Baican, A., Peter, H., Hainzl, A., Schatz, S., Qi, Y., Schlecht, A., Weiss, J. M., Wlaschek, M., Sunderkotter, C. & Scharffetter-Kochanek, K. (2011). *The Journal of clinical investigation* 121, 985-997.
Sutterwala, F. S., Noel, G. J., Clynes, R. & Mosser, D. M. (1997). *J Exp Med* 185, 1977-1985.
Taylor, M., Urquhart, A. J., Zelzer, M., Davies, M. C. & Alexander, M. R. (2007). *Langmuir* 23, 6875-6878.
Urquhart, A. J., Anderson, D. G., Taylor, M., Alexander, M. R., Langer, R. & Davies, M. C. (2007). *Adv Mater* 19, 2486-+.
Vereyken, E. J., Heijnen, P. D., Baron, W., de Vries, E. H., Dijkstra, C. D. & Teunissen, C. E. (2011). *Journal of neuroinflammation* 8, 58.
Verreck, F. A. W., de Boer, T., Langenberg, D. M. L., Hoeve, M. A., Kramer, M., Vaisberg, E., Kastelein, R., Kolk, A., de Waal-Malefyt, R. & Ottenhoff, T. H. M. (2004). *P Natl Acad Sci USA* 101, 4560-4565.
Willenborg, S., Lucas, T., van Loo, G., Knipper, J. A., Krieg, T., Haase, I., Brachvogel, B., Hammerschmidt, M., Nagy, A., Ferrara, N., Pasparakis, M. & Eming, S. A. (2012). *Blood* 120, 613-625.
Xia, C., Braunstein, Z., Toomey, A. C., Zhong, J. & Rao, X. (2018). *Frontiers in immunology* 8.
Xue, J., Schmidt, S. V., Sander, J., Draffehn, A., Krebs, W., Quester, I., De Nardo, D., Gohel, T. D., Emde, M., Schmidleithner, L., Ganesan, H., Nino-Castro, A., Mallmann, M. R., Labzin, L., Theis, H., Kraut, M., Beyer, M., Latz, E., Freeman, T. C., Ulas, T. & Schultze, J. L. (2014). *Immunity* 40, 274-288.

ttp://jgu.garmian.edu.krd https://doi.org/10.24271/garmian.323

Evaluation of some interleukins and immunomodulatory factors in Iraqi scabies patients

Nora.D. Al-Musawi[1] Nagham Y.Al-Bayati[1] Munther, Hussain[2]

[1]College of Education for Pure Science, University of Diyala, Iraq

[2]King's College London, London, UK

E-mail: munther.hussain@kcl.ac.uk

Abstract

Scabies is a contagious skin infection, caused by *Sarcoptesscabiei*. It is one of a neglected parasitic disease. It causes complications that lead to inflammatory and allergic immune response.This study was designed to obtain the role of some cytokines in scabies patients and compare their levels with dermal diseases patients and control (healthy).

The study included one hundred and three patients infected with scabies, seven dermal disease patients (positive controls) as well as 34 healthy individual as control group. The blood samples were collected from scabies and dermal disease patients as well as the control groups.Enzyme linked immunosorbent assay(ELISA) was used to measure Interleukine-4 (IL-4), Interleukin -8 (IL-8), Interleukin-17A (IL-17A), Tumor necrosis factor-α (TNF-α), Interferon-γ (IFN-γ), Monocyte Chemotactic Protein-1 (MCP-1) and Macrophage Inflammatory Protein-1-α (MIP-1- α) in the serum of scabies patients, dermal disease patients and healthy individuals.

The results showed that IL-4, IL-8, IL-17A and TNF- α was higher in scabies patients than in other groups (positive control and healthy), with no significant differences. While both of MIP- α and MCP-1 were higher in scabies patients compared with healthy group, with significant differences. MIP- α was higher in dermal patients individuals than in scabies patients. TNF- α was lower in scabies patients than in healthy group but higher than in dermal disease patient group.There was positive correlation between IL-17A and each of IL-8, TNF- α, MCP-1 and between IL-8 and both of IL-17A and MCP-1, while there was negative correlation between MIP-1- α and both of IL-4 and MCP-1.The results suggested that the scabies infection may induce the systemic and inflammatory immune response.

Keywords: Scabies, IL-4, IL-8, IL-17A, TNF-α, IFN-γ, MCP-1, MIP-1- α

1. Introduction:

Scabies is a disease affecting both sexes at different ages for all ethnic and socio- economic levels without exception (W.H.O., 2005). It remains a certain health problem causes a serious economic loss for cattle breeders and farm animals(Jordan &Verma, 2014). It is cutaneous infestation caused by a tiny obligate parasite belong to scabies mites (*Sarcoptesscabiei*)affects various kinds of domestic and wild animals (Pence &Veckermann, 2002; Walton et al., 2004).

Despite of *Sarcoptesscabiei* worldwide spread and infects over than 40 kinds of mammals including human, it still considersa neglected parasitic disease.The cold weather and high population density are a crucial factors for increase prevalence of disease (Daown et al.,1999; Poulat&Nasirian, 2007). Low temperatures and high relative humidity are suitable environment conditions for increase mites activity and infection (Arlian, 1989;White, 2009).

Scabies has been found to be more prevalent in both developing and developed countries andhas high incidence in crowded and poor populations, such as prisons and civil institutions, nursing and orphans centers as well as army andemigrant and immigrant camps (Routh et al.,1994). Individuals with scabies suffer from severe itching mediated through hypersensitivity reaction caused by mite's antigens and its secretion(Walton, et al., 2004).Liu, et al., (2014) confirmed that mitesmay induce an inflammatory and cell-mediated immune responses in its host. Other studies indicated that Scabies induces immune allergic responseand keratinocytes and lead to secretion of its some cytokines (Arlian et al., 2003; Walton, et al., 2010) in the other hand, Al-Musawi (2014) referred that the disease stimulates both humoral and cellular immune responses.

A numerous studies focus on the humoral and cellular immune response, most of these studies conducted on laboratory animals (mice, rabbits, pigs), either exposed to the parasite antigens or infected with parasite itself (Smets&Vercruysse, 2000; Mounsey, et al.,2015).Despite the availability of a lot of information on the immunology of scabies in human, there is a dearth of studies that address the immunological changes that occur in human systemic immuneresponse. Previously literature obtained that most common cells in the site of lesion areinflammatory cells (eosinophils, lymphocytes and macrophages),while the most predominant cells are T-lymphocyteswhich play a main role in the activation and regulation of immune responses by inducing cytokine production (Bhat el al., 2017).Keratinocytes may also produce pro-inflammatory and immunomodulatory cytokines and they consider to be responsible for systemic effects (Al-Musawi et al., 2014). The present study was conducted to determine IL-4, IL-17A, IL-8, TNF-α, IFN-γ, MCP-1, MIP-1-α levels inscabies patients, dermal disease patients and healthy (control) in Diyala province and to compare cytokines levels in all studied groups.

2. Material and Methods:

2-1. Subjects: The study samples were collected from March to May 2016.One hundred and three patients infected with scabies,(50 males and 53 females), their ages between 1-90 years were including in the present study. The diseaseswere diagnosed by dermatologist, the study included also sevendermal disease patients (five males and two females).Their ages between 2-54 years as apositive control, as well as the healthy group (control) included 34 persons (21 males and 13 females) their ages between (5-63) years. It has been confirmed that all group individuals did not have allergic diseases, helminthic infections, secondary infection, previous attack with scabies, and/or getting any antihistamines drugs were included for cytokines assays.

2-2. Blood sample collection: The blood sampleswere collected from scabies and dermal disease patients as well as the control groups. Five ml of venous blood was taken and leftto clot in room temperaturefor 30-60 minutes. Serum was separated by centrifuging at 3000 rpm for five minutes. Sera were divided into four parts using Eppendorf tubes (0.5ml per each). The samples were kept at -20 C° until it uses.

2-3.Clinical examination: The clinical examination had been done by the dermatologistsin hospital and the scabies and other dermal diseases were diagnosedaccording to clinical features.

2-4.The cytokines assay: The cytokines werequantitatively measured in allgroups individuals. These cytokines were human IL-4, IL-8, IL-17A, TNF-α, IFN-γ, MCP-1 and MIP-1-α by using enzyme linked immunosorbent assay, according to manufacturers' instruction, PeproTech Com, UK.

2-5.Statistical Analysis: The results were statistically analyzed using Statistical Package for Social Sciences (SPSS),version 15. Data were expressed as mean± standard error(SE). Duncan's multiple range test was used for comparison among several means. Pearson Correlation (r) wasused to determine the correlation between criteria. P-value ≤0.05 was considered statistically significant.

3. Results:

3-1.Cytokines levels: The results of the present study showedhigh level concentration of cytokine IL-4 in scabies patients (84.101±23.844 pg/ml) comparing with its levels in dermal diseases patients (77.871± 45.242 pg/ml), and the control group (49.106±16.044 pg/ml) but without significant differences as shown in Table1.

Table (1): Cytokines and chemokines level among individuals infected with scabies, dermal diseases and healthy persons.

Cytokines and chemokines	Groups	Mean ±SE pg/ml	ρ- value
IL-4	Scabies patients	84.101±23.844	0.812(NS)
	Dermal diseases patients	77.871 ± 45.242	
	Control	49.106 ± 16.044	
IL-8	Scabies patients	33.746 ± 9.996	0.755(NS)
	Dermal diseases patients	34.742 ± 14.642	
	Control	14.143 ± 4.379	
IL-17A	Scabies patients	49.738 ± 9.768	0.651(NS)
	Dermal diseases patients	33.285 ± 14.842	
	Control	44.817 ± 7.694	
IFN-γ	Scabies patients	177.864 ± 10.626	0.042*
	Dermal diseases patients	86.142 ± 11.244	
	Control	180.705 ± 19.114	
TNF-α	Scabies patients	75.306 ± 23.321	0.785(NS)
	Dermal diseases patients	49.028 ± 23.361	
	Control	55.217 ± 17.990	
MCP-1	Scabies patients	253.466± 18.979	0.01**
	Dermal diseases patients	332.714 ± 45.531	
	Control	185.750 ± 32.543	
MIP-1-α	Scabies patients	601.194 ± 140.528	0.023*
	Dermal diseases patients	2426.857± 1352.358	
	Control	491.706± 488.358	

*** Significant differences in p<0.05.**

**** Significant differences in p<0.001**

The results showedelevation in IL-8 concentration in both scabies and dermal diseases serum (33.746±9.996 and 34.742 ±14.642pg/ml, respectively)comparedwith in healthy group (14.143 ± 4.379 pg/ml), while IL-17A was increase in scabies patients serum (49.738± 9.768 pg/ml)and healthy group (44.817 ± 7.694 pg/ml) compared with dermal diseases patients (33.285 ± 14.842 pg/ml)as sowed in Table 1.

IFN-γ wasdecreasein scabies patients and dermal patients diseases comparing tohealthy group (177.864 ± 10.626pg/ml, 86.142 ± 11.244pg/ml,180.705 ± 19.114pg/ml, respectively). The present study showed increase in TNF-α levels in scabies patients comparing with dermal diseases patients andhealthy group (75.306 ± 23.321pg/ml, 49.028 ± 23.361pg/ml , 55.217 ± 14.990 pg/ml, respectively)

The current study showed increase in both of MCP-1and MIP-1-αscabies and dermal diseases patients serum comparing with healthy group (253.466 ± 18.979pg/ml , 332.714 ± 45.531pg/mland185.750 ±32.543pg/mlfor MCP-1 and 601.194 ±

140.528pg/ml, 2426.857 ± 1351.358pg/ml and 601.194 ± 140.528 pg/ml, respectively)

3-2.Correlation of cytokines in scabies patients:

The current study showedthat there was positive correlation between IL-17A and each of IL-8, TNF- α, MCP-1 and between IL-8 and both of IL-17A and MCP-1, while there was negative correlation between MIP-1- α and both of IL-4 and MCP-1 as showed in table (2):

Table (2): Cytokines correlation among 103 scabies patients

	IL-4	IL-8	IL-17A	IFN-γ	TNF-α	MCP-1	MIP-1-α
IL-4	1						
IL-8	0.339**	1					
IL-17A	0.011	0.731**	1				
IFN-γ	0.285**	0.128	1.142	1			
TNF-α	0.070	0.093	0.288**	0.110	1		
MCP-1	0.096	0.386**	0.294**	0.132	0.039	1	
MIP-1-α	0.019-	0.050	0.025	0.056	0.351**	0.008-	1
Correlation in P- value 0.01							

4. Discussion:

The current study showed increase in the level of IL-4 in scabies patients serum comparing with dermal diseases patients and healthy group (control). This results agree with Karthikeyan&Ragunatha (2011) , Al-Musawi, et al., (2014) and Mounsey, et al., (2015). They mentioned that there is an increase in IL-4 levels in scabies patients comparing with the healthy group while Arlian et al., (2006) did not record this cytokine in scabies patients. In the other hand Walton, et al., (2010) showed there is no significant differences in the levels of IL-4 between the scabies patients and healthy groups. The increase of this cytokine (IL-4) (which is one of the cytokines expression of Th2) indicates that Th2 cells stimulate in scabies infestation. This cytokince regulates the production of IgE and control the production of mast cell and eosinophils which are stimulating in hypersensitivity reaction (as shown in histological changes obtained in previous study for Almusawi et al, 2018). In addition the stimulating mast cell and eosinophils produce IL-4 (Zamorano et al, 2003). On the other hand, IL-4 play important rols as chemotactic immune response in skin lesion. Many other histological studies use human and animal models had been detected mast cells and basophils in skin lesion of human and animals infected with scabies (Amer et al ., 1995; Ito et al.,2011; Nimmervoll et a l., 2013; Mounsey et al.,2015). Activated mast cells and basophils rapidly produce some cytokines (including Th2 cytokines IL-4) which are the main molecules as well as that the cytotoxicity against keratinocytes mostly release cytokines responsible for amplify the allergic Th2-type inflammatory response (Bhat et al., 2017).

The present study obtained that the levels of IL-8 was increase in scabies and dermal disease patients comparing with healthy group, this results agree with Morgan &Arlian (2010) who showed that monocytes secret IL-8 in high levels after adding Sarcoptesscabiei antigen to the culture media or when exposed skin cells culture media (EpiDerm EFT-400 full-thickness Human Skin Equivalents) to extract of parasites. IL-8 secretes from skin cells (keratinocytes, fibroblasts, and macrophages), and the secretion of IL-8 increase in dermal diseases (Coondoo,2012).

The increase in IL-17A level in scabies patients in the present study agrees with Liu, et al. (2014) and Mounsey, et al. (2015) who reported that IL-17-A was increased in pigs infested with scabies. IL-17A is pro-inflammatory cytokine related with many hypersensitivity , host defense and inflammation diseases (Jin and Dong, 2013). Its secreted from mast cells and Th17 cells .Arlian et al., 2007, Martin et al., (2014) and Mounsey et al., (2015) referred that this cytokine related with IL-23 secreted by dendritic cells, macrophages and keratinocytes, all these cells are recorded in scabies cases, supporting an IL-17environment (Arlian et al., 2007; Martin et al ,2014) . The present study showed that INF-γ was decrease in scabies patients comparing with healthy and patients with dermal diseases groups. This results agree with Zamorano,Walton et al . (20032010) who obtained that there was a clear decreased of IFN-γ production was observed in scabies patients as a response to parasite cystine – proteinase. Arlian et al, (2007) referred that expose mice to live mites lead to decrease the expression of IFN-γ and suggest that the mite produce molecules reduce expression of immune cytokines and chemokine including IFN-γ. In the other hand, Arican, et al. (2005) showed that the cells production of this cytokine downregulates in the blood of dermal disease (such as psoriasis) and lead to aggravation of disease, in the contrary, some studies reported that there was increase in INF-γ in dermal diseases combined with macrophage (Hua, et al ., 2006; Huard, et al., 2017).

In the present study TNF-α level was increase in scabies patients serum and decrease among dermal diseases patients. This result agree with Arlian et al (2004) Morsy, et al., (1995) who demonstrated that TNF-α was increased in monocyte culture media when exposing to culture to scabies mite extract which indicate the ability of the molecules in the extract's molecules to modulate the monocytes and dendritic cells functions. Likewise Portugal, et al. (2007) , Al-Musawi, et al . (2014) and Abd El-Aal, et al. (2016) indicated a higher levels of TNF-α among individuals infested with scabies and suggested that there was an important role of TNF- α in human scabies control . While Portugal, et al. (2007) Levi – Schaffer, et al., (1998) showed that TNF-α production may be due to the physical stimulation by parasite's burrowing in the skin that lead to inflammatory response., Levi – Schaffer, et al., (1998) Mulline, et al . (2009) Morgan, et al., (2013) and Al-Musawi, et al., (2014) suggested that TNF-α associated with presence of eosinophils and its ability to active this cells in scabies patients.

The present results showed increase in MCP-1 level in scabies patient serum. This result agrees with Morgan &Arlian (2010) who indicated that MCP-1 increase in the culture media using (human skin equivalent) human skin cells was that exposed to mite extract and suggested that this result may be due to the physical stimulation resulting from extract's molecules borrowing by the mites which lead to produce this cytokine . Another study observed that salivary secretions and mite's antigen stimulate MCP-1 which in turn attracts lymphocytes, monocytes and dendritic cells to lesion areas result in inflammatory reactions (Kobets, et al., 2012).

This study showed increasing in MIP-1α among dermal diseases patient and scabies patients. These This results agree with Morgam et al, (2013) Kobets, et al. (2012) who suggested that in vivovitro, the interplay between cell media culture and the antigens of parasite is responsible for increase of this some chemokines also including MIP-1α, re MIP-2α and M3P-1α and suggested that the antigen of the parasite stimulates inflammatory immune response. In the other hand ,Kobets, et al. (2012) suggest that the increase of MIP-1α related with increase of TNF- α . MIP-1α was increase in cutaneous leishmaniasis patients this agree with Al-Saadi (2014) who showed increasing this cytokine among individual infected with cutaneous leishmaniasis and related with skin lesion numbers. MIP-1 α produce by macrophages and dendritic cells where Leishmaniatropica proliferation proliferate and increasing numbers of this parasite leading to rupture of these cells and release their contents (including (CCl3) MIP-1 α) . (Kobets, et al.,2012).

The current study showed that there was positive correlation between IL-17A and each of IL-8, TNF- α, MCP-1 and between IL-8 and both of IL-17A and MCP-1, while there was negative correlation between MIP-1- α and both of IL-4 and MCP-1 . These may reflect the complex associate relation in immune response and help explain the delayed inflammatory reaction to infestation with S. scabiei which needs further investigation and study .

Conclusion

The study concluded that the scabies infection may induce the systemic and inflammatory immune response.

References

-Abd El-Aal, A.A.; Hassan, M. A.; Gawdat; M.I.; Ali, M.A. &Barakat, M. (2016). Immunomodulatory impression of anti and pro- inflammatory cytokines relation to humeral immunity in human scabies. International Journal of Immunopathology and Pharmacology, 29(2): 188-194.

-Amer, M.; Mostafa, F.F.; Nasr, A.N.; and el-Harras, M. (1995). The role of mast cells in treatment of scabies. International Journal of Dermatology, 34(3):186–9.

-Al-Musawi, M.A.A. (2014). Evaluation of immune response in scabietic patients in Najaf Governorate. PH. D. Thesis, Kufa University, College of Science, Department of Biology: 102P.

-Al-Musawi, M.M.; Hasan, H.R. and Maluk, A.H,(2014). Relationship between Th1, Th2 immune response and serum SOD activity in scabies. Journal of Advanced Biomedical and Pathobiology Research, 4(1):1-15.

-Al-Saadi; K.H.R, (2014).Cytokines measurements IL-10, IL-17A, IL-4, MIP-1-α among individuals infected with leishmaniasis, M.Sc., College of Education For Pure Sciences, University of Diyala, 200p.

-Arican, O.; Arai, M., Sasmaz ; S. Ciragil, p.(2005). Serum levels of TNF-α, IFN-γ, IL-6, IL-8, IL-12, IL-17 and IL18 in patients with active psoriasis and correlation with disease severity. Mediators of Inflammation, 2005(5):273-279.

-Arlian, L.G. (1989). Biology, host relation and epidemiology of Sarcoptesscabiei. Annual Review of Entomology, 34(1): 139-161.

-Arlian, L.G.; Fall, N. & Morgan, M.S. (2007). In vivo evidence that Sarcoptesscabiei (Acari: Sarcoptidae) is the source of molecule, that modulate splenic gene expression. Journal of Medical Entomology. 44(6):1054-1063.

-Arlian, L.G.; Morgan, M.S. and Neal, J.S. (2004). Extracts of scabies mites (Sarcoptidae: Sarcoptesscabiei) modulate cytokine expression by human peripheral blood mononuclear cells and dendritic cells. Journal of Medical Entomology. 41 (1):69-73.

-Arlian, L.G.; Morgan, M.S & Paul, C.C. (2006). Evidence that scabies mites (Acari, sarcoptidae) influence production of interleukine-10 and function of T-regulatory cells (Trl) in humans. Journal of Medical Entomology, 23(2): 283-287.

-Arlian, L.G.; Morgan, M.S.& Neal, J.S. (2003). Modulation of cytokines expression in human keratinocytes and fibroblasts by extract scabies mites. The American Journal of tropical Medicine and Hygiene, 69(6):652-656.

-Bhat, S.A.; Mounsey, K.E.; Liu, X. & Walton, S. F. (2017). Host immune responses to the itch mite, Sarcoptesscabiei, in humans. Parasites and Vectors,10(1): 10:385 DOI 10.1186/s13071-017-2320-4

-Coondoo, A. (2012). The role of cytokines in the pathomechanism of cutaneous disorder. Indian Journal of Dermatology, 57(2):90-96.

-Downs, A.M.; Harvey, I. & Kennedy, C.T. (1999). The epidemiology of head lice and scabies in UK. Epidemiology and Infection, 122(3):471-477.

-Hua, Z., Feil, H. &Mingming, X. (2006). Evaluation and interferon of serum and skin lesion levels leukotrienes in patients with eczema. Prostaglandins leukotrienes and Essential Fatty Acids, 75(1): 51-55.

-Huard, C.; Gulla, S.V.; Bennett, D.V.; Coyle, A.J.; Velugels, R.A & Greenberg, S.A. (2017). Correlation of cutaneous disease activity with type interferon gene signature and interferon-β in dermatomysil. British Journal of Dermatology, 175(5): 1224-1230.

-Ito. Y.; Satoh, T.; Takayama, K.; Miyagishi, C.; Walls, A.F. and Yokozeki, H. (2011). Basophil recruitment and activation in inflammatory skin diseases. Allergy, 66(8):1107–13

-Jin, W. and Dong, C.(2013). IL-17 cytokines in immunity and inflammation.Emerging Microbes and Infections, 2(9): e60.

-Jordan, E.L. &Verma, S. P. (2014). Invertebrate zoology. Chand Company Ltd, New Delhi: 1127p.

-Karthikeyan, K &Ragunatha, S. (2011). Update on scabies and pediculosis in children, In :Inamadar, A.C. and Palit, A. (Edrs.) Advance in pediatric dermatology. Jawan Brothers Medical publisher (p) Ltd, New Delhi, India: 111-120p.

-Kobets, T.; Havelkova, H.; Grekov, L. Volkova, V.; Vojtiskova, J.; Svobodova, M.; Demank, P. &Lipoldova , M. (2012). Genetic of host response to Leishmaniatropica in mice different control to skin pathology, chemokine reaction and invasion in spleen and liver. POLS Neglected Tropical Disease, 6(6): e1667-e1679.

-Levi- Schaffer, F.; Temkin, V.; Malamud, V.; Feld, S &Ziberman, y. (1998). Mast cells enhance eosinophil survival in vitro: role of TNF- α and granulocyte-macrophage colony stimulating factor. Journal of Immunology, 160(11)5:5554-5562.

-Liu, X.; Walton, S.F.; Murrany, H.C.; king, M. Kelly, A.; Holt, D.C.; Currie , B.J.; Mccarthy, J.S.&Mounsey, K. E.(2014). Crusted scabies in associated with IL17 secretion by skin T cell. Parasite Immunology, 36(11): 594-604.

-Martin JC, Baeten DL, Josien R (2014) Emerging role of IL-17 and Th17 cells in systemic lupus erythematosus. ClinImmunol 154: 1–12. pmid:24858580

-Morgan, M.S. &Arlian, L.G. (2010). Response of human skin equivalent to Sarcoptesscabiei. Journal of Medical Entomology, 47 (5): 877-883.

-Morgan, M.S.; Arlian, L.G & Markey, M.P. (2013). Sarcoptesscabiei mites modulate gene expression in human skin equivalents. PLOS ONE, 8(8): e71143, doi: 10.137/Journal pone.0071143.

-Morsy, T.A.;elAlfy, M.S.; Arafa, M.A.; Salama, M.M & Habib, K.S. (1995). Serum levels of tumor necrosis factor alpha (TNF- α) versus immunoglobulin (IgG, Ig MandIgE) in Egyptian scabitic children. Journal of Egyption Society Parasitology, 25(3):773-788.

-Mounsey , K.E.; Murray, H.C.; Belefeld- Ohmann, H.; Pasay, C., Holt, D.C.; Currie, B.J.; Walton, S.F. &Mccarthy, J.S. (2015) prospective study in a porcine model of Sarcoptesscabiei indicates the association of Th2 and Th1 pathways with the clinical severity of scabies. PLOS Neglected Tropical Diseases Journal, 498: 1-17.

-Mullins, J.S.; Arlian, L. G. & Morgan; M.S. (2009). Extracts of Sarcoptesscabiei down modulate secretion of IL-8 by skin keratinocytes and fibroblast in the presence of proinflammatory cytokines. Journal of Medical Entomology, 46(4): 845-851.

-Nimmervoll, H.; Hoby, S.; Robert, N.; Lommano, E.; Welle, M. and Ryser-Degiorgis, M. P. (2013). Pathology of sarcoptic mange in red foxes (Vulpesvulpes): macroscopic and histologic characterization of three disease stages. Journal of Wildlife Disease, 49(1):91–102.

-Pence, DB &Veekermann,E. (2002). Sarcoptic manage in wild life. Revue Scienifique et Technique deLOIE.,33(2):413-420

-Portugal, M.; Barak, V.: Ginsburg. I. & Kohen, R. (2007). Interplay among oxidants, ant: oxidants, and cytokines in skin disorders: present status and future considerations. Biomedicine and Pharmacotherapy, 61(7):412-422.

-Poulat, A .&Nasirian, H. (2007). Prevalence of pediculosis and scabies in prisoners of Bander Abbas, Hormozgan province, Iran. Pakistan Journal of Biological Sciences, 10(21): 3967-3969.

-Routh, H.B. Mirensky, Y, M.; Parish, C.C. &Witkows, J.A. (1994). Ectoparasites as sexually transmitted diseases. Seminar Dermatology, 13(4):243-244.

-Smets, K. and vercruysse, J. (2000). Evaluation of different methods for the diagnosis of scabies in swine. Veterinary parasitology, 90(2):137-145.

-Toet, H. M.; Fischer, K.; Mounsey, K. E.; Sandeman, R. M., Autoantibodies to iron-binding proteins in pigs infested with Sarcoptesscabiei, Veterinary Parasitology (2014),http://dx.doi.org/10.1016/j.vetpar.2014.07.012

-Walton, S.F.; Holt, D.C.; Currie, B.J. & Kemp, D.J. (2004). Scabies: new future for neglected disease. Advances in Parasitology, 57: 309-317.

-Walton, S.F.; Pizzuto, S.: Slender, A.: Viberg, L.; Holt, D..' Hales, B.J.; kemp, D.J., currie, B.J; Rolland, J.M &O'Hehir, R.(2010). Increased allergic immune response to Sarcoptesscabiei antigens in crusted versus ordinary scabies. Clinical and Vaccine Immunology, 17(9): 1428-1438.

-White, J.J. (2009). The veron community scabies education and eradication program. Ph. D. Thesis, Faculty of Virginia polytechnic institute and state university: 102p.

-Word health organization. (2005). Epidemiology and management of common skin diseases in children in developing countries. Geneva: World Health Organization, Depart men of Child and Adolescent Health and Development. WHO/FCH/CAH/05-12:62p.

-Zamorano, J.: Rivas, M.D.& Perez, M. (2003). Interlukine-4: a multi- functional cytokine. Immunologia, 22(2):215-224.

ttp://jgu.garmian.edu.krd https://doi.org/10.24271/garmian.324

Incidence of Phthiriasis palpebrarum caused by pubic lice *Pthirus pubis*in Al-Sulaimaniyah province, Kurdistan region, Iraq

Omer Mahmood Amin[1*] Nahla Mahmood Ameen[2]

[1]PhD of Parasitology, Biology Depatment, College of Education, University of Garmian, Kalar, Al-Sulaimaniyah, Kurdistan Region, Iraq

[2]High Diploma of Ophthalmology,Shahid Doctor Aso Hospital, Department of Ophthalmology Clinic, Al-Sulaimaniyah, Kurdistan Region, Iraq
Email: nahlajaf@gmail.com

[*]Corresponding author. Email: omer.mahmood@garmian.edu.krd

Abstract

Phthiriasis palpebrarum is a rare infection caused by pubic lice *Pthirus pubis*. This parasite has become a public health problem since itinfestshuman eyes and has been linked with other infections like keratitis, conjunctivitis and blepharitis. The present study was carried out on 2325 patients attended Doctor Shahid Aso Hospital in Al-Sulaimaniyah province, Kurdistan region, Iraq from January to November 2017. Four patients were observed to have symptoms like itching, redness, swollen of the eyelids with the presence of tiny white objects at the base of their eyelashes . Through examination using slit lamp and florescent microscopes, it was observed that the infections were caused by infestation with adults and nymphs of *Pthirus pubis*. Lice and nits were removed mechanically using fine forceps followed by treatment of the patients with erythromycin eye ointment. All the patients were treated successfully. To the best of our knowledge this is the first documentation of phthariasis papebrarum in Kurdistan and Iraq. Further studies are required for better understanding the ecology, phylogeny and the potential of disease transmission of the parasite.

Keywords: Phthiriasis palpebrarum, Pthirus pubis, Al-Sulaimaniyah, Iraq

1.Introduction

Pediculus are obligate ectoparasites feed on blood and skin of human, theybelong to the (Phylum Arthropoda)(Karabela *et al*., 2015).According to the area of infestation, Pediculus can be categorized into three species: *Pediculus capitis* which are usually found on the hairs of the head. Second, *Pediculus corporis* which resemble *pediculus capitis*, and usually infest the hair on the human body, particularly the abdomen and*Pediculus pubis or Pthirus pubis*, found in the human pubic region at the base of pubic hair (Yoon *et al*. 2003, Dehghani *et al*, 2013).

Pthirus pubis isgeographically distributed worldwide and it is estimated of having the potential to infest 2-10% of human populations (Anderson and Chaney, 2009). *Pthirus pubis* has a crab-shaped body and the adults are small around 2-2.5 mm in length and gray in color, having a complete life cycle: eggs, nymphs and adults (Badri and Hafsi, 2017). Pubic lice are typically transmitted through sexual contact. It is also possible to catch pubic lice by using blankets, towels, sheets, or clothing of people who have pubic lice (Castaneda *et al*., 2000). The parasite can also transmit to the areas of human eyelashes and eyelids causing a disease called phthiriasis palpebrarum (Ashraf *et al*., 2014).

The most obvious symptoms of phthiriasis palpebrarumare itchiness of the eyelid margin, eye redness, Tearing, Feeling ill or tired, low-grade fever, small red spots at the bite sites and in some cases conjunctivitis (Wu *et al*., 2016).The parasites are removed from the eyelashes mechanically using forceps. However, in some heavily infested patients, it could be painful, so local treatment with creams or ointment are required (Burkhart *et al*., 2000; Karabela *et al*., 2015).Pediculus lice particularly head lice and body lice are well studied in Iraq and neighboring countries (Mahmood, 2010; Dehghani *et al*., 2013; Abdulla, 2015; Al-Marjan *et al*., 2015; Gharsan et el., 2016; Khidhir *et al*., 2017).However, no studies have been carried outbefore onan infestation of human eyes by *Pthirus pubis*(Phthiriasis palpebrarum) in Iraq particularly in Kurdistan region. This study aims to diagnose and treatphthiriasis palpebrarum among people attendingDoctor Shahid Aso hospital in Al-Sulaimaniyah province.

2.Materials and Methods

Thisstudy was conducted on 2325patients attended Ophthalmology department in Doctor Shahid Aso hospital from January to November2017. Slit lamp microscope, magnifying lenses were used for clinical diagnosis and fineforcepswere used for mechanical removal of the lice and nits.The Parasites were morphologically identified (based on outer morphology, shape of the claws, size and color of the parasite) using florescent microscope in the laboratories of Garmian University depending on identification key (Pratt and Litting., 1973).Patients were treated with erythromycin eye ointment for 5 days once a day to prevent bacterial conjunctivitis. The patients were examinedfor any unremoved lice infestationseven daysafter the first removal to ensure the complete removal of the parasites and were followed up for 30 days afterwards.

3.Results:

The primary results using eye slit microscope indicated the presence of variously sized lice infesting the eyes of four patients. They were two children, a boy aged five years and a girl aged seven years and two adult females aged 35 and 46 years respectively. Itching and redness of the eyelid were observed in the infested patients, two of the patients had the experience of swollen eyelid. Further investigation using high resolution florescent microscope revealed that they were infested with *Pthirus pubis*(Figure 1).All the stages of the parasite (Eggs, Nymphs and adults) were observed in the infested patients. Some of the parasites were observed on the surface of the skin at the bases of the eyelashes and others were partially embedded in the eyelid of the eyes while others were almost completely penetrating the skin.

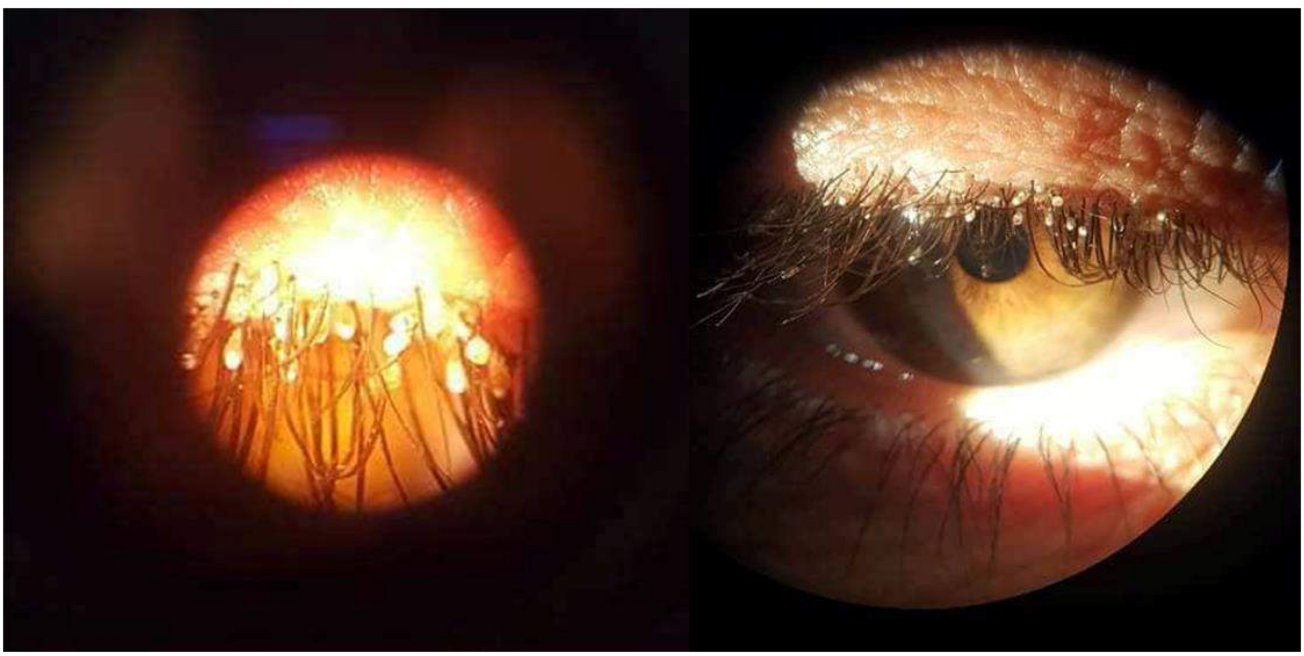

Figure (1): ***Pthirus pubis*** **infesting eyes of a patient examined with slit lamp microscope**

The size of the adults was about 2mm. the parasites transparent bodies were observed red due to the blood they had ingested from the host. No wings were observed. Male and female were hard to distinguish.

Nymphs had dark grayish color, morphologically and structurally exactly resembled the shape of the adults apart from their smaller size 1-1.5mm.

Microscopic examinations showed that eggs had a translucent yellowish brown color about the size of 0.5 mm attached to the eyelashes. Eggs were observed on three of the infested patients (75%). Eggs had oval shapes and the larvae seemingly appeared inside and were covered with an outer egg shells.

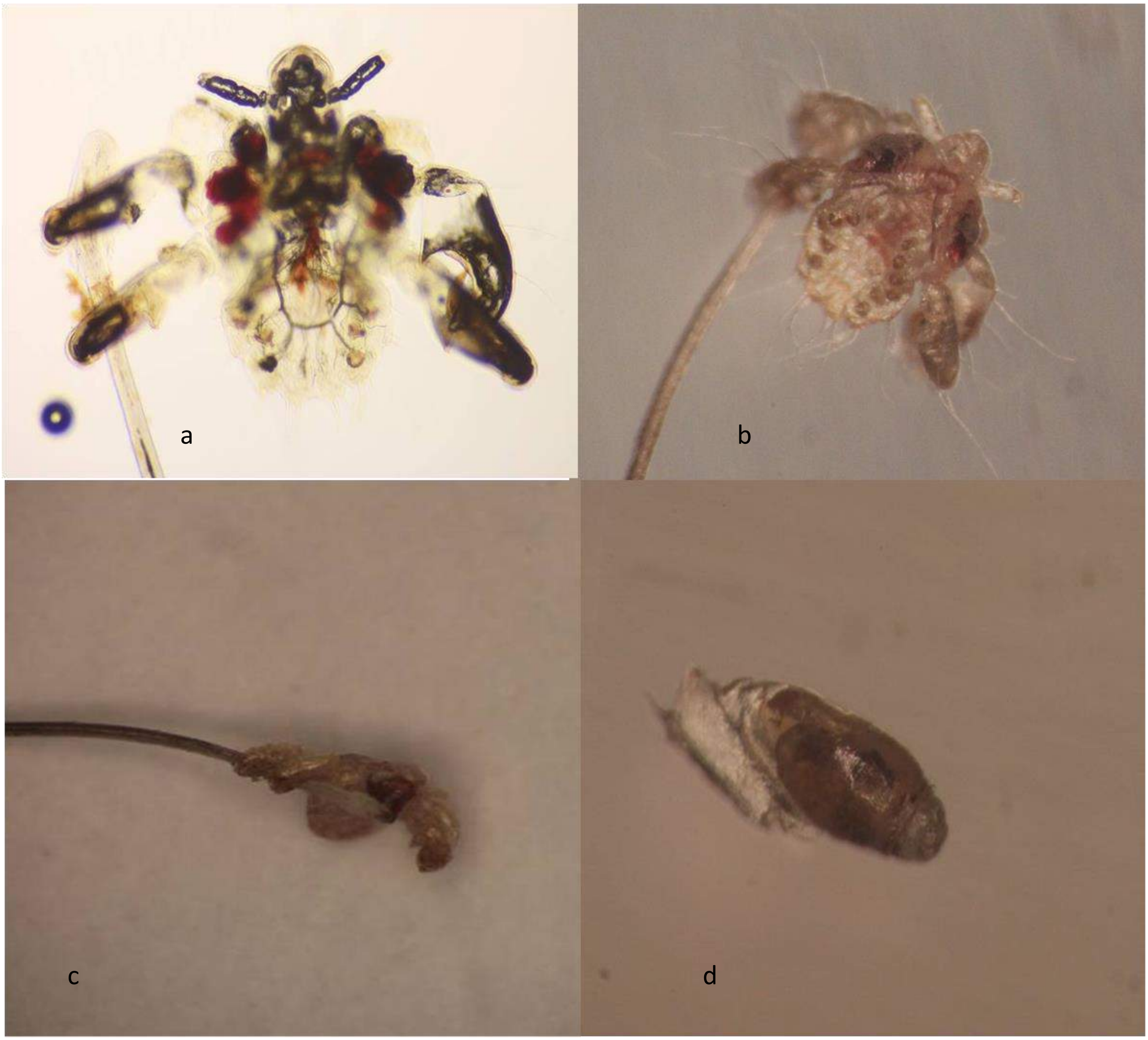

Figure (2): Microscopic views of Different stages of *Pthirus pubis* extracted from patients eyelashes. a and b represent adult lice 25 X, c represents nymph 30 X, and d represents egg 50 X.

In the next clinical examinations under slit lamp microscope after seven days of the first mechanical removal of the parasites and antibiotictreatments, no parasites were observed in the infested eyes.Continuous checkupof the patients for up to 30 days confirmed the complete disappearing of lice after the mechanical treatment.

4. Discussion:

Phthiriasis palpebrarum is a rare infection caused by the parasitic lice *Phthirus pubis* (Ashraf *et al*., 2014). The parasite usually infests adults and reproducein the pubic hair because of their main mode of transmission during sexual contact (Yi *et al*., 2014). The parasites transmitviacontaminated handswith infested pubic hair to the eye area (Castaneda *et al*., 2000). Studies have shown that children can also be infested with the parasite (Yoon *et al*., 2003). Since children lack body hair and are immature for sexual practice, the parasite if present are always seen on the eyelashes. There is a potential of child abuse if the parasitesare diagnosed in children especially if their parents are not infested. In the current study the parasites were observed in both children and adults, it is believed that people in Kurdistan particularly the rural areas havecrowded families live together and in more cases share the same beds with their parents. Cases of Phthiriasis palpebrarum have been reported in countries that have borders with Kurdistan such as Iran and Turkey (Dehghani *et al*, 2013; Karabela, *et al*., 2015; Sundu *et al*., 2015). However, in the records we could not find any studied cases in Kurdistan or Iraq. Studies have shown that travelers could transmit the parasite from one place to another (Diaz, 2006). One of the adult patients in the present study had been recently returned from Iran prior to diagnosis. It is possible that she might caught the parasite from infested people in Iran and then carried them back to Kurdistan. Low hygiene, education level and socio-economicstatus have also been linked to the availability of lice (Mahmood, 2010). Successful treatments of phthiriasis palpebrarum have been achieved using different mechanisms and medications including petroleum Jelly, permethrin, yellow mercuricoxide, vaseline, and recently argon laser (Couch etal., 1982; Jiang *et al*.,2011; Panos *et al*., 2013; Karabela, *et al*., 2015; Sundu *et al*., 2015). In the current study, a special fine forceps was used followed by erythromycin eye ointment and it was successful in eradication of the parasites from the eyes. Head and body lice are difficult to distinguish however pubic lice are different having broad stout legs especially the posterior two pairs and equipped with powerful claws with a round body. In this study, the use of florescent microscope facilitated easy characterization of the external morphology of the parasite.

In conclusion, *Pthirus pubis* can infest human in any country, this is the first study of phthriasis palpebrarum to be documented in Kurdistan and Iraq. Despite the parasites common occurrence in adults, children can also be infested. Mechanical removal of the parasites using fine forceps followed with 30 days follow up can successfully treat patients infected with lice infestation in the eyes. Travelling abroad and low socio economic status could increase the chance of catching the parasite.

References

Abdulla, B.S. (2015). Morphological study and Prevalence of head lice (*Pediculus humanus capitis*) (Anoplura: Pediculidae) infestation among some primary school students in Erbil City, Kurdistan region. *Zanko J applied Science*. 27(5), 29-36.

Al-Marjan, K.S., Koyee,Q.M.K., and Abdulla, S.M. (2015). In Vitro Study On The Morphological Development Of Eggs (Nits) And Other Stages Of Head Lice *Pediculus humanus capitis* De Geer, 1767. *Zanko J applied Science*. 27(3), 35-40.

Anderson, A.L., and Chaney , E. (2009). Pubic lice (*Pthirus pubis*): history, biology and treatment vs. knowledge and beliefs of US college students. *Int J Environ Res Public Health*. 6(2), 592-600.

Ashraf, M., Waris,A., Kumar,A., and Akhtar, N. (2014). A case of unilateral phthiriasis palpebrarum infestation involving the left eye. *BMJ Case Rep*. 6, 1-3.

Badri, T., and Hafsi, W. (2017). Phthiriasis Palpebrarum. StatPearls [Internet]. Treasure Island (FL): StatPearls Publishing; 2017 Jun-. Available from http://www.ncbi.nlm.nih.gov/books/NBK459226/ PubMed PMID: 29083779.

Burkhart, C.N., Burkhart,C.G., MSPH., and Sylvania, M.D. (2000). Oral Ivermectin therapy for phthiriasis palpebrarum. *Arch Ophthalmol*. 51, 1037

Castaneda, A.N., Osorio,R.C., Pomar,J.L., Canales,J.L., and Salas, S.M. (2000). Phthiriasis Palpebrarum. *Rev Fac Med UNAM*. 43(5), 180-184.

Couch, J.M., Green,W.R., Hirst,L.W., and de la Cruz, Z.C. (1982). Diagnosing and treating *Phthirus pubis* palpebrarum. *Surv Ophthalmol*. 26(4), 219-225.

Dehghani, R., Limoee,M., and Ahaki, A.R. (2013). First report of family infestation with pubic louse (*Pthirus pubis*; Insecta: Anoplura: Pthiridae) in Iran--a case report. *Trop Biomed*. 30(1),152-154.

Diaz J.H. (2006). The epidemiology, diagnosis, management, and prevention of ectoparasitic diseases in travelers. *J Travel Med*. 13(2),100-111.

Gharsan F.N., Abdel-Hamed,N.F., Elhassan S.A., and Gubara, N.G. (2016). The prevalence of infection with head lice *Pediculus humanus capitis* among elementary girl students in Albaha region- Kingdom of Saudi Arabia. *Int J Res Dermatol*. 2(1), 12-17.

Jiang J., Shen,T., and Hong, C.Y. (2011). A peculiar case of eye pruritus: phthiriasis palpebrarum initially misdiagnosed as common blepheritis. *Int J Ophthalmol*. 4(6), 676-577.

Karabela Y., Yardimci,G., Yildirim,I., Atalay,E., and Karabela, S.N. (2015). Treatment of Phthiriasis Palpebrarum and Crab Louse: Petrolatum Jelly and 1% Permethrin Shampoo. Case Rep Med.; 2015:287906. doi: 10.1155/2015/287906. Epub 2015 Sep 15.

Khidhir, K.N., C.K. Mahmood and Ali W.K., (2017). Prevalence of infestation with head lice *Pediculus humanus capitis* (De Geer) in primary schoolchildren in the centre of Erbil city, Kurdistan region, Iraq. *Pak. Ent*. 39(2):1-4.

Mahmood S.A. (2010). Head pediculosis among in Baghdad area elementary schoolchildren. *Iraqi J science*. 1(51), 49-55.

Panos G.D., Petropoulos,I.K., D., and Gatzioufas, Z. (2013). Phthiriasis palpebrarum. BMJ Case Rep.; 2013. pii: bcr2013009272. doi: 10.1136/bcr-2013-009272.

Pratt H.D and Litting K.S. (1973). Lice of public health importance. PP 23-26.

Sundu C., Dinc,E., Kurtulus,U.C., and Yildirim, O. (2015). Common blepheritis related to phthiriasis palpebrarum: Argon laser phototherapy. *Turkiye Parazitol Derg*. 39, 252-254.

Wu N., Zhang,H., and Sun, F.Y. (2017). Phthiriasis palpebrarum: A case of eyelash infestation with Pthirus pubis. *Exp Ther Med*. 13(2), 2000-2002.

Yi J.W., Li,L., and Luo da, W. (2014). Phthiriasis palpebrarum misdiagnosed as allergic blepharoconjunctivitis in a 6-year-old girl. *Niger J Clin Pract*. 17, 537-539.

Yoon K.C. Park,H.Y., Seo,M.S., and Park,Y.G. (2003). Mechanical treatment of phthiriasis palpebrarum. *Korean J Ophthalmol*. 17(1), 71-73.

ttp://jgu.garmian.edu.krd https://doi.org/10.24271/garmian.325

Assessment of Sirwan River Water Quality from Downstream of Darbandikhan Dam to Kalar District, Kurdistan Region, Iraq

Azad HamaAli Alshatteri[1*] Abdulmutalib Rafat Sarhat[1] Avesta M. Jaff[2]

[1] Department of Chemistry, College of Education, University of Garmian. Kalar, Al-Sulaimaniyah, Kurdistan Region, Iraq

[2] Research Centre, University of Garmian. Kalar, Al-Sulaimaniyah, Kurdistan Region, Iraq

[*] Corresponding author. Email: Azadalshatteri@garmian.edu.krd

Abstract

This study was performed to evaluate the Siwran River water quality between Darbandikhan Downstream Dam and Kalar city for domestic and irrigation uses. Seven stations from different sites have been selected along the Sirwan River, and four replications from each station were taken. The parameters of water quality used in this work are (Turbidity, pH, Total hardness, Magnesium, Calcium, Sulphate, Nitrate, Chloride, Conductivity µs/cm, TDS). Data analysis shows that the water quality parameters of Sirwan River are not compatible with the drinking water standards especially the concentrations of Aluminum and Iron which show increasing levels than the maximum allowable levels for drinking water standards. In addition, to classifying water quality and evaluation its suitability for irrigation purposes, SAR, RSC, and ESP were calculated following standard equations and found experimentally as 0.5, 1.7, and 5.3 respectively. The results of the study revealed that the Sirwan River water should be used with good irrigation management techniques and soil salinity monitored by laboratory.

Keywords: Water Quality, Sirwan River, Aluminum concentrations, Sodium Adsorption Ratio (SAR), Residual Sodium Carbonate (RSC), Exchangeable Sodium Percentage (ESP).

1. Introduction

Water resources play an important role on population growth in any living area. With increasing inhabitants, water demand growths; meanwhile, the world is facing with severe water crisis. Rivers are most vital resources of fresh water in the world [1]. The water of rivers must be managed in an appropriate way particularly for those rivers pass through numerous countries [2]. Sirwan River is the source of lifeline to almost one million residents of Kurdistan Iraq. The cities along Rirwan River depend mostly on it for domestic, municipal, agriculture and other purposes. Water quality mainly depends on the physical, chemical and biological properties. These characteristics give an indicator on water use for a specific purpose.

Fresher water is important to human health, agriculture, and environments. The quality of water is a critical issue in the world. It is clear that the quantity of chemical composition in water is changed as a result of the changing the quantity of surface and ground water in a specific area [3]. For this reason, monitoring physiochemical properties of water are essential issue to deal with. The appropriate properties of water quality should include the measuring of pH, temperature, dissolved oxygen, essential and toxic cation elements, anions, electrical conductivity, total dissolved solid, chemical oxygen demand, biochemical oxygen demand, total organic carbon, taste, color, and extra [4]. This study has been mainly conducted in order to measure and analyze the water quality parameters of Sirwan River such as electric conductivity EC, total dissolved solids TDS, sodium adsorption ratio SAR, magnesium hazard MH, pH, residual sodium carbonate RSC, that could potentially impact on the quality of water for drinking and irrigation crops.

2. Methodology

2.1 Study Area

The study area consists of seven sites along the river were selected between Darbandikhan downstream dam and Kalar District. Four replications sample from each site were selected. These sites are very important for drinking water as the study area was dense of the population along the banks of the river, as well as the presence of some industrial activities. Also, it includes a number of fallings the wastewater, which are distributed on both sides of the river. Therefore, dangers of various biological, chemical and physical pollutants could be existed, which can affect the quality of the river water as a source of water for processing drinking and irrigation water.

Figure (1) shows the location of sampling stations from downstream of Derbendixan River in Derbendixan area to Shexlenger village at down of Kalar district. Seven stations were selected along Sirwan River which starting from downstream of Darbandikhan Dam, Maydan, Bawanur, Isayi, Qulasutaw, Kalar, and Shekhlanger in south of the Kalar City. Four replication water samples were collected from each of these stations during April 2018 in 1-L Poly ethylene bottles that are rinsed several times before filling.

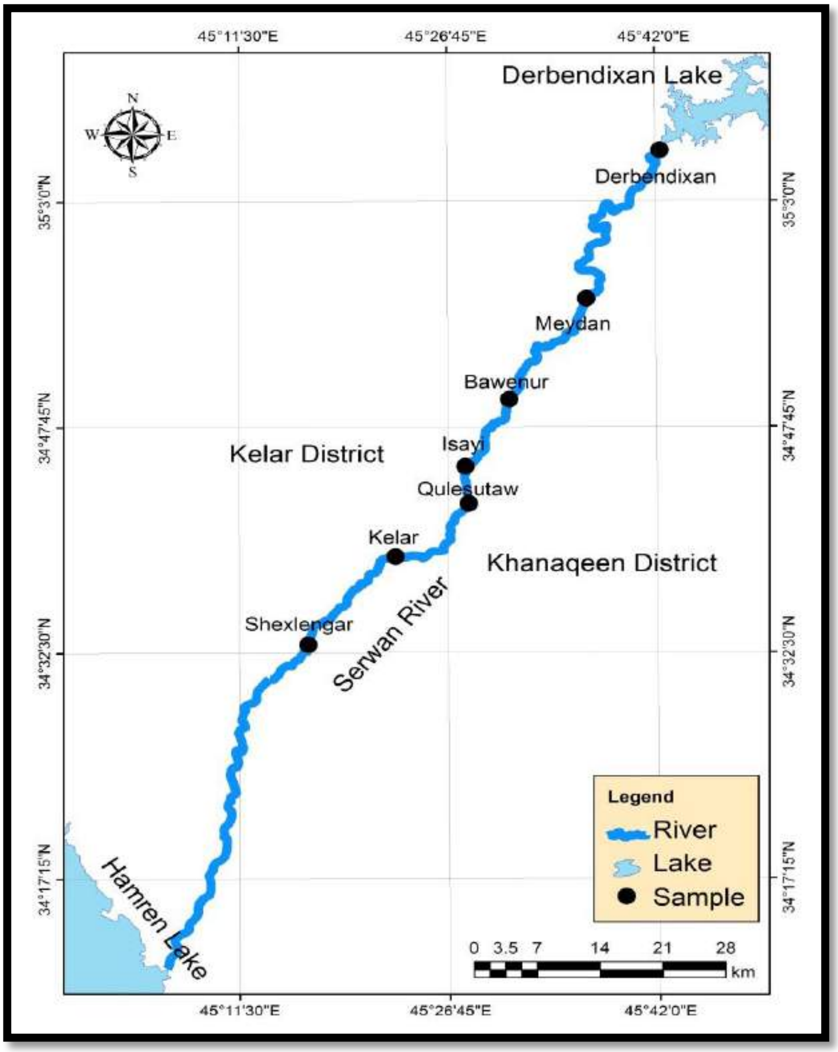

Figure 1: Location of the sampling stations.

2.2 Physicochemical Study

The samples were kept refrigerated and analyzed within 48 hours after collection in the laboratory of Chemistry Science Department in Garmian University. Various tests were conducted according to the Standard Methods for examination of water [5]. Some physicochemical parameters were study in site and composited at laboratory as required. The pH, EC and DO were measured immediately in site by using a portable WTW conductometer and pH meter. TDS was measured using an HANNA instrument EC/TDS meter in a laboratory after the samples were arrived within 24 hours. (SO_4^{2-}), chloride (Cl^-), and (NO_3^-) ion concentrations were measured by means of SENTEK ion selective electrodes after 24 hours from sample collection. Some essential and toxic elements were analyzed using induced coupled plasma optical emission spectroscopy (ICPOES)

(Spectro Arcos Germany). For analysis of water samples by ICPOES, the samples were acidified by 2% HNO_3, and then left for 24 hours before analysis. These parameters mainly consist of certain physical and chemical characteristics of water that are used in the evaluation of agricultural water quality.

3. Results and Discussion

Physicochemical properties were measured and their results can be seen in tables 1, 2, 3 and 4 respectively.

Table 1: Some results of the physicochemical for all samples

Sample	Turbidity (NUT)	pH	EC (µS/cm)	Total Hardness (mg/l)	TDS (mg/l)	D.O (mg/l)	NO_3^- (mg/l)
Darbandixan	1.47	7.80	371	134.74	448.0	7.71	1.51
Maydan	**5.40**	7.60	455	137.02	456.0	7.73	4.56
Bawanur	2.80	7.63	481	141.39	486.0	7.13	3.34
Isayi	2.99	7.88	500	141.42	**611.0**	7.92	2.62
Qulasutyaw	2.88	7.60	485	140.52	485.0	7.45	3.66
Kalar	1.63	7.76	468	135.98	463.0	7.99	2.96
Shexlangar	1.72	7.35	788	143.82	**657.0**	6.70	3.37
Ave.	**2.70**	**7.66**	**506.86**	**139.27**	**515.1**	**7.52**	**3.15**
WHO	**5.00**	**6.5 - 8.5**	**400-800**	**500.00**	**500.0**	**5.00**	**45.00**

3.1 pH of Water

The (pH) plays important roles in evaluating the acid-base balance of water. World Health Organization (WHO) has maximum acceptable limits of pH (6.5-8.5). The pH of the samples in the present study ranges (7.35-7.88) which is falling within the range of WHO limits. The overall results show that the Sirwan River water source is inside required and appropriate range.

3.2 Electrical Conductivity (EC), Total Dissolved Solids (TDS), and Turbidity

Unpolluted water is not a noble conductor of electric current. By increasing ion concentrations, electrical conductivity increases too [6]. Generally, (TDS) has the directly proportional with electrical conductivity. WHO has recommended standard tolerable limits for EC values that should not excessed (400) µS/cm for drinking water [7]. The current study showed that the EC values were between (371-788) µS/cm. the results revealed that most of the results outside the WHO standard limits for drinking. However, for irrigation purpose the sample fall under medium category based on FAO standard.

Capacity of water is high to dissolve a numerous of inorganic and some organic minerals such as Ca^{+2}, K^{+}, Mg^{+2}, CO_3^{-2}, SO_4^{-2}, and NO_3^{-}. These dissolved ions formed undesirable taste and color of water. Water with high TDS may affect persons suffering from heart and kidney diseases. WHO has a recommended maximum permissible limits of TDS which equals to (500) mg/L [8]. The concentration of (TDS) in samples was indicated in the range of (448-657) mg/L with an average of (515) mg/L. Therefore, it is out of the (WHO) standards limit for drinking purpose.

The values of turbidity in the river are ranged between (1.47- 5.4) NTU, with the average value of (2.70) NTU. It can be considered as a safe limit [8]. Most of the samples do not exceed the turbidity limits (5 NTU). The permissible value for total hardness is (500) mg/l according to the WHO [8].

3.3 Dissolved oxygen (DO)

In water body, oxygen is obtainable in a dissolved state. DO is the concentration of oxygen that is dissolved in water [9]. DO is measured as one of the most vital characteristic of aquaculture. It is desirable by fish to breathe and perform metabolic activities. Lower levels of (DO) are frequently connected to fish kill happenings. The deficiency of DO may be owing to temperature, breathing, photosynthesis, aeration, and organic waste [9]. DO in current study water ranged from (6.7-7.99) mg/L, with the mean value of (7.51) mg/L. DO value with more than (5) mg/L is very important for fisheries life and production [10]. The results revealed that the DO is lower than desirable WHO limits in drinking water which equals to (8) mg/L.

3.4 Nitrate NO_3^-

The allowable WHO maximum limits of nitrate is (45) mg/L in drinking water [11]. In current investigation, it is clear that the NO_3^- concentration ranges from (1.51-4.56) mg/L with the mean of (3.15) mg/L. These results show that amount of NO_3^- in the study sites are permissible.

3.5 Cations (Ca^{+2}, Mg^{+2}, Na^+, and K^+)

The concentrations of calcium were between (24.36-24.49) mg/l. All the samples were under acceptable and permissible limit. The concentrations of magnesium were between (17.95-20.17) mg/l. The water samples were within the permissible limits [12].

The samples analysis showed that the concentration of sodium vary between (12.35-17.83) mg/l. These were observed to be within permissible limit. For drinking water the acceptable limit for Na is about (200) mg/l [12]. On the other hand, potassium concentrations vary between (2.17-21.13) mg/l. Therefore, all samples had potassium concentration within the acceptable limit.

3.6 Anions (Cl^-, SO_4^{-2}, and $NaHCO_3^-$)

The present study indicated that the Cl^- values were between (33.67-231.01) mg/L, and the mean is equals to 93.87 mg/L. the results were lower than WHO standard limits [12].

SO_4^{-2} is mainly obtained from the dissolution of salts sulfuric acid and almost in all water bodies found in abundance. Extraordinary concentration of SO_4^{-2} is may be because of oxidation of pyrite and excavation drain [13]. By now not most important negative influence of SO_4^{-2} on human health is informed. In the current investigation, SO_4^{-2} ion concentration was ranged from (135-165) mg/L with the average of (147) mg/L. The results revealed that the quantity of SO_4^{-2} in the study area is acceptable [11].

3.7 Carbonate and Bicarbonate:

They are existed in water because of some carbonate minerals present in water such as limestone, magnesite, and dolomite. This may influence pH values of water [14]. The concentrations of bicarbonate were between (258.64-378.2) mg/l with an average of (293.6) mg/l, or (3.98-5.81) meq/l with an average of (4.51) meq/l. So, all samples were found to be within moderate limits [12].

Table 2: Cations and anions results of the study area

Sample	Ca^{+2}	Mg^{+2}	Na^+	K^+	Cl^-	SO_4^{-2}	HCO_3^-
Darbandixan	24.46	17.95	12.35	2.17	35.10	144.0	268.4
Maydan	24.49	18.49	12.39	2.17	119.70	136.0	258.6
Bawanur	24.45	19.58	15.92	2.27	33.67	156.0	341.6
Isayi	24.36	19.64	17.29	2.47	65.79	152.0	278.2
Qulasutyaw	24.45	19.37	15.59	2.35	43.29	135.0	378.2
Kalar	24.43	18.27	17.12	11.68	128.56	141.0	260.1
Shexlangar	24.45	20.17	17.83	21.13	231.01	165.0	270.0
Ave.	**24.44**	**19.07**	**15.50**	**6.32**	**93.87**	**147.0**	**293.6**

Concentrations are expressed in mg/L.

4. Water Quality Indexes

4.1 Sodium Adsorption Ratio SAR

It is a measure of the suitability of water for agricultural irrigation, as calculated from the ratio of Na^+ to Ca^{+2} and Mg^{+2} by the following formula [15]:

$$SAR = \frac{Na^+}{\sqrt{(Ca^{2+} + Mg^{2+}/2}}$$

Excess sodium in water leads to produce undesirable effects of changing soil properties and reducing soil permeability [16]. All the samples in the study area have SAR values within the excellent class and acceptable for irrigation.

4.2 Magnesium Hazard

It can be calculated through using the flowing equation that was proposed by (Szabolcs and Darb, 1964) [17] :

$$MH\ (meq/l) = \frac{Mg^{2+}}{(Ca^{2+} + Mg^{2+})} \times 100$$

The concentration of Mg^{+2} ion can play an important role in soil productivity. When the value of magnesium hazard is less than (50), the water will be considered as safe and suitable for irrigation. The results of the water samples of the study area observed that all the samples have (MH) values greater than (50). Therefore, it cannot be used directly for irrigation without treatment or water management [17].

4.3 Kelly's ratios KR

It is the concentration of Na^{+} against Ca^{+2} and Mg^{+2} [18]. Water for irrigation uses was classified based on Kelly's ratios. The Kelly's ratio values less than (1) are considered suitable for irrigation [18].

4.4 Residual Sodium Carbonates RSC

It represents the amount of sodium carbonate and sodium bicarbonate in water when the total levels of carbonate and bicarbonate exceed the total amount of Ca^{+2} and Mg^{+2} [19]. Residual carbonate values with less than (1.25) are considered as safe. However, RSC values of (1.25-2.50) are within the marginal range. Those types of water should be used with good irrigation management techniques and soil salinity monitored by laboratory analysis [20]. RSC values of (2.50) or more are considered as high making the water unsuitable for irrigation use. RSC is determined through [19]:

$$RSC = (CO_3^{2-} + HCO_3^{-}) - (Ca^{2+} + Mg^{2+})$$

All ion concentrations are expressed in meq/l.

RSC values in the study area are ranges (1.2-3) with an average of (1.7). Therefore, most of the water samples are within the marginal range for irrigation except Qulasutaw station.

4.5 Exchangeable Sodium Percentage (ESP)

The desired value for ESP is (5) or less. However, values more than (5) mean increasing problems with soil infiltration and permeability, especially in clay soil. ESP value for irrigation water can be calculated from the following empirical relationship [20]:

$$ESP= 100* (-0.0126+0.01475*SAR) / 1+ (-0.0126+0.01475*SAR)$$

Therefore, most of the water samples are unsuitable for irrigation regarding ESP except tow stations (Darbandikhan and Maydan) which they have ESP values of less than (5).

Table 3: Water quality index results of the study area

Sample	SAR	Mg%	KR	RSC	ESP
Darbandixan	0.4	**55.0**	0.2	1.4	3.8
Maydan	0.4	**55.7**	0.2	1.2	3.8
Bawanur	0.5	**57.2**	0.2	**2.4**	**5.5**
Isayi	0.5	**57.3**	0.3	1.4	**6.2**
Qulasutyaw	0.5	**56.9**	0.2	**3.0**	**5.4**
Kalar	0.5	**55.5**	0.3	1.3	**6.2**
Shexlangar	0.5	**57.9**	0.3	1.2	**6.4**
Ave.	**0.5**	**56.5**	**0.2**	**1.7**	**5.3**

5 Heavy metals (total iron and Aluminum)

Although total iron levels low in natural water; however, it can be present in various ionic, organic and mineral forms. The concentration of total iron varied from (0.032-0.506) mg/L. Water samples at Bawanur, Qulasutaw, Kalar, and Shekhlanger showed high iron concentration than the prescribed limit by WHO which is (0.3) mg/L. On the other hand, the concentration of Aluminum in the analyzed samples was in the range of (0.093-2.411) mg/L which also higher than the prescribed limit by WHO. Aluminum levels in drinking water vary according to the levels found in the source water and whether aluminum coagulants are used during water treatment [21]. The sludge of the water treatment units are directly disposed into the river. This ultimately leads to increase the level of Aluminum and Iron in the river.

Therefore, water from the river cannot be used directly for drinking purpose. This is due to the nature of raw materials used in the industry and municipal wastes.

Table 4: The concentration of total Aluminum and Iron of study areas' samples

Sample	T. Al	T. Fe
Darbandixan	0.093	0.032
Maydan	**0.491**	0.149
Bawanur	**2.411**	**0.445**
Isayi	**0.423**	0.086
Qulasutyaw	**2.362**	**0.403**
Kalar	**0.975**	**0.506**
Shexlangar	**1.352**	**0.479**
Ave.	1.158	0.300
WHO	0.200	0.300

6. Conclusion

On the basic of results, it was concluded that physicochemical properties revealed that most of the parameter such as pH, cations, and anions drop under the WHO permissible limits. However, there are some parameters like TDS, total Al, Fe fall outside of the permissible limits, and must be pretreatment before using for drinking. These parameters and. For irrigation purpose, data results show that the water of Sirwan River is medium salinity and may cause saline damages in the future. Also, some indexes including Mg hazards, ESP and RSC are with high values; therefore, water of the river should be used with good irrigation management techniques and soil salinity monitored by laboratory.

References

1. Abdelkader, T. A., and Mohamed H. E.: Hydrological And Environmental of Grand Ethiopian Renaissance Dam on the Nile River, IWTC18, 12-14, March, 2015
2. Latifah, A.M. and Les Met. An Ecological Evaluation Approach for Dam Project Development in Malaysia. Life Sci J 2014;11(7):225-237
3. Ling, T. Y., Soo, C. L., Heng, T. L. E., Nyanti, L., Sim, S. F., and Grinang, J.: Physicochemical Characteristics of River Water Down-stream of a Large Tropical Hydroelectric Dam, Journal of Chemistry, vol.(2016), 7 pages, http://dx.doi.org/10.1155/2016/7895234
4. Roman S., Lukasz W.: The impact of a reservoir on the physicochemical properties of water in a mountain river, Water and Environment Journal, 2013, 22-31 http://dx.doi.org/10.1111/wej.12059

5. APHA, WWA & WEF: "Standard Methods for Examination of Water and Wastewater," 21st Edition, pp. 333, American Public Health Association, Washington, D.C., 2005.
6. Sundaram, S. E. J., Elayaperumal, R., Kiruthika, M., Ramya, V. and Dharmalingam, P., "Effluents of Paper Mill: Physico-Chemical Properties of Water," International Journal of ChemTech Research, vol 6, pp. 3541-3545, 2014.
7. FAO, 1992, the use of saline waters for crop production. Irrigation and drainage paper 48. FAO, Rome. 1992.
8. WHO: Preventing Disease through Healthy Environments, Geneva, Switzerland, 2006, Accessed on 30 Oct. 2017, available at: http://www.who.int/quantifyingehimpacts/ publications/preventing disease /en /print.html.
9. Orebiyi, E. O., Awomeso, J. A., Idowu, O. A., Martins O., Oguntoke O., and Taiwo, A. M., "Assessment of Pollution Hazards of Shallow Well Water in Abeokuta and Environs," Amer. J. Env. Sci., vol 6, pp. 50-56, 2010.
10. Bhatnagar, A. and Singh, G.: Culture fisheries in village ponds: a multi-location study in Haryana, India. Agriculture and Biology Journal of North America, issue: (1), No. (5), pp. 961-968. 2010.
11. WHO: Guidelines for drinking-water quality, 4th edn. Geneva, pp. 96, Switzerland, 2011.
12. WHO: Guidelines for drinking-water quality - 4th ed, pp. 851, World Health Organization 2011.
13. Yirdaw M., and Bamlaku A.: Drinking water quality assessment and its erects on residents health in Wando genet campus, Ethiopia, Meride and Ayenew Environ Syst Res (2016) 5:1, http://dx.doi.org/10.1186/s40068-016-0053-6
14. Natraj, V. M., Katya, D. and Gorntiwar, S: Study of groundwater contamination due to agricultural activity under Paravara laft bank canal, 2014, IJARIIE, ISSN(O)-2395-4396.
15. Haritash, A. K., Kaushik, C.P. and kaushik, A: Suitability assessment of groundwater for drinking, irrigation and industrial use in some North Indian villages, 2008, Environ Monit Assess, 145: pp 397–406.
16. Biswas, S. N., Mohabey, H., Malik, M., L: Assessment of The Irrigation Water Quality Of River Ganga In Haridwar District, 2002, Asian J. Chem., pp 16.
17. Michael, A, M: Irrigation Theory and Practice, 2nd edition, Vikas Publishing House, Pvt. Ltd., New Delhi, 2008.

18. Kelly, W, P: Use of Saline Irrigation Water, Soil Sci., 1963, Vol.(95), Issue (4), pp.(35-39).
19. Rachel, P: Effects of water quality on soil, plants and irrigation equipment, Primary Industries and fisheries, April 2010.
20. Richards, L. A: Diagnosis and improvement of saline and alkali soils U.S. Salinity laboratory staff, USDA Handbook, 1954, pp 60-160.
21. World Health Organization (WHO): Guidelines for drinking-water quality-Aluminum", 2nd ed., 1998b, Addendum to Vol. 2. Health criteria and other supporting information, pp 66-269 World Health Organization, Geneva.

الخلاصة

تم إجراء هذه الدراسة لغرض تقييم جودة مياه نهر سيروان بين مجرى سد دربنديخان ومدينة كلار للاستخدامات المنزلية والري. تم اختيار سبع محطات من مواقع مختلفة على طول نهر سيروان، وتم أخذ أربع نماذج مكررة من كل محطة. إن معايير جودة المياه المستخدمة في هذا البحث هي (التعكر، الدالة الهيدروجينية، العسرة الكلية، المغنيسيوم، الكالسيوم ، الكبريتات، النترات، الكلوريد، التوصلية الكهربائية، المواد الصلبة الذائبة الكلية. يبين تحليل البيانات أن معايير جودة مياه نهر سيروان غير متوافقة مع معايير مياه الشرب خاصة تراكيز الالمنيوم والحديد التي تظهر مستويات متزايدة من الحد المسموح به لمياه الشرب. بالإضافة إلى ذلك ، ولتصنيف جودة المياه وتقييم مدى ملاءمتها لأغراض الري، تم حساب بعض المؤشرات مثل نسبة إمتصاص الصوديوم (SAR) وكربونات الصوديوم المتبقية (RSC) ونسبة الصوديوم المتبادلة (ESP) وتم العثور عليها تجريبياً بمعدلات (0.5، 1.7 , 5.3) على التوالي. وكشفت نتائج الدراسة أن مياه نهر سيروان يجب أن تستخدم مع تقنيات إدارة جيدة للري ومتابعة ملوحة التربة.

الكلمات المفتاحية: جودة المياه، نهر سيروان، تركيز الالمنيوم, نسبة امتزاز الصوديوم (SAR)، نسبة كاربونات الصوديوم المتبقية (RSC) ، ونسبة الصوديوم القابل للتبادل (ESP).

ttp://jgu.garmian.edu.krd https://doi.org/10.24271/garmian.326

Alteration of Some Heavy Metals and Kidney Function Tests in Serum of Crude Oil Station Workers

Vyan A. Qader[1*], Sardar N. Ahmed[2] Ayad F. Palani[3]

[1]Department of Chemistry, Faculty of science and health, Koya University, Daniel Mitterrand Boulevard, Koya KOY45 AB64, Kurdistan Region, Iraq

[2]Department of clinical Biochemistry, Hawler Medical University, Erbil, Kurdistan Region, Iraq

[3]Department of Chemistry, College of science, University, Garmian, Kalar, Kurdistan Region, Iraq

[*]Corresponding Author. Email: vyan.asad@koyauniversity.org

Abstract

Some trace metals have no biological role, are toxic when in a certain form and concentration. The aim of the present study is to study the effects of exposure to the vapors of crude oil (vehicle fuel) on some trace elements value and kidney function tests in serum of crude oil station workers. The study includes (30) men crude oil station workers (group 1), and (30) men non crude oil station workers (group 2). The mean value of serum aluminum (Al), barium (Ba), zinc (Zn), manganese (Mn), iron (Fe), and vanadium (V) were significantly higher in (group 1) compared with (group 2) ($p<0.05$), while the mean value of serum silver (Ag) in group 2 was significantly higher than that of group 1, while {mercury (Hg), and lead (Pb)} in group 1 no significantly higher than that of group2, the serum creatinine and uric acid in group 1 was significantly higher than that of group 2, and serum urea in group 1 was non significantly higher than that of group 2. Based on the findings of the present study, it can be concluded trace elements in serum of crude oil station workers are abnormal and affect dramatically of kidney functions.

***Keywords*:** crude oil station worker, trace elements, urea, creatinine, uric acid

1. Introduction

Crude oil (petrol) is a complex manufactured mixture that does not exist naturally in the environment. It consists mostly of several hundred hydrocarbons obtained by the fractional distillation of petroleum that have boiling points from approximately 40°C to 180°C. The hydrocarbons present in the gasoline mixture include alkanes, or straight chain C5 to C12 compounds or branched-chain compounds of the same size; alkenes, which are unsaturated linear and branched-chain hydrocarbon, also saturated cyclic hydrocarbons. Also included in the gasoline is aromatic compounds (principally benzene, toluene, ethyl-benzene, and xylenes) [1].

Exposure to crude oil occurs by: Breathing, drinking contaminated water and Being close to where gasoline has spilled or leaked into the soil. Certain workers have a greater risk of exposure to gasoline vapors. These include service station attendants, drivers of gasoline, and refinery workers [2].

Heavy metals are described as those metals which, in their standard state, have a specific gravity of more than 5 gm/cm^3, and atomic weight of 63.5 - 200.6 [3]. The heavy metals are responsible for many pernicious effects on human health such as saturnism (lead contamination), immunodepression and skin diseases (zinc and copper contamination), cancer (cadmium), hyperkeratosis (arsenic), neurological disorders (manganese) or blood disorders (iron) [4].

When not digest heavy metals accumulate in the human bodybecomes toxic and cause many problems for human health,including damage to the nerves and the central, bloodcomposition and many organs especially kidneys and these metals become toxicwhen an increase from the normal level allowed. As a rule,acute poisoning is more likely to result from inhalation or skincontact of dust, fumes or vapors, or materials in the workplace [5, 6].

Certain trace elements (TEs) are essential for life and health of the human, they are essential for the metabolism, growth and survival, there are an alteration in the levels TEs caused by air, water, and food contamination by environmental pollution [7].

A lot of TEs have an important influence on risk factors like disorders of blood pressure, blood lipids, glucose intolerance, coagulation and circulating insulin [8], high exposure cause defect of organs especially liver and kidneys.

The kidney is the first target organ of heavy metal toxicity. The extent of renal damage by heavy metals depends on the nature, the dose, route and duration of exposure. Both acute and chronic intoxication have been demonstrated to cause nephropathies [9].

The aim of the work is to obtain the effects of pollution by exposure (crude oil station workers) on serum heavy metals (Hg, Pb, Cd, Ag and V), trace elements (Al, B, Fe, Mn, and Zn) on kidney function tests (urea, creatinine and uric acid).

2. Materials and Methods

A. Subjects

This study was conducted over a period of one year, from January to December 2017, and the subjects included (30) men crude oil station workers (group 1), ages (43.46±9.55), and (30) men non crude oil station workers (control) (group 2), mean ages (45.15±6.5).

B. Sampling

Four to six milliliters venous blood was withdrawn from each individual using disposable syringe. The samples after half hour centrifuged for [10] min at 3000 rpm, and the serum obtained was analyzed directly.

C. Estimation of serum heavy metals and trace elements

The sample was prepared by addingone milliliter of serum into disposable plastic (polystyrene) tube, then added 9 milliliters of 5% nitric acid (Already prepared from Nitric Acid, 67-70%, Fisher Scientific- CAS: 7697-37-2), mixed and incubate for 6 -10 hours at room temperature, centrifuged at 4000g for 10 minutes, separated clear supernatant solutions, used for determination of serum trace and heavy metals by using inductively coupled plasma optical emission spectrophotometer (ICP-OES, Optima 2100 DV, Perkin Elmer-USA).

Preparation of Standard curve

The calibration curve of trace metals were obtained from five different known standard solutions, as (1 mg/L, 2 mg/L, 3 mg/L, 4 mg/L, and 5 mg/L)were prepared from a 100mg/L standard (or stock) solutionand heavy metalswere obtained from five different known standard solutions, as (1 ug/L, 10 ug/L, 30 ug/L, 50 ug/L, and 100 ug/L)were prepared from a 100ug/L standard (or stock) solution(ICP multi-element standard solution VIII, 1.09492 – Merck, Germany). 5% HNO_3 was used for dilution [10, 11].
The following table is limit of detection (LOD) (ug/L), limit of quantization(LOQ) (ug/L), and wave length for each element

Elements	Limit of detection (LOD) (ug/L)	Limit of quantization (LOQ) (ug/L)	Wave length (nm)
Ag	0.5	1.6	328.07
Al	162.2	540.6	308.213
Ba	0.3	1.0	233.523
Cd	3.9	13.2	317.935
Fe	2.7	9.0	259.943
Hg	3.7	22.4	198.023
Mn	0.5	1.2	220.352
Pb	3.4	11.3	196.026
V	0.2	0.5	292.402
Zn	1.1	1.7	213.858

d. Evaluation of kidney function test

The serum urea, creatinine and uric acid were estimated (enzymatic method) by using the Biolabo diagnostic kit with fully automated biochemical analyzer.

e. Statistical analysis

SPSS version 22 for windows was used in the analysis of the data obtained. Statistical analysis was assessed using student t-test. Mean ±SD value was adopted in the determinations. P-values less than 0.05 were considered statistically significant.

3. Results

Mean ± SD of estimated heavy metals are shown in table (I). The results obtained indicated that the mean serum Pb and Hg in group 1 were non significantly higher than that of group2 (P> 0.05), the heavy metal Cd not present in serum of both groups, the serum V in group 1 significantly higher than that of group 2 (P< 0.05), while serum Ag in group 2 was significantly higher than that of group 1 (P<0.001).

.

TABLE I

HEAVY METALS IN CRUDE OIL STATION WORKERS AND CONTROL

Parameters	Control group	Exposure group	P value
Pb (ug/L)	11.4± 6.2	13.3± 4.7	P> 0.05
Hg (ug/L)	35±0.24	36±0.15	P> 0.05
V (ug/L)	1.4 ± 0.57	2.8 ± 0.93	P < 0.05
Cd (ug/L)	0.0	0.0	0.0
Ag (ug/L)	0.8±0.07	0.65±006	P< 0.001

Results expressed as Mean ±SD

P value: probability value

Some serum trace element levels in crude oil station workers and control groups.

Results in the table (II) showed the mean ± SD of trace elements (Ba, Al, Fe, Zn, Zn and Mn) in sera of crude oil station workers and control groups. Significant elevation were found in all the trace elements in crude oil station workers compared with that in normal group with different probably values (Ba and Al p<0.05), but (Fe and Zn P<0.01), while the trace element in crude oil station workers was highly significantly (P<0.001) higher than that of control group.

TABLE II

TRACE ELEMENTS IN CRUDE OIL STATION WORKERS AND CONTROL

Parameters	Control group	Exposure group	P value
Ba (mg/L)	0.47±0.1	0.58±0.18	P< 0.05
Al (mg/L)	0.98±0.21	1.39±0.46	P< 0.05
Fe (mg/L)	0.21±0.043	0.36±0.1	P<0.01
Zn (mg/L)	0.072±0.05	0.175±0.06	P<0.01
Mn (mg/L)	0.006±0.004	0.19±0.1	P< 0.001

Results expressed as Mean ±SD

Concentration of serum urea, creatinine and uric acid in crude oil station workers and control: -

Table (III) provided the mean S.urea, creatinine and uric acid in crude oil station workers and control groups. The results obtained indicated that the mean S.urea in group 1 was not significantly higher than that of group 2, the mean S.creatinine in group 1 was significantly higher than that of group 2,($P< 0.05$), and the mean S.uric acid in group 1 was significantly higher than that of group 2, ($P< 0.01$).

TABLE III

UREA, CREATININE AND URIC ACID IN CRUDE OIL STATION WORKERS AND CONTROL

Parameters	Control group	Exposure group	P value
Serum urea (mg/dl)	27.35± 9.37	30.5± 7.33	P> 0.05
Serum creatinine (mg/dl)	0.53± 0.28	0.85± 0.18	P< 0.05
Serum uric acid (mg/dl)	4.6± 1.4	6.34± 1.25	P<0.001

Results expressed as Mean ±SD

4. Discussion

The toxicity effect of certain metals in some forms and doses on health, certain metals have no biological role, it means are not essential minerals, or are toxic when in a certain form [12], for example the heavy element lead in any amount will affect human health [13], which cause anemia and affect organs especially kidneys [4]. The heavy metals such as lead, mercury and cadmium, all have electron–sharing affinities that can result information of covalent attachments [14]. These attachments are mainly formed between heavy metals and sulfhydryl groups of proteins [15]. In the present the metals the heavy metals Pb and V in exposure group (group 1) was not significantly higher than that of control group (group 2), the same results obtained by Adnan et al [16].

In current study all the trace elements Ba, Al, Fe, Zn and Mn in serum of exposure group were significantly higher than that of control group. Trace elements as Zn, Fe and Mn participate in the regulation of multiple biochemical metabolisms and physiological functions (e.g. nucleic acid and protein synthesis, enzymatic reactions, membrane stabilization, immune system function, antioxidant defenses, oxidative phosphorylation, etc.). These metals are effective at very low concentrations, and their concentration in body fluids must be tightly regulated: deficiency or excess both cause severe illness and death. Thus, urinary excretion by the kidney, together with the gastrointestinal absorption rate, plays an important role in regulating the plasma level of these elements. Although the renal handling of cations is not fully understood, it is probable that each segment of the nephron is involved in their reabsorption; even so 70% of the transport occurs along the proximal tubule [17, 18].

In current study analyzed kidney function tests (urea, creatinine and uric acid), obtained that serum urea and creatinine of exposure group were significantly higher than that of control group ($P< 0.05$), and uric acid in serum of exposure group were significantly higher than that of control group ($P< 0.01$), caused by the body is contaminated by heavy metals Hg, Pb and V, and also high level of trace elements Mn. Zn and Fe. Therefore, the kidney will be confronted with two problems;

1- The entry of the toxic metal into the renal cells
2- The concomitance of the essential trace elements entry due to competition with the toxin [19].

Renal failure occurs were the kidneys cannot ability to remove the body metabolic waste products (urea, creatinine and uric acid), leading to accumulate in the body fluids as a result of impaired renal excretion and lead to a disruption in endocrine and metabolic functions as well as fluid, electrolyte, and acid-based disturbances, all this participative in renal failure [20].

5. Conclusion

This study concluded that human exposure to crude oil cause increase heavy metals in blood circulation especially vanadium and lead, also increase serum essential elements (Mn, Zn and Fe), and each of (Ba and Al) non-essential trace elements was increased, and kidney function tests are elevated especially creatinine and uric acid.

Reference

[1] MA. Mehlman. Dangerous properties of petroleum-refining products: carcinogenicity of motor fuels (gasoline). TeratogenesisCarcinog Mutagen. 1990, (10) pp: 399-408.

[2] H. Carolyn and JL. John. Toxicological profile for gasoline.U.S. Department of Health and Human Services. Public health service agency for toxic substances and disease registry. 1995.

[3] Aslam B, Javed I, Khan H F and Zia-ur-Rahman. Uptake of heavy metal residues from sewage sludge in the goat and cattle during summer season. Pakistan Veterinary Journal.2011, 31(1), 75-77.

[4] allanGow, Michael J. Murphy, Rajeef Srivastava, Robert A. Cowan and Denis St. j. OReilly. Clinical biochemistry, an illustrated color text.fifth edition. Churchill livingstone. Elsevier. Toronto 2013.

[5] Mortada W.I., Sobh M.A., El-Defrawy M.M., FarahatS.E., Study of lead exposure from automobile exhaust as arisk for nephrotoxicity among traffic policemen, *Am JNephro*. 2001,21(4), 274-9

[6] Hong Y.C., Park E.Y., Park M.S., Ko J.A., Oh S.Y. andKim H., et al. Community-level exposure to chemicalsandoxidative stress in adult population. Toxicol Lett. 2009, 184,139–44

[7] Henry A. Schroeder. The role of trace elements in cardiovascular diseases.Medical clinics of North America. 1974, 58(2):381.

[8] Elif Ari, Yuksel Kaya, HalkitDemir, EbruAsicicoglue, SiddikKeskin. The correlation of serum trace elements and heavy metals with carotid artery atherosclerosis in maintenance hemodialysis patients.Biological Trace Element Research. 2011, 144(1-3):351-9.

[9] Liu J, Habeebu SS, Liu Y, Klaassen CD: Acute CdMT injection is not a good model to study chronic Cd nephropathy: Comparison of chronic CdCl2 and CdMT exposure with acute CdMT injection in rats. ToxicolApplPharmacol 1998, 153:48–58.

[10] Massadeh, A., et al., Simultaneous determination of Cd, Pb, Cu, Zn, and Se in human blood of Jordanian smokers by ICP-OES. Biological trace element research, 2010, 133(1): p. 1.

[11] Bakircioglu, D., Y.B. Kurtulus, and G. Ucar, Determination of some traces metal levels in cheese samples packaged in plastic and tin containers by ICP-OES after dry, wet and microwave digestion. Food and Chemical Toxicology, 2011, 49(1): p. 202-207

[12] Dartmouth Toxic Metals Superfund Research Program. 2012-05-30. Archived from the original on 2013-12-30. Retrieved 2013-12-29.

[13] Jump up ^"Announcement: Response to the Advisory Committee on Childhood Lead Poisoning Prevention Report, Low Level Lead Exposure Harms Children: A Renewed Call for Primary Prevention". Centers for Disease Control and Prevention. 2012-05-25. Archived from the original on 2017-04-30.

[14] Bondy, S.C., Oxygen generation as a basis for neurotoxicity of metals. In: Toxicology of metals, Chang, L.W.; Eds,;RCPress, Baco Raton. 1996, pp 699-706

[15] Quig D. Cysteine, metabolism and metal toxicity, Alter.Med.Rev.1998,3, 262-70.

[16] Adnan J. M, AL-Fartosy, Nadhum A, Awad and Sanna K. Shanan. Biochemical correlation between some heavy metals, malondialdehyde and total antioxidant capacity in blood of gasoline station workers.Int. res. J. Environment. Sci. 2014, vol. 3(9); pp 56-60.

[17] Ducoudret O, Barbier O, Tauc M, Fuchs M, Poujeol P: Characterization of Zn2+ transport in Madin-Darby canine kidney cells. BiochimBiophysActa 2003, 1611.pp171–179.

[18] Felley-Bosco E, Diezi J: Fate of cadmium in rat renal tubules: A microinjection study. ToxicolApplPharmacol 1987, 91, pp 204–211.

[19] Gachot B, Tauc M, Morat L, Poujeol P: Zinc uptake by proximal cells isolated from rabbit kidney: Effects of cysteine and histidine. Pflügers Arch 1991, 419.pp 583–7.

[20] Al-Jawadi A. M. Zena. Clinical and biochemical study of acute renal failure disease. Nati.J. of Chemistry. 2006, 21, pp 119-124.

ttp://jgu.garmian.edu.krd https://doi.org/10.24271/garmian.327

Corrosion Prevention of Cast Iron Industrial Water Pipes: A Preliminary Comparative Study of Hexamine and Aniline Inhibitors

Hayder Mohammed Issa[1*] Azad H. Alshatteri[2]

[1]College of Human Sciences, University of Garmian, Kalar, Al- Sulaimaniyah, Kurdistan Region, Iraq

[2]Chemistry Dept., Education College, University of Garmian, Kalar, Al- Sulaimaniyah, Kurdistan Region, Iraq

[*]Corresponding author. Email: hayder.mohammed@garmian.edu.krd

Abstract

Using cast iron pipes in various industrial and water systems is experiencing a major problem of corrosion occurrence. Hence the operation and maintenance of these pipes become costly and infeasible. Corrosion inhibitors have a great role in decreasing pipes corrosion rate. In this study, the inhibition effect by applying two inhibitors of hexamethylenetetramine (hexamine) and aniline on cast iron pipes was studied. Experimental measurements of the corrosion behavior of cast iron pipes was thoroughly examined in three aqueous salt solutions of 2% NaCl, 2% Na_2SO_4 and 2% $CaCO_3$. The corrosion inhibition efficiency of the cast iron pipes by aniline or hexamine in the three aqueous salt aqueous solutions was investigated at constant temperature and for different time intervals. Corrosion rates of the pipes were determined using weight loss technique. It has been found that, for the corrosion of cast iron pipes, a satisfactory inhibition efficiency is observed for a concentration close to 150 ppm hexamine and 150 ppm aniline over the whole aqueous salt solutions tested in the work. The results showed that at the same inhibitor concentration and temperature, aniline exhibits higher inhibition corrosion efficiency on cast iron pipes than the efficiency achieved by hexamine.

Keywords: cast iron pipes; corrosion inhibitors, hexamethylenetetramine; aniline; aqueous salt solution

1. Introduction

Cast iron as an alloy is widely used for water carrying purposes besides mild steel and other metals. Cast iron is also widely used in industrial water piping systems for more than one century. In the past, in industry the pipes were used especially for carrying water were made of cast iron (Mohebbi and Li 2011). The extent and cost of damage caused by corrosion in cast iron water pipes has been rising during recent decades (Mehra and Soni 2002). The use of cast iron in industrial water pipes and potable water distribution systems is essentially suffering from an inevitable corrosion problems

(Atkinson et al. 2002). Actually, this corrosion phenomenon is now considered as the main problem facing cast iron water pipes operation and maintenance in industry, potable water distribution, and wastewater systems (Agatemor and Okolo 2008; Daneshvar-Fatah et al. 2013; Hasan and Sadek 2014; Li et al. 2016; Liang et al. 2013). The corrosion of cast iron pipes is actually varied regarding both material quality and purpose of using (Yang et al. 2012). Corrosion leads to deterioration and failures of those industrial pipes and equipment made of cast iron (Essa 2006; Kuźnicka 2009). The high cost of occurring corrosion in industry and water systems shows the need to improved corrosion measurement and prevention schemes (Reynaud 2010).

Among available solutions of corrosion in engineering materials, inhibitors were found to be of high practical importance, in minimizing metallic waste (Collins et al. 1993). Corrosion protection aims to improve performance of pipes metal (Dwivedi et al. 2017). Methods of Corrosion control are needed to be properly selected according to environment and operational conditions of pipes and equipment (Mannivanan et al. 2012). Corrosion inhibitors are employed as it has been observed the absence of corrosion inhibitors leads always to an exponential increase in corrosion rate of pipe metals (Barmatov et al. 2015). Corrosion inhibitors are commonly single organic components, but mixtures of solvents-compound or compound-surfactant are regularly used (Finšgar and Jackson 2014; Hill and Jones 2003). Various nitrogen or sulfur-containing organic compounds have been used as corrosion inhibitors (Al-Rawajfeh and Al-Shamaileh 2007; Ebenso et al. 2001; Ekpe et al. 1995; Fathima Sabirneeza et al. 2015; Hosseini et al. 2003). The mechanism of corrosion inhibition in surface processes involves adsorption of the inhibitor organic compounds on the metal surface that needed to be protected (Zhu et al. 2015). Inhibition efficiency of organic compounds is usually depends on inhibitor molecular size and the mode of interaction with metal surface (Shirazi et al. 2017).

The corrosion of cast iron in acidic and alkaline mediums was studied in several previous works (Osarolube et al. 2008; Simsek et al. 2010). These studies figured out aqueous salt solutions, at high salt concentrations such as 3.0 M, are the most corrosive for cast iron metal. The corrosion behavior was characterized by two factors of salt and oxygen dissolved in aqueous solutions (Shakir et al. 2018). Many previous works have studied hexamine (hexamethylenetetramine) and aniline or their derivatives inhibition properties to protect metals in different acidic and alkaline mediums. The studies were made for diverse metals and alloys such as copper and iron (Benchikh et al. 2009; Essa 2007; Khaled and Hackerman 2004; Vashi and Naik 2010). It has been found that low molecular mass and high water solubility amines such as hexamine produce higher adsorption and corrosion prevention (Bayol et al. 2007). Aniline and its derivatives are also used as inhibitors as they found to inhibit metal corrosion, especially iron with great extent (Jeyaprabha et al. 2006).

As any obtained information on the rate at which corrosion initiates and progress in cast iron pipes is considered to be important for the attempts to control or reduce the damage caused by corrosion. Moreover, the controlling of deterioration and failures become extremely challenging without a well understanding of the cast iron pipes corrosion. In this work, the aim is to investigate the inhibition effect of aniline and hexamine on cast iron pipes in three different aqueous salt solutions NaCl, Na_2SO_4, and $CaCO_3$. The corrosion rate of cast iron pipe was experimentally determined using weight loss method with and without inhibitors presence.

2. Materials and Method

2.1. Material Preparation and Weight Loss Measurement Specimens were cut from cast iron water pipes of outer diameter 24 mm, a thickness of 2 mm. The arrangement of the cast iron alloy testing was as coupon specimen of 2x2 cm^2 and thickness 0.2 cm, a hole was drilled diameter 0.05 cm at the upper edge. The surface of specimens were cleaned, degreased in benzene, washed using 50% acetone, dried, marked and weighed to a constant weight before exposing to the corrosive medium. The specimens were suspended by a glass hook in a beaker filled with test solution, for different duration of immersion 72, 120, 168, 240, and 288 hours in three aqueous salt corrosive mediums. All test solutions were prepared from analytical grade reagents and double – distilled water. The testing aqueous salt solutions are 2% NaCl, 2% Na_2SO_4 and 2% $CaCO_3$ at room temperature. At the end of each exposure time, the specimens were removed, cleaned, dried and weighed. All specimen metal surfaces, including the edges, were abraded to original ground using grit silicon carbide papers to remove any coated layer to prevent corrosion to pipes like galvanized zinc layer. Figure 1 (a) shows the clean surface of specimen cast iron pipe, as can be seen in Figure 1 (b), the specimen cast iron pipe with a localized corrosion condition is being evident on pipe surface after 288-hour (12 days) immersion in 2% NaCl solution.


(a) (b)

Figure 1.a. The clean surface of specimen cast iron pipe, Figure 1.b. The specimen cast iron pipe with localized corrosion on the surface after 12 days immersion in 2% NaCl solution.

The chemicals aniline and hexamine were used as corrosion inhibitors for this investigation. The inhibitors concentrations were 150 ppm were prepared in 2% NaCl, 2% Na_2SO_4 and 2% $CaCO_3$ aqueous salt solutions at 25 $\pm$ 2 ^oC. The molecular structures of the inhibitors used are displayed in Figure 2 (a), and (b).

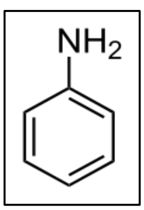

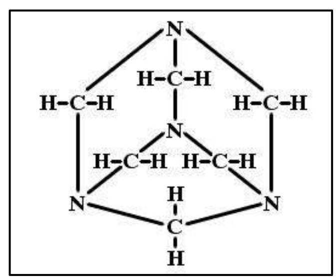

(a) (b)

Figure 2.a. the molecular structure of the aniline inhibitor. Figure 2.b. the molecular structure of the hexamethylenetetramine (hexamine) inhibitor.

2.2. Pipe Metal Analysis

The cast iron pipe specimens were analyzed using ICP-OES: Spectro Arcos in the chemical laboratory at University of Garmian. The chemical composition of the cast iron pipes is shown in Table 1. The instrument conditions used were: Spray chamber is Scott spray; Nebulizer: crossflow; RF power/W: 1400; pump speed: 30 RPM; Coolant flow (L/min): 14; Auxiliary flow (L/min): 0.9; nebulizer gas flow (L/min): 0.8; Preflush (s): 40; Measure time (s): 28; replicate measurement: 3; argon gas (purity ≥ 99.99); multi-elements stock solutions containing 1000 mg/L were obtained from Bernd Kraft (Bernd Kraft GmbH, Duisburg, Germany); standard solutions were diluted by several dilution in 0.5% nitric acid as diluent.

Table 1. Chemical composition of cast iron pipes used for water carrying

Component*	Fe	Si	Mn	S	Ni	Cu	Pb	Mo	V	Mg	Cr
Wt. Percentage (%)	95.00	1.00	1.70	0.02	0.06	0.06	0.01	0.03	0.06	0.02	0.14

*The rest is carbon C.

2.3. Inhibition Efficiency and Degree of Surface Coverage Calculations

After the weight loss of cast iron specimens, efficiency was determined as the difference in the weight before and after each exposure time in test aqueous salt solutions for each inhibitor. The values of percentage corrosion inhibition efficiency of aniline and hexamine inhibitors in the three investigated aqueous salt solutions for the various immersion periods was calculated using the following equation that obtained from literature (Abiola et al. 2013; James and Akaranta 2011; Rafiquee et al. 2009). The definition of each symbol in the following equation is presented in the nomenclature at the end of this paper.

$$IE\% = \left(1 - \frac{W_i}{W_n}\right) * 100\% \quad (1)$$

The degree of surface coverage, θ was determined by the following equation (Daoud et al. 2015; Sirajunnisa et al. 2014);

$$\theta = \left(1 - \frac{W_i}{W_n}\right) \quad (2)$$

2.4. Corrosion Rate Calculations

The corrosion rate of cast iron in different aqueous salt solution mediums was determined for different immersion period from weight loss using the equation below. The same corrosion rate (CR) equation was used for various metals and solutions (Anand and Balasubramanian 2011; Singh and Quraishi 2015):

$$C_R = \frac{87.6\,W}{AtD} \quad (3)$$

Where W (in mg) is the weight loss and calculated as follows:

$$W = W_0 - W_t \quad (4)$$

3. Results and Discussion

3.1. Morphology of Corroded Metal Surface

The corroded metal surface has been changed in appearance and its color was turned into brown for all the specimens of cast iron pipes. As shown in Figure 1 typical changes in the corrosion products on a specimen after 12 days exposure in 2% NaCl. In general, the look of the corroded surface of cast iron specimens was the same for all the investigated aqueous salt solutions, but the thickness of corrosion product varies with exposure time. The localized corrosion occurred on specimen surface is the main form of corrosion of water used cast iron pipes.

3.2. Weight Loss and Corrosion Rates

Results obtained from weight loss and corrosion rate of cast iron pipe specimens in a 2% NaCl, 2% Na_2SO_4, and 2% $CaCO_3$ solutions at 25$\pm$ 2^oC are showed in Tables 2 and 3. From which it can be observed that the weight loss for specimens in the three solutions increases with time, in consequence, the corrosion rate is also increases with time. The corrosion rate of cast iron specimens in the test solutions was calculated from the decrease in weight loss by applying equations 3 and 4.

Table 2. Weight loss (mg / cm^2) of the cast iron specimens in 3 aqueous salt solutions of 2% NaCl, 2% ppm Na_2SO_4 and 2% ppm $CaCO_3$ at 25$\pm$ 2^oC and for different time intervals.

Time (hr.)	24	72	120	168	240	288
NaCl	0.138	0.422	0.774	1.181	1.689	1.882
Na_2SO_4	0.059	0.248	0.493	0.731	0.974	1.134
$CaCO_3$	0.057	0.191	0.322	0.484	0.668	0.748

Table 3. Corrosion rates (mmpy) of the cast iron specimens in three aqueous salt solutions of 2% NaCl, 2% ppm Na_2SO_4 and 2% ppm $CaCO_3$ at 25$\pm$ 2^oC and for different time intervals.

Time (hr.)	24	72	120	168	240	288
NaCl	0.0690	0.0704	0.0774	0.0844	0.0845	0.0784
Na_2SO_4	0.0295	0.0414	0.0493	0.0522	0.0487	0.0473
$CaCO_3$	0.0284	0.0318	0.0322	0.0346	0.0334	0.0312

For the specimens in 2% NaCl solution, the corrosion rate seems to follow a specific trend and it appears to increase with time. But this increase is more drastic and then tends to be less at longer exposure time. For the specimens in 2% Na_2SO_4 solution, the corrosion rate seems to establish a different trend as it decreases at the higher exposure time. For the specimens in 2% $CaCO_3$ solution, the average corrosion rate is close at exposure times longer than 120 hr. Based on the analysis of the corrosion rate results obtained from the three aqueous salt solutions it can be understand that the localized corrosion behavior of cast iron water pipes is the primary form of corrosion degradation. The intensity of the localized corrosion depends on the extent of time exposure. From Tables 2 and 3, where the weight loss and corrosion rate values were listed, it can be observed from corrosion rate in mmpy of cast iron specimens in the three tested aqueous salt solutions are in the order of NaCl > Na_2SO_4 > $CaCO_3$ during time of exposure of 288 hours.

3.3. Effect of Corrosion Inhibitors

The weight loss measurements were carried out of cast iron specimens with aniline and hexamine corrosion inhibitors concentrations of 150 ppm separately. The exposure time was ranging from 24 to 288 hours to study the effect of inhibitor presence and immersion time on the corrosion rate of cast iron water pipes at $25 \pm 2^{o}C$ as seen in Table 4 and 5. It was found that with use of 150 ppm concentration of aniline and hexamine inhibitors causes decreasing of weight loss in all the studied aqueous salt solutions as displayed in Figure 3 to 5.

Figure 3 shows the results of specimen weight loss produced from corrosion of cast iron pipes for different exposure time in three conditions of 2% NaCl aqueous salt solution. In one these conditions 150 ppm of hexamine inhibitor was added and in another, a 150 ppm aniline was added to the solution.

As illustrated in Figure 3, the amount of weight loss was decreased considerably when 150 ppm hexamine was added to NaCl solution. The weight loss of cast iron specimens was more significantly decreased when 150 ppm aniline was added to the solution. The same effect was noticed for the other two aqueous solutions of 2% Na_2SO_4 and 2% $CaCO_3$ as presented in Figures 4 and 5 for the exposure time ranges from 24 hr. to 288 hr.

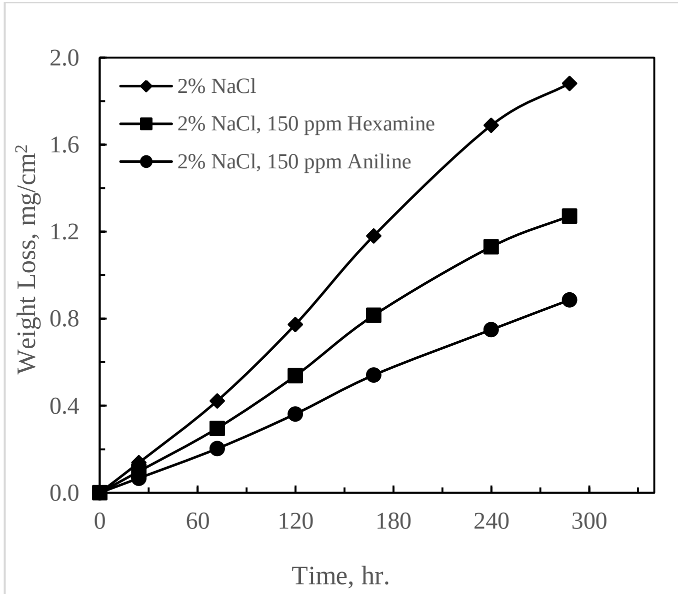

Figure 3. Variation of specific weight loss with time of cast iron specimens in 150 ppm Aniline and 150 ppm hexamine inhibitors added to 2% NaCl solution at 25$\pm$2^{o}C.

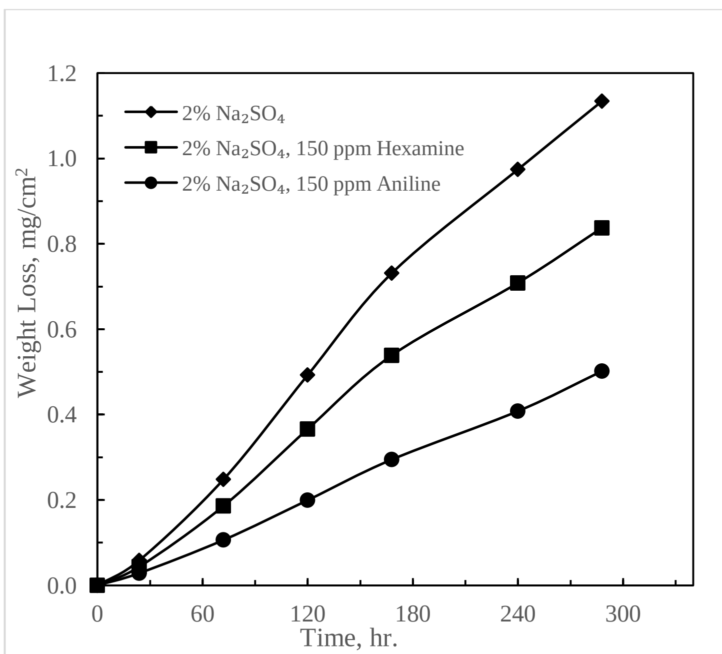

Figure 4. Variation of specific weight loss with time of cast iron specimens in 150 ppm Aniline and 150 ppm hexamine inhibitors added to 2% Na_2SO_4 solution at 25$\pm$2^{o}C.

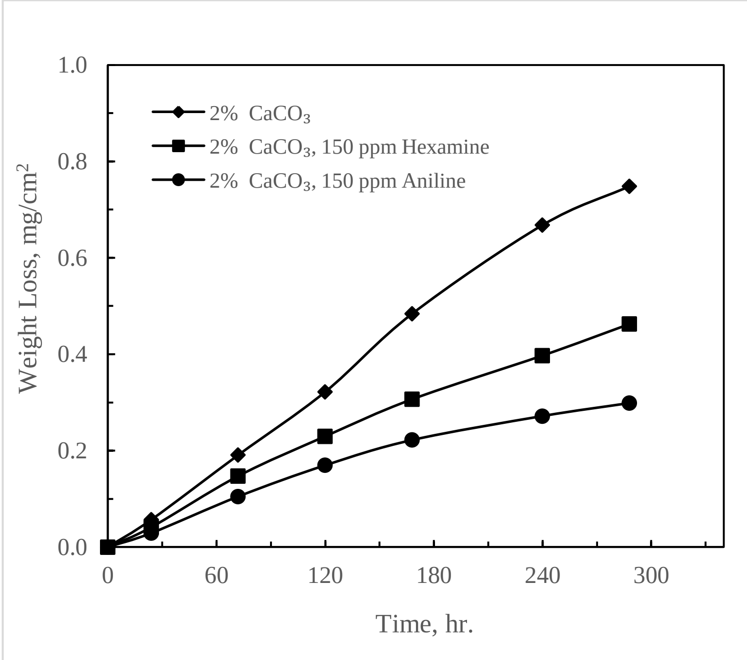

Figure 5. Variation of specific weight loss with time of cast iron specimens in 150 ppm Aniline and 150 ppm hexamine inhibitors added to 2% $CaCO_3$ solution at 25 ± 2^oC.

From Table 4 it was found that with increase in exposure time from 24 to 288 hours, the weight loss decreased and hence the inhibition efficiency increased from 28.95% to 32.41% when 150 ppm hexamine was added to the solution of 2% NaCl (surface coverage increased from 0.289 to 0.324). The increase ranges of efficiency of 2% Na_2SO_4 and 2% $CaCO_3$ were (from 25.46% to 26.16%) and (from 27.37% to 35.38%).

In terms of metal protection, these results indicate that adding 150 ppm of hexamine is the satisfactory concentration to develop acceptable corrosion prevention for cast iron pipe specimens in the investigated salt solutions. The behavior of hexamine inhibitor most probably results from adsorption on metal surface is suitable with this concentration of hexamine and therefore the inhibition efficiency was reasonable.

Table 4 shows the results of 150 ppm aniline added to the tested aqueous salt solutions. It can be observed that the corrosion rate reduced during with time interval from 24 to 288 hours for 2% NaCl, 2% Na_2SO_4, and 2% $CaCO_3$. The reduction of corrosion rate increases higher than that achieved by 150 ppm hexamine. The reason of this difference is most possibly due to the adsorption behavior of anions the electrolyte of aniline at the electrode surface (Luo et al. 1998).

Table 4. Corrosion parameters, obtained from weight loss measurements for cast iron specimens in three aqueous salt solutions of 2% NaCl, 2% Na_2SO_4 and 2% $CaCO_3$ at 25$\pm$ 2^{o}C, containing 150 ppm hexamine inhibitor for different time intervals.

Exposure time (hr.)	Corrosion rate (mmpy)	Inhibition efficiency (%)	Surface coverage (θ)
2%NaCl			
24	0.0490	28.95	0.289
72	0.0494	29.86	0.299
120	0.0538	30.52	0.305
168	0.0583	30.96	0.310
240	0.0565	33.05	0.331
288	0.0530	32.41	0.324
2% Na_2SO_4			
24	0.0220	25.46	0.255
72	0.0310	25.13	0.251
120	0.0366	25.70	0.257
168	0.0385	26.31	0.263
240	0.0354	27.27	0.273
288	0.0349	26.16	0.262
2% $CaCO_3$			
24	0.0206	27.37	0.274
72	0.0246	22.83	0.228
120	0.0230	28.66	0.287
168	0.0219	36.65	0.366
240	0.0209	37.53	0.375
288	0.0202	35.38	0.354

From the results presented in Table 4, it was found with the weight loss increases with time for all three solutions and the corrosion rate remains at certain levels with time for NaCl and Na_2SO_4 solutions. However, for 2% $CaCO_3$ solution, the corrosion rate drops relatively after 168 hours. This declining is perhaps because of the stability of ferric oxide film that formed after corrosion occurrence. The phenomena is known for corrosion inhibitor behavior of anions in aqueous solutions (Xu et al. 2017). In general, it is noticed that the corrosion rate is highly reduced in the solutions contain hexamine or aniline inhibitor. The reduction occurs due to the inhibitor protection for the metals by preventing the direct contact between metals surface and corrosive anions. In the same time, the reduction is also made by decreasing plenty of cations on the metal surface. At 25 ^{0}C $\pm$ 2 and 240 hours with presence 150 ppm hexamine and 150 ppm aniline, the corrosion rate of 2% NaCl solution was lessened to 0.0565 and 0.0375 mmpy respectively. While for Na_2SO_4 and $CaCO_3$ solutions, same thing happened at varying rates of the corrosion. The two anions are reported to have a significant influence on the corrosion characteristics of cast iron are chloride and sulfate ions (Ekpe et al. 2001).

Table 5. Corrosion parameters obtained from weight loss measurements for cast iron specimens in three aqueous salt solutions of 2% NaCl, 2% Na_2SO_4 and 2% $CaCO_3$ at 25$\pm$ 2^oC, containing 150 ppm aniline inhibitor for different time intervals.

Exposure time (hr.)	Corrosion rate (mmpy)	Inhibition efficiency (%)	Surface coverage (θ)
2% NaCl			
24	0.0335	51.50	0.515
72	0.0338	52.00	0.520
120	0.0362	53.20	0.532
168	0.0386	54.20	0.542
240	0.0375	55.62	0.556
288	0.0369	52.90	0.529
2% Na_2SO_4			
24	0.0144	51.08	0.511
72	0.0177	57.20	0.572
120	0.0200	59.50	0.595
168	0.0211	59.70	0.597
240	0.0204	58.12	0.581
288	0.0209	55.77	0.558
2% $CaCO_3$			
24	0.0145	48.79	0.488
72	0.0175	45.06	0.451
120	0.0170	47.30	0.473
168	0.0159	54.12	0.541
240	0.0136	59.31	0.593
288	0.0124	60.08	0.601

The exposure time effect on cast iron corrosion rate from 24 to 288 hours was also explored in this work. For both hexamine and aniline inhibitor in 2% NaCl solution, the inhibition efficiency enhanced (from 28.95 % to 32.41 %), and (from 51.50 % to 52.90 %) respectively.

The increase in inhibition efficiency at longer immersion time is due to anion kinetics in aqueous solutions of strengthening of adsorption that mentioned above. The immersion time with corrosion inhibitors aniline and hexamine scores highest inhibition efficiency of cast iron specimens in 2% NaCl, 2% Na_2SO_4 and 2% $CaCO_3$ at 288 hours as given in Tables 3 and 4.

As a result, the inhibition increased as more inhibitor molecules are adsorbed on the metal surface reduces the surface area available for the attack of the aggressive ions from the salt solution. Inhibition efficiency showed remarkable improvement with addition of 150 ppm to 2% $CaCO_3$ probably for the same reason mentioned above.

Conclusions

The inhibition of corrosion of cast iron alloy by an addition of 150 ppm hexamine and 150 ppm aniline was performed efficiently in salts solutions of 2% NaCl, 2% Na_2SO_4 and 2% $CaCO_3$ at $25\pm 2\ ^oC$.

The aniline showed more effective inhibition efficiency than the hexamine. In 2% NaCl solution the corrosion rate of cast iron pipes was higher than 2% Na_2SO_4 and 2% $CaCO_3$ solutions.

Generally, in aqueous salt solutions, the corrosion rate of cast iron alloy appears to be a function of dissolved salt type, inhibitor type and immersion time.

The work described here lead us to expect the using aniline as a corrosion inhibitor rather than hexamine in prevention the cast iron corrosion in industry, where cast iron pipes still implemented to carry aqueous salt solutions.

Nomenclature

A the area of the specimen (cm^2),
C_R the corrosion rate (CR) of cast iron (mmpy),
t the exposure time (h),
D the density of cast iron (g/cm^3)
IE% the inhibition efficiency (%)
θ the surface coverage (-)
W weight loss (mg),
W_i the weight loss of cast iron in the corrodent – inhibitor system (mg),
W_n the weight loss of cast iron in the corrodent (blank) (mg),
W_0 the weight loss of cast iron in the corrodent (blank) at exposure time 0 (mg),
W_t the weight loss of cast iron in the corrodent (blank) at the end of exposure time (mg),

References

Abiola O, Aliyu A, Phillips A, Ogunsipe A (2013) The effects of Phyllanthus amarus extract on corrosion and kinetics of corrosion process of aluminum in HCl solution Journal of Materials and Environmental Science 4:370-373

Agatemor C, Okolo PO (2008) Studies of corrosion tendency of drinking water in the distribution system at the University of Benin The Environmentalist 28:379-384 doi:10.1007/s10669-007-9152-2

Al-Rawajfeh AE, Al-Shamaileh EM (2007) Inhibition of corrosion in steel water pipes by ammonium pyrrolidine dithiocarbamate (APDTC) Desalination 206:169-178 doi:https://doi.org/10.1016/j.desal.2006.02.065

Anand B, Balasubramanian V (2011) Corrosion Behaviour of Mild Steel in Acidic Medium in Presence of Aqueous Extract of Allamanda Blanchetii E-Journal of Chemistry 8 doi:10.1155/2011/345095

Atkinson K, Whiter JT, Smith PA, Mulheron M (2002) Failure of small diameter cast iron pipes Urban Water 4:263-271 doi:https://doi.org/10.1016/S1462-0758(02)00004-3

Barmatov E, Hughes T, Nagl M (2015) Efficiency of film-forming corrosion inhibitors in strong hydrochloric acid under laminar and turbulent flow conditions Corros Sci 92:85-94 doi:https://doi.org/10.1016/j.corsci.2014.11.038

Bayol E, Kayakırılmaz K, Erbil M (2007) The inhibitive effect of hexamethylenetetramine on the acid corrosion of steel Mater Chem Phys 104:74-82 doi:https://doi.org/10.1016/j.matchemphys.2007.02.073

Benchikh A, Aitout R, Makhloufi L, Benhaddad L, Saidani B (2009) Soluble conducting poly(aniline-co-orthotoluidine) copolymer as corrosion inhibitor for carbon steel in 3% NaCl solution Desalination 249:466-474 doi:https://doi.org/10.1016/j.desal.2008.10.024

Collins WD, Weyers RE, Al-Qadi IL (1993) Chemical Treatment of Corroding Steel Reinforcement After Removal of Chloride-Contaminated Concrete CORROSION 49:74-88 doi:10.5006/1.3316037

Daneshvar-Fatah F, Mostafaei A, Hosseinzadeh-Taghani R, Nasirpouri F (2013) Caustic corrosion in a boiler waterside tube: Root cause and mechanism Eng Failure Anal 28:69-77 doi:https://doi.org/10.1016/j.engfailanal.2012.09.010

Daoud D, Douadi T, Hamani H, Chafaa S, Al-Noaimi M (2015) Corrosion inhibition of mild steel by two new S-heterocyclic compounds in 1 M HCl: Experimental and computational study Corros Sci 94:21-37 doi:https://doi.org/10.1016/j.corsci.2015.01.025

Dwivedi D, Lepkova K, Becker T (2017) Carbon steel corrosion: a review of key surface properties and characterization methods RSC Advances 7:4580-4610 doi:10.1039/C6RA25094G

Ebenso E, Okafor P, Offiong O, Ita B, Ibok U, Ekpe U (2001) Comparative investigation into the kinetics of corrosion inhibition of aluminium alloy AA 1060 in acidic medium Bull Electrochem 17:459-464

Ekpe U, Okafor P, Ebenso E, Offiong O, Ita B (2001) Mutual effects of thiosemicarbazone derivatives on the acidic corrosion of aluminium Bull Electrochem 17:131-135

Ekpe UJ, Ibok UJ, Ita BI, Offiong OE, Ebenso EE (1995) Inhibitory action of methyl and phenyl thiosemicarbazone derivatives on the corrosion of mild steel in hydrochloric acid Mater Chem Phys 40:87-93 doi:https://doi.org/10.1016/0254-0584(94)01464-R

Essa H. M., (2006), Removal of Corrosion Product from Inside Heat Exchanger Tubes Used in Topping Unit in Azzawia Refinery/Libya by Chemical Methods, Journal of Corrosion Science and Engineering, 10:1-10

Essa H. M., (2007), The Influence of Corrosion Inhibitor (Hexamine) Concentration on Heat Exchanger Copper Alloy Tubes, Corrosion Rate Journal of Corrosion Science and Engineering, 10:1-10

Fathima Sabirneeza AA, Geethanjali R, Subhashini S (2015) Polymeric Corrosion Inhibitors for Iron and Its Alloys: A Review Chem Eng Commun 202:232-244 doi:10.1080/00986445.2014.934448

Finšgar M, Jackson J (2014) Application of corrosion inhibitors for steels in acidic media for the oil and gas industry: A review Corros Sci 86:17-41 doi:https://doi.org/10.1016/j.corsci.2014.04.044

Hasan BO, Sadek SA (2014) The effect of temperature and hydrodynamics on carbon steel corrosion and its inhibition in oxygenated acid–salt solution Journal of

Industrial and Engineering Chemistry 20:297-307 doi:https://doi.org/10.1016/j.jiec.2013.03.034

Hill DG, Jones A (2003) An Engineered Approach to Corrosion Control During Matrix Acidizing of HTHP Sour Carbonate Reservoir. Paper presented at the CORROSION 2003, San Diego, California, 2003/1/1/

Hosseini M, Mertens SFL, Arshadi MR (2003) Synergism and antagonism in mild steel corrosion inhibition by sodium dodecylbenzenesulphonate and hexamethylenetetramine Corros Sci 45:1473-1489 doi:https://doi.org/10.1016/S0010-938X(02)00246-9

James A, Akaranta O (2011) Inhibition of corrosion of zinc in hydrochloric acid solution by red onion skin acetone extract Research Journal of Chemical Sciences Vol 1:1

Jeyaprabha C, Sathiyanarayanan S, Venkatachari G (2006) Polyaniline as corrosion inhibitor for iron in acid solutions J Appl Polym Sci 101:2144-2153 doi:10.1002/app.22579

Khaled KF, Hackerman N (2004) Ortho-substituted anilines to inhibit copper corrosion in aerated 0.5 M hydrochloric acid Electrochim Acta 49:485-495 doi:https://doi.org/10.1016/j.electacta.2003.09.005

Kuźnicka B (2009) Erosion–corrosion of heat exchanger tubes Eng Failure Anal 16:2382-2387 doi:https://doi.org/10.1016/j.engfailanal.2009.03.026

Li M, Liu Z, Chen Y, Hai Y (2016) Characteristics of iron corrosion scales and water quality variations in drinking water distribution systems of different pipe materials Water Res 106:593-603 doi:https://doi.org/10.1016/j.watres.2016.10.044

Liang J et al. (2013) Impact of flow rate on corrosion of cast iron and quality of re-mineralized seawater reverse osmosis (SWRO) membrane product water Desalination 322:76-83 doi:https://doi.org/10.1016/j.desal.2013.05.001

Luo H, Guan YC, Han KN (1998) Corrosion Inhibition of a Mild Steel by Aniline and Alkylamines in Acidic Solutions CORROSION 54:721-731 doi:10.5006/1.3284891

Mannivanan M, Rajendran S, Prabha AS (2012) Inhibitors for Prevention of Corrosion of Metals in Sea water–An Overview European Chemical Bulletin 1:317-329 doi:http://dx.doi.org/10.17628/ecb.2012.1.317-329

Mehra R, Soni A (2002) Cast iron deterioration with time in various aqueous salt solutions Bull Mater Sci 25:53-58 doi:10.1007/bf02704595

Mohebbi H, Li CQ (2011) Experimental Investigation on Corrosion of Cast Iron Pipes International Journal of Corrosion 2011:17 doi:10.1155/2011/506501

Osarolube E, Owate I, Oforka N (2008) Corrosion behaviour of mild and high carbon steels in various acidic media Scientific Research and Essay 3:224-228

Rafiquee MZA, Khan S, Saxena N, Quraishi MA (2009) Investigation of some oleochemicals as green inhibitors on mild steel corrosion in sulfuric acid J Appl Electrochem 39:1409-1417 doi:10.1007/s10800-009-9811-8

Reynaud A (2010) 3.02 - Corrosion of Cast Irons A2 - Cottis, Bob. In: Graham M, Lindsay R, Lyon S, Richardson T, Scantlebury D, Stott H (eds) Shreir's Corrosion. Elsevier, Oxford, pp 1737-1788. doi:https://doi.org/10.1016/B978-044452787-5.00088-3

Shakir IK, Alsamurraee A-KMA, Saleh SM (2018) Pitting Corrosion Behavior of 304 SS and 316 SS Alloys in Aqueous Chloride and Bromide Solutions Journal of Engineering:53-69%V 24

Shirazi Z, Keshavarz MH, Esmaeilpour K, Pakniya T (2017) A Novel and Simple Method for the Prediction of Corrosion Inhibition Efficiency without Using Complex Computer Codes Z Anorg Allg Chem 643:2149-2157 doi:10.1002/zaac.201700347

Simsek M et al. (2010) Boronizing Effect on the Corrosion Behaviour of Chilled Cast Iron and AISI 1050 Steel vol 29. doi:10.1515/HTMP.2010.29.4.241

Singh A, Quraishi MA (2015) The extract of Jamun (Syzygium cumini) seed as green corrosion inhibitor for acid media Res Chem Intermed 41:2901-2914 doi:10.1007/s11164-013-1398-3

Sirajunnisa A, Mohamed MF, Subramania A, Venkatraman B (2014) The inhibitive effect of Ziziphus jujuba leaves extract on the alkaline corrosion of aluminium European Journal of Applied Sciences and Technology [EUJAST] Volume 1

Vashi RT, Naik D (2010) Hexamine as Corrosion Inhibitors for Zinc in Phosphoric Acid E-Journal of Chemistry 7: S1-S6 doi:10.1155/2010/402764

Xu Q, Pang X, Gao K (2017) Effects of anions on corrosion behaviour of carbon steel in simulated groundwater in China Corrosion Engineering, Science and Technology 52:84-89 doi:10.1080/1478422X.2017.1294356

Yang F, Shi B, Gu J, Wang D, Yang M (2012) Morphological and physicochemical characteristics of iron corrosion scales formed under different water source histories in a drinking water distribution system Water Res 46:5423-5433 doi:https://doi.org/10.1016/j.watres.2012.07.031

Zhu Y, Free ML, Yi G (2015) Electrochemical measurement, modeling, and prediction of corrosion inhibition efficiency of ternary mixtures of homologous surfactants in salt solution Corros Sci 98:417-429 doi:https://doi.org/10.1016/j.corsci.2015.05.050

ttp://jgu.garmian.edu.krd https://doi.org/10.24271/garmian.328

Effect of Atorvastatin on Vitamin D Levels in Type 2 Diabetic Patients with Hypercholesterolemia

Huda Jaber [1*], Kassim Mohmmed [1], Azhar Abed Flayyih[2] , Amal Rasheed[3]

[1]College of pharmacy, Mustansiriyah University, Baghdad.
[2]Safeer Alimam Al-Hussain (A.S) Surgical Hospital,Karbala.
[3]Institute of medical Technology, Baghdad, Iraq.
[*]Corresponding author .Email: hudaiq84@yahoo.com

Abstract

Objective: The decrement of 25-hydroxy-vitamin D [25-OH-D] concentrations has been increase the severity of cardiovascular disease especially in diabetic patients. The aim of the present study was to assess the effect of atorvastatin on 25-OH-D concentration in diabetic patients with hypercholesterolemia. **Methods and patients:** Forty diabetic patients with hypercholesterolemia were participated in this work. For comparison, thirty healthy subjects were inserted in the present study. Serum vitamin D levels and lipid profile (total cholesterol, triglyceride, HDL, LDL and VLDL) were measured. **Results:** Vitamin D levels significantly decrease ($p<0.05$) in diabetic patients group (22.4±5.1 ng/ml) when compared to healthy group (32.44±4.12 ng/ml) .After 8 weeks from taking atorvastatin (20 mg/day) the mean of serum vitamin D were a slightly increase(26.4± 5.6) but not significant. Total cholesterol significantly decreases after therapy. **Conclusion:** Vitamin D levels significantly decrease in diabetic patients when compared to healthy subjects. There was no significant difference in vitamin D patients before and after lipid lowering therapy.

Key words: T2DM, hypercholesterolemia, vitamin D, atorvastatin.

1. Introduction:

Type 2 diabetic patients are more prone to dyslipidemia and cardiovascular complications. Patients with type 2 diabetes are at high risk for cardiovascular diseases (Benjamin M Leon & Thomas M Maddox, 2015). Previous medical studies recorded that atorvastatin, an inhibitor of 3-hydroxy-3-methylglutaryl coenzyme A reductase, which decreased the Probability of occurrence of cardiovascular complications in diabetic patients (Ahmed Abbas, et al., 2012; Kayama Y, et al., 2015). The advantage of statin using to decrease the incidence of cardiovascular complications in diabetic patients and also noted that the effect of atorvastatin and pravastatin on glycemic control (Manjunath G. Raju, et al., 2013).

Vitamin D is a steroid vitamin, has an important role in several biological functions. Its deficiency consider as a risk factor for osteoporosis and other chronic diseases such as diabetes, thyroid disorders, hypertension and other cardiovascular diseases, metabolic syndrome and ischemic heart disease (Daria M. Adamczak, 2017). Vitamin D is synthesized by exposing the skin to the sun that works on 7-dehydrocolesterol which hydroxylate carbon number 25 by the action of 25-hydroxyvitamin D-1 hydroxylase or CYP27B1,which is enzyme found in the mitochondria of the liver cells. The resulting molecule (25-hydroxyvitamin D) is the best formula to determine vitamin D levels (Matthias Wacker & Michael F. Holick, 2013). Both cholesterol and vitamin D together share by the 7-dehydrocolesterol conversion pathway. Statin is a treatment used for patients with high cholesterol, which inhibits the manufacture of cholesterol inside the body by inhibit 3-hydroxy-3-methylglutaryl coenzyme A (HMG-CoA) reductase (catalyze the rate limiting step in cholesterol synthesis) (Ahmed Abbas, et al., 2012). Statins have significant benefits effect in reducing acute ischemic heart disease degradation (Rose Gilbertab, et al., 2017). These patients often have a vitamin D deficiency and they will undergo statin treatment as secondary prevention (Ulrich Laufs, et al., 2015). This calls attention to the importance of studying the effect of this treatment on the levels of vitamin D, which are often critical in these patients. The aim of the present study was to assess the effect of atorvastatin on 25-OH-D concentration in diabetic patients with hypercholesterolemia.

2. Material and Methods:

Forty T2DM patients with hypercholesterolemia were collected from National Diabetic Center/Al- Al-Mustansiriyah University, Baghdad. Venous blood was drown from fasting diabetic patients and left for 30 min. then centrifuged to separate serum. For comparison, thirty healthy subjects were inserted in the present study. Serum vitamin D levels was measured by Cobas C111, Germany. Lipid profile (total cholesterol, triglyceride, HDL, LDL and VLDL) were measured by reflatron (Roch, Germany) and glycemic status parameters include FPG measured by reflatron(Roch, Germany), insulin hormone measured by ELISA (Diagnostic Automation Company/USA) and variant hemoglobin A_{1c} measured pack for HbA_{1c} mesurment (Bio-Rad Variant, Italy).

Statistical analysis:

Statistical analysis was done by computer program (SPSS-21). Unpaired t test was applied to find the significant difference between studied parameters. $P \leq 0.05$ considered significant.

3. Results:

In the current study, Patients and control group were similar in both age and BMI and there was no significant difference between them [P value >0.05], as shown in table (3.1)

Table (3.1): The characteristics of T2DM patients and control groups

Parameters (mean ± SD)	Controls (n = 30)	Patients (n = 40)	P.value
Age	42.63±5.27	44.47±5.56	0.85
BMI	30.24±1.96	30.83±2.38	0.18
Duration of disease (year)		5.42±3.43	-

Table (3.2) illustrate the mean± **SD** for each studied parameters which include vitamin D, total cholesterol, trigluceride, HDL , insulin hormone , FPG and Hba1c.

Table 2 : the biochemical parameters in studied groups.

Parameters (mean ± SD)	Control (n=30)	Patients (n=40)	
		Baseline	After 8 weeks
Vit D ng/ml	32.44±4.12a	22.4±5.1 b	26.4± 5.6b
Total Cholesterol mg/dl	166±44a	212±43c	186±37b
Triglyceride mg/dl	123±30a	173±41c	142±21b
HDL mg/dl	47±8.6a	36±6.2b	44±9.3a
Insulin hormone IJU/mL	12.4±7.4a	24.1± 5.9b	23.45±6.3b
FPG mg/dl	87.50 ± 1.62a	181.50 ± 9.37b	172.8±8.68b
Hba1c	5.7±0.6a	8.4±0.7b	8.2±0.6b

Means with different subscript letters refer to significant difference (P<0.05)

There is a significant decrement in the levels of vitamin D in diabetic patients when compare to control group (p<0.001), but there was no significant difference in vitamin D levels after treatment (P>0.05), as shown in table 2.

Total cholesterol significantly elevated in patients group when compare to control (P>0.05), as well as there was a significant difference after treatment.

Table 2 also show that there was a significant difference in HDL levels when compare between patients and control groups (P>0.05), also there was a significant difference when compared in patients before and after treatment.

There were a significant difference in all glycemic status parameters (FPG,serum insulin and Hba1c) in patients when compare to healthy subjects but there was no significant differences were found in serum insulin, FPG and Hba1c before and after treatment (P>0.05), as shown in table 2.

4.Discussion:

The current study confirms that vitamin D levels are low in Iraqi society and this means that living in a sunny country such as Iraq does not necessarily lead to adjustment of vitamin D levels.

In agreement with previous studies (Akio Nakashimam et al., 2016; Alvarez JA, et al. 2010) vitamin D levels were significantly lower in diabetic patients when compared to healthy people. Recent study suggests that there is an inverse relationship between levels of vitamin D and blood glucose level. In other words, high blood glucose levels lead to lower vitamin D concentrations (Mattila Mannisto, 2018).

Low vitamin D levels lead to decrease the secretion of insulin secretion (Bourlon PM, et al., 1999). Other study suggest that the indirect effects of vitamin D on the secretion of insulin may be due to the effect of calcium on the secretion of insulin. vitamin D levels maintain on the calcium level outside the cell depending on the permeability characteristic of cell membrane to cross the calcium ion out of the cell (Teresa Martin,2011) . In fact the role of vitamin D in regulation insulin sensitivity and secretion not clear until now. Diabetic patients after 8 weeks of statin treatment also measured vitamin D levels and found there was no significant change on the levels of vitamin D.

Current study recorded that dyslipidemia associated with T2DM and the levels of lipid profile improve after using atorvastatin. Cholesterol improves cell response to insulin and work to amplify GLUT4 / glucose that regulates secretion of insulin. statin-induced PM effect which accurs in skeletal muscle, a site which responsible for approximately 80% from glucose consume and is considered as a major tissue for insulin resistance (Floriana Elvira Ionică, et al., 2010).

In conclusion. Current study found that the vitamin D deficiency association with T2DM . After 8 weeks from atorvastatin the vitamin D levels slightly increase but not significant.

References:

1. Ahmed Abbas, John Milles and Sudarshan Ramachandran. Rosuvastatin and Atorvastatin: Comparative Effects on Glucose Metabolism in Non-Diabetic Patients with Dyslipidaemia. Clin Med Insights Endocrinol Diabetes. 2012; 5: 13–30.
2. Akio Nakashima, Keitaro Yokoyama, Takashi Yokoo, and Mitsuyoshi Urashima. Role of vitamin D in diabetes mellitus and chronic kidney disease. World J Diabetes. 2016 Mar 10; 7(5): 89–100.
3. Alvarez JA, Ashraf A: Role of vitamin D in insulin secretion and insulin sensitivity for glucose Homeostasis. Int J Endocrinal. 2010, 2010: 351-385.
4. Benjamin M Leon and Thomas M Maddox. Diabetes and cardiovascular disease: Epidemiology, biological mechanisms, treatment recommendations and future research. World J Diabetes. 2015 Oct 10; 6(13): 1246–1258.
5. Bourlon PM, Billaudel B, Faure-Dussert A: Influence of vitamin D3 deficiency and 1,25 dihydroxyvitamin D3 on de novo insulin biosynthesis in the islets of the rat endocrine pancreas. J Endocrinol 1999, 160:87–95 .
6. Daria M. Adamczak. The Role of Toll-Like Receptors and Vitamin D in Cardiovascular Diseases—A Review. Int. J. Mol. Sci. 2017,18,2252.
7. Floriana Elvira Ionică, Cătălina Pisoschi , Simona Negreş4 , Rigas F. Nikos5 , Mihai Tărâţă3 , Florica Popescu. Atorvastatin Influence on Glycemic Control in Patients with Type 2 Diabetes Mellitus. FARMACIA, 2010, Vol. 58, 6: 728-734.
8. Kayama Y, Raaz U, Jagger A, Adam M, Schellinger IN , Sakamoto M, Suzuki H, Toyama K, Spin JM, Tsao PS. Diabetic Cardiovascular Disease Induced by Oxidative Stress. Int J Mol Sci. 2015 Oct 23;16(10):25234-63.
9. Manjunath G. Raju; Ajay Pachika; Sujeeth R. Punnam; Joseph C. Gardiner; Mehdi H. Shishehbo; Samir R. Kapadia; George S. Abela . Statin Therapy in the Reduction of Cardiovascular Events in Patients Undergoing Intermediate-Risk Noncardiac, Nonvascular Surgery. Clin. Cardiol.2013, 36, 8, 456–461.
10. Matthias Wacker and Michael F. Holick· Sunlight and Vitamin D. Dermatoendocrinol. 2013 Jan 1; 5(1): 51–108.
11. Mattila Mannisto . Vitamin D as a common supplement for insulin resistance patients. Med Hypotheses. 2018, 78 (2): 123-128.
12. Rose Gilbertab, Ahmed Al-Janabiab, Oren Tomkins-Netzerab,and Sue Lightmanab. Statins as anti-inflammatory agents: A potential therapeutic role in sight-threatening non-infectious uveitis. Porto Biomedical Journal. Volume 2, Issue 2, March–April 2017, Pages 33-39

13. Teresa Martin. Vitamin D and Diabetes. Diabetes Spectrum 2011 May; 24(2): 113-118.
14. Ulrich Laufs, Hubert Scharnagl, Martin Halle, Eberhard Windler, Matthias Endres, and Winfried März. Treatment Options for Statin-Associated Muscle Symptoms. Dtsch Arztebl Int. 2015 Oct; 112(44): 748–755.

ttp://jgu.garmian.edu.krd https://doi.org/10.24271/garmian.329

Enhance the Activities of Hydrogen Production by Changing the Sequence of Preparation the Ternary Composite Pt -TiO_2/MWNT

Firas H. Abdulrazzak[1*] Falah H. Hussein[2]

[1]Chemistry Department, College of education for pure science, Diyala University, Diyala, Iraq

[2]Chemistry Department, College of Science, Babylon University, Hilla, Iraq

[*] Corresponding author. Email: firas_habeb2000@yahoo.com

Abstract

Two types of ternary Pt-TiO_2/MWNT were synthesized by Sonochemical/Hydration–Dehydration methods which include photoplatinazation and supporting with MWNTs. The synthesized materials (Pt-TiO_2)/MWNT and Pt-(TiO_2/MWNT) were characterized by X-ray diffraction, Raman spectroscopy, UV-Vis diffuse reflectance spectroscopy, scanning electron microscopy and transmission electron microscopy. The activity of (0.65 g/L) MWNT/TiO_2/Ptwere estimated by H_2 production from (7.5 vol %) aqueous methanol solution. The results showed that platinizationof TiO_2 than create hybrid with MWNTs was more efficient in hydrogen production than platinazationofMWNT/ TiO_2.The preparation method, homogenous distribution and localized of MWNTs with Pt onto TiO_2 shows sensitively influence in the achieving the best efficient charge separation and transfer in exist the platinum under UV- light (< 420 nm) irradiation.

Keywords: MWNT, TiO_2; Hydrogen Production; Ternary composite; Sequences of Preparation

1-Introduction:

The use of nanotechnology in the field of energy aims to provide energy with taking care on the source of energy, cost, and environmental risks as well as get the maximum amount of energy which can be obtained. Hydrogen gas is an ideal technology of energy for the future to produce clean and friendly sources without any damages for the environmental [Chiari, &Zecca, 2011]. Hydrogen as sources of energy started with electrolysis of water thus the real orientation towards of sustainable technology for hydrogen production [Hashimoto et al., 2005] was developed for a long time ago. Nanomaterials in pristine or compounds and composites showed positive orientations in this field such semiconductors SC, metals M, and carbon nanotubes CNTs [Chen et al., 2010; Ong et al. 2010]. The binary and ternary composites commonly used for synthesizing catalyst used in hydrogen production reactions. The activities of composites depend on nature of bonding which produces maximum value for active sites. The ternary composites represent the ideal case for produce many active sites such Pt-TiO_2/CNTs. TiO_2 is semiconductors with three phases, Rutile, Anatase and Brookite. The first two phases of TiO_2 are both in a tetragonal structure and the last type in an orthorhombic [Nadtochenko et al., 2006].Carbon nanotubes CNTs is graphite or graphene sheets rolling from side to side to forming a tubular structure with specific properties such chiral, armchair and zig-zag with nanometer in diameter [Falah et al., 2018]. Carbon nanotubes can be classified two single-walled SWNTs, double walled DWNTs, few walled FWNTs and multi-walled carbon nanotubes MWNTs [Falah et al., 2018]. Pt as noble metals with specific physical and chemical behavior which encourage widely used activation and enhance the activities of semiconductors [Shaoet al., 2010; Stefano et al., 2012]. The ternary composites Pt-TiO_2/CNTs were used in many applications such Sensors [Stefano et al., 2012] hydrogen production [Firas et al., 2016] converted agent for CO to CO_2 [Lin et al., 2009] degradation of many pollutants [Shih et al., 2017]. The method of synthesized ternary composite technically influences with of preparations methods and the sequence of adding the three materials which rarely studied. This studies concern with the sequences effect for the out- sito addition of Pt and MWNTs in activates of TiO_2 towards hydrogen production. TiO_2 did not show any activities towards the hydrogen production in alcohol/water solution while existing of CNTs or Pt showed abilities to evolve the H_2 gas [Firas et al., 2016].The results from many literature had shown that exits CNTswith TiO_2 increasethe surface area of TiO_2. The contact between the surface of the TiO_2 particle and CNTs or Pt became one of the most important reasoned to accrue the reaction and increase the rate of reaction. The presence of the CNTs or Pt prevents for the recombination the photoexcited electron [Valentin, 2004]. The effect of Pt with TiO_2 in the reaction of hydrogen production [Ren et al., 2007] was shown more effective than two types of CNTs, which is less activates as compare with Pt-TiO_2/MWNT. The greater synergic effect of Pt -TiO_2/ MWNT can be related to the better charge transfer between TiO_2 and Pt and best distribution for three materials [Yang et al., 2012]. In this studies, two types of Pt-TiO_2/MWNTs were synthesized with changing the sequence of addition which characterized by UV-vis reflectance, X-ray diffraction, Raman spectroscopy, TEM images and BET. Activates were tested by using the hydrogen production reaction form 7.5% of methanol aqueous solution.

2-Experimental

2.1 Materials

Multi-walled carbon nanotubes MWNTs, were purchased from Aldrich, which fabricated by chemical vapor deposition method. Thepurities of MWNTs 95% and mode diameter 5.5nm. The TiO_2 sample was purchased from Degussa, Germany (TiO_2-P25) consist of 20% Rutial and 80% Anatase. The source of Pt was hexachloro platonic (IV) acid hexa hydrate ($H_2PtCl_6.6H_2O$) where purchased from Riedel-De-Haen AG, Seelze, Hannover, Germany. Methanol(A.R quality, 99.9%) was supplied from Hayman, England. The work was done in Institute of Technical Chemistry, Leibniz Universität Hannover\Germany.

2.2**Preparation of Binary and ternary composite**

TiO_2/MWNT were prepared by a simple evaporation methodbased on our previous works[Firas et al., 2016a]. Firstly,100mg of MWNTs was treated with 60 ml of mixture HNO_3/H_2SO_4 (1/3) with the assist of ultra-sonic water bath for 7h [Dirk et al., 2010] then washing and drying at 100°C. The required amount of activated MWNTs was dispersed in 200 ml of distilled water by using ultra-sonic system for 20 min then adding the equivalent amount of TiO_2 powder which produces TiO_2/0.5%MWNT. The suspension was filtered by vacuum evaporator (Rota vapor re121 BUSHI 461 water Bath) at 45 °C, then dried overnight in an oven at 100 °C. TiO_2 was platinized, by photo-depositionmethodwhenmixture of 37% formaldehyde: absolute ethanol (4:1) was added to the aqueous suspension of TiO_2 and an equivalent amount of ($H_2PtCl_6.6H_2O$)[Falah et al., 2016]. The deposition was accrued with UV light irradiated for 3hour at 40°C, using a 200-W mercury lampto produce 0.5%Pt-TiO_2. Two types of ternary composites were prepared: the first (0.5%Pt-TiO_2)/0.5%MWNT, while the second 0.5%Pt-(TiO_2/0.5%MWNT). The first ternary composite (0.5%Pt-TiO_2)/0.5%MWNT was prepared by platinized the TiO_2 then loaded with MWNTs under the same conditions of preparation. The second composite 0.5%Pt-(TiO_2/0.5%MWNT) was prepared by loaded MWNTs than platinized process.

2.2.Hydrogen production

The activity of the composites was evaluated by H_2 production from 70 ml of an aqueous methanol solution (7.5 vol %) with (0.65 g/L) of catalyst which was stirred in a Pyrex-glass reactor (ca. 110 ml volume) equipped with a quartz disc for light penetration. Before to irradiation, Argon gas was purged through the suspension for 30 min. A solar simulator equipped with (SUX 1450) Xenonlampenversorg UNG, Muller, was used as a light source. To avoid thermal effects, the reactor was cooled to room temperature with a cooler system Land Nds. Uni Han. During irradiation, the headspace gas (40 ml) of the reactor was intermittently sampled (0.5 μL) and analyzed for H_2 using a gas chromatograph (Shimadzu GC – 8A) equipped with a thermal conductivity detector and a carboxen 1000 packed column.

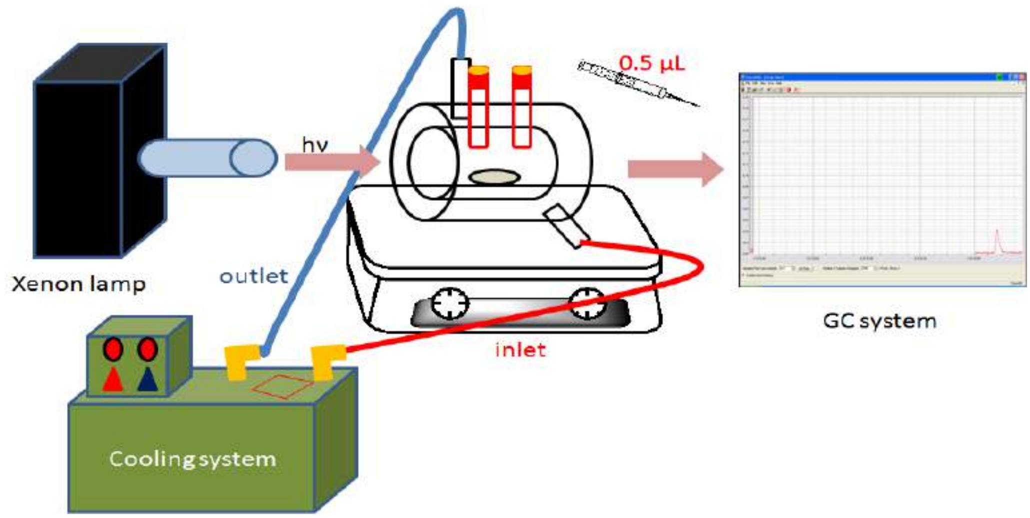

Figure 1. Schematic diagram for the system of hydrogen production

2.3 **Characterization**

UV-Vis diffuse reflectance spectra were recorded over the range of 200–800nm in the absorption mode using a CARY 100 Bio UV-vis spectrophotometer which calibrated with $BaSO_4$. Kubelka–Munk function [Kauffman & Star, 2008] were depend to calculate the band gap energy (E_g) from diffuse reflectance data. The E_g value was determined using the theory of optical absorption for allowed direct transitions: {$h\nu = A\,(h\nu - E_g)^{1/2}$ }where A is the absorption coefficient which relative to the material, (hv) is the discrete photon energy. The linear portion of extrapolating $(FR \times h\nu)^{1/2}$ vs. hν curves to FR = 0 refer to the E_g as reported in Fig. 2. The important consideration for TiO_2 was absorbance occurred at 380 nm, while MWNTs observed broad peaks between 450-1000 nm [Firas, 2016b,c]. In the same time the combined effect of both carbon nanotubes and Pt in the band gap value of TiO_2 will increased[Luma et al., 2014]. Surface area estimation of the TiO_2 has been performed by the Brunauer-Emmett-Teller method, performed on a Micrometrics Automate 23 apparatus. The samples have been previously heated to 125 °C for 30 min to remove possible contaminants and humidity adsorbed on their surfaces. The measurements have been performed using a gas mixture containing 30 % nitrogen and 70 % helium as shown in table 1.

Table 1. Summaries of, surfaces area, particle size and band gap, for pure MWNTs, TiO_2, and modified TiO_2 with Pt and MWNTs.

Samples	BET (m^2/g)	Particle size (nm)	Band gap (e V)
MWNT	282	04.37	0.50
TiO_2	51	23.09	3.18
TiO_2/0.5%MWNT	56	15.41	2.80
0.5%Pt-TiO_2	47	23.13	2.75
(0.5%Pt-TiO_2) /0.5%MWNT	61	18.60	2.60
0.5%Pt-(TiO_2 /0.5%MWNT)	50	25.76	2.80

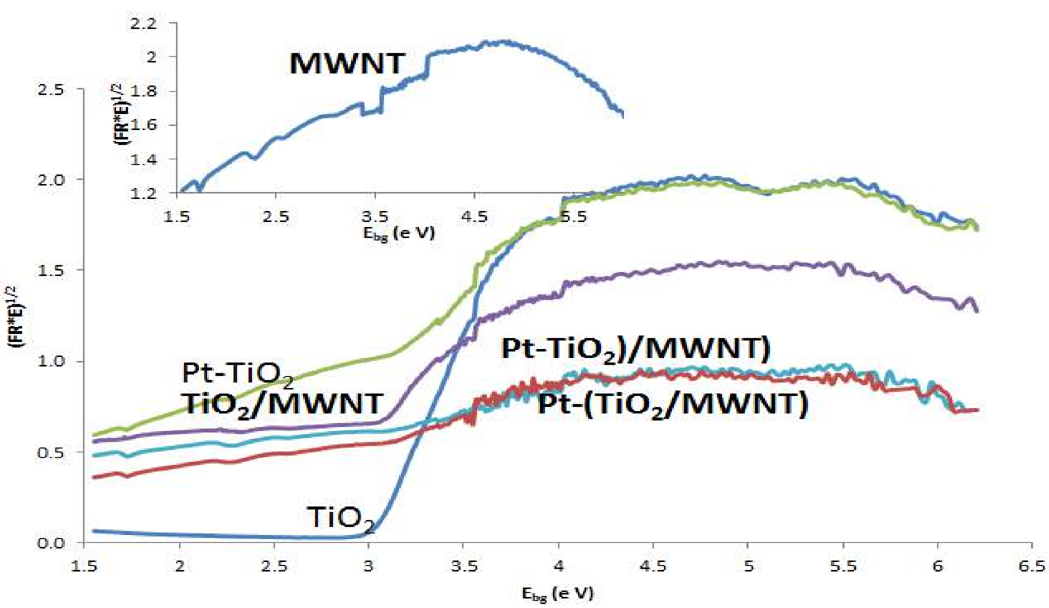

Figure 2. Band gap for pristine and modified TiO2 with MWNTs and Pt in binary and ternary composites.

Table 2. Summaries for activities of binary and ternary composites towards hydrogen productions.

Samples	r (μ mole/h)	Compare r**	k (s^{-1})	R
0.5%Pt-TiO_2	226	TiO_2 0.00	4.42	1
(0.5%Pt-TiO_2)/0.5%MWNT	263	2.17 TiO_2/0.5%MWNT	4.83	1.12
0.5%Pt-(TiO_2/0.5%MWNT)	208		3.94	0.89

The binary and ternary composites were characterized by X-ray diffraction (XRD) on a (RigakuRotalflex) (RU-200B) X-ray diffractometer using Cu Kα radiation at 0.15405 nm) with a Ni filter. The tube current was 100 mA with voltage 40 kV. The

2θ angular regions between 15 and 65° were explored at a scan rate of 5°/min. For all XRD tests, the resolution of the 2θ scans was kept at 0.02°.Fig. 3 shows the XRD patterns of the crystallographic structures of the binary and ternary composites. The influence was limited to the small change in the width of peaks with the shift towards higher 2θ. The 0.5%Pt-TiO_2 , there is only TiO_2 in the anatase form and rutile while no peaks of Pt at $2\theta = 40$ and 48◦ can be notes, maybe can be attributed for low ratios of Pt which used or the homogenous dispersion for Pt on TiO2 [Stefano et al., 2012]. Debye–Scherrer equation ($d = K\lambda / \beta \cos\theta$) [Luma et al., 2014] were depended to determine the average crystallite size (d) which estimation by line broadening measurements. When λ refers to X-ray wavelength which equals to 0.15405 nm, β is the peak width at half maximum height resulting in radians and K mostly equal to 0.9 which related to crystallite shape. The peaks at 25.3° and 27.4° are the characteristic reflection for anatase and rutile, respectively for TiO_2, which did not change in the binary and ternary composite [Stefano et al., 2012]. From Fig. 4, for MWNTs appears two characteristic peaks 2θ=25.9° and 43.2°, from C(100) and C(002) planes of the carbon nanotubes, [Fias et al., 2016a,b].The two peaks for MWNTs disappears in binary and ternary composites because the overlapped for these peaks with the anatase peak of TiO_2 at 25.2° and 43.9∘ [Firas et al., 2016b]. The results show that TiO_2 crystallite size of the binary compound did not significantly affect by Pt [Shao et al., 2010] while with MWNTs there is reduces in size. The ternary composite shows the two properties in crystallite size of Pt and MWNTs with TiO_2. The two types of ternary composites appear variance in particle size which represent less broadening of the XRD peaks found for 0.5%Pt-(TiO_2/0.5%MWNT) compared to (0.5%Pt-TiO_2)/0.5%MWNT. These phenomena make the particle size for pristine and modified TiO2 arranged as the following:Pt-(TiO_2/MWNT)>P25 ≈ P25/Pt > (Pt-TiO_2)/MWNT > TiO_2/MWNT.

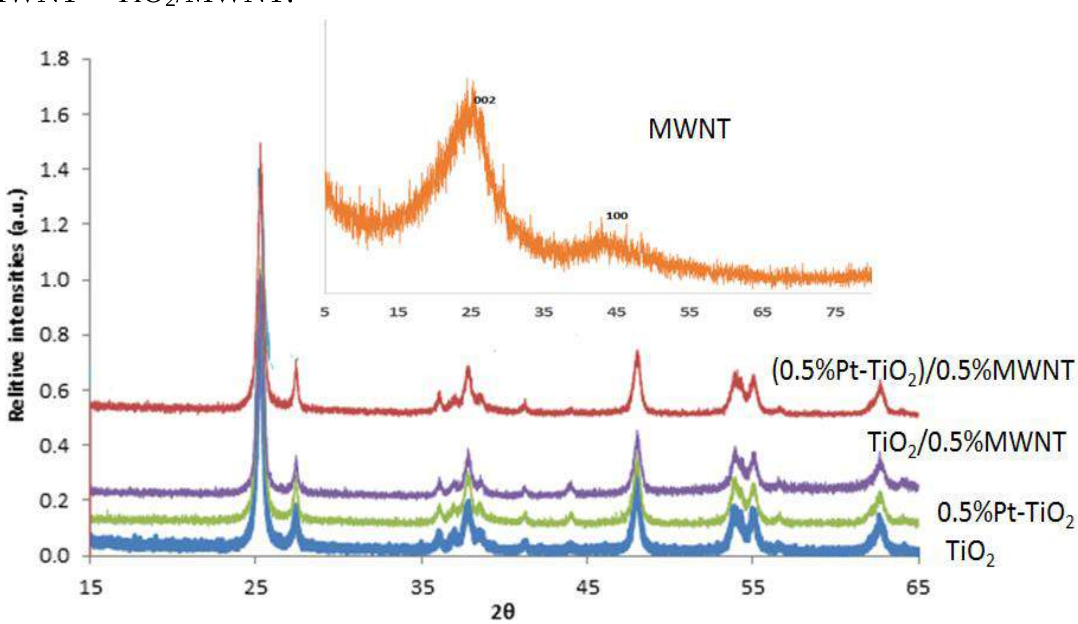

Figure 3. XRD pattern for pristine and modified TiO2 by loading with MWNTs and platinized in binary and ternary composite.

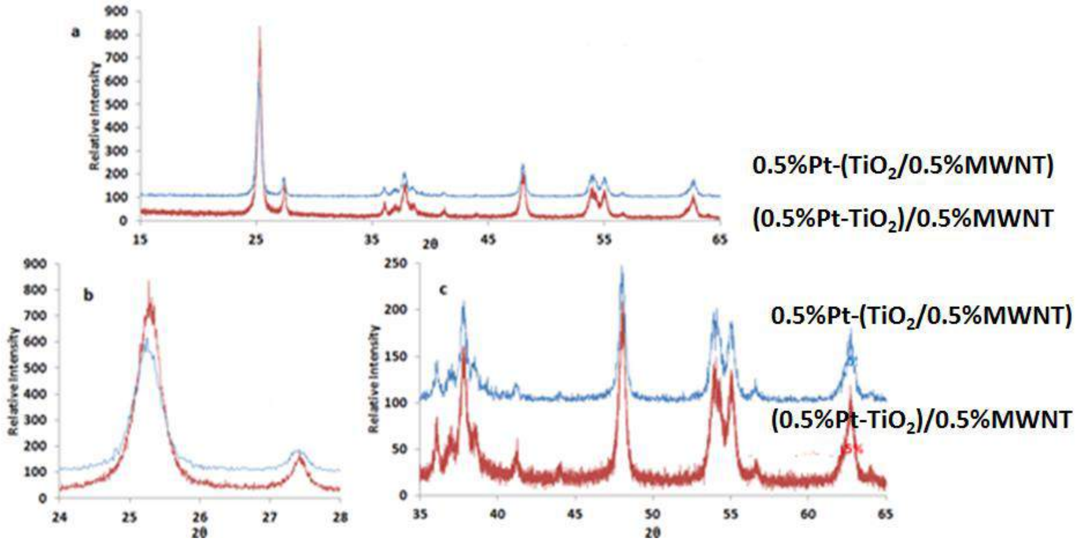

Figure 4. XRD pattern for ternary composite Pt-TiO2/MWNT with different sequence of preparation.

Raman spectroscopy for pure TiO_2 was plotted in Fig. 5, characteristic bands for two phases' anatase and rutile. Anatase modes appears at 150 cm-1 (Eg), 395.1 cm^{-1} (B1g), 512.5 cm^{-1} (A1g + B1g) and 636.7 cm^{-1} (Eg) respectively[Hashimoto et al., 2005 &Firas et al. 2016a]. rutile phase appears at 143, 235 cm-1 which can be ascribed to the B1g, two-phonon scattering, 445 cm^{-1}Eg, and 612 cm^{-1} A_1g, respectively [Zhenhai et al., 2013].The Raman spectra for both binary and ternary composite with MWNTs showed a G band at 1582 cm^{-1} corresponding to the wrapped graphene plane and a D band at 1330 cm-1 for the C-related defects of MWNTs [Falah et al.,2018]. In the case of TiO_2/0.5%MWNT composites, all the Raman bands for anatase and MWNTs remain, except slightly broadened. Table 1 and Fig. 5 shows the peak broadening which is consistent with their decease in the average crystallite size. From the Fig.5, it is seen that Raman spectroscopy for 0.5%Pt-TiO_2, the spectrum shows distortion for TiO_2 between 100-700 cm^{-1} which refer to precipitation Pt on the surfaces of particles TiO_2. The ternary composite shows the two effects for MWNTs and Pt with less distortion for anatase phase before 700 cm^{-1}.

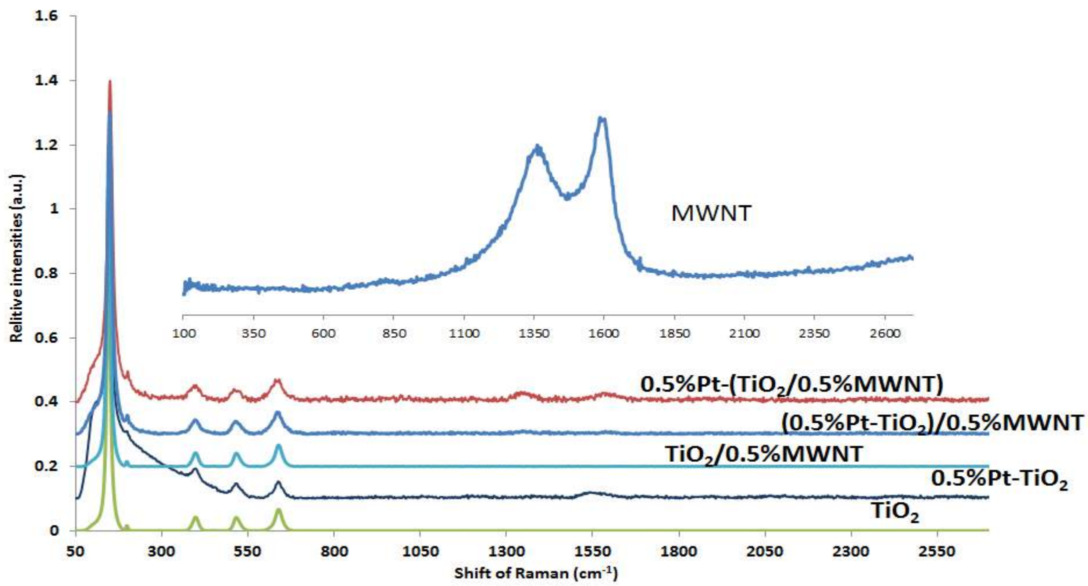

Figure 5. Raman Shift for pristine and modified TiO2 by loading with MWNTs and platinized in binary and ternary composite.

The SEM images in Fig.6(a,b) shows the surface from a TiO_2 agglomerate. The marked area is shown in the micrograph to the right at higher magnification, a single carbon fillement is visible. The Fig.6c shows the TiO_2 particle surface, which were decorated by a lot of small particles (Platinum) with a single carbon nanotube is visible. The interesting imager which shown in Fig. 6d when seen that particles of Pt in the surface of CNTs , and that may reffer to the to increasd the activity of ternary composite as compaer with Pt- TiO_2.

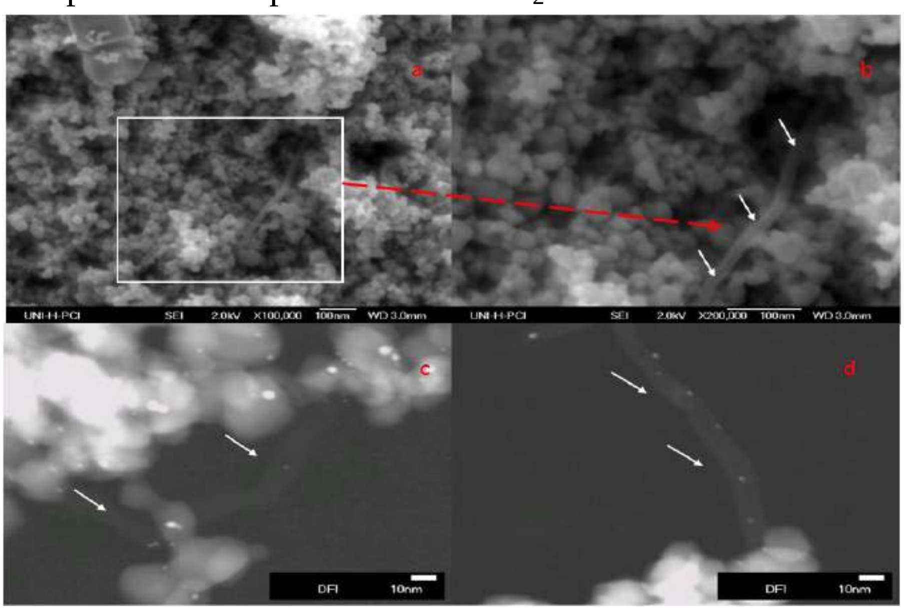

Figure 6. SEM (a,b) and HR-TEM images (c, d) for ternary (Pt-TiO2)/MWNT composites.

3-Results

The activities of synthesized binary and ternary composites were tested in hydrogen production from 7.5 vol % aqueous methanol solution. The catalysts include binary

TiO_2 composites which platinized with 0.5% of Pt or loaded with MWNTs. The last two binary composites were used as control groups against ternary composites. The ternary composites which the aims of this work include two composites with the same ratios and continent but different from each other in the strategy of preparation. The first ternary composite was prepared from platinization of TiO_2 than loaded with MWNTs which is (Pt-TiO_2)/MWNT. The second ternary composite Pt-(TiO_2/MWNT) was loaded with MWNTs than platinized. The brackets refer to the first process of preparations and slash refer to support or impregnated surfaces MWNTs while (-) refer to impregnation Pt onto TiO_2. The results were plotted in Fig.7 and listed in table 1 which shows that pristine TiO_2 without platinization or loading with MWNTs do not show any activity to produce hydrogen under dark or illumination conditions. The results show that effect of Pt towards hydrogen production was larger than MWNTs in binary composites.

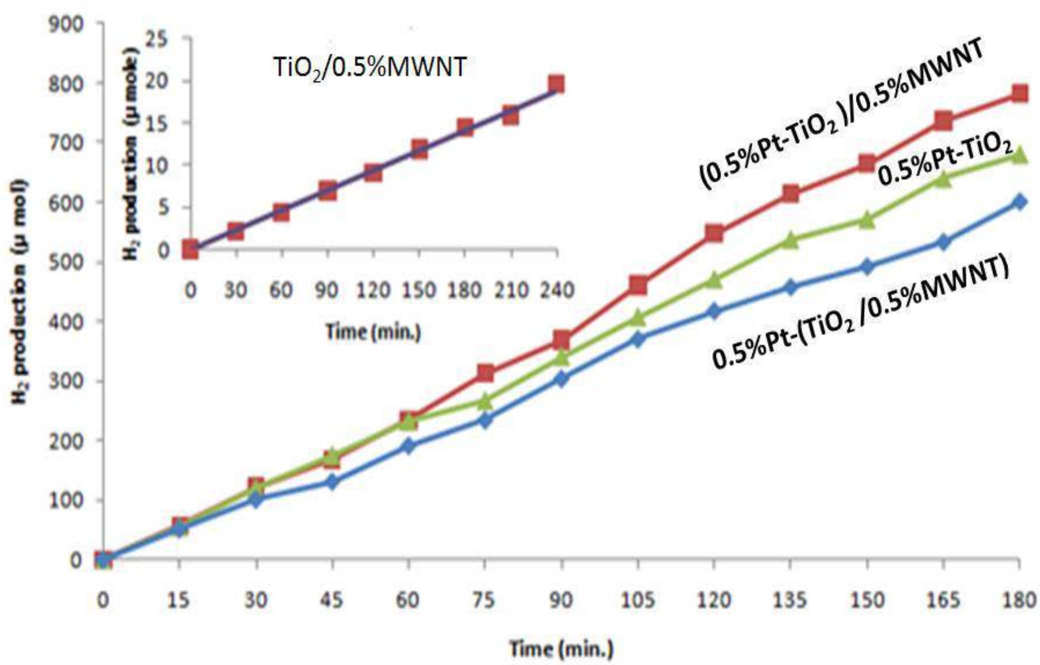

Figure 7. The photocatalytic H_2 production from 7.5vol% methanol aqueous suspended with 65 mg of Pt-TiO_2, TiO_2/MWNT, (Pt-TiO_2)/MWNT and Pt-(TiO_2/MWNT) using 300 W xenon arc lamp as the light source.

Table 2, shows that ternary composite (Pt-TiO_2)/MWNT was succeeded to increase the hydrogen production more than Pt-TiO_2 while Pt-(TiO_2/MWNT) was failed. The evaluations for the results of hydrogen production in two types of ternary composites compare with binary composites, can estimated synergy factor (R). The increase and reduce were calculated by apparent rate constant for Pt-TiO_2/MWNT with Pt-TiO_2 {R = k_{app}Pt-TiO_2/MWNT/ k_{app}Pt-TiO_2}. The R represent the best calculus to valuation effect of loading MWNTs and platinazation towards achievement maximum activities for hydrogen production.

*** These values refer to the rate of hydrogen evaluate for TiO_2/0.5%MWNT which insert with these tables for compare with the same ratios of Pt in Pt-TiO_2 and with Pt-TiO_2 /MWNT.*

4. Discussion The efficiency of Pt-TiO_2/MWNT [Bo et al., 2013] increases with increasing the direct connections between TiO_2 and Pt with interference MWNTs for creating the best transfer of the electrons from TiO_2 to methanol/H_2O mixture. The strong connections between TiO_2/MWNTs occurred when MWNTs penetrated through TiO_2 under the influence of ultrasonic when succeed to break Van Der Waals interaction for MWNTs bundles [Yi et al., 2010]. The results of UV-visible reflectance and XRD refer to change in band gap and particle size which shows variance in size of groups as explain in Figure 8. The activities of Pt- TiO_2 can be related to Pt when removed photoexcited electron from hole because reduce the space charge [18] and forming Schottky barrier for TiO_2 electron in CB to the CB of Pt. the role of MWNT in binary TiO_2/MWNTs was the same action of Pt with less activities which shows in value of product. The different between Pt- TiO_2 and TiO_2/MWNTs were shown in reducing the agglomerations and increase the surface area with MWNTs as compare with Pt as represented in Fig. 8 and table 2.

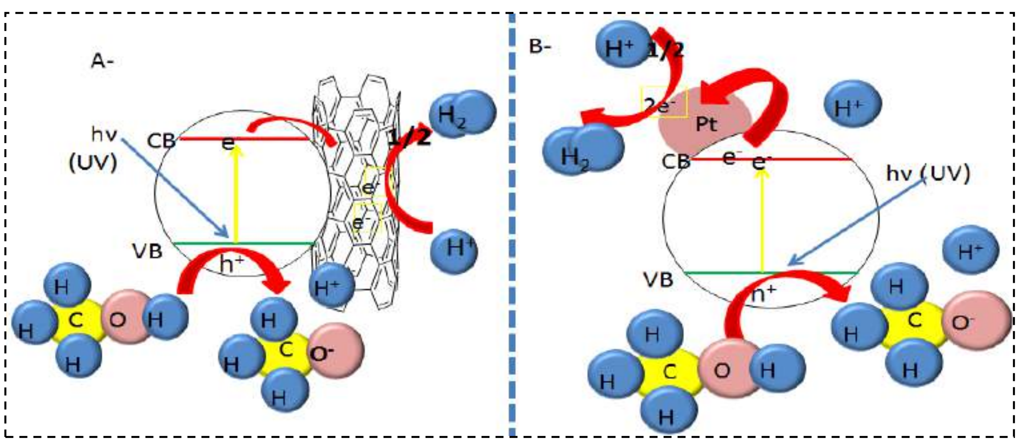

Figure 8.Schematics of synthesized -1, (Pt-TiO2)/MWNT, by platinized than loading by MWNTs -2, Pt-(TiO2/MWNT), by loading with MWNT than platinized.

Fig. 8 refer to the behaviors of ternary composites when accumulations for effect of Pt and MWNTs reduce the surface area SBET for (Pt-TiO_2)/MWNT and increase SBET with Pt-(TiO_2/MWNT). The process of platinization was added many active sites to produce many agglomerations that covered most of the active sites causing reduce the activity. Loading MWNTs within ultra-sonic water bath at least reduce the agglomerations which encourage to shows more active site. All of this change in morphology can be seen in Fig9. When TEM images show redistribution for Pt onto MWNTs and TiO_2 surface under the effect of ultra-sonic [Jimmyet al., 2002].The ternary composite as mentions before shows variance on activities for evaluating hydrogen gas, which appears as a result of appearing or disappears the active site which responsible for activities.

4.1 Mechanism of the reaction

The mechanism depends on transfer of the electrons from TiO_2 to MWNTs as mentions in many works of literature [Rowan & Aidan, 2009] and represents in Fig.9A. When TiO_2 was attached to the surface of MWNTs, the active site of the binary matrix within existing of UV lights, mostly stimulates the transfer of excited electrons from the surface of TiO_2 to the network of MWNTs [Baoet al., 2012] which become a source to convert H^+ to H_2. The effect of Pt was more activities for withdrawn the excited electron as compare with MWNTs as represented in Fig.9B.

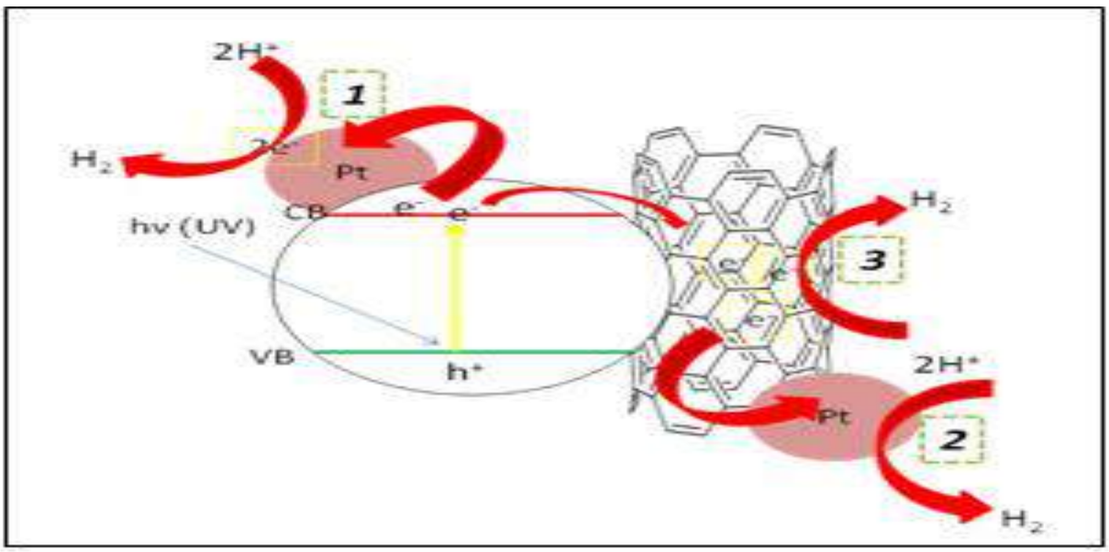

Figure 9.Sckematic diagram for proposal mechanism of A- TiO2/MWNT, and B- Pt-TiO2.

The mechanism depends on transfer of the electrons from TiO_2 to MWNTs as mentions in many works of literature [Rowan & Aidan, 2009]. When TiO_2 was attached to the surface of MWNTs, the active site of the binary matrix removed the exited electrons which forming H_2 gas. In the cases of Pt- TiO_2/MWNT, under the irradiation the electrons were excited to the conduction band CB from valence band VB of TiO_2. The Pt- TiO_2/MWNT, raises two routes for electrons to transfer, the first is from the conduction band of TiO_2 to Pt, and the second is to transfer the electrons to MWNTs. The second routs appear two probabilities, one of them include indirect ways for transfer the electron to Pt which adsorbed on the surfaces of MWNTs. The ether which represents direct ways from the surfaces of MWNTs to H^+ and all of this state causing evaluate the hydrogen gas as shown in Fig. 10. The efficiency of Pt-TiO_2/MWNT may relate to the Pt particles on TiO_2 aggregates were isolated the electrons transport which limited in activity by the insufficient local electronic conductivity of TiO_2 [Lin et al., 2009].The UV lights, mostly stimulates transfer of excited electrons from the surface of TiO_2 to the network of MWNTs [Baoet al., 2012] which become a source to convert H^+ to H_2as shown in Fig.10.

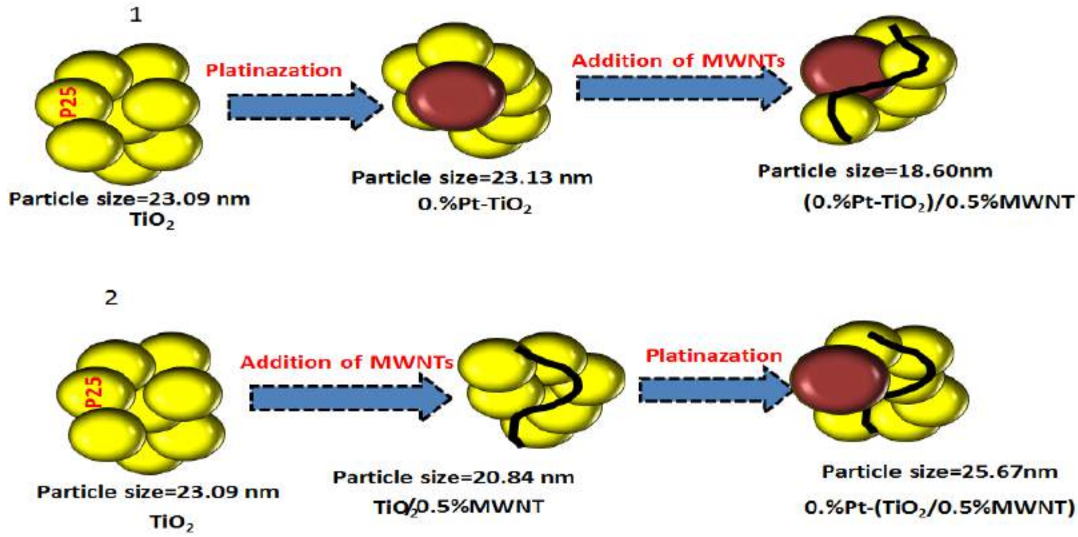

Figure 10. Schematic diagram for the mechanism of ternary composite Pt-TiO2/MWNT.

Conclusion

The binary and ternary composite was successfully synthesized by using simple evaporations methods and platinazation to forming Pt- TiO_2, TiO_2/MWNT and Pt-TiO_2/MWNT. The ability of Pt to evaluate hydrogen in binary composite was more active than MWNTs although, reduce the activities of Pt- (TiO_2/MWNT) when platinazation were done after loading with MWNTs.Ternary composite Pt- (Pt-TiO_2)/MWNT showed the best abilities to increase the activities due todouble effectof MWNTs when reduces the agglomeration, and make with Pt as a bridge to move the electrons from TiO_2freely. Thus chose the best ways for preparations toachieve the ideal transfer of electron can produce the best activities for hydrogen production.

Acknowledgements:

Detlef W. Bahnemann and I. Ivanova acknowledge financialsupport from the BMBF (BundesministeriumfürBildung undForschung), research projectDuaSol (03SF0482C).

References:

Bao Y. X., Shujiang D., Hao B. W., Xin W. &Xiong W. D.(2012). Hierarchically structured Pt/CNT@TiO_2nanocatalysts with ultrahigh stability for low-temperature fuel cells, *RSC Advances*, 2,792–796.

Bo C., Tianyou P., Xiaohu Z., Jing M., Kan L. & Xungao Z.(2013).Synthesis of C60-decorated SWCNTs (C60-d-CNTs) and its TiO2-based nanocomposite with enhanced photocatalytic activity for hydrogen production", Dalton Transactions, 42(10), 3402-3409.

Chen X., Shen S., Guo L., & Samuel S. M. (2010). Semiconductor-based Photocatalytic Hydrogen Generation.*Chemical Reviews*, 110 (11), 6503–6570.

Chiari, L. &Zecca A. (2011). A. Constraints of fossil fuels depletion on global warming projections. Energy Policy, 39(9), 5026–5034.

Dirk M. Guldi& Martín N.(2010). Carbon Nanotubes and Related Structures Synthesis, Characterization, Functionalization, and Applications. WILEY-VCH Verlag GmbH & Co. KGaA, Weinheim. Kauffman D. R. & Star A.(2008).Carbon nanotube gas and vapor sensors. AngewandteChemie International Edition, 47,6550-6570.

Falah H. Hussein, Firas H. Abdulrazzak, and Ayad F. Alkaim, (2018). Nanomaterials: Biomedical and Environmental Applications, chapter 1: Nanomaterials: Synthesis and Characterization,1 ed. Welly .

Firas H. Abdulrazzak , Falah H. Hussein , Ayad F. Alkaim , Irina Ivanova , Alexei V. Emeline & Detlef W. Bahnemann. (2016a) Sonochemical /hydration–dehydration synthesis of Pt–TiO_2 NPs/decorated carbon nanotubes with enhanced photocatalytic hydrogen production activity. Photochemical &PhotobiologicalSciences., 15(11),1347-1357.

Firas H. Abdulrazzak(2016b). Enhance photocatalytic Activity of TiO2 by Carbon Nanotubes. International Journal of ChemTech Research., 9(3) 431-443.

Firas H. Abdulrazzak, Shahad K Esmail, Halimah A. Dawod, Ahmed M. Abbas & Mustafa K. K. Almaliki. (2016c).X-ray Analysis for Purification Process of Synthesized Multi-Walled Carbon Nanotubes by Chemical Vapor Deposition. International Journal of Theoretical & Applied Sciences, 8(1), 432016-432037 .

Hashimoto K., Irie H., &Fujishima A, (2005). TiO_2photocatalysis: a historical overview and future prospects. *Japanese Journal of Applied Physics* , 44(12),8269–8285.

Jimmy C. Yu, Jiaguo Y., Lizhi Z. &Wingkei H.(2002).Enhancing effects of water content and ultrasonic irradiation on the photocatalytic activity of nano-sized TiO2 powders. Journal of Photochemistry and Photobiology. A: Chemistry, 148,263–271.

Lin K.N., Liou W.J., Yang T.Y., Lin H.M., Lin C.K., Chien S.H., Chen W.C.& Wu S.H.(2009). Synthesis of hybrid Pt/TiO2 (anatase)/MWNTs nanomaterials by a combined sol–gel and polyol process. Diamond and Related Materials . 18,312–315.

Luma M. Ahmed, Irina I., Falah H. Hussein, &Detlef W. Bahnemann. (2014). Role of Platinum Deposited on TiO2 in Photocatalytic Methanol Oxidation and Dehydrogenation Reactions. International Journal of Photoenergy.(3):1-9.

Nadtochenko V., Denisov N., Sarjusiv O., Gumy D., Pulgarin C. & Kiwi J.(2006). Laser kinetic spectroscopy of the interfacial charge transfer between membrane cell walls of E. coli and TiO2. *Journal of Photochemistry and Photobiology A: Chemistry*, 181,401–408.

Ong Y. T., Ahmad A.L., Hussein S. Z. & Soon H. T. (2010). A review on carbon nanotubes in an environmental protection and green engineering perspective. *Brazilian Journal of Chemical Engineering*

Ren W. J., Ai Z. H., Jia F. L., Zhang L. Z., Fan X. X. & Zou Z. G. .(2007).Low temperature preparation and visible light photocatalytic activity of mesoporous carbon-doped crystalline TiO2. Applied Catalysis

Rowan L.& Aidan W.(2009). Carbonaceous nanomaterials for the enhancement of TiO2 Photocatalysis. Diamond and Related Materials

Shao F. C., Jian P. L., Kun Q., Wei P. X., Yang L., Wei X. H. & Shu H. Y. (2010). Large Scale Photochemical Synthesis of M@TiO_2 Nanocomposites (M = Ag, Pd, Au, Pt) and Their Optical Properties, CO Oxidation Performance, and Antibacterial Effect. *Nano Res*earch, 3(4),244–255.

Shih-Y. L., Ya-Chu Y., Sheng-Hsin H., & Jon-Yiew G.(2017). Synthesis of Pt@TiO_2@CNTs Hierarchical Structure Catalyst by Atomic Layer Deposition and Their Photocatalytic and Photoelectrochemical Activity",*Nanomat*. (Basel). 7(5)97-112.

Stefano T., Andrea D., Mariangela L., Nicola D., Salvatore G. L. & Giovanni N. (2012). Pt-TiO_2/MWNTs Hybrid Composites for Monitoring Low Hydrogen Concentrations in Air, *Sensors*, 12(9), 12361-12373.

Valentin N. P.(2004). Carbon nanotubes: properties and application. Materials Science and Engineering. R, 43, 61–102.

Yang Z, Du G., Meng Q., Guo Z., Yu X., Chen Z., Guo T. & Zeng R.(2012). Synthesis of uniform TiO2@carbon composite nanofibers as anode for lithium ion batteries with enhanced electrochemical performance. Journal of Materials Chemistry. 22(12), 5848–54.

Yi-Jun X., Yangbin Z. &Xianzhi F.(2010). New insight for enhanced photocatalytic activity of TiO2 by doping carbon nanotubes: A case study on degradation of Benzene and Methyl Orange", The Journal of Physical Chemistry. C , 114, 2669–2676.

Zhenhai W., Suqin C., Shun M., Shumao C., Ganhua L., Kehan Y., Shenglian L.& Zhen H., Junhong C.(2013).TiO2 nanoparticles-decorated carbon nanotubes for significantly improved bioelectricity generation in microbial fuel cells", Journal of Power Sources. 234, 100-106.

ttp://jgu.garmian.edu.krd https://doi.org/10.24271/garmian.330

Photostabilization of Polystyrene Films by Chromium complex

Burak.Kadhim[1*] Ahamed Ahamed[2] Amir Fadhil Dawood[1] Karim H. Hassan[1]

[1]Department of Chemistry, College of Science, University of Diyala, Baquba, Diyala, Iraq.
[2]Department of Chemistry, College of Science, University of Mustansiriyah, Bagdad, Iraq.

Abstract

The photo sensitized degradation of polymer system is occasionally used as a means of solving the problem of environmental pollution, photostabilization of polystyrene films using chrom complexes was investigated. Poly styrene films with a thickness of 80µm and contains complexes concentration of 0.05% wt were produced by the casting method with chloroform being the solvent The photostabilization activities of these complexes were determined by monitoring changes in carbonyl,(I_{CO}) and hydroxyl,(I_{OH}) indices and calculating the photodecomposition rate constant (k_d), the average molecular weight for the studied films The results obtained showed that the photostabilization activity of polystyrene film in the presence of the complexes as additive follows the trends:

$Cr\,[S2CN(C_2H_5)_2]_3 < Cr[C_6H_4NO_2]_3 < PS < Cr(acac)_3$

Keywords: Photostabilization ; Polystyrene; Chromium complexs; Environment.

1. Introduction

Many polymeric materials exposure to ultraviolet (UV) radiation cause a significant degradation as it causes photooxidative degradation which results in breaking of the polymer chains, produces free radical and reduces the molecular weight, causing deterioration of mechanical properties and leading to useless materials, after an unpredictable time

Polystyrene (PS) which is one of the most important material in the modern plastic industry, has been used all over the world, due to its excellent physical properties and low-cost. When polystyrene is subjected to UV irradiation in the presence of air, it undergoes a rapid yellowing and a gradual embrittlement. The mechanism of PS photolysis in the solid state (film) depends on the mobility of free radicals in the polymer matrix and their bimolecular recombination.

The UV-photodegradation of PS films has been studied using fluorescence spectroscopy, excitation and dispersed fluorescence spectra were also collected to monitor the chemical changes in the films. These fluorescence gave direct evidence that degradation products indicated to conjugated double bond along the polystyrene backbone named polyene structures-(C(C6H5)=CH)n. Polyene structure is responsible for color change of PS under UV-exposure].

It is well known that the photo sensitized degradation of polymer system is occasionally used as a means of solving the problem of environmental pollution by plastic litter. The attempts to develop plastics with reduced outdoor stability are based on the syntheses of polymers with light–sensitive groups such as aliphatic ketone groups located predominantly in the main chain or independent (side) groups (Emad Yousif and Raghad Haddad,2013 ; Khalid E. Al Ani and,2015) and also the modification of polymers by the addition of another polymer (H.Omicihi,M.Hagiwara and K.Araki,1979;H.Omicihi,M.Hagiwara,1981) to do so in addition of using or application of photosensitizes which are added to the polymers or the plastic to photosensitize them against degradation process (AL-Niaimi, A. F. D el at ,2018).

A number of research papers have appeared in literature dealing with the photosensitized degradation of polymers by addition of transition–metals salts and complexes (J.F.Rabek .1994; Hameed. K. ALI and Abdulhameed. H. SHUKKUR ,2014). Preliminary it is found that the photodegradation of the polystyrene film was affected by the type of metal, concentration of the complex in addition to the kind of ligand and film thickness (Hameed. K. ALI and Abdulhameed. H. SHUKKUR ,2014; A.F. Dawood.AL-Niaimi2006). It was reported also that the photo-stability of PS was reduced by the addition of bromine containing flame retardant, and appeared to depend upon the chemical structure of the polymeric additives (A.F. Dawood.AL-Niaimi,2002). For PS containing carbonyl group, it was found that the photodegradation increased with increasing in irradiation time. The changes in the average molecular weight in photooxidized PS were produced as consequences of chain dissociation by Norrish Type II reaction

2. Materials and methods

2.1 A Materials used

The organic chemicals used are Polystyrene, Petroleum ether, Picolinic acide, ethanol, Benzene, Urea, sodium diethyl dithiocarbamat whereas the inorganic one are chromium chloride,$CrCl_3$.6H2O.All these starting materials as well solvents were purchased commercially and used without any further purification except the polystyrene which was re-precipitated from chloroform solution with alcohol several times and finally dried under vacuum at room temperature for 24 hours.

2.2 B Instruments used

Accelerated weathering Q.U.V tester (Q-panal company,USA), was used for irradiation of polystyrene films at light intensity flux of 1.8 x 10^{-8} Einstein dm^{-3} sec^{-1} determined by potassium ferri-oxalate actinometrical technique(G.Ganqlize and S.Hubiq ,1989). Infrared spectrophotometer 4200-JASCO was used for monitoring the growth of carbonyl and hydroxyl groups at (1730, 3440 cm^{-1}) respectively whereas the ultraviolet–visible spectrophotometer type V-650-JACSO was used to measure the changes in the UV-visible spectrum during irradiation at a wavelength of maximum absorption (λ_{max}). Film thickness was measured by a micrometer type 2610 a, Germany.

2.3 C Synthesis of complexes

1- Triple (Estelle Asito Neto) Chrome $Cr(C_5H_7O_2)_3$;This complex is attended by the way the world is used (Fernelius and blanch) by adding 2.66 g (0.01) of chromium chloride crystallized to (100) ml of distilled water and after dissolving, add (20) grams of urea. 6 g (0.06) Mol of acetyl acetone covers the reaction blend in an hour bottle and heated on a steam bath for 12 hours. When urea is dissolved, ammonia is released. Dark red crystals (deep maroom), which are filtered and dried with air at room temperature, then dissolve the dried raw compound in (20) gasoline is hot and added (75) ml of hot pure ether slowly and cools to laboratory temperature, and takes its spectrumI R and UV (Buraq Nadhim Kadhim,2018) .

2- Triple (Diethyl Thiayo carbamtu) chromium **$Cr[S_2\,CN(C_2H_5)_2]_3$** :This complexity is prepared by the way suggested by Whitre &co. Workers by mixing of a water solution for (1, 35 mg) (0.005) mol of hexagonal chromium chloride with a water solution of ligand salt Na [S_2CN (C_2H_5) $_2$] (2.57 mg) (0.015) mol with stirring, which consists of a direct deposition of a color (bluish violet) washed with distilled water and dried under pressure and the temperature of the laboratory. The IR and UV spectra are given in the appendix and have a complex melting point (243 °c). (Buraq Nadhim Kadhim,2018).

3- Tri(piclinate) chromium **$Cr[C_6H_4NO_2]_3$** :This complexity is attended by following the method suggested by RAY&co.workers by dissolving (1.8 mg) (0.005) Mole of Cr (acac) $_3$ in 60 ml of ethanol the range is mixed with a(0.62 mg) (0.005) Mole of pycloonic acid in 25 ml of the same solvent where the color crystals are separated (Maronite). Collect and wash and ethanol Dry and I'm in a dry place. It took a spectrum of IR and UV and a complex melting point (216 c^o). (Buraq Nadhim Kadhim,2018)

2.4 D Film preparation

Polystyrene and metal complexes were dissolved in $CHCI_3$ to form polystyrene films which contain 0.05 % wt of additive and have (80µm) thickness. The films were prepared by evaporation technique at room temperature for 24 hours in order to remove the possible residual may present.

2.3 E Irradiation experiments

The films were located (6cm) a part from the UV lamps sources [four fluorescent lamps with 40 watt power)] .These lamps are of the type UV-B 313, giving a spectrum range between 290-360 nm with a maximum being at wavelength 313 nm. The irradiated samples were rotated from time to time to ensure that the intensity of light incident on all samples was the same.

2.4 F Spectrophotometric measurements

For Infrared spectrophotometer and in order to eliminate the effect of sample thickness we adopted the band indexing method (D.Cmellar ,A.B.Mair and G.S.Scott,1973) .A band index, I_s is defined as $I_s = A_s / A_r$,where A_s is the absorbance of the studied band and A_r , the absorbance of the reference band at 1450 cm^{-1} which is the bending mode of –CH- group in polystyrene(Buraq Nadhim Kadhim,2018) .Actual absorbance ,the difference between the absorbance of top peak and the base line one ($A_{Top\ peak}$-$A_{Base\ line}$), is calculated using the base line method (A.F. Dawood.AL-Niaimi,1999). The ultraviolet–visible spectrum was measured during irradiation time for each compound at a wavelength of maximum absorption band (λ_{max}) for calculating the rate photodecomposition constant (k_d).

2.5 G Measuring the photodegradation rate of polymer films using Ultraviolet-visible spectrophotometer

Ultraviolet-visible spectrophotometry technique (Esraa Ismeal Al-Kjateb et .al,2016) was used to measure the changes in the UV-Visible spectrum during different irradiation times for a polymer film at a wavelength (λ_{max}=200-400 nm).The photodegradation rate constant for the Photostabilizer (k_d) was calculated using the first order kinetic equation:

$\ln(a-x) = \ln a - k_d t$ .... (1)

where:

a is the additive concentration before irradiation, x is the additive concentration after irradiation time t which is in second.

If A_o represents the absorption intensity of the polymer film containing additive before irradiation, A_∞ is the intensity at infinite irradiation time and A_t is the absorption intensity after irradiation time t, then :

$a = A_o - A_\infty$ and $x = A_o - A_t$

$a - x = A_o - A_\infty - A_o + A_t = A_t - A_\infty$ .... (2)

Substitution of (a) and (a-x) from equation (2) to equation (1) gives:

$\ln(A_t - A_\infty) = \ln(A_o - A_t) - k_d t$ .... (3)

Thus the plot of $\ln(A_t - A_\infty)$ versus irradiation time (t) gives straight line with a slope equal to (k_d). This indicates that the photodecomposition of the polymer is of first order.

3. Results and discussion

The chrom complexes were used as additive for photostabilization of polystyrene films. During UV irradiation polystyrene films intensity of absorption spectrum increased ,the initial rates of increase in absorbance are relatively rapid at the begining ,however they gradually decline as the film becomes insoluble (crosslinked) and being slightly yellow in colored (due to formation of diene and triene structures) (J.F.Rabek, 1986; A.F. Dawood.AL-Niaimi,1999).The irradiation of polystyrene films led to change in the infrared spectra ,the growth in absorption bands at 3440 and 1730 cm^{-1} which are belong to hydroxyl and carbonyl groups respectively (A.F. Dawood.AL-Niaimi,2006),from these absorptions ,the carbonyl index(I_{CO}) and hydroxyl index (I_{OH}) were calculated with irradiation time. The effectiveness of these complexes on the rate of photodegradation of polystyrene films was monitored by following the (I_{CO}) and (I_{OH}) with irradiation time. In figures 2,3 and 4 ,the (I_{CO}) and (I_{OH}) of complexes shows a lower growth with irradiation time with respect to polystyrene control film without additives. Since the growth of carbonyl and hydroxyl indexes with irradiation time are lower than that of the control ,it is safe to conclude that these additives might be considered as photostabilizers of the polymer. An efficient photostabilizer shows a longer induction period .Therefore ,the Cr $[S2CN(C_2H_5)_2]_3$is the most active photostabilizer ,followed by $Cr[C_6H_4NO_2]_3$, PS and finally the $Cr(acac)_3$which seem to be the least active one.

The change of ln $(A_t- A_\infty)$ versus irradiation time, t for Cr $[S2CN(C_2H_5)_2]_3$ additive in polymer as example is a straight line and is shown in (fig 2). This indicates that the rate is first order for the decomposition of polymer, the slope is equal to the value $(-k_d)$ .The values of the all first order constants of all additives used calculated by the same way are shown in table 1.

The photostabilizers always possess low k_d values ,which mean that theses modified polymer films are stable towards UV light more than polystyrene without additive. Absorption in polystyrene film at 241 ,260 and 305nm have been attributed to acetophenone ,dicarbonyl structures and benzal acetophenone respectively (H.C.Beachell and L.H.Smiley,1967).

Of the results obtained, the efficiency of the organic compounds used as polystyrene stabilizers except Cr $(acac)_3$ acts as a photocatalyst that can be arranged according to the change in the decomposition calculation, the molecular weight ratio(fig 5), Chain cutting(fig 6), decomposition grade(fig 7), polymerization grade(fig 2)., inverse polymerization grade and quantum product for chain cutting as described in all previous forms.

Conclusion

Some of the additives used in this work have behaved successfully as photostabilizers for polystyrene chips

It is found that carbonyl and hydroxyl, $\mathbf{I_{CO},I_{OH}}$ at a thickness film of 80µm , additive concentration , 0.05% wt % increased with time exposed to radiation and this rate of dissociation depends on type of additives used where $Cr(acac)_3$ seem to be initiator while the other seem to be a photo stabilizer and follow :

$Cr\,[S_2CN(C_2H_5)_2]_3 < Cr[(C_6H_4)No_2]_3 < PS < Cr(acac)_3$

Finally degree of polymerization, degree of dissociation, quantum yield value for cutting of polymer chain investigation indicated that all additives behaves as photo stabilizer except $Cr(acac)_3$ which show otherwise and act as a photo initiator.

References

-Yousif, E., & Haddad, R. (2013). Photodegradation and photostabilization of polymers, especially polystyrene. *SpringerPlus*, *2*(1), 398.
-Al Ani, K. E., & Ramadhan, A. E. (2015). Kinetic Study of the Effect of Plasticization on Photodegradation of Polystyrene Solid Films. *Materials Sciences and Applications*, *6*(07), 617.
-H.Omicihi,M.Hagiwara and K.Araki , *Materials Sciences and Applications,180,1923, 1979.*

-H.Omicihi,M.Hagiwara , Polym.Photochem, *15,1981*
-AL-Niaimi, A. F. D., Ahmed, A., & Aliwy, S. B. (2018).Photodegradation Of Poly (Vinyl Chloride) Films With Some Cobalt (111) Complexes And Schiff Bases As Additives. International Journal Of Research In Pharmacy And Chemistry
-Hameed. K. ALI and Abdulhameed. H. SHUKKUR (2014), International Journal of Applied and Natural Science , 3, 3,123-134.

J.F.Rabek,polymer photodegradation Mechanisms and experimental methods Stockholm ,1994.

A.F. Dawood.AL-Niaimi ,Diyala Journal for Applied Researches , 2, 2, 2006

A.F. Dawood.AL-Niaimi, Journal of Diyala , 12, 2002.

G.Ganqlize and S.Hubiq, Chemical Actinometry ," *pure and Appl. Chem .1989, 6, 187.*

Buraq Nadhim Kadhim, (2018). photodegradation of polystyrene doped with some organometallic compounds, Master in Chemistry.

D.Cmellar ,A.B.Mair and G.S.Scott .Eur.Polym.J.1973.9,219.
Esraa Ismeal Al-Kjateb,Ahmed Ahmed and Khaiaf F Alsamarrai,2016,''Pharmaceutical Compounds as Photostabilizers'',Journal of Al-Nahrain University,Vol.19(3),September,34-38.
A.F. Dawood.AL-Niaimi.(1999).Ph.D. Thesis, University of Mustansiria, College of Science.

J.F.Rabek and J.Sanertra ,Macromolecules ,1986.19.167.

H.C.Beachell and L.H.Smiley, J ournal Polym.Sci, 1967,5,1633.

Appendices

Table 1: photodecomposition rate constant (k_d) of polystyrene films of (80µm) thickness and containing 0.05 %wt additives.

K_d (h^{-1})	Film used
0.0031	Polystyrene+**Cr(acac)$_3$**
0.0024	Polystyren +Cr[C_6H_4)NO_2] $_3$
0.0002	Polystyrene+**Cr[$S_2CN(C_2H_4)_2]_3$**
0.0026	Polystyrene

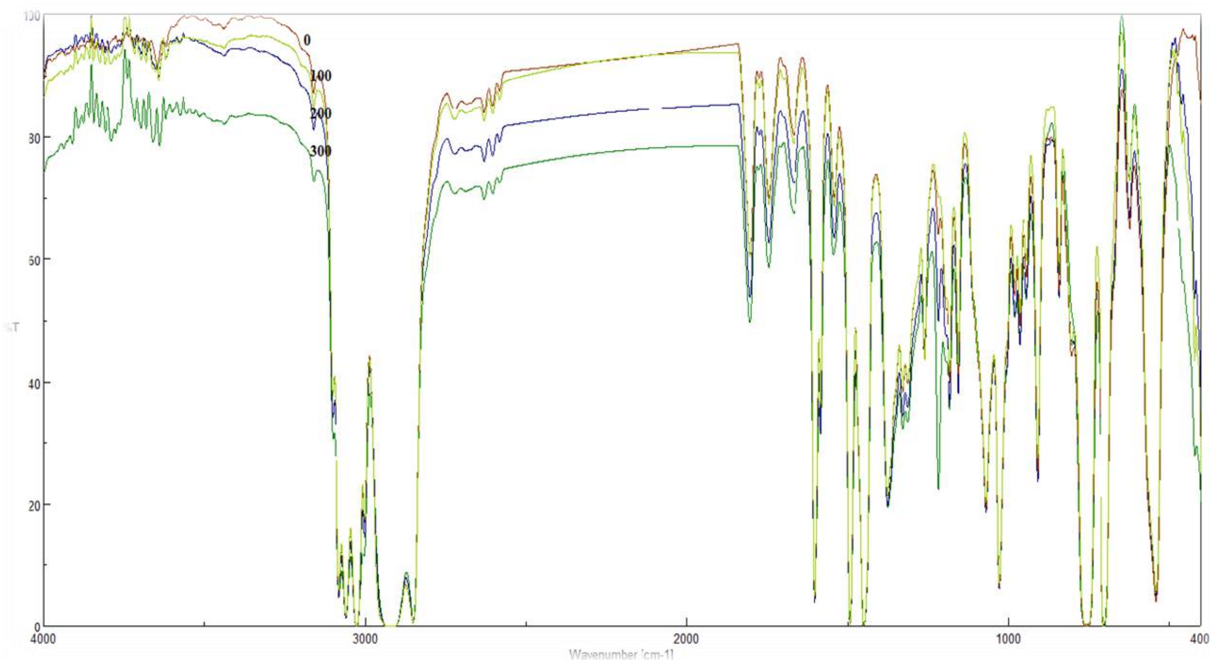

Figure 1:The IR of polystyrene chips with athicness of 80 µn before irradiation and after 300 hours.

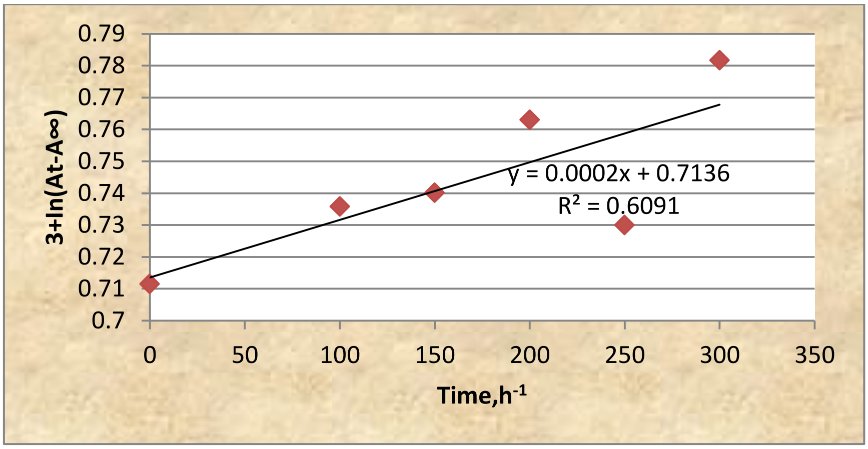

Figure2: Variation $\ln(A_t - A_\infty)$ with time for polystyrene films of (80µm) thickness and containing 0.05% wt of Cr $[S2CN(C_2H_5)_2]_3$as additive.

Figure 3: Change of carbonyl index with irradiation time for polystyrene films, 80 µm thickness and containing 0.05% wt of additives.

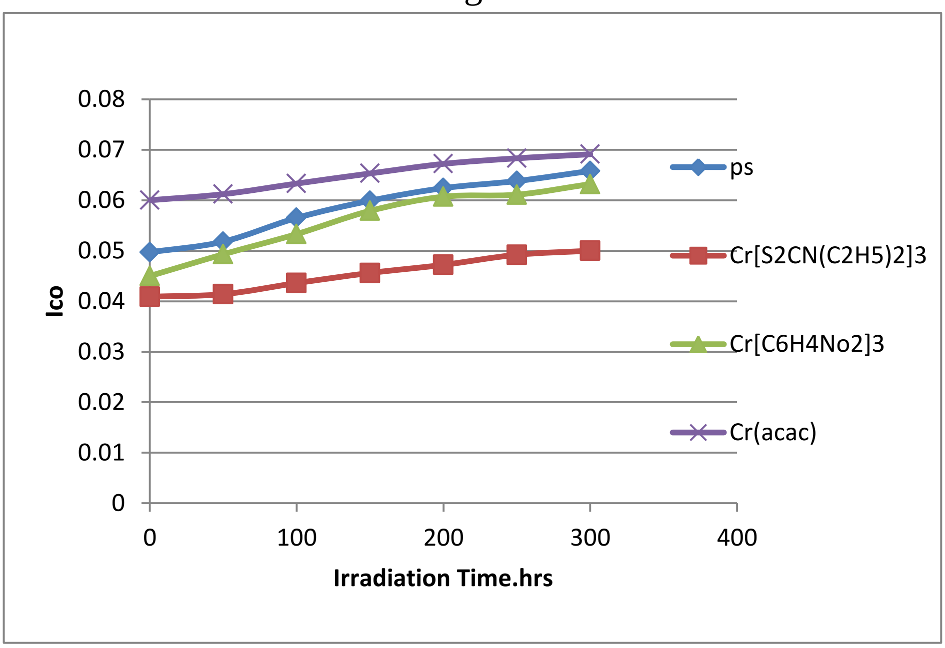

Figure 4: The relationship between the hydroxyl index and irradiation time for polystyrene films of 80 μm thickness and those containing additives with a concentration of 0.05% wt.

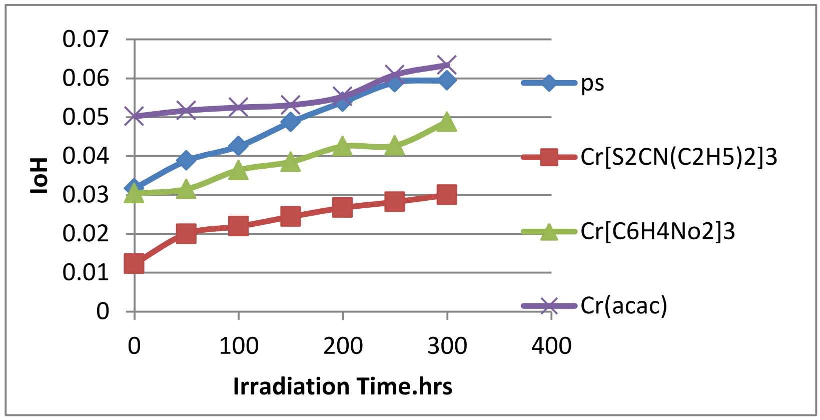

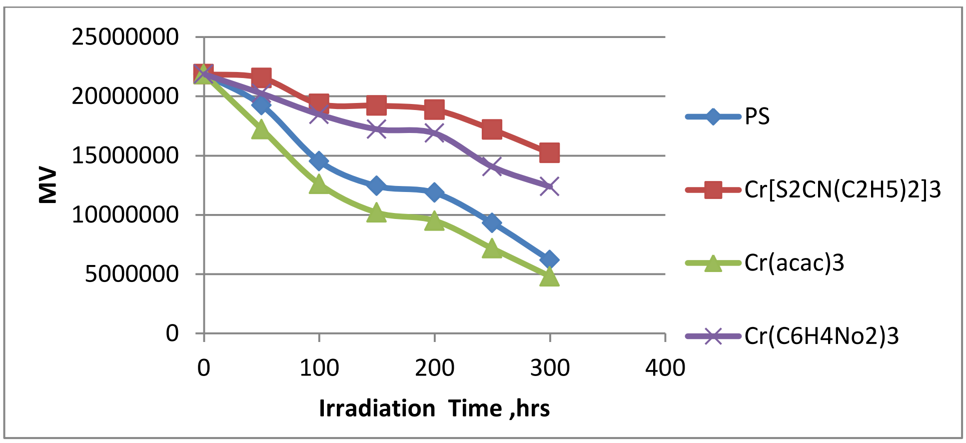

Figure5: Change (v)and irradiation time for polystyrene films of 80 μm thickness and those containing additives with a concentration of 0.05% wt.

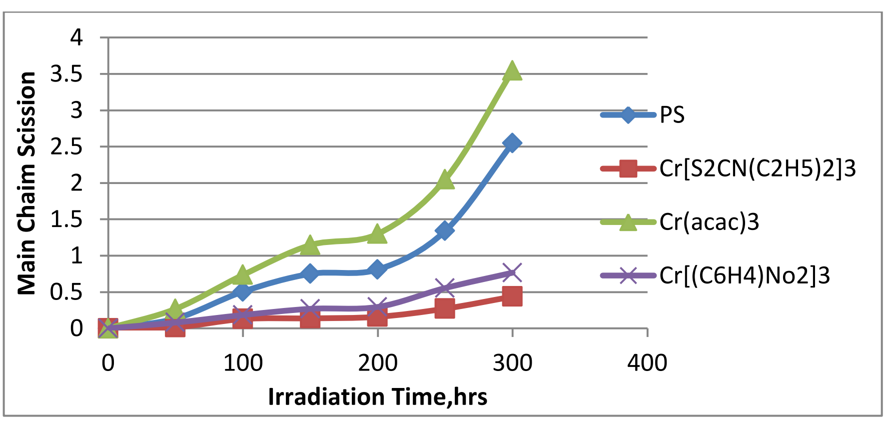

Figure6: Change (S)and irradiation time for polystyrene films of 80 μm thickness and those containing additives with a concentration of 0.05% wt.

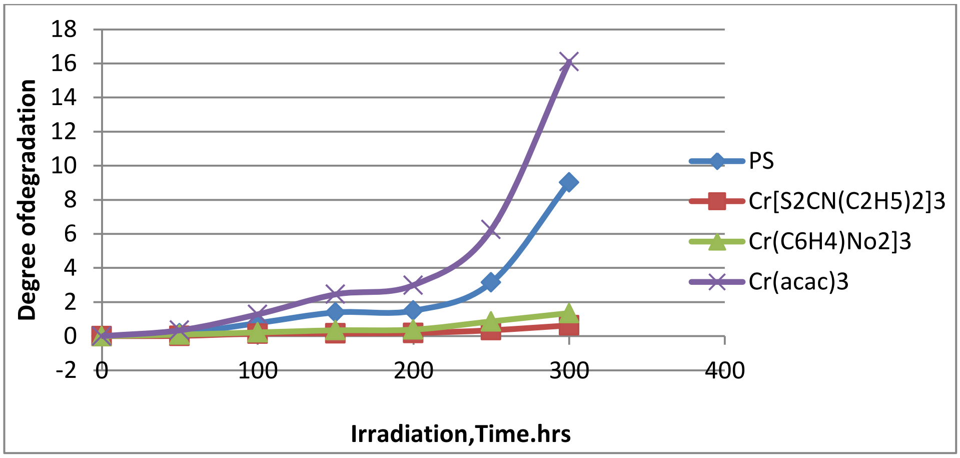

Figure7: Change (α)and irradiation time for polystyrene films of 80 μm thickness and those containing additives with a concentration of 0.05% wt.

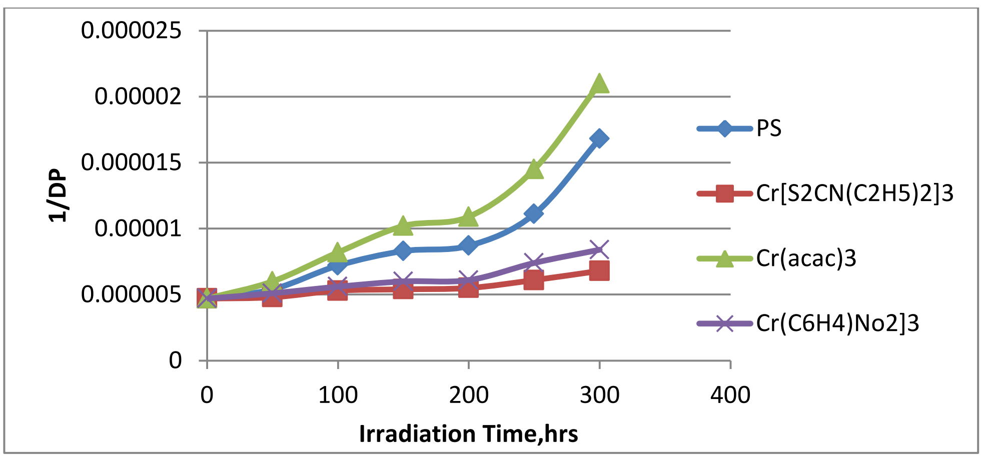

Figure8: Change (1\Dp)and irradiation time for polystyrene films of 80 μm thickness and those containing additives with a concentration of 0.05% wt.

ttp://jgu.garmian.edu.krd https://doi.org/10.24271/garmian.331

Aerodynamic simulation of windflow aroundurban regionsusing different turbulence modeling approaches

Shako A. Mohammed[1*] Saman A. Abdullah[2]

[1]College of Engineering, University of Sulaimani, Sulaymaniyah, Iraq
[2]Civil and Environmental Engineering, University of California, Los Angeles, USA
[*]Corresponding author. Email: Shako.mohammed@univsul.edu.iq

Abstract

There are different turbulent models that have significant impacts on aerodynamic performance and simulation of wind flow over urban areas. A built-up urban area that contains a set of mid- to high-rise buildings was used to highlight theimpact of different turbulence models such asRe-Normalization Group(RNG)k-epsilon, Shear-Stress-Transport (SST)k-omega on the aerodynamic performance of wind flowingin different directions.For both approaches, simulation results such as pressure, mean velocity, and kinetic energy at different directions were obtained and compared. The results demonstrate that, givenan acceptable iterative time andthe same boundary conditions and input variables, both modeling approachesproduce similar resultsfor pressure and velocity around the urban area and slightly different results for the kinetic energy at some location in the urban region, as well as along the height of the buildings considered herein.

Keywords:*Wind flow; winds pressure; wind velocity;Computational Fluid Dynamics (CFD); Turbulence models;k-ε RANS model;k-ω SST model*.

1. Introduction

Aerodynamic characteristics of buildings during wind events is one of the most important considerations in analysis and design of mid- and high-rise buildings because design of such structures is significantly impacted by wind-induced static and dynamic effects. Currently, understanding the true behaviour of buildings subjected to wind pressures as well as investigating the aeroelasticbehaviour of slender and lightweight buildings in urban regions can be cumbersome and expensive as it requires performing wind-tunnel testing procedures. An alternative approach to the time-consuming and costly wind-tunnel experiment is utilizing numerical based approaches of Computational Fluid Dynamics (CFD)(Wang et al., 2014), whichhas recently become the focus of research efforts concerned with aerodynamic controversial issues. CFD is a branch of fluid mechanics commonly used to solve and analyze complex scientific and engineering problemsthrough numerical analyses and algorithms, not only in fluid dynamics but also in other engineering disciplines such as aerodynamic, environmental, and thermodynamicengineering(H. Hu, 2012). Since methods used in CFD are very strict and complex, software such as Fluent, Star, and CFX and platforms to write CFD codes such as OpenFoam are available to aid for analysis. On the other hand, CFD method can be significantly used for solving the Navier Stokes equations (Lee D., 1993).Although, the existing world-leading standards and specifications in the field of aerodynamic engineering (e.g. ASCE, 2013)are using some experimental approaches in dealing with the various impacts of wind on buildings, the wind-tunnel procedure is utilized as a pre-design step for many types of buildings, especially for high rise buildings and those that have irregularities in geometry and/or function. Thus, the numerical turbulence models can be seen as a remarkablealternative to the experimental approaches (Wang et al., 2014).

Reviewing the available literature reveals(e.g. Ping He et al., 1997; A.K. Roy and P.K. Bhargava, 2012 and many others) that most studieshave applied only one turbulence model to simulate the aerodynamic performance of wind flow over a terrain, which can produce inaccurate results(Wang et al., 2014). Therefore, two different turbulence modeling approaches (i.e., RNG k-epsilonandSST k-omega) were studied herein and the results obtained for each approach (such as pressure, velocity, and kinematic energy)were compared for wind blowing in both orthogonal directions.Based on the results of the study, it can be concluded that utilizing more than one turbulence model can effectively increase the reliability of the achieved simulation results.

2. Turbulence Models

The wind flow around urban regions is dealt to have a constant density over the pathway and also belongs to the low flow problems. Hence, the wind can behave as an incompressible fluid in its simulation and/or calculation process. As a result, solving the energy equation is notthe point of interest because consideration of effects of heat transfer in the simulation process is not needed.On the other hand, RANS models calculate the equations of transport only for an average amount of the airflow; therefore, the results are not accurate (Reiter, 2008). Furthermore, the most general and simple model in the RANS approaches is the standard k–epsilon model, which has been employed by many researchers. Alternatively, there are some other reliable modeling approaches in RANS that work more accurately compared to the simple standard k–epsilon model, e.g.,RNG k-epsilondeveloped by Yakhot et al. (1992) andSST k-omegadeveloped by Menter(1993).This studyattempts to utilizeReynoldsaveraged viscous incompressible Navier-Stokes equationsin OpenFOAM toolbox software for both models. Details of each modeling approach are presented next.

2.1. RNG k-epsilon turbulence model

RNG k-epsilon turbulence model is basically an improved version of the standard k-epsilon model with some enhancements to increase the accuracy of the results. It was validated for a wide range of Reynold's number of fluids by providing an analytical formula for turbulent number Prandtl which allows for using a user-supplied constant(Wang et al., 2014). These features make the RNG k-epsilon a more reliable and efficient modelin dealing with wider engineering circumstances than the classic standard k-epsilon approach. Numerical equations of the RNG k-epsilon model are given in Eq. (1) and Eq. (2) as follows:

$$r\frac{Dk}{Dt}=\frac{\partial}{\partial x_i}\left[\left(a_k m_{eff}\right)\frac{\partial k}{\partial x_i}\right]+G_k+G_b-re-Y_M \qquad \text{Eq. (1)}$$

$$r\frac{De}{Dt}=\frac{\partial}{\partial x_i}\left[\left(a_e m_{eff}\right)\frac{\partial k}{\partial x_i}\right]+C_{1e}\frac{e}{k}\left(G_k+C_{3e}G_b\right)-C_{2e}r\frac{e^2}{k}-R \qquad \text{Eq. (1)}$$

Where, Y_M isthe effects of the compressible turbulence expansion on the total dissipation rate, G_k and G_b are the turbulent kinetic energy generated by both average velocity gradient and buoyancy, respectively, α_k and α_ε are the inverse parameters for the turbulent Prandtl number in both the kinetic energy k and dissipation rate ε, respectively.

2.2. SST k-omega turbulence model

This model consists of the two-equation eddy-viscosity models, which are the Wilcox k-omega and the k-epsilon models used to simulate the transit of flow near the wall and remote boundary, respectively,(Wang et al., 2014). It also can be used as a low Reynold's turbulence model without adding any kind of dumping functions (Menter, 1993). Compared to the standard k-omega model, there are some improvements in the SST k-omega model such as adding a special cross-diffusion in the omega (ω) equation and utilizing constants in both models are different. Therefore, compared to the normal k-epsilon model, this model produces a larger turbulence levels, especially in regions of large normal strains. The flow equations of the SST k-omega model are given in Eq. (3) and Eq. (4) in the following:

$$\frac{\partial}{\partial t}\left(rk\right)+\frac{\partial}{\partial x_i}\left(rku_i\right)=\frac{\partial}{\partial x_j}\left(G_k\frac{\partial k}{\partial x_j}\right)+G_k-Y_k+S_k \qquad \text{Eq. (3)}$$

$$\frac{\partial}{\partial t}(\rho\omega)+\frac{\partial}{\partial x_i}(\rho\omega u_i)=\frac{\partial}{\partial x_j}\left(\Gamma_\omega\frac{\partial\omega}{\partial x_j}\right)+G_\omega-Y_\omega+D_\omega+S_\omega \qquad \text{Eq. (4)}$$

Where Γ_k and $\Gamma_\omega$arethe effective diffusion terms of k and ω, respectively, $G_k$and G_ω represent both the kinetic energy and omega equations, respectively, D_ω isthe orthogonal divergent term, and S_k and S_ω are parameters defined by the user.

3. Simulation Model

3.1. Model definition

The idealized prototype urban area developed in this study contains many buildings with various heights ranging mid-rise to high-rise buildings(up to 100 m tall) and various shapes (i.e., regular and irregular cross-sectional shapes) spaced at various distances, as shown in Figure 1. This was to ensure that the prototype region used herein represents a somewhat realistic urban region.

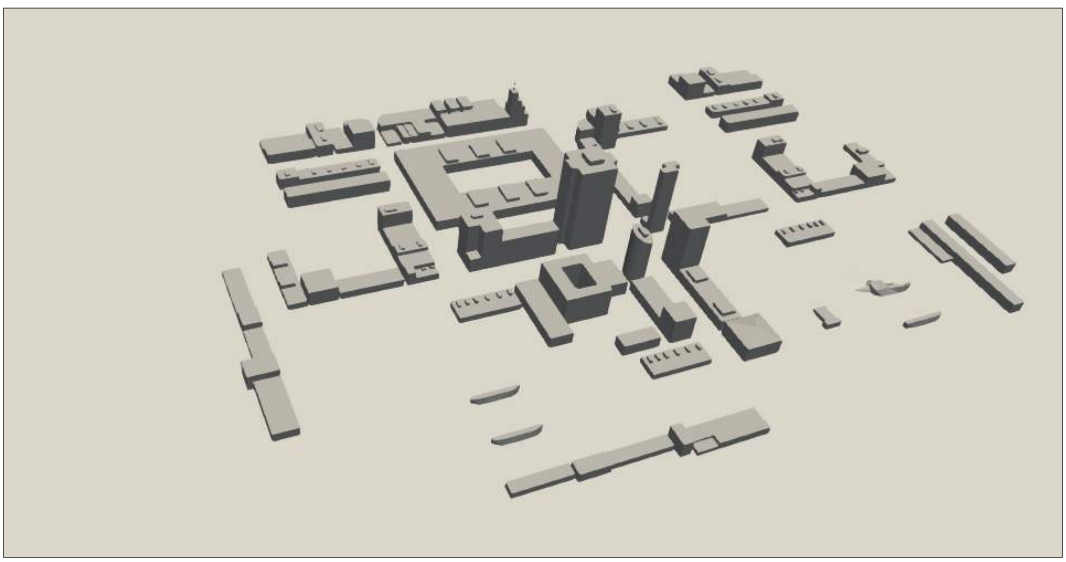

Figure 1: The prototype urban region used in this study.

3.2. Mesh generation

Mesh generation is a crucial step innumerical simulation of any engineering challenge because quality of the mesh can significantly impact the outcomes of the analyses. In this study, the geometry of the idealized urban area wasfirst developedin AutoCAD and was then exported into OpenFOAM simulation tool. Computational structured grid wasutilized to generate meshing of the buildings and surroundings in the form of snappyHexMesh(Figure 2). After that, the meshes were checked for uniformity, aspect ratio, orthogonality, and skewness because these mesh metrics would affect accuracy, robustness, and efficiency of the resulted mesh. As the snappyHexMesh isnot capable of creating sharp edges for the buildings, an approach using surfaceExtractDictfile was employed to generate sharp edges in the analysis.

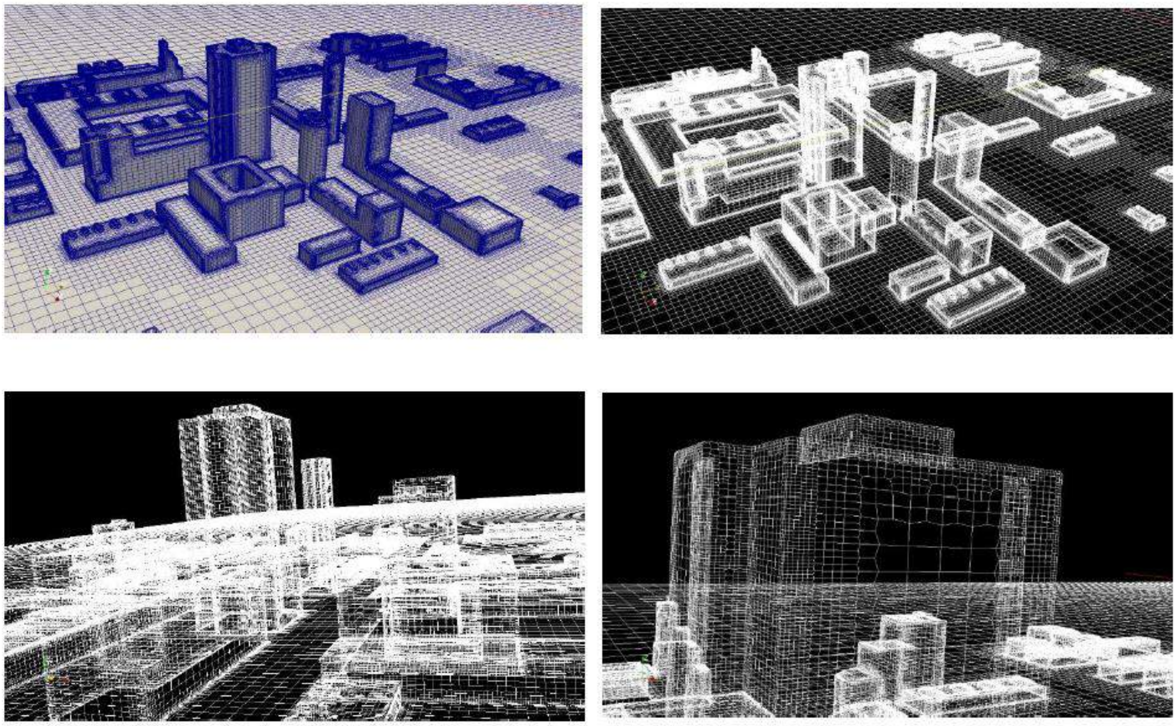

Figure 2: Mesh generation of the urban area by the snappyHexMesh.

4. Domain, Boundary Conditions, and Initial Conditions

Domain means a boundary region bounded by the targeted area, which can imitate the real environmental conditions for the region. In CFD, each issue has its own criteria for size and shape of its domain that are recommended by relevant standard codes or research studies. On the other hand, the urban area should have a domain that could represent the real condition of atmosphere and;

therefore, it must be large enough for simulating the wind flow. There are several recommendations suggested by researchers working in the areaof wind engineering (e.g., Hall, 1997). Depend on that, the domain should have an inlet layer and lateral sides away from the urban region by $5\times H_{max}$, whereH_{max} is the height of the tallest buildingin the region. Furthermore, the out flow sides of the domain should be away from the area by $15\times H_{max}$. The top of the computational domain should also be away from the tallest building by $5\times H_{max}$. Figure 3 shows the recommended domain for the issue. In addition, each domain has some boundary faces bounded by the domain used to describe the inlet/outlet path and sides of the flow through the domain.

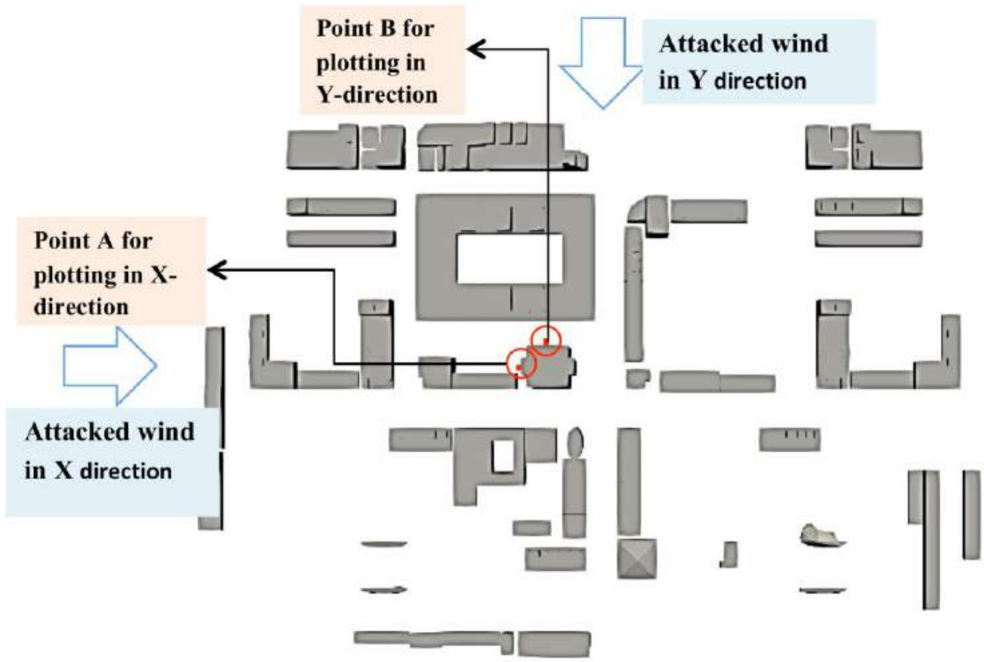

Figure 3: Top view of the urban area

In regards with the initial conditions for the wind flow, this study uses uniform profiles for the velocity and other parameters (e.g., pressure, Reynold number, kinematic energy, and epsilon). However, there is non-uniformity of these parameters in the atmosphere. That is, they have different valuesatdifferent heights above the ground. Thus, a monotonic magnitude of 40 m/secwasemployed for the wind velocity as its initial inlet value into the domain. This leads to calculatingthe Reynold's number and turbulent intensity for the wind flow through the domain. Generally, the turbulent intensity has a value in the range of 1% to 20%. For the wind flow, a small value of turbulent intensity has commonly, been used because Reynold's number of wind is much higher–in some complex situations it could be more than 1 billion. Furthermore, the turbulent intensity plays a major rolein figuring out the initial inlet values of kinetic energy and its dissipation rate. Table 1 shows the calculated values for all the requiredparameters used in the simulation.It is noted that these values are initial physical conditions of the wind flow, and that they would change at any iteration until the simulation reaches the pre-defined convergence value for each of them.

Table 1: Initial input values of theparameters.

Parameter	Mean velocity (m/sec)	Kinetic energy, k (m^2/sec^2)	Epsilon, ε (m^2/sec^3)	Omega, ω (1/sec)
Initial values	40	0.00375	0.0125	3.375

5. Simulation and Results

5.1 Simulation conditions

In order to perform an efficient comparison between RNG k-epsilon and k-omega turbulence models, the same boundary and initial conditions were set for the simulation. Linear SIMPLE algorithms were utilized for both models as the main solvers for the calculation process of velocity, and GAMG(generalized geometric-algebraic multi-grid) solver was used as a pressure solver, whereas Smooth solver was used for the other parameters. Pressure residual control was taken as 0.0001 and a value of 0.001 was set for the other variables in the simulation.Comparison between the two models was carried out in two steps. First, looking at different schemes of the simulated output results on the same sections and/or the same environmental conditions in the Paraview software. For this, a single section was chosen in each attacked wind direction. Second, variation of velocity, pressure, and the kinetic energy was plotted along the height of the building at a location on the face of the tallest building, for each orthogonal direction (i.e., X and Y-directions), as it can be seen in Figure 3.

5.2 Simulation and comparison of turbulence models

Results of variation of velocity, pressure, and kinetic energy at the point A for X-direction and point B for Y-direction of wind flow are compared for both turbulence modeling approaches in Figure 4 and Figure 5, respectively. From these figures, it can clearly be seen that the predicted pressure and velocity profiles obtained from both modeling approaches are identical, whereas significant difference can be seen in the kinetic energy up to 40 m height; the k-epsilon model predicts higher kinetic energy than the k-omega model.

Figures 4a and 4b show that the pressure profile is the reverse of the velocity profile, which indicates that when the wind flow attacks the face of the building, it creates pressure on that face and loses most of its energy; therefore,its speed magnitudefalls down. Another important aspect to be considered in this regard is creating the vortex shading in front of the point A that dissipates the magnitude of the velocity and also falls down the amount of kinetic energy on those zones.

Flow fields of the simulated results obtained from both turbulence models are shown in Figure 6 and Figure 7 for X- and Y-directions, respectively. From these figures, it can be observed that the flow fields turbulence models for both models are also identical for velocity and pressure, except for pressures on the roof of the tall building. However, there are still significant differences in the simulated results of kinetic energy obtained from the two modeling approaches. It can also be seen that there is higher kinetic energy produced around the buildings using the RNG k-epsilon model. Furthermore, compared to the SST k-omega model, the k-epsilon mdels exhibits a higher reduction rate along the height of the building.

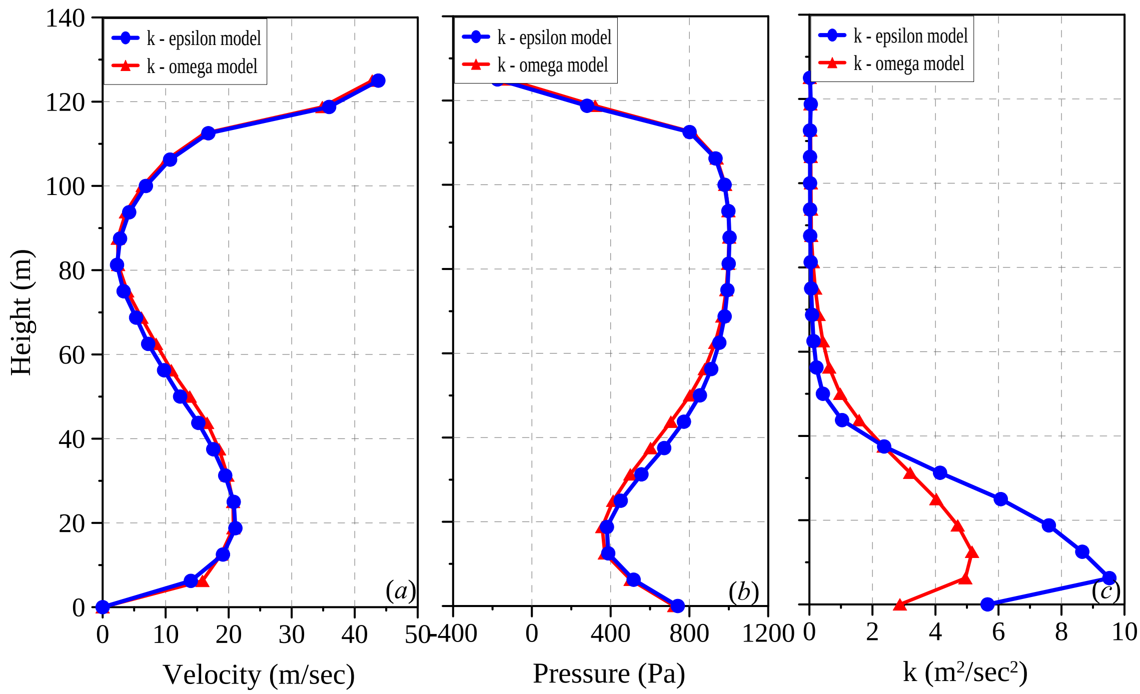

Figure 4: Profiles of (a) velocity, (b) pressure, and (c) kinetic energy at point A in the X-direction.

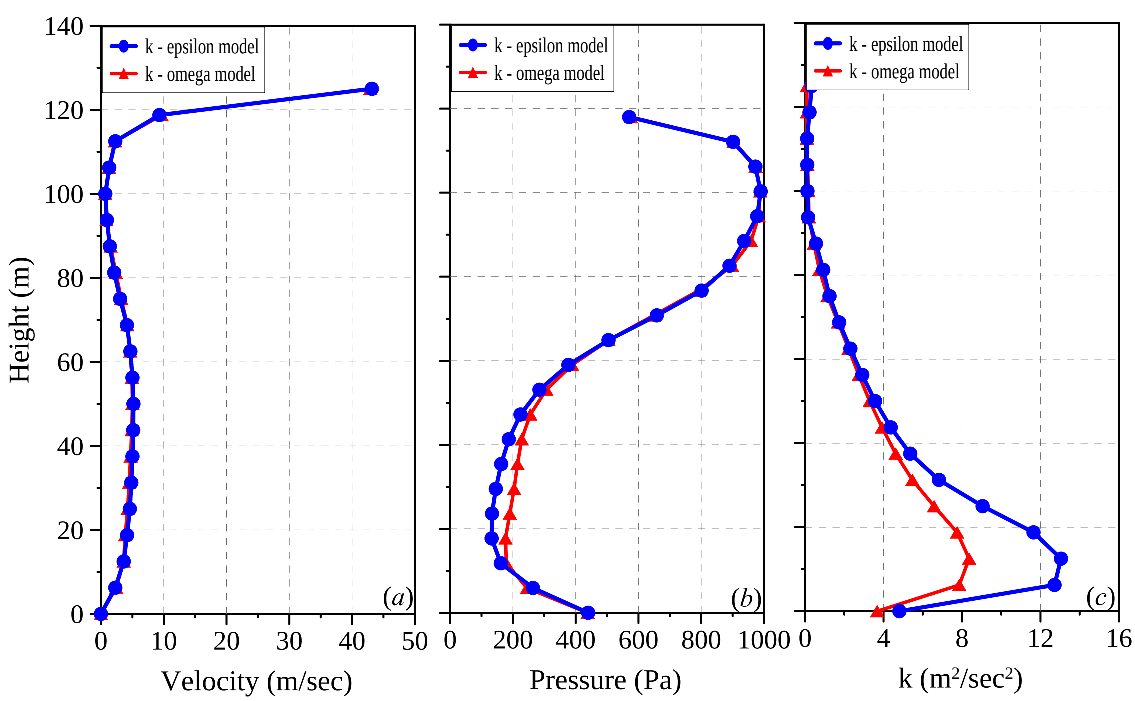

Figure 5: Profiles of (a) velocity, (b) pressure, and (c) kinetic energy at point B in the Y-direction.

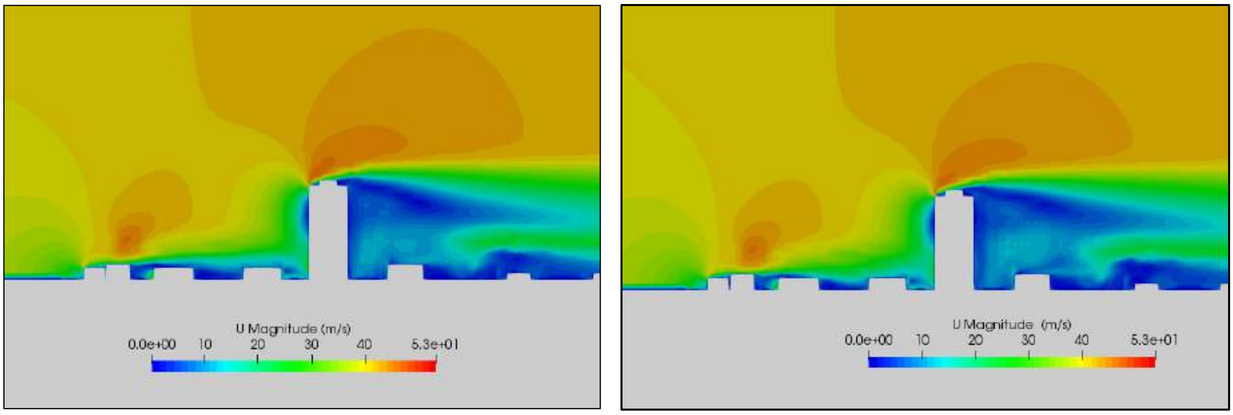

(*a*) Velocity

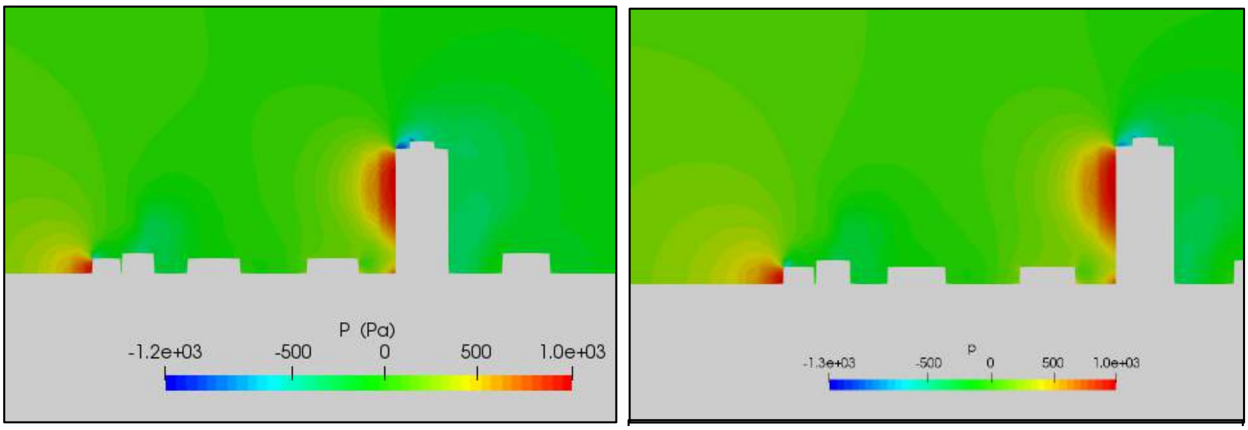

(*b*) Pressure

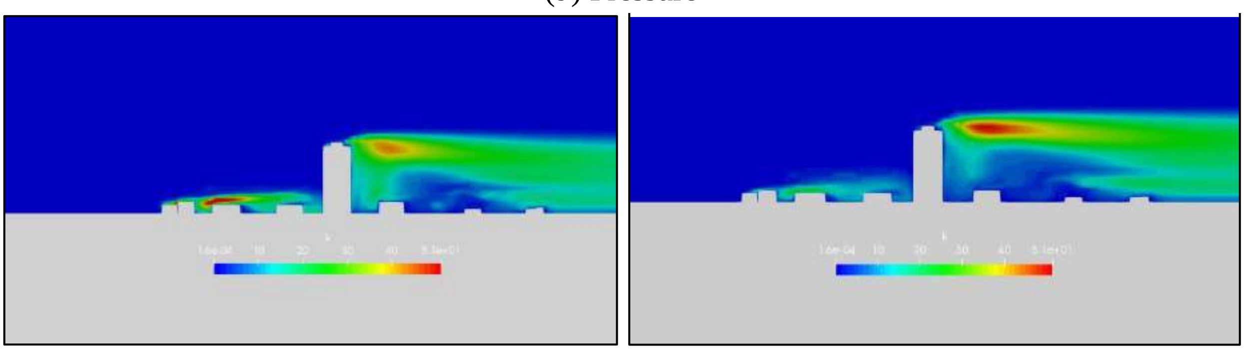

(*c*) Kinetic energy

Figure 6: The comparison of flow field in X-direction for both RNG k-epsilon model (left side) and SST k-omega model (right side).

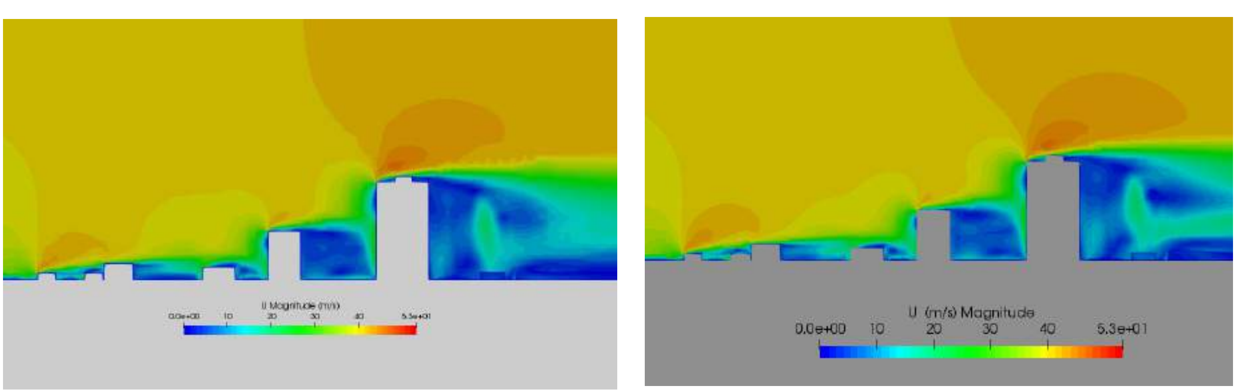

(*a*) Velocity

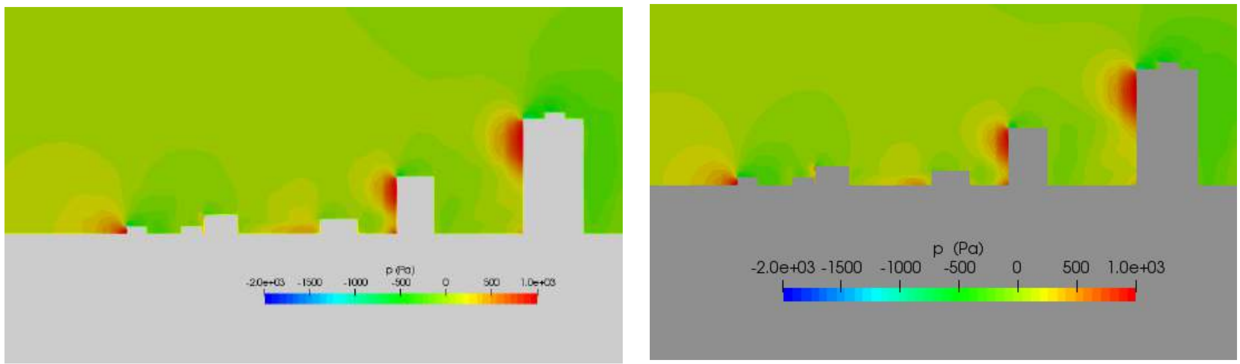

(*b*) Pressure

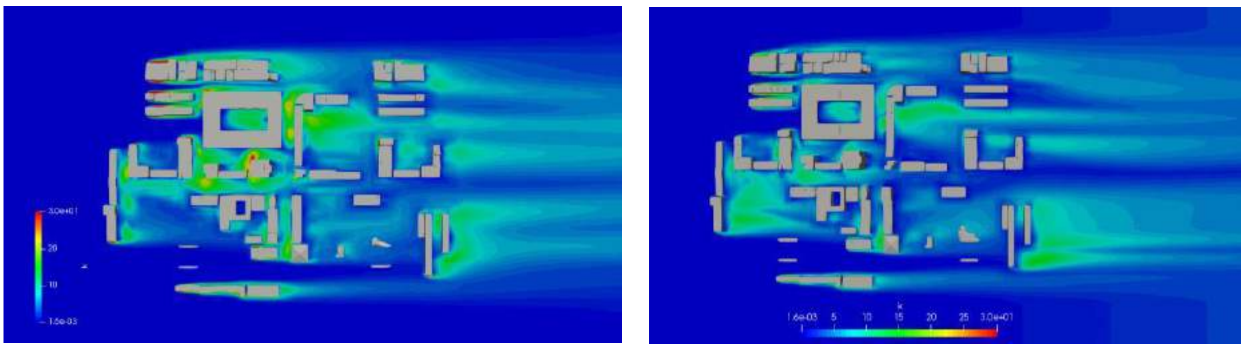

(*c*) Kinetic energy at 2.5 m above the ground (plan view)

Figure 7: The comparison of flow field in Y-direction for both RNG k-epsilon model (left side) and SST k-omega model (right side).

6. Conclusion

In this study, an idealized urban area was generated to investigate the use of different turbulence modeling approaches such as the RNG k-epsilon and k-omega models to simulate the wind flow at different wind directions. The results showed that the predicted pressure and velocity profiles obtained from both modeling approaches are identical, whereas significant difference can be seen in the kinetic energy up to 40 m height; the k-epsilon model predicts higher kinetic energy than the k-omega model.Based on the outcome results, it can be concluded that using two or more turbulence models can be more efficient in reducing the numerical errors and overcome the effects of utilizing only single numerical simulation in the field of aerodynamic engineering.

References

A.K. Roy and P.K. Bhargava. (2012). CFD Modelling of Wind Flow around Buildings for Wind Energy Conversion. *National Conference on Emerging trends of energy conservation in buildings*, (pp. 370-379). Roorkee, India.

ASCE . (2013). *Minimum design loads for building and other structures.* WASHINGTON, D.C.: ASCE (American Society of Civil Engineers).

Hao Wang, Jiaojiao Ding, Bing Ma, Shuaibin Li. (2014, Aauugust 15). Aerodynamic simulation of wind turbine blade airfoil with different turbulence models. *Journal of Vibroengineering, 16*(5), 2474-2483.

Howard H. Hu. (2012). *Chapter 10 – Computational Fluid Dynamics*. Waltham, MA 02451, USA: Elsevier.

Lee D. (1993). *Application of computational fluid dynamics in transonic aerodynamic design.* American Institute of Aeronautics and Astronautics, Aerospace Sciences Meeting and Exhibition.

Menter, F. R. (1993). Zonal Two Equation k-ω Turbulence Models for Aerodynamic Flows. *AIAA Journal*.

Ping He, Tadahisa Katayama, Tetsuo Hayashi, Jun-ichiro Tsutsumi. (1997). Numerical simulation of air flow in an urban area with regularly aligned blocks. *Journal of Wind Engineering*, 281-291.

S.Reiter. (2008). Validation Process for CFD Simulations of Wind Around Buildings. *European Built Environment CAE Conference.* Belgium: University of Liège.

Yakhot, V., Orszag, S.A., Thangam, S., Gatski, T.B. & Speziale, C.G. (1992). Development of turbulence models for shear flows by a double expansion technique. *Physics of Fluids A, 4*(7), 1510-1520.

ttp://jgu.garmian.edu.krd https://doi.org/10.24271/garmian.332

Effect of Freezing and Thawing on Physical and Mechanical Properties of Sedimentary Rock

Safin Bahadin Hama Saeed [1*], Younis M. Alshkane [1]

[1]Civil Department, faculty of Engineering, University of Sulaimani, Al- Sulaimaniyah, KRG/Iraq

[2] Civil Department, faculty of Engineering, University of Sulaimani, Al- Sulaimaniyah, KRG/Iraq
younis.ali@univsul.edu.iq

[*]Corresponding author. Email: safin19@gmail.com

Abstract

Rocks have been used as a building material throughout the history. The Engineering Properties of rocks mainly depends on mineralogical composition and texture of the rock type. Weathering processes influence the rock porosity in cold climate area. This paper studies the effect of weathering (freezing thawing cycles) on physical and mechanical properties of specific types of rock (sedimentary rocks). Freeze–thaw cycles is one of the most important phenomena affecting the engineering properties of rocks. This study was conducted based on literature data to analyze the durability and stability of rocks throughout the physical and mechanical properties such as (density, porosity, Brazilian tensile strength, unconfined compressive strength and point load Index) of sedimentary rock specimens exposed to excessive amount freezing-thawing cycles. Key factors that affecting the strength of frozen rocks were analyzed. Results showed that porosity and the intensity of freezing-thawing cycles influenced Engineering properties of sedimentary rocks significantly. The loss in unconfined compressive strength is an important indicator for rock strength and durability However, this test is extremely expensive and tedious. Therefore, different correlations and Statistical models were developed using multiple regression analyses to predict the mechanical properties of rocks such as unconfined compressive strength and tensile strength from other physical properties and corresponding to specified number of F-T cycles. The models are very reliable with R^2= 95% and can be used to predetermination of unconfined compressive strength and tensile strength of sedimentary rocks.

Keywords Freezing-Thawing cycles, Sedimentary Rocks, UCS, Brazilian tensile strength (BTS), Point Load index ($I_{s(50)}$), Pulse velocity (Vp), Dry density (γd).

1. Introduction

In the history, natural stones were used to construct many amphitheaters, arenas, statues and monuments and nowadays rocks are used in shape of polished slabs for wall cladding of the buildings (Akin and Ozsan, 2011). Sedimentary rocks is one of the most popular types of rock used in constructions, it faces engineers as a foundation material, building stone and as face cladding material. The reason behind using Sedimentary rocks so widely in construction is their abundance in nature (Pettijohn et al., 2012). Another reason is that some sedimentary rocks have high strength and durability (Hale and Shakoor, 2003).

In literature the strength and durability of sedimentary rocks has been studied frequently and considered to be relatively proportional (Shakoor and Bonelli, 1991; and Bell, 1992). Also they reported that density is directly proportional with compressive strength, while porosity and percentage absorption are inversely proportional with compressive strength. Hale and Shakoor, (2003) have stated that the percentage of cementation material are directly proportional with compressive strength.

In general there are many physical processes that affect the strength and durability of rocks and causes disintegration of the rocks as result of the climate changes, such as wetting–drying, heating–cooling, and freezing– thawing (F-T) cycles.

According to another research heating–cooling cycles has less effect on disintegration of rocks while freezing and thawing cycles is the most detrimental physical processes that affect rock durability and disintegration (Erguler and Shakoor, 2009).

Researchers have indicated that disintegration in rocks that caused by freeze-thaw cycles has the most paramount importance on projects such as roads, building construction, railroads and pipelines (Nicholson., 2001; Zhang et al., 2004; Chen et al., 2004; Mutluturk et al., 2004; Yavuz et al., 2006; Grossi et al., 2007; Ruedrich and Siegesmund, 2007; Tan et al., 2011). Freezing-thawing action can changing the mechanical properties of rocks rapidly. Therefore, the rock's durability should be studied prior to the selection of an appropriate building stone (Zappia et al., 1998).

Water get in to the rock's pores and freezes when temperature drop to below 0 ^{o}C, as a result the volume of the water increase up to 9% and this will generate excessive pressure inside the rock pores which is greater than the tensile strength of the rock: thus the generated pressure is quite enough to disintegrate the rock and causes primarily fractures (Lienhart, 1988). Kolay, (2016) proposed that the frozen pore water can generate a pressure up to 200 MPa.

Successive freezing-thawing cycles can cause fatigue and lead to damages of the stone (Lienhart and Stransky, 1981; Lienhart, 1988).

Many parameters has been studied by researchers to investigate the physical and mechanical properties of rocks. Compressive strength is one of the most essential parameters in designing most of the geo-engineering projects (Nazir et al., 2013; Akram and Bakar, 2016).

The method for evaluating the compressive strength in laboratory is time consuming and costs a lot, nevertheless it is not easy to obtain intact samples from highly weathered rock mass (Hyam et al., 2017). Due to the mentioned reasons other indirect testy are proposed to predict the engineering properties and durability of rocks such as Point Load Index (Is(50)), indirect tensile strength (BTS) and pulse velocity (VP) (Cargill and Shakoor, 1990; Sharma and Singh, 2008).

(Topal and Sözmen, 2000) has investigated the effect of freezing-thawing cycles on compressive strength, dry density (ρd), porosity (n) and Pulse velocity (Vp), also they have reported many relationship between the freezing-thawing (F-T) cycles and the engineering parameters of rock. Accordingly many correlation and prediction equations has been developed to predict important engineering parameters of rock such as compressive strength and tensile strength (Kolay, 2016).

This study was conducted to investigate the effect of freezing-thawing cycles on physical and mechanical properties of sedimentary rocks based on data collected from literature. Various engineering parameters of rocks has been studied such as Unconfined compressive strength (UCS), Brazilian tensile strength (BTS), Point

Load index ($I_{s(50)}$), Pulse velocity (Vp) and Dry density (ρd). simple and multiple regression analysis has been developed to predict the effect of F-T cycles on the engineering properties of sedimentary rocks.

2. Modeling

In this study different correlation and relationships has been evaluated to propose models to predict the engineering properties of rock after successive amount of F-T cycles. The proposed equation presented in Table 2.

2.1 Testing the Model's Accuracy

In order to investigate the accuracy of the proposed models in this study both the coefficient of determination (R^2) and root mean square error (RMSE) has been calculated using equations Eq. 1 and Eq. 2.

$$R^2 = \left(\frac{\sum i(xi-\bar{x})\,(yi-\bar{y})}{\sqrt{\sum i\,(xi-\bar{x})^2} * \sqrt{\sum i\,(yi-\bar{y})^2}}\right)^2 \quad (1)$$

$$\text{RMSE} = \sqrt{\frac{\sum_{i=1}^{n}(yi-xi)^2}{N}} \quad (2)$$

Where

yi = actual test value.

x_i = calculated value from the model.

$\bar{y}$ = mean of actual test values.

$\bar{x}$ = mean of calculated values and

N = is the number of data points.

3. Methodology

This study was conducted depending on data from literature to investigate the physical and mechanical properties of sedimentary rocks and their changes due to successive amount of freezing-thawing cycles. The tests from the literature studies was conducted according to both standards ASTM and ISRM.

3.1 Point Load Index $I_{s(50)}$

Point load test (Points load index Is(50)) has been widely used as a quick and simple method to identify the strength of rocks. The test procedure is very simple since no need regular form specimens, ether it can be done on field. Rock specimens are tested by applying concentrated point load using two steel cones end. According to the test procedure which given by ASTM (ASTM, 2002). The load should be applied in increment so that failure should occur within 1 minute. The rock specimen will fail and crack parallel to the applied load axis due to the development of tensile strength.

4.2 Pulse velocity (Vp)

Pulse velocity techniques (Vp) have been used by many researchers for many years to analyses the rock strength parameters (Vasconceloset al., 2007). Pulse velocity can be used to evaluate the porosity as well as the rock strength. It can be correlated to predict the most important engineering parameters such as uniaxial compressive strength (UCS) with a very low costs and efforts. The test procedure and specification have been given by both standards ASTM and ISRM (Vasconceloset al., 2007).

4.3 Brazilian Tensile Strength (BT)

Brazilian Tensile Strength (BTS) is an indirect method to evaluate the engineering parameters of rocks. This test can be used to predict the tensile strength of rock and also to determine the rate of damage that can be caused by successive amount of Freezing-thawing cycles. According to the test procedure which given by ASTM (ASTM, 2008) specimens in a shape of circular disk loaded and compressed across its diameter.

4.4 Unconfined compressive strength (UCS)

The Unconfined compressive strength is one of the most essential strength parameters. It has been desired by researchers to determine the engineering strength parameters. This test can be conducted according to the standard test procedure given by ISRM (Bieniawski and Bernede, 1979). Many studies has been conducted to evaluate the effect of F-T cycles on the strength and durability of stones.

5. Results and Discussion

In order to better understand the reasons that affect the strength and durability of sedimentary rocks, each parameters has been studied separately. The collected data from literature were analyzed to determine Mean, Median, Standard deviation, Variance and coefficient of variance using statistical tools. The results are presented in Table 1. The results of this study has showed that the engineering parameters of rock such as Dry density, Porosity, Tensile strength and compressive strength are mainly affected by successive amount of freezing-thawing actions. Different correlational and regression analysis has been evaluated between the index properties and the essential engineering parameters such as compression strength and tensile strength. Also different prediction equations has been developed to predict the changes in each parameters due to successive amount of freezing-thawing actions and to predict rock strength (compression and tensile) from the physical properties such as Dry density, Porosity, Pulse velocity, Point load index. The Equations are summarized in Table 2. The results and the relationships are discussed in detail as follows:

5.1 Relationship between Porosity (n%) and Freezing-Thawing Action (F-T).

Statistical analysis has been conducted for 107 data which has been collected from literature, accordingly the data has standard deviation of 6.1 % and coefficient of variation (COV) of 47.16 %, with a mean and median of 12.93 % and 12.78 %, respectively. The results are summarized in Table 2. Fig. 1 show that the porosity ratio raised up after successive amount of F-T cycles and the prediction equation Eq. 3 is highly reliable with R^2 = 91% that can be used to predict the increases in porosity ratio accurately up to 30 F-T cycles. The model parameters are summarized in Table 2.

$$n_{(\%)} = 11.022 + \frac{N}{(0.738 + 0.381N)} \qquad (3)$$

Where

N = Freezing-Thawing Number.

5.2 Relationship between compressive strength (UCS) and Freezing-Thawing Action

Statistical analysis has been conducted for 67 data which has been collected from literature, accordingly the data has standard deviation of 26.22 MPa and coefficient of variation (COV) of 71.57 %, with a mean and median of 36.64 MPa and 28.42 MPa, respectively. The results are summarized in Table 2. Fig. 2 show that the UCS dropped sharply after successive amount of F-T cycles and the prediction equation Eq. 4 is highly reliable with R^2 = 95% that can be used to predict UCS value accurately up to 30 F-T cycles. The model parameters are summarized in Table 2.

$$UCS_{\ (MPa)} = 0.027\ N^2 - 1.33\ N + 47.7 \qquad (4)$$

5.3 Relationship between Point load index ($I_{s(50)}$) and Freezing-Thawing Action.

Statistical analysis has been conducted for 45 data which has been collected from literature, accordingly the data has standard deviation of 1.74 MPa and coefficient of variation (COV) of 46.72 %, with a mean and median of 3.76 MPa and 4.1 MPa, respectively. The results are summarized in Table 2. Fig. 3 show that the point load index has affected by successive amount of F-T cycles and the prediction equation Eq. 5 is less reliable with R^2 = 43% that can be used only to have a rough idea on the point load index value up to 30 F-T cycles. The model parameters are summarized in Table 2.

$$I_{s(50)(MPa)} = 0.0015\ N^2 - 0.0514\ N + 4.06 \qquad (5)$$

5.4 Relationship between Pulse velocity (Vp) and Freezing-Thawing Action (F-T)

Statistical analysis has been conducted for 67 data which were collected from literature, accordingly the data has standard deviation of 949 m/s and coefficient of variation (COV) of 45.9%, with a mean and median of 2069 m/s and 2147 m/s, respectively. The results are summarized in Table 2. Fig. 4 show the correlation between pulse velocity and F-T cycles and the prediction equation Eq. 6 is moderately reliable with R^2 = 84 % that can be used to predict the pulse velocity value up to 30 F-T cycles. The model parameters are summarized in Table 2.

$$Pv_{m/s} = 0.015\,N^2 - 23.86\,N + 2380.6 \quad (6)$$

5.5 Relationship between Compressive strength (UCS) and Dry density (ρd)

Statistical analysis has been conducted for 44 data which has been collected from literature, accordingly the data has standard deviation of 0.37 g/cm^3 and coefficient of variation (COV) of 18.7 %, with a mean and median of 2.02 g/cm^3 and 2.04 g/cm^3, respectively. The results are summarized in Table 2. Fig. 5 show the correlation between UCS and Dry Density and the prediction equation Eq. 7 is moderately reliable with R^2 = 74 % that can be used to predict the UCS from dry density ranged between (1.41 to 2.47) g/cm^3. The model parameters are summarized in Table 2.

$$UCS = 5.53 + \frac{\rho_d}{(0.256 + 0.076\rho_d)} \quad (7)$$

5.6 Relationship between Tensile strength (BTS) and Point load Index ($I_{s(50)}$).

Statistical analysis has been conducted for 45 data which has been collected from literature, accordingly the data has standard deviation of 3.96 MPa and coefficient of variation (COV) of 63.76 %, with a mean and median of 6.22 MPa and 5 MPa, respectively. The results are summarized in Table 2. Fig. 6 show the correlation between tensile strength and point load index and the prediction equation Eq. 8 is highly reliable with R^2 = 94 % that can be used to predict the tensile strength from ($I_{s(50)}$) ranged between (1.34 to 6.7) MPa. The model parameters are summarized in Table 2.

$$BTS_{MPa} = -0.023 + \frac{I_{S(50)}}{(0.968 + 0.076\, I_{S(50)})} \quad (8)$$

5.7 Relationship between Dry density (ρd) and Pulse velocity (Vp)

Prediction equation Eq. 9, has been proposed. The model and its parameters are summarized in Table 2 and shown in Fig. 7. The accuracy of the model was tested; accordingly, the coefficient of determination (R^2) and root mean square error (RMSE) for the proposed model were 72% and 0.17, respectively.

$$\rho d_{g/cm^3} = 0.42\ (\ln Vp) - 1.27 \quad (9)$$

5.8 Relationship between Porosity (n) and Dry Density (ρd)

Prediction equation Eq. 10, has been proposed. The model and its parameters are summarized in Table 2 and shown in Fig. 8. The accuracy of the model was tested; accordingly, the coefficient of determination (R^2) and root mean square error (RMSE) for the proposed model were 50% and 4.19, respectively.

$$n = 11.8\,\rho_d{}^2 - 33.23\,\rho_d + 33.47 \qquad (10)$$

6. Conclusion

The freezing-Thawing test is the most effective test to determine the loss in strength of rocks due to Freezing-Thawing action. However, it is not easy to conduct this test as it is very laborious and costly. In this study different correlation and prediction models has been developed to predict compression and tensile strength of rock and their loss due to successive amount of freezing-thawing actions the result of this study can be summarized as:

1. In general Freezing-Thawing cycles affect porosity and increased the rock's disintegration. Especially the first 5 F-T cycles that mostly affected porosity (n) and increased it from 11% up to 13%. Also the result of the pulse velocity test confirm that the disintegration and cracks has been increased wildly after subjecting the rock specimens to successive amount of F-T actions.
2. The result of this study has shown that the F-T action affect the rock strength. The UCS of the tested specimens has dropped sharply from almost 47 MPa to less than 32 MPa after 25 successive F-T cycles.
3. Multiple regression analysis were performed and different correlation and prediction equations has been developed between the rock strength parameters (Compressive and tensile) and the index properties. This prediction equations can be used easily to predict the loss in rocks strength parameters due to the effect of F-T actions without conducting F-T test.
4. The UCS has been correlated with dry density and modeled. The developed model is moderately reliable with R^2 = 74% and can predict USC value accurately up to 30 F-T cycles.

5. The tensile strength of sedimentary rocks has been correlated with point load index. The developed model is highly reliable with R^2 = 95% that can predict tensile strength value accurately up to 30 F-T cycles.

References

Akin, M., & Özsan, A. (2011). Evaluation of the long-term durability of yellow travertine using accelerated weathering tests. *Bulletin of Engineering Geology and the Environment*, *70*(1), 101-114.

Akram, M., & Bakar, M. A. (2016). Correlation between uniaxial compressive strength and point load index for salt-range rocks. *Pakistan Journal of Engineering and Applied Sciences*.

ASTM, D. (2002). 5731, Standard test method for determination of the point load strength index of rock. *ASTM International, West Conshohocken, PA*.

ASTM, D. (2008). 3967, Standard Test Method for Splitting Tensile Strength of Intact Rock Core Specimens. *ASTM International, West Conshohocken, PA*.

BELL, R. G. (1992). The durability of sandstone as building stone, especially in urban environments. *Bulletin of the Association of Engineering Geologists*, *29*(1), 49-60.

Bieniawski, Z. T., & Bernede, M. J. (1979, April). Suggested methods for determining the uniaxial compressive strength and deformability of rock materials: Part 1. Suggested method for determination of the uniaxial compressive strength of rock materials. In *International Journal of Rock Mechanics and Mining Sciences & Geomechanics Abstracts* (Vol. 16, No. 2, p. 137). Pergamon.

Cargill, J. S., & Shakoor, A. (1990, December). Evaluation of empirical methods for measuring the uniaxial compressive strength of rock. In *International Journal of Rock Mechanics and Mining Sciences & Geomechanics Abstracts* (Vol. 27, No. 6, pp. 495-503). Pergamon.

Chen, T. C., Yeung, M. R., & Mori, N. (2004). Effect of water saturation on deterioration of welded tuff due to freeze-thaw action. *Cold Regions Science and Technology*, *38*(2-3), 127-136.

Erguler, Z. A., & Shakoor, A. (2009). Relative contribution of various climatic processes in disintegration of clay-bearing rocks. *Engineering Geology*, *108*(1-2), 36-42.

Grossi, C. M., Brimblecombe, P., & Harris, I. (2007). Predicting long term freeze–thaw risks on Europe built heritage and archaeological sites in a changing climate. *Science of the Total Environment*, *377*(2-3), 273-281.

Hale, P. A., & Shakoor, A. (2003). A laboratory investigation of the effects of cyclic heating and cooling, wetting and drying, and freezing and thawing on the compressive strength of selected sandstones. *Environmental & Engineering Geoscience*, *9*(2), 117-130.

Hyam, S. D., Younis, M. A., & Kamal, A. R. (2017). Prediction of Uniaxial Compressive Strength and Modulus of Elasticity for Some Sedimentary Rocks in Kurdistan Region-Iraq using Schmidt Hammer. Journal of Zankoy Sulaimani, 19 – 3-4, pp. 57-72.

Ingham, J. P. (2005). Predicting the frost resistance of building stone. *Quarterly Journal of Engineering Geology and Hydrogeology*, *38*(4), 387-399.

Jamshidi, A., Nikudel, M. R., & Khamehchiyan, M. (2013). Predicting the long-term durability of building stones against freeze–thaw using a decay function model. *Cold Regions Science and Technology, 92*, 29-36.

Khanlari, G., Sahamieh, R. Z., & Abdilor, Y. (2015). The effect of freeze–thaw cycles on physical and mechanical properties of Upper Red Formation sandstones, central part of Iran. *Arabian Journal of Geosciences*, *8*(8), 5991-6001.

Kolay, E. (2016). Modeling the effect of freezing and thawing for sedimentary rocks. *Environmental Earth Sciences*, *75*(3), 210.

Lienhart, D. A. (1988). The geographic distribution of intensity and frequency of freeze-thaw cycles. *Bulletin of the Association of Engineering Geologists*, *25*(4), 465-469.

Lienhart, D. A., & Stransky, T. E. (1981). Evaluation of potential sources of riprap and armor stone—methods and considerations. *Bulletin of the Association of Engineering Geologists*, *18*(3), 323-332.

Mutlutürk, M., Altindag, R., & Türk, G. (2004). A decay function model for the integrity loss of rock when subjected to recurrent cycles of freezing–thawing and heating–cooling. *International journal of rock mechanics and mining sciences*, *41*(2), 237-244.

Nazir, R., Momeni, E., Armaghani, D. J., & Amin, M. M. (2013). Correlation between unconfined compressive strength and indirect tensile strength of limestone rock samples. *Electr J Geotech Eng*, *18*, 1737-1746.

Nicholson, D. T. (2001). Pore properties as indicators of breakdown mechanisms in experimentally weathered limestones. *Earth surface processes and landforms*, *26*(8), 819-838.

Nuri, T. M., Awad, M. A., & Msbah, A. M. A. (2011). Effect of Freezing-Thawing Cycles on the Physical and Mechanical Properties of Some Sedimentary Rocks Located Near Mosul City. *Engineering and Technology Journal*, *29*(16), 3388-3404.

Pettijohn, F. J., Potter, P. E., & Siever, R. (2012). *Sand and sandstone*. Springer Science & Business Media.

Ruedrich, J., & Siegesmund, S. (2007). Salt and ice crystallisation in porous sandstones. *Environmental Geology*, *52*(2), 225-249.

SHAKOOR, A., & BONELLI, R. E. (1991). Relationship between petrographic characteristics, engineering index properties, and mechanical properties of selected sandstones. *Bulletin of the Association of Engineering Geologists*, *28*(1), 55-71.

Sharma, P. K., & Singh, T. N. (2008). A correlation between P-wave velocity, impact strength index, slake durability index and uniaxial compressive strength. *Bulletin of Engineering Geology and the Environment*, *67*(1), 17-22.

Tan, X., Chen, W., Yang, J., & Cao, J. (2011). Laboratory investigations on the mechanical properties degradation of granite under freeze–thaw cycles. *Cold Regions Science and Technology*, *68*(3), 130-138.

Vasconcelos, G., Lourenço, P. B., Alves, C. A., & Pamplona, J. (2007). Prediction of the mechanical properties of granites by ultrasonic pulse velocity and Schmidt hammer hardness.

Yavuz, H., Altindag, R., Sarac, S., Ugur, I., & Sengun, N. (2006). Estimating the index properties of deteriorated carbonate rocks due to freeze–thaw and thermal shock weathering. *International Journal of Rock Mechanics and Mining Sciences*, *43*(5), 767-775.

Zappia, G., Sabbioni, C., Riontino, C., Gobbi, G., & Favoni, O. (1998). Exposure tests of building materials in urban atmosphere. *Science of the total environment*, *224*(1-3), 235-244.

Zhang, S., Lai, Y., Zhang, X., Pu, Y., & Yu, W. (2004). Study on the damage propagation of surrounding rock from a cold-region tunnel under freeze–thaw cycle condition. *Tunnelling and Underground Space Technology*, *19*(3), 295-302.

Appendices

Table 1. Statistical analysis of the main parameters.

Variable	Mean	St. Dev	Variance	Coef. of Var.	Minimum	Q1	Median	Q3	Maximum
[1]ρd	2.02	0.37	0.14	18.70	1.39	1.73	2.04	2.38	2.67
[2]n	12.93	6.10	37.21	47.16	1.40	7.72	12.78	17.41	23.84
[3]F-T	19.80	12.14	147.38	61.30	5.00	10.00	20.00	25.00	50.00
[4]Vp	2069	949	901430	45.90	576	1308	2147	2729	4185
[5]$I_{s(50))}$	3.76	1.74	3.03	46.27	1.25	1.97	4.10	5.25	6.700
[6]BTS	6.22	3.96	15.73	63.76	1.09	2.70	5.0	10.15	12.90
[7]UCS	36.64	26.22	687.48	71.57	8.09	18.74	28.42	42.45	127.34

[1]ρd Dry density, [2]n Porosity, [3]F-T Freezing-thawing cycles, [4]Vp Pulse velocity

[5]$I_{s(50)}$ Point load index, [6]BTS Brazilian tensile strength, [7]UCS Unconfined compressive strength

Table 2. Proposed models

Proposed Equation	Independent Parameter	Dependent Parameter	RMSE	Coefficient of determination R^2
n = 11.022 + N/(0.738+ 0.381N)	[1]F-T cycle (N)	Porosity (n)	0.26	91 %
UCS = 0.027 N2 - 1.33 N + 47.7	F-T cycle (N)	[2]UCS	1.33	95 %
Is(50) = 0.0015 N2 - 0.0514 N + 4.06	F-T cycle (N)	Point load $I_{s(50)}$	0.17	43 %
Vp = 0.01 N2 - 23.86 N + 2380.6	F-T cycle (N)	Pulse velocity Vp	104.37	84 %
UCS = 5.53 + ρd/(0.256 - 0.076 ρd)	Dry density (ρd)	UCS	4.73	74%
BTS = -0.023 + I s(50) /(0.968 - 0.076 $I_{s(50))}$	Point load $I_{s(50)}$	Tensile strength [3]BTS	0.88	95%
ρd = 0.42 lnVp- 1.27	Pulse velocity Vp	Dry density (ρd)	0.17	72 %
n = 11.8 ρd 2 -33.23 ρd +33.47	Porosity (n)	Dry density (ρd)	5.32	50 %

[1]F-T cycles: Freezing-Thawing cycles, [2]UCS: Unconfined compressive strength

[3]BTS: Brazilian tensile strength

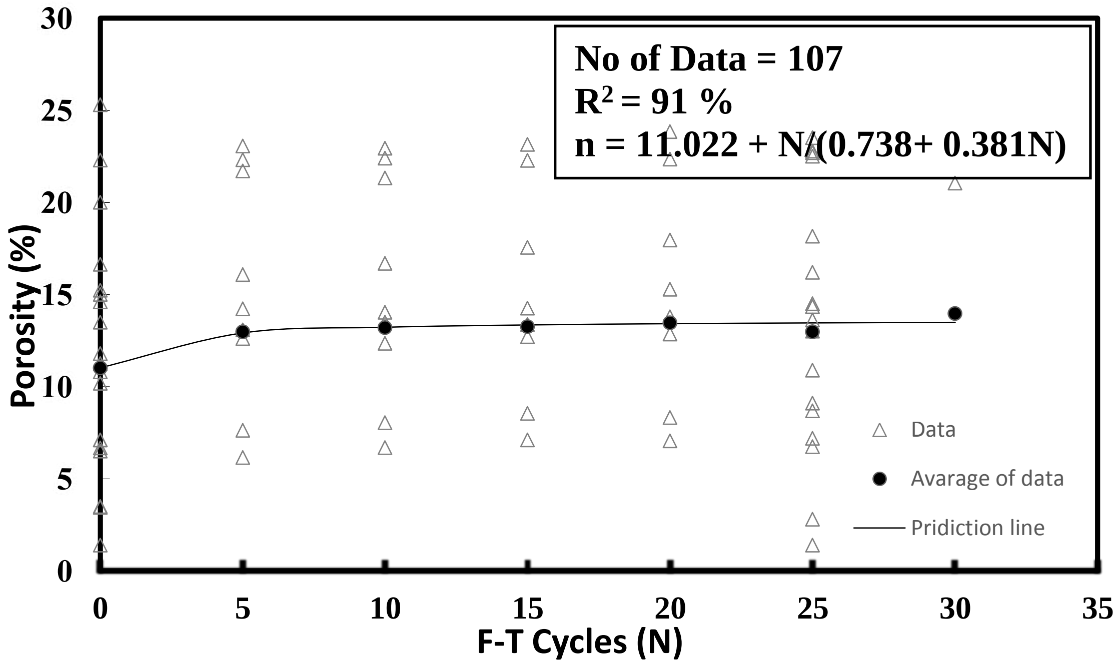

Fig1. Variation of Porosity with the number of Freezing-Thawing cycles.

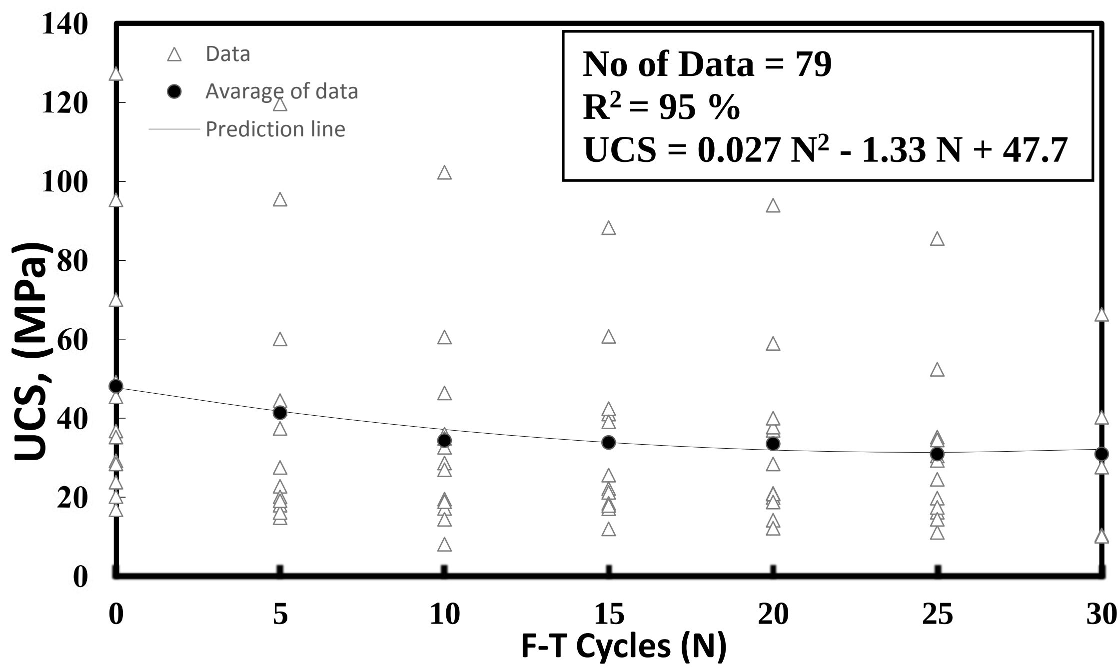

Fig 2. Variation of Unconfined compressive strength with the number of Freezing-Thawing cycles.

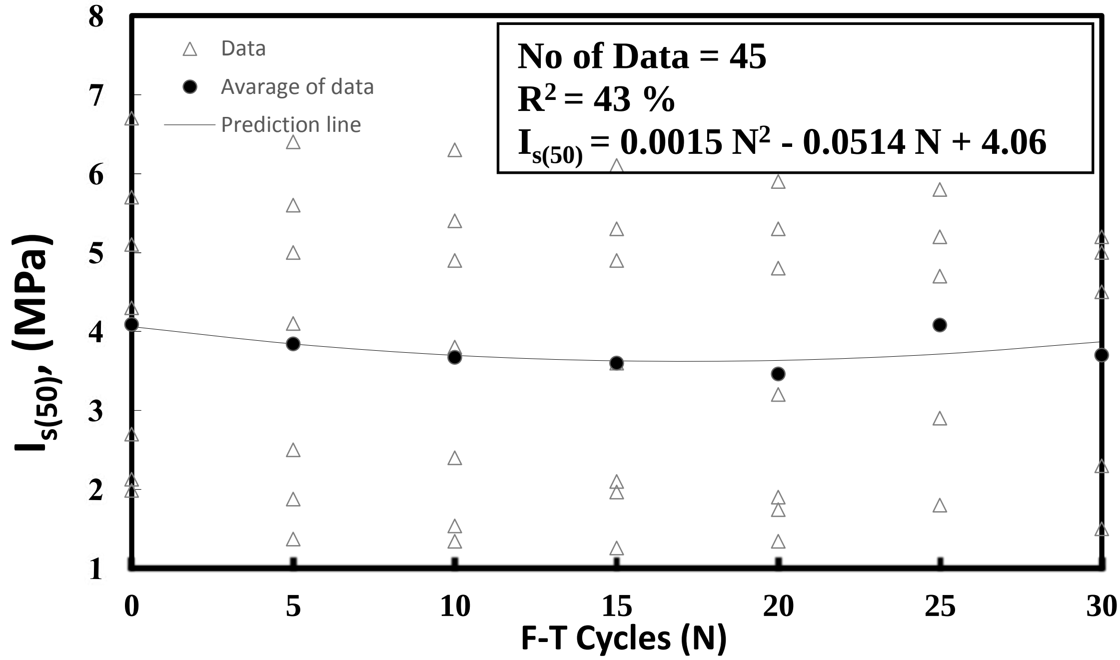

Fig 3. Variation of Point load index with the number of Freezing-Thawing cycles.

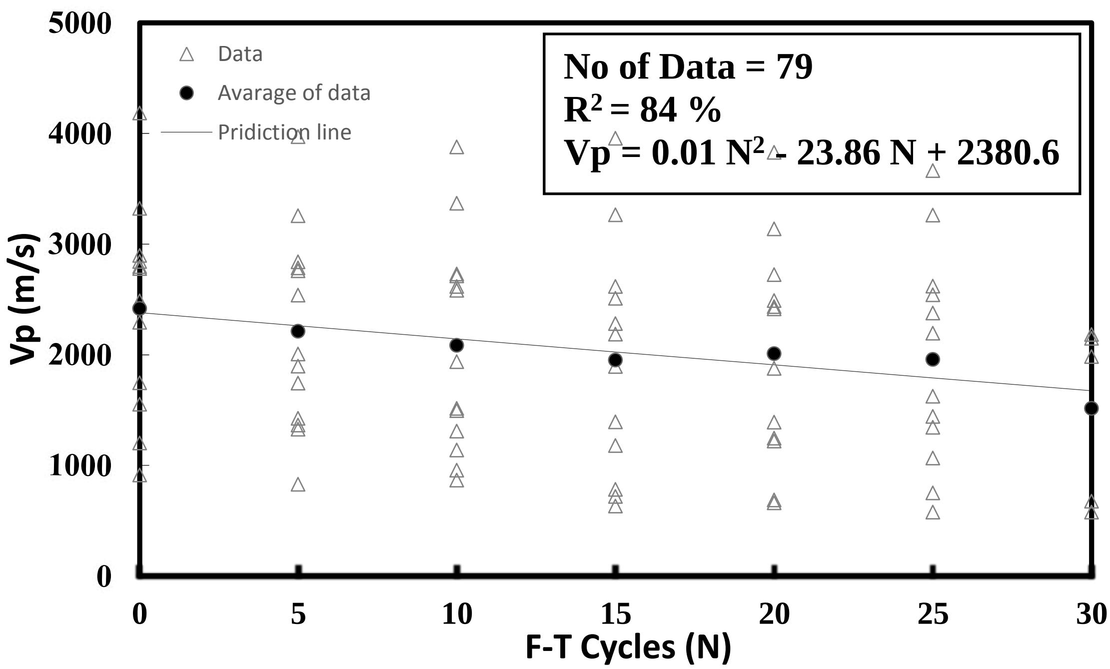

Fig 4. Variation of Pulse velocity with the number of Freezing-Thawing cycles.

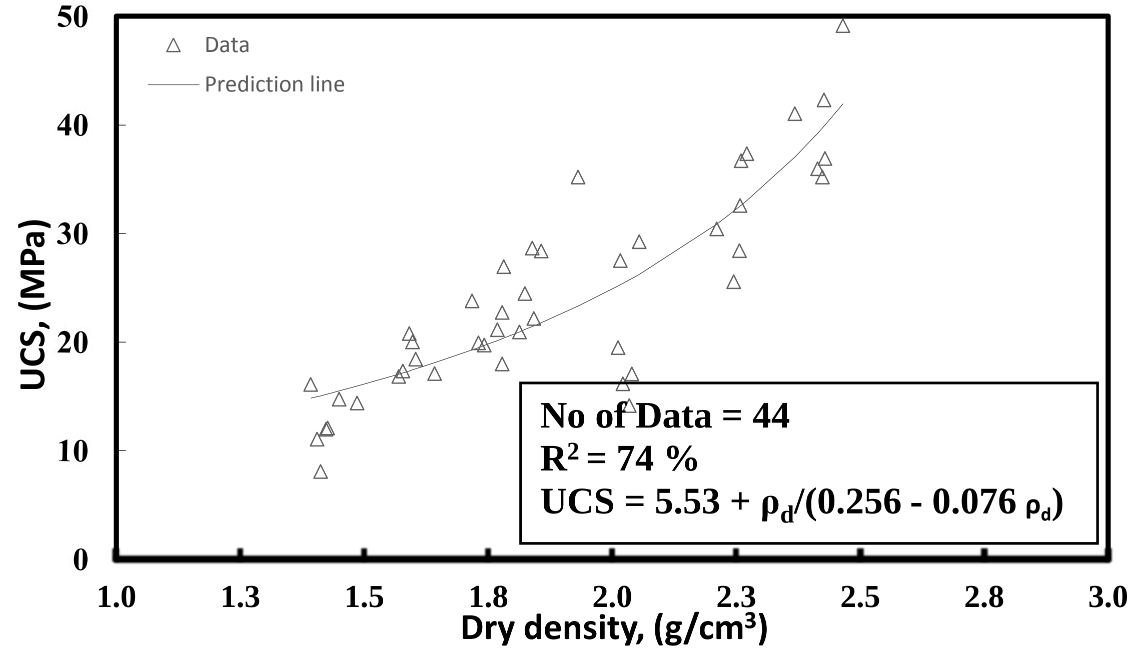

Fig 5. Relationship between Unconfined compressive strength with Dry Density.

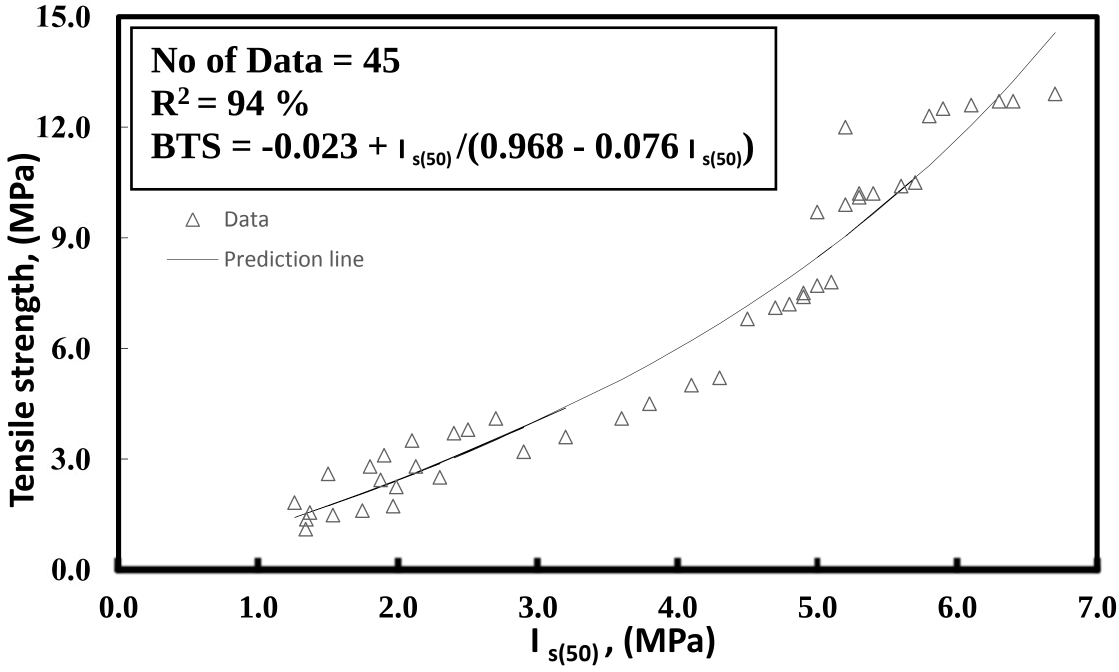

Fig 6. Relationship between Tensile strength and point load index.

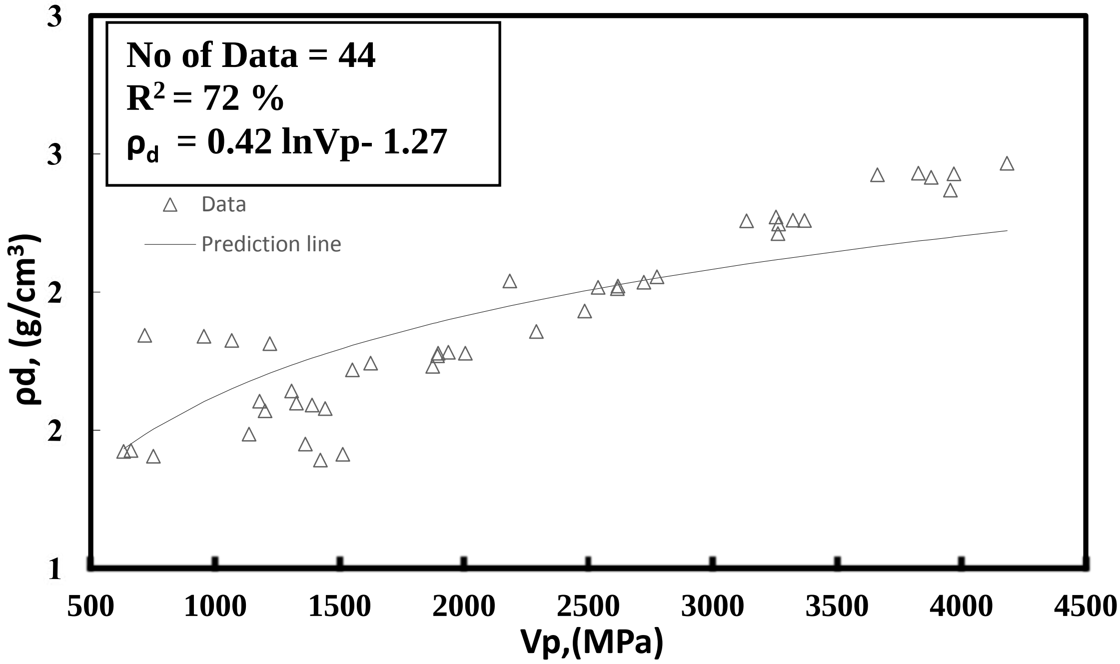

Fig 7. Relationship between Dry densities and Pulse velocity.

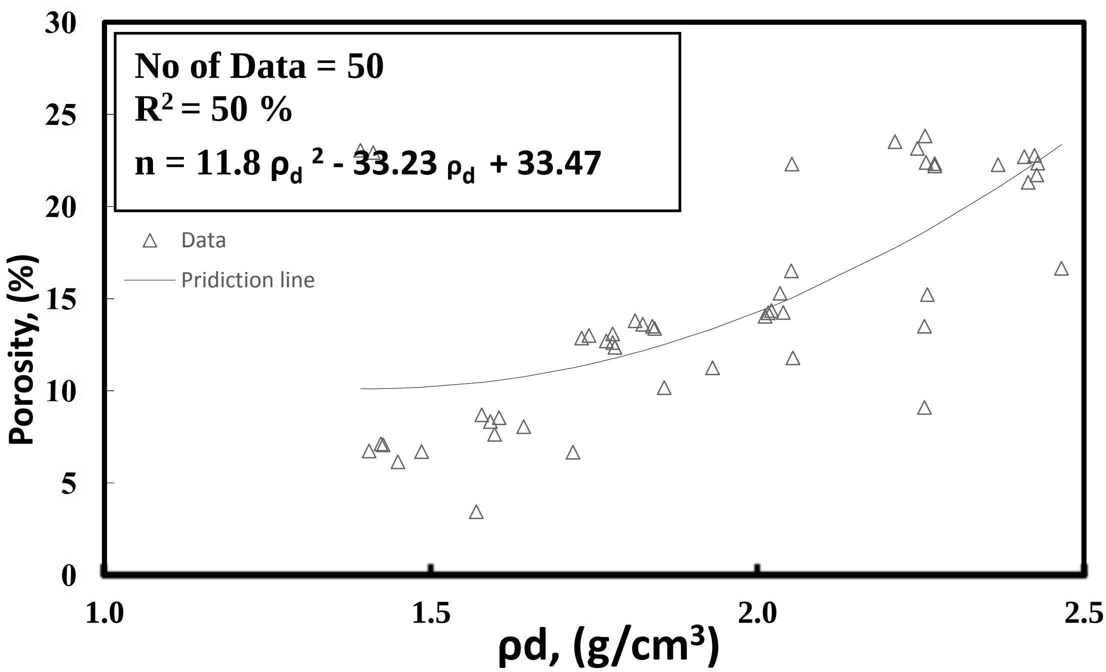

Fig 8. Relationship between Porosity and dry density.

ttp://jgu.garmian.edu.krd https://doi.org/10.24271/garmian.333

Legal Sanction of Construction Projects

Suzan Othman Qadir [1*] Payjor Ali Shonm [2]

[1] College of Law, University of Sulaimaniyah, Kurdistan Region, Iraq

[2] Construction Management Department, College of Engineering, University of Sulaimaniyah, Kurdistan Region, Iraq

Email: payjor.shonm@univsul.edu.iq

[*]Corresponding author. Email: susanalsaraf@yahoo.com

Abstract

The projects and implementer contractors in Sulaimaniyah area sometimes faced to the legal sanctions due to several reasons, like quality control, safety, health, security, financial, the legal aspects of the contract and the delay in the implementations or change in the design of the projects during the implementation of the projects which is the most frequent and important reason that happen in the projects and causes the sanction of the parties either contractor or the employer staff , , this study conducted to define the type and the responsible persons of the sanctions, and then to reduce or prevent the reasons that causes' sanctions, therefore particularly it was focused on the reasons that have related to the Iraqi General Conditions Contract (IGCC) gaps, which is all the contracts depends on, and signing the contracts accordingly. There are some items in the IGCC indicated the fault of the contractor and severe penalty that causes sanction of the contractor specially the item that related to the delay of and over passing the time scheduled duration. Those items were sometimes caused bankruptcy of the contractors during the in implementations of several constructional projects. There were some characteristics and parameters have direct effects on the variation orders and that changes, but the IGCC did not specialized any item for sanction with the responsible persons.

This study was focused on the reasons that have related to the legal aspects, specially the sanction of the contractor and the faults of the designer which goes straight without taking any legal action against the Engineer. Therefore tried to collect information and indicate characteristics to help or facilitate to trying to decrease the delay, minimize and prevent the sources and making suggestion to modify that items that have affect on the delay of the projects in design and implementation stages of the projects and finally have effect on the sanction of the contractors and the designers. The data collection for this study depended on reviews which collected from various projects in constructional fields, some informationn were collected from the actual implemented projects and other some from the experience of contractors and engineers that have implemented projects and faced to the delay and suffered from the side effects of the variations during the implementation of the projects, in

other hand there are some other different causes also has effects on the delaying and sanction like financial causes, quality control, risk controlling safety and health that causes sanction of the contractors and designers.

Keywords: Constructional projects contract, Contractor and designer sanction, Iraqi general contract conditions, Legal aspects, Punishment, Reasons of variation order

1. Introduction

Taking legal action against any faults with any clients is very necessary to manage and control the quality of the work and monitoring the time schedule during or after implementation of the projects this legal action called sanction of the contract. This study focused on some items in the IGCC that have very severe sanction against the contractor due to his faults and some items that had not appointed any sanction or action against employer clients, specially the faults of the designer which causes variation orders in the design and delay in projects and causes elapsing the time from the planned time scheduled duration.

There are many different reasons causes sanction, moreover there are various stages occurring mistakes and faults, each stage have its own reasons and characteristics as classified below:[1]

Stags that occurs mistakes and faults with or without sanction in projects as detailed below and shown in Fig 1.

1. Forecasting and budgeting stage.
    a. Finding a suitable project to be match with the budget and necessity of the project for the selected area.
    b. Getting necessary routine approvals.
    c. Performing phisability study
2. Planning design and scheduling stage.
    a. Planning for the project
    b. Time scheduling.
    c. Selecting a suitable location, land and area
    d. Selecting a suitable designing staff
    e. Considering safety and health for all the stages of the project.
    f. Considering the risks and planning for the risks.
    g. Selecting a suitable method for implementation like tendering, direct implementation.
    h. Selecting a liable contractor or staff to perform the job.
    i. Consideration of insurance
    j. Quality control consideration.
    k. Financial capability of the company implementer.
    l. Designing the project

3. Implementation stage
    a. Planning for implementation the project
    b. Monitoring the implementation and observation the project by the employer.
    c. Selecting a suitable implementation staff.
    d. Selecting a capable and suitable grade and special contractor.
    e. Considering safety and health for all the stages of implementation.
    f. Considering the risks and planning for decreasing the risks.
    g. Consideration of insurance.
    h. Type of the contract between the contractor and employer.
    i. Financial capability of the company implementer.
    j. Obey to all items of the general conditions of contract by both parties.
    k. Paying the payments according to the time schedule

    Several of the projects in Sulaimaniyah, were faced to temporary stopping and arranging the variation orders for the changes due to the availability of deficiencies in the design in the contract, therefore most of the projects to be stopped from the beginning for several months.

    For identifying the exact reasons of the delay, the old projects that had been completed should be taken in to consideration and study. Therefore this study depended on questionnaires review, among engineers that have actual experience about the site supervision and implementation of constructional projects, those who have experience about the contractors that actually suffered from delays and their projects were delayed because of different reasons. The result of questionnaires had been collected and tabulated then through using some statistical equations have been analyzed and summarized in Table 1 and 2, then accordingly explained the effects of the related characteristics as shown in the Figure 2 and 3 [2].

According to the Iraqi law sanctions had been specialize and applied for all types of the faults according to the size and their circumstances, below some of the sanctions that related to the constructional works.

The authority has the full power to face the contractors and undergo in the following fields:

First: The authority of observation and direction. The employer has the authority to make continuous observation and direct the contractor from time to time.

Second: The authority of modification of the contracts. The employer has the authority to modify the contract whenever or wherever needs modifications.

Third: The authority of sanctions of the contractor: The employer has authority to apply three types of sanctions:

A. Financial Sanctions;
   a. Includes the penalty: for the delay beyond the deadline of the contract.
   b. Compensation for damages:
   c. Confiscation of contract
B. Nonfinancial Sanctions ore obligatory.
   a. Put the hand on the site.
   b. Purchase on contractor's account.
   c. Withdraw the work from the contractor.
C. Termination of Contract: either with or without fault of contract.

Fourth: The authority of termination of the contract.

Types of termination of Contract:

A. Abolition by agreement.
B. Judicial dissolution of the contract.
C. Administrative termination of Contract [3].

2. Literature Review:

1. According to the FIDIC, various types of sanctions applied to the contractor faults, but there were not applied any sanction towards employer's clients. Two types of sanctions applied on contractor, financial and personal sanctions, the financial sanction applied for delay, performing unqualified works, withdraw of works, confiscation of insurance, while the employer delays the contractor payment without having power to take any action against the employer, and the routine system let the works complex and difficult to implement. The personal sanctions prison of the contractor on the site [4].
2. According to the General Contractors Conditions (GCCI), various types of sanctions applied to the contractor faults, but there were not applied any sanction towards employer's clients. Two types of sanctions applied on contractor, financial and personal sanctions, the financial sanction applied for delay, performing unqualified works, withdraw of works, prison of the contractor on the site, while the employer delays the contractor payment without having power to take any action against, or due to the routine the works would complex and to be difficult to implement [5]. While only some limited small administrative regulations applied as sanctions on the employers clients like (warning letter, rebuke letter, notification letter, transfer between the locations, unpaid working.)[6].

3. The study mentioned all the types of sanctions towards the contractor, the designer engineer and any person whom start construction without license, decreasing the routine system and time limitation for the to perform any approval documents, sanctions to by applied on the contractor that implement the projects with lack of quality or not match the specifications, in addition the insurances, but the research never mentioned the sanctions towards the employer's faults [7].
4. The Law applied the sanction towards the responsibility on both contractor and the architectural designer engineers, if the whole building fails or a part of the building fails during first 10 years of completion, both of the engineer and the contractor is responsible of the fault, according to the article no. 870 of the Iraqi civil law no. 40 on 1951[6]. The same sanction is available in the Jordan law no. 43 on 1976 article no. 788, 651 in Egypt law no. 131 on 1948 and 1792 in francs law, and article 744 of the Palestine civil law no. 4 of 2012, the sanction may be financial and/or personal prison[8].
5. Algerian law in 1975 applied the sanctions in article 554 towards the responsibility on both contractor and the architectural designer engineers, if the whole building fails or a part of the building fails during first 10 years of completion, both of the engineers and the contractor is responsible of the fault, according to the article no. 554 [9].
6. Britain law applied the sanction at 1939 towards the responsibility on both contractor and the architectural designer engineers, if the whole building fails or a part of the building fails during first 6 years of completion, or after 12 years of completion, both of the engineer and the contractor be responsible of the fault, according to the article no. 554 [10].
7. The author detailed in all the types of sanction due to the fail a part or all the building, but did not mention any sanction against the employer towards their faults [11].
8. A Study conducted in the United States of America, due to setting a high level of sanctions has the impact of triggering a defense by the labors, that causes shifting the mechanism, from managers of the firms that supervising production to the verifying legality of the law, this situation had effect of the production and caused decreasing the productions, therefore the managers modified the labor contracts from the long term to the short terms, daily basis, weekly basis or monthly basis. The side effect of modifying the contracts was to decrease the products [12].
9. Internal Policy for the Engineers Union in Iraq, not applied any sanction on government clients for any unfair action towards the contractors [13].

10. In the case of default delays of contractor payments by the government side more than 28 days, there is no any sanction towards the default client, but law let the contractor to claim and ask for financial compensation of the delayed payment, the payment consider as an official interest which is between 4%-7% in a year [4], [5], [14].
11. Criminal punishment applied in Kuwaiti law, the punishment may be execution, permanent prison, temporary imprisonment, or the sanction may be financial, like penalty or confiscation [15].
12. The Sanction Law no, 111 and all the modifications, were not mentioned applying any sanction towards whom make the routine system more complex or to whom delay the contractor projects works [16].
13. The Iraqi legal system regulation 1929 for disciplining the governmental employees had not specialized any article to punish any client towards obstacle contractors [17].
14. The research explained the sanctions that applied towards the failure of a part or whole the building, but did not mention any sanction towards employer clients who delay the contractor's payments or make the routine system more complex for the contractor [18].
15. The report in very comprehensive and investigated about deficiency in the law, and made a suggestion list to modify the regulation and instructions, but did not mention any suggestion of modify the routine system and not suggested any sanction towards the clients who delay the payment or be an obstacle for the contractor [19].
16. The law of retirement and social insurance for workers or privet sector and all the amendments, specialized articles to reiteration of all employees in the private sector with the director of the companies, but the law not included the owners or who has shears or participants in the companies or the contractors, therefore the contractors considers that it is as a punishment for working in the private sectors [20].
17. Pre advanced payment, if the contractor been paid for a pre advanced payment, could provide the materials on time and pay for the workers and labors on time and success on the work, vies versa could not goes according the plan and finally delayed and face to the sanctions [21].
18. The Law applied the sanction towards the responsibility on both contractor and the architectural designer engineers, if the whole building fails or a part of the building fails during first 10 years of completion, both of the engineers and the contractor is responsible of the fault [22].

3. Objectives:

Explaining the applied sanctions and applying unfair legal sanctions during the implantation of the projects, or during the design of the projects towards the contractors, and suggesting some suitable points to modify the IGCC and the legal instruction in order to decrease or prevent the delay or mistakes in the projects in the stages of forecasting, designing, planning and implementation of the projects and avoiding applying unfair sanctions on the responsible clients.

This study focused on finding the main reasons that causes sanctions that faced to the contractors which leads to delay, stopping the works of projects, bankruptcy of the contractors or losing a huge amount of contractor's money in constructional projects, in other words trying to decrease the limit of the range or avoid making variation orders during the implementations stage which happens resulting from the deficiencies of the design or the contract.

4. Methodology:

This study depended on theoretical and practical data reviews, for collecting of the theoretical data 20-related papers has been reviewed as summarized in Table 3, and for collecting the practical data 30-no. of questionnaire forms had been distributed among various scientific level of engineers that have experience in construction field , residential engineers and the site engineers. Each form was consists of two parts of clients for review as follow:

1. Employer's client related questionnaire forms. 7-related sensitive factors had been selected and distributed through Google form's facility among the academic class of society, the engineers could vote for the impact of the answers from (1 to 5), which means (un available, low importance, neutral, important, very important) in sequence, then analyzed the data's as summarized in the Table 1.
2. Contractor's client related questionnaire forms. 6-related sensitive factors had been selected and distributed through Google form's facility among the academic class of society, the engineers could vote for the impact of the answers from (1 to 5), which means (un available, low importance, neutral, important, very important) in sequence, then analyzed the data's as summarized in the Table 2.

The voted answers were analyzed through an important sensitive statist equation 1, which called the Relative Important Index (RII) equation, then the RII was been found as summarized in the last column of the same Tables 1 and 2.

$$\text{RII} = \frac{\sum_{i=1}^{5} \quad Wi * Xi}{A * N} \qquad (1)$$

Where:

RII – Relative Importance Index
W –Weighting given to each factor by the respondents and ranges from 1 to 5
X – Frequency of the response given for each cause
A – Highest weight (i.e. 5 in this case)
N – Total number of respondents.

5. Results and Discussion:

70-questionnaire related forms had been distributed among the engineers' voters.

30-questionnaire forms that were related to vote of 30 engineers were completely returned for each of the employer's client and the contractor's related clients, and the result summarized as follow:

5-1: Employer's Related Factors:

The five most important related factors had been selected according to the RII factors. The results were sorted according to the RII impact factor's as shown in figure 2:

- The impact of routine system's effect in the directorates was 0.87.
- The impact of Designer's Engineer's effect was 0.89
- The impact of lack of trusting in Banks effect was 0.82
- The impact of weakness of laws and regulations effect was 0.75
- The impact of financial sectors effect was 0.63
- The effects of contract monitoring engineers and the resident engineers were poor; the impacts were only 0.59 and 0.55 in sequence.

While the delays occurs in the projects, the employer should investigate about the reasons and find the reasons that have related to the employer faults especially if the fault was include one of the 5-important impact factors that have been mentioned in the Table 1, The employer should take action and make sanctions for the defective client

5-2: Contractor's Related Factors:

The five most important related factors had been selected according to the RII factors. The results were sorted according to the RII factor's impact as shown in figure 3:

- The impact of financial ability effect was 0.86.
- The impact of contractor himself effect was 0.75
- The impact of lack of logistics section effect was 0.72
- The impact of project manager effect was 0.71

- The impact of monitor effect was 0.66
- The effects of monitors and the site engineers poor; the impacts were only 0.66 and 0.64 in sequence.

While the delays occurs in the projects, the Contractor should investigate about the reasons and find the reasons that have related to the Contractor especially if the fault was within one of the 5-important impact factors that have been mentioned in the Table 2. The contractor should take action and make sanctions for the defective client in order to avoid frequent repetition and continuous delays.

5-3: Sanctions Result:

After reviewing 20 numbers of papers, noticed that 16 of papers mentioned the applied sanctions on contractor, designer and the employees which is 70%, and other 6-papers mentioned the power of employer to have ability to make financial and/or personal actions towards the contractors without any sanctions which is 30%, as summarized in Table 4.

The Clients who were already sanctions applied on were 70%, and the other 30% which is the employer client were not applied any sanction of towards their faults as shown in Figure 4.

6. Conclusions:

The study conducted to manage the legal sanctions towards the employer’s and contractor’s clients that were not performed their duties in an accepted range, and caused deficiencies and faults in the projects. The legal aspects were taken in to consideration in this study; there were two main parties;

1. **Employer Clients:** The impact factors for the employer’s clients were very effective, especially the 5-most clients that had RII between (0.87 – 0.63), as shown in Fig. 2
   - The impact of routine system’s effect in the directorates was 0.87.
   - The impact of Designer's Engineer’s effect was 0.89
   - The impact of lack of trusting in Banks effect was 0.82
   - The impact of weakness of laws and regulations effect was 0.75
   - The impact of financial sectors effect was 0.63

   The study focused on managing legal sanctions towards the employers’ clients’ faults that may not applied a fair or eligible punishment that caused losses of the contractors or leads to bankruptcy due to occurring small mistakes in the implemented works by the contractor. The graphs explained that routine system had the main roll for dealing the projects while there was no any sanction towards the routine system, in addition the government proud of the routine system which caused delays and cost losses by several contractors.

The designer engineers takes the second rank in rolling responsibilities for delaying through occurring a lot of deficiencies and performing unqualified designs, that caused delays or implementing un suitable work, while no any sections applied towards the faults of designers neither in GCCI, FIDIC no in Civil Laws No. 40.[4], [5], [6].

2. **Contractor Clients:** The impact factors for the contractor's clients were effective, especially the 5-clients that had RII between (0.86 – 0.66), as shown in Fig. 3
   - The impact of financial ability effect was 0.86.
   - The impact of contractor himself effect was 0.75
   - The impact of lack of logistics section effect was 0.72
   - The impact of project manager effect was 0.71
   - The impact of monitor effect was 0.66

This study focused on the contractors faults especially the reasons that shown in the graphs, and noticed that the legal articles sanctions available and they are accurate against any delay or unqualified performed items. Therefore the contractor subjected to the punishment due to his faults. [4], [5], [6]

3. Sanctions Applied:

70% of all the faults related to the contractor and the designer sanctions applied for as shown in Fig. 4

30% of the faults related to the employer were not applied legal sanctions for.

Recommendations:

1. The design section should use local or foreign experts to assist them towards decreasing or avoiding to making variation orders that resulted from designers faults.

2. Modify article no, 62 of the GCCI, involving sanction to be applied on the employer in case causes to delay of contractor's payments, and compensation to the contractor and offers the right to the contractor to temporary stop the works.

The existing sanctions should be reviewed, and the Sanctions suggested to be applied for the employer's faults as summarized in the table 1.

References:

[1] Murali Sambasivan, Yau Wen Soon, Causes and effects of delays in Malaysian construction industry, International Journal of Project Management 25, 517–526, 2007.

[2] A.A. Aibinu, G.O. Jagboro, The effects of construction delays on project delivery in Nigerian construction industry, International Journal of Project Management 20 , 593–599, 2002.

[3] د. نجيب خلف أحمد الجبوري, "القانون الأداري", كتاب صادر من جامعة السليمانية, الطبعة الأولى ، ص 340-352 ، 2015.

[4] FIDIC, article (8.4 and 8.4) page 31, 2006.

[5] IGCC, article (7, 8, 22, 25, 27, 40, 41, 48, 54, 89.).

[6] Iraqi Civil Laws no. 40, Article   , modified on 1951.

[7] د.سوزان عثمان قادر ، أطرحة دكتورا مقدمة الى مجلس كلية القانون و السياسة جامعة صلاح الدين – أربيل ، ص 221-229 ، 2015

[8] Iraqi Civil Laws no. 40, Article 868, 869, 870, 871, modified on 1951.

[9] أ: عايدة مصطفاوي ، الضمان العشري و الضمانات الخاصة لمشيدي البناء في التشريع الجزائري والتشريع المقارن ، دفاتر السياسة و القانون ، 2012.

[10] خالد حسن عبدعلي ، دراسة عن الضمان العشري لعقود مقاولات الإنشاء استنادا للمادة (٨٧٠) من القانون المدني العراقي رقم (٤٠) المعدل ، 1951

[11] د. محمد جابر الدوري، مسؤلية المقاول و المهندس في مقاولات البناء و المنشأت الثابتة بعد أنجاز العمل و تسليمه، 1985.

[12] Oded, Marcin Jakubek, Employer sanctions, and the welfare of native workers, Economics Letters 117, 533-536, 2012.

[13] Internal Policy for the Engineers Union in Iraq.

[14] Iraqi Civil Laws no. 40, Article Iraqi Civil Laws no. 40.

[15] أ.د.سامي محمد فريج ، التخطيط للعقد، ص109، 2007.

[16] قانون العقوبات رقم 111 المعدل – الكتاب الثاني – الجرائم المضرة بالمصلحة العامة، لسنة 1969

[17] النظام القانوني لتأديب الموظف العام في القانون العراقي، 1929

[18] مروه خالد خنطيل ، ضمان المقاول والمهندس في التشريع العراقي الضمان الخاص، بحث مقدم إلى مجلس كلية القانون / جامعة القادسية، 1929

[19] تقرير لجنة قطاع البناء والتشييد ، تحليل الوضع الراهن للقطاع من الجانب الاقتصادي و و الأقتراحات و التوصيات العامة لتطوير قطاع التشييد

[20] قانون التقاعد والضمان الاجتماعي للعمال المعدل رقم 39 لسنة 1971.

[21] الشروط العامة للمقولات و والأعمال الهندسية المادة ( ).

[22] عادل عبد العزيز عبد الحميد سماره ,مسؤولية المقاول والمهندس عن ضمان متانة البناء في القانون المدني الأردني" دراسة مقارنة ,"جامعة النجاح الوطنية ,كلية الدراسات العليا، ص 73-77، 2007.

Table 1: Delay Management Templates (Responsible Persons), Weight, frequency and impacts due to the Contractor faults.

			Impacts					
No.	Employer	Templates	1	2	3	4	5	RII
1	Routine system	to what extent the contractor should subject to the government complex Routine system without considering size and priority of the project by the government.	1	0	3	6	20	**0.89**
2	Designer's Engineer	To what extent the Design, Bill of quantities, Drawings and the tender documents are includes deficiencies	0	1	2	12	15	**0.87**
3	Lack of Trust in Bank	To what extent the banks have the lack of facilitation, not paying the lone to the contractors and they do not payback even the contractors deposits	0	1	7	10	12	**0.82**
4	Weakness of laws and Regulations	To what extent the week of laws and regulations are not support the legal rights of the contractor	0	2	8	15	5	**0.75**
5	Financial Sector	To what extent the Employer's financial sector delay the contractor payments even all the related documents are legal without any deficiencies	4	5	7	11	3	**0.63**
6	Contract Monitoring Manager	To what extent the contract monitoring employer's manager delay, ignore and be an obstacle towards the contractor's requirements even all the requirements are legal.	4	5	11	9	1	**0.59**
7	Resident Engineers	To what extent the Employer's Resident Engineers to be an obstacle towards progressing of the projects and they do not let the works to go on normally even all the events pursuits according to the lows.	3	4	21	2	0	**0.55**

Table 2, Literature Review Table

Reference No.	Author	Volume and page	Title of the research	Client	Fault	Sanction	Recommendation
[1]	Murali Sambasivan Yau Wen Soon	25 517–526 2007	Causes and effects of delays in Malaysian construction industry	Contractor	delay shortening unqualified Failure	withdraw of works, confiscation of insurance	Deducting the penalty according to the Priority of the Projects
[2]	A.A. Aibinu, G.O. Jagboro	20 593–599, 2002	The effects of construction delays on project delivery in Nigerian construction industry	Contractor	delay shortening unqualified Failure	withdraw of works, confiscation of insurance	Deducting the penalty according to the Priority of the Projects
[3]	د. نجيب خلف أحمد الجبوري	-340 352 2015	القانون الأداري	Contractor & Architectural Designer	Failure within 10 years	Financial Personal	Stay the law as it is
[4]			FIDIC	Contractor & Architectural Designer	Failure within 10 years	Financial Personal	Stay the law as it is
[5]			IGCC	Contractor & Architectural Designer	Failure within 10 years	Financial Personal	Stay the law as it is
[6]		Article 40 1951	Iraqi Civil Laws no. 40	Contractor & Architectural Designer	Failure within 10 years	Financial Personal	Stay the law as it is
[7]	عادل عبد العزيز عبد الحميد سماره		مسؤولية المقاول والمهندس عن ضمان متانة البناء في القانون المدني الأردني	Contractor & Architectural Designer	Failure within 10 years	Financial Personal	Stay the law as it is
[8]	Article 868, 869, 870, 871, modified on 1951		Iraqi Civil Laws no. 40	Contractor & Architectural Designer	Failure within 10 years	Financial Personal	Stay the law as it is

Reference No.	Author	Volume and page	Title of the research	Client	Fault	Sanction	Recommendation
[9]	أ:عايدة مصطفاوي		الضمان العشري و الضمانات الخاصة لمشيدي البناء في التشريع الجزائري	Contractor & Architectural Designer	Failure within 10 years	Financial Personal	Stay the law as it is
[10]	خالد حسن عبدعلي	870 1951	دراسة عن الضمان العشري لعقود مقاولات الإنشاء استنادا للمادة (٨٧٠ من القانون) المدني العراقي رقم (٤٠)المعدل ، 1951	Contractor & Architectural Designer	Failure within 6 years or 12 years	Financial Personal	Stay the law as it is
[11]	د. محمد جابر الدوري	1985	مسؤلية المقاول و المهندس في مقاولات البناء و المنشأت الثابتة بعد أنجاز العمل و تسليمه	Contractor & Architectural Designer	Failure within 10 years	Financial Personal	Stay the law as it is
[12]		117 533-536, 2012	Oded, Marcin Jakubek	Employees	Severe Sanction	Limitation contract from long term to short term contract	Stay the law as it is
[13]			Employer sanctions, and the welfare of native workers	Contractor & Architectural Designer	Failure within 10 years	Financial Personal	Stay the law as it is
[14]		Iraqi Civil Laws no. 40	Iraqi Civil Laws no. 40	Employer	Delaying the payments	No Sanction	Sanction to be applied
[15]	أ.د.سامي محمد فريج	109 2007	التخطيط للعقد	Contractor	Failure within 10 years	Financial Personal (Prison or execution)	Stay the law as it is
[16]		1969	قانون العقوبات رقم 111 المعدل – الكتاب الثاني – الجرائم المضرة بالمصلحة العامة	Employer	make the routine system more complex	No Sanction	avoiding routine system

Reference No.	Author	Volume and page	Title of the research	Client	Fault	Sanction	Recommendation
[17]		1929	النظام القانوني لتأديب الموظف العام في القانون العراقي	Employer	make the routine system more complex been as an obstacle to contractor	No Sanction	Sanction to be applied
[18]	مروه خالد خنطيل	1929	ضمان المقاول والمهندس في التشريع العراقي الضمان الخاص	Employer	make the routine system more complex	No Sanction	Sanction to be applied
[19]			تقرير لجنة قطاع البناء والتشييد ، تحليل الوضع الراهن للقطاع من الجانب الاقتصادي و و الأقتراحات و التوصيات العامة لتطوير قطاع التشييد	Employer	make the routine system more complex	No Sanction	Sanction to be applied
[20]		1979	قانون التقاعد والضمان الاجتماعي للعمال المعدل رقم 39	Employer	make the routine system more complex	No Sanction	Sanction to be applied

Table 3: Summary of Clients made Faults and Availability of Sanctions applied

Total Client made Faults	Detailed Client made faults	Frequency sanctions in Reviews	Availability of Sanction	Frequency of Sanction %	Accumulative Frequency of Sanctions **%**
Contractor, Designer and Employees	Contractor	3	Applied	15	**70**
	Contractor and Designer	10	Applied	50	
	Employees	1	Applied	5	
Employer	Employer	6	Not Applied	30	**30**

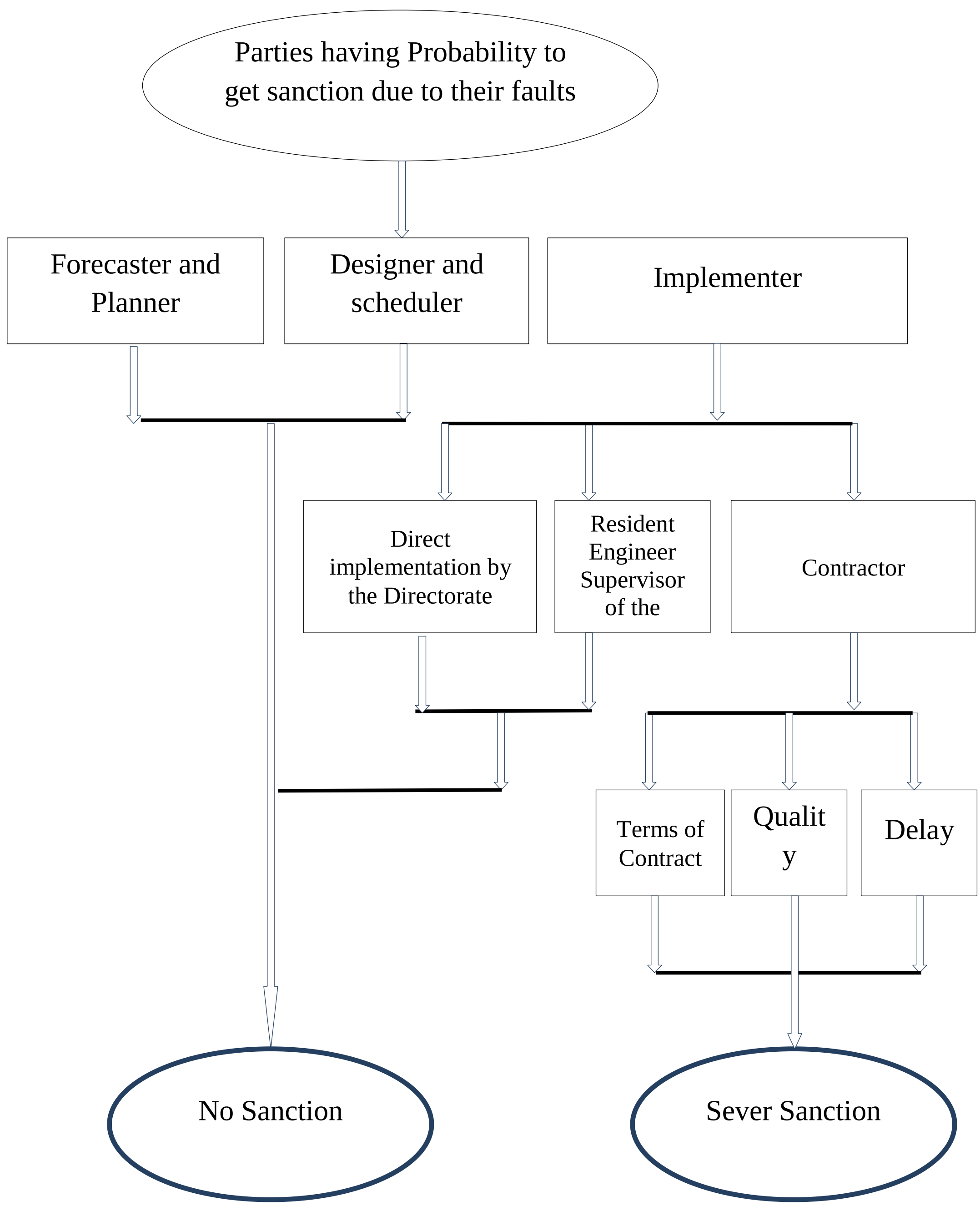

Figure. 1: Clients having probability to get Sanction and actual clients that really gets sanctions due to their faults.

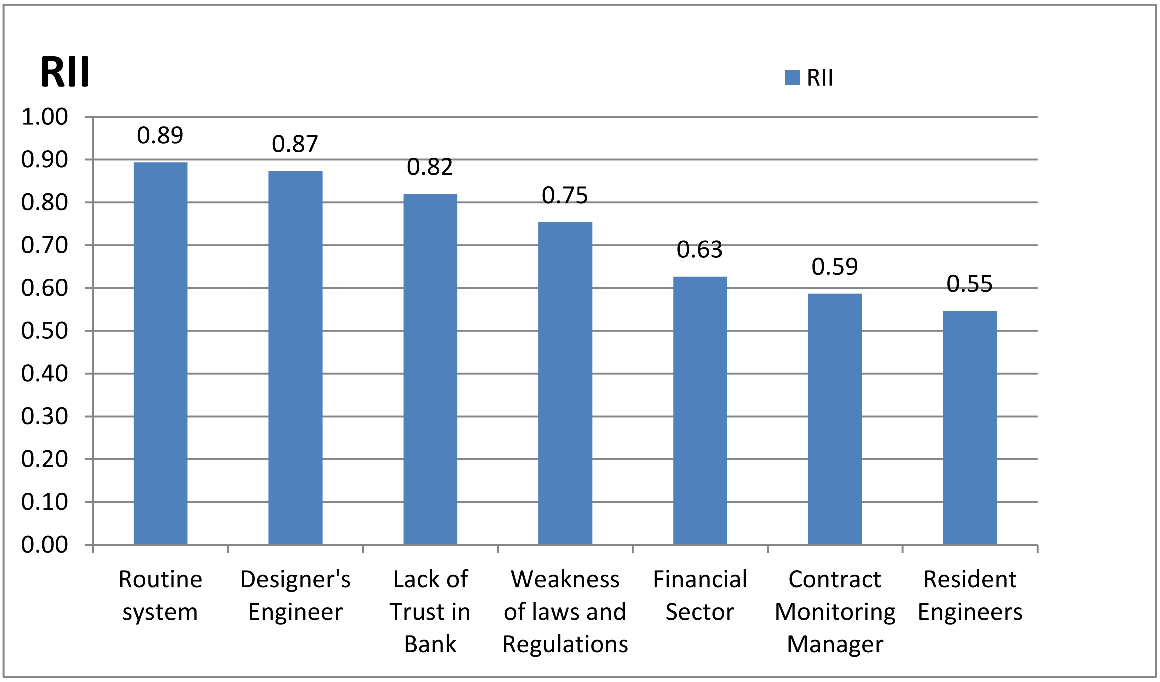

Figure 2, Employer's Parameters Impact

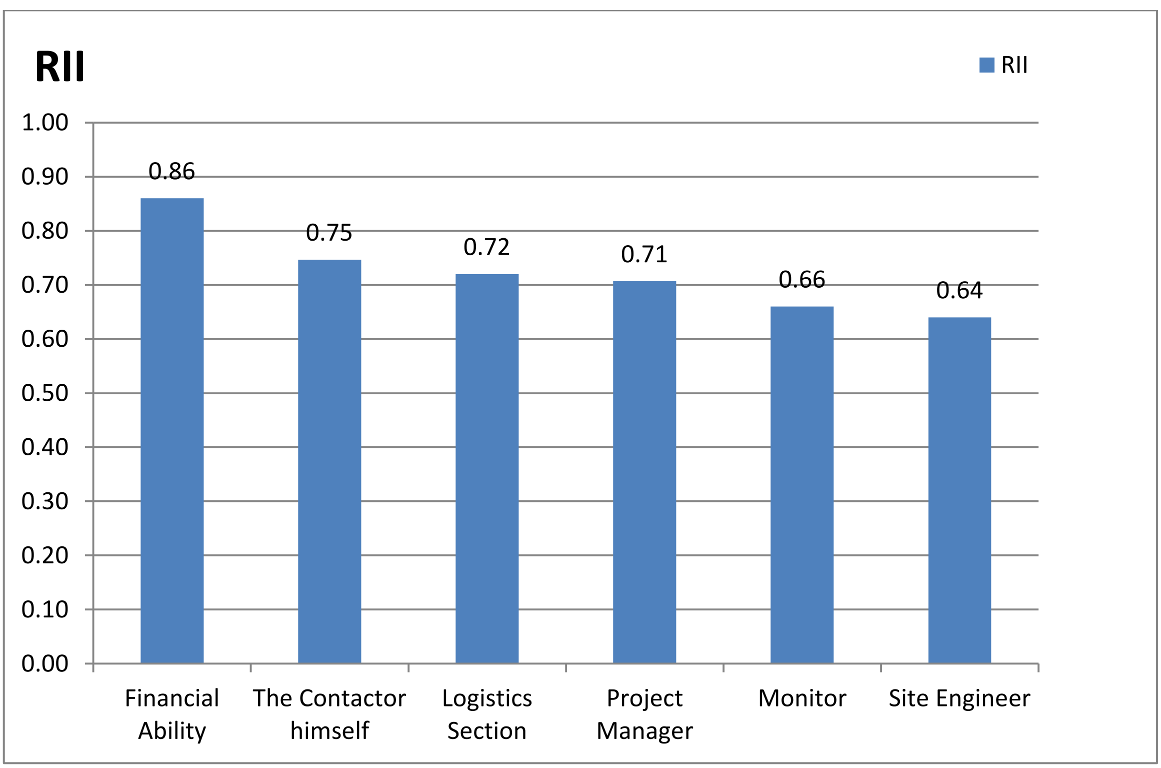

Figure 3, Contractor's Parameters Impact

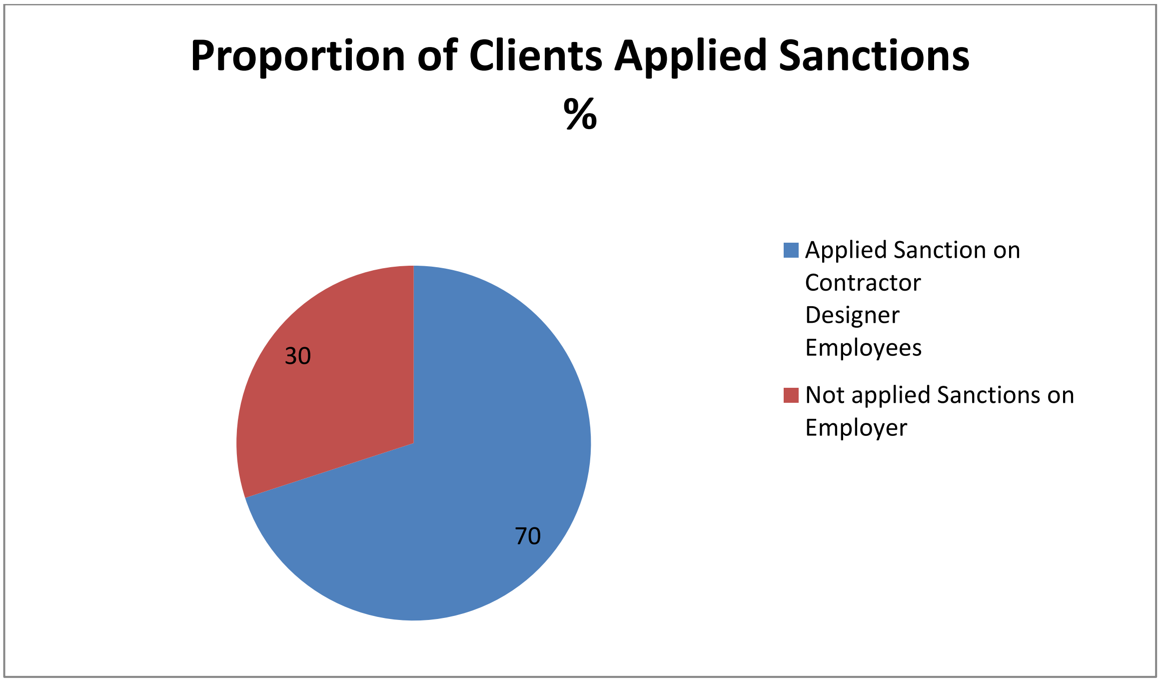

Figure 4, Proportion Clients Applied Sanctions

ttp://jgu.garmian.edu.krd https://doi.org/10.24271/garmian.334

Physical and Mechanical Properties of Metamorphic Rocks

Zozk Kawa Abdaqadir [1*] Younis Mustafa Alshkane[2]

[1] Civil Engineering Department, College of Engineering, University of Sulaimani, Al- Sulaimaniyah, Kurdistan Region, Iraq

[2]Civil Engineering Department, College of Engineering, University of Sulaimani, Al- Sulaimaniyah, Kurdistan Region, Iraq
Email: younis.ali@univsul.edu.iq

[*]Corresponding author. Email: Zozk.abdalqadir@univsul.edu.iq

Abstract

In this study, the relationships between the physical and mechanical properties of metamorphic rocks have been investigated based on data that were collected from previous studies. The data for the physical and mechanical properties of metamorphic rocks such as (Density, Young's modulus, Uniaxial Compressive Strength *(*UCS*)*, Porosity, Tensile strength, Specific Gravity) for some types of metamorphic rocks (Gneiss, Schist, Phyllite , Slate , Marble, Amphibolite, Hornfels and Quartzite) were collected from previous studies. The statistical analysis has been investigated in order to find the valuable relationships between physical and mechanical properties of the studied rock.. The results revealed linear relationships between those properties. Based on the coefficient of determination (R^2), the best linear correlations were obtained between Young's modulus and Porosity with R^2 of 0.86 whereas, the weak relationship was found between UCS and Specific Gravity of R^2=0.22. This indicates that there is not a direct relationship between UCS and specific gravity.

***Keywords*:** Metamorphic rocks; UCS; porosity; specific gravity; Physical Properties; Mechanical Properties.

1. Introduction

Metamorphic rocks are the rocks that formed from other rocks. They are sedimentary rocks or pyrotechnics that have changed due to extreme pressure and heat. The configured name defines where "meta" means change and "morph" means "form". Thus, mutated rocks are those whose shapes have been altered through a geological process

such as large tectonic movements and magma penetrations. Transient transformation occurs mainly due to changes in temperature; pressure exerted, and the introduction of chemically active fluids. For metamorphism to occur, there are some conditions which speed up the process that is the geologic events that happen on large scales such as the movement of the global lithospheric plate, the seduction of the lithosphere of the ocean, the collision of the continents and the spreading of the ocean floor. All the mentioned three have the consequence of rocks that are moving transport heat; these changes in pressure and temperature are the important variables in the changes in the rock texture (Owaid et al., 2015). In the North East corner of Arabia, Peninsula lays the country of Iraq. The country island to different contrasting geography that consists of the arid desert in the west of mountains that are rugged of Taurus and Zagros in the northeast; the two regions are separated by the fertile depression of Mesopotamia. In geology, Iraq is said to lie in the transition between the Arabian Shelf and the damaged areas of Taurus and Zagros Zones in the North and North East (Al-Juboury et al., 2009).
The design of underground structures such as road tunnels and rail tunnels depends on the data collected through the physical and mechanical properties of the rocks. These geotechnical properties of rocks play an important role in design, safety, stability and rock structures when they are exposed to heterogeneous areas in situ resulting from excess stresses, tectonicity and gravity, which are locally complicated by water pressure and pressure , Persuaded by the excavations. The physical and mechanical parameters play a very important role in a precise forecast of rock behavior under such inconsistent conditions. The mechanical properties of rocks change with density, porosity, UCS, specific gravity, grain size, texture and effective pressures acting on them. Changes in physical and mechanical properties in metamorphic rocks lead to corresponding variations in failure pattern (Singh et al., 2017). In this study, the linear relationships between physical and mechanical properties of metamorphic rocks were investigated based on data collected from the previous studies.

2. Objective

This study aimed to investigate the correlations between the physical and mechanical properties of metamorphic rocks.

3. Materials and Methods

3.1 Materials

In this study based on literature different types of metamorphic rocks such as (gneiss, phyllite, schist, slate, hornfels, marble, quartzite, novaculite and amphibolite) were used for the correlation between the physical and mechanical properties of metamorphic rocks.

3.2 Methods

Based on previous studies for the physical and mechanical properties of metamorphic rocks such as (Young's modulus, E), (Density, ρ), (Uniaxial compressive strength, UCS), (Porosity, n), (Tensile Strength, σt),(Specific Gravity, Gs) data were collected as summarized in Table (1). and the correlation between those properties were conducted.

Table 1: Literature Review for the Physical and Mechanical Properties of Metamorphic Rocks

Reference	Location	Number of data collected from previous studies					
		Density ρ (g/cm^3)	Young's modulus E (GPa)	UCS (MPa)	Porosity n (%)	Tensile strength σt (MPa)	Specific Gravity Gs
Ozcelik, (2011)	Turkey	-	-	16	-	16	-
Jayawardena, (2011)	Sri Lanka	-	-	14	-	14	-
Siegesmund et al., (2011)	Germany	27	13	-	27	13	-
Kahraman et al., (2012)	Turkey	-	-	15	-	15	-
Tandon et al., (2013)	India	42	-	42	-	-	-
Benayad et al., (2013)	Korea						
Perras et al., (2014)	Switzerland	-	-	6	-	-	-
Talabi et al., (2014)	Nigeria	-	-	22	22	-	22
Barros et al., (2014)	Portugal	5	-	-	5	-	-
Gholami et al., (2014)	Malaysia	3	-	-	3	14	-
Khanlari et al., (2014)	Iran	6	-	-	6	-	6
El–Hamid et al., (2015)	Egypt	3	-	3	3	-	-
Mustafa et al., (2015)	Pakistan	-	-	10	-	10	-
Gegenhuber, (2016)	Australia	12	-	-	12	-	-
Chen et al., (2016)	China	35	-	-	35	-	-
Fereidooni, (2016)	Iran	8	8	8	8	-	-
Singh et al., (2017)	India	3	3	3	3	3	3
Udagedara et al., (2017)	Sri Lanka	5	-	5	5	-	5
Motra et al., (2017)	Germany	28	28	-	-	-	-
Su et al., (2017)	USA	-	9	-	-	9	-
Mishra et al., (2017)	India	-	11	-	-	-	-
Özbek et al., (2018)	Turkey	4	-	-	4	-	-

4. Results and discussions

4.1 Physical and mechanical properties

4.1.1 Density (ρ) (g/cm^3)

The density of the metamorphic rocks as summarized in Table 1. Based on total of 181 data varied from 2.04 to 3.29 g/cm^3 with a mean of 2.71, the standard deviation of 0.20**,** variance of 0.04, median of 2.7 and the coefficient of variation (C.O.V) of 7.35 as summarized in Table 2.

4.1.2 Young's modulus, E (GPa)

The young's modulus of the metamorphic rocks as summarized in Table 1. Based on total of 72 data varied from 10.44 to 217.44 GPa, with a mean of 74.22, standard deviation of 48.75, variance of 2377, median of 58.7 and the coefficient of variation (C.O.V) of 65.7 as summarized in Table 2.

4.1.3 Uniaxial compressive strength (UCS), (MPa)

The uniaxial compressive strength of the metamorphic rocks as summarized in Table 1. Based on total of 169 data varied from 8 to 355 MPa, with a mean of 104, standard deviation of 62.10, variance of 3857, median of 96 and the coefficient of variation (C.O.V) of 60 as summarized in Table 2.

4.1.4 Porosity (n), (%)

The porosity of the metamorphic rocks as summarized in Table 1. Based on total of 182 data varied from 0.02 – 10.95 %, with a mean of 3.1, standard deviation of 3.14, variance of 9.9, median of 1.9 and the coefficient of variation (C.O.V) of 101 as summarized in Table 2.

4.1.5 Tensile strength (σt), (MPa)

The tensile strength of the metamorphic rocks as summarized in Table 1. Based on total of 78 data varied from 2.3 to 18.1 MPa, with a mean of 8.61, standard deviation of 3.68, variance of 13.52, median of 8.35 and the coefficient of variation (C.O.V) of 43 as summarized in Table 2.

4.1.6 Specific Gravity, Gs

The specific Gravity of the metamorphic rocks as summarized in Table 1. Based on the total of 36 data varied from 1.72 to 2.84 with a mean of 2.61, the standard deviation of 0.26, variance of 0.068, median of 2.68 and the coefficient of variation (C.O.V) of 10 as summarized in Table 2.

4.2 Correlation between Physical and mechanical properties

Based on the collected data from previous for physical and mechanical properties for metamorphic rocks statistical analysis were studied as summarized in Table 2 and 13 linear relationships between those properties were investigated as presented in Table 3. And the graph for each relationships as shown in Fig. 1,2,3,4,5,6,7,8,9,10,11,12 and 13.

Table 2 Statistical Analysis for Metamorphic Rocks

Statistical Parameters	Density	Young's modulus	UCS	Porosity	Tensile strength	Specific Gravity
Range(Min,Max)	2.04 – 3.29	10.45 – 217.50	8 - 355	0.02 – 10.95	2.3 – 18.1	1.72 – 2.84
Mean	2.71	74.22	104	3.1	8.61	2.61
Std. Deviation	0.20	48.75	62.10	3.14	3.68	0.26
Median	2.7	58.7	96	1.9	8.35	2.68
Variance	0.04	2377	3857	9.9	13.52	0.068
C.O.V (%)	7.35	65.7	60	101	43	10
No. of Data	181	72	169	182	78	36

Table 3 Summary of Correlations between Physical and Mechanical Properties of Metamorphic Rocks

No.	Dependent variables	Independent variables	Equations	R^2	No. of Data	No of graph
1	Density , ρ (g/cm^3)	Young's modulus , E (GPa)	E = 189.41 ρ - 460.65	0.77	68	1
2	Density , ρ (g/cm^3)	UCS (MPa)	UCS = 179 ρ - 394.38	0.30	138	2
3	Density , ρ (g/cm^3)	Porosity,n (%)	N = -6.9915 ρ + 20.159	0.58	90	3
4	Density , ρ (g/cm^3)	Tensile strength (MPa)	σt = 15.616 ρ - 35.261	0.83	54	4
5	Tensile strength (MPa)	UCS (MPa)	UCS = 10.847 σt + 10.841	0.71	70	5
6	Tensile strength (MPa)	Young's modulus , E (GPa)	E = 4.3448 σt + 0.4039	0.66	47	6
7	Young's modulus , E (GPa)	UCS (MPa)	UCS = 0.9437 E + 31.621	0.72	72	7
8	Density , ρ (g/cm^3)	Young's modulus/Tensile strength	E / $σ_t$ = 34.214 ρ - 85.763	0.78	52	8
9	Young's modulus , E (GPa)	Porosity, n (%)	n = -0.0047 E + 0.951	0.86	58	9
10	Specific Gravity , Gs	Density , ρ (g/cm3)	ρ = 1.5366 Gs - 1.4632	0.54	33	10
11	UCS (MPa)	Specific Gravity , Gs	Gs = = -0.0004 UCS+ 2.743	0.22	32	11
12	Tensile strength (MPa)	Specific Gravity , Gs	Gs = 0.0049 σt + 2.6401	0.48	36	12
13	UCS (MPa)	Young's modulus / Density	E / ρ= 0.1602 UCS + 8.5131	0.60	72	13

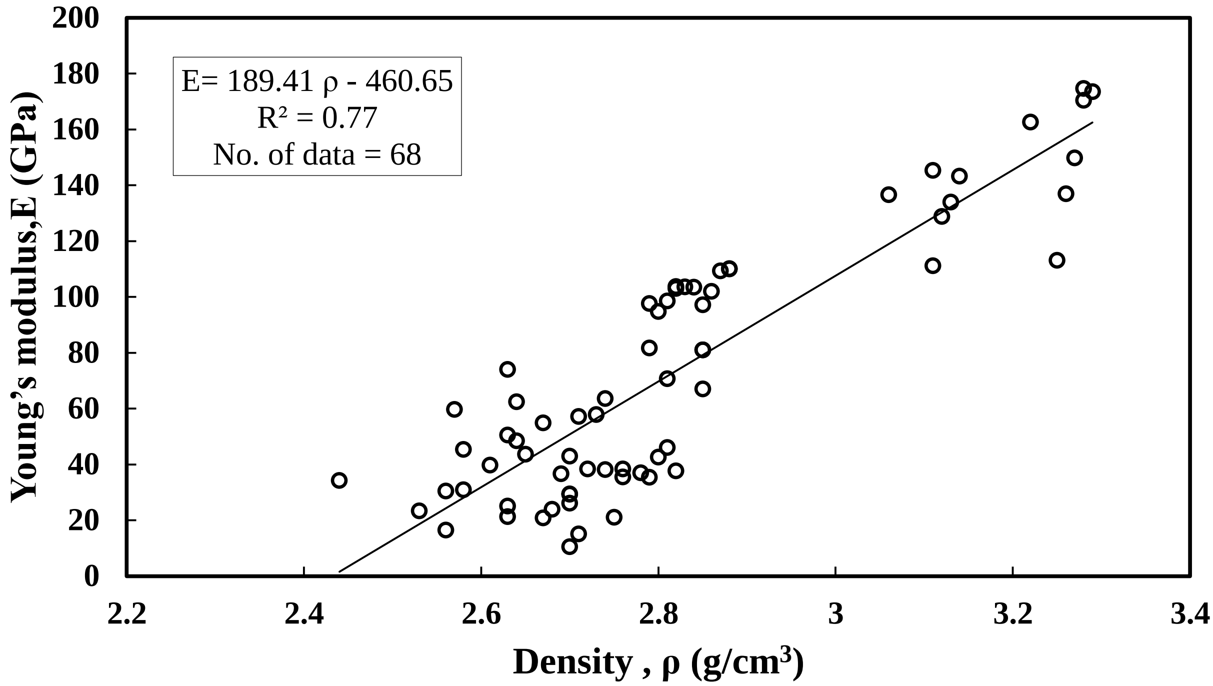

Fig. 1 linear variation between density (ρ) and Young's modulus (E)

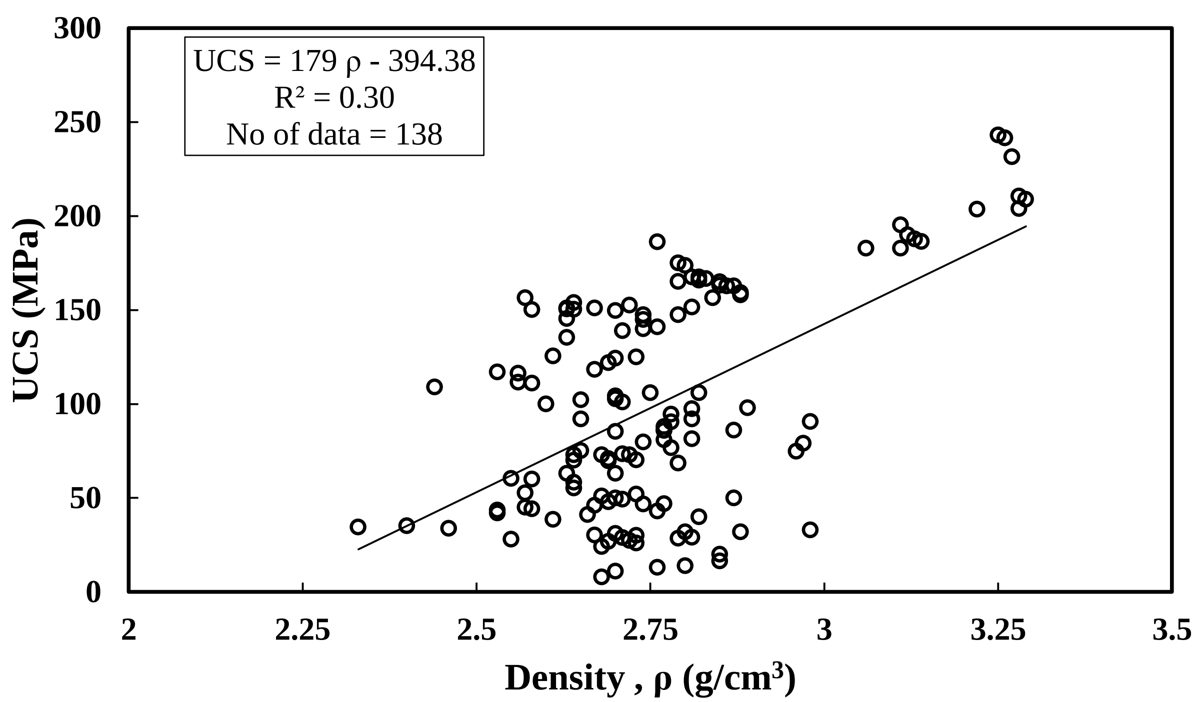

Fig. 2 linear variation between density (ρ) and UCS (MPa)

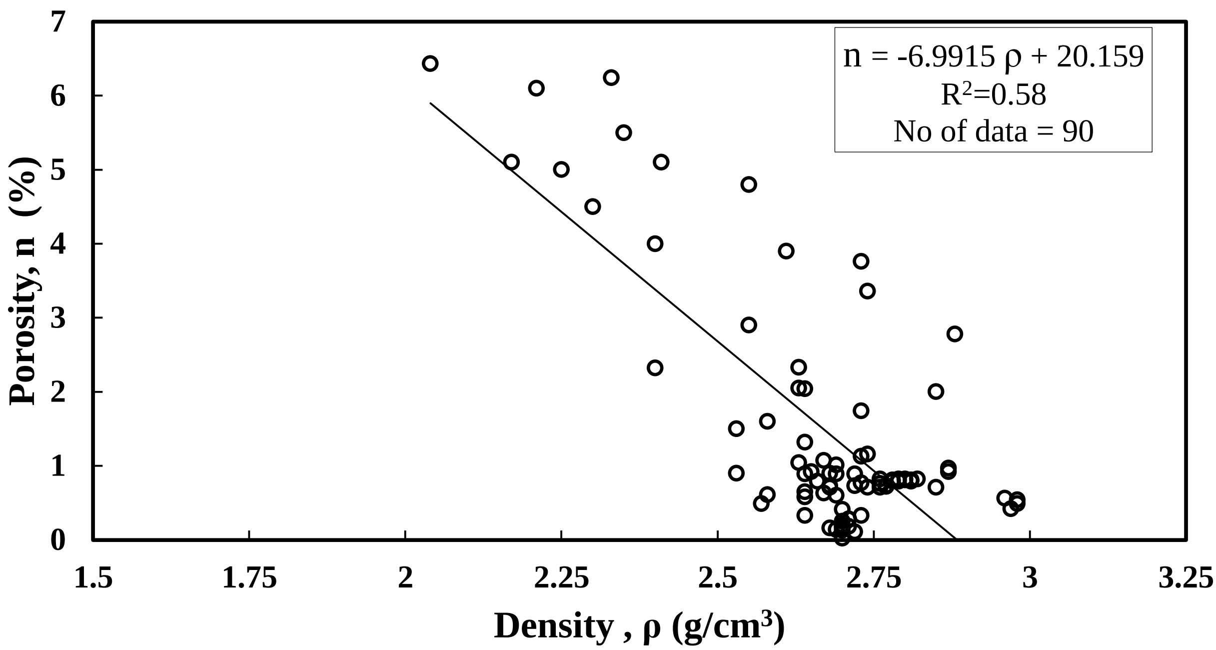

Fig. 3 linear variation between density (ρ) and Porosity, n (%)

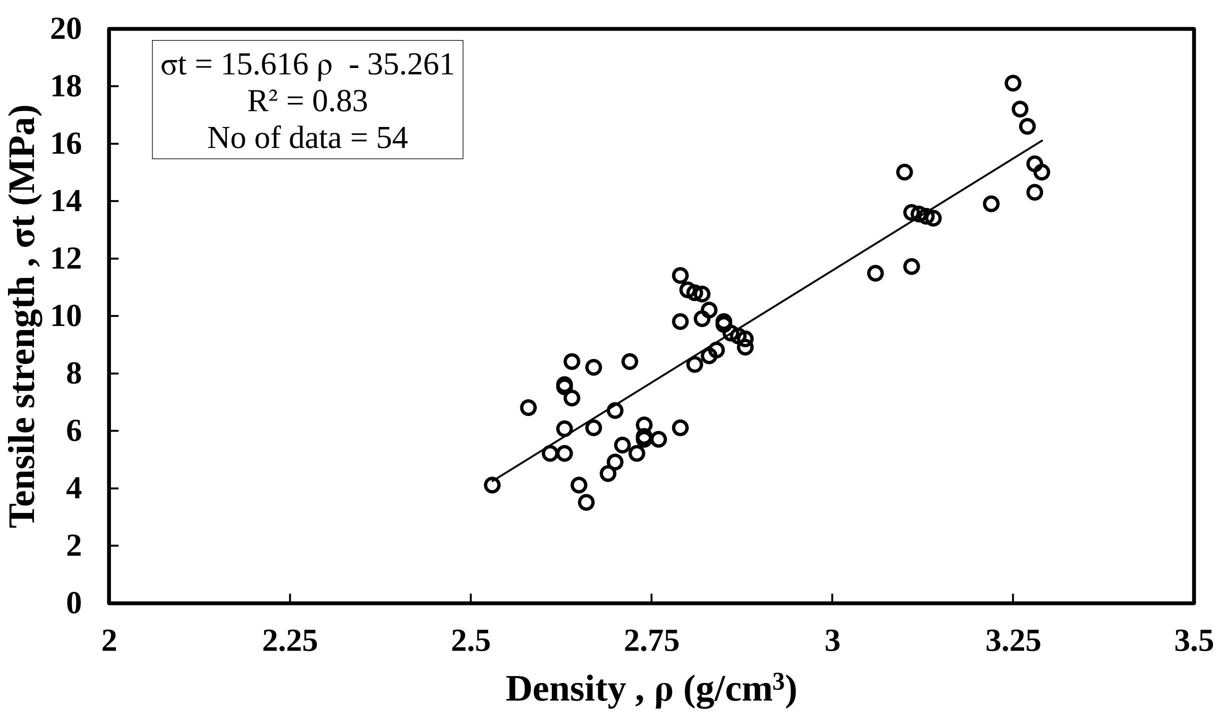

Fig. 4 linear variation between density (ρ) and Tensile strength, σ_t (MPa)

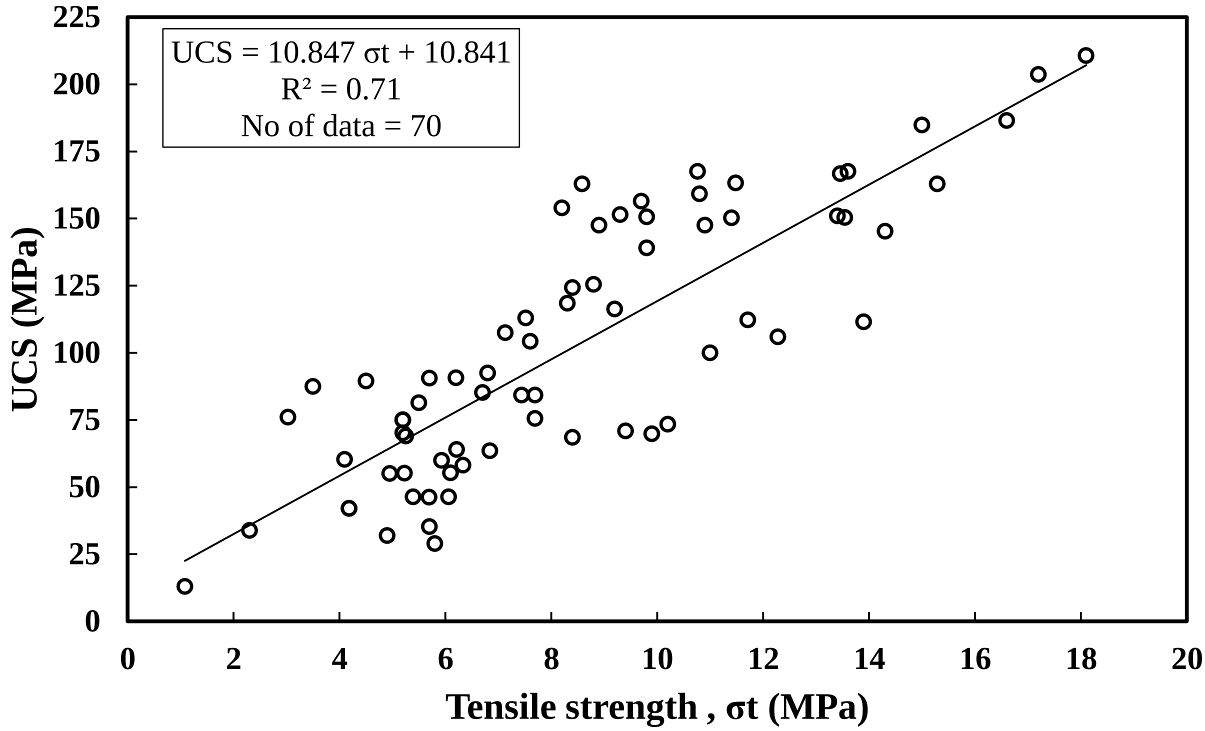

Fig. 5 linear variation between Tensile strength, σ_t (MPa) and UCS (MPa)

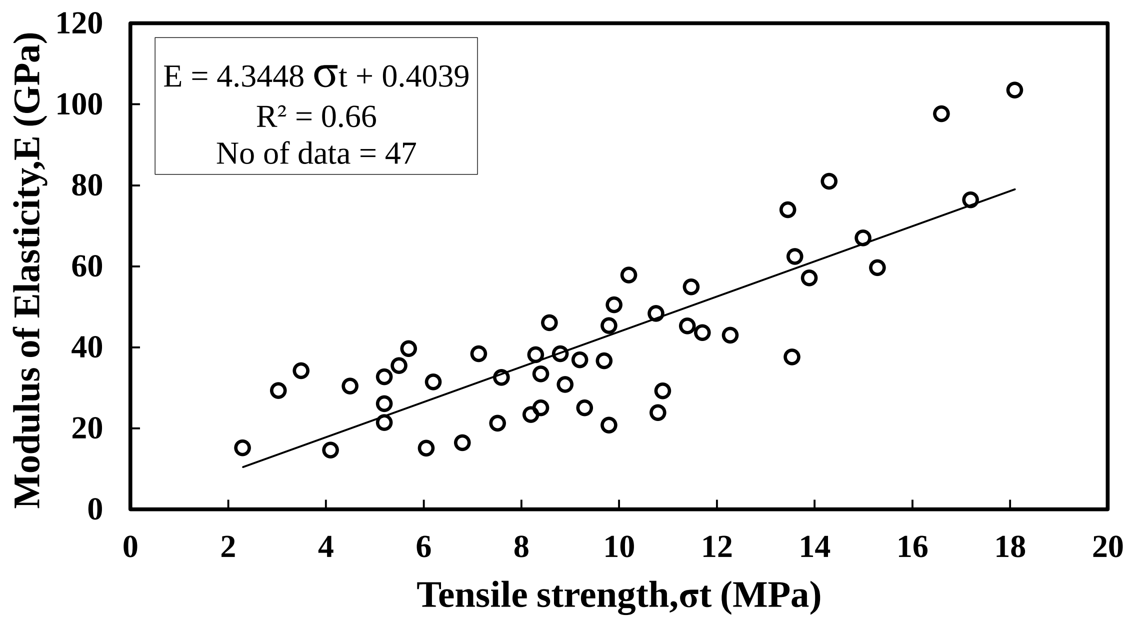

Fig. 6 linear variation between Tensile strength, σ_t (MPa) and Young's modulus,E (GPa)

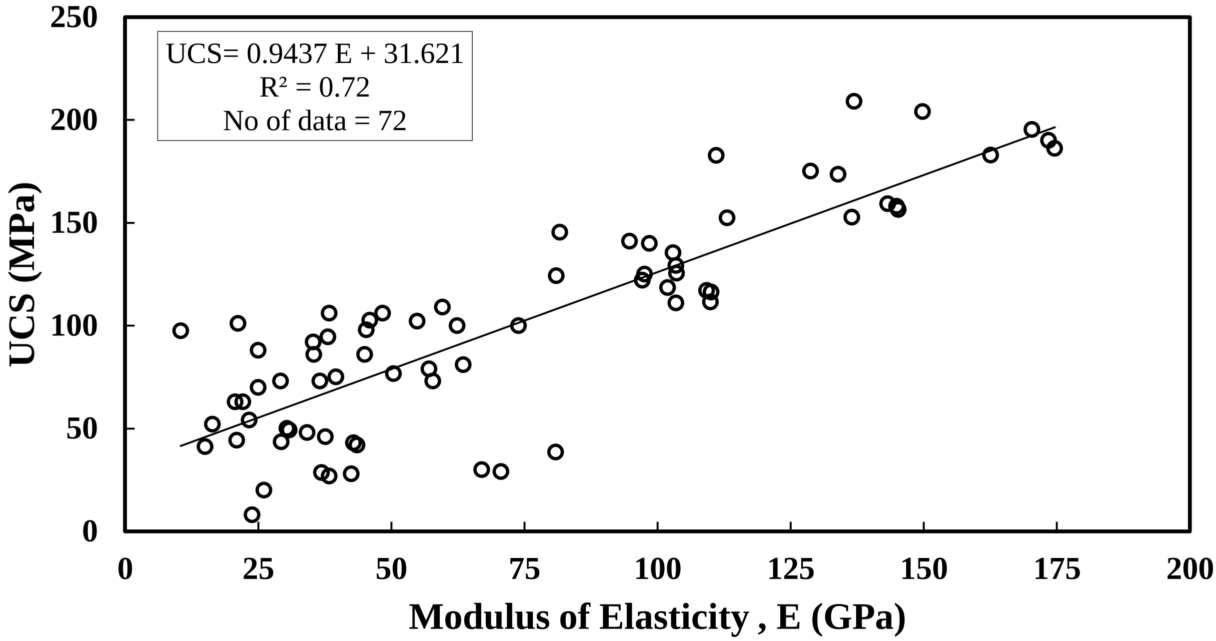

Fig. 7 linear variation between Young's modulus, E (GPa) and UCS (MPa)

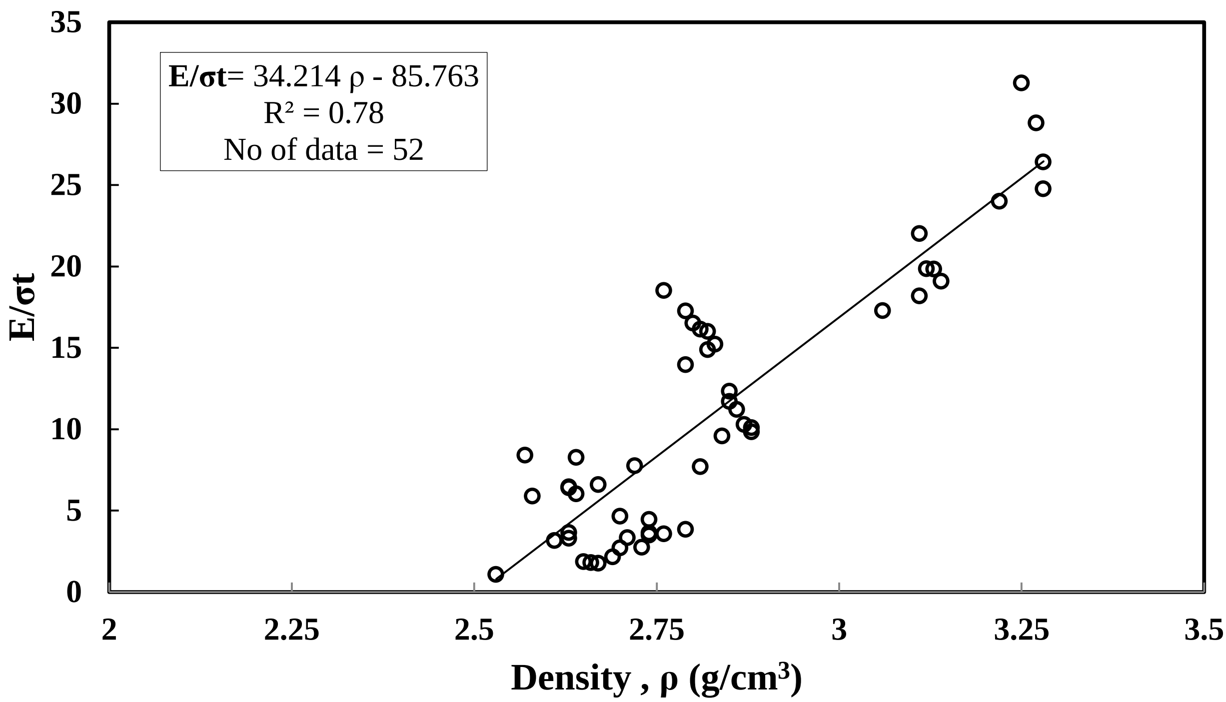

Fig. 8 linear variation between Density, ρ (g/cm^3) and E / σ_t

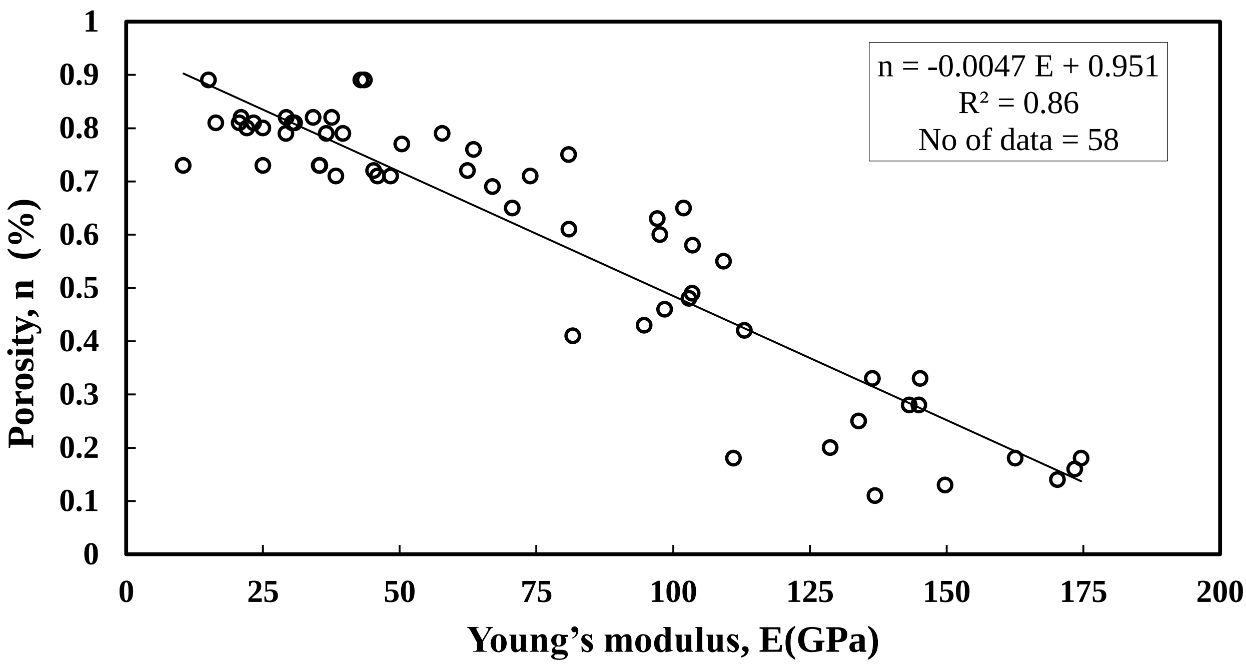

Fig. 9 linear variation between Young's modulus, E (GPa) and Porosity, n (%)

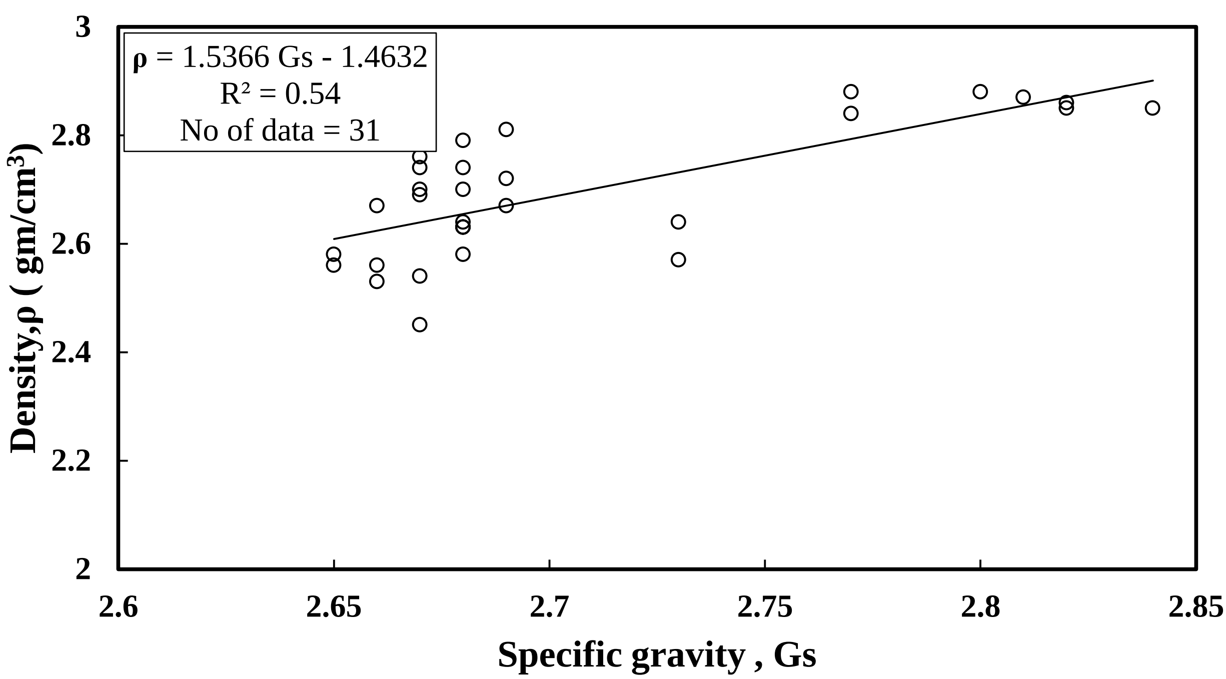

Fig. 10 linear variation between Specific gravity, Gs, and density, ρ (gm/cm^3)

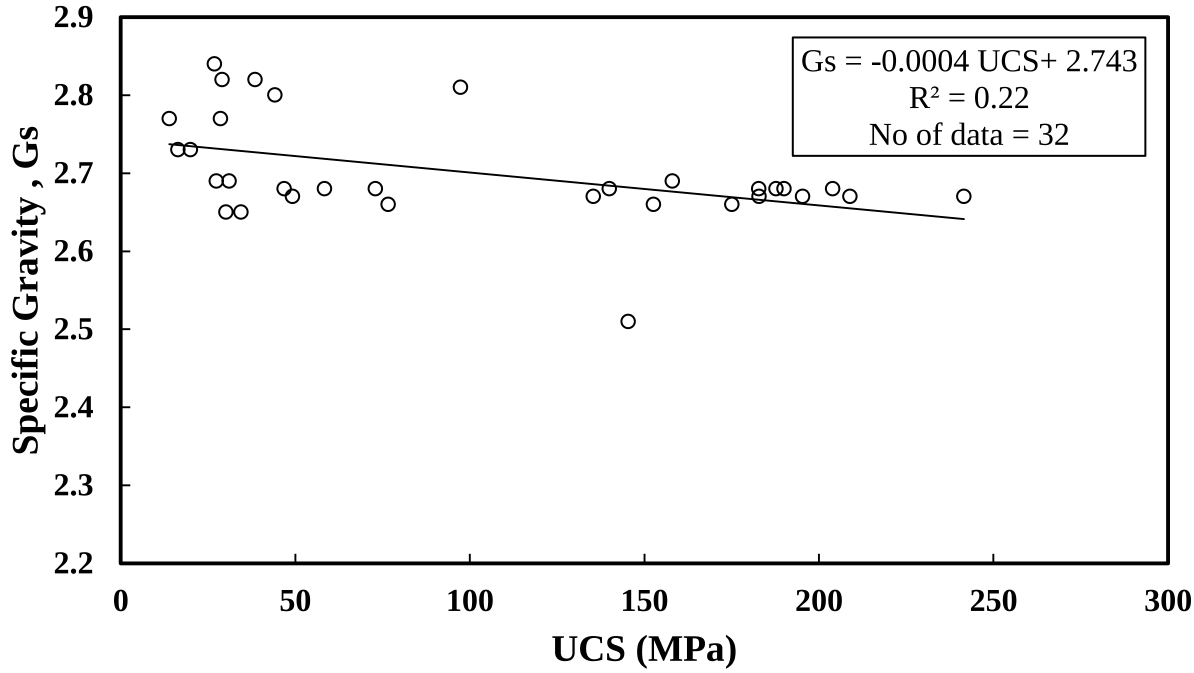

Fig. 11 linear variation between UCS (MPa) and Specific Gravity, Gs

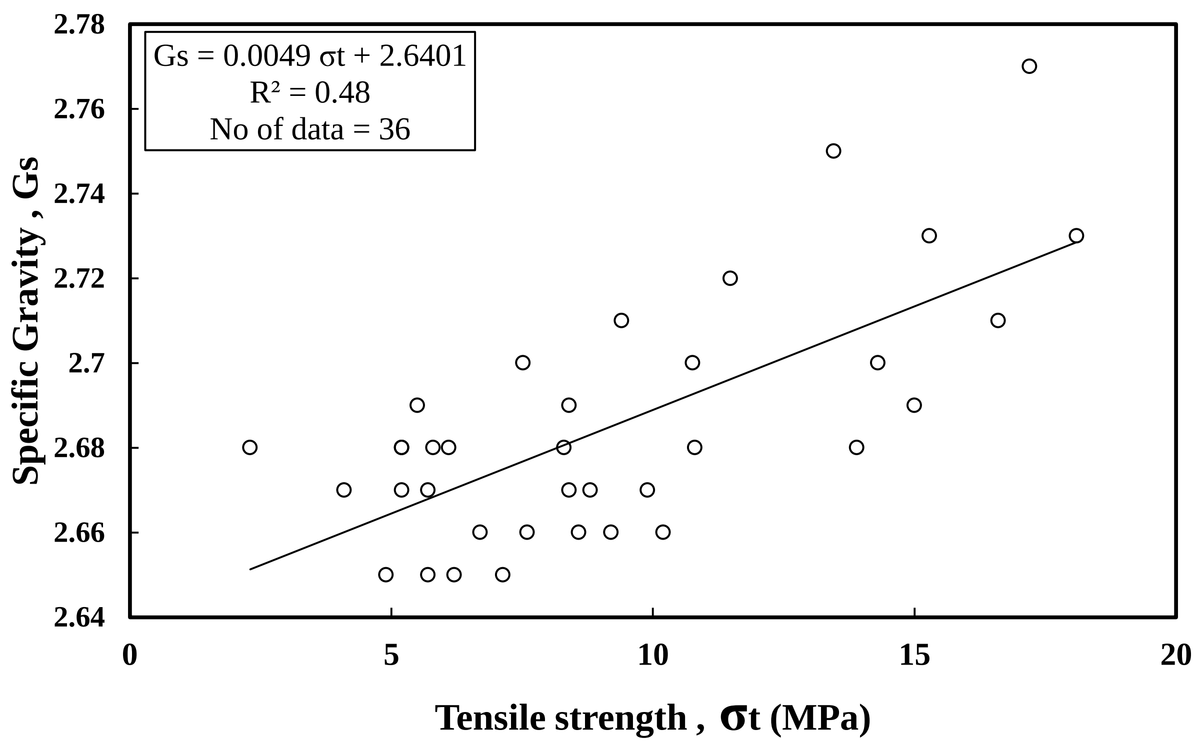

Fig. 12 linear variation between Tensile strength, σt (MPa) and Specific Gravity, Gs

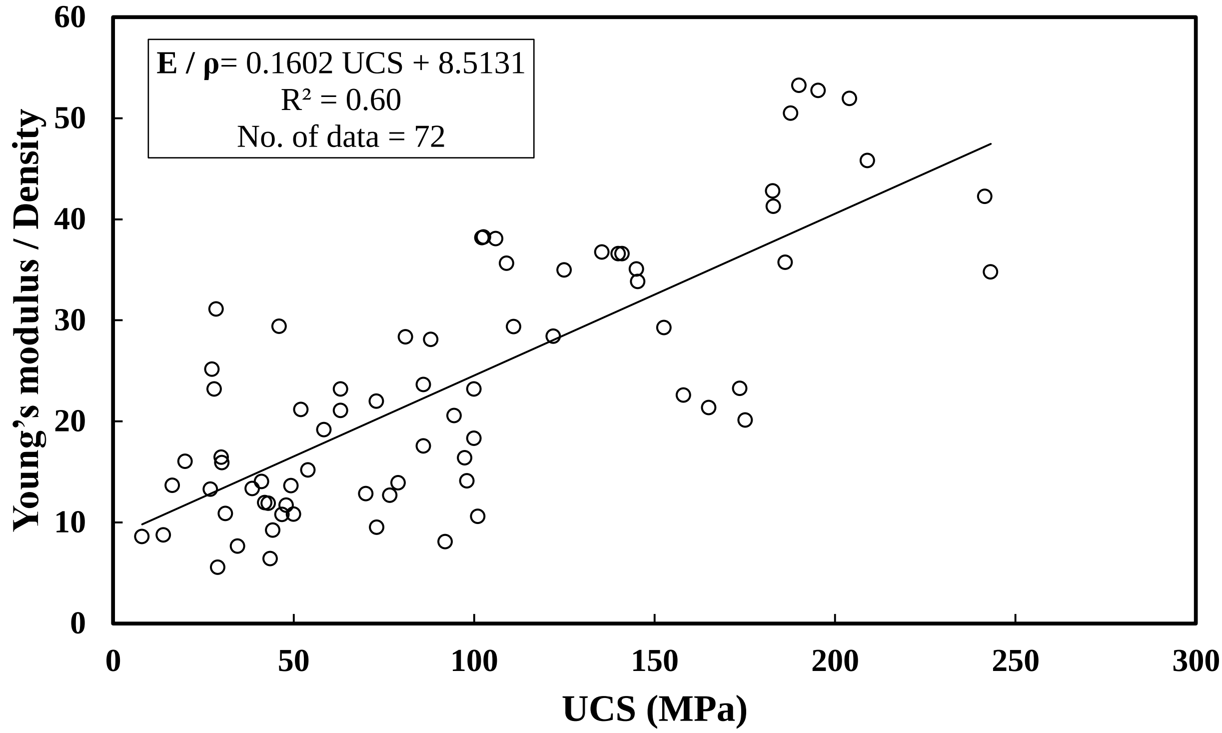

Fig. 13 linear variation between UCS (MPa) and Young's modulus / Density

5. Conclusions

This study aimed to investigate the relationship between the physical and mechanical properties of metamorphic rocks. The statistical analyses of metamorphic rocks were studied. Correlation between geotechnical properties of metamorphic rocks was examined based on data was collected from literature; the following conclusions can be drawn:

1. The best linear relationships have been found between Young's modulus with Porosity with $R^2 = 0.86$.

2. Density with Tensile strength has a linear correlation with $R^2 = 0.83$.

3. UCS and Specific Gravity has a weak linear correlation with $R^2 = 0.22$.

4. Linear correlation between Density and UCS with $R^2 = 0.30$.

5. It would be better for future to work on the relationships between UCS with Specific Gravity and Density with UCS.

References

Al-Juboury, A. I., & Al-Hadidy, A. H. (2009). Petrology and depositional evolution of the Paleozoic rocks of Iraq. Marine and Petroleum Geology, 26(2), 208-231.

Barros, R. S., Oliveira, D. V., Varum, H., Alves, C. A., & Camões, A. (2014). Experimental characterization of physical and mechanical properties of schist from Portugal. Construction and Building Materials, 50, 617-630.

Benayad, S., Park, Y.-S., Chaouchi, R., & Kherfi, N. (2013). Unconventional resources in Algeria: appraisal result from the Hamra Quartzite reservoir. Geosciences Journal, 17(3), 313-327.

Chen, Y.-F., Wei, K., Liu, W., Hu, S.-H., Hu, R., & Zhou, C.-B. (2016). Experimental characterization and micromechanical modeling of anisotropic slates. Rock Mechanics and Rock Engineering, 49(9), 3541-3557.

El–Hamid, M. A., Draz, W., Ismael, A., Gouda, M., & Sleem, S. (2015). Effect of Petrographical Characteristics on the Engineering Properties of Some Egyptian Ornamental Stones. International Journal of Scientific & Engineering Research, 6(7).

Fereidooni, D. (2016). Determination of the geotechnical characteristics of Hornfelsic rocks with a particular emphasis on the correlation between physical and mechanical properties. Rock Mechanics and Rock Engineering, 49(7), 2595-2608.

Gegenhuber, N. (2016). Interpretation of elastic properties for magmatic and metamorphic rock types. International Journal of Rock Mechanics and Mining Sciences(88), 44-48.

Gholami, R., & Rasouli, V. (2014). Mechanical and elastic properties of transversely isotropic slate. Rock Mechanics and Rock Engineering, 47(5), 1763-1773.

Kahraman, S., Fener, M., & Kozman, E. (2012). Predicting the compressive and tensile strength of rocks from indentation hardness index. Journal of the Southern African Institute of Mining and Metallurgy, 112(5), 331-339.

Khanlari, G.-R., Heidari, M., Sepahigero, A.-A., & Fereidooni, D. (2014). Quantification of strength anisotropy of metamorphic rocks of the Hamedan province, Iran, as determined from a cylindrical punch, point load, and Brazilian tests. Engineering Geology, 169, 80-90.

Mishra, S., Chakraborty, T., & Matsagar, V. (2017). Dynamic Characterization of Himalayan Quartzite Using SHPB. Procedia engineering, 191, 2-9.

Motra, H. B., & Zertani, S. (2017). Influence of loading and heating processes on elastic and geomechanical properties of eclogites and granulites. Journal of Rock Mechanics and Geotechnical Engineering.

Mustafa, S., Khan, M. A., Khan, M. R., Hameed, F., Mughal, M. S., Asghar, A., & Niaz, A. (2015). Geotechnical study of marble, schist, and granite as dimension stone: a case study from parts of Lesser Himalaya, Neelum Valley Area, Azad Kashmir, Pakistan. Bulletin of engineering geology and the environment, 74(4), 1475-1487.

Owaid, M. N., & Abed, I. A. (2015). Mineral analysis of phosphate rock as Iraqi raw fertilizer. International Journal of Environment, 4(2), 413-415.

Özbek, A., Gül, M., Karacan, E., & Alca, Ö. (2018). Anisotropy effect on strengths of metamorphic rocks. Journal of Rock Mechanics and Geotechnical Engineering.

Ozcelik, Y. (2011). Predicting Los Angeles abrasion of rocks from some physical and mechanical properties. Scientific Research and Essays, 6(7), 1612-1619.

Perras, M. A., & Diederichs, M. S. (2014). A review of the tensile strength of rock: concepts and testing. Geotechnical and geological engineering, 32(2), 525-546.

Siegesmund, S., & Dürrast, H. (2011). Physical and mechanical properties of rocks Stone in architecture (pp. 97-225): Springer.

Singh, T., Jain, A., & Rao, K. (2017). Physico-mechanical Behaviour of Metamorphic Rocks in Rohtang Tunnel, Himachal Pradesh, India. Procedia engineering, 191, 419-425.

Su, O., & Momayez, M. (2017). Indirect estimation of electrical resistivity by abrasion and physicomechanical properties of rocks. Journal of Applied Geophysics, 143, 23-30.

Tandon, R. S., & Gupta, V. (2013). The control of mineral constituents and textural characteristics on the petrophysical & mechanical (PM) properties of different rocks of the Himalaya. Engineering Geology, 153, 125-143.

Statistical Analysis of Mechanical and Physical Properties of Igneous Rocks

Soran Jabbar H. Salih[1*] Younis M. Alshkane[2]

[1]Department of Civil Engineer, Faculty of Engineering, University of Sulaimni, Al- Sulaimaniyah, Kurdistan Region, Iraq
[2]Department of Civil Engineer, Faculty of Engineering, University of Sulaimni, Al-Sulaimaniyah, Kurdistan Region, Iraq
Email: younis.ali@univsul.edu.iq

[*]Corresponding author. Email: Soran.hama@univsul.edu.iq

Abstract

One of the modern finishing materials for building construction is igneous rock. This study was focused on determining the relationships between mechanical and physical properties of igneous rocks. This incorporates point load strength index $Is_{(50)}$, Unconfined Compression Strength (UCS), flexural strength, poisons ratio, dry density, porosity, Schmidt rebound values and P-wave velocity for a wide range of igneous rocks. The study was performed on data collected from the literature. The results showed that the porosity has a significant negative effect on the dry density of rock samples. The best relationship was observed between modulus of elasticity and temperature with the coefficient of determination (R^2) of 0.89; it means that the temperature had a great influence on the modulus of elasticity so that increasing temperature causes to decrease in modulus of elasticity of igneous rock. In addition, the weakest relationship was observed between flexural strength and p-wave velocity with R^2 of 0.42; whereas, there was no relationship between UCS and Poisons ratio.

Keywords: Igneous rock; mechanical properties; physical properties; modulus of elasticity; temperature.

1. Introduction

Solidification of partly molten or molten magma produced from Earth's crust caused to generate igneous rocks. On the word of their formation condition, igneous rocks are classified to two main types, intrusive (plutonic), this type of rock formed from slow cooling of magma deeply inside the earth crust and then start solidification. The second type of igneous rock is volcanic (extrusive) formed from flowing of lava, causing fine grained or glassy material as a result of quick cooling at the earth's surface. Main mineral components and grain size are the main characteristics to classified volcanic and plutonic rocks. In most case the maximum mechanical strength comes from unweathered igneous rock(Harker, 2011; McBirney, 1993; Zhou & Li, 2000). In geotechnical engineering, high mechanical strength generally due to small grained size, while, the alteration of minerals, joints, cavities, and faults cause reduce mechanical strength(Bowen, 1956; Maitre, 1989). Several factors affect the properties of igneous rock, such as the fabric (voids and minerals' arrangement) mineral composition, texture (shape and size of grain), and the condition of the weather (Irfan, 1996). Igneous rocks vary in their petrographic properties, mineralogy, and engineering features for instance shape and size of grain, interlocking degree, and type of contact and composition of the minerals can affect the rock's mechanical properties. The combination of texture and mineral, provide good elastic deformation strength properties for synthetic (fresh) igneous rock (Irfan & Dearman, 1978; Mendes, Aires-Barros, & Rodrigues, 1966; Onodera & Asoka Kumara, 1980; Tuğrul & Zarif, 1999; Willard & McWilliams, 1969; Yusof & Zabidi, 2016). According to the literature the strength of igneous rock increases with increasing fine grain in the rock. In general, the mechanical properties (strength and stiffness) of igneous rock decrease with decreasing grain size (Crawford, DeDontney, Alramahi, & Ottesen, 2012; Singh, Kainthola, & Venkatesh, 2012; Tuğrul & Zarif, 1999). Quartz is one of the main compositions of igneous rock, the more quartz in the rock give higher strength. Meanwhile, if the rock contain feldspar, weakens the rock's strength (Merriam, Rieke III, & Kim, 1970; Tuğrul & Zarif, 1999). The composition of igneous rock and mineral crystal frame changes under the influence of temperature, Pores and cracks of igneous rock and its structure changes as well. Micro-cracking occurs with increasing temperature. This is due to the change of the rock's grain size (Rao, Wang, Xie, & Xie, 2007; Takarli, Prince, & Siddique, 2008). Thermal damage is mainly caused by minerals' differential thermal expansion(Keshavarz, Pellet, & Loret, 2010). Various researches have been conducted to deal with the effect of high temperature on the mechanical properties of rock under mechanical loads by utilizing numerical simulation(Jing, 2003; Takarli et al., 2008). Numerous studies have developed empirical equations to determine Young modulus and UCS in rocks depending on point load index $Is_{(50)}$, Schmidt hammer rebound (Rn) and P-wave velocity (P_v) (Çobanoğlu & Çelik, 2008; Palchik & Hatzor, 2004; Singh et al., 2012; Thuro, Plinninger, Zah, & Schutz, 2001). The objectives of this study were to correlate some physical and mechanical properties of Igneous rocks as well as develop a useful empirical equations between igneous rock properties.

2. Materials and methods

2.1. Data collection

In this study, the following geotechnical properties were collected from literature: Unconfined Compression Strength (UCS), Flexural strength, P-wave velocity, porosity, Dry density, Modulus of elasticity, Point load strength index, Schmidt hammer and the effect of Temperature on the geotechnical properties of Igneous rocks.

2.2. Igneous rock properties

In this study, more than 1000 data points were obtained from literature so as to investigate the relationships between the geotechnical properties of igneous rock. .. All tests have been conducted according to American Society for Testing and Materials (ASTM) and International Society for Rock Mechanics (ISRM). The data were analyzed using linear and nonlinear regression models.

3. Results and discussion

3.1. Unconfined Compressive Strength, UCS (MPa)

Based on the total of 240 UCS data for Igneous rocks, the range of data was from 6.0 to 212 MPa with a mean value of 93.0 MPa, standard deviation of 45 MPa and coefficient of variation COV of 60 % as summarized in Table 1.

3.2. Tensile strength, σt (MPa)

The σt of previous studies is presented in Table 1. based on the total of 88 σt data for Igneous rocks, the range of data was from 1.5 to 29 MPa with a mean of 13.75 MPa, standard deviation of 8.35 MPa and COV of 60 % as summarized in Table 1.

3.3. P-wave velocity, Pv (m/s)

The data of Pv are collected from other studies as summarized in Table 1. Based on the total of 188 Pv data for Igneous rocks, the data varied from 2300 to 8000 m/s with a mean of 4918 m/s, standard deviation of 1154 m/s and COV of 23 % as summarized in Table 1.

3.4. Porosity, n (%)

The statistical analysis of total collected data of 87 n for Igneous rocks collected from the literature presented a variation from 0.14 to 50 % with a mean of 4.8 %, standard deviation of 9.80% and COV of 2.0.0 % as summarized in Table 1.

3.5. Dry Unit Weight, γdry (kN /m3)

data of 73 were collected from previous studies for γdry for Igneous rocks collected from the literature gave a variation from 1.50 to 28.0 kN/m3 with a mean of 20.50 kN/m3, standard deviation of 9.50 kN/m3 and COV of 46 % as summarized in Table 1.

3.6. Modulus of elasticity, E (GPa)

A total of 101 data points of E were collected from literature for Igneous rocks. The range of data was from 2.0 to 13.0 GPa with a mean of 36.25 GPa, standard deviation of 19.19 GPa and COV of 53 % as summarized in Table 1.

3.7. Point load strength index, Is(50) (MPa)

A data of 119 for Is(50) was collected from other studies for Igneous rocks are presented in Table 1. The range of Is(50) was from 1.0 to 13.0 MPa with a mean value of 4.32 MPa, standard deviation of 2.90 MPa and COV of 67 % as summarized in Table 1.

3.8. Schmidt hammer, (Rn)

The Rn of other research studies is presented in Table 1. The total of 119 data for Rn of Igneous rocks were obtained from literature. The range of data was from 18 to 72 with a mean of 45.70, standard deviation of 14.25 and COV of 31 % as summarized in Table1.

3.9. Poisson ratio, v

A total of 61 data of v for igneous rocks were collected from literature is presented in Table 1. The minimum and maximum values were 0.10 and 0.40, respectively, with average of 0.25, standard deviation of 0.064 and COV of 25 % as summarized in Table1.

3.10. Effect of Temperature change , T (C°)

The effect of temperature on mechanical properties was studied based literature. The minimum and maximum values of T was 20 to 1130 C° out of 19 data from literature and the mean and standard deviation were 278, 369 C° respectively and COV was 75 % as summarized in Table 1.

3.11. Relationships between Unconfined Compression Strength and P-wave velocity

The correlation between UCS and P-wave was investigated using data collected from previous studies using 172 data points using simple regression model, the best relationships between UCS and Pv was a nonlinear model as presented in Fig. 1. The coefficient of determination (R2) and Root Mean Square Error (RMSE) for the relationship were 0.55 and 28.80respectively. Eq.1 shows the developed equation.

$.UCS = 0.0008\ P_v^{1.37}$ (1)

3.12. Relationships between tensile strength and P-wave velocity

A total of 65 data points were collected from various research studies. The data collected from the literature were quantified using (Eq. 2) as shown in Fig. 2. The change in the X with Y was represented using relationship shown in Eq. 2. It is clear that as Pv increases, the tensile strength increases. R^2 and RMSE were 0.45 and 5.3 respectively.

$\sigma t = 3.138 \exp^{0.0003pv}$ (2)

3.13. Relationships between Porosity and P-wave velocity

Data points of 61were collected from numerous research studies. The collected data from the studies were calculated using (Eq. 3) as shown in Fig. 3. The change in the X with Y was shown using the relationship (Eq. 3) and the model parameters A and B are summarized in Table 2. It is obvious that increasing of sound velocity decreased porosity. R^2 and RMSE for the relationship were 0.69 and 1.55 as summarized in Table 2.

$n = 127.42\exp^{-9E-04\ Pv}$ (3)

3.14. Relationships between Modulus of Elasticity and Temperature

From various research studies 13 data were collected. The collected data from the studies were calculated using (Eq. 4) as shown in Fig.4. The change in the X with Y was shown using the relationship (Eq. 4) and the model parameters A and B are summarized in Table 2. The change in temperature had a great effect on modulus of elasticity increase of temperature lead to decrease modulus of elasticity. R^2 and RMSE were 0.89 and 6.84 as summarized in Table 2.

$E = -0.062\ T + 74.65$ (4)

3.15. Relationships between Unconfined Compression Strength and Modulus of Elasticity

A total of 66 data were collected from various research studies. The collected data from the studies were calculated using (Eq. 5) as shown in Fig.5. The change in the X with Y was shown using the relationship (Eq. 5) and the model parameters A and B are summarized in Table 2. R^2 and RMSE were 0.88 and 21.0 respectively as summarized in Table 2.

$$UCS = 6.30\ E^{0.7893} \quad (5)$$

3.16. Relationships between Unconfined Compression Strength and Point load

From numerous research studies 129 data were collected. The collected data from the studies were calculated using (Eq. 6) as shown in Fig.6. The change in the X with Y was shown using the relationship (Eq. 6) and the model parameters A and B are summarized in Table 2. R^2 and RMSE for the relationship were 0.53and 29.40 as summarized in Table3.

$$UCS = 53.821\ I_s^{0.51} \quad (6)$$

3.17. Relationships between Unconfined Compression Strength and Flexural strength

A total of 89 data were collected from different research studies. The data collected from the literature were quantified using (Eq. 7) as shown in Fig. 7. The change in the X with Y was represented using relationship (Eq. 7) it can be seen that increased Flexural strength caused to increase Unconfined Compression Strength and the model parameters, A and B are summarized in Table 2. R2 and RMSE for the relationship were 0.63 and 28.6 as summarized in Table 2.

$$UCS= 4.4877\sigma t + 23.683 \quad (7)$$

3.18. Relationships between Unconfined Compression Strength and Schmidt hammer

119 data were collected from different research studies. The collected data from the studies were calculated using (Eq. 8) as shown in Fig. 8. The change in the X with Y was shown using the relationship (Eq. 8) and the model parameters A and B are summarized in Table 2. It is obvious that increasing of Schmidt hammer values lead to increase unconfined Compression Strength. R2 and RMSE for the relationship were 0.73 and 22.25 as summarized in Table 2.

$$UCS = 1.4467\ Rn1.1066 \quad (8)$$

3.19. Relationships between Dry density and Porosity

From various research studies 58 data were collected. The collected data from the studies were calculated using (Eq. 9) as shown in Fig.9. The change in the X with Y was shown using the relationship (Eq. 5) and the model parameters A and B are summarized in Table 2. R2 and RMSE for the relationship were 0.90 and 0.78 as summarized in Table 2.

$$\gamma\ dry = 26.97\exp -0.033\ n \qquad (9)$$

3.20. Relationships between Unconfined Compression Strength and Poisson's ratio

From various research studies 61 data were collected. Based on R2 and RMSE no relationship was observed as shown in Fig. 10.

4. Conclusions

Based on statistical analysis on data obtained from literature, the following conclusions were drawn:

1. The UCS – Rn relationship was stronger than the UCS–$Is_{(50)}$ Relationship for Igneous rocks.
2. P_v have a good relationship with n, compared to UCS and σt based on RMSE and R^2.
3. The inverse relationship observed between n and γ dry, as well as with P_v have been proven.
4. Low correlation coefficients were achieved between σt and P_v , nevertheless good correlation coefficients were trended between UCS and σt.
5. Temptature change (T) have a great effect on UCS, increasing 35 times of T caused to decrease UCS 35 times.
6. Based on Root Mean Square Error (RMSE) and coefficient of determination (R^2) values, the acceptable relationships were observed between igneous rock properties.

References:

Bowen, N. L. (1956). The evolution of the igneous rocks: Dover Publications.

Çobanoğlu, İ., & Çelik, S. B. (2008). Estimation of uniaxial compressive strength from point load strength, Schmidt hardness and P-wave velocity. Bulletin of Engineering Geology and the Environment, 67(4), 491-498.

Crawford, B., DeDontney, N., Alramahi, B., & Ottesen, S. (2012). Shear strength anisotropy in fine-grained rocks. Paper presented at the 46th US Rock Mechanics/Geomechanics Symposium.

Harker, A. (2011). The natural history of igneous rocks: Cambridge University Press.

Irfan, T. (1996). Mineralogy, fabric properties and classification of weathered granites in Hong Kong. Quarterly Journal of Engineering Geology and Hydrogeology, 29(1), 5-35.

Irfan, T., & Dearman, W. (1978). Engineering classification and index properties of a weathered granite. Bulletin of the International Association of Engineering Geology-Bulletin de l'Association Internationale de Géologie de l'Ingénieur, 17(1), 79-90.

Jing, L. (2003). A review of techniques, advances and outstanding issues in numerical modelling for rock mechanics and rock engineering. International Journal of Rock Mechanics and Mining Sciences, 40(3), 283-353.

Keshavarz, M., Pellet, F., & Loret, B. (2010). Damage and changes in mechanical properties of a gabbro thermally loaded up to 1,000 C. Pure and Applied Geophysics, 167(12), 1511-1523.

Maitre, L. (1989). A classification of igneous rocks and glossary of terms. Recommendations of the international union of geological sciences subcommission on the systematics of igneous rocks, 193.

McBirney, A. R. (1993). Igneous petrology: Jones & Bartlett Learning.

Mendes, F. M., Aires-Barros, L., & Rodrigues, F. P. (1966). The use of modal analysis in the mechanical characterization of rock masses. Paper presented at the 1st ISRM Congress.

Merriam, R., Rieke III, H. H., & Kim, Y. C. (1970). Tensile strength related to mineralogy and texture of some granitic rocks. Engineering Geology, 4(2), 155-160.

Onodera, T., & Asoka Kumara, H. (1980). Relation between texture and mechanical properties of crystalline rocks. Bull Int Assoc Eng Geol, 22, 173-177.

Palchik, V., & Hatzor, Y. (2004). The influence of porosity on tensile and compressive strength of porous chalks. Rock mechanics and rock engineering, 37(4), 331-341.

Rao, Q.-h., Wang, Z., Xie, H.-f., & Xie, Q. (2007). Experimental study of mechanical properties of sandstone at high temperature. Journal of Central South University of Technology, 14(1), 478-483.

Singh, T., Kainthola, A., & Venkatesh, A. (2012). Correlation between point load index and uniaxial compressive strength for different rock types. Rock mechanics and rock engineering, 45(2), 259-264.

Takarli, M., Prince, W., & Siddique, R. (2008). Damage in granite under heating/cooling cycles and water freeze–thaw condition. International Journal of Rock Mechanics and Mining Sciences, 45(7), 1164-1175.

Thuro, K., Plinninger, R., Zah, S., & Schutz, S. (2001). Scale effects in rock strength properties. Part 2: Point load test and point load strength index. Paper presented at the Rock Mechanics-A Challenge for Society.-881 p., Proceedings of the ISRM Regional Symposium Eurock.

Tuğrul, A., & Zarif, I. (1999). Correlation of mineralogical and textural characteristics with engineering properties of selected granitic rocks from Turkey. Engineering Geology, 51(4), 303-317.

Willard, R., & McWilliams, J. (1969). Microstructural techniques in the study of physical properties of rock. Paper presented at the International Journal of Rock Mechanics and Mining Sciences & Geomechanics Abstracts.

Yusof, N., & Zabidi, H. (2016). Correlation of mineralogical and textural characteristics with engineering properties of granitic rock from Hulu Langat, Selangor. Procedia Chemistry, 19, 975-980.

Zhou, X., & Li, W. (2000). Origin of Late Mesozoic igneous rocks in Southeastern China: implications for lithosphere subduction and underplating of mafic magmas. Tectonophysics, 326(3-4), 269-287.

Appendices

Table 1. Statistical Variation of Igneous rock properties

	Igneous Rock				
Statistical Parameters	No. of Data	Range	Mean (μ)	Std. Deviation (σ)	COV (%)

USC (MPa)	240	6.0 - 212	93.0	45.0	48
Flexural strength(MPa)	88	1.50 -29	13.75	8.35	60
P-wave velocity, P_v (m/s)	188	2300-8000	4918	1154	23
Porosity, n(%)	87	0.14 - 50.0	4.80	9.80	2.0
Dry density, γ_{dry} (kN /m^3)	73	1.50 - 28.0	20.50	9.50	46
Modulus of elasticity, (Gpa)	105	2.0 – 75.0	36.25	19.19	53
Point load strength index, $Is_{(50)}$ (Mpa)	119	1.0 – 13.0	4.32	2.90	67
Schmidt hammer (Rn)	119	18 -72	45.70	14.25	31
Poisson's ratio, υ	61	0.10 – 0.40	0.25	0.064	25
Temperature, T (C°)	19	20 - 1130	369	278	75

Table 2. Model parameters for Expansive soil properties

depended Variable (Y-axis)	In depended Variable (X-axis)	A	B	R^2	RMSE	No. of Data	Fig. No.
Unconfined Compression Strength ,USC(kPa)	P-wave velocity, P_v(m/s)	0.0008	1.37	0.55	28.8	172	Fig.1
Flexural strength, σt (MPa)	P-wave velocity, P_v(m/s)	3.138	0.0003	0.45	5.30	65	Fig.2
Porosity, n (%)	P-wave velocity, P_v(m/s)	127.42	-0.0009	0.69	1.55	61	Fig.3
Modulus of Elasticity, E (Gpa)	Temperature, T(c̊)	74.65	-0.062	0.89	6.84	13	Fig.5
Unconfined Compression Strength	Modulus of Elasticity, E	6.30	0.7893	0.85	21.0	66	Fig.4

,USC(kPa)	(Gpa)						
Unconfined Compression Strength ,USC(kPa)	Point load, $Is_{(50)}$ (Mpa)	53.821	0.51	0.56	29.40	119	Fig.6
Unconfined Compression Strength ,USC(kPa)	Flexural strength, σt (MPa)	23.68	4.49	0.63	28.60	89	Fig.7
Unconfined Compression Strength ,USC(kPa)	Schmidt hammer, (Rn)	1.4467	1.1066	0.73	22.25	119	Fig.8
Dry density, γ dry (kN/m3)	Porosity , n	26.97	-0.033	0.90	0.78	58	Fig.9
Unconfined Compression Strength ,USC(kPa)	Poisson's ratio, υ	No relation was observed				61	Fig.10

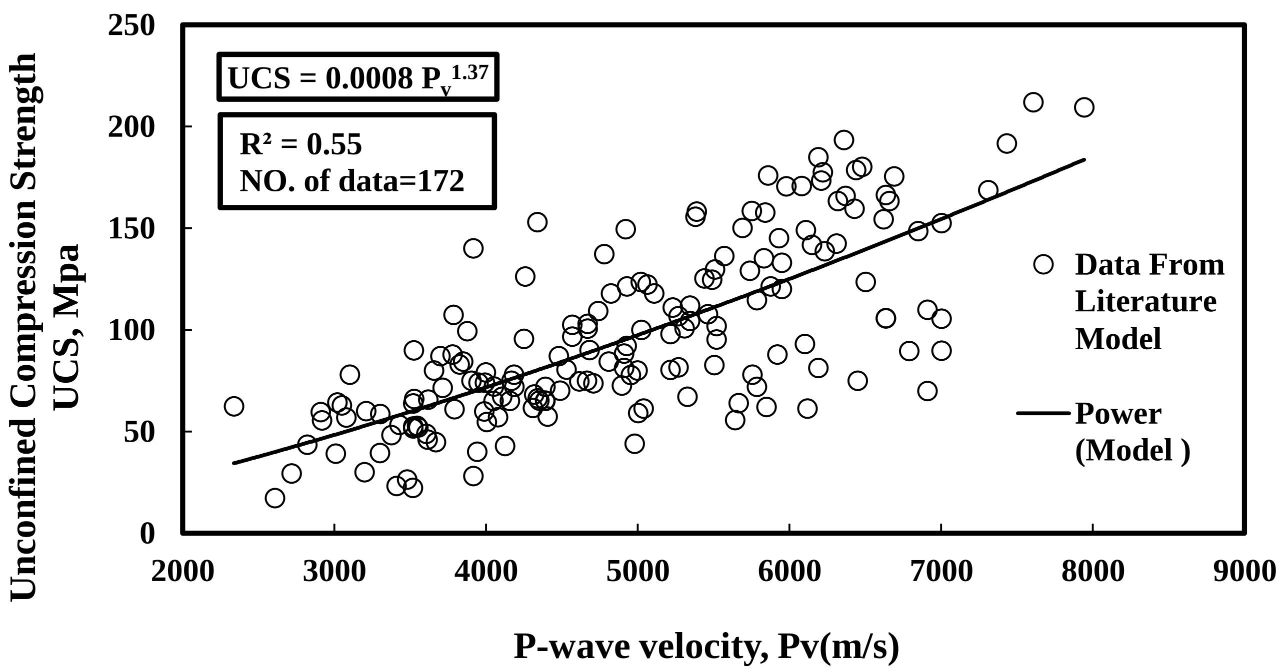

Fig. 1 Unconfined Compression Strength vs P-wave velocity

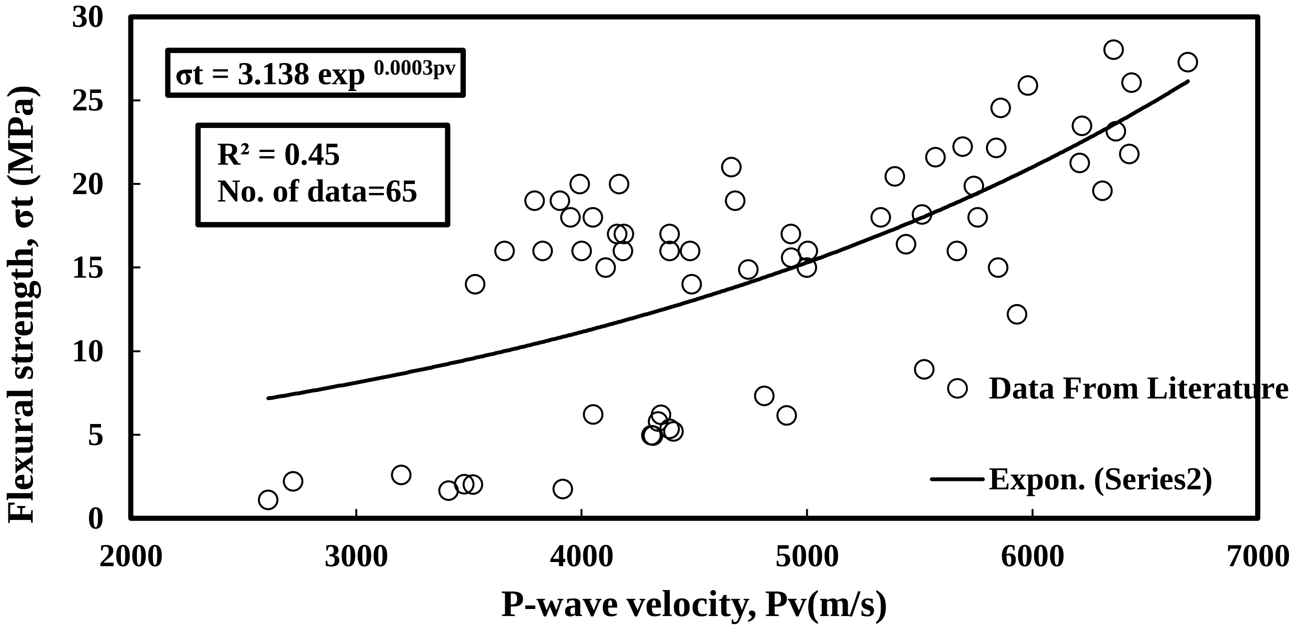

Fig. 2 Flexural strength vs P-wave velocity

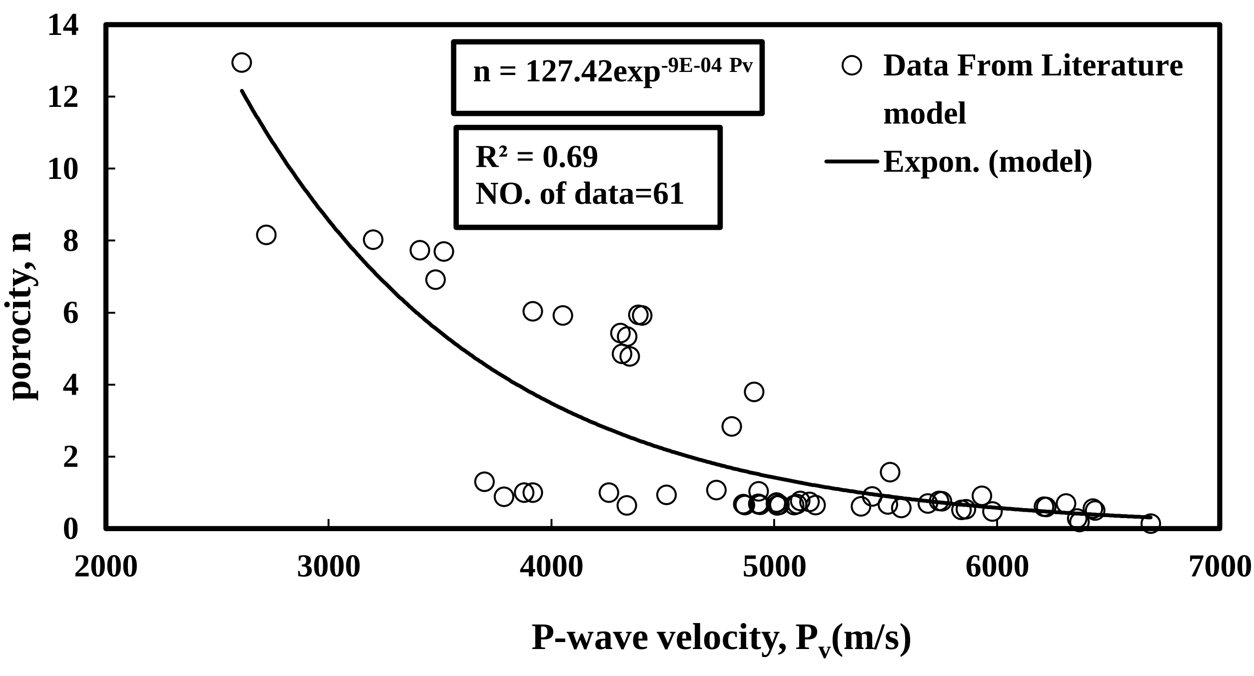

Fig. 3 Flexural strength vs P-wave velocity

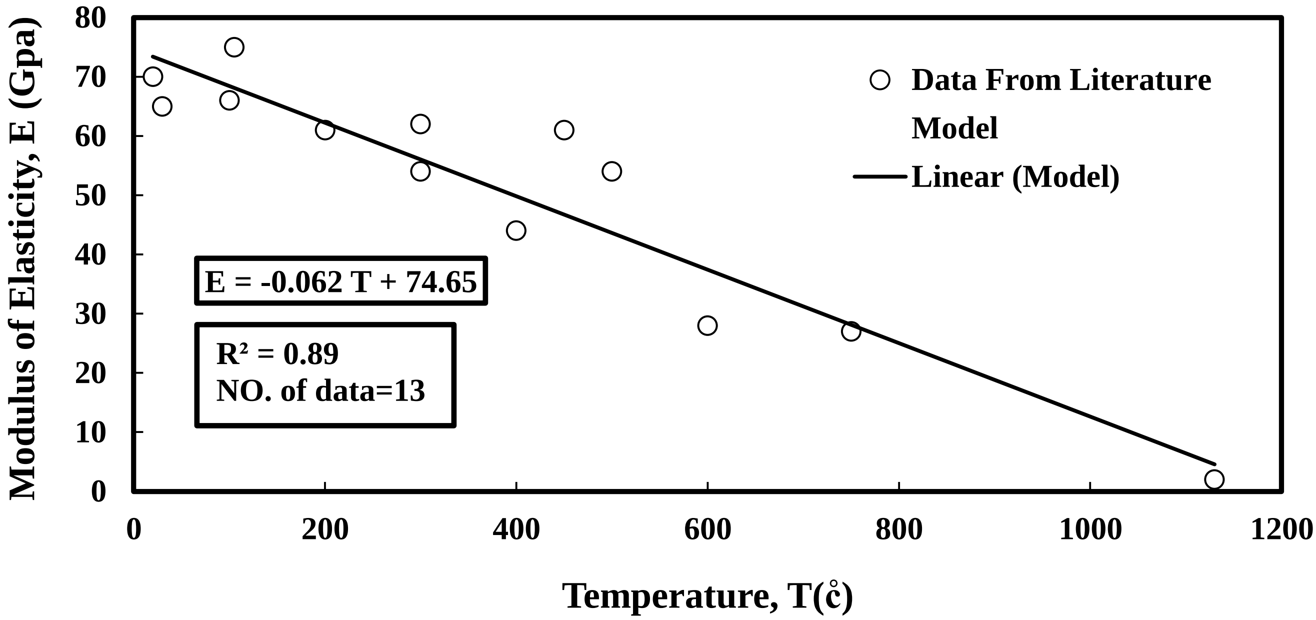

Fig. 4 Modulus of Elasticity vs Temperature

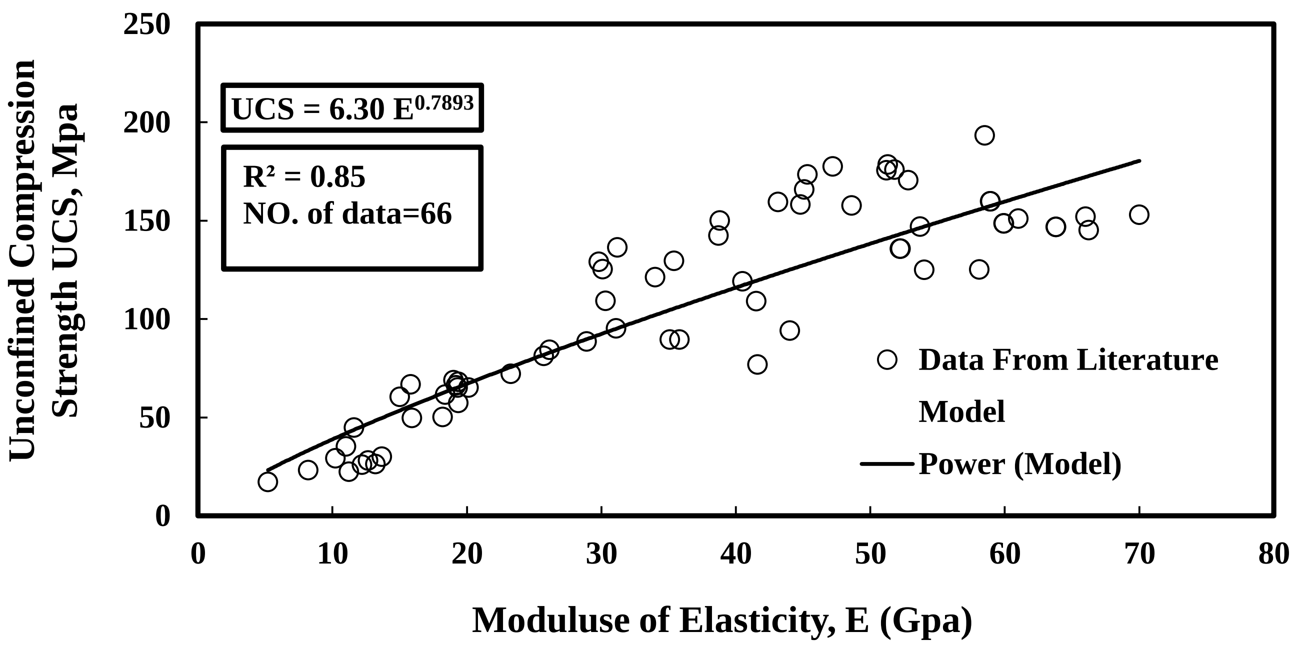

Fig. 5 Unconfined Compression Strength vs Modulus of Elasticity

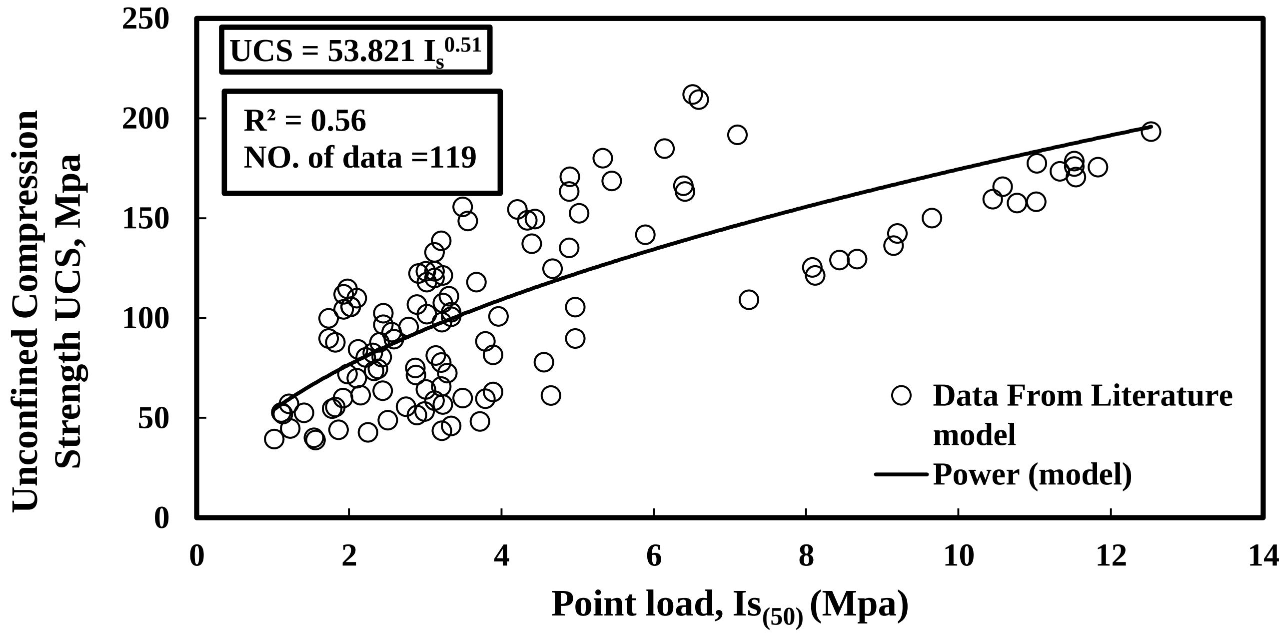

Fig. 6 Unconfined Compression Strength vs Point load

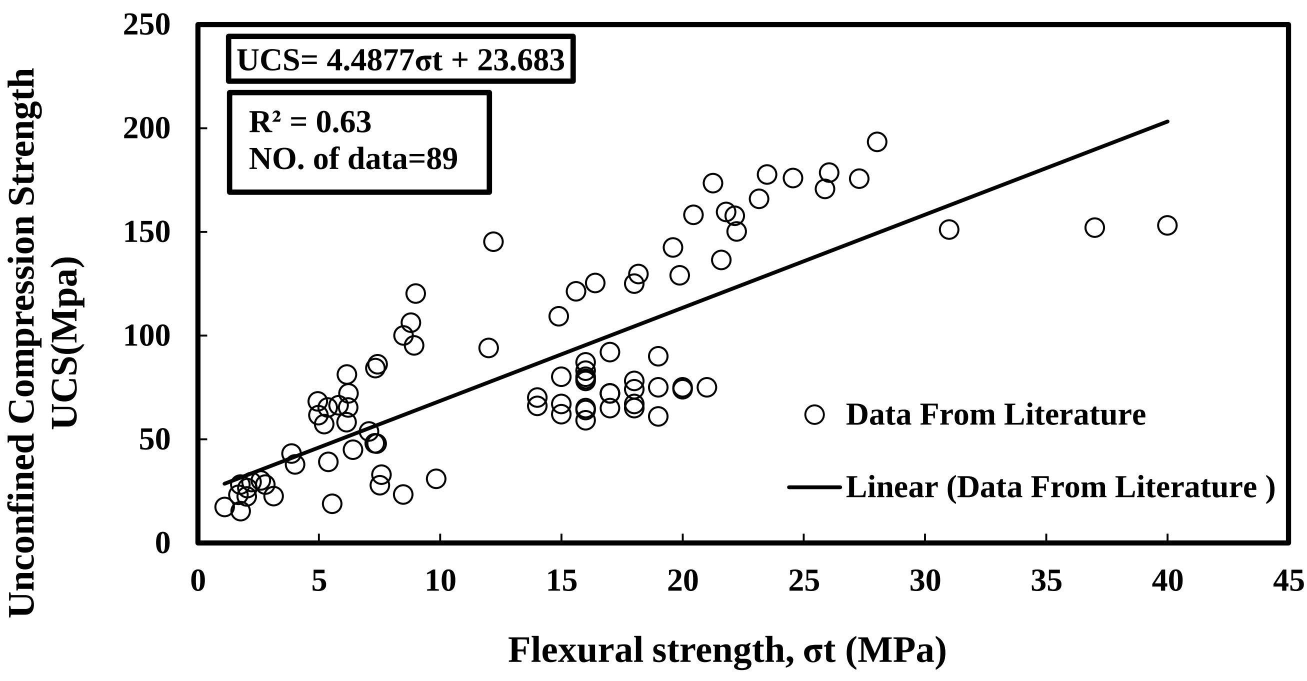

Fig. 7 Unconfined Compression Strength vs Flexural strength

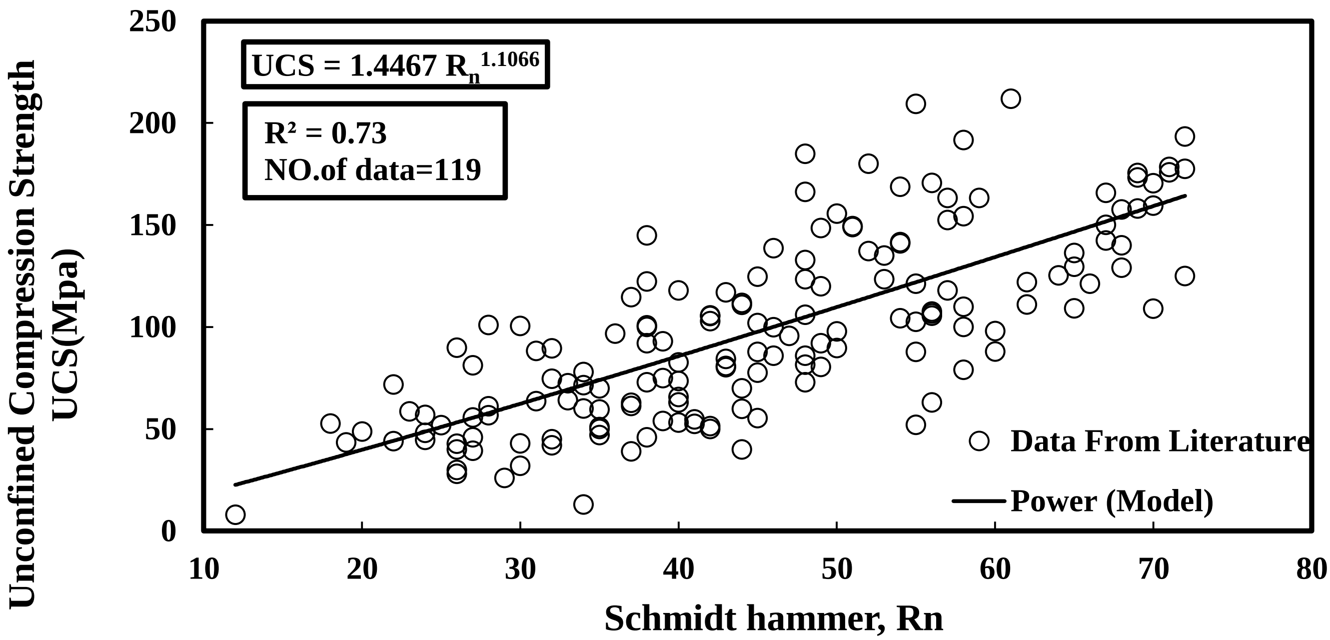

Fig. 8 Unconfined Compression Strength vs Schmidt hammer

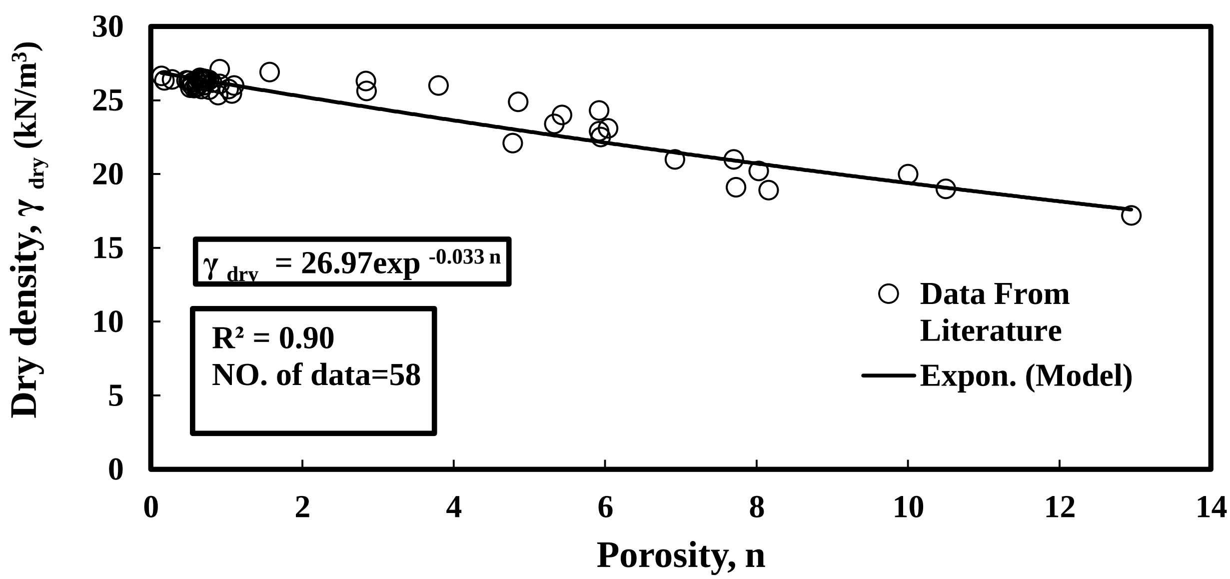

Fig. 9 Dry density vs Porosity

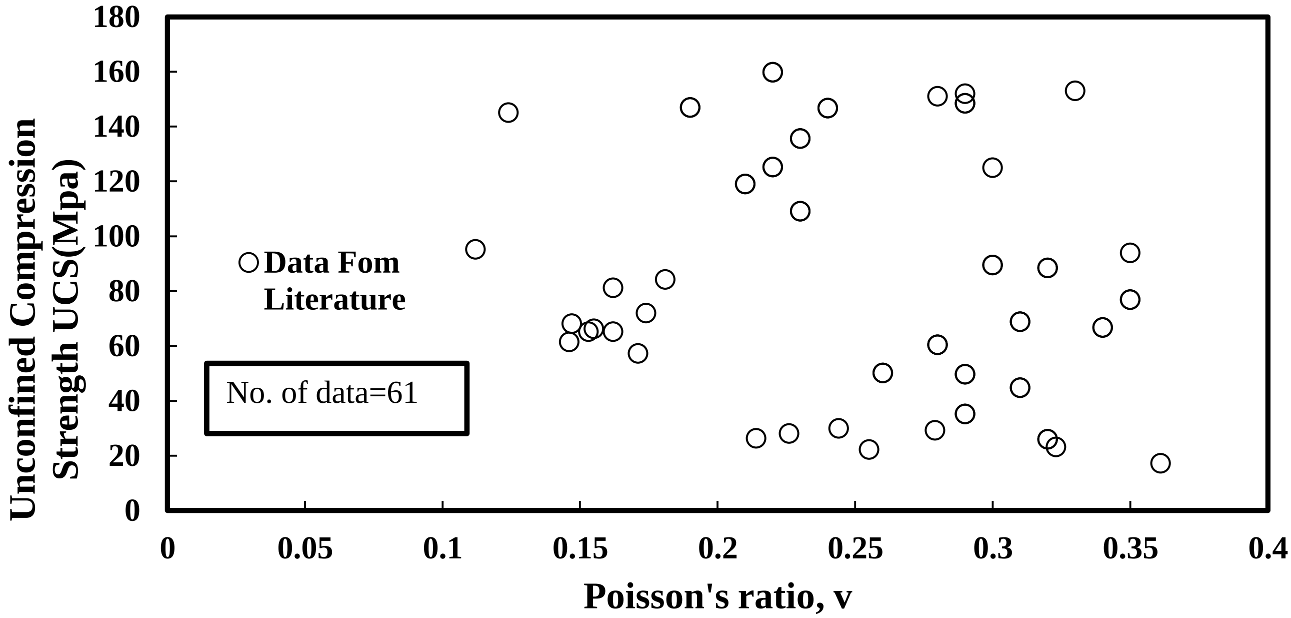

Fig. 8 Unconfined Compression Strength vs Poisson's ratio

The effect of superplasticizer dosage on fresh properties of self-compacting lightweight concrete produced with coarse pumice aggregate

Nadhim Abdulwahid Hamah Sor
Building and Construction Engineering Department, University of Garmian, Kalar, Kurdistan Region, Iraq.
Email: Nadhim.abdulwahid@garmian.edu.krd

Abstract:
The use of superplasticizer in the manufacture of self-compacting concrete is gradually more common. Each type of superplasticizer available in the market has different compositions, causing differences in dosage requirement. Also, superplasticizer affect the fresh and hardened properties of concrete. In this experimental study the effect of different dosage of superplasticizer (SP) on fresh properties of self-compacting lightweight concrete (SCLC) containing coarse aggregate pumice were studied by using five different percentages for (SP) (1%, 1.3%, 1.5%, 1.7% and 2%) of the binder weight. (SCLCs) were produced with constant binder content of 550 kg/m^3 and at a water-to-binder ratio of 0.26. 20% of portland cement was replaced with fly ash by weight. The workability of SCLCs was quantitatively evaluated by slump flow time and diameter, V-funnel flow time, and L-box height ratio. Moreover, compressive strength of hardened SCLCs was measured at 28 days by using compression machine and Rebound hammer test. The results show that with the increase of (SP) dosage in the concrete mixture, the flowability increased. However, there is an optimum value of (SP). The increase of (SP) dosage is accompanied by decreasing of T_{500} slump flow and V-funnel time until it reaches the optimum level. Nevertheless, excessive use of (SP) lead to increase of slump flow diameter.

Keywords: Self-compacting lightweight concrete, superplasticizer dosage, pumice aggregate, fresh properties, Compressive strength.

1. Introduction:

Self compacting concrete (SCC) is another type of high performance concrete that was invented by the Japanese researchers in the late of the 1980’s which has good segregation resistance, deformability and can consolidate into the congested reinforcement, narrow and deep sections by its self-mass to completely fill the formwork without demanding external mechanical vibration and can be pumped through long distances (Okamura & Ouchi, 2003; Ozawa, 1989). Actually, the combination of SCC with lightweight aggregate (LWA) to produce self compacting lightweight concrete (SCLC) can maximize the applications and benefits of SCC (Kim et al, 2010; Hwang & Hung, 2005). Well-designed SCLC mixtures can fill the formwork and surround the reinforcement without any bleeding or segregation (Wu, Z., Zhang et al., 2009). Furthermore, using lightweight concrete (LWC) leads to the reduction of the dead weight in a building that related to the reduction in the size of structural reinforced concrete such as foundation, beams, columns, and slabs (Topcu, 1997). Furthermore, LWC has some advantages such as; increasing the strength-to-weight ratio, reducing the modulus of elasticity, enhancing the thermal and sound insulation and fire resistance properties (Dhir et al., 1984). Pumice is available in the nature from volcanic origin produced by the release of gases during the solidification of lava, and it has been used as lightweight aggregate in the production of lightweight concrete in many countries around the world. So far, the use of pumice was dependent on the availability and limited to the countries where it is locally available or easily imported. Approximately, 7.4 billion m^3 (40%) of the total 18 billion m3 of pumice reserve is located in Turkey (Mor, A. 1993).

Lightweight aggregates were primarily used to reduce the weight of concrete structures. However, these aggregates were usually saturated prior to use in concrete to ensure adequate workability, since it was recognized that dry porous aggregates could absorb some of the mix water in fresh concrete (Cusson & Hoogeveen, 2008). The workable concrete mixtures become stiff within a few minutes of mixing Because of high water absorption. So, it’s a standard practice to pre-soak lightweight aggregates before batching (Craig & Wolfe, 2012). Actually, the aggregates will be soaked in water for 24 h prior to mixing is commonly used. So, it’s a standard practice to pre-soak lightweight aggregates before batching (Craig & Wolfe, 2012).

In self compacting concrete and high strength concrete, superplasticizers are used as an essential ingredient for achieving higher workability at a very low water-to-powder (w/p) ratio (Matsumoto et al., 2009). The effect of superplasticizer in concrete fresh mixture depends on its dosage and distribution in the mixture. Very low dosage will not affect the rheological behavior of the fresh mixture, and on the other hand very high dosage may cause detrimental effect such as bleeding and segregation. Yamada et al., (2001) remark that there are critical dosage and saturation dosage of SP in the concrete mixture. Critical dosage is defined as minimal dosage needed to cause overall effect of SP in the mixture.

Many studies (Brencich et al., 2013; Pucinotti, 2015) have investigated the reliability of the compressive strength estimates from the rebound hammer test. Lower W/C ratio provides higher rebound value. However, variation of the rebound value with the W/C ratio is similar to the general variation of concrete compressive strength with the W/C ratio, but less pronounced (Katalin, S., 2013). Moisture in the concrete can decrease the rebound by up to 20 percent (A. Samarin, 2004).

The purpose of this study was to examine the superplasticizer dosage on SCLCs produced by pumice lightweight coarse aggregates by using five different percentages for (SP) (1%, 1.3%, 1.5%, 1.7% and 2%) of the binder weight. Consequently, a total of five SCLC mixes were designed at a constant w/b ratio of 0.26 and the total binder content of 550 kg/m^3. For fresh properties (Slump flow time and diameter, V-funnel and L-box height ratio) and Rebound Number, compressive strengths were measured at the age of 28 days.

2 Experimental study:

2.1 Materials:

In this study, CEM I 42.5 R type portland cement (PC) with Blaine fineness of 326 m^2/kg and specific gravity of 3.15 and class F fly ash (FA) with Blaine fineness of 379 m^2/kg and specific gravity of 2.05 were used for manufacturing both the artificial lightweight aggregates and the concrete mixtures. The chemical compositions and physical properties of the Portland cement and fly ash are presented in Table 2.1. A polycarboxylic ether based superplasticizer with a specific gravity of 1.10 g/cm^3 was used in all mixtures as shown in (Fig. 2.1).

The mixture grading curve illustrated in (Fig. 2.2) of crushed stone and river sand with a maximum particle size of 4 mm was used as normal fine aggregate and pumice lightweight gravel with a maximum particle size of 16 mm was used as normal lightweight coarse aggregate as illustrated in (Fig. 2.3). The sieve analyses as well as the physical properties of the normal and lightweight aggregates are given in Table 2.2.

2.2 Mix proportions:

After materials preparation, the self-compacting lightweight concretes (SCLC) with a total binder content of 550 kg/m^3 and at a water-to-binder ratio of 0.26 were produced by replacing superplasticizer (SP) dosage to investigate the influence of superplasticizer on the fresh properties of SCLC (slump flow time and diameter, V-funnel, L-box) as well as on compressive strengths and rebound hammer number. In all mixtures, the class F fly ash was used by 20% of the total binder content. In the mix design, the total aggregate volume was designated as 50% fine and 50% coarse aggregates by volume. Five different self-compacting lightweight concrete were designed in this study by using five different percentages for (SP) (1%, 1.3%, 1.5%, 1.7% and 2%) of the binder weight. However, all mixes made with lightweight pumice aggregates as coarse aggregates. Totally 5 self-compacting concrete mixtures were designed and produced. The detailed mix proportions of the mixtures are tabulated in Table 2.3. In the Mix ID; SP is the abbreviation of superplasticizer. For example, $SP_{1.5\%}$ means that the SCLC mixture containing superplasticizer dosage as 1.5% of the binder weight.

2.3. Specimens preparation and curing:

All concrete mixtures were mixed in power-driven revolving pan mixer with capacity of 30 liter. Mixing and batching procedure suggested by (Khayat et al., 2000) was followed in this study to achieve the same homogeneity and uniformity in all SCLCs due to the fact that the mixing sequence and duration are very important in the SCC production. However, for the concrete mixture produced with pumice lightweight aggregates, before each mixing, sufficient amount of coarse pumice lightweight aggregates were immersed in water for 24 hr for saturation. Then, coarse pumice aggregates lightweight were taken out of water and put on the mesh for the outflow of excessive surface water for about 30 s. The extra water on the surface of pumice aggregate was rubbed out manually by a dry towel as shown in (Fig. 2.4). This is an effective way to obtain SSD condition for the lightweight pores aggregates (Gesoğlu, 2004). Regarding to this procedure, the fine and coarse aggregates were poured in a power-driven revolving pan mixer and allowed to mix homogeneously for 30 seconds. After that about one-third of the mixing water was added into the mixer and it was allowed to proceed the mixing for one more minute. The aggregates, then, were left to absorb the water for 1 minute. Afterwards, the powder materials (cement and fly ash) were added to the wetted aggregate mixture for mixing another minute. After that SP with remaining water was poured into the mixer, the concrete was mixed for 3 min and then left to rest for a 2 min. Finally, the concrete was mixed for additional 2 min to complete the production. The quantity of superplasticizer was arranged for all mixtures to obtain the desired workability. To determine the fluidity and workability properties of SCC, V-funnel tests were performed to gather information about flowing ability and viscosity with flow diameter and time of fresh concrete.

Besides, the L-box tests were performed to determine the passing ability from narrow sections of fresh concrete. These fresh concrete tests were conducted according to the standards of (EFNARC, 2005), prepared by the European Working Group on Self-Compacting Concrete. For each mixture, the flow diameter, time to flow a diameter of 500 mm (T_{500} time), V-funnel flow time and L-box ratio were measured. As well as, the concrete mixtures were poured in the plastic moulds and kept in the casting room at

20±2 ºC for 24 hours. After the demoulding, 28-day water curing was applied to the compressive strength and rebound hammer test specimens of the SCLCs.

2.4. Test procedure:

Slump flow diameter, T_{500mm} slump flow time, V-funnel flow time, and L-box height ratio tests were done according to the procedure recommended by (EFNARC, 2005). Slump flow value describes the flowability of a fresh mix. It is an important test for self compacting concretes as the primary check that the fresh concrete meets the specification in terms of flow. T_{500mm} is the time measured that shows the concrete has flowed to a diameter of 500 mm (EFNARC, 2005). According to EFNARC, there are three typical slump flow classes for the range of applications according to their flow diameter as shown in (Fig. 2.5). Their typical application fields as well as the upper and lower limits are illustrated in Table 2.4.

Viscosity of the produced SCLCs can be characterized with the T_{500mm} slump flow time and V-funnel flow time. These values do not measure the viscosity directly but they are related to the rate of flow. In the case of V-funnel test, a V shaped funnel is filled with fresh concrete (Fig. 2.6) and the time taken for the concrete to flow out of the funnel is measured and recorded as the V-funnel flow time. According to (EFNARC, 2005) there are two viscosity classes to measure V-funnel and T_{500mm} slump flow times. Viscosity classification was given in Table 2.4. For checking passing ability of the fresh mixes by using L-box test (Fig. 2.7) to show the flow through confined spaces and narrow openings such as areas of congested reinforcement without segregation. Another important test for SCC is L-box test, a limited volume of fresh concrete is allowed to flow horizontally through the gaps between vertical, smooth reinforcing bars and the height of the concrete beyond the reinforcement is measured. Table 2.4 presents the passing ability types on the basis of L-box height ratio.

Testing for compressive strengths and rebound number (Figs. 2.8 and 2.9) were done at 28 days of age. According to (ASTM C 39, 2012) the test was conducted on three 150 * 150 * 150 mm cubes by means of a 4000 kN capacity testing machine (ASTM C 39, 2012). Also, according to (ASTM C805, 2013) the three cubs were tested for rebound hammer.The average of three test specimens was computed.

3. Experimental results:

3.1. Fresh properties:

The concretes produced in this study, approximately had similar fresh and dry densities for all mixes of 1930 kg/m^3 and 1815 kg/m^3, respectively.

According to (EFNARC, 2005) standard, the flow diameter, time to flow a diameter of 500 mm (T_{500mm}), V-funnel flow time and L-box ratio were measured.

The flow diameters of SCLC containing 5 l/m^3 of superplasticizer (SP) for the first mix ($SP_{1\%}$) was measured as 700 mm and gradually increased with increasing SP dosage while for using 10 l/m^3 of SP the flow diameter reach 750 mm (Halim et al., 2017). However, flow diameter for the other mixes $SP_{1.3\%}$, $SP_{1.5\%}$ and $SP_{1.7\%}$ were increased by 2.86%, 4.29% and 5%, respectively compared with the first mix. Figure 3.1 illustrated the relationships between flow diameter and SP dosages. The mixtures have satisfied 660 – 750 mm value of flow diameter is the second class SF2, proposed by (EFNARC, 2005).

The time required to reach 500 mm slump-flow and the time required to flow through the V-funnel apparatus of produced SCLCs were presented in (Figs. 3.2 and 3.3), respectively. These parameters can be used to evaluate the segregation resistance of SCLCs (Kim et al., 2010). It was observed that both the time required to reach 500 mm slump-flow and the time required to flow through the V-funnel apparatus decreased as the dosage of SP was increased up to 1.5% of the binder weight after this point the time required to reach 500 mm slump flow and V-funnel were increased . T_{500mm} slump flow for $SP_{1\%}$, $SP_{1.3\%}$, $SP_{1.5\%}$, $SP_{1.7\%}$ and $SP_{2\%}$ was recorded as 3.2, 2.9, 2.7, 3.3 and 3.5 s respectively. However, the time obtained from V-funnel for all mixes were out of recommended by EFNARC (20) except $SP_{1.5\%}$ was 25 s. Furthermore, the other mixes ($SP_{1.3\%}$ and $SP_{1.7\%}$) and ($SP_{1\%}$ and $SP_{2\%}$) their time extend from $SP_{1.5\%}$ time by 50% and 100%, respectively.

According to Table 2.4, the viscosity classes of the produced SCLCs are shown in Figure 3.4. EFNARC (2005) recommended that viscosity should be indicated only in special cases such as best surface finish and in limiting the formwork pressure or improving the segregation resistance. As obviously seen in (Fig. 3.4), all SCLCs mixtures were classified as VS2/VF2.

The L-box test can be used to measure the passing ability of SCLC mixes such that the ratio of H2/H1 represents a measure of the passing ability among the reinforcing bars. The variation in the three bar L-box height ratio with superplasticizer dosage is presented in (Fig. 3.5) for the SCLCs. To confirm that SCLC has the passing ability, L-box height ratio must be equal to or greater than 0.8. According to (Fig. 3.5), H2/H1 ratio met the (EFNARC, 2005) limitation for all mixes. As clearly seen, the first mixture $SP_{1\%}$ has the lowest H2/H1 ratio of 0.92. Especially, a perfect fluid behavior was observed in $SP_{1.5\%}$ due to having H2/H1 ratio being 0.97. However, for the mixes $SP_{1.3\%}$ and $SP_{1.7\%}$ were calculated as 0.96 and for $SP_{2\%}$ was 0.95.

3.2. Compressive strength and rebound number:

The effect of SP dosage on the 28-day compressive strength for SCLCs were presented in (Fig. 3.6). It is shown that the presence of SP certainly has positive influence in increasing the compressive strength of concrete with the increase of workability and it is agreement with (Halim et al., 2017). There is an optimum dosage of 8.25 kg/m^3 to achieve higher strength. Further dosage increment reduces the strength. The 28- day compressive strength of the $SP_{1.5\%}$ was 45.67 MPa while that of $SP_{1\%}$ being 37.1 MPa. In particular, the 28-days compressive strength of SCLC containing 7.15 kg/m^3 of SP was 16.1% lower than that of the $SP_{1.5\%}$ mix, while the 28-days compressive strength of $SP_{1.7\%}$ and $SP_{2\%}$ mixes were measured as 44.62 and 43.95 MPa, respectively.

According to RELEM/CEB (Clarke, 1993) the compressive strengths recorded in this SCLC experiments were satisfy the minimum value for structural lightweight concrete is 15 MPa and the density was as (1805 kg/m^3) is in the range (1600 – 2000) kg/m^3 that illustrated in Table 3.1.

On the other hand, the influence of SP dosage on the rebound number on cubes of SCLCs at 28-day were shown in (Fig. 3.7). The rebound number of SCLCs were recoded as 38.5, 39.6, 43.3, 42.1 and 41.3 for the mixes $SP_{1\%}$, $SP_{1.3\%}$, $SP_{1.5\%}$, $SP_{1.7\%}$ and $SP_{2\%,}$ respectively. Furthermore, the estimated compressive strengths that obtained from the chart that delivered with the rebound hammer instrument were presented in (Fig. 3.8). The maximum estimated compressive strength was measured as 52.1 MPa for $SP_{1.5\%}$ mixture.

Correlating the experimental data is an important practice for the researchers to evaluate of the determined results. Theoretically, the major parameter controlling the mechanical characteristics of concrete is its quality and the increasing the compressive strength lead to improve other mechanical behavior. Therefore, the relationship between rebound number and estimated compressive strength from the chart depending on the rebound number as well as compressive strength measured from the cubes of SCLCs at 28 days were illustrated in (Fig. 3.9). The iteration between test results was evaluated in terms of R-square values. It was noticed that there are strong relationship between the compressive and estimated compressive strengths with the rebound number of the SCLC mixtures.

4. Conclusions

From this study, the following conclusions can be summarized:

- Slump flow diameter increased with increasing of superplasticizer dosage.
- Both the time required to reach 500 mm slump-flow and the time required to flow through the V-funnel apparatus decreased as the SP dosage increased up to 8.25 kg/m^3 dosage then both of them increased with increasing SP dosage.

- It was observed that increasing the SP amount resulted in a gradual increase in the L-box height ratio of SCLCs mixes up to an amount 8.25 kg/m^3 which recorded 0.97 after that decreased by increasing SP amount.
- The increased dosage of SP caused an increment in the compressive strength of SCLCs up to the third dosage in the $SP_{1.5\%}$ mixture then slightly decreased.
- The rebound number consequently the estimated compressive strength were increased by increasing SP amount till to 8.25 kg/m^3 then decreased.
- The analysis of the iteration of the compressive and estimated compressive strength with rebound number indicated that there is a strong relationship between these tests in terms of R-square value of 0.95 and 0.97 respectively.
- It is very clear from the test results that the mix $SP_{1.5\%}$ of SCLCs produced by coarse pumice lightweight aggregate satisfy the requirements of SCC with respect to (EFNARC, 2005) and its compressive strength was 45.67 MPa greater than the minimum value indicated in RELEM/CEB.

References:

A. Samarin, (2004). Handbook on Nondestructive Testing of Concrete, second ed., CRC Press LLC.

ASTM C 805 (2013). Test Method for Rebound Number of Hardened Concrete, ASTM International, West Conshohocken, PA.

ASTM C39/C39M (2012). Standard test method for compressive strength of cylindrical concrete specimen's annual book of ASTM Standard, Philadelphia, vol. 04–02.

Brencich, A., Cassini, G., Pera, D., & Riotto, G. (2013). Calibration and reliability of the rebound (Schmidt) Hammer test. *Civil Engineering and Architecture*, *1*(3), 66-78.

Clarke JL. (1993). Structural lightweight aggregate concrete. Blackie Academic and Professional, Berkshire.

Craig, P., Wolfe, B. (2012). Another look at the drying of lightweight concrete: A comparison of drying times for normal weight and lightweight floors. Concrete international, January 2012, pp. 53–56.

Cusson, D., & Hoogeveen, T. (2008). Internal curing of high-performance concrete with pre-soaked fine lightweight aggregate for prevention of autogenous shrinkage cracking. *Cement and Concrete Research*, *38*(6), 757-765.

Dhir K, Mays RGC, Chua HC (1984) Lightweight structural concrete with aglite aggregate: mix design and properties. Int J Cem Comp Lightweight Concr 6(4):249– 261. doi: 10.1016/0262-5075(84)90020-4.

Euroguide, EFNARC (2005). The European guidelines for self-compacting concrete specification, production and use. SCC European group formed by BIBM, CEMBUREAU, ERMCO, EFCA.

Gesoğlu, M. (2004). Effects of lightweight aggregate properties on mechanical, fracture, and physical behavior of lightweight concretes (Doctoral dissertation, PhD thesis, Boğaziçi University, İstanbul).

Halim, J. G., Kusuma, O. C., & Hardjito, D. (2017). Optimizing Polycarboxylate Based Superplasticizer Dosage with Different Cement Type. *Procedia engineering*, *171*, 752-759.

Hwang, C. L., & Hung, M. F. (2005). Durability design and performance of self-consolidating lightweight concrete. Construction and Building Materials, 19(8), 619-626.

Katalin, S. (2013). *Rebound surface hardness and related properties of concrete* (Doctoral dissertation, Ph. D. thesis, Budapest Univ. of Technology and Economics, Dept. of Construction Materials and Engineering, Budapest, Hungary).

Khayat KH, Bickley J, Lessard M (2000) Performance of self-consolidating concrete for casting basement and foundation walls. ACI Mater J, 97(3):374–80

Kim, Y. J., Choi, Y. W., & Lachemi, M. (2010). Characteristics of self-consolidating concrete using two types of lightweight coarse aggregates. *Construction and Building Materials*, *24*(1), 11-16.

Matsumoto, T., Sugiyama, T., & Ohta, A. (2009). Study of the Application of Viscosity Reducing Type Superplasticizers for Low Water-Binder Ratio Concrete. *Special Publication*, *262*, 177-186.

Mor, A. (1993). Steel-concrete bond in high-strength lightweight concrete. ACI Materials Journal, 89(1).

Okamura, H., & Ouchi, M. (2003). Self-compacting concrete. Journal of advanced concrete technology, 1(1), 5-15.

Ozawa, K. (1989). High performance concrete based on the durability design of concrete structures. In The Second East Asia-Pasific Conference on Structural Engineering & Construction.

Pucinotti, R. (2015). Reinforced concrete structure: Nondestructive in situ strength assessment of concrete. *Construction and Building Materials*, *75*, 331-341.

Topcu, I.B., (1997), "Semi-Lightweight Concretes Produced by Volcanic Ash", Cement and Concrete Research, Vol. 27, Issue. 1, pp. 15-21.

Wu, Z., Zhang, Y., Zheng, J., Ding, Y. (2009). An experimental study on the workability of self-compacting lightweight concrete. Construction and Building Materials. 23, 2087-2092.

Yamada, K., Ogawa, S., & Hanehara, S. (2001). Controlling of the adsorption and dispersing force of polycarboxylate-type superplasticizer by sulfate ion concentration in aqueous phase. *Cement and Concrete Research*, *31*(3), 375-383.

Appendices

Table 2.1 Chemical compositions and physical properties of Portland cement and fly ash

Analysis report (%)	**Cement**	**Fly ash**
CaO	62.58	2.24
SiO2	20.25	57.2
Al2O3	5.31	24.4
Fe2O3	4.04	7.1
MgO	2.82	2.4
SO3	2.73	0.29
K2O	0.92	3.37
Na2O	0.22	0.38
Loss on ignition	2.96	1.52
Specific gravity	3.15	2.05
Blaine fineness (m^2/kg)	**326**	**379**

Table 2.2 Physical properties and Sieve analysis of lightweight and normal weight aggregates

Sieve size (mm)	**Natural weight aggregate**		**Lightweight aggregate**
	River sand	Crushed sand	Coarse 4-16mm
16	100	100	100
8	99.7	100	79.9
4	94.5	99.2	0
2	58.7	62.9	0
1	38.2	43.7	0
0.5	24.9	33.9	0
0.25	5.4	22.6	0
Specific gravity (g/cm^3)	**2.60**	**2.63**	**1.10**

Table 2.3 Concrete mix proportions in kg/m^3

Code number	W/b	Cement	Fly Ash	Water	Lightweight Coarse Aggregate LWCA		Normal weight fine aggregate NWFA		HRWRA
					(4 – 8) mm	(8 – 16) mm	Normal sand	Crushed sand	
$SP_{1\%}$	0.26	440	110	143	108.2	252.4	598.2	259.3	5.5
$SP_{1.3\%}$	0.26	440	110	143	108.2	252.4	598.2	259.3	7.15
$SP_{1.5\%}$	0.26	440	110	143	108.2	252.4	598.2	259.3	8.25
$SP_{1.7\%}$	0.26	440	110	143	108.2	252.4	598.2	259.3	9.35
$SP_{2\%}$	0.26	440	110	143	108.2	252.4	598.2	259.3	11

Table 2.4: Slump flow, viscosity, and passing ability classes with respect to EFNARC (2005).

Class	Slump flow diameter (mm)
Slump flow classes	
SF1	550–650
SF2	660–750
SF3	760–850

Class	T50 (s)	V-funnel time (s)
Viscosity classes		
VS1/VF1	⩽2	⩽8
VS2/VF2	>2	9–25
Passing ability classes		
PA1	⩾0.8 with two rebar	
PA2	⩾0.8 with three rebar	

Table 3.1 Classification of lightweight concretes according to compressive strength-density relationship (Clarke, 1993)

Property	Class and Type		
	Structural	Structural/Insulating	Insulating
Compressive strength (MPa)	>15	>3.5	>0.5
Density range (kg/m^3)	1600-2000	<1600	≪ 1450

Figures

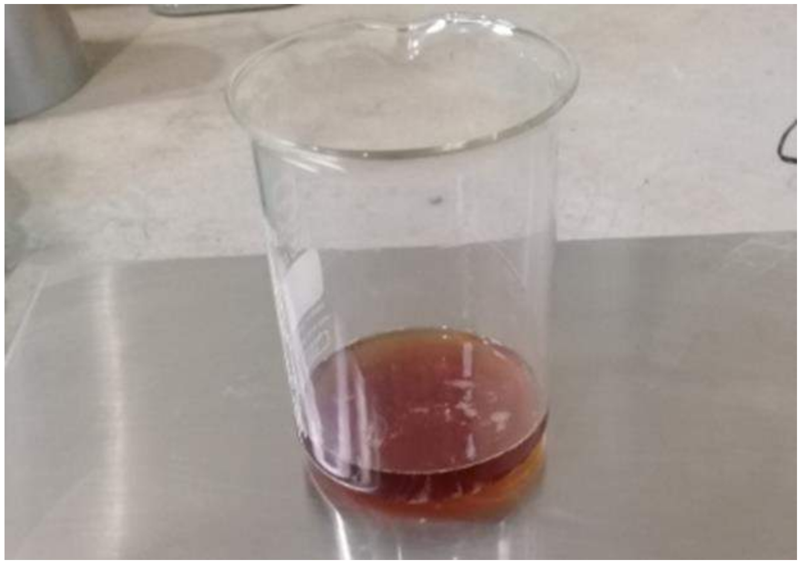

Figure 2.1 Photographic view of HRWRA

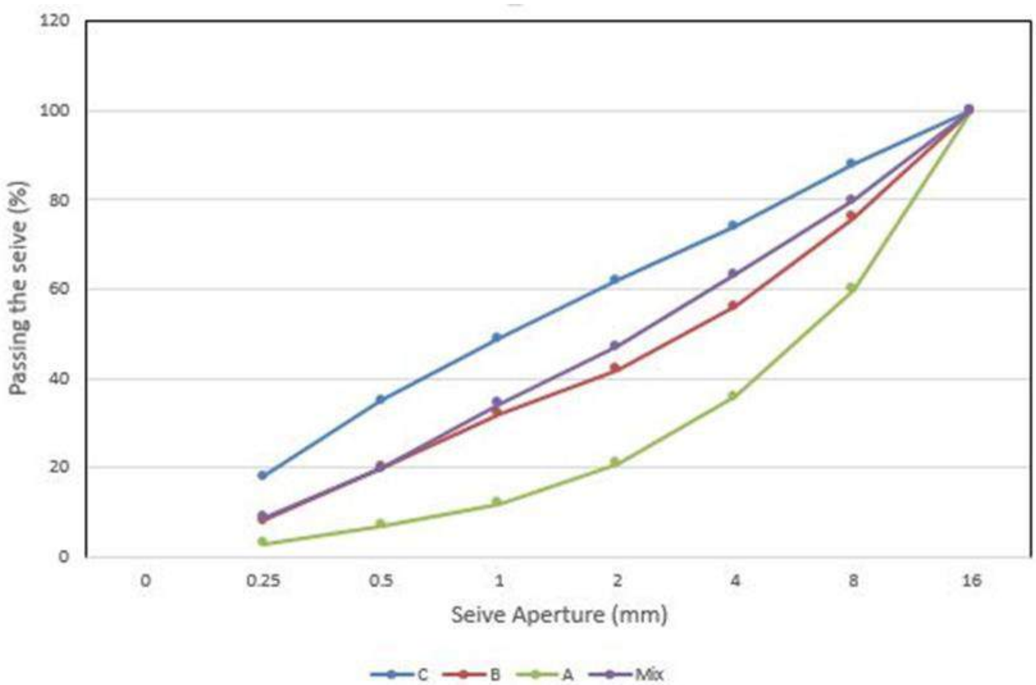

Figure 2.2 Grading curves of coarse pumice lightweight and normal sand aggregates used in experiments.

Figure 2.3 Lightweight coarse pumice

Figure 2.4 LWAs in SSD condition

Figure 2.5 Slump flow test

Figure 2.6 V-funnel test

Figure 2.7 L-box test

Figure 2.8 Compression test

Figure 2.9 Rebound hammer test

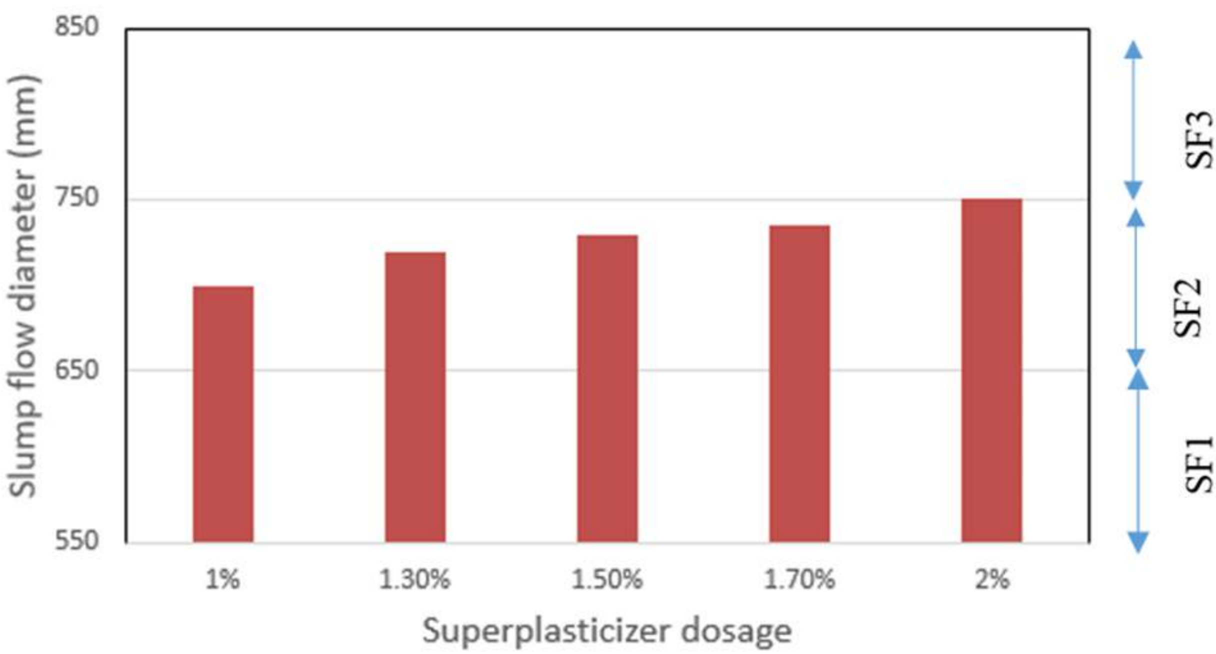

Figure 3.1 Variation of slump flow diameter and slump flow classes for SCLCs.

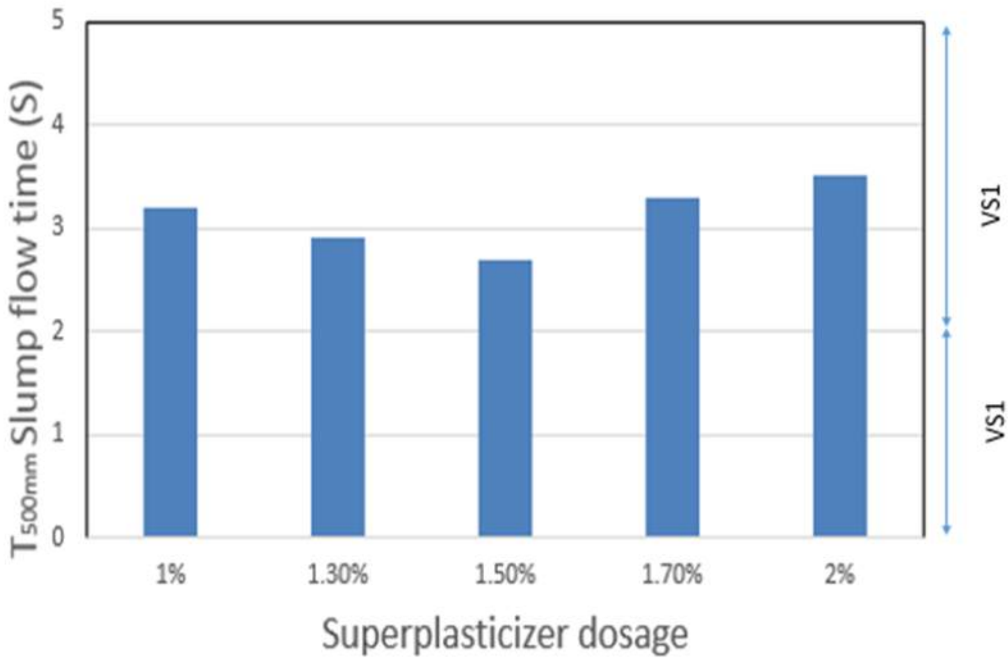

Figure 3.2 Variation of $T_{500\ mm}$ slump flow time and viscosity classes for SCLCs.

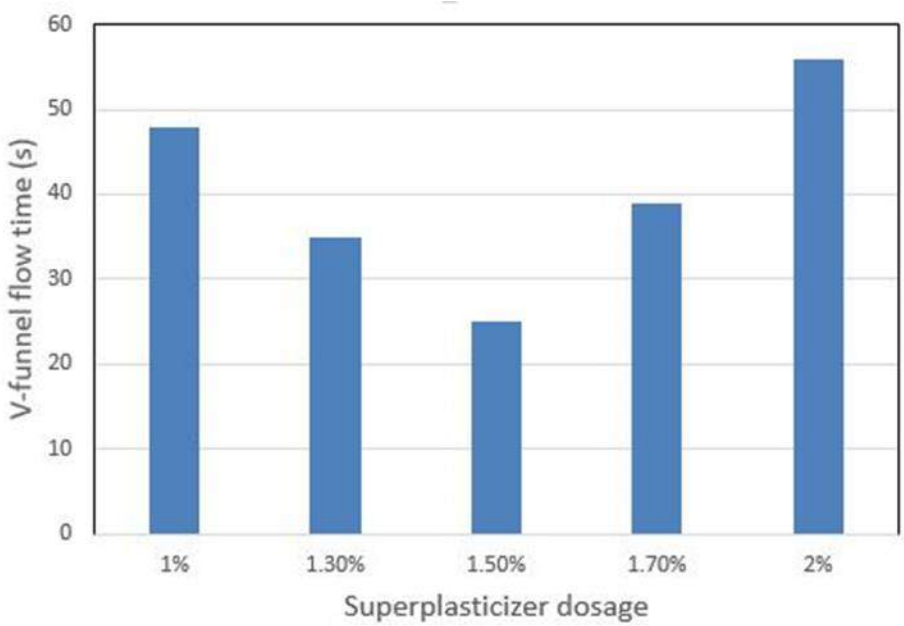

Figure 3.3 Variation of V-funnel flow time for SCLCs.

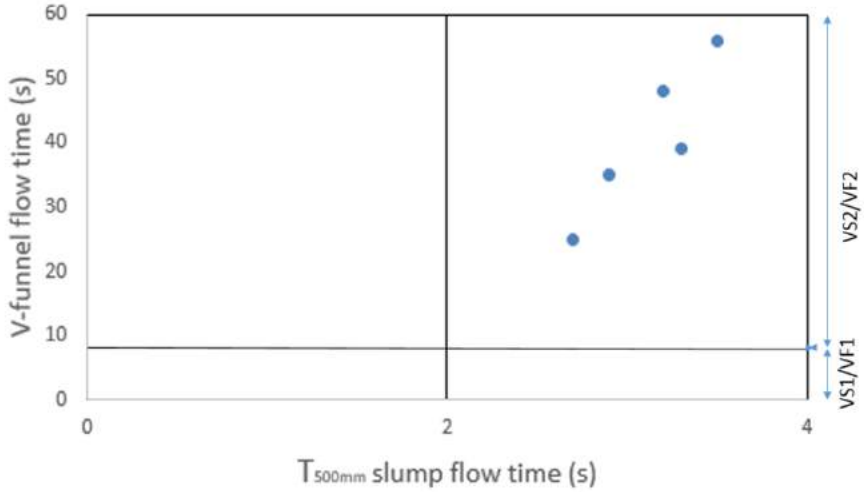

Figure 3.4 Variation of viscosity classes with T500 mm slump flow and V-funnel times for SCLCs.

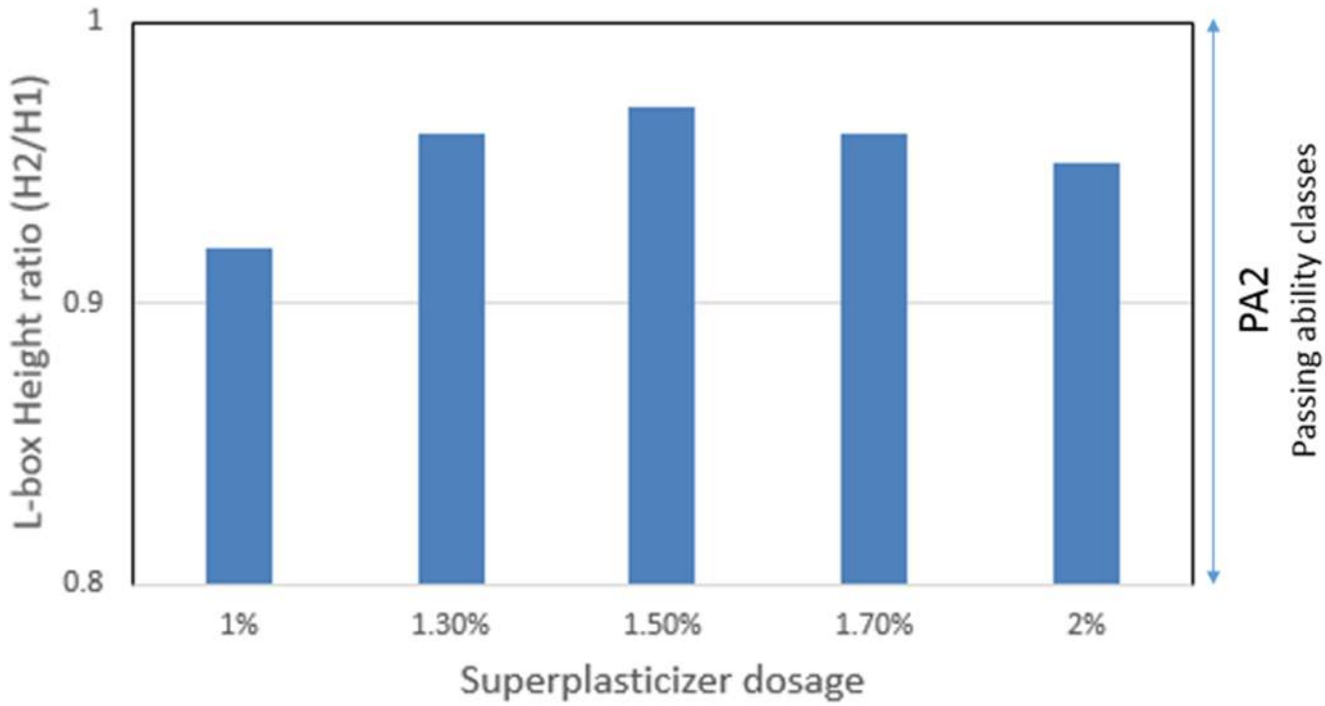

Figure 3.5 Variation of L-box height ratio values for SCLCs.

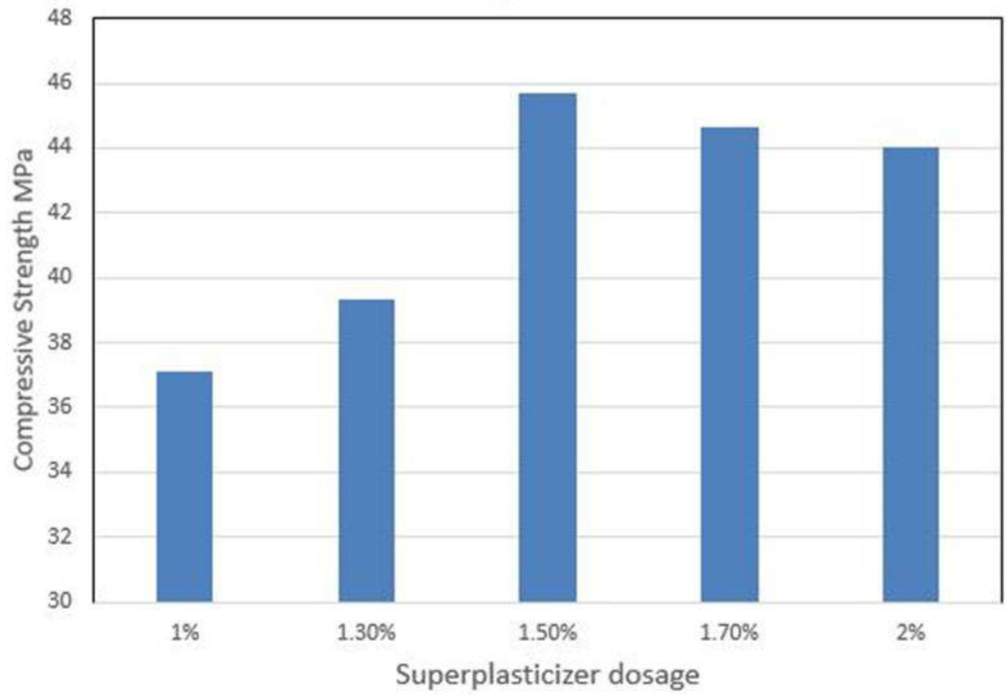

Figure 3.6 Compressive strength of SCLCs at 28 days

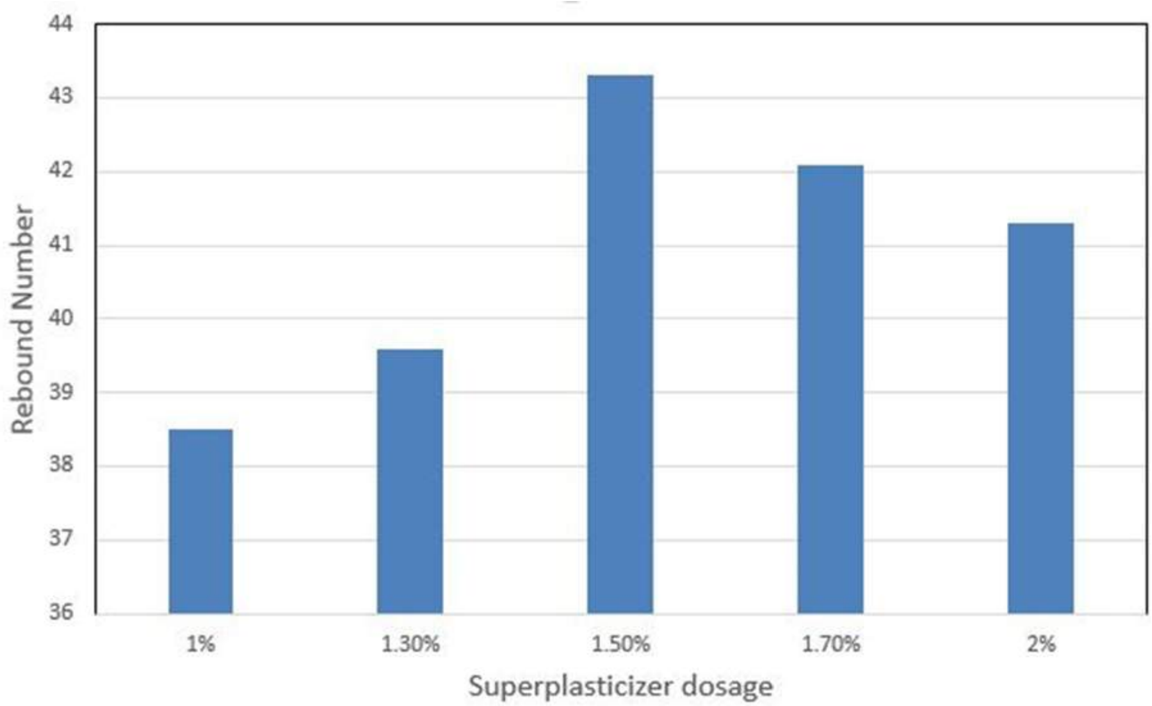

Figure 3.7 Rebound number of SCLCs at 28 days

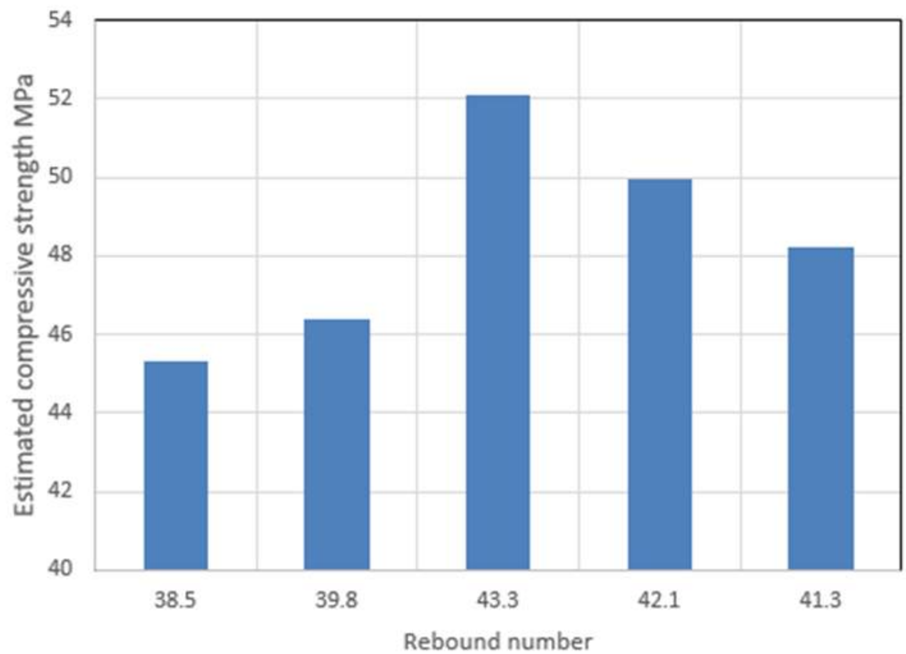

Figure 3.8 Estimated compressive strength of SCLCs

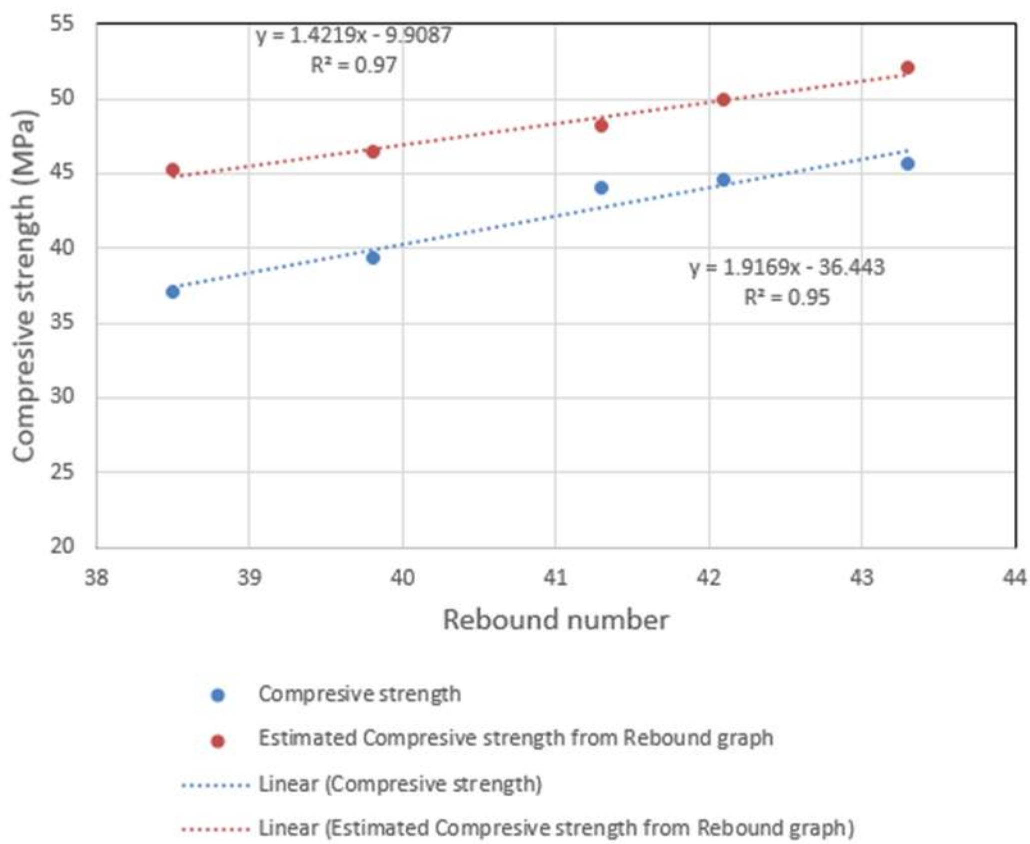

Figure 3.9 Correlation between compressive and estimated compressive strength with rebound number

ttp://jgu.garmian.edu.krd https://doi.org/10.24271/garmian.337

On Minimal λ_{bc}-Open Sets

Sarhad F. Namiq
Mathematics Department, College of Education, University of Garmian, Kurdistan Region, Iraq
Email:sarhad.faiq@garmian.edu.krd

Abstract

In this paper, we introduce and discuss minimal λ_{bc}-open sets in topological spaces. We establish some basic properties of minimal λ_{bc}-open. We obtain an application of a theory of minimal λ_{bc}-open sets and we defined a λ_{bc}-locally finite space.

1.Introduction

The study of semi open sets in topological spaces was initiated by Levine[1]. The complement of A is denoted by $X \setminus A$. In the space (X, τ), a subset A is said to be b-open[2]if $A \subseteq Cl(Int(A)) \cup Int(Cl(A))$. The family of all b-open sets of (X, τ) is denoted by $BO(X)$. The concept of operation γ was initiated by Kasahara[3]. He also introduced γ -closed graph of a function. Using this operation, Ogata[4]introduced the concept of γ -open sets and investigated the related topological properties of the associated topology τ_γ and τ. He further investigated general operator approaches of closed graph of mappings. Further Ahmad and Hussain[5] continued studying the properties of γ –open(γ-closed) sets. In 2009, Hussainand Ahmad[6], introduced the concept of minimal γ-open sets. In 2011[7] (resp., in 2013[8]) Khalafand Namiq defined an operation λcalled s-operation. They defined λ*-open sets[9] which is equivalent to λ-open set[7] and λ_s- open set[8] by using s-operation. They work in operation in topology in[10-22]. They defined $\lambda_{\beta c}$-open setby using s-operation and β-closed set and also investigated several properties of $\lambda_{\beta c}$-derived, $\lambda_{\beta c}$-interior and $\lambda_{\beta c}$-closure points in topological spaces.

In this paper, we introduce and discuss minimalλ_{bc}-open sets in topological spaces. We establish some basic properties of minimal λ_{bc}-open sets and provide an example to illustrate that minimal λ_{bc}-open sets are independent of minimal open sets.

First, we recall some definitions and results used in this paper.

2. Preliminaries

Throughout, X denotes a topological space. Let A be a subset of X, then the closure and the interior of A are denoted by $Cl(A)$and $Int(A)$respectively. A subset A of a

topological space (X,τ) is said to be semi open [1] if $A \subseteq Cl(Int(A))$. The complement of a semi open set is said to be semi closed [1]. The family of all semi open (resp. semi closed) sets in a topological space (X,τ) is denoted by $SO(X,\tau)$or $SO(X)$ (resp. $SC(X,\tau)$or$SC(X)$). We consider λ as a function defined on $SO(X)$into $P(X)$ and $\lambda: SO(X) \longrightarrow P(X)$ is called an s-operation if $V \subseteq \lambda(V)$ for each non-empty semi open set V. It is assumed that $\lambda(\phi) = \phi$and $\lambda(X) = X$for any s-operation λ. Let X be a topological space and $\lambda: SO(X) \longrightarrow P(X)$ be an s-operation, then a subset A of X is called a λ^*-open set [9]which is equivalent to λ –open set[7] and λ_s-open set[8] if for each $x \in A$ there exists a semi open set U such that $x \in U$and $\lambda(U) \subseteq A$.
The complement of a λ^*-open setis said to be λ^*-closed. The family of all λ^*-open (resp., λ^*-closed) subsets of a topological space $(X,\tau)$is denoted by $SO_\lambda(X,\tau)$ or $SO_\lambda(X)$ (resp. , $SC_\lambda(X,\tau)$ or $SC_\lambda(X)$).

Definition 2.1.A λ^*-open[9](λ -open[7], λ_s-open[8]) subset A of a topological space X is called $\lambda_{\beta c}$-open [23]if for each$x \in A$there exists a β-closed set F such that $x \in F \subseteq A$. The complement of a $\lambda_{\beta c}$-open set is called $\lambda_{\beta c}$-closed[23]. The family of all $\lambda_{\beta c}$-open (resp., $\lambda_{\beta c}$-closed) subsets of a topological space $(X,\tau)$is denotedby $SO_{\lambda_{\beta c}}(X,\tau)$ or $SO_{\lambda_{\beta c}}(X)$(resp. $SC_{\lambda_{\beta c}}(X,\tau)$or $SC_{\lambda_{\beta c}}(X)$)[23].

We get the following results in [23]

Proposition 2.2. For a topological space X, $SO_{\lambda_{\beta c}}(X) \subseteq SO_\lambda(X) \subseteq SO(X)$.

The following example shows that the converse of the above proposition may not be true in general.

Example 2.3. Let $X = \{a,b,c\}$, and $\tau = \{\phi,\{a\},X\}$.We define an s-operation $\lambda: SO(X) \longrightarrow P(X)$ as $\lambda(A) = A$ if $b \in A$ and $\lambda(A) = X$ otherwise. Here, we have $\{a,c\}$ is semi open but it is not λ^*-open. And also $\{a,b\}$ is λ^*-open set but it is not λ_{bc}-open .

Definition 2.4. An s-operation λ on X is said to be s-regular which is equivalent to λ -regular [8]if for every semi open sets $U$and V of $x \in X$, there exists a semi open set Wcontaining x such that $\lambda(W) \subseteq \lambda(U) \cap \lambda(V)$.

Definition 2.5. Let A be a subset of X. Then:

(1) The $\lambda_{\beta c}$-closure of A ($\lambda_{\beta c}Cl(A)$) is the intersection of all $\lambda_{\beta c}$-closed sets containing A.

(2) The $\lambda_{\beta c}$-interior of A ($\lambda_{\beta c}Int(A)$) is the union of all $\lambda_{\beta c}$-open sets of X contained in A.

Proposition 2.6. For each point $x \in X, x \in \lambda_{\beta c}Cl(A)$if and only if $V \cap A \neq \phi$ for every $V \in SO_{\lambda_{\beta c}}(X)$ such that $x \in V$.

Proposition 2.7. Let $\{A_\alpha\}_{\alpha\in I}$be any collection of $\lambda_{\beta c}$-open sets in a topological space (X,τ), then $\bigcup_{\alpha\in I} A_\alpha$is a $\lambda_{\beta c}$-open set.
Proposition 2.8. Let λ bean s-regular s-operation. If A and B are $\lambda_{\beta c}$-open sets in X, then $A\cap B$is also a $\lambda_{\beta c}$-open set.

The proof of the following two propositions are in [24].

Proposition 2.9. Let $\{A_\alpha\}_{\alpha\in I}$be any collection of λ^*-open sets in a topological space (X,τ), then $\bigcup_{\alpha\in I} A_\alpha$is a λ^*-open set.
Proposition 2.10. Let λ besemi-regular operation. If A and B are λ^*-open sets in X, then $A\cap B$ is also aλ^*-open set.
Definition 2.11.A λ^*-open[9](λ -open[7], λ_s-open[8]) subset A of a topological space X is called λ_{bc}-open if for each $x\in A$ there exists a b-closed set F such that $x\in F\subseteq A$. The complement of a λ_{bc}-open set is called λ_{bc}-closed. The family of all λ_{bc}-open (resp., λ_{bc}-closed) subsets of a topological space$(X,\tau)$is denoted by $SO_{\lambda_{bc}}(X,\tau)$ or $SO_{\lambda_{bc}}(X)$(resp. $SC_{\lambda_{bc}}(X,\tau)$or $SC_{\lambda_{bc}}(X)$).
Proposition 2.12. For a topological space $X, SO_{\lambda_{bc}}(X)\subseteq SO_\lambda(X)\subseteq SO(X)$.
Proof.Obvious.
The following example shows that the converse of the above proposition may not be true in general.
Example 2.13. In Example 2.3**,** we have $\{a,c\}$ is semi open but it is not λ^*-open. And also $\{a,b\}$ is λ^*-open set but it is not λ_{bc}-open .
Definition 2.14. An s-operation λ on X is said to be s-regular which is equivalent to λ -regular [8] if for every semi open sets U and V of $x\in X$, there exists a semi open set Wcontaining x such that $\lambda(W)\subseteq\lambda(U)\cap\lambda(V)$.
Definition 2.15. Let A be a subset of X. Then:
(3) The λ_{bc}-closure of A ($\lambda_{bc}Cl(A)$) is the intersection of all λ_{bc}-closed sets containing A.

(4) The λ_{bc}-interior of A ($\lambda_{bc}Int(A)$) is the union of all λ_{bc}-open sets of Xcontained in A.

Proposition 2.16. For each point $x\in X, x\in\lambda_{bc}Cl(A)$if and only if $V\cap A\neq\phi$ for every $V\in SO_{\lambda_{bc}}(X)$ such that $x\in V$.
Proof. Obvious
Proposition 2.17. Let $\{A_\alpha\}_{\alpha\in I}$be any collection of λ_{bc} -open sets in a topological space (X,τ), then $\bigcup_{\alpha\in I} A_\alpha$is a λ_{bc}-open set.
Proof. Obvious

Proposition 2.18. Let λ bean s-regular s-operation. If A and B are λ_{bc}-open sets in X, then $A \cap B$is also a λ_{bc}-open set.

Proof. Obvious

3. Minimal λ_{bc}-Open Sets

Definition 3.1. Let X be a space and $A \subseteq X$ bea λ_{bc}-open set. Then A is called a minimal λ_{bc}-open set ifϕ and A are the only λ_{bc}-open subsets of A.

Example 3.2. Let $X = \{a, b, c\}$, and $\tau = P(X)$.We define an s-operation $\lambda: SO(X) \longrightarrow P(X)$ as $\lambda(A) = A$ if $A = \{a, c\}$ and $\lambda(A) = X$ otherwise. The λ_{bc}-open sets are $\phi, \{a, c\}$and X.We have $\{a, c\}$ is minimal λ_{bc}-open set.

Proposition 3.3. Let A be a nonempty λ_{bc}-open subset of a space X. If $A \subseteq \lambda_{bc}Cl(C)$, then $\lambda_{bc}Cl(A) = \lambda_{bc}Cl(C)$, for any nonempty subset C of A.

Proof. For any nonempty subset C of A,we have $\lambda_{bc}Cl(C) \subseteq \lambda_{bc}Cl(A)$. On the other hand, by supposition we see $\lambda_{bc}Cl(A) = \lambda_{bc}Cl(\lambda_{bc}Cl(C))$=$\lambda_{bc}Cl(C)$ implies $\lambda_{bc}Cl(A) \subseteq \lambda_{bc}Cl(C)$.

Therefore we have $\lambda_{bc}Cl(A) = \lambda_{bc}Cl(C)$ for any nonempty subset $C$of A.

Proposition 3.4. Let A be a nonempty λ_{bc}-open subset of a space X.If$\lambda_{bc}Cl(A) = \lambda_{bc}Cl(C)$, for any nonempty subset C of A, then A is a minimal λ_{bc}-open set.

Proof. Suppose that A is not a minimal λ_{bc}-open set. Then there exists a nonempty λ_{bc}-open set B such that $B \subseteq A$ and hence there exists an element $x \in A$ such that $x \notin B$.Then we have $\lambda_{bc}Cl(\{x\}) \subseteq X \setminus B$ implies that $\lambda_{bc}Cl(\{x\}) = \lambda_{bc}Cl(A)$.This contradiction proves the proposition.

Remark 3.5. In the remainder of this section we suppose that λ is an s–regular operation defined on a topological space X.

Proposition 3.6. The following statements are true:

(1) If A is a minimal λ_{bc}-open set and B a λ_{bc}-open set. Then $A \cap B = \phi$or $A \subseteq B$.

(2) If B and C are minimal λ_{bc}-open sets. Then $B \cap C = \phi$or $B = C$.

Proof.(**1**) Let B be a λ_{bc}-open set such that $A \cap B \neq \phi$. Since A is a minimal λ_{bc}-open set and $A \cap B \subseteq A$, we have $A \cap B = A$. Therefore $A \subseteq B$.

(**2**) If $A \cap B \neq \phi$, then by (1), we have $B \subseteq C$and $C \subseteq B$. Therefore, $B = C$.**Proposition 3.7.**Let A be a minimal λ_{bc}-open set. If$x$is an element of$A$,then$A \subseteq B$for any λ_{bc}-open neighborhood$B$of$x$.

Proof. Let$B$ be a λ_{bc}-open neighborhood of x such that$A \not\subset B$. Since where λ is λ–regularoperation, then$A \cap B$is λ_{bc}-open set such that$A \cap B \subseteq A$and$A \cap B \neq \phi$.This contradicts our assumption that$A$is a minimal λ_{bc}-open set.

Proposition 3.8. Let$A$be a minimal λ_{bc}-open set. Then for any element$x$of$A$, $A = \bigcap\{ B: B$ is λ_{bc}-open neighborhoodof$x$ }.

Proof. By Proposition 3.4, and the fact that$A$ is λ_{bc}-open neighborhood of$x$,we have $A \subseteq \bigcap\{ B: B$ is λ_{bc}-open neighborhood of$x$ } $\subseteq A$.Therefore, the result follows.

Proposition 3.9. If$A$is a minimal λ_{bc}-open set in$X$not containing $x \in X$.Then for any λ_{bc}-open neighborhood$C$of$x$, either$C \cap A = \phi$or$A \subseteq C$.

Proof. Since$C$ is a λ_{bc}-open set, we have the result by Proposition 3.3.

Corollary 3.10. IfA is a minimal λ_{bc}-open set in$X$ not containing $x \in X$ such that$x \notin A$.If $A_x = \bigcap\{ B: B$is λ_{bc}-open neighborhood of$x$ }.Theneither$A_{\mathrm{x}} \cap A = \phi$or$A \subseteq A_x$.

Proof. If$A \subseteq B$ for any λ_{bc}-open neighborhood$B$ of$x$, then$A \subseteq \bigcap\{ B: B$ is λ_{bc}-open neighborhood of$x$ }. Therefore$A \subseteq A_{\mathrm{x}}$.Otherwise there exists a λ_{bc}-open neighborhood B of$x$ such that$B \cap A = \phi$.Then we have$A_{\mathrm{x}} \cap A = \phi$.

Corollary 3.11. If$A$is a nonempty minimal λ_{bc}-open set of$X$, then for a nonempty subset$C$of A, $A \subseteq \lambda_{bc}Cl(C)$.

Proof. Let$C$be any nonempty subset of$A$.Let$y \in A$and$B$be any λ_{bc}-open neighborhood of y. By Proposition 3.4, we have$A \subseteq B$and$C = A \cap C \subseteq B \cap C$.Thus we have$B \cap C \neq \phi$and hence$y \in \lambda_{bc}Cl(C)$.This implies that$A \cap \lambda_{bc}Cl(C)$.This completes the proof.

Combining Corollary 3.11 and Propositions 3.3 and 3.4, we have:

Theorem 3.11. Let A be a nonempty λ_{bc}-open subset of space X. Then the following are equivalent:

(1) A is minimal λ_{bc}-open set, where λ is s-regular.

(2) For any nonempty subset C of A, $A \subseteq \lambda_{bc}Cl(C)$.

(3) For any nonempty subset C of A, $\lambda_{bc}Cl(A) = \lambda_{bc}Cl(C)$.

4. Finite λ_{bc} -Open Sets

In this section, we study some properties of minimal λ_{bc}-open sets in finite λ_{bc}-open sets and λ_{bc}-locally finite spaces.

Proposition 4.1. Let(X, τ)be a topological space and$\phi \neq B$a finite λ_{bc}-open set in$X$. Then there exists at least one (finite) minimal λ_{bc}-open set$A$ such that$A \subseteq B$.

Proof. Suppose that$B$ is a finite λ_{bc}-open set in$X$. Then we have the following two possibilities:

(1) B is a minimal λ_{bc}-open set.

(2) B is not a minimal b-open set.

In case (1), if we choose$B = A$, then the proposition is proved. If the case (2) is true, then there exists a nonempty (finite) λ_{bc}-open setB_1which is properly contained in$B$. If$B_1$is minimal λ_{bc}-open, we take$A = B_1$. If$B_1$is not a minimal λ_{bc}-open set, then there exists a nonempty (finite) λ_{bc}-open set B_2 such that $B_2 \subseteq B_1 \subseteq B$. We continue this process and have a sequence of λ_{bc}-open sets $\ldots \subseteq B_{\mathrm{m}} \subseteq \cdots \subseteq B_2 \subseteq B_1 \subseteq B$. Since B is a finite, this process will end in a finite number of steps. That is, for some natural number k, we have a minimal λ_{bc}-open set B_k such that $B_k = A$. This completes the proof.

Definition 4.2. A space X is said to be a λ_{bc}-locally finite space, if for each $x \in X$ there exists a finite λ_{bc}-open set A in X such that $x \in A$.

Corollary 4.3. Let X be a λ_{bc}-locally finite space and B a nonempty λ_{bc}-open set. Then there exists at least one (finite) minimal λ_{bc}-open set A such that $A \subseteq B$, where λ is $semi$-regular.

Proof. Since B is a nonempty set, there exists an element x of B. Since X is a λ_{bc}-locally finite space, we have a finite λ_{bc}-open set B_x such that $x \in B_x$. Since $B \cap B_x$ is a finite λ_{bc}-open set, we get a minimal λ_{bc}-open set A such that $A \subseteq B \cap B_x \subseteq B$ by Proposition 4.1.

Proposition 4.4. Let X be a space and for any $\alpha \in I, B_\alpha$ a λ_{bc}-open set and $\phi \neq A$ a finite λ_{bc}-open set. Then $A \cap (\bigcap_{\alpha \in I} B_\alpha)$ is a finite λ_{bc}-open set, where λ is $semi$-regular.

Proof. We see that there exists an integer n such that $A \cap (\bigcap_{\alpha \in I} B_\alpha) = A \cap (\bigcap_{i=1}^{n} B_{\alpha i})$ and hence we have the result.

Using Proposition 4.4, we can prove the following:

Theorem 4.5. Let X be a space and for any $\alpha \in I, B_\alpha$ a λ_{bc}-open set and for any $\beta \in J, B_\beta$ a nonempty finite λ_{bc}-open set. Then $(\bigcup_{\beta \in J} B_\beta) \cap (\bigcap_{\alpha \in I} B_\alpha)$ is a λ_{bc}-open set, where λ is $semi$-regular.

5. More Properties

Let A be a nonempty finite λ_{bc}-open set. It is clear, by Proposition 3.3 and Proposition 4.1, that if λ is $semi$-regular, then there exists a natural number m such that $\{A_1, A_2, \ldots, A_m\}$ is the class of all minimal λ_{bc}-open sets in A satisfying the following two conditions:

(1) For any ι, n with $1 \leq \iota, n \leq m$ and $\iota \neq n, A_\iota \cap A_n = \phi$.

(2) If C is a minimal $\lambda_{\alpha c}$-open set in A, then there exists ι with $1 \subseteq \iota \subseteq m$ such that $C = A_\iota$.

Theorem 5.1. Let X be a space and $\phi \neq A$ a finite λ_{bc}-open set such that A is not a minimal λ_{bc}-open set. Let $\{A_1, A_2, \ldots, A_m\}$ be a class of all minimal λ_{bc}-open sets in A and $y \in A \setminus (A_1 \cup A_2 \cup \ldots \cup A_m)$. Define $A_y = \bigcap\{ B{:}\, B$ is $\lambda_{\alpha c}$-open neighborhood of $x \}$. Then there exists a natural number $k \in \{1,2,3, \ldots, m\}$ such that A_k is contained in $A_{y,}$ where λ is $semi$-regular.

Proof. Suppose on the contrary that for any natural number $k \in \{1,2,3, \dots, m\}, A_k$is not contained in$A_y$. By Corollary 3.7, for any minimal λ_{bc}-open set$A_k$in$A$, $A_k \cap A_y = \phi$. By Proposition 4.4,$\phi \neq A_y$ is a finite λ_{bc}-open set. Therefore by Proposition 4.1, there exists a minimal λ_{bc}-open set C such that$C \subseteq A_y$.Since$C \subseteq A_y \subseteq A$,we have C is a minimal λ_{bc}-open set in A. By supposition, for any minimal λ_{bc}-open setA_k, we have$A_k \cap C \subseteq A_k \cap A_y = \phi$.Therefore, for any natural number$k \in \{1,2,3, \dots, m\}, C \neq A_k$.This contradicts our assumption. Hence the proof.

Proposition 5.2. Let X be a space and$\phi \neq A$ be a finite λ_{bc}-open set which is not a minimal λ_{bc}-open set. Let$\{A_1, A_2, \dots, A_m\}$be a class of all minimal λ_{bc}-open sets in$A$ and$y \in A \setminus (A_1 \cup A_2 \cup \dots \cup A_m)$. Then there exists a natural number$k \in \{1,2,3, \dots, m\}$,such that for any λ_{bc}-open neighborhood$B_y$of y, A_k is contained inB_y, where λ is λ-regular.

Proof. This follows from Theorem 5.1, as $\bigcap\{ B: B$ is λ_{bc}-open of $y \} \subseteq B_y$.Hence the proof.

Theorem 5.3. Let X be a space and$\phi \neq A$ be a finite λ_{bc}-open set which is not a minimal $\lambda_{\alpha c}$-open set. Let $\{A_1, A_2, \dots, A_m\}$ be the class of all minimal λ_{bc}-open sets in $A$and $y \in A \setminus (A_1 \cup A_2 \cup \dots \cup A_m)$.Then there exists a natural number$k \in \{1,2,3, \dots, m\}$, such that $y \in \lambda_{bc}Cl(A_k)$.where λ is λ-regular.

Proof. It follows from Proposition 5.2, that there exists a natural number$k \in \{1,2,3, \dots, m\}$such that$A_k \subseteq B$for any λ_{bc}-open neighborhood$B$ of$y$. Therefore $\phi \neq A_k \cap A_k \subseteq A_k \cap B$implies$y \in \lambda_{bc}Cl(A_k)$.This completes theproof.

Proposition 5.4. Let$\phi \neq A$be a finite λ_{bc}-open set in a space$X$ and for each $k \in \{1,2,3, \dots, m\}, A_k$is a minimal λ_{bc}-open sets in A. If the class$\{A_1, A_2, \dots, A_m\}$ contains all minimal λ_{bc}-open sets in A, then for any$\phi \neq B_k \subseteq A_k, A \subseteq \lambda_{bc}Cl(B_1 \cup B_2 \cup B_3 \cup \dots \cup B_m)$, where λ is$semi$-regular.

Proof. If A is a minimal λ_{bc}-open set, then this is the result of Theorem 3.11 (2). Otherwise, when$A$ is not a minimal λ_{bc}-open set. If x is any element of$A \setminus (A_1 \cup A_2 \cup \dots \cup A_m)$,then by Theorem 5.3, $x \in \lambda_{bc}Cl(A_1) \cup \lambda_{bc}Cl(A_2) \cup \dots . \cup \lambda_{bc}Cl(A_m)$. Therefore, by Theorem 3.11 (3), we obtain that$A \subseteq \lambda_{bc}Cl(A_1) \cup \lambda_{bc}Cl(A_2) \cup \dots . \cup \lambda_{bc}Cl(A_m) = \lambda_{bc}Cl(B_1) \cup \lambda_{bc}Cl(B_2) \cup \dots . \cup \lambda_{bc}Cl(B_m) = \lambda_{bc}Cl(B_1 \cup B_2 \cup B_3 \cup \dots \cup B_m)$.

Proposition 5.5. Let$\phi \neq A$be a finite λ_{bc}-open set and $A_k$is a minimal λ_{bc}-open set in$A$, for each $k \in \{1,2,3, \dots, m\}$.If for any$\phi \neq B_k \subseteq A_k, A \subseteq \lambda_{bc}Cl(B_1 \cup B_2 \cup B_3 \cup \dots \cup B_m)$then $\lambda_{bc}Cl(A) = \lambda_{bc}Cl(B_1 \cup B_2 \cup B_3 \cup \dots \cup B_m)$.

Proof. For any $\phi \neq B_k \subseteq A_k$ with $k \in \{1,2,3,\dots,m\}$, we have $\lambda_{bc}Cl(B_1 \cup B_2 \cup B_3 \cup \dots \cup B_m) \subseteq \lambda_{bc}Cl(A)$. Also, we have $\lambda_{bc}Cl(A) \subseteq \lambda_{bc}Cl(B_1) \cup \lambda_{bc}Cl(B_2) \cup \dots \cup \lambda_{bc}Cl(B_m) = \lambda_{bc}Cl(B_1 \cup B_2 \cup B_3 \cup \dots \cup B_m)$. Therefore, $\lambda_{bc}Cl(A) = \lambda_{bc}Cl(B_1 \cup B_2 \cup B_3 \cup \dots \cup B_m)$ for any nonempty subset B_k of A_k with $k \in \{1,2,3,\dots,m\}$.

Proposition 5.6. Let $\phi \neq A$ be a finite λ_{bc}-open set and for each $k \in \{1,2,3,\dots,m\}$, A_k is a minimal λ_{bc}-open set in A. If for any $\phi \neq B_k \subseteq A_k$, $\lambda_{bc}Cl(A) = \lambda_{bc}Cl(B_1 \cup B_2 \cup B_3 \cup \dots \cup B_m)$, then the class $\{A_1, A_2, \dots, A_m\}$ contains all minimal λ_{bc}-open sets in A.

Proof. Suppose that C is a minimal λ_{bc}-open set in A and $C \neq A_k$ for $k \in \{1,2,3,\dots,m\}$. Then we have $C \cap \lambda_{bc}Cl(A_k) = \phi$ for each $k \in \{1,2,3,\dots,m\}$. It follows that any element of C is not contained in $\lambda_{bc}Cl(A_1 \cup A_2 \cup \dots \cup A_m)$. This is a contradiction to the fact that $C \subseteq A \subseteq \lambda_{bc}Cl(A) = \lambda_{bc}Cl(B_1 \cup B_2 \cup B_3 \cup \dots \cup B_m)$. This completes the proof.

Combining Propositions 5.4, 5.5 and 5.6, we have the following theorem:

Theorem 5.7. Let A be a nonempty finite λ_{bc}-open set and A_k a minimal λ_{bc}-open set in A for each $k \in \{1,2,3,\dots,m\}$. Then the following three conditions are equivalent:

(1) The class $\{A_1, A_2, \dots, A_m\}$ contains all minimal λ_{bc}-open sets in A.

(2) For any $\phi \neq B_k \subseteq A_k, A \subseteq \lambda_{bc}Cl(B_1 \cup B_2 \cup B_3 \cup \dots \cup B_m)$.

(3) For any $\phi \neq B_k \subseteq A_k$, $\lambda_{bc}Cl(A) = \lambda_{bc}Cl(B_1 \cup B_2 \cup B_3 \cup \dots \cup B_m)$, where λ is *semi*-regular.

References

1. Levine, N., *Semi-open sets and semi-continuity in topological spaces.* Amer. Math.Monthly, 1963. **70**(1): p. 36-41.
2. Andrijevic, D., *On b-open sets.* Mat. Vesnik, 48 1996. : p. 59 - 64.
3. Kasahara, S., *Operation-Compact Spaces.* Math. Japon, 1979(24): p. 97-105.
4. Ogata, H., *Operations on Topological Spaces and Associated Topology.* Math. Japon, 1991. **36**(1): p. 175-184.
5. Ahmad, B. and S. Hussain, *Properties of γ-Operations on Topological Spaces.* Aligarh Bull.Math, 2003. **1**(22): p. 45-51.
6. Hussain, S. and B. Ahmad, *On Minimal γ -Open Sets.* Eur. J. Pure Appl. Maths, 2009. **3**(2): p. 338-351.
7. Khalaf, A.B. and S.F. Namiq, *New types of continuity and separation axiom based operation in topological spaces.* M. Sc. Thesis, University of Sulaimani, 2011.
8. Khalaf, A.B. and S.F. Namiq, *Lammda sub c-Open Sets and Lammda sub c-Separation Axioms in Topological Spaces.* Journal of Advanced Studies in Topology, 2013. **4**(1): p. 150-158.

9. Namiq, S.F., *Lammda-R0 and Lammda-R1 Spaces*. Journal of Garmyan University, 2014. **4**(3).
10. F.Namiq, S., *Contra 〚(λ,γ)〛^*-Continuous Functions*. Journal of Garmyan University, 2017.
11. B.Khalaf, A. and S.F. Namiq, *Generalized Lammda-Closed Sets and (Lammda,Gamma)^*-Continuous* Journal of Garmyan University, 2017: p. 2310-0087.
12. Namiq, S.F., *Generalized λ_c-Open Set*. International Journal of Scientific & Engineering Research, June-2017. **8**(6).
13. B.Khalaf, A. and S.F. Namiq, *λ_βc-Connected Spaces and λ_βc-Components*. Journal of Garmyan University, 2017.
14. Khalaf, A.B., H.M. Darwesh, and S.F. Namiq, *λ_c-Connected Space Via λ_c-Open Sets*. Journal of Garmyan University, 2017.
15. Namiq, S.F., *λ_sc-open sets and topological properties*. Journal of Garmyan University, 2014.
16. B.Khalaf, A. and S.F. Namiq, *ON Minimal λ^*-Open Sets*, . International Journal of Scientific & Engineering Research, October-2014. **5**(10).
17. Namiq, S.F., *λ_c-Separation Axioms Via λ_c-open sets*. International Journal of Scientific & Engineering Research May-2017. **8**.
18. Namiq, S.F., *λ_sc-Connected Spaces Via λ_sc-Open Sets*. Journal of Garmyan University, 2017.
19. Darwesh, H.M., S.F. Namiq, and W.K. Kadir, *Maximal λc-Open Sets*. ICNS-2016, 2017.
20. Namiq, S.F., *λ-Connected Spaces Via λ-Open Sets*. Journal of Garmyan University, 2015.
21. Darwesh, H.M. and S.F. Namiq, *On Minimal λ_βc-Open Sets* Journal of Garmyan University, 2017.
22. Namiq, S.F., *On Minimal λ_αc-Open Sets*. Journal of Garmyan University, 2017(accepted).
23. F.Namiq, S., *Lammda sub beta c-Open Sets and Topological Properties*. Journal of Garmyan University, 2017(2310-0087).
24. B.Khalaf, A. and S.F. Namiq, *Generalized lammda-Closed Sets and (Lammda,Gamma)^*-Continuous Functions* International Journal of Scientific & Engineering Research, 2012. **3**(12).

ttp://jgu.garmian.edu.krd https://doi.org/10.24271/garmian.338

On Minimal $\lambda_{\alpha c}$-Open Sets

Sarhad F. Namiq
Mathematics Department, College of Education, University of Garmian, Kurdistan Region, Iraq
Email: sarhad.faiq@garmian.edu.krd

Abstract

In this paper, we introduce and discuss minimal $\lambda_{\alpha c}$-open sets in topological spaces. We establish some basic properties of minimal $\lambda_{\alpha c}$-open. We obtain an application of a theory of minimal $\lambda_{\alpha c}$-open sets and we defined a $\lambda_{\alpha c}$-locally finite space.

1. Introduction

The study of semi open sets in topological spaces was initiated by Levine[1]. The complement of A is denoted by $X\backslash A$. In the space (X,τ), a subset A is said to be α-open [2] if $A \subseteq Int(Cl(Int(A)))$. The family of all b-open sets of (X,τ) is denoted by $BO(X)$. The complement of α-open is called α-closed. The concept of operation γ was initiated by Kasahara [3]. He also introduced γ -closed graph of a function. Using this operation, Ogata[4] introduced the concept of γ -open sets and investigated the related topological properties of the associated topology τ_γ and τ. He further investigated general operator approaches of closed graph of mappings. Further Ahmad and Hussain[5] continued studying the properties of γ –open(γ-closed) sets. In 2009, Hussainand Ahmad [6], introduced the concept of minimal γ-open sets. In 2011[7] (resp., in 2013[8]) Khalaf and Namiq defined an operation λ called s-operation. They defined λ*-open sets [9] which is equivalent to λ-open set[7] and λ_s- open set[8] by using s-operation. They work in operation in topology in [10-22]. They defined $\lambda_{\beta c}$-open set by using s-operation and β-closed set and also investigated several properties of $\lambda_{\beta c}$-derived, $\lambda_{\beta c}$-interior and $\lambda_{\beta c}$-closure points in topological spaces.

In this paper, we introduce and discuss minimal $\lambda_{\alpha c}$-open sets in topological spaces.
We establish some basic properties of minimal $\lambda_{\alpha c}$-open sets and provide an example to illustrate that minimal $\lambda_{\alpha c}$-open sets are independent of minimal open sets.
First, we recall some definitions and results used in this paper.

2. Preliminaries

Throughout, X denotes a topological space. Let A be a subset of X, then the closure and the interior of A are denoted by $Cl(A)$ and $Int(A)$ respectively. A subset A of a topological space (X,τ) is said to be semi open [1] if $A \subseteq Cl\big(Int(A)\big)$. The complement

of a semi open set is said to be semi closed [1]. The family of all semi open (resp. semi closed) sets in a topological space (X,τ) is denoted by $SO(X,\tau)$ or $SO(X)$ (resp. $SC(X,\tau)$ or $SC(X)$). We consider λ as a function defined on $SO(X)$ into $P(X)$ and $\lambda: SO(X) \longrightarrow P(X)$ is called an s-operation if $V \subseteq \lambda(V)$ for each non-empty semi open set V. It is assumed that $\lambda(\phi)=\phi$ and $\lambda(X)=X$ for any s-operation λ. Let X be a topological space and $\lambda: SO(X) \longrightarrow P(X)$ be an s-operation, then a subset A of X is called a λ^*-open set [9]which is equivalent to λ –open set[7] and λ_s-open set [8] if for each $x \in A$ there exists a semi open set U such that $x \in U$and $\lambda(U) \subseteq A$.
The complement of a λ^*-open set is said to be λ^*-closed. The family of all λ^*-open (resp., λ^*-closed) subsets of a topological space $(X,\tau)$is denoted by $SO_\lambda(X,\tau)$ or $SO_\lambda(X)$ (resp. , $SC_\lambda(X,\tau)$ or $SC_\lambda(X)$).

Definition 2.1.A λ^*-open[9](λ -open[7], λ_s-open[8]) subset A of a topological space X is called $\lambda_{\beta c}$-open [23] if for each $x \in A$ there exists a β-closed set F such that $x \in F \subseteq A$. The complement of a $\lambda_{\beta c}$-open set is called $\lambda_{\beta c}$-closed[23]. The family of all $\lambda_{\beta c}$-open (resp., $\lambda_{\beta c}$-closed) subsets of a topological space (X,τ) is denoted by $SO_{\lambda_{\beta c}}(X,\tau)$ or $SO_{\lambda_{\beta c}}(X)$(resp. $SC_{\lambda_{\beta c}}(X,\tau)$or $SC_{\lambda_{\beta c}}(X)$) [23].

We get the following results in [23]

Proposition 2.2. For a topological space X, $SO_{\lambda_{\beta c}}(X) \subseteq SO_\lambda(X) \subseteq SO(X)$.

The following example shows that the converse of the above proposition may not be true in general.

Example 2.3. Let $X=\{a,b,c\}$, and $\tau=\{\phi,\{a\},X\}$. We define an s-operation $\lambda: SO(X) \longrightarrow P(X)$ as $\lambda(A)=A$ if $b \in A$ and $\lambda(A)=X$ otherwise. Here, we have $\{a,c\}$ is semi open but it is not λ^*-open. And also $\{a,b\}$ is λ^*-open set but it is not $\lambda_{\alpha c}$-open .

Definition 2.4. An s-operation λ on X is said to be s-regular which is equivalent to λ -regular [8]if for every semi open sets $U$and V of $x \in X$, there exists a semi open set Wcontaining x such that $\lambda(W) \subseteq \lambda(U) \cap \lambda(V)$.

Definition 2.5. Let A be a subset of X. Then:

(1) The $\lambda_{\beta c}$-closure of A ($\lambda_{\beta c}Cl(A)$) is the intersection of all $\lambda_{\beta c}$-closed sets containing A.

(2) The $\lambda_{\beta c}$-interior of A ($\lambda_{\beta c}Int(A)$) is the union of all $\lambda_{\beta c}$-open sets of X contained in A.

Proposition 2.6. For each point $x \in X, x \in \lambda_{\beta c}Cl(A)$ if and only if $V \cap A \neq \phi$ for every $V \in SO_{\lambda_{\beta c}}(X)$ such that $x \in V$.

Proposition 2.7. Let $\{A_\alpha\}_{\alpha\in I}$be any collection of $\lambda_{\beta c}$-open sets in a topological space (X,τ), then $\bigcup_{\alpha\in I} A_\alpha$is a $\lambda_{\beta c}$-open set.

Proposition 2.8. Let λ bean s-regular s-operation. If A and B are $\lambda_{\beta c}$-open sets in X, then $A\cap B$is also a $\lambda_{\beta c}$-open set.

The proof of the following two propositions are in [24].

Proposition 2.9. Let $\{A_\alpha\}_{\alpha\in I}$ be any collection of λ^*-open sets in a topological space (X,τ), then $\bigcup_{\alpha\in I} A_\alpha$ is a λ^*-open set.

Proposition 2.10. Let λ be semi-regular operation. If A and B are λ^*-open sets in X, then $A\cap B$ is also a λ^*-open set.

Definition 2.11. A λ^*-open[9](λ -open[7], λ_s-open[8]) subset A of a topological space X is called $\lambda_{\alpha c}$-open if for each $x\in A$ there exists a b-closed set F such that $x\in F\subseteq A$. The complement of a $\lambda_{\alpha c}$-open set is called $\lambda_{\alpha c}$-closed. The family of all $\lambda_{\alpha c}$-open (resp., $\lambda_{\alpha c}$-closed) subsets of a topological space(X,τ) is denoted by $SO_{\lambda_{\alpha c}}(X,\tau)$ or $SO_{\lambda_{\alpha c}}(X)$(resp. $SC_{\lambda_{\alpha c}}(X,\tau)$or $SC_{\lambda_{\alpha c}}(X)$).

Proposition 2.12. For a topological space $X, SO_{\lambda_{\alpha c}}(X)\subseteq SO_\lambda(X)\subseteq SO(X)$.

Proof. Obvious.

The following example shows that the converse of the above proposition may not be true in general.

Example 2.13. In Example 2.3**,** we have $\{a,c\}$ is semi open but it is not λ^*-open. And also $\{a,b\}$ is λ^*-open set but it is not $\lambda_{\alpha c}$-open .

Definition 2.14. An s-operation λ on X is said to be s-regular which is equivalent to λ -regular [8] if for every semi open sets U and V of $x\in X$, there exists a semi open set Wcontaining x such that $\lambda(W)\subseteq\lambda(U)\cap\lambda(V)$.

Definition 2.15. Let A be a subset of X. Then:

(3) The $\lambda_{\alpha c}$-closure of A ($\lambda_{\alpha c}Cl(A)$) is the intersection of all $\lambda_{\alpha c}$-closed sets containing A.

(4) The $\lambda_{\alpha c}$-interior of A ($\lambda_{\alpha c}Int(A)$) is the union of all $\lambda_{\alpha c}$-open sets of X contained in A.

Proposition 2.16. For each point $x\in X, x\in\lambda_{\alpha c}Cl(A)$ if and only if $V\cap A\neq\phi$ for every $V\in SO_{\lambda_{\alpha c}}(X)$ such that $x\in V$.

Proof. Obvious

Proposition 2.17. Let $\{A_\alpha\}_{\alpha\in I}$be any collection of $\lambda_{\alpha c}$ -open sets in a topological space (X,τ), then $\bigcup_{\alpha\in I} A_\alpha$is a $\lambda_{\alpha c}$-open set.

Proof. Obvious

Proposition 2.18. Let λ bean s-regular s-operation. If A and B are $\lambda_{\alpha c}$-open sets in X, then $A \cap B$ is also a $\lambda_{\alpha c}$-open set.

Proof. Obvious

3. Minimal $\lambda_{\alpha c}$-Open Sets

Definition 3.1. Let X be a space and $A \subseteq X$ be a $\lambda_{\alpha c}$-open set. Then A is called a minimal $\lambda_{\alpha c}$-open set if ϕ and A are the only $\lambda_{\alpha c}$-open subsets of A.

Example 3.2. Let $X = \{a, b, c\}$, and $\tau = P(X)$. We define an s-operation $\lambda: SO(X) \longrightarrow P(X)$ as $\lambda(A) = A$ if $A = \{a, c\}$ and $\lambda(A) = X$ otherwise. The $\lambda_{\alpha c}$-open sets are $\phi, \{a, c\}$and X. We have $\{a, c\}$ is minimal $\lambda_{\alpha c}$-open set.

Proposition 3.3. Let A be a nonempty $\lambda_{\alpha c}$-open subset of a space X. If $A \subseteq \lambda_{\alpha c}Cl(C)$, then $\lambda_{\alpha c}Cl(A) = \lambda_{\alpha c}Cl(C)$, for any nonempty subset C of A.

Proof. For any nonempty subset C of A,we have $\lambda_{\alpha c}Cl(C) \subseteq \lambda_{\alpha c}Cl(A)$. On the other hand, by supposition we see $\lambda_{\alpha c}Cl(A) = \lambda_{\alpha c}Cl(\lambda_{\alpha c}Cl(C))$=$\lambda_{\alpha c}Cl(C)$ implies $\lambda_{\alpha c}Cl(A) \subseteq \lambda_{\alpha c}Cl(C)$.

Therefore we have $\lambda_{\alpha c}Cl(A) = \lambda_{\alpha c}Cl(C)$ for any nonempty subset $C$of A.

Proposition 3.4. Let A be a nonempty $\lambda_{\alpha c}$-open subset of a space X.If $\lambda_{\alpha c}Cl(A) = \lambda_{\alpha c}Cl(C)$, for any nonempty subset C of A, then A is a minimal $\lambda_{\alpha c}$-open set.

Proof. Suppose that A is not a minimal $\lambda_{\alpha c}$-open set. Then there exists a nonempty $\lambda_{\alpha c}$-open set B such that $B \subseteq A$ and hence there exists an element $x \in A$ such that $x \notin B$.Then we have $\lambda_{\alpha c}Cl(\{x\}) \subseteq X \setminus B$ implies that $\lambda_{\alpha c}Cl(\{x\}) = \lambda_{\alpha c}Cl(A)$.This contradiction proves the proposition.

Remark 3.5. In the remainder of this section we suppose that λ is an s–regular operation defined on a topological space *X*.

Proposition 3.6. The following statements are true:

(1) If A is a minimal $\lambda_{\alpha c}$-open set and B a $\lambda_{\alpha c}$-open set. Then $A \cap B = \phi$ or $A \subseteq B$.

(2) If B and C are minimal $\lambda_{\alpha c}$-open sets. Then $B \cap C = \phi$ or $B = C$.

Proof.(**1**) Let B be a $\lambda_{\alpha c}$-open set such that $A \cap B \neq \phi$. Since A is a minimal $\lambda_{\alpha c}$-open set and $A \cap B \subseteq A$, we have $A \cap B = A$. Therefore $A \subseteq B$.

(**2**) If $A \cap B \neq \phi$, then by (1), we have $B \subseteq C$ and $C \subseteq B$. Therefore, $B = C$.

Proposition 3.7. Let A be a minimal $\lambda_{\alpha c}$-open set. If x is an element of A, then $A \subseteq B$ for any $\lambda_{\alpha c}$-open neighborhood B of x.

Proof. Let B be a $\lambda_{\alpha c}$-open neighborhood of x such that $A \not\subset B$. Since where λ is λ–regular operation, then $A \cap B$ is $\lambda_{\alpha c}$-open set such that $A \cap B \subseteq A$ and $A \cap B \neq \phi$. This contradicts our assumption that A is a minimal $\lambda_{\alpha c}$-open set.

Proposition 3.8. Let A be a minimal $\lambda_{\alpha c}$-open set. Then for any element x of $A, A = \bigcap\{ B: B$ is $\lambda_{\alpha c}$-open neighborhood of $x \}$.

Proof. By Proposition 3.4, and the fact that A is $\lambda_{\alpha c}$-open neighborhood of x, we have $A \subseteq \bigcap\{ B: B$ is $\lambda_{\alpha c}$-open neighborhood of $x \} \subseteq A$. Therefore, the result follows.

Proposition 3.9. If A is a minimal $\lambda_{\alpha c}$-open set in X not containing $x \in X$. Then for any $\lambda_{\alpha c}$-open neighborhood C of x, either $C \cap A = \phi$ or $A \subseteq C$.

Proof. Since C is a $\lambda_{\alpha c}$-open set, we have the result by Proposition 3.3.

Corollary 3.10. If A is a minimal $\lambda_{\alpha c}$-open set in X not containing $x \in X$ such that $x \notin A$. If $A_x = \bigcap\{ B: B$is $\lambda_{\alpha c}$-open neighborhood of $x \}$. Then either $A_{\mathrm{x}} \cap A = \phi$ or $A \subseteq A_x$.

Proof. If $A \subseteq B$ for any $\lambda_{\alpha c}$-open neighborhood B of x, then $A \subseteq \bigcap\{ B: B$ is $\lambda_{\alpha c}$-open neighborhood of $x \}$. Therefore $A \subseteq A_{\mathrm{x}}$. Otherwise there exists a $\lambda_{\alpha c}$-open neighborhood B of x such that $B \cap A = \phi$. Then we have $A_{\mathrm{x}} \cap A = \phi$.

Corollary 3.11. If A is a nonempty minimal $\lambda_{\alpha c}$-open set of X, then for a nonempty subset $C$of $A, A \subseteq \lambda_{\alpha c}Cl(C)$.

Proof. Let C be any nonempty subset of A. Let $y \in A$ and B be any $\lambda_{\alpha c}$-open neighborhood of y. By Proposition 3.4, we have $A \subseteq B$ and $C = A \cap C \subseteq B \cap C$. Thus we have $B \cap C \neq \phi$ and hence $y \in \lambda_{\alpha c}Cl(C)$. This implies that $A \cap \lambda_{\alpha c}Cl(C)$. This completes the proof.

Combining Corollary 3.11 and Propositions 3.3 and 3.4, we have:

Theorem 3.11. Let A be a nonempty $\lambda_{\alpha c}$-open subset of space X. Then the following are equivalent:

(1) A is minimal $\lambda_{\alpha c}$-open set, where λ is s-regular.

(2) For any nonempty subset C of $A, A \subseteq \lambda_{\alpha c}Cl(C)$.

(3) For any nonempty subset C of A, $\lambda_{\alpha c}Cl(A) = \lambda_{\alpha c}Cl(C)$.

4. Finite $\lambda_{\alpha c}$ -Open Sets

In this section, we study some properties of minimal $\lambda_{\alpha c}$-open sets in finite $\lambda_{\alpha c}$-open sets and $\lambda_{\alpha c}$-locally finite spaces.

Proposition 4.1. Let (X, τ) be a topological space and $\phi \neq B$ a finite $\lambda_{\alpha c}$-open set in X. Then there exists at least one (finite) minimal $\lambda_{\alpha c}$-open set A such that $A \subseteq B$.

Proof. Suppose that B is a finite $\lambda_{\alpha c}$-open set in X. Then we have the following two possibilities:

(1) B is a minimal $\lambda_{\alpha c}$-open set.

(2) B is not a minimal b-open set.

In case (1), if we choose $B = A,$ then the proposition is proved. If the case (2) is true, then there exists a nonempty (finite) $\lambda_{\alpha c}$-open set B_1 which is properly contained in B. If B_1 is minimal $\lambda_{\alpha c}$-open, we take $A = B_1$. If B_1 is not a minimal $\lambda_{\alpha c}$-open set, then there exists a nonempty (finite) $\lambda_{\alpha c}$-open set B_2 such that $B_2 \subseteq B_1 \subseteq B$. We continue this process and have a sequence of $\lambda_{\alpha c}$-open sets... $\subseteq B_{\mathrm{m}} \subseteq \cdots \subseteq B_2 \subseteq B_1 \subseteq B$. Since B is a finite, this process will end in a finite number of steps. That is, for some natural number $k,$ we have a minimal $\lambda_{\alpha c}$-open set B_k such that $B_k = A$. This completes the proof.

Definition 4.2.A space X is said to be a $\lambda_{\alpha c}$-locally finite space, if for each $x \in X$ there exists a finite $\lambda_{\alpha c}$-open set A in X such that $x \in A$.

Corollary 4.3. Let X be a $\lambda_{\alpha c}$-locally finite space and B a nonempty $\lambda_{\alpha c}$-open set. Then there exists at least one (finite) minimal $\lambda_{\alpha c}$-open set A such that $A \subseteq B,$ where λ is $semi$-regular.

Proof. Since B is a nonempty set, there exists an element$x$ of B. Since X is a $\lambda_{\alpha c}$-locally finite space, we have a finite $\lambda_{\alpha c}$-open set B_x such that $x \in B_x$. Since$B \cap B_x$ is a finite $\lambda_{\alpha c}$-open set, we get a minimal $\lambda_{\alpha c}$-open set A such that $A \subseteq B \cap B_x \subseteq B$ by Proposition 4.1.

Proposition 4.4. Let X be a space and for any $\alpha \in I, B_\alpha$ a $\lambda_{\alpha c}$-open set and $\phi \neq A$ a finite $\lambda_{\alpha c}$-open set. Then $A \cap (\bigcap_{\alpha \in I} B_\alpha)$ is a finite $\lambda_{\alpha c}$-open set, where λ is $semi$-regular.

Proof. We see that there exists an integer n such that $A \cap (\bigcap_{\alpha \in I} B_\alpha) = A \cap (\bigcap_{i=1}^{n} B_{\alpha i})$ and hence we have the result.

Using Proposition 4.4, we can prove the following:

Theorem 4.5. Let X be a space and for any $\alpha \in I, B_\alpha$ a $\lambda_{\alpha c}$-open set and for any $\beta \in J, B_\beta$ a nonempty finite $\lambda_{\alpha c}$-open set. Then $(\bigcup_{\beta \in J} B_\beta) \cap (\bigcap_{\alpha \in I} B_\alpha)$ is a $\lambda_{\alpha c}$-open set, where λ is $semi$-regular.

5. More Properties

Let A be a nonempty finite $\lambda_{\alpha c}$-open set. It is clear, by Proposition 3.3 and Proposition 4.1, that if λ is $semi$-regular, then there exists a natural number m such that$\{A_1, A_2, \dots, A_m\}$is the class of all minimal $\lambda_{\alpha c}$-open sets in A satisfying the following two conditions:

(1) For any ι, n with $1 \leq \iota, n \leq m$ and $\iota \neq n, A_\iota \cap A_n = \phi$.

(2) If C is a minimal $\lambda_{\alpha c}$-open set in $A,$ then there exists ι with $1 \subseteq \iota \subseteq m$ such that $C = A_\iota$.

Theorem 5.1. Let X be a space and $\phi \neq A$ a finite $\lambda_{\alpha c}$-open set such that A is not a minimal $\lambda_{\alpha c}$-open set. Let $\{A_1, A_2, \dots, A_m\}$ be a class of all minimal $\lambda_{\alpha c}$-open sets in A and $y \in A \setminus (A_1 \cup A_2 \cup \dots \cup A_m)$. Define $A_y = \bigcap\{ B: B$ is $\lambda_{\alpha c}$-open neighborhood of x }.Then there exists a natural number $k \in \{1,2,3, \dots, m\}$ such that A_k is contained in A_y, where λ is $semi$-regular.

Proof. Suppose on the contrary that for any natural number $k \in \{1,2,3, \dots, m\}, A_k$ is not contained in A_y. By Corollary 3.7, for any minimal $\lambda_{\alpha c}$-open set A_k in $A, A_k \cap A_y = \phi$. By Proposition 4.4, $\phi \neq A_y$ is a finite $\lambda_{\alpha c}$-open set. Therefore by Proposition 4.1, there exists a minimal $\lambda_{\alpha c}$-open set C such that $C \subseteq A_y$. Since $C \subseteq A_y \subseteq A$, we have C is a minimal $\lambda_{\alpha c}$-open set in A. By supposition, for any minimal $\lambda_{\alpha c}$-open set A_k, we have $A_k \cap C \subseteq A_k \cap A_y = \phi$. Therefore, for any natural number $k \in \{1,2,3, \dots, m\}, C \neq A_k$.This contradicts our assumption. Hence the proof.

Proposition 5.2. Let X be a space and $\phi \neq A$ be a finite $\lambda_{\alpha c}$-open set which is not a minimal $\lambda_{\alpha c}$-open set. Let $\{A_1, A_2, \dots, A_m\}$ be a class of all minimal $\lambda_{\alpha c}$-open sets in A and $y \in A \setminus (A_1 \cup A_2 \cup \dots \cup A_m)$. Then there exists a natural number $k \in \{1,2,3, \dots, m\}$, such that for any $\lambda_{\alpha c}$-open neighborhood $B_y$of y, A_k is contained in B_y, where λ is λ-regular.

Proof. This follows from Theorem 5.1, as $\bigcap\{ B: B$ is $\lambda_{\alpha c}$-open of y } $\subseteq B_y$. Hence the proof.

Theorem 5.3. Let X be a space and $\phi \neq A$ be a finite $\lambda_{\alpha c}$-open set which is not a minimal $\lambda_{\alpha c}$-open set. Let $\{A_1, A_2, \dots, A_m\}$ be the class of all minimal $\lambda_{\alpha c}$-open sets in A and $y \in A \setminus (A_1 \cup A_2 \cup \dots \cup A_m)$. Then there exists a natural number $k \in \{1,2,3, \dots, m\}$, such that $y \in \lambda_{\alpha c}Cl(A_k)$. where λ is λ-regular.

Proof. It follows from Proposition 5.2, that there exists a natural number $k \in \{1,2,3, \dots, m\}$ such that $A_k \subseteq B$ for any $\lambda_{\alpha c}$-open neighborhood B of y. Therefore $\phi \neq A_k \cap A_k \subseteq A_k \cap B$ implies $y \in \lambda_{\alpha c}Cl(A_k)$. This completes the proof.

Proposition 5.4. Let $\phi \neq A$ be a finite $\lambda_{\alpha c}$-open set in a space$X$ and for each $k \in \{1,2,3, \dots, m\}, A_k$is a minimal $\lambda_{\alpha c}$-open sets in A. If the class$\{A_1, A_2, \dots, A_m\}$ contains all minimal $\lambda_{\alpha c}$-open sets in A, then for any$\phi \neq B_k \subseteq A_k, A \subseteq \lambda_{\alpha c}Cl(B_1 \cup B_2 \cup B_3 \cup \dots \cup B_m)$, where λ is$semi$-regular.

Proof. If A is a minimal $\lambda_{\alpha c}$ -open set, then this is the result of Theorem 3.11 (2). Otherwise, when A is not a minimal $\lambda_{\alpha c}$-open set. If x is any element of $A \setminus (A_1 \cup A_2 \cup \dots \cup A_m)$, then by Theorem 5.3, $x \in \lambda_{\alpha c}Cl(A_1) \cup \lambda_{\alpha c}Cl(A_2) \cup \dots . \cup \lambda_{\alpha c}Cl(A_m)$. Therefore, by Theorem 3.11 (3), we obtain that $A \subseteq \lambda_{\alpha c}Cl(A_1) \cup$

$\lambda_{\alpha c}Cl(A_2) \cup \dots . \cup \lambda_{\alpha c}Cl(A_m) = \lambda_{\alpha c}Cl(B_1) \cup \lambda_{\alpha c}Cl(B_2) \cup \dots . \cup \lambda_{\alpha c}Cl(B_m) = \lambda_{\alpha c}Cl(B_1 \cup B_2 \cup B_3 \cup \dots \cup B_m)$.

Proposition 5.5. Let $\phi \neq A$ be a finite $\lambda_{\alpha c}$-open set and A_k is a minimal $\lambda_{\alpha c}$-open set in A, for each $k \in \{1,2,3, \dots, m\}$. If for any $\phi \neq B_k \subseteq A_k, A \subseteq \lambda_{\alpha c}Cl(B_1 \cup B_2 \cup B_3 \cup \dots \cup B_m)$ then $\lambda_{\alpha c}Cl(A) = \lambda_{\alpha c}Cl(B_1 \cup B_2 \cup B_3 \cup \dots \cup B_m)$.

Proof. For any $\phi \neq B_k \subseteq A_k$ with $k \in \{1,2,3, \dots, m\}$, we have $\lambda_{\alpha c}Cl(B_1 \cup B_2 \cup B_3 \cup \dots \cup B_m) \subseteq \lambda_{\alpha c}Cl(A)$. Also, we have $\lambda_{\alpha c}Cl(A) \subseteq \lambda_{\alpha c}Cl(B_1) \cup \lambda_{\alpha c}Cl(B_2) \cup \dots . \cup \lambda_{\alpha c}Cl(B_m) = \lambda_{\alpha c}Cl(B_1 \cup B_2 \cup B_3 \cup \dots \cup B_m)$. Therefore, $\lambda_{\alpha c}Cl(A) = \lambda_{\alpha c}Cl(B_1 \cup B_2 \cup B_3 \cup \dots \cup B_m)$ for any nonempty subset B_k of $A_k$with $k \in \{1,2,3, \dots, m\}$.

Proposition 5.6. Let $\phi \neq A$ be a finite $\lambda_{\alpha c}$-open set and for each $k \in \{1,2,3, \dots, m\}, A_k$is a minimal $\lambda_{\alpha c}$-open set in A. If for any $\phi \neq B_k \subseteq A_k$, $\lambda_{\alpha c}Cl(A) = \lambda_{\alpha c}Cl(B_1 \cup B_2 \cup B_3 \cup \dots \cup B_m)$, then the class $\{A_1, A_2, \dots, A_m\}$ contains all minimal $\lambda_{\alpha c}$-open sets in A.

Proof. Suppose that C is a minimal $\lambda_{\alpha c}$-open set in A and $C \neq A_k$ for $k \in \{1,2,3, \dots, m\}$. Then we have $C \cap \lambda_{\alpha c}Cl(A_k) = \phi$ for each $k \in \{1,2,3, \dots, m\}$. It follows that any element of C is not contained in $\lambda_{\alpha c}Cl(A_1 \cup A_2 \cup \dots \cup A_m)$.Thisis a contradiction to the fact that $C \subseteq A \subseteq \lambda_{\alpha c}Cl(A) = \lambda_{\alpha c}Cl(B_1 \cup B_2 \cup B_3 \cup \dots \cup B_m)$. This completes the proof.

Combining Propositions 5.4, 5.5 and 5.6, we have the following theorem:

Theorem 5.7. Let$A$ be a nonempty finite $\lambda_{\alpha c}$-open set and A_k a minimal $\lambda_{\alpha c}$-open set in A for each $k \in \{1,2,3, \dots, m\}$. Then the following three conditions are equivalent:

(1) The class $\{A_1, A_2, \dots, A_m\}$ contains all minimal $\lambda_{\alpha c}$-open sets in A.

(2) For any $\phi \neq B_k \subseteq A_k, A \subseteq \lambda_{\alpha c}Cl(B_1 \cup B_2 \cup B_3 \cup \dots \cup B_m)$.

(3) For any $\phi \neq B_k \subseteq A_k$, $\lambda_{\alpha c}Cl(A) = \lambda_{\alpha c}Cl(B_1 \cup B_2 \cup B_3 \cup \dots \cup B_m)$, where$\lambda$ is $semi$-regular.

References

1. Levine, N., *Semi-open sets and semi-continuity in topological spaces*. Amer. Math.Monthly, 1963. **70**(1): p. 36-41.
2. Njastad, O., *On some classes of nearly open sets*. Pacific J.Math, 1965. **15** p. 961-970.
3. Kasahara, S., *Operation-Compact Spaces*. Math. Japon, 1979(24): p. 97-105.
4. Ogata, H., *Operations on Topological Spaces and Associated Topology*. Math. Japon, 1991. **36**(1): p. 175-184.

5. Ahmad, B. and S. Hussain, *Properties of γ-Operations on Topological Spaces.* Aligarh Bull.Math, 2003. **1**(22): p. 45-51.
6. Hussain, S. and B. Ahmad, *On Minimal γ -Open Sets.* Eur. J. Pure Appl. Maths, 2009. **3**(2): p. 338-351.
7. Khalaf, A.B. and S.F. Namiq, *New types of continuity and separation axiom based operation in topological spaces.* M. Sc. Thesis, University of Sulaimani, 2011.
8. Khalaf, A.B. and S.F. Namiq, *Lammda sub c-Open Sets and Lammda sub c-Separation Axioms in Topological Spaces.* Journal of Advanced Studies in Topology, 2013. **4**(1): p. 150-158.
9. Namiq, S.F., *Lammda-R0 and Lammda-R1 Spaces.* Journal of Garmyan University, 2014. **4**(3).
10. F.Namiq, S., *Contra 〚(λ,γ)〛^*-Continuous Functions.* Journal of Garmyan University, 2017.
11. B.Khalaf, A. and S.F. Namiq, *Generalized Lammda-Closed Sets and (Lammda,Gamma)^*-Continuous* Journal of Garmyan University, 2017: p. 2310-0087.
12. Namiq, S.F., *Generalized λ_c-Open Set.* International Journal of Scientific & Engineering Research, June-2017. **8**(6).
13. B.Khalaf, A. and S.F. Namiq, *λ_βc-Connected Spaces and λ_βc-Components.* Journal of Garmyan University, 2017.
14. Khalaf, A.B., H.M. Darwesh, and S.F. Namiq, *λ_c-Connected Space Via λ_c-Open Sets.* Journal of Garmyan University, 2017.
15. Namiq, S.F., *λ_sc-open sets and topological properties.* Journal of Garmyan University, 2014.
16. B.Khalaf, A. and S.F. Namiq, *ON Minimal λ^*-Open Sets, .* International Journal of Scientific & Engineering Research, October-2014. **5**(10).
17. Namiq, S.F., *λ_c-Separation Axioms Via λ_c-open sets.* International Journal of Scientific & Engineering Research May-2017. **8**.
18. Namiq, S.F., *λ_sc-Connected Spaces Via λ_sc-Open Sets.* Journal of Garmyan University, 2017.
19. Darwesh, H.M., S.F. Namiq, and W.K. Kadir, *Maximal λc-Open Sets.* ICNS-2016, 2017.
20. Namiq, S.F., *λ-Connected Spaces Via λ-Open Sets.* Journal of Garmyan University, 2015.

21. Darwesh, H.M. and S.F. Namiq, *On Minimal λ_βc-Open Sets* Journal of Garmyan University, 2017.
22. Namiq, S.F., *Lammda sub alpha c-Open Sets and Topological Properties*. pre-print
23. F.Namiq, S., *Lammda sub beta c-Open Sets and Topological Properties.* Journal of Garmyan University, 2017(2310-0087).
24. B.Khalaf, A. and S.F. Namiq, *Generalized lammda-Closed Sets and (Lammda,Gamma)*^**-Continuous Functions* International Journal of Scientific & Engineering Research, 2012. **3**(12).

ttp://jgu.garmian.edu.krd https://doi.org/10.24271/garmian.339

Some Properties of Preopen Set in Closure Spaces

Halgwrd M. Darwesh[1*] Sarhad F.Namiq[2]

[1]Department of Mathematics, College of Science, University of Sulaimani, 46001, Sulaimani, Kurdistan Region, Iraq.

Email: halgwrd.darwesh@univsul.edu.iq

[2]Department of Mathematics, College of education, University of Garmian, Kalar, Kurdistan Region, Iraq.

Email: sarhad.faiq@garmian.edu.krd

[*] Corresponding author.

Abstract

Using the concept of preopen set, we introduce and study closure properties of pre-limit points, pre-derived sets, pre-interior and pre-closure of a set, pre-interior points, pre-border, pre-frontier and pre-exterior in closure space. The relations between pre-closure of a set and pre-interior (point) in closure spaces and pre-closure of a set and pre-interior (point) in topological space are investigated.

Keywords: Pre-limit point, Pre-derived set, Pre-closure, Pre-interior points, Pre-border of sets, Pre- frontier of sets, Pre-exterior points.

Introduction

The notion of (X,c)(closure space) was introduced by Khampakdee [1]. He introduced open set and closed set in closure space [1]. And also he introduced *Semi-open sets in biclosure spaces* [2]. The notion of preopen set was introduced by Mashhour et al [3]. In [4] Halgwrd M. Darwesh defined preopen set in closure space which is different of preopen set in topological space, he introduced and studied some properties of preopen sets in closure space. They work in operation in topology in [5-28]. In this paper, we introduce the notions of pre-limit points, pre-derived sets, pre-interior of sets. We study some results of topological spaces in [29] & [30].

2.Preliminaries

Through this paper, (X,τ) (resp. (X,c)) always mean topological spaces (closure spaces). The intersection of all closed sets in topological spaces which contain A, is called closure of set denoted by $Cl(A)$. And also the union of all open sets which contain in A is called interior of A which is denoted $Int(A)$. A subset A of X is said to be preopen [3] if $A \subseteq Int(Cl(A))$. The complement of a preopen set is called a preclosed set.

Definition 2.1 [1]

A function $c: P(X) \to P(X)$ defined on the power set $P(X)$ of a set X is called a closure operator on X and the pair (X, c) is called a closure space if the following axioms are satisfied:

$(A1)$ $c(\phi) = \phi$.
$(A2)$ $A \subseteq c(A)$ for every $A \subseteq X$.

$(A3)$ $A \subseteq B \Rightarrow c(A) \subseteq c(B)$ for all $A, B \subseteq X$. A closure operator c on a set X is called additive (respectively, idempotent) if $A, B \subseteq X$, $c(A \cup B) = c(A) \cup c(B)$ (respectively, for all $A \subseteq X \Rightarrow cc(A) = c(A)$. A subset $A \subseteq X$ is closed in the closure space (X, c) *if* $c(A) = A$. It is called open, if its complement in X is closed. The empty set and the whole space are both open and closed.

Definition 2.2 [4]

A subset A of a space (X, c) is said to be a preopen set, if there exists an open set G such that $A \subseteq G \subseteq c(A)$. The complement of a preopen set is called preclosed. The family of all preopen sets denoted by $PO(X, c)$. The family of all preclosed sets denoted by $PC(X, c)$.

Theorem 2.1 [4]

A subset A of a space (X, c) is preclosed if and only if there exists a closed set F such that $X \backslash c(X \backslash A) \subseteq F \subseteq A$.

Proposition 2.1 [4]

The union (intersection) of any family of preopen (preclosed) sets in a space(X, c) is preopen (preclosed).

Definition 2.3 [4]

The interior operator $i: P(X) \to P(X)$ corresponding to the closure operator c on X is given by; $i(A) = X \backslash c(X \backslash A)$.

Theorem 2.2 [4]

Let A be a subset of a closure (X, c). If $x \in c(A)$, then $G \cap A \neq \phi$, for each open subset G of X containing x.

Theorem 2.3 [4]

Let A be a subset of a closure (X, c) and c is idempotent on X, then $x \in c(A)$ if and only if $G \cap A \neq \phi$, for each open subset G of X containing x.

Proposition 2.2 [4]

Let c be an idempotent closure operator on a set X. If A is preopen in X and $B \subseteq A \subseteq c(B)$, then B is preopen.

Theorem 2.4 [4]

Let c be an idempotent closure operator on X. A subset A of X is preopen if and only if $A \subseteq X \backslash c(X \backslash cA) = ic(A)$.

Proposition 2.3 [4]

If A is closed and preopen in a space (X, c), then A is open.

3 Some Properties of Preopen Sets

Definition 3.1

Let (X, c) be a closure space, $x \in X$ and N be a subset of X. Then N is called a pre-neighborhood of x in X, if there exists a preopen set V_x such that $x \in V_x \subseteq N$.

Definition 3.2

Let A be a subset of a closure space (X, c). A point $x \in X$ is said to be pre-limit point of A, if it satisfy the following assertion:

$V \cap (A \setminus \{x\}) \neq \phi$, for every preopen set V such that $x \in V$.The set of all pre-limit points of A is called the prederived set of A and is denoted by $D_P(A)$.

Note that for a subset A of X, a point $x \in X$ is not a pre-limit point of A if and only if there exists a preopen set V in X such that $x \in V$ such that $V \cap (A \setminus \{x\}) = \phi$, or (equivalently, $x \in V$ and $V \cap A = \phi$ or $V \cap A = \{x\}$).

Theorem 3.1

Let c_1 and c_2 be two closure operator on X such that $PO(X, c_1) \subseteq PO(X, c_2)$. For any subset A of X, every pre-limit point of A with respect to c_2 is a pre-limit point of A with respect to $c_{1.}$

Proof.

Let x be a pre-limit point of A with respect to c_2.Then $V \cap (A \ \{x\}) \neq \phi$, for every preopen set V with respect to c_2, such that $x \in V$. But $c_1 \subseteq c_2$, so, in particular, $V \cap (A \ \{x\}) \neq \phi$, for every preopen set V with respect to c_1, such that $x \in V$. Hence x is a pre-limit point of A with respect to c_1.

The converse of Theorem 3.1 is not true in general as seen in the following example.

Example 3.1

Let $X=\{a,b,c,d\}$ and defined closure operator $c_1: P(X) \longrightarrow P(X)$ by:

$$c_1(A)=\begin{cases} \phi & \text{if } A=\phi \\ \{b,c,d\} & \text{if } \phi \neq A \subseteq \{b,c,d\} \\ X & otherwise \end{cases}$$

So $PO(X,c_1)=\{\phi,\{a\},\{a,b\},\{a,c\},\{a,d\},\{a,b,c\},\{a,b,d\},\{a,c,d\},X\}$.

And also defined closure operator $c_2: P(X) \longrightarrow P(X)$ by:

$$c_2(A)=\begin{cases} \phi & if\ A=\phi \\ X & if\ \phi \neq A \subseteq X. \end{cases}$$

So $PO(X,c_2)=P(X)$. We have $PO(X,c_1) \subseteq PO(X,c_2)$. Let $A=\{a,b\}$, then $D_P(A)=\{b,c,d\}$ with respect $PO(X,c_1)$ and $D_P(A)=\phi$ with respect $PO(X,c_2)$. Note that d is pre-limit point of A with respect $PO(X,c_1)$, but it is not a pre-limit point of A with respect $PO(X,c_2)$.

Theorem 3.2

For any subsets A and B of $(X,c\ )$, the following assertions are valid:

(1) If $A \subseteq B$, then $D_P(A) \subseteq D_P(B)$.

(2) $D_P(A) \cup D_P(B) \subseteq D_P(A \cup B)$.

(3) $D_P(A \cap B) \subseteq D_P(A) \cap D_P(B)$.

(4) $D_P(D_P(A)) \backslash A \subseteq D_P(A)$.

(5) $D_P(A \cup D_P(A)) \subseteq A \cup D_P(A)$.

Proof. (**1**): Let $x \in D_P(A)$. Then $x \in X$ is a pre-limit point of A. So $V \cap (A \setminus \{x\}) \neq \phi$, for every preopen set V. But $A \subseteq B$, so $V \cap (B \setminus \{x\}) \neq \phi$, then x is a pre-limit point of B, that is $x \in D_P(B)$. Hence, $D_P(A) \subseteq D_P(B)$.

(**2**) We have $A \subseteq A \cup B$ and $B \subseteq A \cup B$, then by(1) $D_P(A) \subseteq D_P(A \cup B)$ and $D_P(B) \subseteq D_P(A \cup B)$. Hence, $D_P(A) \cup D_P(B) \subseteq D_P(A \cup B)$.

(**3**)We have $A \cap B \subseteq A$ and $A \cap B \subseteq B$, then by(2) $D_P(A \cap B) \subseteq D_P(A)$ and $D_P(A \cap B) \subseteq D_P(B)$.Hence, $D_P(A \cap B) \subseteq D_P(A) \cap D_P(B)$.

(**4**) Let $x \in D_P\big(D_P(A)\big)\backslash A$. So $x \in D_P\big(D_P(A)\big)$ and $x \notin A$. Then, x is a pre-limit point of $D_P(A)$. That is, $V \cap (D_P(A) \setminus \{x\}) \neq \phi$, for every preopen set V. Then, there exists $y \in V \cap (D_P(A) \setminus \{x\})$. So $y \in V$ and $y \in D_P(A) \setminus \{x\}$. Then, $y \in D_P(A)$ and $y \neq x$. Thus, y is a pre-limit point of A. Then, $V \cap (A \setminus \{y\}) \neq \phi$ and $y \neq x$. If we take $z \in V \cap (A \setminus \{y\})$, so $x \neq z$ because $x \notin A$. Hence, $V \cap (A \setminus \{x\}) \neq \phi$, then x is a pre-limit point of A. Therefore $x \in D_P(A)$. Thus $D_P(D_P(A))\setminus A \subseteq D_P(A)$.

(**5**) Let $x \in D_P\big(A \cup D_P(A)\big)$. Then x is a pre-limit point of $A \cup D_P(A)$. If $x \in A$, the result is obvious. Assume that $x \notin A$. Then, $V \cap (A \cup D_P(A)\setminus \{x\}) \neq \phi$, for all preopen set V.This means that, $V \cap (A \setminus \{x\}) \neq \phi$ or $V \cap (D_P(A)\setminus \{x\}) \neq \phi$. The first case implies $x \in D_P(A)$. If $V \cap (D_P(A)\setminus \{x\}) \neq \phi$, then $x \in D_P\big(D_P(A)\big)$. Since $x \notin A$, it follows similarly from (4)that $x \in D_P(D_P(A))\setminus A \subseteq D_P(A)$. Therefore (5) is valid.

In general, neither inclusion of Theorem 3.2 is true as we will seen in the following examples.

Example 3.2

Let $X = \{a, b, c, d\}$ and defined closure operator $c: P(X) \longrightarrow P(X)$ by: $c(A) =$

$$\begin{cases} A & \text{if } A \in \{\phi, \{b\}, \{c\}, \{b, c\}\} \\ \{a, b\} & \text{if } A \in \{\{a\}, \{a, b\}\} \\ \{c, d\} & \text{if } A \in \{\{d\}, \{c, d\}\} \\ \{a, b, c\} & \text{if } A \in \{\{a, c\}, \{a, b, c\}\} \\ \{b, c, d\} & \text{if } A \in \{\{b, d\}, \{b, c, d\}\} \\ X & otherwise \end{cases}$$

Hence $PO(X, c) = \{\phi, \{a\}, \{d\}, \{a, b\}, \{a, d\}, \{c, d\}, \{a, b, d\}, \{a, c, d\}, X\}$. For two subsets $A = \{a, c\}$ and $B = \{a, b, d\}$ of X, we get $D_P(A) = \{b\} \subseteq \{b, c\} = D_P(B)$, but $A \nsubseteq B$. This shows that the converse of Theorem 3.2(1) is not valid.

Example 3.3

Let $X = \{a, b, c, d, e\}$ and defined closure operator $c: P(X) \longrightarrow P(X)$ by:

$$c(A) = \begin{cases} A & \text{if } A \in \{\phi\} = \mathcal{F} \\ \{b, e\} & \text{if } A \in \{\{b\}, \{e\}, \{b, e\}\} = \mathcal{G} \\ \{a, b, e\} & \text{if } A \in \{\{a\}, \{a, e\}, \{a, b\}, \{a, b, e\}\} = \mathcal{H} \\ \{b, c, d, e\} & \text{if } A \notin \{\mathcal{F}, \mathcal{G}, \mathcal{H}\} \text{and } A \subsetneq \{b, c, d, e\} \\ X & otherwise \end{cases}$$

$PO(X, c) = \{\phi, \{a, b\}, \{a, c\}, \{a, d\}, \{c, d\}, \{a, b, c\}, \{a, b, d\}, \{a, c, d\}, \{a, c, e\},$

$\{a, d, e\}, \{a, b, c, d\}, \{a, b, c, e\}, \{a, b, d, e\}, \{a, c, d, e\}, X\}$. Now consider two subsets $A = \{a, b\}$ and $B = \{b, c, d\}$ of X. Then $D_P(A) = \{b, e\}$, $D_P(B) = \{a, e\}$, and so $D_P(A \cap B) = \phi$, but $D_P(A) \cap D_P(B) = \{e\} \nsubseteq \phi = D_P(A \cap B)$. Thus the equality in Theorem 3.2 (5)is not valid.

Example 3.4

Let $X = \{a, b, c, d\}$ and defined closure operator $c: P(X) \longrightarrow P(X)$ by:

$$c(A) = \begin{cases} A & \text{if } A \in \{\phi, \{a\}, \{d\}, \{a, d\}\} \\ X & otherwise \end{cases}$$

Hence

$PO(X, c) =$

$\{\phi, \{b\}, \{c\}, \{a, b\}, \{a, c\}, \{b, c\}, \{b, d\}, \{c, d\}, \{a, b, c\}, \{a, b, d\}, \{a, c, d\}, \{b, c, d\}, X\}$.

Let $A=\{a,b\}$ and $B=\{a,c\}$ be subsets of X. Then $D_P(A)=\phi=D_P(B)$. $D_P(A)\cup D_P(B)=\phi$, $D_P(A\cup B)=\{a,d\}$ but $D_P(A\cup B)=\{a,d\}\nsubseteq\phi=D_P(A)\cup D_P(B)$. Thus the equality in Theorem 3.2(2) **Error! Reference source not found.** is not valid. For a subset $A=\{a,b,c\}$of X, we have $D_P\big(D_P(A)\big)=D_P(\{a,d\})=\phi$. But $D_P(A)=\{a,d\}\nsubseteq D_P\big(D_P(A)\big)\backslash A=\phi$, and so the equality in Theorem 3.2(4) is not valid. Now for a subset $B=\{b,c\}$ of X, we get $D_P(B)=\{a,d\}$, and so $B\cup D_P(B)=X$ and $D_P(X)=\{a,d\}$, but $B\cup D_P(B)=X\nsubseteq D_P\big(B\cup D_P(B)\big)=\{a,d\}$. This shows that $D_P(A\cup D_P(A))=A\cup D_P(A)=X$. Hence the equality in Theorem 3.2(5) is not valid.

Definition 3.3

Let (X,c) be a closure space and $A\subseteq X$. The intersection of all preclosed sets containing A is called the pre-closure of A, denoted by $Cl_P(A)$.

Theorem 3.3

Let (X,c) be a closure space, $A,B\subseteq X$ then the following properties are true:

(1) $Cl_P(A)$ is preclosed set.

(2) $A\subseteq Cl_P(A)$.

(3) $Cl_P(A)$ is smallest preclosed set which containing A.

(4) If $A\subseteq B$, then $Cl_P(A)\subseteq Cl_P(B)$.

(5) $Cl_P(A)\cup Cl_P(B)\subseteq Cl_P(A\cup B)$.

(6) $Cl_P(A\cap B)\subseteq Cl_P(A)\cap Cl_P(B)$.

(7) A is preclosed set if and only if $A=Cl_P(A)$.

(8) $Cl_P\big(Cl_P(A)\big)=Cl_P(A)$.

Proof:

1. It follows from Definition 3.3 and Proposition 2.1.

2. Obvious.

3. From (1) and (2), we get $Cl_P(A)$ is preclosed set which containing A. It is enough to show $Cl_P(A)$ is smallest preclosed. Let L be any preclosed set with $A\subseteq L$. Then, L is one of the preclosed sets in which the intersection is taken it is mean $Cl_P(A)=\bigcap\{K, K$ is preclosed set and $A\subseteq K\}$. Hence $Cl_P(A)$ is the smallest preclosed set containing A.

4. BY (2) $\boldsymbol{B\subseteq Cl_P(B)}$, since$\boldsymbol{A\subseteq B}$, so $\boldsymbol{A\subseteq Cl_P(B)}$, but $\boldsymbol{Cl_P(A)}$ is the smallest preclosed set containing $\boldsymbol{A}$. So $\boldsymbol{Cl_P(A)\subseteq Cl_P(B)}$.

5. It follows from (4).
6. It follows from (4).
7. Let $A = Cl_P(A)$.Since $Cl_P(A)$ is preclosed set by (1), then A is a preclosed set. Conversely: Let A be a preclosed set. Then A is the smallest preclosed set which contains A. So $A = Cl_P(A)$ by (3).
8. Let $L = Cl_P(A)$. So L is a preclosed set by (1), then by (7) $L = Cl_P(L)$. Thus $Cl_P(A) = Cl_P\big(Cl_P(A)\big)$.

Theorem 3.4

Let (X, c) be a closure space and $A \subseteq X$. Then $x \in Cl_P(A)$ if and only if $A \cap V \neq \phi$, for all preopen set V which contains x.

Proof.

Let $x \in Cl_P(A)$ and suppose that $A \cap V = \phi$, for some preopen set V which contains x. This implies that X/V is a preclosed set and $A \subseteq X/V$. So $Cl_P(A) \subseteq Cl_P(X/V) = X/V$. This implies that $x \in X/V$, which is a contradiction. Therefore, $A \cap V \neq \phi$, for all preopen set V, Which contains x.

Conversely. If $x \notin Cl_P(A)$, then there exists a preclosed set K such that $A \subseteq K$ and $x \notin K$. Hence $X \setminus K$ is a preopen set which containing x and $A \cap (X \setminus K) \subseteq A \cap (X \setminus A) = \phi$. Which is a contradiction. Hence, $x \in Cl_P(A)$is valid.

Corollary 3.1

For any subset A of a closure space (X, c), we have $D_P(A) \subseteq Cl_P(A)$.

Proof.

Let $x \in D_P(A)$. Then, $A/\{x\} \cap V \neq \phi$, for all preopen set V which contains x. So $A \cap V \neq \phi$, for all preopen set V that contains x. Thus, by Theorem 3.4 $x \in Cl_P(A)$.

Theorem 3.5

For any subset A of a closure space (X, c), we have $Cl_P(A) = A \cup D_P(A)$.

Proof.

Let $x \in Cl_P(A)$. Assume that $x \notin A$ and let V be a preopen set with $x \in V$. Then, $A/\{x\} \cap V \neq \phi$, and so $x \in D_P(A)$. Hence $Cl_P(A) \subseteq A \cup D_P(A)$. The reverse inclusion is valid by $A \subseteq Cl_P(A)$ and Corollary 3.1.

Theorem 3.6

For a subset A of a closure space (X, c), we have A is preclosed if and only if $D_P(A) \subseteq A$.

Proof.

Assume that A is preclosed. Let $x \notin A$, i.e., $x \in X \setminus A$. Since $X \setminus A$ is preopen, so x is not a pre-limit point of A, i.e., $x \notin D_P(A)$, because $(X \setminus A) \cap (A \setminus \{x\}) = \phi$. Hence, $D_P(A) \subseteq A$. The reverse implication is followed by Theorem 3.5.

Corollary 3.2

Let A be a subset of a closure space (X, c). If F is a preclosed superset of A, then $D_P(A) \subseteq F$.

Proof.

By Theorem 3.2 (1) and Theorem 3.6, $A \subseteq F$ implies $D_P(A) \subseteq D_P(F) \subseteq F$.

Theorem 3.7

Let A and B be any subsets of a closure space (X, c) such that A is preopen. If the family of all preopen subsets of X is form a topology on X, then $A \cap Cl_P(B) \subseteq Cl_P(A \cap B)$.

Proof.

Let $x \in A \cap Cl_P(B)$. Then, $x \in A$ and $\in Cl_P(B) = B \cup D_P(B)$. If $x \in B$, then $x \in A \cap B \subseteq Cl_P(A \cap B)$. If $x \notin B$, then $x \in D_P(B)$ and so $B/\{x\} \cap V \neq \phi$, for all preopen set V containing x. Since A is preopen and $V \cap A$ is also a preopen set containing x. Hence, $V \cap (A \cap B) = (V \cap A) \cap B \neq \phi$, and consequently $x \in Cl_P(A \cap B)$. Therefore, $A \cap Cl_P(B) \subseteq Cl_P(A \cap B)$.

Example 3.5

Let $X = \{a, b, c, d\}$ and defined closure operator $c: P(X) \longrightarrow P(X)$ by:

$$c(A) = \begin{cases} A & \text{if } A \in \{\phi, \{a\}\} = \mathcal{F} \\ \{a, d\} & \text{if } A \in \{\{d\}, \{a, d\}\} = \mathcal{G} \\ \{a, c, d\} & \text{if } A \notin \{\mathcal{F}, \mathcal{G}\} \text{ and } A \subseteq \{a, c, d\} \\ X & otherwise \end{cases}.$$

Hence $PO(X, c) = \{\phi, \{b\}, \{a, b\}, \{b, c\}, \{b, d\}, \{a, b, c\}, \{a, b, d\}, \{b, c, d\}, X\}$

which is a topology on X. Consider the subset $A = \{a, b\}$ and $B = \{b, c\}$ of X, then $A \cap$

$Cl_P(B) = \{a,b\} \neq X = Cl_P(A \cap B)$. This shows that the equality in Theorem 3.7 is not true in general.

Example 3.6

The family of all preopen subsets of Example 3.4 does not form a topology on X and since for subsets $A = \{a,b\}$ and $B = \{b,c\}$ of the closure space X $A \cap Cl_P(B) = \{a,b\} \nsubseteq \{b\} = Cl_P(A \cap B)$. This shows that the conditions that the family of all preopen sets of X form a topology, in Theorem 3.6 is necessary and it can not be dropped.

Definition 3.4

A closure space(X,c) is said to be discrete if every subset of X is open set.

Note that

(1) An closure spaces (X,c) is discrete if and only if every subset of X is closed.
(2) If A is a subset of a discrete closure space (X,c), then $D_P(A) = \phi$.

Proposition 3.1

Let A be a subset of a closure space (X,c). If a point $x \in X$ is a pre-limit point of A, then x is also a pre-limit point of $A\backslash\{x\}$.

Proof. Obvious.

Definition 3.5

Let A be a subset of a closure space (X,c). A point $x \in X$ is called a pre-interior point of A, if there exists a preopen set V such that $x \in V \subseteq A$. The set of all pre-interior points of A is called the pre-interior of A and is denoted by $Int_P(A)$.

Proposition 3.2

For subsets A and B a closure space (X,c), the following assertions are valid.

(1) $Int_P(A)$ is the union of all preopen subsets of A.
(2) $Int_P(A)$ is the largest preopen set contained in A.
(3) A is preopen if and only if $A = Int_P(A)$.
(4) $Int_P(Int_P(A)) = Int_P(A)$.
(5) $Int_P(A) = A\backslash D_P(X\backslash A)$.
(6) $X\backslash Int_P(A) = Cl_P(X\backslash A)$.
(7) $X\backslash Cl_P(A) = Int_P(X\backslash A)$.
(8) If $A \subseteq B$, then $Int_P(A) \subseteq Int_P(B)$.
(9) $Int_P(A) \cup Int_P(B)) \subseteq Int_P(A \cup B)$.
(10) $Int_P(A \cap B) \subseteq Int_P(A) \cap Int_P(B)$.

Proof:

1. Let $\{V_i : i \in \Lambda\}$ be the collection of all preopen subsets of X contained in A. If $x \in Int_P(A)$, then, there exists $j \in \Lambda$ such that $x \in V_j \subseteq A$. Hence, $x \in \bigcup_{i\in\Lambda} V_i$, and so $Int_P(A) \subseteq \bigcup_{i\in\Lambda} V_i$. On the other hand, if $y \in \bigcup_{i\in\Lambda} V_i$, then $y \in V_k \subseteq A$ for some $k \in \Lambda$. Thus, $y \in Int_P(A)$, and so $\bigcup_{i\in\Lambda} V_i \subseteq Int_P(A)$. Accordingly, $Int_P(A) = \bigcup_{i\in\Lambda} V_i$.

2. Since $Int_P(A) = \bigcup_{G\subseteq A}\{G, G \text{ is preopen set}\}$, so by Proposition 2.1 $Int_P(A)$ is a preopen set. Also $Int_P(A) \subseteq A$. Now, to prove $Int_P(A)$ is the largest preopen set contained in A. Let H be any other preopen set that contained in A. Since H is a preopen set and $H \subseteq A$. So $H \subseteq \bigcup_{G\subseteq A}\{G, G \text{ is preopen set}\} = Int_P(A)$. That is $H \subseteq Int_P(A)$. Thus, $Int_P(A)$ is the largest preopen set contained in A.

3. Let A be a preopen set. Since $Int_P(A)$ is largest preopen contained in A and $A \subseteq A$, so $A \subseteq Int_P(A)$. And since $Int_P(A) \subseteq A$. Thus, $A = Int_P(A)$.Conversely: It follows from part(1).

4. Let $U = Int_P(A)$.So U is preopen set, then $U = Int_P(U)$ by (3). Thus, $Int_P(A) = Int_P\big(Int_P(A)\big)$.

5. If $x \in A\backslash D_P(X\backslash A)$, then $x \notin D_P(X\backslash A)$ and so there exists a pre-open set V containing x such that $V \cap (X\backslash A) = \phi$. Thus, $x \in V \subseteq A$ and hence $x \in Int_P(A)$. This shows that $A\backslash D_P(X\backslash A) \subseteq Int_P(A)$. Now let $x \in Int_P(A)$. Since $Int_P(A) \cap (X\backslash A) = \phi$, we have $x \notin D_P(X\backslash A)$. Therefore, $Int_P(A) = A\backslash D_P(X\backslash A)$.

6. Using (4) and Theorem 3.5, we have $X\backslash Int_P(A) = X\backslash(A\backslash D_P(X\backslash A)) = (X\backslash A) \cup D_P(X\backslash A) = Cl_P(X\backslash A)$.

7. Using (4) and Theorem 3.5, we have $Int_P(X\backslash A) = (X\backslash A)\backslash D_P(A) = X\backslash(A \cup D_P(A)) = X\backslash Cl_P(A)$.

8. Let $x \in Int_P(A)$, then x is pre-interior of A, so there exists a preopen set V such that $x \in V \subseteq A$, but $A \subseteq B$. So $x \in V \subseteq B$, then x is pre-interior of B. Hence, $x \in Int_P(B)$. Thus $Int_P(A) \subseteq Int_P(B)$.It follows from part (8).

9. It follows from part (8).

The converse of (8) in Proposition 3.2. is not true in general as seen in the following example:

Example 3.7

Let $X = \{a, b, c, d, e\}$ and defined closure operator $c: P(X) \longrightarrow P(X)$ by:

$$c(A)=\begin{cases} A & \text{if } A\in\{\phi,\{a\},\{b,c,d,e\}\}=\mathcal{F} \\ \{b,e\} & \text{if } A\in\{\{b\},\{e\},\{b,e\}\}=\mathcal{G} \\ \{a,b,e\} & \text{if } A\in\{\{a,b\},\{a,e\},\{a,b,e\}\}=\mathcal{H} \\ \{b,c,d,e\} & \text{if } A\notin\{\mathcal{F},\mathcal{G},\mathcal{H}\} \text{ and } A\subseteq\{b,c,d,e\} \\ X & otherwise \end{cases}$$

Let $A=\{a,b\}$ and $B=\{a,c,d\}$ be subsets of X. Then $Int_P(A)=\{a\}\subseteq Int_P(B)=\{a,c,d\}$.

Definition 3.6

For a subset A of a closure space (X,c), the set

(1) $B_P(A)= A\backslash Int_P(A)$ is called the pre-border of A.

(2) $Fr_P(A)= Cl_P(A)\backslash Int_P(A)$ is called the pre-frontier of A.

Remark 3.1

If A is a preclosed subset of X, then $B_P(A)=Fr_P(A)$.

Example 3.8

Let (X,c) be the closure space which is described in Example 3.7. Let $A=\{a,b,e\}$ be a subset of X. Then $Int_P(A)=\{a\}$, and so $B_P(A)=\{b,e\}$. Since $A=\{a,b,e\}$ is pre-closed, $Cl_P(A)=\{a,b,e\}$ and thus $Fr_P(A)=\{b,e\}$.

Example 3.9

Consider the closure space (X,c)which is given in Example 3.3. For a subset $A=\{b,c,d\}$ of X, we have $Int_P(A)=\{c,d\}$ and $Cl_P(A)=\{b,c,d,e\}$. Hence $B_P(A)=\{b\}$ and $Fr_P(A)=\{b,e\}$.

Proposition 3.3

For a subset A of a closure space (X,c), the following statements hold:

(1) $A=Int_P(A)\cup B_P(A)$.

(2) $Int_P(A)\cap B_P(A)=\phi$.

(3) A is a preopen set if and only if $B_P(A)=\phi$.

(4) $B_P(Int_P(A))=\phi$.

(5) $Int_P(B_P(A))=\phi$.

(6) $B_P\big(B_P(A)\big)=B_P(A)$.

(7) $B_P(A)=A\cap Cl_P(X\backslash A)$.

(8) $B_P(A) = A \cap D_P(X\backslash A)$.

Proof:

1. Obvious.

2. Obvious.

3. It follows from Proposition 3.2 (3) and Definition 3.5 (1).

4. Since $Int_P(A)$ is preopen, it follows from (3) that $B_P(Int_P(A)) = \phi$.

5. If $x \in Int_P(B_P(A))$, then $x \in B_P(A) \subseteq A$, and then $x \in Int_P(A)$. Thus, $x \in B_P(A) \cap Int_P(A) = \phi$, which is a contradiction. Hence, $Int_P(B_P(A)) = \phi$.

6. Using (5), we get $B_P(B_P(A)) = B_P(A)\backslash Int_P(B_P(A)) = B_P(A)$.

7. Using Proposition 3.2 (6) we have $B_P(A) = A\backslash Int_P(A) = A\backslash(X\backslash Cl_P(X\backslash A)) = A \cap Cl_P(X\backslash A)$.

8. Applying (7) and Theorem 3.5, we have we have to show $Cl_P(A) \subseteq A$. To this end, let $x \notin A$. Then $x \notin Fr_P(A)$. So $x \notin Cl_P(A)\backslash Int_P(A)$. But since $Int_P(A) \subseteq A$ and $x \notin A$, so $x \notin Cl_P(A)$. This means that, $Cl_P(A) \subseteq A$. So A is preclosed.

Lemma 3.1

For a subset A of a closure space (X, c), A is preclosed if and only if $Fr_P(A) \subseteq A$.

Proof.

Assume that A is preclosed. Then $Fr_P(A) = Cl_P(A)\backslash Int_P(A) = A\backslash Int_P(A) \subseteq A$. Conversely suppose that $Fr_P(A) \subseteq A$, then $Cl_P(A)\backslash Int_P(A) \subseteq A$.To show A is preclosed.. In view of Theorem 3.3(7). We have to show $Cl_P(A) \subseteq A$. To this end, let $x \notin A$. Then $x \notin Fr_P(A)$. So $x \notin Cl_P(A)\backslash Int_P(A)$. But since $Int_P(A) \subseteq A$ and $x \notin A$, so $x \notin Cl_P(A)$. This means that, $Cl_P(A) \subseteq A$. So A is preclosed.

Theorem 3.8

For a subset A of a closure space (X, c), the following assertions are valid:

(1) $Cl_P(A) = Int_P(A) \cup Fr_P(A)$.

(2) $Int_P(A) \cap Fr_P(A) = \emptyset$.

(3) $B_P(A) \subseteq Fr_P(A)$.

(4) $Fr_P(A) = B_P(A) \cup (D_P(A)\backslash Int_P(A))$.

(5) A is a preopen set if and only if $Fr_P(A) = B_P(X\backslash A)$.

(6) $Fr_P(A) = Cl_P(A) \cap Cl_P(X\backslash A)$.

(7) $Fr_P(A) = Fr_P(X\backslash A)$.

(8) $Fr_P(A)$ is preclosed.

(9)$Fr_P(Fr_P(A)) \subseteq Fr_P(A)$.
(10)$Fr_P(Int_P(A)) \subseteq Fr_P(A)$.
(11)$Fr_P(Cl_P(A)) \subseteq Fr_P(A)$.
(12)$Int_P(A) = A \backslash Fr_P(A)$.

Proof:

1. Obvious.
2. Obvious.
3. Obvious.
4. Using Theorem 3.5, we obtain $Fr_P(A) = Cl_P(A) \backslash Int_P(A) = (A \cup D_P(A)) \cap (X \backslash Int_P(A)) = (A \backslash Int_P(A)) \cup (D_P(A) \backslash Int_P(A)) = B_P(A) \cup (D_P(A) \backslash Int_P(A))$.
5. Assume that A is preopen. Then $Fr_P(A) = B_P(A) \cup (D_P(A) \backslash Int_P(A)) = \phi \cup (D_P(A) \backslash A) = D_P(A) \backslash A = B_P(X \backslash A)$ by using (4), Proposition 3.3 (3), Proposition 3.2 (3) and Proposition 3.3 (8).
Conversely; suppose that $Fr_P(A) = B_P(X \backslash A)$. Then $\phi = Fr_P(A) \backslash B_P(X \backslash A) = \left(Cl_P(A) \backslash Int_P(A)\right) \backslash \left((X \backslash A) \backslash Int_P(X \backslash A)\right) = A \backslash Int_P(A) = B_P(A)$. By (5) and (6) of Proposition 3.2, and so by Proposition 3.3(3), A is preopen.
6. It follows from Proposition 3.2(6).
7. It is followed from (6).
8. we have $Cl_P(Fr_P(A)) = Cl_P(Cl_P(A) \cap Cl_P(X \backslash A)) \subseteq Cl_P(Cl_P(A)) \cap Cl_P(Cl_P(X \backslash A)) = Cl_P(A) \cap Cl_P(X \backslash A) = Fr_P(A)$. Obviously $Fr_P(A) \subseteq Cl_P(Fr_P(A))$, and so $Fr_P(A) = Cl_P(Fr_P(A))$. Hence $Fr_P(A)$ is preclosed.
9. This is by (8) and Lemma 3.1.
10. Proposition 3.2 (4), we get $Fr_P(Int_P(A)) = Cl_P(Int_P(A)) \backslash Int_P(Int_P(A)) \subseteq Cl_P(A) \backslash Int_P(A) = Fr_P(A)$.
11. We obtain $Fr_P(Cl_P(A)) = Cl_P(Cl_P(A)) \backslash Int_P(Cl_P(A)) \subseteq Cl_P(A) \backslash Int_P(A) = Fr_P(A)$.
12. We get $A \backslash Fr_P(A) = A \backslash (Cl_P(A) \backslash Int_P(A)) = A \cap ((X \backslash Cl_P(A)) \cup Int_P(A)) = \phi \cup (A \cup Int_P(A)) = Int_P(A)$.

The converse of (3) is not true in general as seen in the following example.

Example 3.10

Example 3.9 shows that the reverse inclusion of Theorem 3.9 (3) is not valid in general.

Definition 3.7

For a subset A of a closure space (X, c), the pre-interior of $X\backslash A$ is called the pre-exterior of A, and it is denoted by $Ext_P(A)$, that is, $Ext_P(A) = Int_P(X\backslash A)$.

Example 3.11

Consider the closure space (X, c)which is given in Example 3.7. For subsets $A = \{a, b, c\}$ and $B = \{b, d\}$ of X, we have $Ext_P(A) = \{d, e\}$ and $Ext_P(B) = \{a, c, e\}$.

Theorem 3.9

For subsets A and B of a closure space (X, c), the following assertions are valid.

(1) $Ext_P(A)$ is preopen.

(2) $Ext_P(A) = X\backslash Cl_P(A)$.

(3) $Int_P(A) \subseteq Int_P\big(Cl_P(A)\big) = Ext_P\big(Ext_P(A)\big)$.

(4) If $A \subseteq B$ then $Ext_P(B) \subseteq Ext_P(A)$.

(5) $Ext_P(A \cup B) \subseteq Ext_P(A) \cap Ext_P(B)$.

(6) $Ext_P(A) \cup Ext_P(B) \subseteq Ext_P(A \cap B)$.

(7) $Ext_P(X) = \phi, Ext_P(\phi) = X$.

(8) $Ext_P(A) = Ext_P(X\backslash Ext_P(A))$.

(9) $X = Int_P(A) \cup Ext_P(A) \cup Fr_P(A)$.

Proof.

1. It follows from Lemma 3.1 and Proposition 3.2(1).
2. It is straightforward by Proposition 3.2(7).
3. Applying (6) and (8) of Proposition 3.2, we get $Ext_P(Ext_P(A)) = Ext_P(Int_P(X\backslash A)) = Int_P(X\backslash Int_P(X\backslash A)) = Int_P(Cl_P(A)) \supset Int_P(A)$.
4. Assume that $A \subset B$, then $Ext_P(B) = Int_P(X\backslash B) \subseteq Int_P(X\backslash A) = Ext_P(A)$ by using Proposition 3.2(8).
5. Applying Proposition 3.2 (10), we get $Ext_P(A \cup B) = Int_P(X\backslash(A \cup B)) = Int_P((X\backslash A) \cap (X\backslash B)) \subseteq Int_P(X\backslash A) \cap Int_P(X\backslash B) = Ext_P(A) \cap Ext_P(B)$.
6. Using Proposition 3.2 (9), we obtain $Ext_P(A \cap B) = Int_P(X\backslash(A \cap B)) = Int_P((X\backslash A) \cup (X\backslash B) \supseteq Int_P(X\backslash A) \cup Int_P(X\backslash B) = Ext_P(A) \cup Ext_P(B)$.
7. $Ext_P(X) = Int_P(X\backslash X) = Int_P(\phi) = \phi$. Also $Ext_P(\phi) = Int_P(X\backslash \phi) = Int_P(X) = X$.
8. Using Proposition 3.2 (4), we have $Ext_P(X\backslash Ext_P(A)) = Ext_P(X\backslash Int_P(X\backslash A)) = Int_P(X\backslash A) = Ext_P(A)$.

9.
$Int_P(A) \cup Ext_P(A) \cup Fr_P(A) = X \backslash Fr_P(A) \cup Fr_P(A) = X$.

Example 3.12

Let (X, c) be a closure space which is given in Example 3.7. Let $A = \{b, e\}$ and $B = \{c, d, e\}$. Then $Ext_P(B) = \{a\} \subseteq \{a, c, d\} = Ext_P(A)$. This shows that the converse of (4) in Theorem 3.9 is not valid. Now let $A = \{d, e\}$ and $B = \{c\}$. Then $Ext_P(A \cup B) = \{a\} \neq \{a, b\} = \{a, b, c\} \cap \{a, b, d, e\} = Ext_P(A) \cap Ext_P(B)$ which shows that the equality in Theorem 3.9 (5) is not valid. Finally let $A = \{a, b\}$ and $B = \{c, d, e\}$. Then $Ext_P(A \cap B) = \{a, b, c, d, e\}$ and $Ext_P(A) \cup Ext_P(B) = \{a, c, d, e\}$. This shows that the equality in Theorem 3.9 (6) is not valid.

Theorem 3.10

Let (X, c) be idempotent closure space and $A, B \subseteq X$, if $A \subseteq B$, then $i(A) \subseteq i(B)$.

Proof.

Since $A \subseteq B$, then $X \backslash B \subseteq X \backslash A$, so $c(X \backslash B) \subseteq c(X \backslash A)$ (since c is closure operator), then $X \backslash c(X \backslash A) \subseteq X \backslash c(X \backslash B)$, so $i(A) \subseteq i(B)$.

Theorem 3.11

Let (X, c) be idempotent closure space and $A \subseteq X$, then $i(i(A)) = i(A)$.

Proof. Let $i(A) = X \backslash c(X \backslash A)$, so $i(i(A)) = i\big(X \backslash c(X \backslash A)\big) = X \backslash c(X \backslash (X \backslash c(X \backslash A))) = X \backslash c(X \backslash (X \backslash c(X \backslash A))) = X \backslash c(c(X \backslash A))) = X \backslash c(c(X \backslash A))) = X \backslash c(c(X \backslash A))) = X \backslash c(X \backslash A) = i(A)$.

References

1. Khampakdee, J., *Semi-open sets in closure spaces.* Ph. D. thesis, BRNO University of technology, 2009.
2. J.Khampakdee, *Semi-open sets in biclosure spaces.* Discussiones Mathematicae, General Algebra-accepted..
3. Mashhour, A.S., M.E.A. El-Monesf, and S.N. El-Deeb, *On pre-continuous and weak pre continuous mappings.* Proc. Math. Phys. Soc. Egypt 53, 1982: p. 47-53.
4. Darwesh, H.M., *Almost-continuity, Pre-continuity and Preopen sets in Closure Spaces.* (submit).
5. Ahmad, B. and S. Hussain, *Properties of γ-Operations on Topological Spaces.* Aligarh Bull.Math, 2003. **1**(22): p. 45-51.

6. B.Khalaf, A. and S.F. Namiq, *Generalized lammda-Closed Sets and (Lammda,Gamma)*^**-Continuous Functions* International Journal of Scientific & Engineering Research, 2012. **3**(12).
7. B.Khalaf, A. and S.F. Namiq, *Generalized Lammda-Closed Sets and (Lammda,Gamma)*^**-Continuous* Journal of Garmyan University, 2017: p. 2310-0087.
8. B.Khalaf, A. and S.F. Namiq, *λ_βc-Connected Spaces and λ_βc-Components.* Journal of Garmyan University, 2017.
9. B.Khalaf, A. and S.F. Namiq, *ON Minimal λ^*-Open Sets, .* International Journal of Scientific & Engineering Research, October-2014. **5**(10).
10. Darwesh, H.M. and S.F. Namiq, *On Minimal λ_βc-Open Sets* Journal of Garmyan University, 2017.
11. Darwesh, H.M., S.F. Namiq, and W.K. Kadir, *Maximal λc-Open Sets.* ICNS-2016, 2017.
12. F.Namiq, S., *Lammda sub beta c-Open Sets and Topological Properties.* Journal of Garmyan University, 2017(2310-0087).
13. F.Namiq, S., *Contra 〖(λ,γ)〗^*-Continuous Functions.* Journal of Garmyan University, 2017.
14. Hussain, S. and B. Ahmad, *On Minimal γ -Open Sets.* Eur. J. Pure Appl. Maths, 2009. **3**(2): p. 338-351.
15. Kasahara, S., *Operation-Compact Spaces.* Math. Japon, 1979(24): p. 97-105.
16. Khalaf, A.B., H.M. Darwesh, and S.F. Namiq, *λ_c-Connected Space Via λ_c-Open Sets.* Journal of Garmyan University, 2017.
17. Khalaf, A.B. and S.F. Namiq, *New types of continuity and separation axiom based operation in topological spaces.* M. Sc. Thesis, University of Sulaimani, 2011.
18. Khalaf, A.B. and S.F. Namiq, *Lammda sub c-Open Sets and Lammda sub c-Separation Axioms in Topological Spaces.* Journal of Advanced Studies in Topology, 2013. **4**(1): p. 150-158.
19. Namiq, S.F., *Lammda-R0 and Lammda-R1 Spaces.* Journal of Garmyan University, 2014. **4**(3).
20. Namiq, S.F., *λ_sc-open sets and topological properties.* Journal of Garmyan University, 2014.
21. Namiq, S.F., *λ-Connected Spaces Via λ-Open Sets.* Journal of Garmyan University, 2015.
22. Namiq, S.F., *λ_sc-Connected Spaces Via λ_sc-Open Sets.* Journal of Garmyan University, 2017.

23. Namiq, S.F., *Generalized λ_c-Open Set.* International Journal of Scientific & Engineering Research, June-2017. **8**(6).
24. Namiq, S.F., *λ_c-Separation Axioms Via λ_c-open sets.* International Journal of Scientific & Engineering Research May-2017. **8**.
25. Namiq, S.F., *Lammda sub αc-Open Sets and Topological Properties.* pre-print.
26. Ogata, H., *Operations on Topological Spaces and Associated Topology.* Math. Japon, 1991. **36**(1): p. 175-184.
27. Namiq, S.F., *On Minimal λ_bc-Open Sets* Journal of Garmyan University, 2018-accepted.
28. Namiq, S.F., *On Minimal λ_αc-Open Sets* Journal of Garmyan University, 2018-accepted.
29. Sharma, J.N *"Topology",.* Krishna Prakashna Mandir, India., 1977.
30. Sharma, J.N. and J.P. Chauhan, *"Topology(General and Algebraic".* Krishna Prakashna Media, India, 2011.

ttp://jgu.garmian.edu.krd https://doi.org/10.24271/garmian.340

Study the Effect of Indium on the Urbach Energy and Dispersion Parameters of CdO Thin Films

Tahseen H. Mubarak[1∞] Sami Salman Chiad[2*] Mahmood M. Kareem[3] Nadir Fadhil Habubi[2#] Mohamed Odda Dawod[4~] Ehssan S. Hassan[4^]

[1]Department of Physics, College of Science, University of Diyala, Diyala, Iraq [2]Department of Physics, College of Education, Mustansiriyah University, Baghdad, Iraq

[*] Email: dr.sami@uomustansiriyah.edu.iq

[#]nadirfadhil@uomustansiriyah.edu.iq

[3]Department of Physics, College of Education, University of Garmian, Kalar, Iraq

Email: mahmood.mohammed@garmian.edu.krd

[4]Department of Physics, College of Science, Mustansiriyah University, Baghdad, Iraq

[~] Email: mohammedodda2017@uomustansiriyah.edu.iq

[^] Email: ehsanphysicyan@uomustansiryah.edu.iq

[∞] Corresponding author. Email: dean@sciences.uodiyala.edu.iq

Abstract

CdO thin films have been deposited onto glass substrate by chemical spray pyrolysis. Transmittance and reflectance spectra in the range300-900 nm were recorded via UV-Visible spectrophotometer for various In-content in the CdO:In thin films. Transmittance decreased with increasingIn-content in the CdO:In thin films, while the reflectance slightly increased in the wavelength more than 480 nm. Urbach energy decreased with increasing In-content in the CdO:In thin films. Dispersion parameters are calculated, and find that E_d, E_o, ε_∞, n(0), S_o,M_{-1} and $M_{-3}$are increased with increasing In-content in the CdO:In thin films.

***Keywords*:** Thin films**,** Cdo:In, Spray pyrolysis, reflectance, Dispersion,

Introduction

Transparent conducting oxide (TCO) thin films have great importance in electronic device applications and among these TCOs, cadmium oxide (CdO), an n-type semiconductor with band gap of 2.5 eV [1].

Inthethinfilmform,itfindsapplicationsingassensordevices,photodiodes,transparentelectrodes, phototransistors and solar cells[2].

Various techniques have been employed to prepare CdO thin films such as spray pyrolysis [3], sputtering [4,5], solution growth [6], activated reactive evaporation [7], pulsed laser deposition [8] and sol-gel method [9].
Urbach energy and dispersion parameters of CuO thin films were calculated and study the effect of In contenton these films.

Experimental Part
0.1M of $Cd(CooCH_3)_2$(supplied from Sigma-Aldrich Chemicals) dissolve in re-distilled water and an aqueous solution of 0.1M of $InCl_3$(2% and 4% volume) (supplied from Sigma-Aldrich Chemicals) were used as precursormaterials to obtain the deposited films by chemical spray pyrolysis on to glass substrate. The optimum conditions were arrived at the following parameters:Substrate temperature was kept at 350 ^{o}C during deposition process, the distance between nozzle and substrate was 28 cm, compressed air was used as a carrier gas ,and rate of depositon was 2 ml/min. Thickness wasobtained bygravimetricmethod was about 350 nm. Double beam UV-Visible spectrophotometer was used in order to record the absorbance spectra and calculate the optical parameters..

Results and Discussion:
The obtained results measured that recorded from UV-Visible spectrophotometer is plotted in Fig.1 for In-doped CdO thin films prepared by chemical spray pyrolysis. From this figure, it can notice the decreases of transmittance with increasing In-doping in the CdO thin films, and also decreased with decreasing wavelength (at high photon energy, the absorbance of films increases leads to decreasing transmittance).

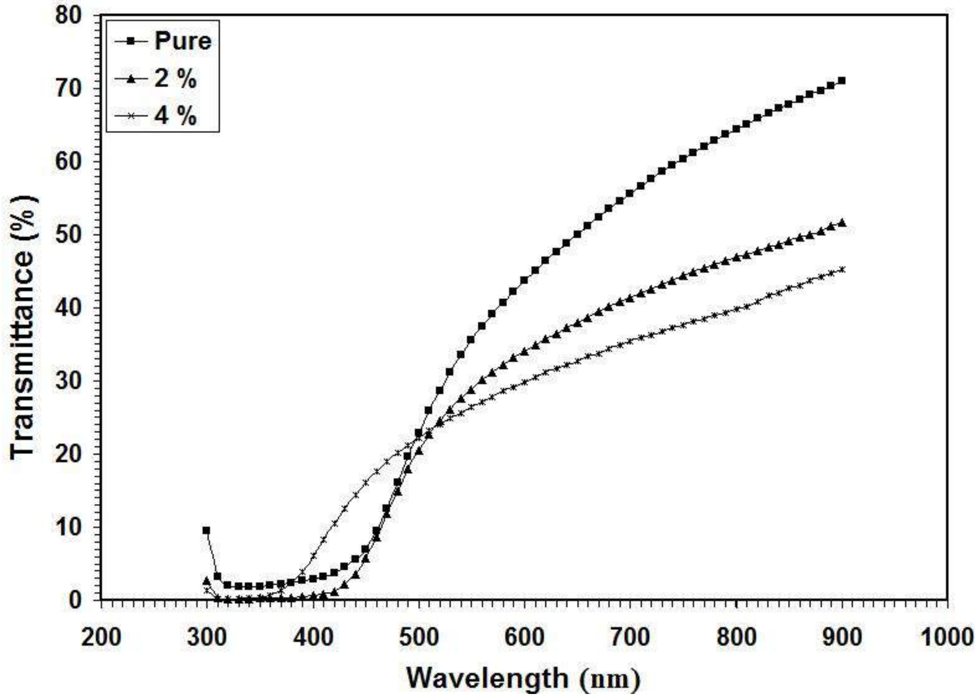

Fig.1: Transmittance spectra of CdO:In thin films with various In-doping.

The reflectance (R) has been found by using the relationship:

$$R + T + A = 1 \quad \dots \ (1)$$

where T and A is the transmittance and absorbance respectively. The reflectance spectra versus wavelength was plotted in Fig. 2. The reflectance increased slightly with increasing In-doping at wavelength more than 480 nm.

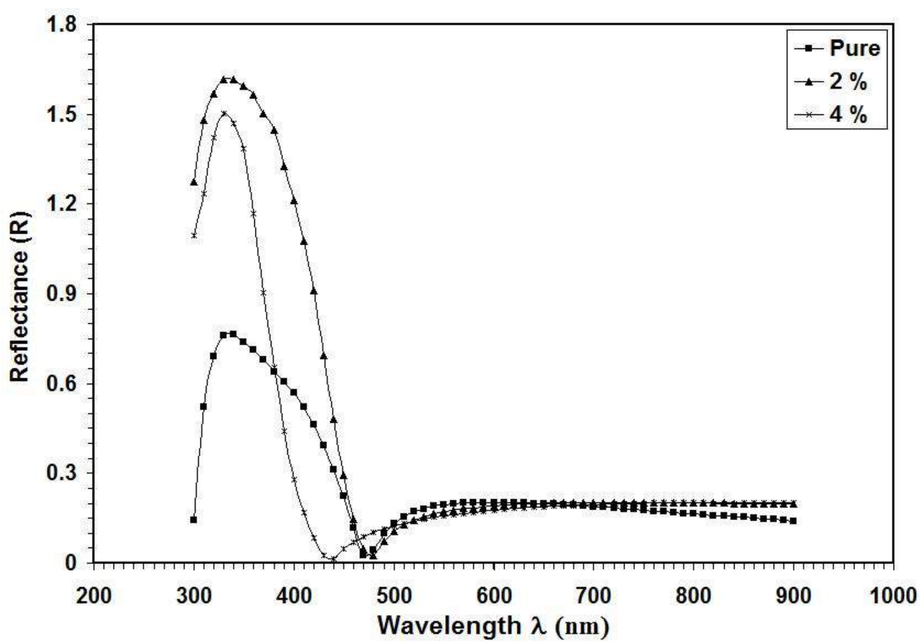

Fig.2: Reflectance spectra of CdO:In thin films with various In-doping.

The optical conductivity was calculated using the relation [10]:

$$Q = \frac{\alpha\, n\, c}{4\pi} \quad \dots \ (2)$$

where α is absorption coefficient, n is refractive index, and c is speed of light. The optical conductivity as a function of wavelength was plotted in Fig.3. From this figure, it can notice the slight decreases with increasing In-doping at wavelength more than 480 nm for pure and In-doped CdO thin films.

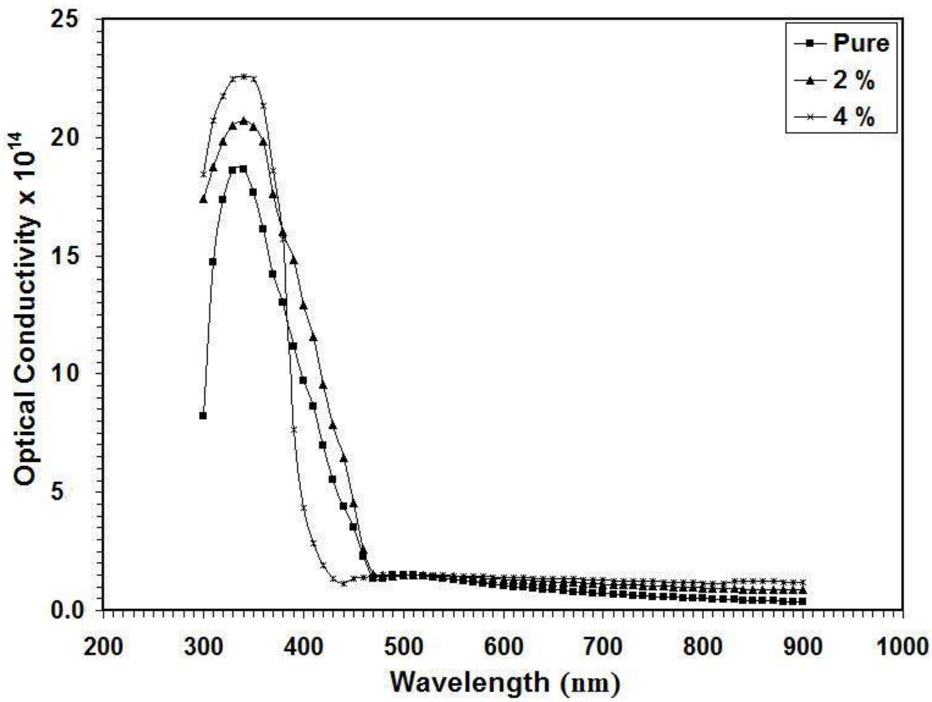

Fig.3: Optical conductivity of CdO:In thin films with various In-doping.

The absorption edge gives a measure of the energy band gap and the exponentialdependence of the absorption coefficient, in the exponential edge region Urbach rule is expressed as[11]:

$$\alpha = \alpha_o \exp\left(\frac{h\nu}{E_U}\right) \quad \dots \ (3)$$

where $\alpha_\circ$ is aconstant, E_U is the Urbach energy, which characterizes the slope of the exponential edge. The values of E_U are obtained from plotting relation between lnα versus photon energy (hυ) as in Fig. 4, the slope value represent the Urbachenergy.

These values are listed in Table 1.The absorption in this region is due to the transitions between the extended states in one band and the localized statesin the exponential tail of the other band. From the Table, the Urbach energy decreased with increasing In-content in CdO thin films.

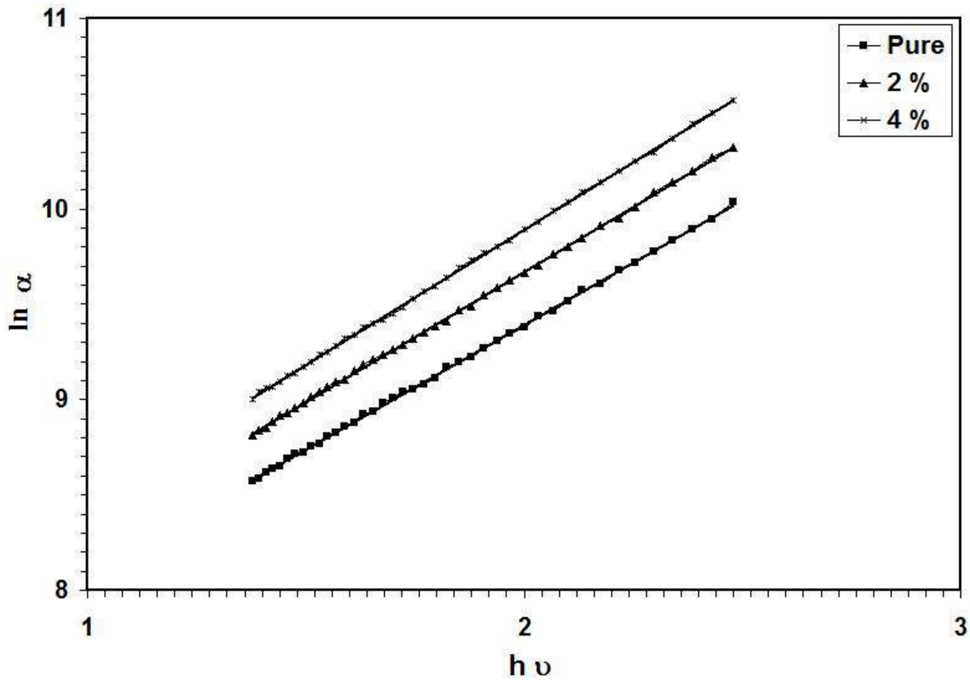

Fig.4: Lnα versus hυ of CdO:In thin films with various In-doping.

The refractive index dispersion for crystallized and amorphousmaterials can be expressed as [12]:

$$n^2 - 1 = \frac{E_o E_d}{E_o^2 - E^2} \quad .....(4)$$

Where n is the real part of refractive index, hυ is the photon energy, E_o is the average excitation energy for electronictransitions and E_d is the dispersion energy, which is ameasure of the strength of interband optical transitions.This model describes the dielectric response for transitionsbelow the optical gap.

By plotting $(n^2-1)^{-1}$vs. $(h\upsilon)^2$and fittinga straight line, the values of the parameters E_o and E_d were calculated from (E_o/ E_d) represents the intercept onthe vertical axis and $(E_oE_d)^{-1}$is the slope of the plot, this shown in Fig. 5.

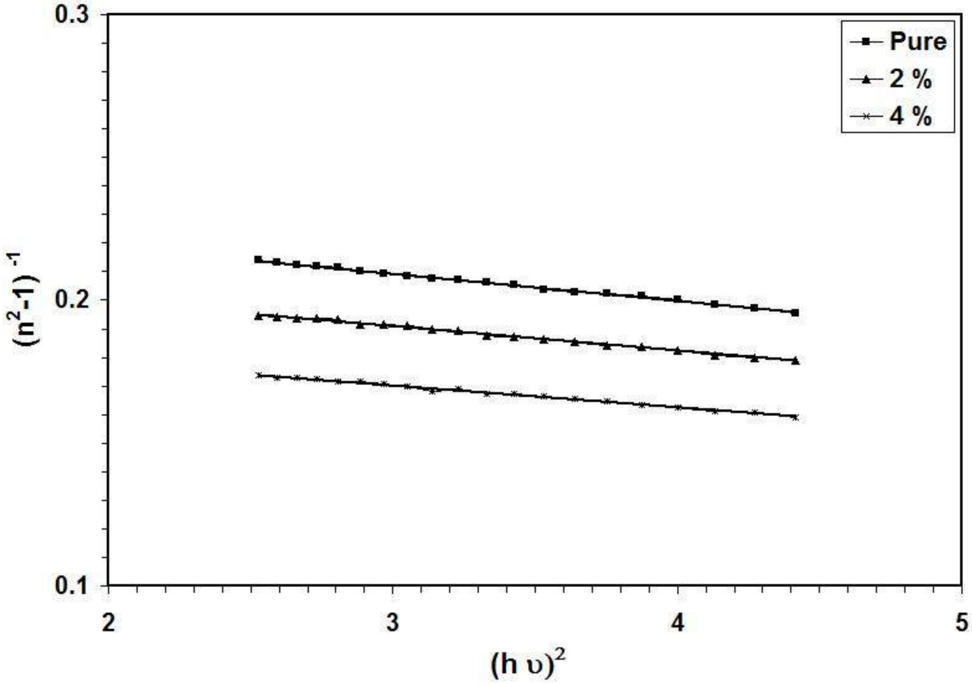

Fig.5: $(n^2\text{-}1)^{-1}$ versus $(h\upsilon)^2$ of CdO:In thin films with various In-doping.

The refractive index at infinite wavelength (n_∞) can be determined from the following relation [13]:

$$\frac{n_\infty^2-1}{n^2-1}=1-\left(\frac{\lambda_o}{\lambda}\right)^2 \quad ...(5)$$

The plot of $(n^2\text{-}1)^{-1}$versus$\lambda^{-2}$was plotted to find the values of (n_∞) of CdO:In thin films. These values are shown in Table 1.

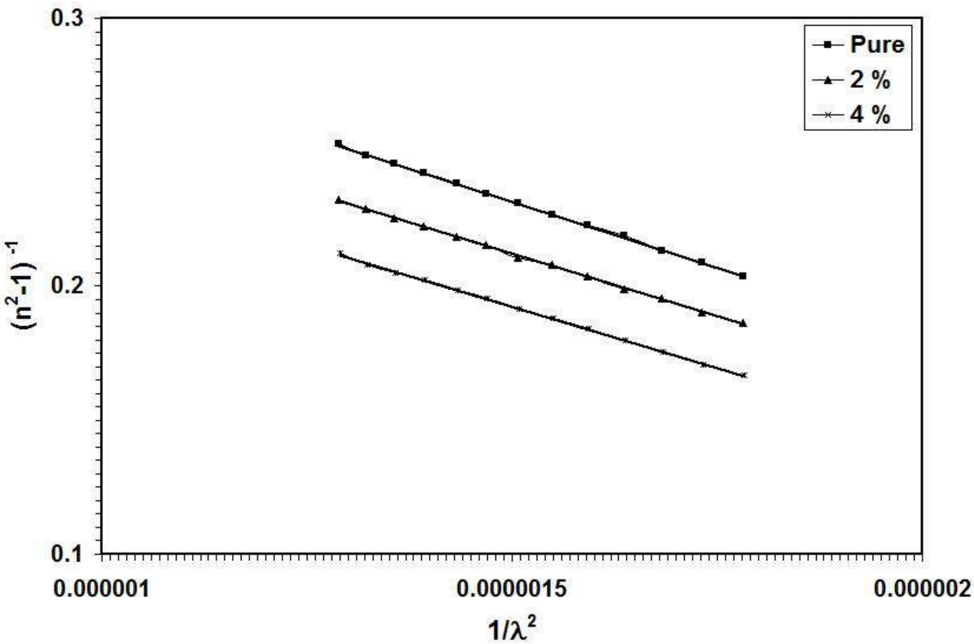

Fig.6: $(n^2-1)^{-1}$ versus $1/\lambda^2$ of CdO:In thin films with various In-doping.

The M_{-1} and M_{-3} moments of the optical spectra have obtained from the following relations [14]:

$$E_d^2 = \frac{M_{-1}^3}{M_{-3}} \quad \text{and} \quad E_o^2 = \frac{M_{-1}}{M_{-3}} \quad \dots (6)$$

The values of M_{-1} and M_{-3} moments of the optical spectra are increased with increasing In-content in the CdO:In thin films as shown in Table 1.

Table 1: Some optical parameters of CdO:In thin films.

Sample	E_d (eV)	E_o (eV)	E_g (eV)	ε_∞	n(o)	M_{-1}	M_{-3} eV^{-2}	S_o x10^{13} m^{-2}	λ_o nm	U_Em eV
Pure	21.87	4.81	2.406	5.545	2.35	4.54	0.196	1.01	592	769
2 %	24.25	4.85	2.425	6.000	2.45	5.00	0.212	1.07	599	740
4 %	27.47	5.03	2.517	6.560	2.56	5.50	0.219	1.10	615	704

Conclusions

CdO thin films with various amounts of In-content have been deposited onto glass substrate by chemical spray pyrolysis. Transmittance spectra in the range of 300-900 nm decreased with increasingIn-content in the CdO:In thin films. Urbach energy decreased with increasing In-content in the CdO:In thin films, while the energy gap increased from 2.406 eV to 2.517 eV after additive of 4% In in the CdO:In thin films. Dispersion parameters such as: E_d, E_o, ε_∞, n(0), S_o,λ_o, M_{-1} and $M_{-3}$are decreased with increasing In-contain in the CdO:In thin films.

References

[1] N.Manjula,K.Usharani,A.R.Balu, V.S.Nagarethinam, Studies on the physical properties of three potentially important TCO thin films fabricated by a simplified spray technique and a same deposition conditions Int. J.chemTech. Res.6, 705-718, (2014).

[2] C. Sravani,K.T.R. Reddy, O.Md. Hussain,P.J. Reddy,J.SolarEnergySoc.

India 6, 1 (1996).

[3] M. D. Uplane, P. N. Kshirsagan, B. J. Lokhande, C. H. Bhosale, Materials Chemistry and Physics, p.64, 75, (2000).

[4]T. K. Subramanyam, S. Uthanna, B. Sinivasulu Naidu, Materials Letters 35 (1998) 214, and Appl. Surface Science, p.169,529, (2001).

[5] K. Gurumurugan, D. Mangalaraj, Sa. K. Narayandass, J. Electron. Mater, p.25, 765, (1996). |

[6] A. J. Varkey, A. F. Fort, (Thin Solid Films)pp:239, 211(1994). |

[7] K. T. Ramakrishna Reddy, C. Sravani, R. W. Miles, J. Cryst. Growth p. 184/185, 1031, (1998). |

[8] Xiaonan Li, Timothy Gessert, Clay DeHart, Teresa Barnes,(A Comparison of Composite Transparent Conducting Oxides Based on the Binary Compounds CdO and SnO_2) National Renewable Energy Laboratory 14-17 October (2001).

[9] D. M. Carballeda-Galicia, R. Castanedo-Perez, O. Jimenez-Sandoval, S. Jimenez-Sandoval, G. Torres-Delgado, C.I. Zuniga-Romero, (Thin Solid Films), p: 371,105 ,(2000).

[10] J. I. Pankove,"Optical processes in semiconductors", Dover Publications, Inc. New York, pp. 91, (1975).

[18]J. Tauc,"Amorphous and Liquid Semiconductors", Plenum Press, New York, 1974.

[11] M. DiDomenico and S.H. Wemple, “Oxygen-octahedra ferroelectrics. I. theory of electro-optical and nonlinear optical effects”, J. Appl. Phys.40, 720 (1969)

[12] F. Yakuphanoglu and C. Viswanathan, "Electrical conductivity and single oscillator model properties of amorphous CuSe semiconductor thin film", Journal of Non-crystalline Solids, Vol. 353, pp. 2934-2937, (2007).

[13] S.H. Wemple, M. DiDomenico, "Optical Dispersion and the Structure of solid", Phys. Rev. Litt. 23, 20, 1156-1160, (1969).

ttp://jgu.garmian.edu.krd https://doi.org/10.24271/garmian.341

Analyzing the interactions between fluid and solid particles

Sherko Ahmad Flamarz Al-Arkawazi

Sulaimani Polytechnic University (SPU), Al- Sulaimaniyah, Kurdistan Region, Iraq
Email: sherko.flamarz@spu.edu.iq

Abstract

This study focuses on analyzing and modeling the interactions between fluid and solid particles. A model based on the detection of contacts in granular medium is developed from a Discrete Elements approach (DEM) for solid phase, coupled with a Computational Fluid Dynamics (CFD) for fluid phase. The objective of this work is to investigate the interactions occurs between the fluid and solid particles in fluidized beds, and to better understand the various characteristic of these interactions which is the base of work of unit operations in a set of industrial processes. A comparison between different models of fluid flow (laminar model, k-ε model, and k-ω SST model) in CFD code is showed that; the k-ε model is most appropriate for calculation of fluid flow in industrial applications. The interaction between the fluid and each particle is performed through a drag force. The effect of the local particle concentration on the drag force is modeled by a porosity function. The simulations results are revealed that the value of exponent of porosity shows substantial dependence on the size of the Representative Volume Element (REV), tortuosity and the velocity of the fluid flow. Finally, the comparison between numerical simulation results with experimental results, in terms of fluidized bed height are showed that the bed expansion height of the fluidized bed is increased with an increase of fluid velocity, and this presents already a very good fit, which eventually achieve an optimization of fluidization processes.

Keywords: Interaction fluid-solid; Drag force; Fluidization; Coupling DEM-CFD

1. Introduction

The multiphase flow is essential in the work of many of industrial operations and processes, in which a close contact between the fluid and the solid particles. Therefore, the fluid-solid interaction plays a major role in unit processes, including, fluidization, catalytic cracking, sedimentation, particle classification, pharmaceutical, food processing, water treatments, chemical reactions, pneumatic conveying, crystallization, and so on (Matheson et al., 1949; Richardson & Zaki, 1954; Hartge & Werther, 1986; Bürger & Wendland, 2001; Hirano et al., 2013). The fluidization processes or fluidized beds are a typical example of fluid-solid particle interaction; therefore, the fluidized beds are suited for chemical reactions as they allow exchanging the hydrodynamic and mechanic energies between the fluid and the solid particles. These conditions make it possible obtaining better yields and also greater selectivity. Besides, the use of fluidized beds makes it possible to obtain a high homogeneity of distribution of the solid phase and a high efficiency of the exchanges of energies.

Since 1920, the fluidization processes are used in the industrial applications, so a large number of researches are having been provided to improve and develop the fluidization units. The majority of the researches were experimental investigations of the characteristics and transport phenomena in the fluidization processes. The practical experiments include; devices and probes of measurements that disturb the fluidized beds and there behaviors and herewith they effect the result of the measurement. The practical limitations had overcome through computer models, since the development of the computer science in early of 1990s. The computers models are able to study and simulate from inside (microscopic interactions between particle-particle and fluid-particle) without disturb the fluidized beds.

The numerical study of fluidized beds through coupling the discrete code (discrete element method DEM) with continuum code (computational fluid dynamics CFD), enables to simulate (measure) many of properties, such as particle velocity, porosity, height of the fluidized beds and the interactions forces, as well as the velocity of the fluid, which are very difficult, if not impossible, to obtain by direct experimental probes.

Many of researchers are proposed models to combine the DEM model with the CFD codes, such as Tsuji et al. (1993) and Hoomans et al. (1996), in which they are reported the coupling of the DEM with a finite volume description of the gas-phase based on the Navier–Stokes equations for the soft-sphere model and the hard sphere model respectively. Yu & Xu (2003), are studied the vital role of the interaction forces between the particles in expanded bed. Zhu et al., (2008) are achieved to work in the particle scale simulation by combining DEM approach with CFD approach, respectively for solid and fluid phases. The coupling models of DEM-CFD have proved an ability to achieve and reproduce most of the features of the fluidized beds for complex units that includes multiphase flows (Chavan et al., 2018; Di Maio & Di Renzo, 2007; Gidaspow, 1994; Apostolou & Hrymak, 2008; Wang et al., 2010; Chu et al., 2018; Al-Arkawazia et al., 2017).

Although the advantages of the numerical models, but they are still need to more analysis in large scale industrial units of fluid-solid particles, to well understanding of the fundamentals of fluid-particle flows (Deen et al., 2007). Especially the behaviors which are related to the collision forces that results from the inter-particle reactions and the drag force produced from fluid-particle interaction.

In this work, the coupling of the two approaches (DEM-CFD) is used for analyzing and simulating the hydrodynamics behaviors of fluid-solid particles, through the fluidization process. The motion of the solid particles are treated by the discrete element method (DEM) is based on the Newtonian equations of motion, and the collision forces between the particle-particle (and wall) are modeled by hard particle approach (Fortain & De Saxcé, 1999). The fluid flow is calculated by using the computational fluid dynamics (CFD), which is based on the Navier-Stokes equations (Archambeau et al., 2004). This is why we analyze and study numerically the interaction between fluid-solid particles through the drag force during the fluidization process, in order to propose a model of estimation of the best size of REV and value of the exponent of porosity correction. In a second step, we will integrate this model with a complete calculation of fluidization, which will be confronted with experimental results, in terms of height of bed expansion according to the inlet velocity of the fluid.

The work presented herein is arranged as follows; we gives and introduction of general principles relating to the discrete element method (DEM), the computational fluid dynamics (CFD), the coupling of DEM-CFD, and the governing equations in section 2. We validate the DEM-CFD model by simulating a single particle, for different models of flow in CFD (laminar, k- ε, and k-w SST) for a range of fluidization velocities, and compare the value of drag force calculated by these models of CFD with the value of drag calculated by theoretical equation. Then we simulate and evaluate the hydrodynamics behaviors of the fluid-solid particles interactions through a comparison between the numerical results with the experimental results to find the best size of REV and the exponent of porosity value (n) in section 3. Finally, we discuss and analyze the results and conclude the points that are carried out in the presented work.

2. Material and Methods

A good prediction of the characteristics of a fluid-solid mixture requires the knowledge to understand, and analyze the governing equations of fluid phase and solid phase. The behavior of fluidized beds is controlled by the effective forces acting on the motion of the solid particles; these forces are mainly the inter-particle contact forces, gravitational force, buoyancy force, and drag force, as shown in Fig.1. In present work, the DEM code is developed in our laboratory, and the CFD code is the open source software code Saturne (version 4), which is developed by electricity of France (EDF) (Archambeau et al., 2004).

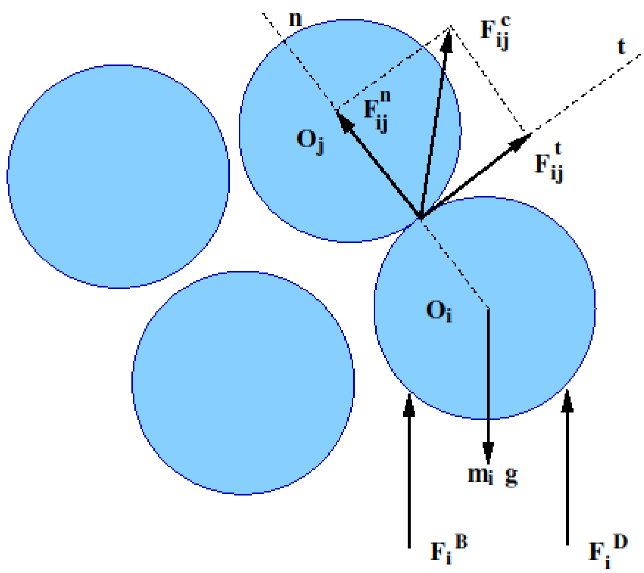

Figure 1: Schematic of the forces acting on particle *i* from contacting particle *j* and fluid-particle interactions.

2.1 Governing equations of particle motion

In the DEM code, the motion of each individual particle is governed by Newton's second law (linear momentum conservation and angular momentum), expressed, for the *i*-particle, by:

$$m_i \frac{d\vec{v}_i}{dt} = \sum_j^{nc} \left(\vec{F}_{ij}^n + \vec{F}_{ij}^t \right) + m_i \vec{g} + \vec{F}_i^B + \vec{F}_i^D \qquad (1)$$

$$I_i \frac{d\vec{\omega}_i}{dt} = \sum_j^{nc} \left(\vec{r}_i \times \vec{F}_{ij}^t \right) \qquad (2)$$

where m_i, $\vec{v}_i$ represent, mass, velocity of the (*i* th) particle respectively, *nc* is the number of contacts, $\vec{F}_{ij}^n$ and $\vec{F}_{ij}^t$ are the normal and tangential contact forces exerted by the neighboring particles on particle *i* which is calculated by the DEM code, $\vec{g}$ is the gravitational acceleration, $\vec{F}_i^B$ is the buoyancy force, $\vec{F}_i^D$ is the drag force exerted by the fluid on the particle, I_i, $\vec{\omega}_i$, and $\vec{r}_i$ are the moment of inertia, angular velocity, and radius of a particle respectively.

2.2 Governing equations of fluid flow

The CFD code used in this work is the open source code Saturne, which solves the Reynolds-Averaged Navier-Stokes (RANS) equations (Archambeau et al., 2004). The continuity and momentum equations are governing the fluid flow, and can be written as:

$$\frac{\partial \rho_f}{\partial t} + \vec{\nabla}.\left(\rho_f \vec{v}_f\right) = 0 \tag{3}$$

$$\frac{\partial\left(\rho_f \vec{v}_f\right)}{\partial t} + \vec{\nabla}.\left(\rho_f \vec{v}_f \otimes \vec{v}_f\right) = \vec{\nabla} \cdot (\vec{\sigma}) + S_u \tag{4}$$

where ρ_f, $\vec{v}_f$ *are* the density and velocity vector for the flow fluid respectively, $\vec{\sigma}$ is the stress tensor. For a turbulent flow, the stress tensor σ includes the effect of pressure, viscous stress τ, the turbulent Reynolds stress tensor R_{ij} , and S_u represents additional momentum source terms. In the present work, it was chosen to use; laminar model, k-ε model and k-ω SST (Shear Stress Transport) model (Menter, 1994). The laminar model is used the Navier-Stokes equations, Among the turbulence closure models available in the code, it was made the choice of using the first order two-equation models, k-ε model and k-ω, largely applied for their simplicity. The transport of the turbulent kinetic energy k and dissipation rate ε is examples of equations commonly used as closure, leading to the well-known standard k-ε turbulence model (Mohammadi & Pironneau, 1994).

$$\rho_f \frac{\partial k}{\partial t} + \nabla \cdot \left(\rho_f \vec{v}_f k - (\mu_f + \frac{\mu_t}{\sigma_k}) grad\, k \right) = P + G - \rho_f \varepsilon \tag{5}$$

$$\frac{\partial \varepsilon}{\partial t} + \nabla \cdot \left(\rho_f \vec{v}_f \varepsilon - (\mu_f + \frac{\mu_t}{\sigma_\varepsilon}) grad\, \varepsilon \right) = C_{\varepsilon 1} \frac{\varepsilon}{k}\left[P + \left(1 - C_{\varepsilon 3}\right)G\right]P - \rho_f C_{\varepsilon 2} \frac{\varepsilon^2}{k} \tag{6}$$

$$\nu_t = \frac{\mu_t}{\rho_f} = C_\mu \frac{k^2}{\varepsilon} \tag{7}$$

k is the turbulent kinetic energy, ε the turbulent dissipation, μ_f the fluid dynamic viscosity, μ_t the turbulent viscosity, P accounts for the production of the kinetic energy through mean shear stresses, G the production term related to gravity effects and finally $\sigma_k = 1$, $\sigma_\varepsilon = 1.3$, $C_{\varepsilon 1} = 1.44$, $C_{\varepsilon 2} = 1.92$ and $C_\mu = 0.09$ defined constants. $C_{\varepsilon 3} = 0$ if $G \geq 0$ and $C_{\varepsilon 3} = 1$ if $G \leq 0$. In the (k-w) SST model (Menter, 1994), the equation 6 is solved for k, and the dissipation ω is a ratio between ε and k so called specific turbulence dissipation ($\omega = \varepsilon/k$).

2.3 Governing equations of fluid-particle interaction

The essential base of the combined of discrete approach (DEM) with continuum approach (CFD), is the interaction force between the fluid and the solid particles. This interaction force consists of two forces; buoyancy force and drag force. The buoyancy force is produced accuse the fluid pressure gradient around each individual particle (Kafui et al., 2011), expressed in this work as,

$$F_i^B = \frac{4\pi}{3} r_i^3 \rho_f g \tag{8}$$

While the drag force is the viscous shearing stresses effect of fluid on the particle. The drag force (Helland et al., 2000) is expressed by:

$$F_i^D = \frac{\pi}{2} C_{D,i} r_i^2 \rho_f \left(\vec{v}_f - \vec{v}_i\right)^2 \varepsilon^{2-n} \tag{9}$$

where $C_{D,i}$ is the drag coefficient, ε_i^{-n} is porosity correction function to consider the effect of presence of other particles in neighbors of the particle *i*, and *n* is exponent, it is an important factor in fluid-solid flows and educe from the experimental results on sedimentation and fluidization of Richardson & Zaki, (1954) :

$$\frac{v_r}{v_{o,i}} = \varepsilon_i^n \tag{10}$$

where v_r is the relative settling velocity between the fluid and the particle, $v_{o,i}$ is the terminal falling velocity of the particle and is obtained from Stokes' law of sedimentation (Stokes, 1901), and expressed as,

$$v_{o,i} = \frac{g d_i^2 \left(\rho_i - \rho_f\right)}{18 \mu_f} \tag{11}$$

The drag force coefficient used herein the coupling DEM-CFD is the correlation proposed by Brown and Lawler, (2003), expressed as:

$$C_{D,i} = \frac{24}{Re_i}\left(1 + 0.15 Re_i^{0.681}\right) + \frac{0.407}{1 + \frac{8710}{Re_i}} \tag{10}$$

where $Re_i = \rho_f \varepsilon_i d_i \left|v_f - v_i\right| / \mu_f$ is the particle Reynolds number, d_i is the diameter of the particle, and μ_f is the dynamic viscosity.

The interstitial velocity of the fluid is evaluated from the velocity calculation by CFD code:

$$\vec{v}_f = K \frac{\vec{v}}{\varepsilon_i} \tag{13}$$

where *K* is a geometric factor that takes into account including the tortuosity of the solid phase (Gilbilaro, 2001). The tortuosity is the ratio of the actual path length through the pores to the euclidean distance, ($K = l_{actual}/l_{euclidean}$). Other thing, the calculation of the porosity in this work is calculated by REV method (Representative Element Volume), which centered on the particle (Sherko, 2017), and expressed as,

$$\varepsilon = \frac{V_{REV} - V_{i,REV}}{V_{REV}} \qquad (14)$$

where V_{REV} is the volume of the REV and calculated as,

($V_{REV} = (l_r \times l_r) \times d_i$, $l_r = y \times d_i$, $y = 1,2,3,..etc.$) and $V_{i,REV}$ is the volumes of the particles in the REV ($V_{i,REV} = N \times V_i$), where N is the number of particles in the REV, and V_i is the volume of particle.

3. Results

3.1 Validation of the coupling DEM-CFD

A numerical simulation of one particle (d_i =2 mm) in a parallelepiped, which is designed by using Salome platform (version 7), each side of the base has a length of 25 times the diameter of sphere (d_i = 2mm), therefore the base is (0.05 m × 0.05 m) to prevent the effect of the walls with fluid flow in z-direction, and a height of 1.0 m, the geometry is shown in Fig.2. The physical parameters used in the simulation are listed in Table 1.

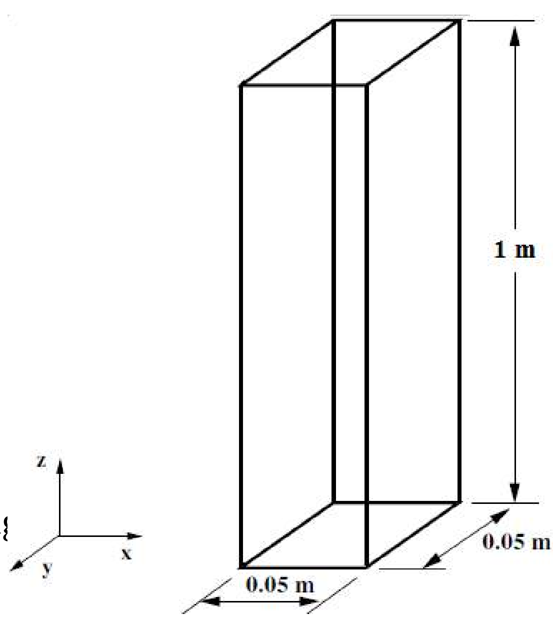

Fi el.

Table 1: Physical parameters used in the simulation.

Parameter	Value
Particle diameter [mm]	2
Density of particle [kg/m^3]	2500
Young's modulus [GPa]	70
Poisson coefficient	0.35
Coefficient of friction	0.3
Coefficient of restitution	0.9
Density of water [kg / m^3]	1000
Dynamic viscosity of water [Pa.s]	0.001
DEM time step [s]	1x10^{-5}

3.2 The relationship between the hydrodynamics characteristics

To analyze the behaviors of fluid-solid particle interactions, it is necessary to understand the relationships between the hydrodynamics characteristics of the fluidized bed, such as the drag force, porosity of the bed, tortuosity, and height of the bed in the fluidization process. The relation between the tortuosity and the size of REV is depicted in Fig.3, it shows that value of the tortuosity is decreasing and approaches to 1 when the size of REV is increased.

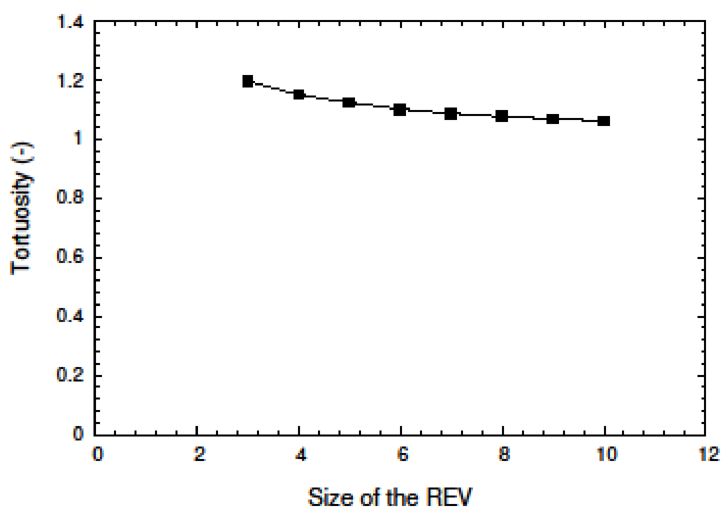

Figure 3: Relationship between the tortuosity and the size of REV.

In other hand, Fig. 4 depicted that the value of porosity for the fluid is increased with the increase the size of REV. From Fig.4, it is obvious that size of REV beyond the size of (5x5), changing the size of REV does not significantly change the value of porosity approaching to 1. The numerical results show that the values of drag force increase with the increase of velocity of the inlet fluid. The results for a single sphere with d_i = 2 mm, are presented in Fig. 5, a comparison between the results of theoretical drag force calculated from equation 15, with several models that used (laminar, *k-ε* and *k-ω* SST).

$$F_{th}^{D} = \frac{1}{2} C_{D,i} \rho_f \pi r_i^2 v_r^2 \qquad (15)$$

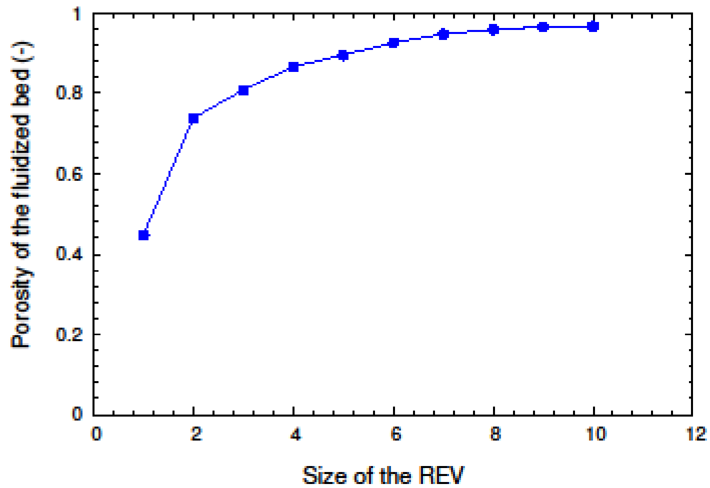

Figure 4: Relationship between the porosity local and the size of REV.

The curves in Fig.5, are depicted that the curve of drag force of *k-ε* model is the nearest to the theoretical curve of drag force.

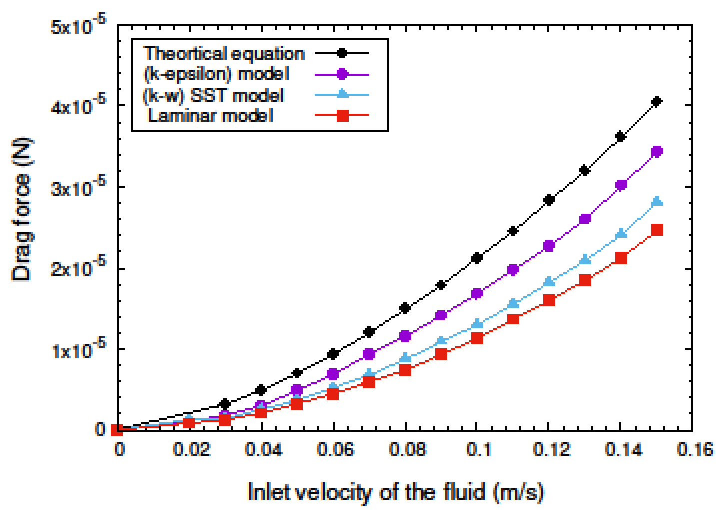

Figure 5: Relation between the drag force and inlet velocity of the fluid.

The Fig.6 depicts the values of exponent of porosity, which are calculated from equation 10, are plotted with different inlet velocity of the fluid for different sizes of REV. The four curves show that the value of the exponent doesn't depend on the inlet velocity but is strongly dependent on the sizes of REV.

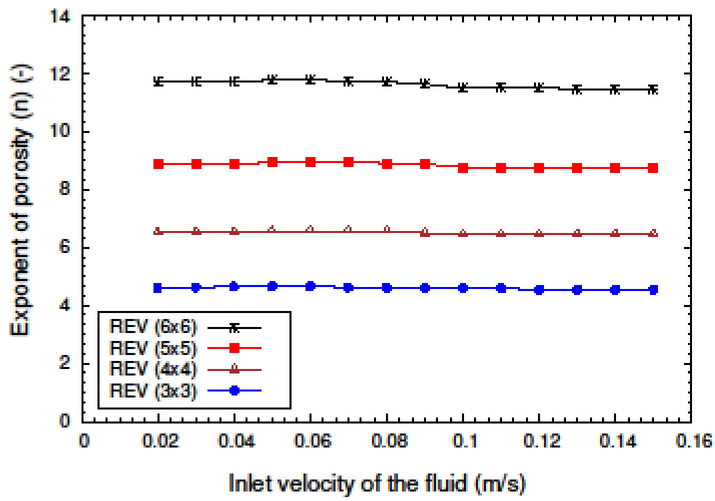

Figure 6: Relationship between the exponent of porosity and the inlet velocity of the fluid

3.3 Results of coupling DEM-CFD (fluidization)

In order to attest the feasibility of the DEM-CFD model, a comparison for the numerical simulation of coupling DEM-CFD model with experimental data (Al-Arkawazi et al., 2017) has been done. For this purpose, a geometry of fluidizing column (pipe) with dimensions; diameter of the pipe (D = 96 mm) and height (H =1 m), as depicted in (Fig.7). The physical parameters used in the simulation are listed in Table 2.

Then, two size of REV (3x3), with exponent of porosity (n = 4.6), and REV (4x4), with exponent of porosity (n = 6.5) are tested. In the fluid side, k-ε model for a range of inlet water velocity (0-0.14 m/s) has been used. The results are plotted in Fig. 7; the results of size of REV (3x3) are the nearest and consistent with the experimental results more than the other size of REV (4x4).

Table 2: Physical parameters of the simulation.

Parameter	Value
Particle diameter [mm]	2
Number of particles	2640
Density of particle [kg/m^3]	2500
Young's modulus [GPa]	70
Poisson coefficient	0.35
Coefficient of friction	0.3
Coefficient of restitution	0.9
Density of water [kg / m^3]	1000
Dynamic viscosity of water [Pa.s]	0.001
DEM time step [s]	1x10^{-5}

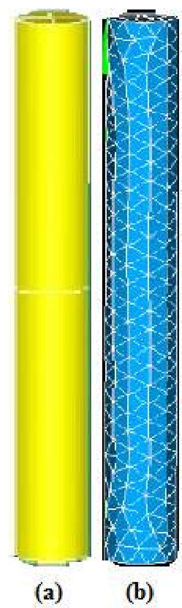

Figure 7: Sketch of fluidized bed, a) geometry 3D, b) meshing

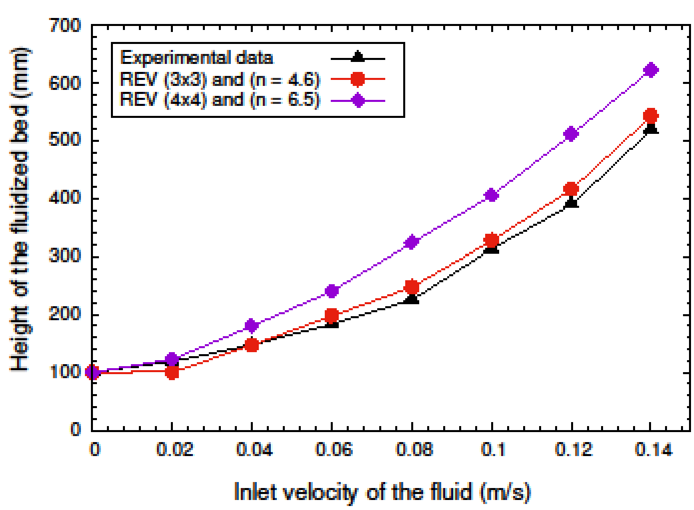

Figure 8: Comparison between the numerical results with the experimental results.

Then, an example of simulation (coupling DEM-CFD) for the fluidization process has been done. The snapshots of fluidization process are presented in Fig. 9, for REV size (3x3) with exponent of porosity (n = 4.6), and inlet velocity of the water is 0.12 m/s. The bed is initially at static (t = 0), then the flow of the water from the inlet of the pipe in upward direction causes fluidization of the particles, as it can be seen the bed start to expanded at t = 0.25 s, and the bed expansion is maximal at about t = 5.0 s and the height of fluidized bed is remained fluctuating at this height as shown in the Fig. 9 for the rest of the time. It can notice in Fig. 9 that a heterogeneous distribution of particles in the cylinder, that can be related to a forming of clusters that mounting upward the fluidized bed before falling back slightly.

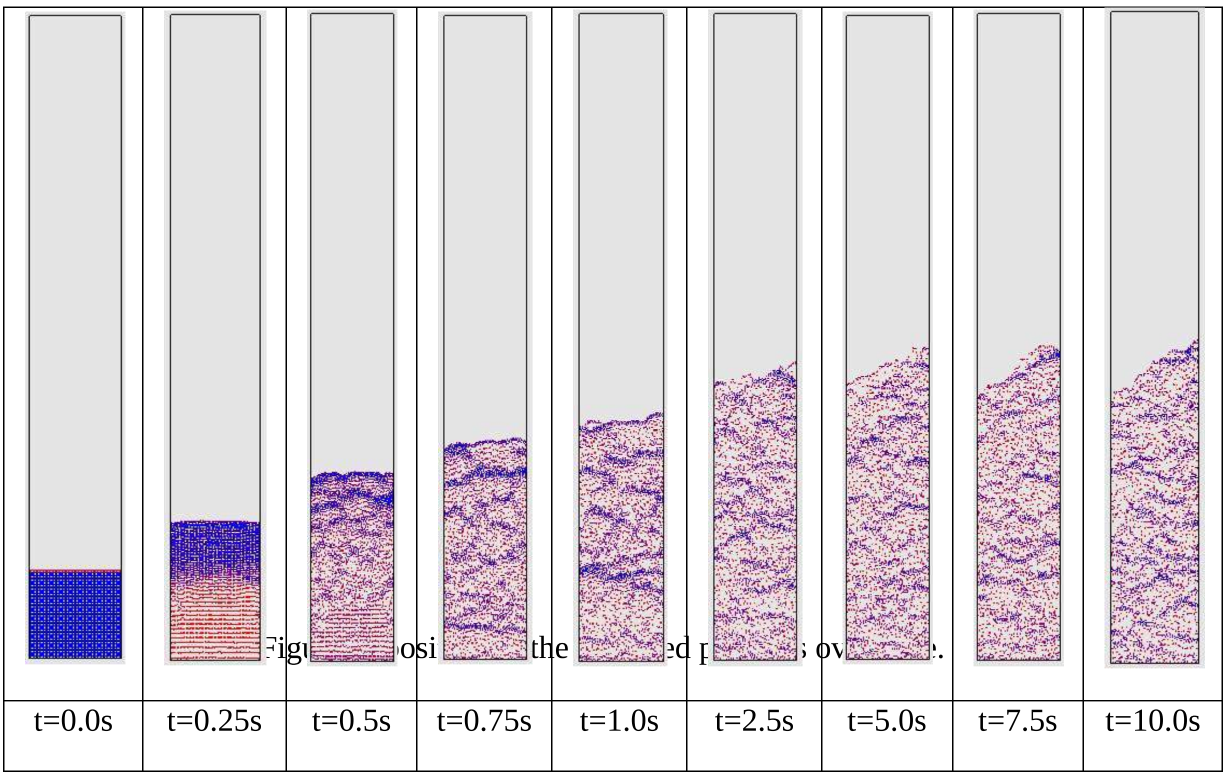

4. Discussion

The study presents an attempt in analyzing and modeling the hydrodynamic behavior of a fluidized bed by means of a coupling between a discrete element code (DEM), and Computational Fluid Dynamics (CFD) calculation. The action of the fluid on the particles is expressed in terms of drag force requiring a good estimation of the exponent of porosity, which is considering the group effects of particles on the global and local flow structures in a fluid-particle circulating fluidized bed. For this reason, we studied the influence of the size of the REV (Representative Volume Element), tortuosity and porosity on the value of the exponent of porosity. The comparison between the numerical results with the experimental ones, attests of a very good agreement. We found that the best size of REV is (3x3) with the exponent of porosity (*n* = 4.6), which approach to other values of (*n*) that proposed by other researchers, for example Helland et al., (2007) who proposed (*n* = 4.7). The good results of the coupling DEM-CFD model for the fluidized bed, will allow us in the longer term; to add heat transfer models and mass transfer ones between the fluid and particles in simulations.

References

Matheson, G. L., Herbst, W. A., & Halt, P. H. (1949). Characteristics of Fluid-Solid Systems. *Industrial Engineering Chemical*, 41, 1099.

Richardson, J.F., & Zaki, W.N. (1954).Sedimentation and fluidization: part I. *Trans. Inst. Chem. Eng*. 32, 35-53.

Hartge, E., & Werther, J. (1986). Analysis of the local structure of the two-phase flow in a fast fluidized bed. In, Circulating Fluidized Bed Technology. *Chemical Engineering Technology*, 58, 153-160.

Bürger, R., &Wendland, W.L. (2001). Sedimentation and suspension flows: historical perspective and some recent developments. *Journal Engineering Mathematic*, 41 (2), 101–116.

Hirano, Y., Kai, T., Tsutsui, T., & Nakazato, T. (2013). Decrease in the fluidization quality of fluidized beds containing binary mixtures of different catalyst particles. *Chemical Engineering Science*, 96 (7), 98-105.

Tsuji, Y., Kawaguchi, T., & Tanaka, T. (1993). Discrete particle simulation of two dimensional fluidized beds. *Powder Technology*, 77, 79–87.

Hoomans, B.P.B., Kuipers, J.A.M., Briels, W.J., & Van Swaaij, W.P.M. (1996). Discrete particle simulation of bubble and slug formation in a two-dimensional gas-fluidized bed: a hard- sphere approach. *Chemical Engineering Science*, 51, 99-118.

Yu, A.B., & Xu, B.H. (2003). Particle-scale modelling of gas-solid flow in fluidisation. *J. Chem. Technol. Biotechnol*, 78, 111-121.

Zhu, H.P., Zhou, Z.Y., Yang, R.Y., & Yu, A.B. (2008). Discrete particle simulation of particulate systems: a review of major applications and findings. *Chemical Engineering Science*, 63, 5728-5770.

Chavan, P. V., Thombare, M. A., Bankar, S. B., Kalaga, D. V., & Patil-Shinde, V. A. (2018). Novel multistage solid-liquid circulating fluidized bed: Hydrodynamic characteristics. *Particuology,* 38, 134-142.

Di Maio, F. P., & Di Renzo, A. (2007). DEM-CFD Simulations of fluidized beds with application in mixing dynamics. *KONA Journal*, 25, 205-216.

Gidaspow, D. (1994). Multiphase flow and fluidization, Academic Press, NewYork.

Apostolou, K., & Hrymak, A.N. (2008). Discrete element simulation of liquid-particle flows. *Computers and Chemical Engineering*, 32, 841-856.

Wang, J.W., van der Hoef, M.A., & Kuipers, J.A.M. (2010). CFD study of the minimum bubbling velocity of Geldart A particles in gas-fluidized beds. *Chemical Engineering Science*, 65, 3772-3785.

Chu, K.W., Kuang, S.B., Zhou, Z.Y., Yu A.B. (2018). Model A vs. Model B in the modelling of particle-fluid flow. *Powder Technology*, 329, 47-54.

Al-Arkawazia, S., Marieb, C., Benhabibb, K., & Coorevits, P. (2017). Modeling the hydrodynamic forces between fluid-granular medium by coupling DEM-CFD. *Chemical Engineering Research and Design*, 117, 439-447.

Deen, N.G., Van Sint Annaland, M., Van der Hoef, M.A., & Kuipers, J.A.M. (2007). Review of discrete particle modeling of fluidized beds. *Chemical Engineering Science*, 62, 28-44.

Fortin, J., & De Saxcé, G. (1999). Modélisation numérique des milieux granulaires par l'approche du bi-potentiel. *C. R. Academic Science*, 327,721–724.

Archambeau, F., Méchitoua, N., & Sakiz, M. (2004). Code Saturne: a finite volume method for the computation of turbulent incompressible flow-industrial applications. *Int. J. Finite*, 1 (1), 1-62.

Menter, F.R. (1994). Two-equation eddy-viscosity turbulence models for engineering applications. *AIAA Journal*, 32(8), 1598-1605.

Mohammadi, B., & Pironneau, O. (1994). Analysis of the k-ε turbulence model, J. Wiley & Sons.

Kafui, D.K., Johnson, S., Thornton, C., & Seville, J.P.K. (2011). Parallelization of a Lagrangian–Eulerian DEM/CFD code for application to fluidized beds. *Powder Technology*, 207 (1-3), 270–278.

Helland, E. , Occelli, R., &Tadrist, L. (2000). Numerical study of cluster formation in a gas–particle circulating fluidized bed. *Powder Technology*, 110, 210–221.

Kl0Stokes, G.G. (1901). Mathematical and Physical Papers. Cambridge University Press, Cambridge.

Brown, P., & Lawler, D. (2003). Sphere drag and settling velocity revisited.

Journal Environment Engineering, 129 (3), 222-231.

Gilbilaro, L.G. (2001). Fluidization-Dynamics: The Formulation and Applications of a Predictive Theory for the Fluidized State. Butterworth–Heinemann.

Sherko Ahmad Flamarz (2017). Comparison of porosity models for fluidized beds. *Kurdistan Journal of Applied Research*, 2 (1), 74-83.

Helland, E., Bournot, H., Occelli, R., & Tadrist, L. (2007). Drag reduction and cluster formation in a circulating fluidized bed. *Chemical Engineering Science*, 62, 148-158.

ttp://jgu.garmian.edu.krd https://doi.org/10.24271/garmian.342

Forward-backward asymmetries of $B \to \phi\ell^+\ell^-$ decay in the SM4

H. Mehranfar

Physics Department, University of Garmian, Kalar, Kurdistan Region, Iraq

Email: hmehranfar@garmian.edu.krd

Abstract

In this paper, we investigate the effects of fourth generation quarks in the unpolarized and polarized forward-backward asymmetries of $B \to \phi\ell^+\ell^-$ decay. The fourth generation quarks change the values of Wilson coefficients in effective Hamiltonian which is the main part of differential decay rate. Taking the $|V_{t'b}V^*_{t's}|$~{0.02} with phase $\{90^o\}$, we conclude that the forward-backward asymmetries of $B \to \phi l^+ l^-$decay is very sensitive to existing of new parameters of fourth generation quarks for both (μ, τ) leptons. In the end, It seems that the study of the forward-backward asymmetries can be a very useful tool for establishing new physics beyond Standard model as well as B-physics experiments.

Keywords: Fourth generation quarks, Forward-backward asymmetries, Effective Hamiltonian, Wilson coefficients.

1 Introduction

Fourth generation standard model (denoted SM4) is an attractive and new version of Standard Model (SM) with three generation of fermions (i.e. quarks and leptons) [1,2]. Although the LHC (Large Hadron Corridor) researches have not discovered directly the heavy fourth generation t' and b' quarks so far. One of the efficient ways to establish the existence of the 4th generation is via their indirect manifestations in loop diagrams. There are many works in various field that approve the existence of fourth generation quarks for instance Higgs and neutrino physics, Cosmology and dark matter [3-8].

In this paper we investigate the possibility of new physics in the heavy baryon decays $B \to \phi\ell^+\ell^-$ using the Standard Model with fourth generation t' and b' quarks. The fourth quark (t′), like u, c, t quarks, contributes in the b → s(d) transition at loop level. It would, Clearly, change the branching ratio and asymmetries such as forward-backward, CP-violation and polarizations. The sensitivity of the CP asymmetry, double lepton polarization and single lepton polarization asymmetries to the existence of fourth generation quarks in $B \to \phi\ell^+\ell^-$ decay is investigated in [9-11] and it is obtained that these asymmetries are very sensitive to the fourth generation parameters $(m_{t'}, r_{sb}, \phi_{sb})$.

One of the most important experimental quantity for searching the new physics (NP) and new signs about particles is forward-backward asymmetry. In this work, we study the forward-backward asymmetries for $B \to \phi\ell^+\ell^-$ decay with four generation of quarks.

This paper is organized as follows. In Section II, we drive the differential decay rate using effective Hamiltonian in the presence of fourth generation quarks (t', b'). Section III devoted to calculation of the analytic expressions for the forward-backward asymmetries. Finally, the numerical analysis of forward-backward asymmetries for $B \to \phi\ell^+\ell^-$ decay with our consequences have been presented in section IV.

2 Differential decay rate

For investigation of any physical quantity in particle physics such as CP violation, Polarization asymmetry and other experimental quantities, we need to calculate the differential decay rate. The differential decay rate of $B \to \phi\ell^+ \ell^-$ decay will be determine via effective Hamiltonian at level quark for $b \to s\ell^+\ell^-$ transition as

$$\mathcal{H}_{eff} = \frac{4G_F}{\sqrt{2}} V_{tb} V_{ts}^* \sum_{i=1}^{10} \mathcal{C}_i(\mu)\, \mathcal{O}_i(\mu)\ , \tag{1}$$

Where $\mathcal{O}_i$ and $\mathcal{C}_i$ are the full set operators and the corresponding Wilson coefficients respectively which are given in [12]. Considering above items, matrix element for the $b \to s\ell^+\ell^-$ transition can be writing in the following form

$$\begin{aligned}
\mathcal{M}(b \to s\ell^+\ell^-) &= \ < s\ell^+\ell^- |\mathcal{H}_{\rm eff}| b > \\
&= -\frac{G_F}{\sqrt{2}} V_{tb} V_{ts}^* \sum_i C_i^{\rm eff}(\mu) < s\ell^+\ell^- |\mathcal{O}_i| b >^{tree} . \\
&= -\frac{G_F \alpha}{2\pi\sqrt{2}} V_{tb} V_{ts}^* \Bigg[\tilde{C}_9^{\rm eff} \bar{s}\gamma_\mu (1-\gamma_5) b\, \bar{\ell}\gamma_\mu \ell \\
&\qquad + \tilde{C}_{10}^{\rm eff} \bar{s}\gamma_\mu (1-\gamma_5) b\, \bar{\ell}\gamma_\mu \gamma_5 \ell \\
&\qquad - 2C_7^{\rm eff} \frac{m_b}{q^2} \bar{s}\sigma_{\mu\nu} q^\nu (1+\gamma_5) b\, \bar{\ell}\gamma_\mu \ell \Bigg],
\end{aligned} \tag{2}$$

Where effective Wilson coefficients $\tilde{C}_7^{eff}$, $\tilde{C}_9^{eff}$ and $\tilde{C}_{10}^{eff}$ at μ scale with details are given in [9].

The fourth generation changes the values of the Wilson coefficients $\tilde{C}_7^{eff}$, $\tilde{C}_9^{eff}$ and $\tilde{C}_{10}^{eff}$, via virtual exchange of the fourth generation up type quark t'. The above mentioned Wilson coefficients will explicitly change as

$$\begin{aligned} C_i^{\text{eff new}}(\mu) &= C_i^{\text{eff}}(\mu) + \frac{\lambda_{t'}}{\lambda_t} C_i^{\text{eff SM4}}(\mu), \qquad i = 7, \\ \tilde{C}_i^{\text{eff new}}(\mu) &= \tilde{C}_i^{\text{eff}}(\mu) + \frac{\lambda_{t'}}{\lambda_t} \tilde{C}_i^{\text{eff SM4}}(\mu), \qquad i = 9, 10. \end{aligned} \tag{3}$$

In the above equation, $\lambda_f = V_{fb}^* V_{fs}$ and $\lambda_{t'}$ can be parameterized as:

$$\lambda_{t'} = V_{t'b} V_{t's}^* = r_{sb} e^{i\phi_{sb}}. \tag{4}$$

The unitary of the 4×4 CKM matrix lead to

$$\lambda_u + \lambda_c + \lambda_t + \lambda_{t'} = 0. \tag{5}$$

Consequently, as required by GIM mechanism, the factor $\lambda_t C_i^{new}$ should be modified to $\lambda_t C_i$ when $m_{t'} \to m$ or $\lambda_{t'} \to 0$ (see [12, 13]). We can easily check the validity of this condition by using Eq.(5):

$$\begin{aligned} \lambda_t C_i^{\text{new}} = \lambda_t C_i + \lambda_{t'} C_i^{\text{SM4}} &= -(\lambda_u + \lambda_c) C_i + \lambda_{t'} (C_i^{\text{SM4}} - C_i) \\ &= -(\lambda_u + \lambda_c) C_i \\ &= \lambda_t C_i. \end{aligned} \tag{6}$$

Now, in order to obtaining differential decay rate width for this decay, we must calculate the matrix element at hadron level as

$$
\begin{aligned}
\mathcal{M}(B_s \to \phi \ell^+ \ell^-) &= \frac{G\alpha}{4\sqrt{2}\pi} V_{tb} V_{ts}^* \\
&\times \Bigg\{ \bar{\ell}\gamma^\mu (1-\gamma_5)\ell \Big[-2B_0 \epsilon_{\mu\nu\lambda\sigma} \varepsilon^{*\nu} p_\phi^\lambda q^\sigma - iB_1 \varepsilon_\mu^* \\
&\qquad + iB_2 (\varepsilon^* q)(p_{B_s} + p_\phi)_\mu + iB_3 (\varepsilon^* q) q_\mu \Big] \\
&\quad + \bar{\ell}\gamma^\mu (1+\gamma_5)\ell \Big[-2C_1 \epsilon_{\mu\nu\lambda\sigma} \varepsilon^{*\nu} p_\phi^\lambda q^\sigma - iD_1 \varepsilon_\mu^* \\
&\qquad + iD_2 (\varepsilon^* q)(p_{B_s} + p_\phi)_\mu + iD_3 (\varepsilon^* q) q_\mu \Big] \Bigg\} ,
\end{aligned} \tag{7}
$$

Where

$$
\begin{aligned}
B_0 &= (\tilde{C}_9^{\rm eff} - \tilde{C}_{10}^{\rm eff}) \frac{V}{m_{B_s} + m_\phi} + 4(m_{B_s} + m_s) C_7^{\rm eff} \frac{T_1}{q^2} , \\
B_1 &= (\tilde{C}_9^{\rm eff} - \tilde{C}_{10}^{\rm eff})(m_{B_s} + m_\phi) A_1 + 4(m_{B_s} - m_s) C_7^{\rm eff} (m_{B_s}^2 - m_\phi^2) \frac{T_2}{q^2} , \\
B_2 &= \frac{\tilde{C}_9^{\rm eff} - \tilde{C}_{10}^{\rm eff}}{m_{B_s} + m_\phi} A_2 + 4(m_{B_s} - m_s) C_7^{\rm eff} \frac{1}{q^2} \left[T_2 + \frac{q^2}{m_{B_s}^2 - m_\phi^2} T_3 \right] , \\
B_3 &= 2(\tilde{C}_9^{\rm eff} - \tilde{C}_{10}^{\rm eff}) m_\phi \frac{A_3 - A_0}{q^2} - 4(m_{B_s} - m_s) C_7^{\rm eff} \frac{T_3}{q^2} , \\
C_1 &= B_0(\tilde{C}_{10}^{\rm eff} \to -\tilde{C}_{10}^{\rm eff}) , \\
D_i &= B_i(\tilde{C}_{10}^{\rm eff} \to -\tilde{C}_{10}^{\rm eff}) , \quad (i = 1,\ 2,\ 3).
\end{aligned}
$$

Above coefficients parametrized in term of form factor as

$$
F(q^2) \in \{V(q^2), A_0(q^2), A_1(q^2), A_2(q^2), A_3(q^2), T_1(q^2), T_2(q^2), T_3(q^2)\} , \tag{8}
$$

are fitted to the following function [14,15]:

$$
F(q^2) = \frac{F(0)}{1 - a_F \frac{q^2}{m_{B_s}^2} + b_F (\frac{q^2}{m_{B_s}^2})^2}, \tag{9}
$$

where the parameters $F(0), a_F$ and $b_F$are shown in the table1.

Table 1: The form factors for $B \to \phi \ell^+ \ell^-$ in a three–parameter fit [14].

	$A_0^{B_s \to \phi}$	$A_1^{B_s \to \phi}$	$A_2^{B_s \to \phi}$	$V^{B_s \to \phi}$	$T_1^{B_s \to \phi}$	$T_2^{B_s \to \phi}$	$T_3^{B_s \to \phi}$
$F(0)$	0.382	0.296	0.255	0.433	0.174	0.174	0.125
a_F	1.77	0.87	1.55	1.75	1.82	0.70	1.52
b_F	0.856	−0.061	0.513	0.736	0.825	−0.315	0.377

From the above expression for matrix element, we can get the following result for the differential decay rate width

$$\frac{d\Gamma^{\phi}}{d\hat{s}}(B_s \to \phi\ell^+\ell^-) = \frac{G^2\alpha^2 m_{B_s}}{2^{14}\pi^5}\left|V_{tb}V_{ts}^*\right|^2 \lambda^{1/2}(1,\hat{r},\hat{s})v\Delta(\hat{s}) \ , \tag{10}$$

With

$$\begin{aligned}\Delta \;=\; & \frac{2}{3\hat{r}_\phi\hat{s}} m_{B_s}^2 Re[-12m_{B_s}^2 \hat{m_l}^2\lambda\hat{s}\{(B_3-D_2-D_3)B_1^* - (B_3+B_2-D_3)D_1^*\} \\ & +12m_{B_s}^4\hat{m_l}^2\lambda\hat{s}(1-\hat{r}_\phi)(B_2-D_2)(B_3^*-D_3^*) \\ & +48\hat{m_l}^2\hat{r}_\phi\hat{s}(3B_1D_1^* + 2m_{B_s}^4\lambda B_0C_1^*) \\ & -16m_{B_s}^4\hat{r}_\phi\hat{s}\lambda(\hat{m_l}^2-\hat{s})\{|B_0|^2+|C_1|^2\} \\ & -6m_{B_s}^4\hat{m_l}^2\lambda\hat{s}\{2(2+2\hat{r}_\phi-\hat{s})B_2D_2^* - \hat{s}|(B_3-D_3)|^2\} \\ & -4m_{B_s}^2\lambda\{\hat{m_l}^2(2-2\hat{r}_\phi+\hat{s})+\hat{s}(1-\hat{r}_\phi-\hat{s})\}(B_1B_2^*+D_1D_2^*) \\ & +\hat{s}\{6\hat{r}_\phi\hat{s}(3+v^2)+\lambda(3-v^2)\}\{|B_1|^2+|D_1|^2\} \\ & -2m_{B_s}^4\lambda\{\hat{m_l}^2[\lambda-3(1-\hat{r}_\phi)^2]-\lambda\hat{s}\}\{|B_2|^2+|D_2|^2\}],\end{aligned}$$

Where $\hat{r}_\phi = m_\phi^2/m_{B_s}^2, \quad \hat{s} = q^2/m_{B_s}^2, \quad \lambda(a,b,c) = a^2+b^2+c^2-2ab-2ac-2bc,$

$\hat{m}_\ell = m_\ell/m_{B_s}$ and $v = \sqrt{1-4\hat{m}_\ell^2/\hat{s}}$ is the final lepton velocity. For more detail about calculating above relations for $B \to \phi l^+ \, l^-$ decay see [9-11].

3 Forward-Backward Asymmetry of $B \to \phi l^+ \, l^-$ Decay

The definition of the unpolarized and normalized differential forward–backward asymmetry is [16-18]

$$\mathcal{A}_{FB} = \frac{\displaystyle\int_0^1 \frac{d^2\Gamma}{d\hat{s}dz} - \int_{-1}^0 \frac{d^2\Gamma}{d\hat{s}dz}}{\displaystyle\int_0^1 \frac{d^2\Gamma}{d\hat{s}dz} + \int_{-1}^0 \frac{d^2\Gamma}{d\hat{s}dz}} \ , \tag{11}$$

where $z = cos\theta$ is the angle between B meson and ℓ^- in the center of mass frame of leptons. For the spins of both leptons, the A_{FB}^{ij} will be a function of the spins of the final leptons as

$$
\begin{aligned}
\mathcal{A}^{ij}_{FB}(\hat{s}) \;=\; & \left(\frac{d\Gamma(\hat{s})}{d\hat{s}}\right)^{-1}\left\{\int_0^1 dz - \int_{-1}^0 dz\right\}\left\{\left[\frac{d^2\Gamma(\hat{s},\vec{s}^- = \vec{i},\vec{s}^+ = \vec{j})}{d\hat{s}dz} - \frac{d^2\Gamma(\hat{s},\vec{s}^- = \vec{i},\vec{s}^+ = -\vec{j})}{d\hat{s}dz}\right]\right. \\
& - \left.\left[\frac{d^2\Gamma(\hat{s},\vec{s}^- = -\vec{i},\vec{s}^+ = \vec{j})}{d\hat{s}dz} - \frac{d^2\Gamma(\hat{s},\vec{s}^- = -\vec{i},\vec{s}^+ = -\vec{j})}{d\hat{s}dz}\right]\right\}, \\
=\; & \mathcal{A}_{FB}(\vec{s}^- = \vec{i},\vec{s}^+ = \vec{j}) - \mathcal{A}_{FB}(\vec{s}^- = \vec{i},\vec{s}^+ = -\vec{j}) - \mathcal{A}_{FB}(\vec{s}^- = -\vec{i},\vec{s}^+ = \vec{j}) \\
& + \mathcal{A}_{FB}(\vec{s}^- = -\vec{i},\vec{s}^+ = -\vec{j})\ . \qquad (12)
\end{aligned}
$$

Where $i, j = L, N\ and\ T$ refer to the longitudinal, normal and transversal polarization. Using these definition for the double lepton forward-backward asymmetries after calculating we get the following results:

$$
\begin{aligned}
A^{NN}_{FB} &= 0 \\
A^{TT}_{FB} &= 0 \qquad (13)
\end{aligned}
$$

$$
\begin{aligned}
A^{TN}_{FB} &= \frac{2}{\hat{r}_\phi \Delta\hat{s}} m_B^2\sqrt{\lambda} Im[-2m_B^4 \hat{m_l}^2 \hat{s}\lambda(B_2+D_2)(B_3^*-D_3^*) \\
&+ 4m_B^4\hat{m_l}^2\lambda(1-\hat{r}_\phi)B_2D_2^* \\
&+ 2m_B^2\hat{m_l}^2\hat{s}(1+3\hat{r}_\phi-\hat{s})(B_1B_2^*-D_1D_2^*) \\
&+ \hat{m}_l(1-\hat{r}_\phi-\hat{s})\{-2\hat{s}m_B^2\hat{m}_l(B_1+D_1)(B_3^*-D_3^*) \\
&+ 4\hat{m}_lB_1D_1^*\} \\
&+ 2m_B^2\hat{m_l}^2[\lambda+(1-\hat{r}_\phi-\hat{s})(1-\hat{r}_\phi)](B_1^*D_2+B_2^*D_1)] \qquad (14)
\end{aligned}
$$

$$
\begin{aligned}
A^{NT}_{FB} &= \frac{2}{\hat{r}_\phi \Delta\hat{s}} m_B^2\sqrt{\lambda} Im[-2m_B^4 \hat{m_l}^2 \hat{s}\lambda(B_2+D_2)(B_3^*-D_3^*) \\
&+ 4m_B^4\hat{m_l}^2\lambda(1-\hat{r}_\phi)B_2D_2^* \\
&+ 2m_B^2\hat{m_l}^2\hat{s}(1+3\hat{r}_\phi-\hat{s})(B_1B_2^*-D_1D_2^*) \\
&+ \hat{m}_l(1-\hat{r}_\phi-\hat{s})\{+2\hat{s}m_B^2\hat{m}_l(B_1+D_1)(B_3^*-D_3^*) \\
&+ 4\hat{m}_lB_1D_1^*\} \\
&+ 2m_B^2\hat{m_l}^2[\lambda+(1-\hat{r}_\phi-\hat{s})(1-\hat{r}_\phi)](B_1^*D_2+B_2^*D_1)] \qquad (15)
\end{aligned}
$$

$$
\begin{aligned}
A^{TL}_{FB} &= \frac{4}{3\hat{r}_\phi \Delta\hat{s}} m_B^2\sqrt{\hat{s}}\lambda Re[\hat{m}_l\{|B_1+D_1|^2 + m_B^4\lambda|B_2+D_2|^2\} \\
&- 4m_B^4\hat{m}_l\hat{s}\hat{r}_\phi\{|B_0+C_1|^2\} \\
&- 2m_B^2\hat{m}_l(1-\hat{r}_\phi-\hat{s})(B_1+D_1)(B_2^*+D_2^*)] \qquad (16)
\end{aligned}
$$

$$
\begin{aligned}
A^{LT}_{FB} &= \frac{4}{3\hat{r}_\phi \Delta\hat{s}} m_B^2\sqrt{\hat{s}}\lambda Re[-\hat{m}_l\{|B_1+D_1|^2 + m_B^4\lambda|B_2+D_2|^2\} \\
&+ 4m_B^4\hat{m}_l\hat{s}\hat{r}_\phi\{|B_0+C_1|^2\} \\
&+ 2m_B^2\hat{m}_l(1-\hat{r}_\phi-\hat{s})(B_1+D_1)(B_2^*+D_2^*)] \qquad (17)
\end{aligned}
$$

$$A_{FB}^{NL} = \frac{8}{3\hat{r}_\phi \Delta \hat{s}} m_B^2 \sqrt{\hat{s}} \lambda v Im[-\hat{m}_l(B_1 D_1^* + m_B^4 \lambda B_2 D_2^*) + 4 m_B^4 \hat{m}_l \hat{r}_\phi \sqrt{\hat{s}} B_0 C_1^* + m_B^2 \hat{m}_l (1 - \hat{r}_\phi - \hat{s})(B_1 D_2^* + B_2 D_1^*)] \quad (18)$$

$$A_{FB}^{LN} = \frac{8}{3\hat{r}_\phi \Delta \hat{s}} m_B^2 \sqrt{\hat{s}} \lambda v Im[-\hat{m}_l(B_1 D_1^* + m_B^4 \lambda B_2 D_2^*) + 4 m_B^4 \hat{m}_l \hat{r}_\phi \sqrt{\hat{s}} B_0 C_1^* + m_B^2 \hat{m}_l (1 - \hat{r}_\phi - \hat{s})(B_1 D_2^* + B_2 D_1^*)] \quad (19)$$

$$A_{FB}^{LL} = \frac{2}{\hat{r}_{\phi^*} \Delta} m_B^3 \sqrt{\lambda} v Re[8 m_B \hat{r}_\phi \hat{s} (B_0 B_1^* - C_1 D_1^*)] \quad (20)$$

4 Numerical Analysis

In this section, we examine the dependence the polarized forward-backward asymmetry to the fourth quark parameters ($m_{t'}, r_{sb} e^{i\phi_{sb}}$). The main input parameters we use in our numerical calculation as follow as:

$$m_{B_s} = 5.37\,\mathrm{GeV}\,,\ m_b = 4.8\,\mathrm{GeV}\,,\ m_c = 1.5\,\mathrm{GeV}\,,\ m_\tau = 1.77\,\mathrm{GeV}\,,$$
$$m_\mu = 0.105\,\mathrm{GeV},\ m_\phi = 1.020\,\mathrm{GeV}\ ,\ |V_{tb}V_{ts}^*| = 0.0385\,,\ \alpha^{-1} = 129\,,$$
$$G_f = 1.166 \times 10^{-5}\,\mathrm{GeV}^{-2}\,,\ \tau_{B_s} = 1.46 \times 10^{-12}\,s\,.$$

For quantitative analysis of the forward-backward asymmetry of $\rightarrow \phi \ell^+ \ell^-$, the values of fourth-generation parameters ($m_{t'}, r_{sb}, \phi_{sb}$) are needed. Using the experimental values of $B \rightarrow X_s \gamma$ and $B \rightarrow X_s \ell^+ \ell^-$decays [19,20], we insert bounds on r_{sb}~{0.01-0.03} for $\phi_{sb} \sim \{0^0 - 360^0\}$ and $m_{t'} \sim \{200 - 600\}$ GeV. Accordingly, we took this new parameters taking into account all the above constraints as:

$$r_{sb} = 0.02,\ \phi_{sb} = 90^0, m_{t'} = 200 \leq m_{t'} \leq 600$$

Now before performing numerical analysis, we should solve a problem about dependencies of the Forward-Backward asymmetry formula (A_{FB}^{ij}) on both $\hat{s}$ and new parameters ($m_{t'}, r_{sb}, \phi_{sb}$), because it may be experimentally difficult to investigate these dependencies at the same time. One way to deal with this problem is to integrate over q^2 and study the averaged Forward-Backward asymmetry. The total branching ratio (B_r) and average A_{FB}^{ij}over $q^2$are defined as:

$$B_r = \int_{4\hat{m}_\ell^2}^{(1-\sqrt{\hat{r}_\phi})^2} \frac{d\mathcal{B}}{d\hat{s}} d\hat{s}\ , \quad (21)$$

$$\langle A_{FB}^{ij} \rangle = \frac{\displaystyle\int_{4\hat{m}_\ell^2}^{(1-\sqrt{\hat{r_\phi}})^2} A_{FB}^{ij} \frac{d\mathcal{B}}{d\hat{s}} d\hat{s}}{B_r} \ . \qquad (22)$$

Figure 1-6 show the dependence of forward-backward asymmetris on r_{sb} =0.02, $\phi_{sb} = 90^0$ in term of $m_{t'}$ for μ and τ leptons. All figures dedicate that values $< A_{FB}^{ij} >$ strongly sensitive to fourth generation quark mass for both τ and μ channels. Moreover, the maximum deviation from SM in τ case is much more than that in μ case for $< A_{FB}^{LL} >$, $< A_{FB}^{LT} >$, $< A_{FB}^{TL} >$,$< A_{FB}^{TN} >$, and $< A_{FB}^{NT} >$. These results can be interesting since the maximum deviation from SM happens for $m_{t'}{\sim}\{300 - 400\}$ GeV. Therefore, the measurement of forward-backward asymmetry of $B \to \phi \ell^+ \ell^-$ decay in this range can used as a good tool when looking for the fourth generation quark and new physics.

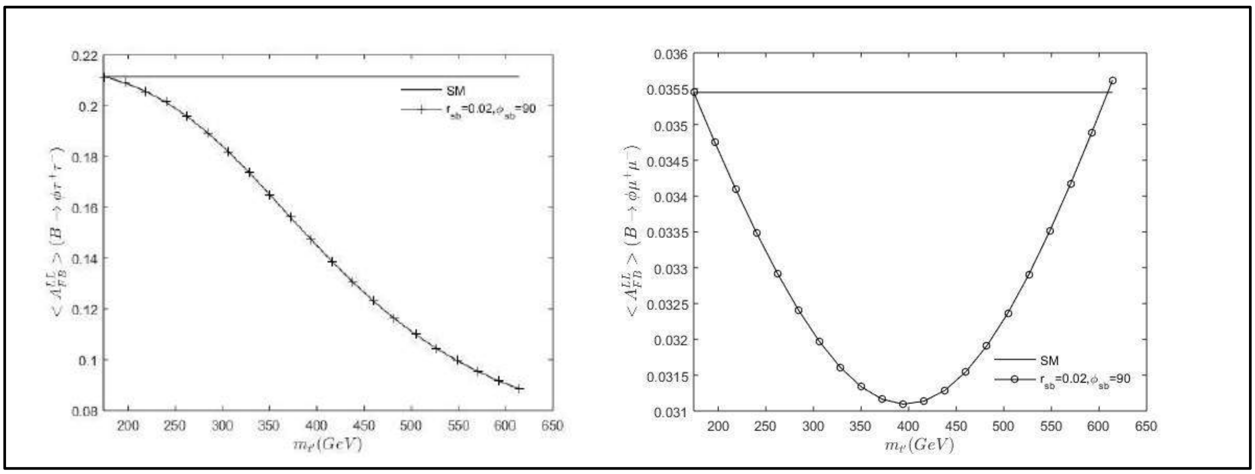

Figure 1: The dependence of the $< A_{FB}^{LL} >$ on the fourth generation quark mass $m_{t'}$ for the μ and τ leptons.

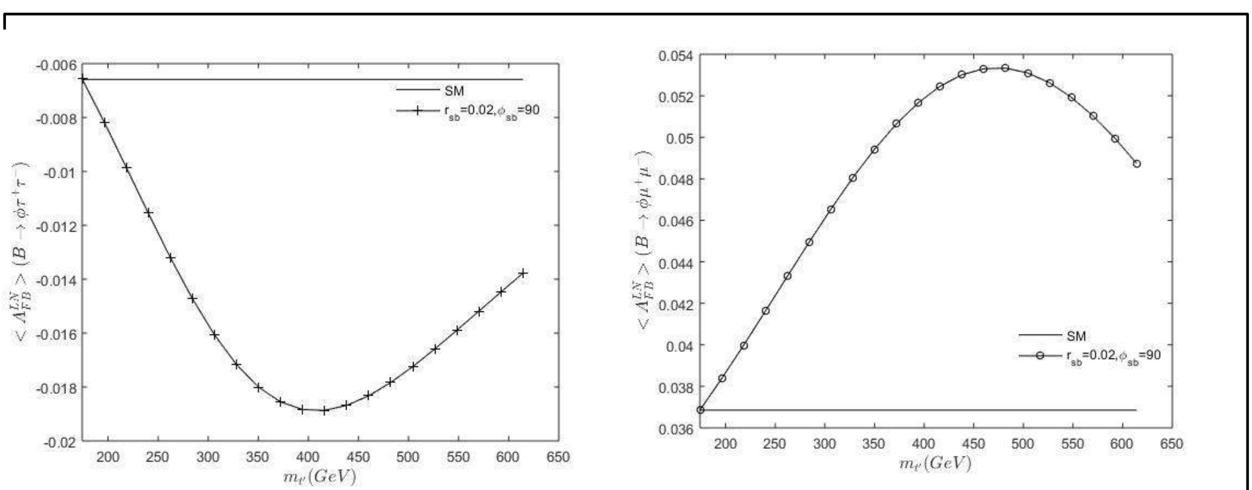

Figure 2: The dependence of the $< A_{FB}^{LN} >$ on the fourth generation quark mass $m_{t'}$ for the μ and τ leptons.

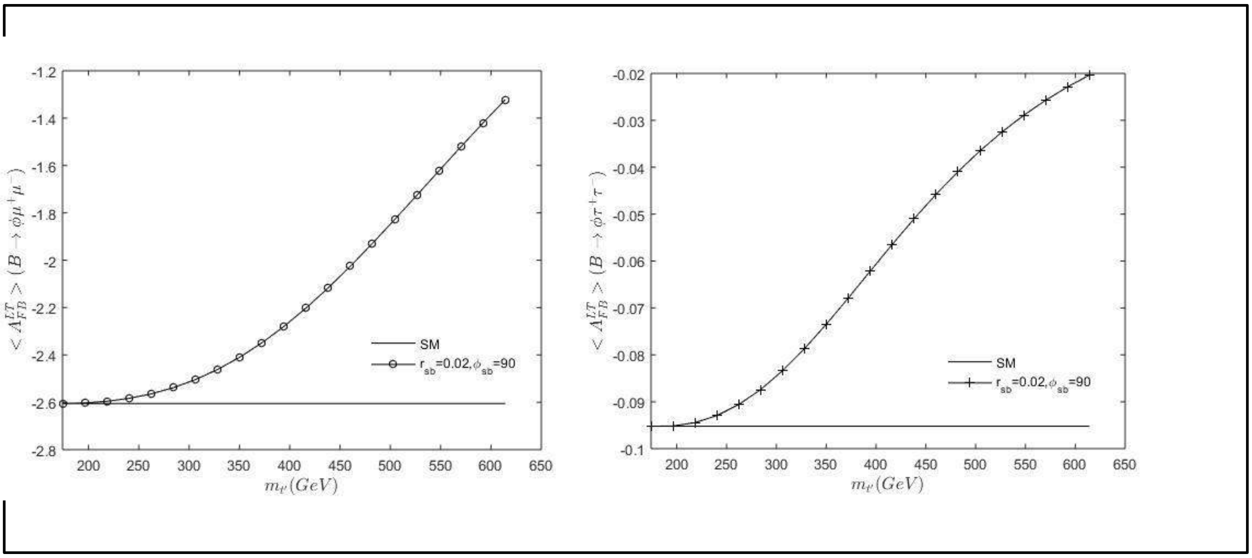

Figure 3: The dependence of the $< A_{FB}^{LT} >$ on the fourth generation quark mass $m_{t'}$ for the μ and τ leptons.

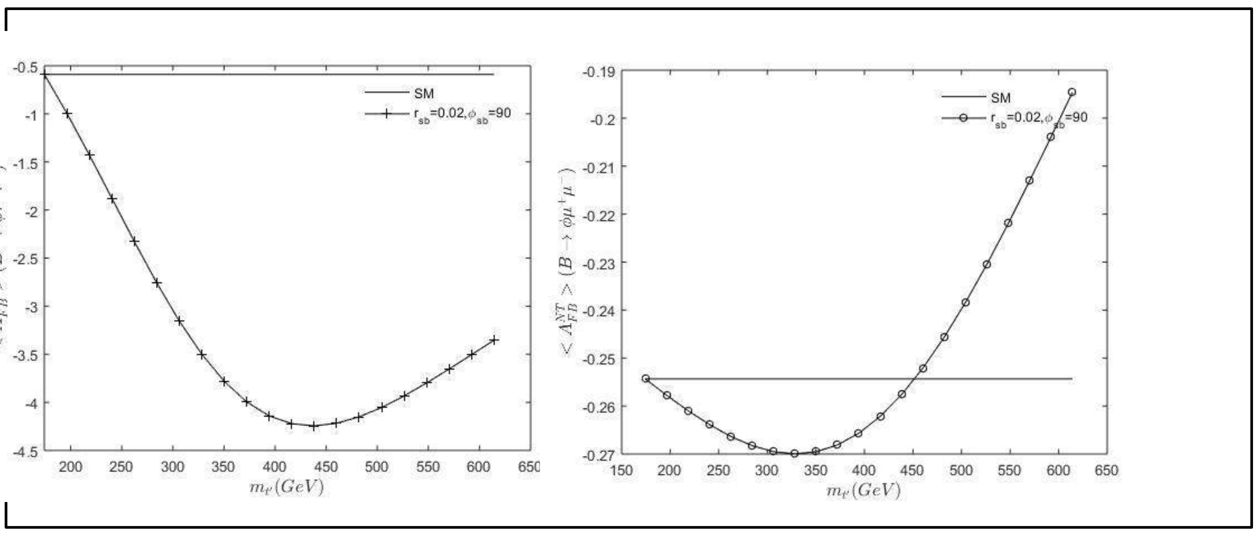

Figure 4: The dependence of the $< A_{FB}^{NT} >$ on the fourth generation quark mass $m_{t'}$ for the μ and τ leptons.

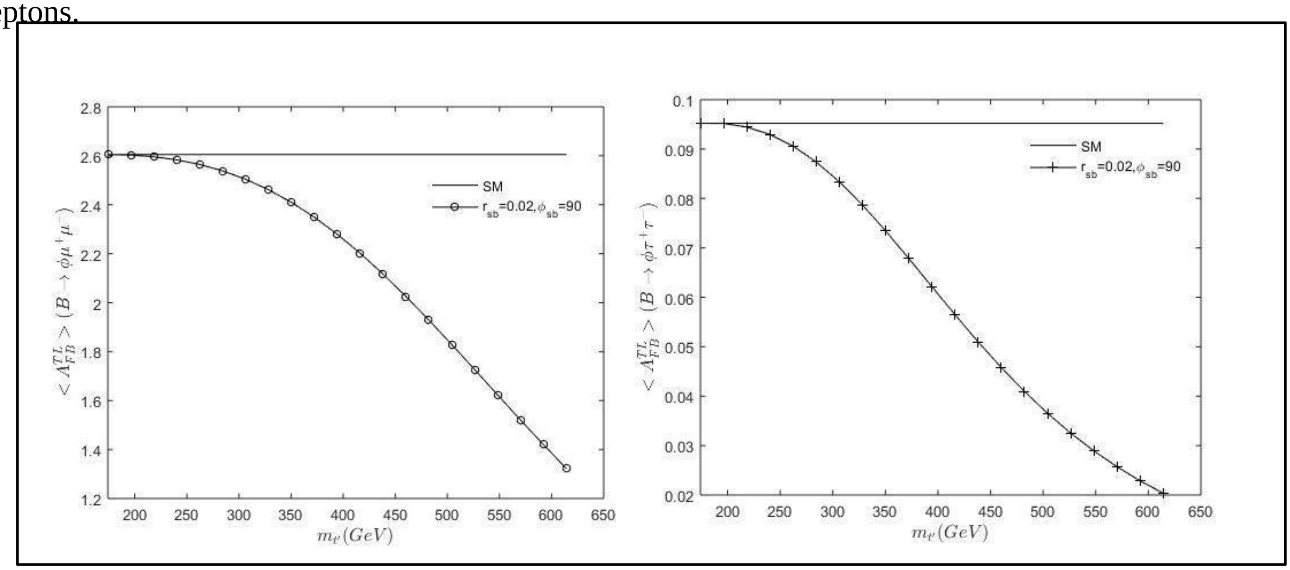

Figure 5: The dependence of the $< A_{FB}^{TL} >$ on the fourth generation quark mass $m_{t'}$ for the μ and τ leptons.

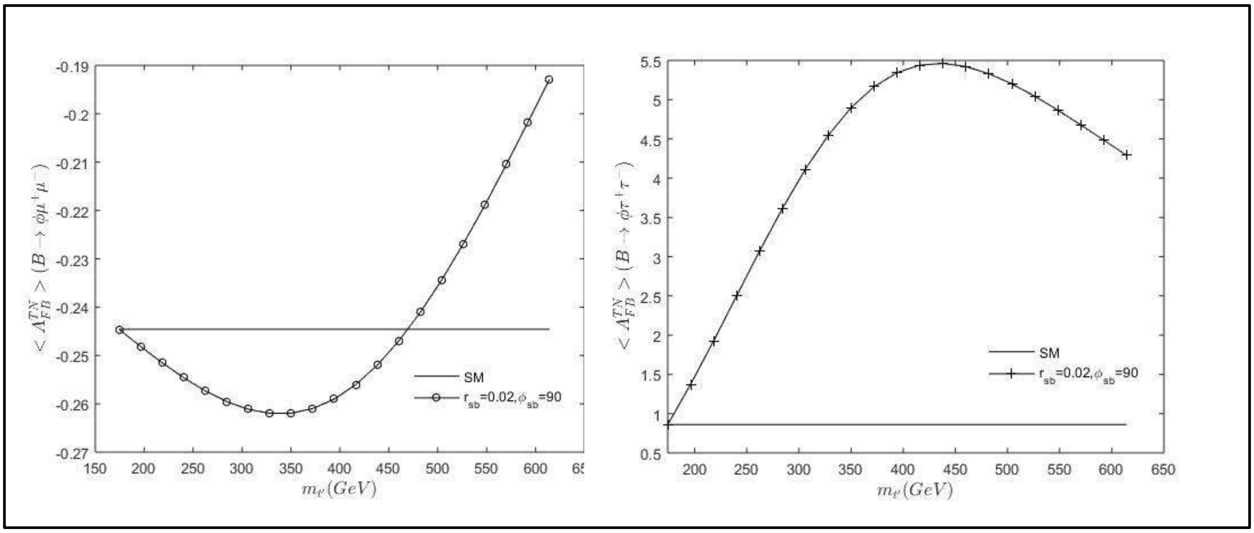

Figure 6: The dependence of the $< A_{FB}^{TN} >$ on the fourth generation quark mass $m_{t'}$ for the μ and τ leptons.

Conclusion

To conclude, we investigate effects of fourth generation quark on the forward-backward asymmetries for $B \to \phi\ell^+\ell^-$ decay. All $< A_{FB}^{ij} >$ showed intensive dependency on the fourth generation parameters. In the other hand, we found that this dependency in τ lepton is greater than μ lepton and probability of finding this new generation for $m_{t'} \sim \{300 - 400\}$ GeV in high energy physics laboratories is more expectant.

Acknowledgment

Support of The university of Garmian is gratefully acknowledged.

References

[1] B. Holdom et al., PMC Phys. A3, 4 (2009), 0904.4698.

[2] M. S. Carena, A. Megevand, M. Quiros, and C. E. Wagner, Nucl.Phys. B716, 319 (2005), hep-ph/0410352.

[3] H. J. He, N. Polonsky and S. F. Su, Phys. Rev. D68 (2001) 052004.

[4] K. M. Belotsky, M. Yu. Khlopov and K. I. Shibaev, Proceedings of 12th Lomonosov Conference on Elementary Particle Physics (Moscow, 2005), astro-ph/0602261.

[5] K. Belotsky, D. Fargion, M. Khlopov, R. Konoplich, K. Shibaev, Phys. Rev. D68 (2003) 054027.

[6] K. Belotsky, D. Fargion, M. Khlopov, R. Konoplich, hep-ph/0411093.

[7] M. Yu. Khlopov, Pisma v ZhETF 83 (2006) 3; JETP Lett. 83 (2006) 1.

[8] I. F. Ginzburg, I. P. Ivanov, A. Schiller, Phys. Rev. D60 (1999) 095001, hep-ph/9802364.

[9] S. M. Zebarjad, F. Falahati, H. Mehranfar, Phys. Rev. D79 (2009) 075006.

[10] H. Mehranfar, The 5th international conference on basic science, Kalar, Iraq, 624-636, 2017. DOI: 10.24271/garmian.171

[11] H. Mehranfar, The 5th international conference on basic science, Kalar, Iraq, 637-659, 2017. DOI: 10.24271/garmian.172

[12] A. J. Buras and M. M¨unz, Phys. Rev. D52 (1995) 186.

[13] B. Grinstein, M. J. Savage and M. B. Wise, Nucl. Phys. B319 (1989) 271.

[14] P. Ball, V. M. Braun, Phys. Rev. D58 (1998) 094016.

[15] P. Ball, JHEP 9809 (1998) 005.

[16] A. Ali, E. Lunghi, C. Greub and G. Hiller, Phys. Rev. D66 (2002) 034002 [hep–ph/0112300].

[17] H. M. Asatrian, K. Bieri, C. Greub and A. Hovhannisyan, Phys. Rev. D66 (2002) 094013 [hep–ph/0209006].

[18] A. Ghinculov, T. Hurth, G. Isidori and Y.P. Yao, Nucl. Phys. B648 (2003) 254 [hep–ph/0208088].

[19] F. Zolfagharpour and V. Bashiry, Nucl. Phys. B796, 294, (2008).

[20] A. Arhrib and W. S. Hou, Eur. Phys. J. C27 (2003) 555.

ttp://jgu.garmian.edu.krd https://doi.org/10.24271/garmian.343

Measurement of the Average Cross-Section Values for Neutron Reaction with the Elements (Mg , Al, Fe, Ni, Zn , Cu) from the Neutron Source ^{241}Am/Be.

Faissal G. Hammody* Firas M. Hady Omar. A. Muwafaq

Department of Physics, College of Science, University of Diyala.

* Corresponding author. Email: faissal_hammody@sciences.uodiyala.edu.iq

Abstract

The average cross- section for fast neutron reactions with the elements (Mg , Al, Fe, Ni, Zn , Cu) in ^{65}Cu(n, p)^{65}Ni, ^{64}Zn(n, p)^{64}Cu, ^{58}Ni(n, p)^{58}Co, ^{56}Fe(n, p)^{56}Mn, ^{57}Al(n, p)^{57}Mg and ^{24}Mg(n, p)^{24}Na reactions has been calculated by using the numerical – graphical method for ^{241}Am/Be neutron source according to the intensity distribution of the source as a function of neutron energy. The corresponding neutron cross-section values at certain energies are taken from neutron cross-sections curves.

Furthermore, the average neutron cross-sections for each of these reactions have been measured using the activation method. A $(5'' \times 5'')$ well-type NaI(Tℓ) detector was used for measuring the radiation activity.

The cross-sections for these reaction were measured by using of ^{27}Al(n, p)^{27}Mg reaction as a reference for short-lived activity arising in the different reactions. For long - lived activities the ^{27}Al(n, α)^{24}Na, and ^{56}Fe (n, p)^{56}Mn are used. It is found that the cross – section for the ^{65}Cu isotope is σ =826.29±62 mb while the standard value is σ =962±60 mb for the same.We have found the relative neutron activation method is more accurate than the absolute neutron activation method to stabilize the value of neutron flux through the use of the monitor reaction.

Keywords: Neutron source, neutron activation , cross-section .

1. Introduction

It is known that the Neutron Activation Analysis technique (NAA) has a great importance in nuclear physics because it is widely used in different scientific applications.

The scientific basis for the analyzing technique by Neutron Activation Analysis (NAA) is based on the concept of making reactions inside the nuclei of radioactive elements by bombardment these with flux of neutrons which can be taken from the available neutron sources so as to make these nuclei activated isotopes which it can these decay according to the half-life for each one by gamma radiation. Analyzing the spectrum of gamma radiation is made by measuring the radioactivity for these isotopes by using the nuclear detectors for gamma ray like high purity germanium

detector (HPGe) which has the ability of high resolving power or by using scintillation detector like NaI(Tℓl) with high efficiency in measuring [1].
The studying of cross-section of fast neutron reaction with the elements is done for its applications in the fields of reactors, academic studies designing breast plate protectors, and producing radioactive isotopes [2].

2. Theoretical Part:

This study used the neutron activation method for measuring the cross section of neutron interaction with elements.
When irradiating a sample that contains stable isotope (A) for time (t_{irr}) and the stable isotope will be radioactive isotope with activity (A_1) thus this falls down into (A_2) after that it falls during delay time (t_d) , then it falls during measuring into (A_3) as follows in the diagrams [3,4]:

$$A(Isotope) \xrightarrow{t_{irr}} A_1 \xrightarrow{t_d} A_2 \xrightarrow{t_c} A_3$$

Where (t_c) is a counting time where as the part which can be measured of radial activation can be represented as :

$$A' = A_2 - A_3$$

(A_1) is related to radiating time of the following relation:

$$A_1 = A_O(1 - e^{-\lambda t_{irr}}) \ldots\ldots\ldots\ldots\ldots\ldots\ldots\ldots \quad (1)$$

Where is A_o in the equation represents the number of radio active nuclei.
(A_2) is take the form :

$$A_2 = A_O(1 - e^{-\lambda t_{irr}}) e^{-\lambda t_d} \quad \ldots\ldots\ldots\ldots\ldots \quad (2)$$

and (A_3) has the form :

$$A_3 = A_O(1 - e^{-\lambda t_{irr}}) e^{-\lambda t_d} e^{-\lambda t_c} \quad \ldots\ldots\ldots \quad (3)$$

so (A') becomes :

$$A' = A_O(1 - e^{-\lambda t_{irr\ t}}) e^{-\lambda t_d} (1 - e^{-\lambda t_c}) \quad \ldots\ldots\ldots \quad (4)$$

Equation (4) represents the analysis by neutron activation .
In considering group of affecting factors represented by neutron flux , cross sections relative of the isotopes and the intensity of the radiation sent from the sample and the adequacy of the used detector in measuring .
We can write equation (4) as follows [1,5,6]:

$$A = (WN_{av}K / \lambda A_w)\sigma \xi I\gamma \phi_n (1 - e^{-\lambda t_{irr}})(1 - e^{-\lambda t_c}) e^{-\lambda t_d} \ldots\ldots\ldots (5)$$

Where:

(A) is the radioactivity measured during the counting time (t_c) through is the net area under the photo peak of gamma radiation .

$N=N_{av}\, wK/A_w$ is nuclei number of the target atoms.

N_{av} is Avogadro number (atom , mole)= 6.023×10^{23} for each gram of the material.

(w) is mass of the sample in (g).

(A_w) is the atomic weight of the sample in (g/mole).

(K) is the isotope abundance in nature by percentage (%).

(λ) is the decay constant $\lambda = 0.693/T_{1/2}$

$T_{1/2}$ is the half life of the produced nucleus [in seconds (s)].

(σ) is the cross section of interaction in (barn).

(ϕ_n) is the neutron flux ($n.cm^{-2}.s^{-1}$).

(ξ) is the efficiency of the used detector in the measuring [percentage (%)].

(I_γ) is the percentage of gamma radiation submitted from radioactive nucleus (%).

(t_d) is the time delay between the end of irradiation and the beginning of measurement

When the irradiating time is quite long in comparison with the half life of the nucleus produced from interaction then:

$$t_{irr} \rightarrow \infty \;\; and \;\; e^{-\lambda t_{irr}} \cong 0 \;\; with \;\; (1-e^{-\lambda t_{irr}}) \cong 1$$

The radioactivity reaches the saturation value when the average radioactivity produced equals the average of decay and this happens when (t_{irr}> 6 $T_{1/2}$) and the last equation becomes [2] :

$$A = \left(\frac{N \sigma \xi I_\gamma \; \phi_n}{\lambda} \right) (1 - e^{-\lambda t_c}) e^{-\lambda t_d} \quad \text{........} \quad (6)$$

The equation can be written as :

$$A = \alpha \beta \phi_n \sigma \quad \text{..} \quad (7)$$

$$\text{where} \quad \left\{ \begin{array}{l} \alpha = \left(\dfrac{N \xi I_\gamma}{\lambda} \right), \\ \beta = (1 - e^{-\lambda t_c}) e^{-\lambda t_d} \end{array} \right\}$$

If the process of irradiating the sample is achieved through irradiate the sample and standard together, the neutron flux of the sample keeps stability and measuring of cross section can be done using the formula

$$\sigma_u = \frac{A_u \alpha_r \beta_r}{A_r \alpha_u \beta_u} \sigma_r \quad \text{......................} \quad (8)$$

where the suffixes

r and u denote the standard and measured values respectively.

3. Average Cross – section Calculation:

We have calculated the average cross – section of the elements in this paper because the neutron source ^{241}Am/Be has uniform intensity and multi- energies. The cross-section values are taken from the curves which describe the relation between the cross-section ( ) and neutron energy (E_n) [7].

The average cross-section for any reaction in continuous neutron spectra is defined by the following relation [8]:

$$\sigma_{av} = \frac{\int_0^{E\max} \sigma(E) N(E) dE}{\int_0^{E\max} N(E) dE} \quad \ldots\ldots\ldots\ldots\ldots\ldots \quad (9)$$

Where:-

$\sigma(E)$ is the cross-section of reaction as a function of energy and $N(E)$ is the energy distribution of neutrons.

Equation (9) can be approximated to the following formula for discrete values of energy [8]:

$$\sigma_{av} = \frac{\sum_{j=1}^{n} \sigma_j N_j}{\sum_{j=1}^{n} N_j} \quad \ldots\ldots\ldots\ldots\ldots\ldots \quad (10)$$

Where:-

σ_j is the cross-section at a given neutron energy and N_j is the relative intensity of neutron at the same energy.

Moreover, the relative intensity of neutrons is taken from energy spectra of the radioisotope neutron source ^{241}Am/Be as shown in figures (7) and (8).

4. Preparation of Samples:

Samples of the elements (Cu, Zn, Ni, Fe, Al, Mg) have been taken in the form of foils and powder. The powder samples were compressed in the form of pellets. Diameter (2-3 cm). Were put inside smooth nylon bags for irradiating to avoid polluting the samples and losing part of their weight before and after irradiating.

The following is an explanation of radioisotope samples irradiated by using the radio isotope neutron source (^{241}Am/Be).

The samples as foils and thicknesses (0.5-1 mm) to isotopes their irradiated from the radioisotope as shown in Table (1).

5. Results and Discussion:

In this research, the technique of neutron activation is used for its accuracy in measuring cross- section. Whereas the vibration in neutron flux was dealt with by using Monitor Reaction and the use of Mixture Powder Method to guarantee irradiating both the studied sample and the standard sample under same conditions.

The reaction $^{27}Al(n, p)^{27}Mg$ is used as standard reaction in finding the cross-sections through interactions having results of short half –lifes And for long half life, the reactions $^{27}Al (n ,\alpha)^{24}Na$ was used as standard reaction, We list the elements studied as follows.

5.1.Aluminum

The reason of the importance of this element is its high purity (99.99%) and its possession of neutron interactions with long and short half-lives and the possession of not overlapped gamma line.

So it is possible to depend on in nuclear research like the calculation of neutron flux and as parallel and standard element for calculating a lot of cross – section.

Aluminum is used in this study as a parallel and standard element for the reasons mentioned

As Fig (1) illustrates the photo peak of gamma radiation for the reaction $^{27}Al (n, p)^{27}Mg$ (E_γ = 843.8 keV, 1014.4 keV) and the reaction $^{27}Al (n, \alpha)^{24}Na$ (E_γ = 1368.6 keV, 2754 keV)

The average of cross- section value of reaction $^{27}Al (n,p)\ ^{24}Mg$ was (20± 4) mb and this value is in agreement with the value reported by (Rieppo) [8].

The average of cross section value for the interaction $^{27}Al (n,\alpha)\ ^{24}Mg$ which is calculated as a rate for interaction $^{27}Al (n,p)\ ^{24}Mg$ with a flow (100%) and gamma line (843.8 keV) with intensity (72%) and half life (9.45 min) and the 286rradiation in time (24 h) calculated with NaI(Tℓl) a flow delay time (55 s) was σ_{av} = (5.21 ± 1.4) mb.

5.2. Magnesium

The average value of cross – section for the interaction $^{24}Mg (n,p)\ ^{24}Na$ with flux (78.99%) gamma line (1368.6 keV) and with high intensity(100%) and half life (15.02 h) which is measured as a rate for interaction $^{27}Al (n, \alpha)^{24}Na$ (Eγ = 1363.6 keV) and the result was (26.29 ± 3.41 mb) and which is measured value in this study as shown in Table (3).the values of are $^{24}Mg (n, p)^{24}Na$ comparison with ref [1] and we get a good agreement and matching .

Fig. (2) the spectrum of gamma radiation for the interaction $^{24}Mg (n, p)^{24}Na$ which is produced by irradiating (MgO) during the irradiation time (6.78 d) and measured by detector NaI(Tℓ) after delay time (75 s) .

5.3. Iron

The average value of cross section for the interaction $^{56}Fe (n, p)^{56}Mn$ with a flow (91.7%) and gamma line (846.6 keV) with intensity (99%) and half life (2.582 h) as a rate of interaction(843.8 keV) $^{27}Al (n, p)^{27}Mg$ which is measured by the detector NaI(Tℓ) after irradiating time (5.01 d) and delay time (60 sec) was (10.3 ± 2.29) mb) and which is the calculated value in this study and the mentioned value (46) as in

Table (3) the values of are ^{56}Fe (n, p)^{56}Mn comparison with ref [1] and we get a good agreement and matching .

Fig.(3) the spectrum of gamma line produced from irradiating (Fe_2O_3) as we notice the photo peaks of gamma radiation for the interaction above is (E_γ = 846.6 keV, 1811.2 keV, 2112.6 keV).

5.4. Nickel

The average value of cross section for the interaction ^{58}Ni (n, p)^{58}Co with a flow (67.88%) and gamma line (810.6 keV) with intensity (99.4%) as a rate of interaction $^{27}Al(n, \alpha)^{24}Na$ (E_γ = 1368.6 keV) and the result was (112.74 ± 2.64) mb and which is the calculated value in this study as shown in Table(3), the values of are ^{58}Ni (n, p)^{58}Cocomparison with ref [1] and we get a good agreement and matching.

Fig. (4) the spectrum of gamma radiation for the interaction of ($NiCl_2$) time (3.953 d) and the photo peaks of gamma radiation for the interaction above are (Eγ = 810.6 keV, 1636 keV).

5.5. Zinc

The average value of cross – section for the interaction $^{64}Zn(n, p)^{64}Cu$ with a flow (48.9%) and gamma line (511 keV) of intensity (37%) and half life (12.74 h) was calculated as a rate of interaction $^{27}Al(n, \alpha)^{24}Na$ and the result was (43.7 ± 4.54) mb and which is measured value in this study as shown in Table (3).

Fig. (5) the spectrum of gamma line produced from irradiating zinc power (Zn) for (22 h). (NaI(Tℓ) detector was used to measure the activity for zinc radioisotope (^{64}Zn) after delaying time (50 s). The photo peaks E_γ = 511 keV belong to reaction $^{64}Zn(n, p)^{64}Cu$ and the energy is E_γ = 1039 keV for reaction $^{66}Zn(n, p)^{66}Cu$ energy is E_γ = 366.5 keV for the reaction $^{68}Zn(n, \alpha)^{65}Ni$.

5.6. Copper

The average value of cross section for the interaction of $^{65}Cu(n, p)^{65}Ni$ with a flow (30.9%) and gamma line (1481.7 keV) of intensity (25.4%) and half life (2.520 h) was calculated as a rate of interaction (1368.6 keV) $^{27}Al(n, \alpha)^{24}Na$ and the result was (5.59 ± 1.17) mb and result was close to the calculated value in this study as shown in Table (3).

Fig. (6) the spectrum of gamma line produced from irradiating thin plate of copper in for (4 d) where the radio activity was measured by the detector NaI(Tℓ) after decay time (120 s), and photo peaks of gamma line calculated were (E_γ = 511 keV) that belongs to interaction $^{65}Cu(n, 2n)^{64}Cu$ whereas the energies (E_γ = 1115.5 keV, 1481.7 keV) belong to interaction $^{65}Cu(n, p)^{65}Ni$.

6. Conclusions:

1- (Numerical – Graphical) technique was used and it is found that the obtained results are measured by neutron activation technique.

2- The measured values in this study are measured values reported by other studies [8].

3- The analyzing technique by relative neutron activation is more accurate than the technique of analyzing by using the absolute neutron activation because of the stability value of neutron flow through using (Monitor Reaction)

4- (Numerical – Graphical) technique is good method for identifying the average of cross – section practically.

References:

1. Al-jobori .S.M., Ahmed .M. Ulaiwi,Saad Saleh Dawod and A.H.Murbat.**2010**.Jurnal of Madenat Alelm College. pp.38-50Vol.2.No.1.

2. Ali,M.A.:2nd Conference on Nuclear and Particle Physics ,13-17 Nov.1999,Cairo,Egypt.

3. Soete. De,. Gibjels D.R., and Hoste, J.**1972,**.(1972) A series of Monographs on Analytical Chemistry and its Applications. . Neutron Activation Analysis .Vol.34.

4. Glasstone,S.&Sesonske,A . 1**994** Van Nostrand Reiiold Company4th Editon,(). Nuclear Reactor Engineering .

5. Tsoulfaninds,N.**2015**. Hemisphere Publishing Corporation. Washington,4th Editon. Measurement and Detection of Radiation.

6. . Baumgärtner, F. **1977**. Erdtmann .G.1977. Verlag Chemie, Weinheim, New York 1976. 146 S., Preis: DM 78.-. Berichte der Bunsengesellschaft für physikalische Chemie,: Neutron Activation Tables. 81: 353. DOI:10.1002/bbpc.19770810324

7. McLane, Victoria, Charles L. Dunford, and Philip F. Rose.**1988**. Neutron cross sections: Volume 2, Neutron cross section curves. No. BNL-325 (ed. 4)(Vol. 2). Brookhaven National Lab., Upton, NY (USA).

8. Rieppo, R.**1979**. "A method to measure average neutron activation cross-sections by neutron sources: The average neutron activation cross-section of some (n, p) reactions for a 241Am-Be source..*Nuclear Instruments and Methods*. pp. 449-453. vol.159, No. 2-3

9. .Lorch,E.A.**1973**.Neutron Spectra Of ^{241}Am/B,^{241}Am/Be,^{241}Am/F,^{242}Cm/Be, ^{238}Pu/^{13}C and Isotopic Neutron Soures .Int.J.Appl.Rad.and Isotopes . pp.585.Vol.24.

10. De Guamni,F.&Malaroda,R.**1970**. two different technique Measurments OF The Neutron Spectrum Of An Am/Be Source .Nucl.Inst.and Meth. pp.277.Vol.92.

11.Geiger,K.W.and L.Vande Zwan.**1970**.The Neutron Spectrum Of a Am-Be(α,n) Source as Simulated by Accelerator Produced α-rticles.Int.J.Appl.Rad.Isotopes. pp193. Vol.21.

قياس متوسط قيم المقاطع العرضية لتفاعل النيوترون مع العناصر (Mg، Al، Fe، Ni، Zn، Cu) من المصدر النيوتروني ^{241}Am/Be

أ.م.فيصل غازي حمودي أ.م.فراس محمود هادي م.د.عمر احمد موفق
جامعة ديالى /كلية العلوم / قسم الفيزياء

الخلاصة

تم حساب قيم متوسط المقاطع العرضية لتفاعل النيوترونات السريعة مع العناصر (Cu, Zn, Ni, Fe, Al, Mg) في التفاعلات ^{24}Mg(n, p)^{24}Na ،^{27}Al(n, p) ^{27}Mg ،^{56}Fe(n, p)^{56}Mn ، ^{58}Ni(n, p)^{58}Co ، ^{64}Zn(n, p)^{64}Cu ، ^{65}Cu(n, p)^{65}Ni باستخدام الطريقة العددية التخطيطية لطيف المصدر النيوتروني ^{241}Am/Be طبقاً إلى توزيع الشدة للمصدر كونها دالة لطاقة النيوترون وكذلك على قيم المقاطع العرضية المناظرة لتلك الطاقة المأخوذة من منحنيات المقاطع العرضية.

تم قياس متوسط المقاطع العرضية لتلك التفاعلات باستخدام طريقة التنشيط النيوتروني. واستخدم كاشف أيوديد الصوديوم البئري (5" × 5") لقياس النشاط الشعاعي.

تم قياس المقطع العرضي للتفاعلات الآنفة الذكر نسبة إلى التفاعل ^{27}Al(n, p)^{27}Mg للنواتج ذات عمر النصف القصير ونسبة للتفاعلين ^{27}Al(n, α)^{24}Na ،^{56}Fe(n, p)^{56}Mn للنواتج ذات عمر النصف الأطول. فعلى سبيل المثال تم اخذ نظير النحاس (^{65}Cu) ووجد أن المقطع العرضي $\sigma = (826.29 \pm 62)mb$ مقارنة مع المقطع العرضي القياسي للنحاس (^{65}Cu) $\sigma = (926 \pm 60)mb$. وقد وجدنا ان طريقة التحليل بالتنشيط النيوتروني النسبية هي أكثر دقة من طريقة التحليل بالتنشيط النيوتروني المطلقة وذلك لثبات قيمة الفيض النيوتروني خلال استخدام تفاعل مرقاب.

الكلمات المفتاحية : *المصدر النيوتروني ، التنشيط النيوتروني ، المقطع العرضي.*

Appendices

Table(1): Data of studying for compound material for the neutron source.

Chemical Compound	Compound Weight (gm)	Compound Purity (%)	Weight of Investigated Element (gm)
Mgo	**1.0268**	**99.80**	**0.61919**
Fe_2O_3	**5.0**	**98.0**	**3.4784**
$NiCl_2$	**1.7111**	**99.98**	**0.7751**

Table(2) Data of studying for average cross-sections values measured by (Numerical - Graphical)method according to the spectra of the neutron source ^{241}Am/Be

Reaction	This Work			Ref [8]			
	σ_{av1}[9] (mb)	σ_{av2}[10] (mb)	$\sigma_{av}^{mean}{}_1$ (mb)	σ_{av3}[9] (mb)	σ_{av5}[10] (mb)	σ_{av4}[11] (mb)	$\sigma_{av}^{mean}{}_2$ (mb)
$^{24}Mg\ (n,p)^{24}Na$	26.96	27.23	27.09	-	-	-	-
$^{27}Al\ (n,p)^{27}Mg$	30.58	31.85	31.21	35	25	28	29.33
$^{56}Fe\ (n,p)^{56}Mn$	14.10	15.82	14.96	11	8.9	9.0	9.63
$^{58}Ni\ (n,p)^{58}Co$	159.56	163.29	161.42	-	-	-	-
$^{64}Zn\ (n,p)^{64}Cu$	39.76	41.26	40.50	-	-	-	-
$^{65}Cu\ (n,p)^{65}Ni$	4.11	4.38	4.24	-	-	-	-

Counts

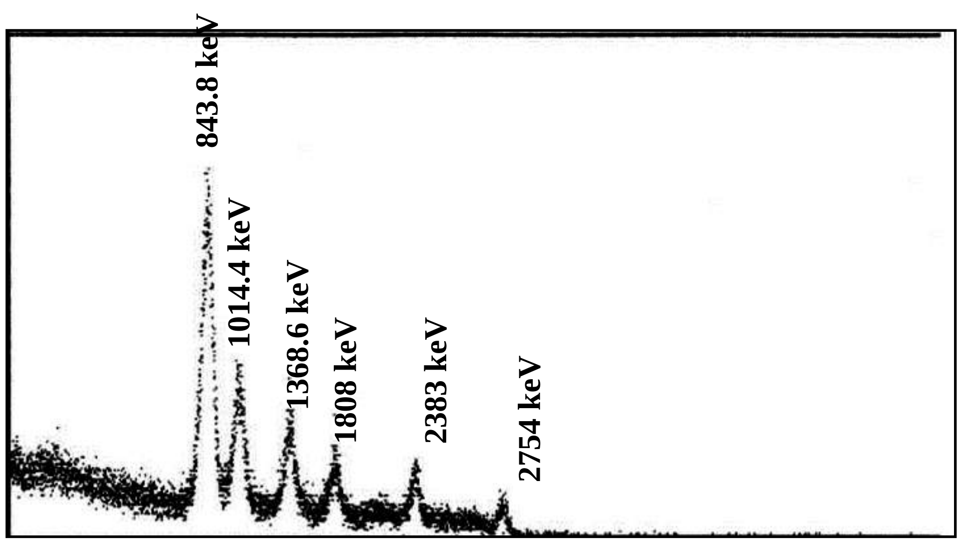

Channel

Channel

Fig (1) Spectrum of gamma ray for two reactions $^{27}Al(n,\alpha)^{24}Na$, $^{27}Al(n,P)^{27}Mg$ after collection time (15 minutes).

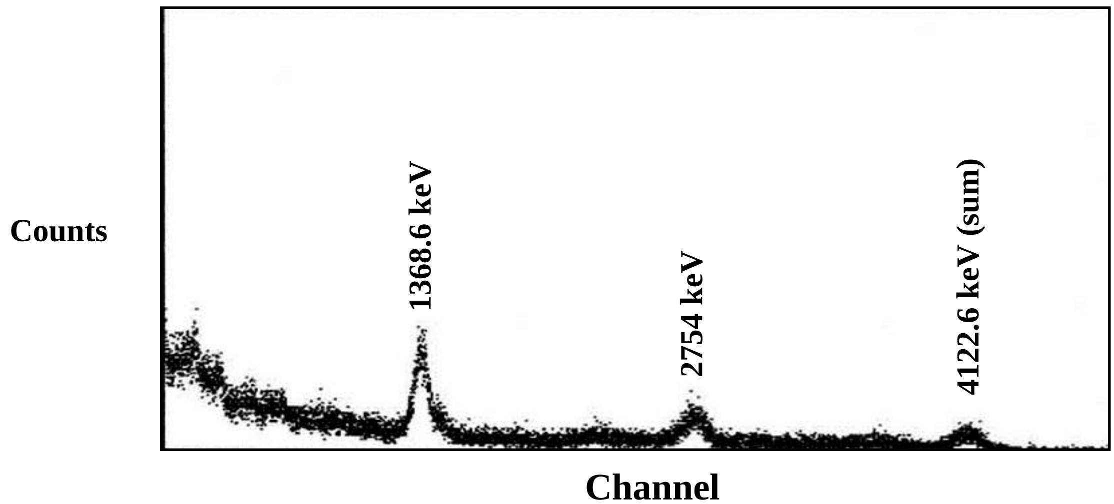

Fig (2) Spectrum of gamma ray for reaction $^{24}Mg\ (n,p)^{24}Na$ after collection time (60 minutes).

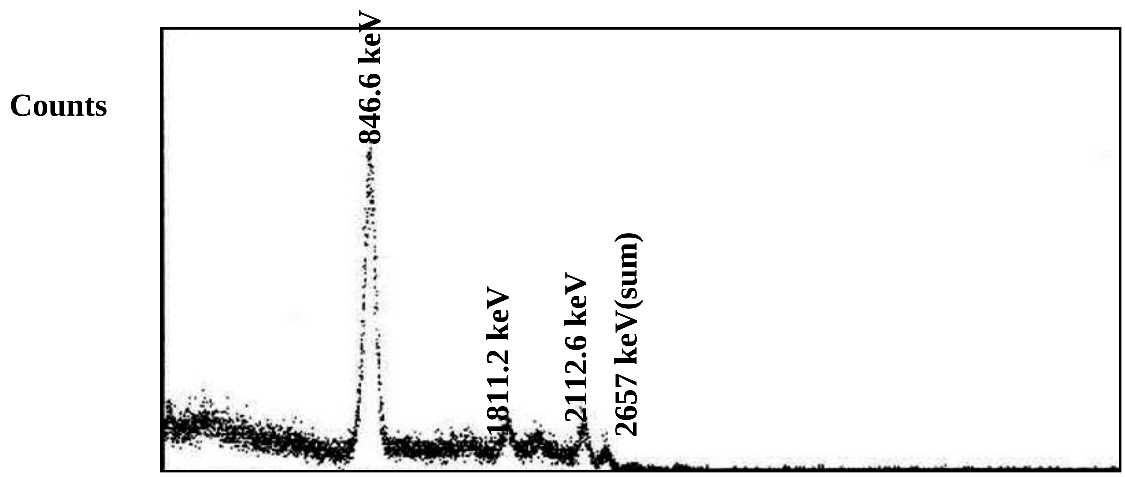

Fig (3) Spectrum of gamma ray for reaction $^{56}Fe\ (n,p)^{56}Mn$after collection time (16 minutes).

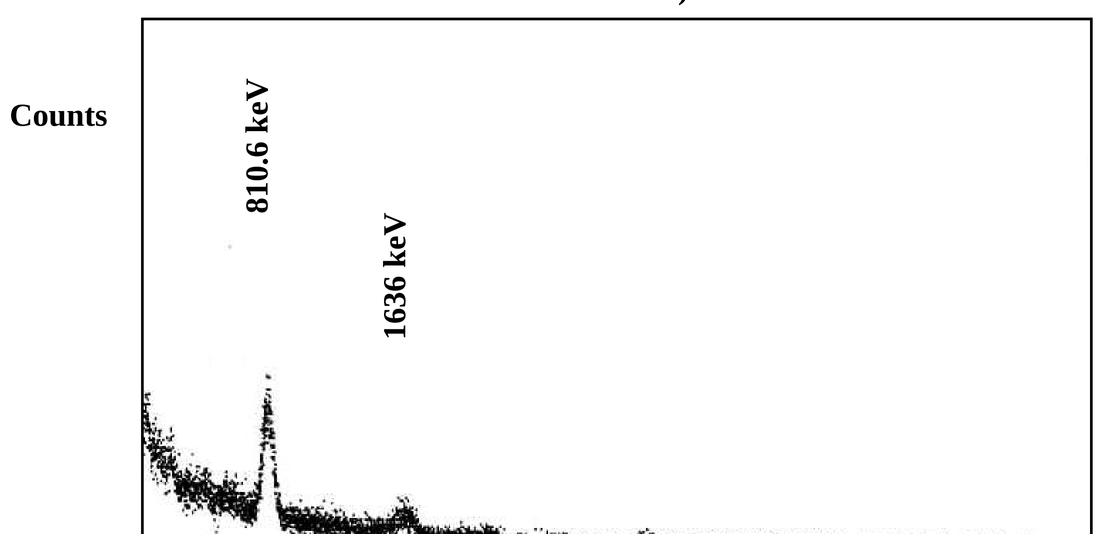

Fig(4) Spectrum of gamma ray for two reactions $^{58}Ni(n,p)^{58}Co$, $^{64}Ni(n,\alpha)^{61}Fe$ after collection time (60 minutes).

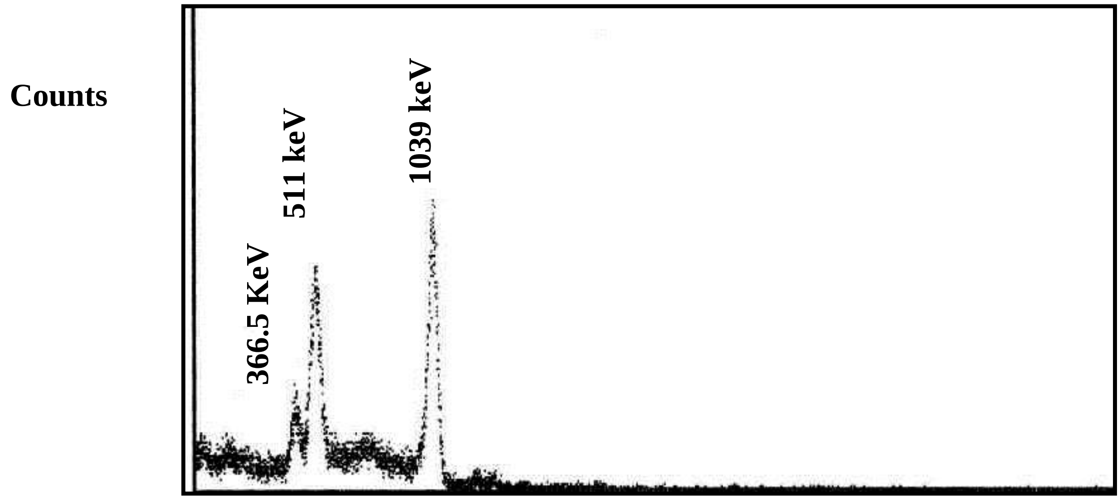

Fig (5) Spectrum of gamma ray for reactions $^{68}Zn(n,\alpha)^{65}Ni$, $^{64}Zn(n,p)^{64}Cu$ ، $^{66}Zn(n,p)^{66}Cu$ **after collection time (10 minutes).**

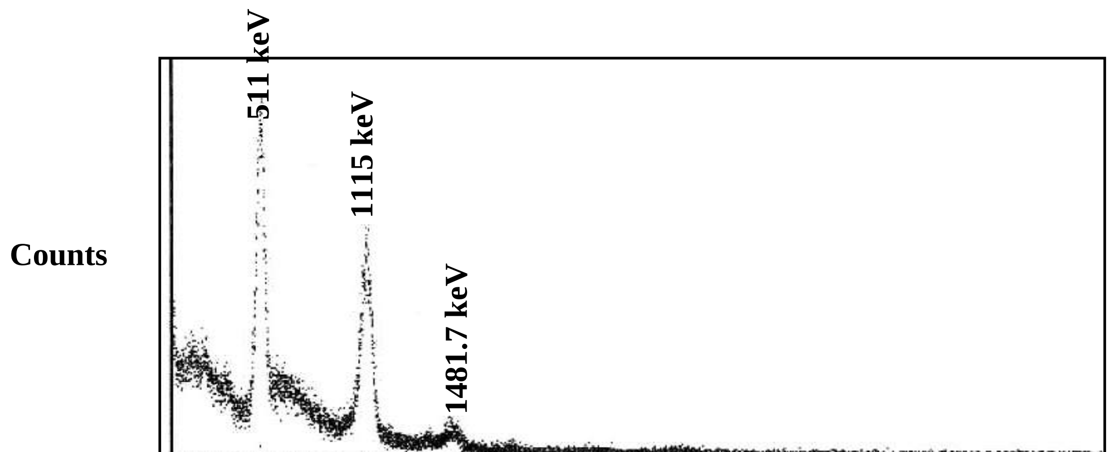

Fig (6) Spectrum of gamma ray for reactions $^{65}\boldsymbol{Cu}(\boldsymbol{n},\boldsymbol{p})^{65}\boldsymbol{Ni}$, $^{63}\boldsymbol{Cu}(\boldsymbol{n},\boldsymbol{\gamma})^{64}\boldsymbol{Cu}$, $^{65}\boldsymbol{Cu}\ (\boldsymbol{n},\boldsymbol{\gamma})^{66}\boldsymbol{Cu}$**after collection time (60 minutes).**

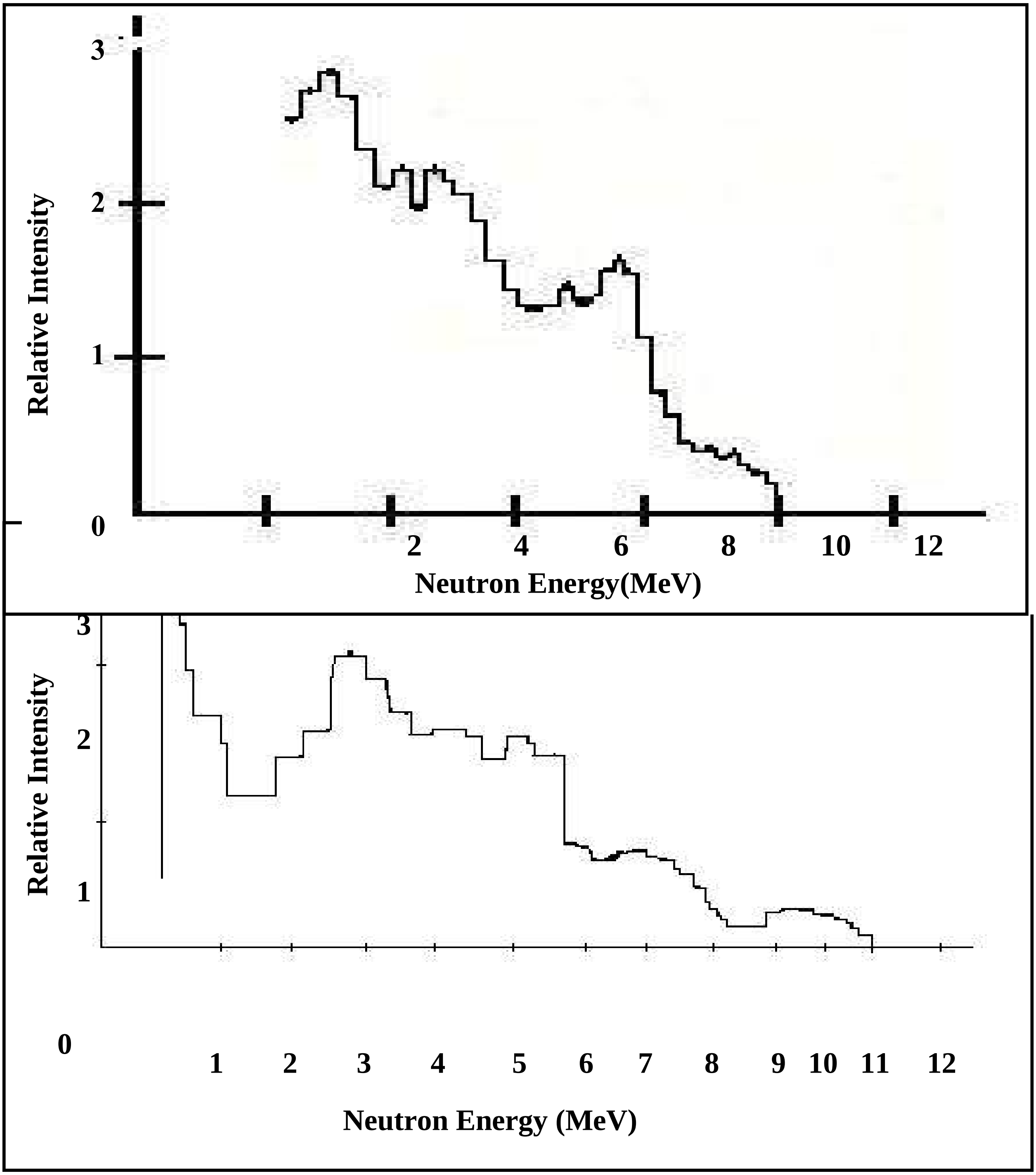

Fig.(8): **The spectrum of the neutron source $^{241}Am/Be$ [10]**

ttp://jgu.garmian.edu.krd https://doi.org/10.24271/garmian.344

دراسة مقارنة لمستوى كفاية العمل البدنية بالحد الاقصى لاستهلاك الأوكسجيني مابين لاعبي بعض الالعاب الجماعية

جميل محمد علي[*١] قادر ابراهيم غيدان علي[١]

[١] قسم التربية الرياضة ، كلية التربية الاساسية، جامعة كرميان

[*] jameel.mohammed@garmian.edu.krd

الملخص

يهدف البحث الى التعرف على الفروق الإحصائية في مستوى الكفاية العمل البدني والحد الاقصى لاستهلاك الأوكسجين ما بين لاعبي بعض الالعاب الجماعيةفي منطقة إدارة كرميان , أذ تكونت عينة البحث من (36) لاعباً من لاعبي بعض الألعاب الجماعية, يشمل لعبة الكرة الطائرة لنادي شيروانة الرياضي ,وكرة القدم, وكرة اليد لنادي رزكاري الرياضي، بواقع (12) لاعباً من كل لعبة.استخدمة الباحثان المنهج الوصفي،اختارا الباحثان مجتمع وعينة البحث بشكل عمدية وتم استخدمةبأجراء اختبار الكفاية العمل البدني عند النبض(170)لعينة البحث، بعد قياس معدل النبض في الدقيقة الواحدة باحتساب عدد نبضات القلب خلال (30ثوان ثم ضرب الناتج × 2)، إذ تم قياس معدل النبض اثناء الراحة وبعد حملين من المقاومة على الخطوة السلم الخشبي بأرتفاع(40)سم, بحيث يكون الحمل الثاني اكبر من الحمل الاول، كما تم تحديد قيمتي للكفاية العمل البدني (170) والحدالاقصى لاستهلاك الأوكسجين بواسطةمعادلة(كاربمان)،كما تم أيضًا تحديد قيمتي الكفاية العمل البدني(170)النسبي والحدالاقصى الاستهلاك الأوكسجين النسبي وقد خلصت نتائج الدراسة إلى ما ياتي:

- عدم وجود فروق ذات دلالة إحصائية في معدل النبض في اثناء الراحة وبعد الحمل الأول والثاني مابين لاعبي بعض الالعاب الجماعية .

-عدم وجود فروق ذات دلالة إحصائية في تحديد قيمتي الكفاية العمل البدني(170) والحد الاقصى لاستهلاك الأوكسجين ما بين لاعبي بعض الالعاب الجماعية .

-عدم وجود فروق ذات دلالة إحصائية في قيمتي الكفاية العمل البدني (170) النسبي و الحد الاقصى لاستهلاك الأوكسجين النسبي ما بين لاعبي بعض الالعاب الجماعية.

وعلى ضوء النتائج المحققة يوصى الباحثان: يجب على كوادر التدريبية الاعتماد على القياسات الفسيولوجية للتعرف على اهم التغيرات التي تحدث لأجهزة والاعضاء الداخلية لجسم اللاعبين لتنمية مستوى الذي يحدث نتيجة لاستمرارية التدريب للاستفادة منها وتقنين الوحدات التدريبية وتحديدها اعتماداً عليها لبناء الأسس العلمية بشكل جيد.

-يجب أن يهتم مدربي فرق الألعاب الجماعية في اقليم كردستان في أثناء تنفيذ البرامج التدريبية بتنمية الكفاية العمل البدنية والحد الاقصى لاستهلاك الأوكسجين بما يتناسب ومتطلبات الفعاليات الرياضية المختلفة .

-أجراء دراسات مشابهة على فعاليات رياضية مختلفة على الحقائق العلمية المتعلقة بالمتغيرات الفسيولوجية التي تناولها البحث للأخذ بنظر الاعتبار في أثناء تنفيذ البرامج التدريبية .

كلمات المفتاحية: الكفاية العمل البدني, الاستهلاك الأوكسجين, الالعاب الجماعية .

1-1 مقدمة البحث وأهميته

ظهرت في الآونة الأخيرة تطورات واضحة في النتائج الرقمية للألعاب الرياضية المختلفة ومن ضمنها فرق الالعاب الجماعية ,وأن هذه التطورات جاءت نتيجة تأثير التدريب الرياضي ,على الأجهزة الفسيولوجية للجسم الرياضي ونتيجة لإستمرار التدريب لفترات طويلة مما أدى ذلك إلى حدوث تكيف في الأجهزة والأعضاءالداخلية لجسم اللاعب,فأن ممارسة التمارين الرياضية بأستمرار في عملية التدريب تؤدي الى حدوث تغيرات فسيولوجية , وان هذه التغيرات تنعكس على مستوى كفاية العمل البدني وهذا بدوره سوف يؤثر بشكل كبير على مستوى الاداء المهاري والبدني وخاصة عند اداء المهارات المتنوعة خاصة للعبة.

وتعد لعبة كرة الطائرة وكرة القدم وكرة اليد هي من تلك الألعاب التي شهدت تطوراً ملحوظاً وأحتلت مكاناً بارزاً في اغلب بلدان العالم لإمتيازهم بالتشويق والاثارهم وتعدد المهاراتها الاساسية . وتتميز الألعاب الفرق الجماعية بانها تتطلب أمكانيات البدنية عالية بصورة عامة وتحتاج الى مستوى مميز من الكفاية العمل البدني والحد الاقصى لاستهلاك الأوكسجين بصورة خاصة والتي له الأثر الكبير والمباشر على العمل البدنية وأثناء تنفيذ أداء المهارات الفنية بشكل جيد ومميز ويخدم المهارات الدفاعيةوالهجومية بزمن المباراة .

ويجدر بالذكر أن مؤشرات الكفاية العمل البدني والحد الاقصى لاستهلاك الأوكسجين من المواضوعات المهمة ذات العلاقة المباشرة في علوم التربية والتي يجب على الجميع ان يهتموا بها ويدرس بدقة وموضوعية" لكونها احدى العوامل الأساسية التي يعتمد عليها التدريب الحديث لرفع مستوى الأداء"[1]. وتتجلى أهمية البحث في تقويم الكفاية العمل البدنية والحد الاقصى لاستهلاك الأوكسجين مابين لاعبي بعض الالعاب الجماعيةمختلفة بهدف تقديم المزيد من المعلومات والحقائق لاستكمال الجوانب العلمية المتعلقة، واضافة حقيقة من الحقائق العلمية لحصيلة المعلومات التي حصل عليها الباحثان، للاستفادة منها من قبل المعنيين في مجال فسيولوجيا للتدريب الرياضي .

1-2مشكلة البحث

تتميز كل لعبة من فرق الألعاب الجماعية بمتطلبات وواجبات مركبة تستدعي قدراً متبايناً من الحركة ويترتب على أساسها وجود الكفاءةالعمل البدنية متفاوتة نسبيًا لتلبية هذه المتطلبات والواجبات واحداث التغيرات الفسيولوجية المطلوبة نتيجة الجهد الذي يبذله اللاعبون اثناء المباراة والذي ينعكس على الاداء المتميز بعناصر اللياقة االبدنية المتنوعة . ومن هنا تكمن مشكلة الدراسة من خلال اطلاعهم على المصادر والمراجع والدراسات السابقة في فسلجة التدريب الرياضي لم يجدوا الدراسات التقويمية التي تتناول المقارنة بين الأنشطة والفعاليات الرياضية الاوكسجينية في الكفاية العمل

البدنية و الحد الاقصى لاستهلاك لأوكسجين ولم يهتمُ الباحثين في دراساتهم وا بحاثهم على المقارنة بين الأنشطة الرياضية الأوكسجينةواللاأوكسجينيةفي مستوى كفاية العمل البدني والحد الاقصى لاستهلاك الاوكسجين، وهذا ما شجع الباحثان لاجراء دراسة مقارنة في مستوى الكفاية العمل البدنية و الحد الاقصى لاستهلاك الأوكسجين ما بين لاعبي الفرق بعض الالعاب الجماعية .

1 -3 هدف البحث

-التعرف على دلالة الفروق في مستوى الكفاءة العمل البدنية و الحد الاقصى لاستهلاك الأوكسجين مابين لاعبي بعض الالعاب الجماعية .

4-1 فرضية البحث

-لا توجد فروق ذات دلالة معنوية في مستوى الكفايةالعمل البدني و الحد الاقصى لاستهلاك الأوكسجين مابين لاعبي بعض الالعاب الجماعية .

5-1 مجالات البحث

المجال المكاني : ملعب نادي رزكاري ضيا الر,القاعةالمغلقة لنادي شيروانةالرياضي .

المجال البشري: لاعبي الكرة الطائرة لنادي شيروانة,كرةالقدم و كرة اليد لنادي رزكاري الرياضي .

المجال الزماني: تم أجراء الدراسة ما بين الفترة 4/3 / 2018 - 4/25/ 2018 .

6-1 تحديد مصطلحات

- **الكفاية العمل البدنية(pwc 170)**:بانها قدرة على العمل البدني عند معدل نبض 170 ضربة/دقيقة أو مقدار الشغل الذي يمكن ان ينجزه اللاعب بأقصى شدة او كفية انتاجية الجهازالدوري التنفسي والدم وكفاءة العضلات عبر استهلاك الاوكسجين وانتاج الطاقة حيث ان تطوير كفاءة الاداء البدني تعكس لنا مدى تكيف اجهزة الجسم تحت تأثير التدريب الرياضي كما يستخدم لتقييم حالة الرياضي[(2)] .
- **بالحد الاقصى لاستهلاك الأوكسجيني** (VO2MAX) : ويشير هذا المصطلح إلى أقصى معدل تستخدمه الفرد من الأوكسجين عند الاداء للمجهود البدني الأقصوى مقاساَ عند مستوى سطح البحر و هذا المؤشر يعكس الخصوصية التامة الكفايةالعمل البدنية القصوى للجهازين الدوري-التنفسي في الفعاليات الرياضية التي تزيد مدتها عن(3-4 دقيقة)[(3)].

2-الاطار النظري والدراسات السابقة

1-2 الاطار النظري

يعد التدريب الرياضي من العلوم الحديثة التي حققت تقدماَكبيراَ من خلال أرتباطها بالعلوم الاخرى, حيث يهدف التدريب الرياضي الحديث الى تطوير قابليات الرياضي والوصول بها الى اعلى مستوى لتحقيق الا نجاز العالي ويتم ذلك من خلال احداث التكيفات الفسيولوجية المناسبة في اجهزة الجسم الحيوية عن طريق الاحمال التدريبية المناسبة والمنظمة .وأن البرامج التدريبية المقننة والتي يتم تنفيذها بشكل منتظم تحدث تطورات سريعة منتظمة في الكفاية العمل الفسيولوجية والبدنية والمهارية لدى الرياضي, وتصل الى تحقيق اهداف العلمية وفي العملية التدريبية ، ويقاس نجاح البرنامج التدريبية بمدى التقدم الذي يحققه اللاعب في نوع النشاط الممارس, لغرض وضع البرامج التدريبية للفعاليات الرياضية المختلفة . وبهذا الخصوص على ان برامج التدريب يجب ان تبنى من اجل تحقيق تنمية القدرات الفسيولوجية الخاصة والمطلوبة لاداء النشاط الرياضي الذي يمارسه لاعب، والتدريبب الرياضي الحديث يعتمد على تركيز اهدافه لتنمية وظائف وأعظاء اجهزة الجسم اللاعب من أجل أن يحدث التغيرات الوظيفية المصاحبة لها ، فكلما تحسنت امكانية العمل البدنية للرياضي فأنه انعكست ذلك بشكل مباشر على مستوى الاداء البدني والمهاري للاعب(4).

ويؤكدالباحثان ان لعبة كرة الطائرة وكرة القدم والكرة اليد من تلك الالعاب التي حققت انتشاراً واسعاً في ا نحاء العالم لميزاتها التربوية والبدنية والفنية الكبيرة, ولقد تطورة الاداء فيها بشكل كبير وواضح , وهذا من اهم مقومات النجاح فيهم ليشكل القاعدة المناسبة لأداء الفني والخططي الرفيع لمستوى من الفعاليات الفرقية التي تتطلب اعداداً بدنيا والوفسيولوجياَ ونفسياَ من اجل رفع الكفاية العمل البدنية للاعب في ممارسة اللعبة .

2-2 مفهوم الحد الأقصى الاستهلاك للأوكسجين

يعتبر مؤشر الحد الاقصى لاستهلاك الاوكسجين من أهم المؤشرات الفسيولوجيةللاعبين وبالأخص بالانشطة التي تحتل التمثيل الغذائي الهوائي الجانب الاكبر في عملية توفر الطاقة فيه. فأن الحد الأقصى لاستهلاك الأوكسجين واحد من أهم القياسات الوظيفية المعتمدة، إذ يعدأهم مقايس موضوعي لكفاية البدنية للاعب(5)

إذ تتحدد الإمكانية الفرد البدنية تبعاً لمقدرته على استيعاب ونقل واستخدام الأوكسجين في عضلاته العاملة كما أن معرفة الحد الأقصى لاستهلاك الأوكسجين يمكن أن يعطي مؤشراً للحالة الوظيفية للجهازين الدوري والتنفسي إذ أن أقصى استهلاك للأوكسجين يعد أقصى معدل لعمل هذين الجهازين, فمن خلال هذا الاختبار يمكن تحديد الأمكانية العامة لوظيفة سلسلة التنفس القلبية الرئوية وبالتالي يدل على صلاحية الفرد وقدرته على تحمل أعباء الاحمال التدريبية . بأن حد أقصى الاستهلاك مؤشرًا جيدًا للامكانية الوظيفية للجسم ودليلاً على اللياقة التنفسية للفرد(6).لذلك فلا بد من معرفة هذه المتطلبات الوظيفية لدى اللاعبين في الألعاب الفرقية لكي يتمكنوا من الاستمرار في العمل البدني طوال وقت المباراة(7).

فإن الكفاية انتاجية الجهازين الدوري والتنفسي وكفاية عمل العضلات عبر استهلاك الاوكسجين وانتاج الطاقة حيث يساعد بتطوير الكفاية عمل الاداء البدني تعكس لنا مدى تكيف اجهزة الجسم تحت تأثير التدريب الرياضي كما يستخدم لتقييم حالة الرياضي,من المهم من تلك الامور الواجبة مراعاتها عند لاعبي كرة الطائرة وكرة القدم وكرةاليد وأنشطةالفعاليات الرياضية الأخرى اذ انها تدل على الكفاية عمل الجسم الاعب , وتطور الكفاية العمل البدني من خلال

التدريب اذ يرتفع مستواها بزيادة الكفايةالعمل الجهازين الدوري والتنفسي لذا فأن الكفايةالعمل البدني هنا تعد مقياساً كلياً للكثير من الوظائف المهمة لاعضاء جسم اللاعب للتعبير عن مقدرة الرياضي على اداء عمل عضلي وبشدة متوسطةالعالية ولفترة طويلة. كما تعطي للاعب جوانب واضحة لبعض المتغيرات الفسيولوجية،وهذا يساعدنا على التعرف إلى طبيعة الفروق بمستوى الفكايةالعمل البدني للاعبي العبة كرة الطائرة , وكرة القدم, وكرةاليد .

2-3بعض التغيرات فسيولوجيةالعمل البدني على الجهاز التنفسي

هنالك عدة تاثيرات فسيولوجية تصاحب العمل البدني ، وتختلف باختلاف مكونات الاحمال التدريبية ، وكذلك نوع النشاط الرياضي الممارس[8]،ومما لا شك فيه ان العمل البدني يترك اثره الواضح على الجهاز التنفسي ، وان عمل الجهاز التنفسي هو عملية تبادل الغازات بين أعضاء الجسم المختلفة والهواء الجوي والتي بمقتضاها يحصل الجسم على الأوكسجين ويتخلص من ثاني أو كسيد الكاربون وتعد وظيفة التنفس إحدى الوظائف التي يؤديها الجهاز التنفسي والجهازالدوري إذ يقوم الجهاز التنفسي بكثير من المتطلبات المهمة خلال النشاط الرياضي وذلك بالتعاون مع الجهاز الدوري بشكل فعال, لذا يعد الجهاز التنفسي عاملاً مساعداً في عملية نقل وأستهلاك الأوكسجين بالجسم اللاعب خلال النشاط الرياضي وتتضمن وظيفة التنفس عمليتين إحداهما التنفس الخارجي ويقصد بها التبادل الغازي بين التهوية الرئوية فضلاً عن حجم التنفس , ويؤدي زيادة هذين العاملين معاً أو زيادة التهوية الرئوية . ويتكون التنفس من عمليتين متعاقبين هما الشهيق والزفير وهناك تأثيرات مختلفة تحدث في جهاز التنفسي للإنسان وهي معدل التنفس الطبيعي لدى الإنسان ليس ثابتا(14-16) مرة في الدقيقة, وتحدث التغيرات وتزداد في حالة التمرين الفعلي,وينخفض بشكل واضح الدى الرياضيين المتمرنين بشكل منظم بمختلف الفعاليات الرياضية بدونة الاستثناء, وان ارتفاع التبادل الغازات من نحو(20-30)ضعف حالة الراحة في حالة الجهد البدني المفرط(الشاق),وان زيادة السرعةوعمق التنفس, ممايؤدي الى زياد معدل التهوية وزيادة كبيرة يتراوح ما بين(150-200)لترهواء اوأكثرفي دقيقة لدى الرياضيين المتميزين,وأن تأثيرات مهمة تحدث ارتفاع استهلاك الاوكسجين في الجهاز التنفسي من(250-350) ملليلتر/دقيقةفي حالة الراحة,الى من(4500-5000)ملليلتر/دقيقة في حالة المجهود البدني[9].

2-4مفهوم المستوى الكفاية العمل البدنية

تعد الكفاية العمل البدني مهمة في الطب الرياضي وفسيولوجيا الرياضة حيث تدرس الكفاية الأداء البدني في العديد من مجالات التطبيق الفسلجي والطبي وتعني الكفاية العمل البدنية(pwc170) بأنهاالقدرة على العمل البدني عند معدل نبض(170)ضربة/ دقيقة.حيث يذكر عمار عبد الرحمن بأن الكفاءة العمل البدنية"مقدار الشغل الذي يمكن ان ينجزه اللاعب بأقصى شدة[10]

ويعد الكفاية انتاجية الجهازالدوري التنفسي والدم وكفاية العضلات العاملة من خلال نقل استهلاك الاوكسجين و الطاقة لتطوير الكفايةالاداء عمل البدني تعكس لنا مدى تكيف اجهزة الجسم تحت تأثير التدريب الرياضي(الحمل التدريب) كما يستخدم لتقييم حالة الرياضي[11].

يوضح الباحثان بأنة تطوير الكفايةالعمل البدنية من الامور الواجبة مراعاتها عند لاعبي الفرق الالعاب الجماعية,اذ انها تدل على الكفاية الجسم في انتاج الطاقة الهوائية واللاهوائية خلال النشاط البدني ولكونها تشتمل على كلا الاتجاهين في الكفاية انتاج الطاقة, وكما تعد جزءاً من اللياقة البدنية. وكذلك يرى الباحثون فأنة التنمية الكفاية العمل البدنية من خلال التدريب اذ يرتفع مستواها في زيادة الكفاية العمل الجهازين الدوري والتنفسي لذا فأن الكفاية البدنية هنا تعد مقياساً كلياً للكثير من الوظائف المهمة لاعضاء الجسم للتعبير عن مقدرة الرياضي على اداء عمل عضلي وبشدة عالية ولفترة طويلة . كما تعطي للرياضي جوانب واضحة لبعض المتغيرات الوظبفية .

2-5 ماهية الكفايةالعمل البدنية

تعد الكفاية العمل البدني الوظيفية القصوى للجهاز الدوري و التنفسي أذ تقع بين 170- 200 ضربة/ دقيقة وهذه الحالة يمكن معرفة اقصى عمل وظيفي للقلب والدورة الدموية باستخدام جهد دون القصوي ويعتبر كاف لايصال الجهازين الدوري والتنفسي لكفائتهما القصوى ,وهناك علاقة خطية بين معدل ضربات القلب من جهة والجهد الفيزياوي المنجز في ثانية من جهة أخرى حيث وجد ان بعد نبض(170)ض/د تتخذ العلاقة بينهما شكلاً اخر, أن هذا الاختبار ضروري للكشف عن الكفاية العمل البدني[12] .

2-6 معدل ضربات القلب

يعبر قياس نبض القلب عن نشاط القلب في حالة الراحة وعند المجهود (يسمى الإيقاع المنتظم مابين انقباض وانبساط عضلة القلب بضربات القلب، فعند الانقباض يندفع الدم خارجًا بقوة إلى الشرايين، مما يسبب ضغطًا على جدرانها يمكن الإحساس به من على سطح الجسم وفي بعض المواضع، وعند الانبساط يقل هذا الضغط وإذا ما تم حصر هذه النبضات فإن ذلك يعبر عن معدل القلب[13]. وللقلب شبكة محكمة من ألياف العضلات التي توصل نبضات القلب وتسيطر عليها وتتم السيطرة على نبضات القلب في العقدة الجيبية الأذينية وتسير منها عبر طريق خاص يسير به النبضة الى البطين. إن معدل تغييرات نبض القلب أثناء الجهد وبعده مباشرة وهو المؤشر الحقيقي لقابلية جهاز القلب والدورة الدموية، فالزيادة التي تحصل له أثناء الجهد وزمن عودته إلى حالته الطبيعية بسرعة بعد انتهاء الجهد مباشرة هي علامة مميزة لجسم الرياضي ودلالة واضحة على تعود جهاز القلب والدورة الدموية . وتعد التغييرات التي تحصل للنبض أثناء الجهد وبعده هي المقياس الحقيقي الذي يبين مدى تحمل الجسم للجهد البدني وبالأخص جهازي القلب و الدوران فارتفاع النبض إلى حد معين أثناء الجهد ثم عودته إلى حالته السابقة قبل الجهد والفترة الزمنية التي يقضيها النبض في الرجوع إلى حالته قبل الجهد هي مؤشر هام يعتمد عليه في العديد من الفحوص الطبية لتقدير قابلية ولياقة الجسم وأنخفاض معدل النبض مع مزاولة التدريب يبين مدى التكييف الجيد فالقدرة على استخدام المزيد من الأوكسجين في الدم تسمح با نخفاض معدل تدفق الدم إلى العضلات النشطة وبذلك تنخفض سرعة ضربات القلب،فالتدريب الطويل للتحمل يخفض السرعة القصوى لنبضات القلب وأيضًا سرعة وقت الراحة و تحقق نبض بمعدل[14] .

2-7 الدراسات السابقة

دراسة قام بها جاك ويلمور (20012)[15] , هدفت الدراسة الى التعرف على العلاقة بين الحد الاقصى لاستهلاك الاوكسجين وكفاءة التحمل على العجلة الثابتة على عينة من طلاب الجامعة (30) طالباً إذ أجرى كل طالب اختبارين للكفاءة البدنية على الارجومتري مع استمرار حساب استهلاك الاوكسجين وقبضة يد كانت المقاومة (كم/ م) و سرعة التبديل ثابتة . كانت من نتائج هذه الدراسة وجود ارتباط عال (0.84)بين الحد الاقصى لاستهلاك الاوكسجين وكفاءة التحمل وتؤكد هذه الدراسة مدى الارتباط بين الحد الاقصى لاستهلاك الاوكسجين والكفاءة البدنية .

دراسة(كمال عارف ,وسعاد عبدالكريم(2011)[16] , هدفت الدراسة الى التعرف على مقارنة مستوى الكفاءة الوظيفية والحد الاقصى لاستهلاك الاوكسجين لدى لاعبات كرة الطائرة وكرة اليد. شملت عينة البحث 44 لاعبة من منتخب كليةالتربيةالرياضية للبنات في جامعة بغداد , بواقع 22 لاعبة من منتخب كرة الطائرة و 22 لاعبة من منتخب كرة اليد . اما في منهج البحث والاجراءات الميدانية، فقد استخدم الباحثان المنهج الوصفي لملائمة طبيعة مشكلة البحث، كما استخدم الباحثان الوسائل الاحصائية التالية : الوسط الحسابي و الا نحراف المعياري و الارتباط البسيط. إختبار T Test و معامل الصدق الذاتي . وفضلا عن المصادر والمراجع المهمة في هذا المجال وبعد اجراء المعالجات الاحصائية توصل الباحثان الى الاستنتاجات الاتية :

- وجود فروق دالة احصائياَ بين لاعبات كرة الطائرة وكرة اليد في الكفاءة الوظيفية المطلقة والنسبية والحد الاقصى لاستهلاك الاوكسجين المطلق والنسبي ولصالح لاعبات كرة اليد .

- وعلى ضوء النتائج المحققة أوصى الباحثان بضرورة الاهتمام ببرامج التدريب لتنمية الكفاءة الوظيفية ومستوى الحد الاقصى لاستهلاك الاوكسجين لدى اللاعبات .

3-منهجية البحث واجراءته الميدانية

3-1- منهجية البحث

هو الطريقة التي يستخدمها الباحث في دراسته للمشكلة لاكتشاف الحقيقة[17], وقد استخدم الباحثان المنهج الوصفي في هذه الدراسة لملائمته لطبيعة المشكلة و هدف الدراسة .

3-2- مجتمع وعينة البحث

اختارا الباحثان مجتمع وعينة البحث بشكل عمدية من لاعبي كرة الطائرة لنادي شيروانة الرياضي ولاعباً كرة القدم وكرة اليد لنادي رزكاري الرياضي في اقليم كوردستان في إدارة منطقة كرميان، تكونت عينة الدراسة من(36)لاعباً، بمعدل (12)لاعبين من كل لعبة بعد استثناء واستبعاد اللاعبين حيث أنهم لم يستطيعوا إجراء الاختبارات بسبب الإصابة . "والعينة " هي النموذج الذي يجري الباحث مجمل محور عمله عليها"[18]. والجدول (1, 2) يوضح مواصفات العينة الدراسة .

جدول الرقم (1) أسماء الأندية المشاركين فيوعدد الاختبار كل ناد تبعاً للعب, لعينة الدراسة

الرقم	النادي	اللعبة	التكرار	النسبة المئوية
1	شيروانه	الكرة الطائرة	12	٪33
2	رزكاري	كرة القدم	12	٪33
3	رزكاري	الكرة اليد	12	٪33
4	المجموع	—	36	٪100

الجدول الرقم (2) يوضح الاوساط الحسابية والا نحرافات المعيارية لمواصفات عينة الدراسة

الرقم	المعالم الأحصائية / المتغيرات والفعالية	العمر		الطول		الوزن	
1		وحدة القياس (سنة)		وحدة القياس (سم)		وحدة القياس (كغم)	
		س	ع±	س	ع±	س	ع±
2	كرة الطائرة	23.7	1.54	179.7	1.86	79	1.49
3	كرة القدم	22.5	0,12	169.6	1.67	67.4	1.43
4	كرة اليد	21.4	1.37	178.9	1.53	76.5	1.82

3-3 الأجهزة والادوات المستخدمة في البحث:

- سماعة طبية لقياس معدل ضربات القلب في الدقيقة الواحدة ,الألماني الصنع (Healtho Meter) .
- ميزان قياس الوزن .
- شريط قياس طول الجسم .
- ساعة توقيت الكترونيةنوع ياباني الصنع (SEWAN) .
- السلم الصندوق الخشبي(40)سم .
- استمارة تسجيل البيانات .

3-4- إجراءات البحث الميدانية:

3-4-1- التجربة الاستطلاعية:

تم اجراء تجربة استطلاعية بتاريخ (2018/4/6) على (4)لاعبين الذين تم اختيارهم من مجتمع البحث بطريقة عشوائية أثنين منهم متخصص في الكرة اليد وأثنين الأخرين متخصص في كرة القدم , وتم استبعادهم عند تنفيذ التجربة الرئيسة وكان اختيارهم بالطريقة العشوائية ومن خارج عينة البحث الرئيسة وكانت الغاية من التجربة الاستطلاعية :

1-التعرف على مدى ملاءمة الاختبارات للعينة المختارة وكانت ملاءمة .

2-التأكد من صلاحية وكفاءة الأجهزة والأدوات المستخدمة في البحث وكانت صالحة للاختبار .

3- التعرف على الوقت الذي يستغرقه كل اختبار فضلاً عن الاختبارات الكلية وحصل ذلك بحيث أصبح لدينا معلومات عن الوقت المستغرق للاختبار .

5- وتم تطبيق جميع قياسات واختبارات البحث عليهم .

3-4-2-التجربة الرئيسة :

وقد قام الباحثان بأجراء التجربة الرئيسية بتاريخ (13-14-2018/4/15) على عينةالدراسة, تكونت عينة الدراسة من(36)لاعباً, وبواقع(12)لاعب لكل لعبة, (12)لاعباً الكرة الطائرة لنادي شيروانة الرياضي, و(12)لاعب كرة القدم لنادي رزكاري الرياضي, و(12)لاعب كرة اليد لنادي رزكاري الرياضي, وقد استغرقت الاختبارات الرئيسية مدة(3) أيام حصل الباحثان من خلالها على انتائج والارقام الخامة من الاختبار .

3-4-3-الاختبارات والقياسات المستخدمةفي البحث:

3-5-1- الكفايةالعمل البدنية(PWC_{170}):

يسمى اختبار الكفايةالعمل البدني(170) وهو من الاختبارات المهمة لتحديد مقدار القابلية البدنية للمختبر وقد تم استخدام اختبار خطوة السلم الخشبي بارتفاع (40) سم لتحديد الكفايةالعمل البدني للجهازين الدوري والتنفسي ويتم ذلك من خلال اعطاء جهدين مختلفين الشدة مدة الجهد الاول (3 دقائق) وفي نهاية الـ(30)ثواني الاخيرة يتم حساب النبض بعد قياس معدل النبض في الدقيقة الواحدة باحتساب عدد نبضات القلب في خلال (30ثوان ثم ضرب الناتج × 2)، لاجل استخراج معدل النبض في الجهد الاول ثم يؤدي الجهد الثاني ايضا ب(3 دقائق) وفي نهاية (30) ثوانية, يتم باحتساب عدد نبضات القلب في الجهد الثاني ايضا خلال (30 ثانية ثم ضرب الناتج × 2) لاستخراج معدل النبض في الجهد الثاني أي أن تكون مدة اختبار المشترك الواحدة (6 دقائق) كاملة ,مع راحة قدرها (3-5) دقائق بين حمل الاول والثاني .

يتم استخراج قيمة الجهد الاول والثاني وفق المعادلة الاتية(19) :

$$N = 1.5 \times W.T \times H \times n$$

اذ ان: N = الجهد ، 1.5 = قيمة ثابتة ، W.T = وزن الشخص ، H = ارتفاع السلم ، n = عدد مرات الصعود والنزول:

اذ ان : N1 = الجهد الاول ، N2 = الجهد الثاني ، PS1 = النبض الاول ، PS2 = النبض الثاني

ب- أختبار الحد الاقصى لاستهلاك الأوكسجين(Vo2Max) : تم تقويم الحد الأقصى لاستهلاك الأوكسجين لعينة البحث بعد التعرف على قيمة الكفايةالعمل البدني (Pwc170) واستخدام احدى معادلات (كاربمان) الخاصة في الرياضات التي تتطلب القوة المميزة بالسرعة بعد استخراج قيمة (Pwc170) وهي كما يأتي :

$$1240 + (\mathbf{Pwc170}) \times 1.7 = (\mathbf{Vo2Max})$$

- **ويتم استخراج الحد الأقصى لاستهلاك الأوكسجين (Vo2Max) النسبية بقسمةناتج ال (Vo2Max)على وزن الجسم بالكيلوغرام لتصبح القيمة تمثل ملليتر/بالدقيقة كيلوغرام من وزن الجسم (ملليتر.د/كغم) .**
- **اما قياس الكفاية العمل البدنية(PWC_{170}) النسبي يتم قياسه بتقسيم PWC_{170} المطلق على وزن المختبر .**

PWC_{170} **النسبي** = / **W.T** PWC_{170} [17] .

3-5-2-الأسس العلمية لاختيار الاختبارات :

لقدتم ايجاد الثقل العلمي للاختبارات المرشحة (الصدق، الثبات، الموضوعية) لمتغيرات الدراسة سابقا ولاسيما (الكفاية العمل البدني عند النبض(PWC_{170})اذ كان يتمتع بمعاملات علمية عاليةجداً، فضلا عن تطبيق (الكفاية العمل البدني باستخدام اختبار الخطوة),إضافة إلى ذلك تم تأكد من الكثير من الدراسات والبحوث التي تناولت على الكفاية العمل البدني والتي تم إجراءها في مجال الاختبارات الفسيولوجية لدى لاعبي كرة الطائرة وكرة القدم والكرة اليد وغيرها من الفعاليات الرياضيةالمختلفة مثل لدراسة(أياد محمد عبدالله,1997 [20],وغصون فاضل هادي,2004[21] , وفاء صباح محمد كريدي الخفاجي,2010[22], كمال عارف ,سعاد عبد الكريم,2001[23] , احمد عبد الغني,والأخرون 2001 [24].

3-6- المعالجات الإحصائية :

استخدمة الباحثان الوسائل الاحصائية الملائمة من خلال الحقيبة الاحصائية(SPSS)والمتمثلة بالقوانين الأتية :

- **الوسط الحسابي .**
- **الا نحراف المعياري .**
- **تحليل التباين .**
- **النسبة المئوية .**

4- عرض و تحليل النتائج ومناقشتها :

4-1 عرض وتحليل النتائج و مناقشتها

لقد تم عرض الاوساط الحسابية والانحرافات المعيارية لاختبارات قام الباحثان بعرض وتحليل ومناقشة النتائج التي توصلوا إليها من خلال اجراء القياسات الفسيولوجية، والجدول (3) يوضح قيم هذه القياسات .

الجدول الرقم (3)

المعالم الأحصائية / والقياسات الفسيولوجية	كرة الطائرة		كرة القدم		كرة اليد	
	الوسط الحسابي	الانحراف المعياري	الوسط الحسابي	الانحراف المعياري	الوسط الحسابي	الانحراف المعياري
معدل النبض في أثناء الراحة(ن/د)	67.3	1.78	66.3	1.5	71.01	2.64
معدل النبض بعد الحمل الأول(ن/د)	126.2	2.61	114.2	4.51	120.1	3.06
معدل النبض بعدالحمل الثاني (ن/د)	140	2.91	128.4	5.32	130.43	21.5
كفاية االعمل البدني(170) (كغم .م/د)	4.59	24.88	4.41	23.19	240.43	20.69
الحدالاقصى الاستهلاك الأوكسجين (مللتر/د)	80.2	21.29	374.66	26.12	.6.01	22.66
كفاية االعمل البدني(170) النسبي(كغم .م/د)	46.99	8.69	59.71	14.05	40.16	9.16
الحدالاقصى الاستهلاك الأوكسجين النسبي(كغم .م/د)	89.82	10.56	13.32	12.21	64.11	10.32

يتبين من للجدول (3) أن الوسط الحسابي للنبض في اثناء الراحة لدى لاعبي كرة الطائرة هو (67.3) ن/د بانحراف معياري قدره (±1.78)، بينما كان الوسط(66.3) ن/د لدى لاعبي كرة القدم وبانحراف معياري (±1.5)، أما كرة اليد فكان الوسط الحسابي للنبض (71.01) ن/د بانحراف معياري (±2.64) وبلغ معدل النبض بعد الحمل الأول لدى لاعبي كرة الطائرة (126.2) ن/د بانحراف معياري قدره(± 2.61)، بينما كان (114.2) ن/د لدى لاعبي كرة القدم بانحراف معياري (±4.51)، أما الكرة اليد (120.1) ن/د وبانحراف معياري (±3.06) وكان معدل النبض بعد الحمل الثاني لدى لاعبي كرة الطائرة (140) ن/د بانحراف معياري قدره(± 2.91)، بينما كان (128.4) ن/د لدى لاعبي كرة القدم بانحراف معياري (±5.32)، أما كرة اليد(130.43)فكان ن/د بانحراف معياري (±21.5) وظهر ان الوسط الحسابي لهذه القيمة (الكفاية االعمل البدني(كغم .م/د) وبعد استخدام القانون الخاص لاستخراج قيمة (170) لدى لاعبي كرة الطائرة (4.59) كغم.م/د، بانحراف معياري قدره (±24.88)، بينما كان(4.41) كغم.م/د لدى لاعبي كرة القدم بانحراف معياري (±23.19)، أما لاعبي كرة اليد فكان(240.43) كغم.م/د بانحراف معياري (±20.69) , أما الحدالاقصى الاستهلاك الأوكسجين (مللتر/د) لدى لاعبي كرة الطائرة بعد استخدام المعادلة الخاصة بلغ الوسط الحسابي

لقيمة(80.2) مللتر/د، بانحراف معياري (±21.29)، بينما كان (374.66) مللتر/د لدى لاعبي كرة القدم بانحراف معياري قدره (± 26.12)، أما لاعبي كرة اليد فكان (6.01) مللتر/د بانحراف معياري (±22.66) .

أما بالنسبةلقيمة الكفاية االعمل البدني النسبي (170)(كغم .م/د) وبعد قسمة قيمة بالنسبةلقيمة الكفايةالعمل البدني النسبي (170)(كغم .م/د) على وزن الجسم ظهر لنا ان الوسط الحسابي لدى لاعبي كرة الطائرة (46.99) كغم.م/كغم، بانحراف معياري قدره (±8.69) بينما كان الوسط الحسابي (59.71) كغم.م/كغم لدى لاعبي كرة القدم بانحراف معياري (±14.05)، أما لاعبي كرة اليد فكان (40.16) كغم.م/كغم بانحراف معياري (±9.16) . وبعد قسمة قيمة الحدالاقصى لاستهلاك الأوكسجين النسبي(كغم .م/د) على وزن الجسم ظهرت لنا ان الأوساط الحسابية الحدالاقصى لاستهلاك الأوكسجين النسبي(كغم .م/د) , فكان الوسط الحسابي لدى لاعبي الكرة الطائرة (89.82) مللتر.د/كغم، بانحراف المعياري قدره (±10.56)، بينما كان الوسط الحسابي لدى لاعبي كرة القدم (13.32) مللتر.د/كغم (بانحراف معياري (±12.21)، أما الوسط الحسابي لدى لاعبي كرة اليد فكان (64.11) (مللتر.د/كغم بانحراف معياري (±10.32) .

ومن اجل معرفة نوعية الدلالة بين لاعبي كرة الطائرة و كرة القدم و كرة اليد لعينة البحث ونوعية الاختبار المختار استتخدمة الباحثان التحاليل الأحصائية المرتبطة بالبحث وكما هو موضح في الجدول رقم (3.2,1), وجود فروق دالة إحصائياَ بين لاعبين والتي تنص على انه توجد فروق ذات دلالة إحصائية في مستوى الكفاية العمل البدني والحد الاقصى لاستهلاك الأوكسجين بين لاعبي الطائرة وكرة القدم و كرة اليد للتعرف على دلالة الفروق بين لاعبي فرق الالعاب الجماعية تم استخدام تحليل التباين للتعرف على دلالة الفروق بين اللاعبين لعينة البحث في المتغيرات التي تناولها البحث وكما هو موضح في الجدول (4) .

الجدول الرقم (4)

المتغيرات	مصدر التباين	درجة الحرية	مجموع المربعات	متوسط المربعات (التباين)	(ف) المحسوبة	(ف) الجدولية
معدل النبض بعد الحمل الأول(ن/د)	بين مجموعات	2	138	69	0.45	
	داخل المجموعات	12	320	160		
	المجموع الكلي	14	458			
معدل النبض بعد الحمل الثاني(ن/د)	بين مجموعات	2	178,01	94,4	2.04	
	داخل المجموعات	12	1102.9	79,2		
	المجموع الكلي	14	1280,91			
كفايةالعمل البدني (170)(كغم .م/د)	بين مجموعات	2	3927701	15102160	1.12	
	داخل المجموعات	12	6454382	21010232		
	المجموع الكلي	14	10382083			
الحدالاقصىالاستهلاك الأوكسجين (مللتر/د)	بين مجموعات	2	897	356	1.56	2.94
	داخل المجموعات	12	4023	289		
	المجموع الكلي	14	4920			
كفايةالعمل البدني (170) النسبي(كغم .م/د)	بين مجموعات	2	30973402	11023150	2.17	
	داخل المجموعات	12	6785273	3543201		
	المجموع الكلي	14	37758675			
الحدالاقصى الاستهلاك الأوكسجين النسبي(كغم .م/د)	بين المجموعات	2	7598	2345	3.09	
	داخل المجموعات	12	4563	11.40		
	المجموع الكلي	14	12161			

2-4مناقشة نتائج الدراسة :

من خلال ملاحظتنا في ضوء نتائج الجدول(4) تيبين لنا عدم وجود فروق ذات دلالة معنوية في جميع القياسات التي تناولها البحث وهي معدل النبض بعد الحمل الأول والثاني والحدالاقصى لاستهلاك الأوكسجين (مللتر/د), والكفاية العمل البدنية (170) الحدالاقصى الاستهلاك الأوكسجين النسبي والكفاية العمل البدنية(170) النسبي(كغم .م/د), بين لاعبي الكرة الطائرة وكرة القدم و كرة اليد، ويعزو الباحثان عدم معنوية الفروق مابين لاعبي كرة الطائرة وكرة القدم وكرة اليد التي تعتمد على نظام انتاج الطاقة اللاأوكسجينية[25]. فان تدريبات اللاأوكسجينية في الفعاليات تتركز في تطوير انظمة أنتاج الطاقة المسيطرة على هذه الألعاب، ولكن هذا لا يعني عدم حاجة الألعاب اللاأوكسجينية إلى الكفايةالعمل البدني واستهلاك الأوكسجين, وذلك لان النظام اللاأوكسجينية هو الأساس في اعادة خزن مصادر الطاقة في فترة استعادة

الشفاء لانظمة انتاج الطاقة، ولذلك فانه يكون من الضروري توافر التدريبات الهوائية عند تطوير اللياقة البدنية في كل الفعاليات[26] .

ومن خلال ملاحظتنا للجدول(4)نرى ان هناك فروقاً واضحة في الاوساط الحسابية للقياسات الفسيولوجية التي تناولها البحث وهي (معدل النبض في أثناء الراحة، ومعدل النبض بعد الحمل الأول، ومعدل النبض بعد الحمل الثاني , وقيمة الحدالاقصى الاستهلاك الأوكسجين (مللتر/د), وقيمةالكفاية االعمل البدنية(170) وقيمة الحدالاقصى الاستهلاك الأوكسجين النسبي و قيمةالكفايةالعمل البدنية(170) النسبي ولصالح لاعبي كرة القدم، على الرغم من ان جميع الالعاب تعد من الالعاب اللاهوائية، وهو يدل على ان الحالة الفسيولوجية والكفاية العمل البدني لدى لاعبي كرة القدم قد تكون افضل من لاعبي الكرة الطائرة ويليها لاعبي الكرة اليد .

ويعزو الباحثان ذلك البرامج التدريبية المعدة للاعبي كرة القدم تولي اهتمامًا أكبر لتمرينات القابلية الأوكسجينية واللاأوكسجينية مقارنة بلعبة كرة الطائرة و كرة اليد، والذي يعمل على زيادة الناتج القلبي وكبر حجم الضربة للقلب، و والأقتصادية في عمل القلب، وبالتالي تحسين الكفاية العمل البدني والفسيولوجية. بأنة كبر كمية الدم المدفوع في الضربة الواحدة للقلب تلاحظ عندما تكون سرعة القلب بطيئة، وعلى العكس يلاحظ انخفاض نسبي لكمية الضربة لدى الاعبين الذي لديهم زيادة في معدل القلب,ويوضح الباحثان أن سبب ذلك تكيف الاجهزة الداخلية للاعب والناتج من تأثير استمرار حمل التدريب وهذا بدوره ينعكس على مستوى الاداء المهاري وخاصة مهارات المتنوعة فرق الألعاب الجماعية وهذا يتفق مع اغلب المصادر التي تشير"الى ان الكفاية العمل البدنية هي الطريقة الوحيدة للكشف عن الكفاية العمل البدنية للرياضيين وتقييم حالات التكيف لدى الرياضيين [27].

نستدل مما سبق ذكره أن الرياضيين المتدربين جيداً يكون عدد ضربات القلب لديهم قليلا قياساً الى لأشخاص غير المتدربين فقد يصل الى 40 ضربة في الدقيقة أو أقل لأبطال راكضي المسافات الطويلة والماراثون[28]. فمعدل ضربات القلب لدى الرياضي المتدرب جيد عند اعطائه حملاً يكون أقل من نظيره غير المتدرب ، و الزيادة العظمى لنتاج قلب الرياضي يكون سببها الرئيسي حجم الضربة[29].و كذلك فان للتدريب الرياضي له تاثير على ضغط الدم حيث يختلف الفرق بين الضغط الانقباضي الذي يرتفع عن معدله وبين الضغط الانبساطي الذي ينخفض عن معدله وهو يتراوح عندالرياضيين (105-130) للانقباص وبين (60-89) للانبساط[30]. فأن النشاط الرياضي والتدريب الرياضي المنتظم تاثير واضح في الكفاءة العمل البدنيةلجهازالقلب والدورة الدموية، فان للاعبين الذين يمارسون التدريبات الرياضية المنتظمة يكون لديهم عدد ضربات القلب في الدقيقة أقل من الذين لاينتظمون في التدريب بشكل الجسد سواء كان ذلك في حالة الراحة ام خلال الجهد البدني ، كما ان نتاج القلب من الدم يكون كبيراً قياساً لغيرهم[31] .

وجدير بالذكر فأن الالعاب ذات شدا عالية تلعب دوراً في التكيفات الفسيولوجية التي تحدث للاعبين، وان انخفاض معدل النبض يعد مؤشراً في أمكانية العمل البدنية ومستوى الأداء الفسيولوجي للاعبين، ويعكس الكفاية العمل البدنية للجهازين الدوري التنقسي ,وان الحد الاقصى لاستهلاك الأوكسجينة يعد من العوامل المهمة لدى اللاعبين الذين يمارسون الانشطة اللاأوكسجينية وخاصةَ لاعبي كرة القدم لانها ذات فائدة كبيرة في أثناء فترات استعادة الشفاء عند تنفيذ الوحدات التدريبية التي تحتوي على تكرارات ومجاميع تدريبية وكذلك له في نقل الأوكسجين وله تأكثيراً كبيراً على

نقل الأوكسجين إلى العضلات، وهذا يتفق مع ما ذكره مؤيد عبدالحميد[32] في ان الكفاية الجهازين الدوري والتنفسي هي أحد المكونات الأساسية والمهمة لممارسة جميع الألعاب الرياضية المختلفة لقيامهما بنقل الأوكسجين والوقود إلى كافة الخلايا العضلية لجسم اللاعب، والتي لا يمكن استمرار العضلات بالانقباض إلا إذا زودت بها .

5-الاستنتاجات والتوصيات:

5-1 الاستنتاجات

- وجود فروق ذات دلالة إحصائية في معدل النبض في اثناء الراحة وبعد الحمل الأول والثاني مابين لاعبي كرة الطائرة وكرة القدم و كرة اليد .

- وجود فروق ذات دلالة إحصائية في تحديد قيمتي الكفاية العمل البدني(Pwc170) والحد الاقصى لاستهلاك الأوكسجين ما بين لاعبي كرة الطائرة وكرة القدم و كرة اليد .

-وجود فروق ذات دلالة إحصائية في قيمتي الكفاية العمل البدني(Pwc170)النسبي والحد الاقصى لاستهلاك الأوكسجين النسبي ما بين لاعبي كرة الطائرة وكرة القدم و كرة اليد .

5-2-التوصيات

- يجب أن يهتم مدربو فرق الألعاب الجماعية في اقليم كوردستان في أثناء تنفيذ البرامج التدريبية بتنمية الكفاية العمل البدني والحد الاقصى لاستهلاك الأوكسجين بما يتناسب ومتطلبات الفعاليات الرياضية المختلفة .
- يجب على كوادر التدريبية على القياسات الفسيولوجية للتعرف على اهم التغيرات التي تحدث للاجهزة والاعضاء الداخلية لجسم لاعب لتنمية مستوى الذي يحدث نتيجة لاستمرارية التدريب للاستفادة منها تقنين الوحدات التدريبية وتحديدها اعتماداً عليها لبناء الأسس العلمية بشكل جيد .
- أجراء دراسات مشابهة على فعاليات رياضية مختلفة على الحقائق العلمية المتعلقة بالمتغيرات الفسيولوجية التي تناولها البحث للأخذ بنظر الاعتبار في أثناء تنفيذ البرامج التدريبية .

الهوامش

1- عبد الفتاح، أبو العلا احمد،(1999): تنمية مقياس الحد الأقصى لاستهلاك الأوكسجين لمتسابقي الجري للمسافات الطويلة والمتوسطة، مجلة ألعاب القوى، العدد 24 ، مصر .

2- عمار عبد الرحمن,(1998) : الطب الرياضي بغداد ، مطبعة جامعة بغداد ، ص25 .

3-هزاع بن محمد الهزاع: (2000),التهيئة البدنية والأسس العلمية لوصفة النشاط البدني بغرض الصحة واللياقة البدنية,الرياض .

4- سيد,احمدنصرالدين,ابوالعلاعبدالغني,(1993): فسيولوجيا اللياقة البدنية،ط 1،دار الفكرالعربي, القاهرة .

5- فاروق عبد الوهاب ,(1983): مبادئ فسيولوجيا الرياضة , ط1,مطبعةبيت الحكمة, بغداد .

6- عبد العظيم عبد الحميد,(1995): دراسة لبعض الاستجابات الوظيفية للحمل البدني المقنن لدى عدائي و سباحي المسافات القصيرة، مجلة بحوث التربية الرياضية,جامعة حلوان, مصر .

7--Bernard, M Astrand P.O. (1997). Quanticication oF Exercise Capability and Evaluation of Physical Capacity in Man. (progress in cardiov. Dis. 19 (1): 51.

8- بهاء الدين إبراهيم سلامة ,(1988): فسيولوجيا الرياضة،دار الفكر العربي،القاهرة، ١٩٨٨ .

9- عمار عبد الرحمن ,(1989): الطب الرياضي بغداد ، مطبعة جامعة بغداد .

10- العلا عبدالفتاح ومحمد حسن علاوي,(1995): فسيولوجيا التدريب الرياضي، ط2،دار الفكرالعربي، القاهرة .

11-محمود داود الربيعي, وسوسن هدود عبيد,(2007):مقارنة لبعض مؤشرات القدرة الهوائية واللاهوائية بين لاعبي الألعاب الفرقية, بحث منشور, جامع بابل, مجلةدراسات،العلوم التربوية،المجّلد34،العد2 ,العراق.

12-محمد سمير سعد الدين:علم وظائف الأعضاء ،ط ٣،منشاة المعارف، الأسكندرية، ٢٠٠٧ .

13- محمد عادل رشدي:الطب الرياضي في الصحة والمرض،منشأة المعارف،الاسكندرية، ١٩٩٧ .

14-Jack H. Wilmare (20012): Maximal oxygen in take and its relation ship to endurang capacity on abicycle ergometer the res , qus: V. uo, N1, PP. 203.

15- كمال عارف ,سعاد عبد الكريم,(2001): دراسة مقارنة لمستوى الكفاءة الوظيفية والحد الأقصى لاستهلاك الأوكسجين للاعبات الكرةالطائرةوكرةاليد, بحث منشور, مجلة التربية الرياضية, المجلد العاشر,العدد الرابع, جامعةبغداد

16-وجيه محجوب وقاسم المندلاوي،(1989):طرائق البحث العلمي ومناهج في التربية الرياضية،بغداد،مطبعة وزارة التعليم العالي .

17-محمد الغريب عبد الكريم,(1983):البحث العلمي،المناهج،التصمي الاجراءاث،المكتب الجامعي الحديث،ط 3,العراق .

18 - Karpnman B. o.p. cit. 1987, p.144-145 .

19- أبو العلا احمد عبد الفتاح ومحمد صبحي حسنين,(1993): فسيولوجيا ومورفولوجيا الرياضي وطرق القياس والتقويم, ط1,القاهرة: دار الفكر العربي، 1993 .

20- أيادمحمد عبدالله,(1997): دراسةمقارنة في مستوى الكفاءة البدنيةوالحدالاقصى لاستهلاكالأوكسجين بين عدائي المسافات القصيرةوالمسافات الطويلة، بحث منشورفي مجلةالرافدين للعلوم الرياضية،المجلد ٣، العدد ٧ .

21-غصون فاضل هادي,(2000): تأثير تدريبات المطاولة ومركبات الحديد على بعض مؤشرات الدم وكفاءة الجهاز الدوري التنفسي. رسالة ماجستير. جامعة بغداد. كلية التربية الرياضية، 2000 .

22- وفاء صباح محمد كريدي الخفاجي,(2010): تأثير استخدام التدريب المتقاطع في تطوير الكفاية البدنية الخاصة بالسباحة عند النبض(pwc170) والكفاية البدنية النسبية, بحث غير منشور, كلية التربية الرياضية جامعة بغداد .

23- كمال عارف ,سعاد عبد الكريم, مصدر سابق ذكره ,(2001) .

24-احمد عبد الغني,والأخرون,(2001): دراسة مقارنة في مستوى الكفاءة البدنية و الحد الاقصى لاستهلاك الأوكسجين بين فعاليات المبارزة وكرة القدم وعدو المسافات القصيرة, مجلة التربية الرياضية –المجلدالعاشر- العدد الأول .

25-Fox, E.L. et al. (1990): The Physiological Basic oF Physical Education and Athletics, 4 th. Ed. Saunders

26-محمود داود الربيعي, وسوسن هدود عبيد,(2007):مقارنة لبعض مؤشرات القدرة الهوائية واالأوكسجينية بين لاعبي الألعاب الفرقية, بحث منشور, جامع بابل, مجلة دراسات، العلوم التربوية،المجّلد 34 ، العدد2 ,العراق .

27-ابو العلا عبدالفتاح ومحمد حسن علاوي,مصدر سابق ذكره,(1995).

28-Frank D. Davis, J,(1980): Medicine for sport London year book Derries H . physiology of exercise, third edition medical publishers,. 29 .

29 - Steven M,.C.:(1992) : Legtenngth, Inequality-Implication for running- 1- Sport Medicine., Injury. prevention .

30-قاسم حسن حسين,(1990):الفسيولوجيا مبادئها وتطبيقاتهافي المجال الرياضي, دارالحكمة للطباعة والنشر, الموصل .

31-رافد مهدي,(1990): منهج مقترح لتحسين مستوى الكفاءة الوظيفية للجهازين الدوري والتنفسي لطياري ,رسالة ماجستير غير منشورة , كلية التربية الرياضية ,جامعة بغداد .

32-مؤيد عبدالحميد الحيالي,(1997): أثر ممارسة بعض الانشطة الرياضية اللاصفية في مستوى الكفاءة الوظيفية للجهازين الدوري والتنفسي للطلاب، رسالة ماجستير غير منشورة، جامعة بغاد، كلية التربية . الرياضية .

المصادر

1-احمد عبد الغني,والأخرون,(2001): دراسة مقارنة في مستوى الكفاءة البدنية و الحد الاقصى لاستهلاك الأوكسجين بين فعاليات المبارزة وكرة القدم وعدو المسافات القصيرة, مجلة التربية الرياضية –المجلدالعاشر- العدد الأول .

2-أياد محمد عبدالله,(1997):دراسةمقارنة في مستوى الكفاءة البدنيةوالحدالاقصى لاستهلاكالأوكسجين بين عدائي المسافات القصيرةوالمسافات الطويلة، بحث منشورفي مجلةالرافدين للعلوم الرياضية،المجلد ٣، العدد ٧ .

3- أبو العلا احمد عبد الفتاح ومحمد صبحي حسنين,(1997): فسيولوجيا ومورفولوجيا الرياضي وطرق القياس والتقويم, ط1, القاهرة: دار الفكر العربي، 1997 .

4- أبو العلا احمد عبد الفتاح ومحمد صبحي حسنين,(1993): فسيولوجيا ومورفولوجيا الرياضي وطرق القياس والتقويم, ط1,القاهرة: دار الفكر العربي، 1993 .

5-ابو العلا عبدالفتاح ومحمد حسن علاوي,(1995): فسيولوجيا التدريب الرياضي،ط2،دار الفكرالعربي، القاهرة .

6- بهاء الدين إبراهيم سلامة ,(1988): فسيولوجيا الرياضة،دار الفكر العربي،القاهرة .

7- سيد,احمدنصرالدين,ابوالعلاعبدالغني,(1993): فسيولوجيا اللياقة البدنية،ط 1،دار الفكرالعربي, القاهرة .

8-رافد مهدي,(1990): منهج مقترح لتحسين مستوى الكفاءة الوظيفية للجهازين الدوري والتنفسي لطياري ,رسالة ماجستير غير منشورة , كلية التربية الرياضية ,جامعة بغداد .

9- عبد الفتاح، أبو العلا احمد،(1999): تنمية مقياس الحد الأقصى لاستهلاك الأوكسجين لمتسابقي الجري للمسافات الطويلة والمتوسطة، مجلة ألعاب القوى، العدد 24 ، مصر .

10- عبد العظيم عبد الحميد,(1995): دراسة لبعض الاستجابات الوظيفية للحمل البدني المقنن لدى عدائي و سباحي المسافات القصيرة، مجلة بحوث التربية الرياضية,جامعة حلوان, مصر .

11- عمار عبد الرحمن,(1998) : الطب الرياضي بغداد ، مطبعة جامعة بغداد ، ص25 .

12- فاروق عبد الوهاب ,(1983): مبادئ فسيولوجيا الرياضة , ط1,مطبعةبيت الحكمة, بغداد .

13-قاسم حسن حسين,(1990):الفسيولوجيا مبادئها وتطبيقاتهافي المجال الرياضي, دارالحكمة للطباعة والنشر, الموصل .

14- كمال عارف ,سعاد عبد الكريم,(2001): دراسة مقارنة لمستوى الكفاءة الوظيفية والحد الأقصى لاستهلاك الأوكسجين للاعبات الكرة الطائرة وكرة اليد,, بحث منشور,مجلة التربية الرياضية ,المجلد العاشر, العدد الرابع , جامعةبغداد .

15- عمار عبد الرحمن ,(1989): الطب الرياضي بغداد ، مطبعة جامعة بغداد .

16-غصون فاضل هادي,(2000): تأثير تدريبات المطاولة ومركبات الحديد على بعض مؤشرات الدم وكفاءة الجهاز الدوري التنفسي. رسالة ماجستير. جامعة بغداد. كلية التربية الرياضية، 2000 .

17- محمود داود الربيعي, وسوسن هدود عبيد,(2007):مقارنة لبعض مؤشرات القدرة الهوائية واللاهوائية بين لاعبي الألعاب الفرقية, بحث منشور,جامع بابل, مجلةدراسات،العلوم التربوية،المجّلد34،العد2 ,العراق.

18-محمد سمير سعد الدين :علم وظائف الأعضاء ،ط ٣،منشاة المعارف، الأسكندرية، ٢٠٠٧ .

19- محمد عادل رشدي:الطب الرياضي في الصحة والمرض،منشأة المعارف،الاسكندرية، ١٩٩٧ .

20-محمد الغريب عبد الكريم,(1983):البحث العلمي،المناهج،التصمي الاجراءات،المكتب الجامعي الحديث،ط 3,العراق .

21-مؤيد عبدالحميد الحيالي,(1997): أثر ممارسة بعض الانشطة الرياضية اللاصفية في مستوى الكفاءة الوظيفية للجهازين الدوري والتنفسي للطلاب، رسالة ماجستير غير منشورة، جامعة بغداد، كلية التربية . الرياضية .

22-وجية محجوب وقاسم المندلاوي،(1989):طرائق البحث العلمي ومناهج في التربية الرياضية،بغداد،مطبعة وزارة التعليم العالي .

23- وفاء صباح محمد كريدي الخفاجي,(2010): تأثير استخدام التدريب المتقاطع في تطوير الكفاية البدنية الخاصة بالسباحة عند النبض(pwc 170) والكفاية البدنية النسبية, بحث غير منشور, كلية التربية الرياضية جامعة بغداد .

24-هزاع بن محمد الهزاع: (2000),التهيئة البدنية والأسس العلمية لوصفة النشاط البدني بغرض الصحة واللياقة البدنية,الرياض .6

25-Bernard, M Astrand P.O. (1997). Quanticication oF Exercise Capability and Evaluation of Physical Capacity in Man. (progress in cardiov. Dis. 19 (1): 51.

26-Jack H. Wilmare (20012): Maximal oxygen in take and its relation ship to endurang capacity on abicycle ergometer the res , qus: V. uo, N1, PP. 203.

27-Fox, E.L. et al. (1990): The Physiological Basic oF Physical Education and Athletics, 4 th. Ed. Saunders .

28-Frank D. Davis, J,(1980): Medicine for sport London year book Derries H . physiology of exercise, third edition medical publishers,. 29.

29-Steven M,.C.:(1992):Legtenngth, Inequality-Implication for running-1- Sport Medicine.,Injury. prevention .

30-Karpnman B. o.p. cit. 1987, p.144-145

A study on the level of physical work efficiency compared to the maximum consumption of oxygen Between the players of some of the group games

Abstract

The objective of theis research was to identify the statistical differences in the level of physical work efficiency and the maximum oxygen consumption among Between the players of some of the group games in the area of the administration of Garamyan. The research sample consisted of (36) (12) players from each game. The researchers used the descripttive method, and used the test of the physical work efficiency at pulse (170) of the sample of the study, after measuring the pulse rate per minute by calculating the number of heartbeat During (30 mutiplimg it by The rate of pulse that measured during rest and after two pregnancies of resistance on the step of the wooden ladder at a height of 40 cm. The second load was greater than the first one load . The two values of physical labor efficiency (170Pwc) and maximum oxygen consumption (170 Pwc) and the relative maximum relative oxygen consumption. The results of the study were as follows :

-There were no statistically significant differences in the rate of pulse during the rest and after the first pregnancy and the second Between the players of some of the group games .

- There were no statistically significant differences in the values of the physical work efficiency values (170Pwc) and the maximum oxygen consumption Between the players of some of the group games.

There were no statistically significant differences in the relative physical work efficiency (170Pwc) values and the maximum relative oxygen consumption among Between the players of some of the group games.

In light of the results achieved, the two researchers recommended: Emphasize the trainers based on physiological measurements to identify the changes that occur to the body organs players to keep pace with the level of development that occurs as a result of the continuity of training to take advantage of the standardization of load training and identification based on scientific grounds. And conducting a similar study on sports activities and events on different scientific facts related to the physiological variables addressed in the research to take into account in the course of the implementation of training programs

Keywords: Physical work efficiency, maximum oxygen consumption, group games.

ttp://jgu.garmian.edu.krd https://doi.org/10.24271/garmian.345

بعض القياسات الجسمية وعلاقتها بدقة الارسال المستقيم بالتنس الارضي للاعبي فريق كلية التربية الرياضية في خانقين

جعفر حسين علي[1] ازاد علي حسن[2]

[1،2]كلية التربية الرياضية ، خانقين ، جامعة كرميان

[1]jaafar.hussein@garmian.edu.krd

الملخص

الباب الاول: التعريف بالبحث تضمن المقدمة واهمية البحث وتم استعراض لعبة التنس الأرضي وهي واحدة من الألعاب الرياضية التي شهدت تطورا ملحوظا باستخدام التطبيق العلمي الصحيح وخاصة القياسات الأنثروبومترية من الخصائص الفردية التي يتميز بها الإنسان عن غيرة سواء قياسات للجسم البشري ككل أو أقسامة وكلمة مقاييس الجسم البشري الأنثروبومترية فرع من الأنثروبولوجيا . وهو علم يبحث في أصل قياس الجسم البشري وللقياسات الأنثروبومترية أو الجسمية عدة اهتمامات فهي تقيس (الأطوال والكتل والأعراض والمحيطات والأعماق وسمك الدهن والأنماط الجسمية والقوة العضلية للكتف والرجلين). وتكمن أهمية البحث في تناول القياسات الجسمية بدراسة من خلال منهج وصفي يجمع بين القياسات الجسمية ودقة الارسال المستقيم في التنس الارضي. اذ تتجلى مشكلة البحث من هنا يبرز التسأول التالي حول العلاقة الجدية في دقة الارسال المستقيم بالتنس الارضي فضلا عن العتلات والروافع الناتجة عن أطوال أجزاء الجسم وخاصة الإطراف العليا ومن هنا تبرز مشكلة البحث في تناول القياسات الجسمية من خلال منهج وصفي يجمع بين القياسات الجسمية ودقة الارسال المستقيم في التنس الارضي وكانت اهم الاهداف هي1 - -التعرف على بعض القياسات الجسمية السائدة لدى لاعبي فريق كلية التربية الرياضية في خانقين 2-التعرف على نوعية العلاقة بين بعض القياسات الجسمية بدقة الارسال المستقيم لدى لاعبي فريق كلية التربية الرياضية في خانقين.اما المجالات البحـــــث فقد تضمنت المجال البشري لاعبي منتخب كلية التربية الرياضي في خانقين لعام 2017-2018 .اماالمجال المكاني القاعة الرياضية لكلية التربية الرياضية في خانقين .والمجال ألزماني للفترة من 15/2 /2018 ولغاية 15\ 4\2018 .

الباب الثاني : فتضمن الدراسات النظرية والمشابهة ذات الصلة والعلاقة بموضع البحث.

وكان **الباب الثالث** قد احتوى على منهجية البحث واجراءاته الميدانية اذ استخدم الباحث المنهج الوصفي وكانت العينة تتألف من لاعبي المنتخب كلية التربية الرياضية في خانقين .واستخدم الباحث الاختبارات المقننة لضمان دقة النتائج، وقد أجريت الاختبارات لمتغيرات البحث على عينة البحث في يوم الاحد الموافق 1/4/ 2018، في الساحات خاصة للتنس الارضي وبعد ان تم معالجة النتائج احصائياً، تم عرضها وتحليلها ومناقشتها في الباب الرابع

اما في الباب الخامس فاستنتج الباحث عدم وجود ارتباط معنوي بين القياسات الجسمية (طول الجسم ، وزن الجسم ، طول الذراع ، طول الساعد ، طول العضد ، طول الكف ، مدى الكف ، عرض الصدر ، عرض الكتف) ومهارة الارسال المستقيم

للاعبي منتخب كلية التربية الرياضية في خانقين وكانت اهم التوصيات 1- التأكيد في البرامج التدريبية للاعبين الذين لديهم ضعف في مهارة الارسال المستقيم.

1-1 ألمقدمة وأهمية البحث

يعد التفوق في مختلف الأنشطة الرياضية التي يمارسها الإنسان من الأمور التي تستوجب توفر عدد من المتطلبات التي تتيح للفرد أن يقوم بهذا النشاط على الوجه الأكمل ويعد النشاط الرياضي ميزة من مميزات هذا العصر والذي بدورة يحتاج إلى كثير من المتطلبات الأساسية سواء كان نشاط جماعياً أو فردياً وهناك اختلاف بين هذه المتطلبات من حيث الدرجة والنوع من نشاط رياضي إلى أخر. وعادةً تنعكس هذه المتطلبات على المواصفات الواجب توفرها لدى الممارسين ولا شك ان توفر تلكَ المتطلبات يمكنها ان تعطي فرصة أكبر لاستيعاب وأداء مهارات اللعبة وفنونها ضمن أطار القانوني .

وتعد القياسات الأنثروبومترية من الخصائص الفردية التي يتميز بها الإنسان عن غيرة سواء قياسات للجسم البشري ككل أو أقسامة وكلمة مقاييس الجسم البشري الأنثروبومترية فرع من الأنثروبولوجيا . وهو علم يبحث في أصل قياس الجسم البشري وللقياسات الأنثروبومترية أو الجسمية عدة اهتمامات فهي تقيس (الأطوال والكتل والأعراض والمحيطات والأعماق وسمك الدهن والأنماط الجسمية والقوة العضلية للكتف والرجلين) . أن القياسات الأنثروبومترية مهمة في المجال الرياضي والعملي المرتبط بشكل كبير لنوع النشاط الرياضي الذي يزاوله الفرد وتحقيق الانجازات الرياضية فلاعب التنس ثناء الارسال يمتاز بطول القامة فالانجاز أذاً يتعلق بالطول والنمط وبقية العوامل الأخرى . إذا فطول القامة للاعب شرط أساسي في بداية الاختبار لهذه الرياضة وبالأخص طول القسم العلوي للجسم والسبب يعود إلى ان كل نشاط رياضي له متطلبات بدنية خاصة تميزه عن غيرة من الألعاب الأخرى خاصة الألعاب االفردية فلاعب التنس يختلف عن لاعب كرة القدم ولكل لعبة مميزات خاصة بها وتنعكس هذه الصفات على عناصر اللياقة البدنية الواجب توفرها لكي تصاحب متطلبات تلك اللعبة فطول القامة وطول مدى الكف وسعة الصدر وطول القسم العلوي للجسم وخاصة الأذرع هي من الأمور المهمة الواجب توفرها في كرة الطائرة مثلا أو حامي الهدف في كرة اليد ومما لا شك فيه أن توفر الصفات الانثروبومترية تعطي فرصة أكبر لتحقيق الفوز والوصول إلى الانجاز ويسهل الطريق لاستيعاب وفهم مهارات اللعبة ومتطلباتها لقد أصبح مهما اليوم توافر القياسات المناسبة والأجسام الملائمة بوصفها الدعامات الأساسية للوصول إلى مستويات ممكنة وعلى اللاعبين أن يتجهوا إلى الألعاب التي تتلائم وأطوالهم وكتلهم وبقية أقسام جسمهم فلاعب قصير القامة لا نحتاجه بالتنس مثل كرة القدم والعكس صحيح وهكذا يختص كل نشاط رياضي بالمقاييس الجسمية الملائمة لهذا النشاط بل أظهرت الدراسات الانثروبومترية ان المقاييس الجسمية تختلف باختلاف البيئات الجغرافية حيث تؤثر عوامل بيئية مختلفة في مقاييس وشكل جسم الإنسان وقد أدى ذلك إلى تفوق بعض الأجناس في رياضيات معينة هي سبب لهذه القياسات كتفوق الزنوج في مسابقات الجري والعدو لمسافات طويلة وكذلك نلاحظ ان سكان جنوب شرق أسيا كونهم يمتازون بكتل صغيرة لايصلون إلى درجة البطولة في العاب القوى كالرمي أو لعبة كرة اليد نسبة إلى الرقعة الجغرافية كأوروبا مثلا الذين يمتازون بالكتل البشرية الضخمة وتؤدي القياسات الانثروبومترية أهمية بالغة في عملية التنبؤ والانتقاء الرياضي والاختيار واهم هذه القياسات طول الجسم والوزن ونسبة الشحوم والسعة الحيوية ومحيطات الأجسام العلاقة المتبادلة بين أقسام هذه القياسات .

ان لعبة التنس تعد إحدى الألعاب الفردية التي تعتمد الفوز والخسارة كأسلوب لتحديد لاعب الفائز في المباراة وهذا ناتج عن عدد النقاط التي يحرزها احد الاعبين في ساحة االمنافس لذا كان للارسال أهمية كبيرة في هذه اللعب هذا و أنه يعد المهارة الأساس والاهم من بين مهارات اللعبة الأخرى لذا فان كل المبادئ الأساسية المدروسة تصبح عديمة الفائدة إذ هي لم تتوج في النهاية بإصابة ساحة المنافس لذا كان الارسال المستقيم هو المبدأ الأساسي الذي يعطيه معظم المدربين وقت أكثر من غيرة فضلاً عن أجادة اللاعبين لأنواع الارسال والدقة وضع الكرة في ساحة المنافس . وتمثل القياسات الانثروبومترية دوراً فعالا في لعبة التنس خاصة طول الإطراف وقوة الوثب والطول الكلي للجسم وكذلك النمط المميز للتنس وهو النحيف والعضلي وهو السائد خاصة في الارسال إذ يحتاج لاعب التنس ان يتميز في الطول والرشاقة وقوة القفز عالياً اثناء الارسال المستقيم . فضلا عن ان قياسات الجسم المتمثلة بالوزن الخفيف نسبة إلى مرحلة القفز ومن هنا تبرز أهمية البحث في تناول القياسات الجسمية بدراسة من خلال منهج وصفي يجمع بين القياسات الجسمية ودقة الارسال المستقيم في التنس الارضي

1-2 مشكلة البحث

بالنظر لأهمية القياسات الجسمية وتأثيراتها على الأنشطة الرياضية والألعاب المختلفة ومن خلال ما شاهدناه ان هناك قصورا في اهتمام بعض المدربين لأهمية القياسات الجسمية والجانب البدني وتأثيره بدقة الارسال المستقيم بالتنس الارضي .من هنا يبرز التسأول التالي حول العلاقة الجدية في دقة الارسال المستقيم بالتنس الارضي فضلا عن العتلات والروافع النا تجة عن أطوال أجزاء الجسم وخاصة الإطراف العليا ومن هنا تبرز مشكلة البحث في تناول القياسات الجسمية من خلال منهج وصفي يجمع بين القياسات الجسمية ودقة الارسال المستقيم في التنس الارضي

1-3 هدفا البحث

1-التعرف على بعض القياسات الجسمية السائدة لدى لاعبي فريق كلية التربية الرياضية في خانقين

2-التعرف على نوعية العلاقة بين بعض القياسات الجسمية بدقة الارسال المستقيم لدى لاعبي فريق كلية التربية الرياضية في خانقين

1-4- فروض البحث

1-4-1 هناك علاقة ذات دلالة إحصائية بين القياسات الجسمية ودقة الارسال المستقيم بالتنس الارضي

1-5 مجالات البحث

1-5-1 المجال البشري :لاعبي منتخب كلية التربية الرياضي في خانقين لعام 2017-2018 و هم عشرة لاعبين

1-5-2 المجال المكاني :القاعة الرياضية لكلية التربية الرياضية في خانقين

1-5-3 المجال الزماني : 15/2/ 2018 ولغاية 15\ 4\2018

2-1-الإطار النظري

2-1-1مدخل تأريخي للقياسات الجسمية واستخداماتها :

ان من الأمور البديهية عند محاولة دراسة إي موضوع يجب التوغل في أعماقه التاريخية .

كي نتمكن من سبر أغواره واستيعاب مضامينه وما وصل آلية اليوم .فعلى الرغم من المفهوم الحديث للقياس ،ألا أن الإنسان القديم مارسه بالعديد من الهيئات ابتداءا منت المرحلة البدائية الفطرية حتى وقتنا هذا ،إذ أن الأساليب المستخدمة قديما كانت من النوع الخام عند موازنتها بما وصل آلية القياس حديثا ،إذ لم يكن من الممكن التخلص من الذاتية وقد استمر الحال كذلك إلى وقت متأخر نسبياً.

ويرجع الاهتمام بقياسات جسم الإنسان إلى العصور القديمة ،فقد استخدم السومريون و الإغريق أقدامهم كوحدة لقياس ساحات الجري على وفق المقاييس السائدة (الشبر والذراع والفتر)في ذلك الوقت التي لم يتفق على دقتها في القياس لاختلافها من فرد إلى أخر

،في حين ان المصريين القدماء استخدموا طول الإصبع الوسطى لليد كوحدة للقياس كما قاموا بتقسيم الجسم إلى 19 جزءا متساويا ،كما كان كل من الرسامين والنحاتين وذوي الاختصاص في الرياضيات من الهنود القدماء متفقين على ضرورة إيجاد جزء من أجزاء الجسم يمكن الاعتماد علية كوحدة قياس لكل أجزاء الجسم الأخرى فنجدهم قد قسموا الجسم إلى 480جزءااما الإغريق القدماء فقد اهتموا بالمقاييس الجسمية وكانت لهم محاولات رائدة في هذا المجال، إذ عدت معايير الجسم المثالي هي مقاربة لقياسات أجسام الآلهة التي صورت على هيئة تماثيل جميلة ولكنها ضخمة ومع مرور الوقت تراجعوا عن هذه النظرة وعدوا الرجل الرشيق الخفيف الوزن هو الرجل المثالي فالمهارة والرشاقة أصبحتا أكثر أهمية من القوة

وكان القياس الجسمي مؤشر الاهتمام باللياقة البدنية ويرجع ذلك إلى القرن السابع عشر وأبان النهضة الصناعية في أوربا في القرن الثامن عشر ونظرا للتطور الذي شمل الحياة كلها من المتغيرات سريعة وتقدم علمي وفني ازداد الاهتمام بالمقاييس الجسمية،إذ يعد رينولدز وهو احد الرسامين فضلا عن انه أول من شجع هذا الاتجاه واهتم به في العصر الحديث ففي عام 1854م اقترح الألماني كراش لأول مرة استخدام بعض الأسس التشريحية لتحديد العلاقات النسبية بين أجزاء الجسم المختلفة وقد استخدم طول الكف.

وفي العام نفسه قام الألماني كارلوس باستخدام العمود الفقري كوحدة للقياسات الجسمية ،حين قسم العمود الفقري إلى 24 جزءا على وفق عدد الفقرات محددا لها قيما متساوية

اما في العام 1961 فظهر للمرة الأولى في أمريكا الاهتمام بالقياسات الجسمية ،ويعد العالم ادوارد هتشكوك أبا روحيا للقياس في التربية الرياضية وقد استخدم القياسات الجسمية في القرن الثامن عشر عام 1800م وكان طبيبا بشريا وقد انصبت اهتماماته على تناسق الجسم البشري والتمرينات التعويضية للجسم ثم توالت البحوث والدراسات وظهر علماء آخرين مثل سارجنت بجامعة هارفد جاليون وهيرقل في الدنمارك وكي في السويد وجربلير في المانيا وبوديش وجودارد في الولايات المتحدة الأمريكية .

ومن الجدير بالذكر ان أول من قام بدراسة أنماط الأجسام هو ابقراط ويعد رائدا في هذا المجال ويرجع ذلك 400 قبل الميلاد . وان أول استخدام لجهاز السكن فولد كاليبر عام 1051م لقياس سمك ثنايا الجلد وتقير نسبة الدهون في الجسم. من الملاحظ ان المتتبع لتاريخ القياسات الجسمية يجد ان الهدف من ذلك التطور كان لأغراض علمية و عملية تطبيقية لكل من

الفنانين والمهتمين في مجال صنع الملابس ،ومع تطور وتعقد الحياة أصبحت القياسات الجسمية أكثر أهمية وأوسع استخداما ولا سيما بالنسبة للمهندسين المختصين في وضع التصميمات الخاصة وصنع الأجهزة والأدوات اللازمة للإنسان ومنها الأجهزة الرياضية ، وكذلك الأطباء في مختلف اختصاصاتهم العلاجية والتقويمية .كما تستخدم مجموعة من القياسات الجسمية للمفاضلة بين مجموعة من الأفراد عند العمل في بعض الميادين ومنها الميدان الرياضي لاختيار وانتقاء اللاعبين للفعاليات الرياضية المختلفة وصولا بهذا الانتقاء للمستويات العليا.

2-1-2 مفهوم القياسات (الانثروبومترية) :

والقياسات الانثروبومترية ذات أهمية كبيرة في تقويم نمو الفرد ،والتعرف على الوزن والطول في المراحل السنية المختلفة ، ويعد احد المؤشرات التي تعبر عن حالة النمو عند الأفراد .كما ان للقياسات الانثروبومترية علاقات عالية بالعديد من المجالات الحيوية ، فالنمو الجسماني له علاقة بالصحة والتوافق الاجتماعي والانفعالي ، كما ان له علاقة بالتحصيل والذكاء وهناك علاقة بين النمو الجسمي والنمو العقلي للأطفال السويون جسميا.اما بالنسبة للمجال الرياضي فقد ثبت ارتباط المقاييس الجسمية بالعديد من القدرات الحركية والتفوق في الأنشطة المختلفة ...فقد أثبتت بعض البحوث ان هناك علاقة طردية بين قوة القبضة والطول والوزن ، كما اثبت كيورتن ان الرياضيين في بعض الألعاب يتميزون عن أقرانهم العاديين في العديد من المقاييس الجسمية كطول الجذع وعرض الكتفين وضيق الحوض

يعرف الباحثان إجرائيا القياسات الجسمية :هي الأبعاد البدنية التي يمتلكها الإنسان التي تدل على كتلة الجسم وأجزاءه فهي وصفا له ، وهي نتاج العوامل الوراثية والبيئية التي يمكن أن يتميز بها الإنسان عن غيره.لقد أصبح من الأهمية توفر الأجسام المناسبة كأحد الأساسيات الواجب توافرها للوصول باللاعب إلى أعلى المستويات الرياضية الممكنة .فالمدرب مهما بلغت مقدرته الفنية لن يستطيع ان يعد بطلا من أي جسم ، وان يختار القياسات المناسبة قبل محاولة التدريب .ومن هذا المنطق فأن السعي لمعرفة السمات البدنية للألعاب والمسابقات المختلفة سيقدم فائدة كبيرة للمدربين والمعنيين في اختيار العناصر المناسبة التي يمكن ان تثمر فيها جهودهم وبذلك يتحقق الاقتصاد في الجهد والوقت والمال .

3-1-2 القياسات الجسمية الانثروبومترية في المجال الرياضي :

أ-العمر

ب-الطول

-الطول الكلي للجسم.

-طول الذراع.

-طول الكف .

-طول الطرف السفلي.

-طول الساق والفخذ .

-طول القدم .

- طول الجذع .

- طول الطرف العلوي

ج- الوزن

د-الأعراض وتتضمن :

-عرض المنكبين .

-عرض الصدر .

- عرض الحوض .

- عرض الكف و القدم .

- عرض جمجمة الرأس.

ه-المحيطات وتتضمن :

- محيط الصدر.

- محيط الوسط .

- محيط الحوض .

- محيط مفصلي المرفق والفخذ .

- محيط العضد .

-محيط الفخذ .

- محيط سمانة الساق .

-محيط الرقبة.

و- ألأعماق وتتضمن :

- عمق (سمك)الصدر.

- عمق الحوض .

- عمق البطن .

-عمق الرقبة .

ز -قوة القبضة .

ح- السعة الحيوية .

ط- سمك الدهن .

4-1-2 شروط وطرق القياس الانثروبومتري :

ان للعمل في مثل هذا المجال (القياسات الجسمية)يرى الباحثان انه يتطلب من القائمين بالعمل الإلمام التام بشروط وطرق القياس ومعرفة النقاط التشريحية التي يتم عندها القياس لأجراء قياسات دقيقة وعلمية والتي يمكن من خلالها استخراج معايير للتميز ،المقارنة ، الاختيار والانتقاء ،...الخ من أهداف القياس المتعددة .

وهناك شروط للقياس الانثروبومتري الناجح هي :

1-المعرفة التامة بالنقاط التشريحية التي تحدد أماكن القياس .

2-الإلمام التام بالأوضاع التي يتخذها المختبر أثناء القياس .

3-الإلمام التام بطرق استخدام الأجهزة المستعملة في القياس.

ولكي يحقق القياس الدقة المطلوبة منة يجب ان تراعي النقاط التالية :

أ-نظرا لتأثر بعض القياسات الجسمية بدرجة الحرارة (كالطول مثلا)، وجب توحيد ظروف القياس لجميع المختبرين (الزمن و درجة الحرارة) .

ب-توحيد القائمين بالقياس قدر الإمكان .

ج-توحيد الأجهزة المستخدمة في القياس .

د- تجريب الأجهزة المستخدمة في القياس للتأكد من صلاحيتها .

الأطوال:

لضمان أداء القياسات المتعلقة بالا طوال يجب ان يلم المحكمون بالنقاط التشريحية التي يتم عندها القياس بالنسبة للأطوال وهي :

1-اعلي نقطة في الجمجمة

2-الحافة الوحشية للنتوء الاخرومي

3-الحافة الوحشية للرأس السفلي لعظم العضد

4-النتوء الابري لعظم الكعبرة

5-النتوء المرفقي

6-النتوء الابري لعظم الزند

7-منتصف عظمة القص

8-الحافة الوحشية لعظم الحرقفة

9-مفصل الارتقاق العاني

10-المدور الكبير للرأس العليا لعظم الفخذ

11-الحافة الوحشية لمنتصف مفصل الركبة

12-البروز الانسي للكعب

13-البروز الوحشي للكعب

الطول الكلي للجسم :

يستخدم لقياس الطول الكلي جهاز الرستاميتر ،وهو عبارة عن قائم مثبت عموديا على حافة قاعدة خشبية ، والقائم طوله (250)سم ، بحيث يكون الصفر في مستوى القاعدة الخشبية ،كما يوجد حامل مثبت أفقيا على القائم بحيث يكون قابلا للحركة للأعلى والأسفل .يقف المختبر على القاعدة الخشبية وظهره مواجه للقائم بحيث يلامسه في ثلاث نقاط هي المنطقة الواقعة بين اللوحين ، وابعد نقطة لسمانة الساقين ، ويجب ان يراعي المختبر شد الجسم للأعلى ، والنظر للإمام .يتم إنزال الحامل حتى يلامس الحافة العليا للجمجمة حيث يعبر الرقم المواجه للحامل على طول المختبر.

طول الذراع :

يستخدم شريط القياس (بالسنتمتر أو البوصة)لقياس طول الذراع وذلك ان الحافة الوحشية للنتوء الاخرومي حتى نهاية الإصبع الأوسط وهو مفتوح .

طول العضد :

يتم قياس طول العضد باستخدام شريط القياس من الحافة الوحشية للنتوء الاخرومي حتى الحافة الوحشية للرأس السفلي لعظم العضد .

طول الساعد :

يتم قياس طول الساعد باستخدام شريط القياس اما من النتوء المرفقي لعظم الزند وحتى النتوء الابري لنفس العظم ،أو من اعلي نقطة في رأس عظم الكعبرة حتى النتوء الابري العظم .

طول الكف :

يتم قياس طول الكف باستخدام شريط القياس من منتصف الرسغ حتى نهاية الإصبع الأوسط وهو ممدود

طول الطرف السفلي :

يتم قياس طول الطرف السفلي من المدور الكبير للرأس العليا الفخذ حتى الأرض.

2-1-5 القياسات الجسمية وأهميتها في المجال الرياضي :

تعد القياسات الجسمية مؤهلات خاصة لدى الأفراد يمكن الاستدلال عليها رقميا وتتميز بالاستقرار النسبي ولها علاقة كبيرة بالتطور في مختلف الألعاب الرياضية ،إذ ان للقياسات الجسمية أهمية واضحة عند أداء إي نشاط رياضي ،لأن اللاعبين يؤدون الحركات الرياضية بأجسامهم المختلفة في قياسا تها من فرد إلى آخر مما يؤدي ذلك إلى اختلاف مستوى الأداء .

ومما لاشك فيه ان القدرة على أداء الحركات الرياضية تعتمد على ملائمة المقاييس الجسمية للاعب للقيام بمتطلبات ذلك الأداء الممارس .فأن لهذه القياسات تأثيرا في ظهور القوة العضلية والسرعة والتحمل والمرونة وكذلك تجاوب جسم اللاعب لمختلف الظروف المحيطة به ، وزيادة كفايته البدنية ، وتحقيق النتائج الرياضية الباهرة.

- **3- منهج البحث وإجراءاته الميدانية :**

3-1 منهج البحث:

ان مناهج البحث العلمي هي التي تبين الطريقة العلمية التي يتبعها الباحث في بحثه إذ إنَّ المنهج العلمي هو "أسلوب للتفكير والعمل يعتمده الباحث لتنظيم أفكاره وتحليلها وعرضها ومن ثم الوصول الى نتائج وحقائق معقولة حول الظاهرة موضوع الدراسة"(1).

لذا استخدم الباحث المنهج الوصفي باسلوب دراسة العلاقات الارتباطية وتهتم هذه الدراسة "بالكشف عن العلاقات بين متغيرين او اكثر لمعرفة مدى الارتباط بين هذين المتغيرين والتعبير عنها بصورة رقمية " (1)" وتم اختيار العينة بصورة عمدية .

(1) . ربحي مصطفى عليان (وآخرون) ؛ مناهج وأساليب البحث العلمي ، ط1 .عمان: دارصفاء للنشر والتوزيع ، 2000 ، ص53.

2-3 مجتمع البحث وعينته :

1-2-3 مجتمع البحث:

" مجتمع البحث هو جميع الأفراد أو الأشخاص أو الأشياء الذين يكونون موضوع مشكلة البحث" (1) لذلك حدد الباحث مجتمع البحث والمتمثل بلاعبي المنتخب كلية التربية الرياضية في خانقين.

2-2-3 عينة البحث:

تعرف العينة بانها "مجموعة من الوحدات أو المشاهدات التي يتم أخذها من مجتمع البحث بطرق مختلفة يطلق عليها اسم طرق المعاينة "(2) ، وبناءً على هذا فقد كانت عينة البحث تشتمل على 10 لاعبين من لاعبي المنتخب كلية التربية الرياضية في خانقين , و من اجل الحصول على القياسات والنتائج المطلوبة في البحوث البايوميكانيكية يجب اختيار عينة البحث بالطريقة العمدية، إذ إن العينة العمدية "يكون الاختيار فيها على أساس حر من قبل الباحث وبحسب طبيعة بحثه ، بحيث يحقق هذا الاختيار هدف الدراسة أو أهداف الدراسة المطلوبة".(3) , وقد اشتملت عينة البحث على لاعبين يمثلون المنتخب كلية التربية الرياضية في خانقين.

3-3- وسائل جمع المعلومات : من أجل الوصول إلى نتائج البحث تم استخدام بعض القياسات الجسمية واختيار الارسال المستقيم بالتنس الارضي والملاحظة العلمية المباشرة كوسائل لجمع المعلومات

3-3-1- القياسات الجسمية : قام الباحثان بأجراء عدد من القياسات الجسمية من خلال أتباع عدة شروط ذكرت في الإطار المرجعي .

3-3-2- تحديد القياسات المستخدمة : قام الباحثان بالاطلاع عل مجموعة من المصادر العلمية والانترنت لغرض التعرف على أهم القياسات الجسمية التي سوف يتضمنها البحث بعد ذلك قام الباحثان بعرض القياسات الجسمية (*) باستبيان على مجموعة من المختصين لبيان رأيهم حول أهم القياسات (*) وقد اقروا وأجمعوا على القياسات التالية :

1- **طول الجسم**

2- **وزن الجسم**

3- **طول الذراع**

4- **طول العضد**

5- **طول الساعد**

6- **طول الكف- -7- عرض الصدر 8- عرض الكتفين**

3-3-3- تم تحديداختبار دقة الارسال المستقيم بالتنس الارضي

---

(1). نوري ابراهيم الشوك ورافع صالح فتحي الكبيسي ؛ دليل الباحث لكتابة الابحاث في التربية الرياضية . المطبعة المركزية ,جامعة ديالى ,2004 , ص57 .

(2). زوغان عبيدان وآخران؛ البحث العلمي– مفهومة– أدواته– اساليبه. عمان, الأردن , دار مجدلاوي للنشر والتوزيع, 1982, ص105.

(3) . محمد نصر الدين رضوان ؛ الإحصاء اللابارامتري . القاهرة , دار الفكر للطباعة والنشر ، 1988 ، ص48.

(4) .عامر ابراهيم قنديلجي؛ البحث العلمي واستخدام مصادر المعلومات،ط1.عمان , دار البازوري العلمية للنشر والتوزيع, 1999, ص147.

2-6- اختبار جونس لقياس دقة مهارة الارسال[1]

اسم اختبار:

اختبار جونس لقياس دقة مهارة الارسال

الغرض من الاختبار:

قياس دقة الارسال .

تطبيق الاختبار

الاجراءات :

- يتم تخطيط منطقة الارسال كما هو موضح في شكل (13)
- يبلغ طول المنطقة المحصورة بين الشبكة والخط الاول (3) قدم والمنطقة التي تليها (12) قدم والمنطقة الثالثة (3) قدم , اما المنطقة الاخيرة فهي المسافة المتبقية بين خط الارسال والمنطقة الثالثة وقدرها (3) قدم ايضا (ويشمل هذا التخطيط منطقتي الارسال اليمين واليسار).
- يوضع حبل فوق الشبكة بارتفاع (10) قدم فوق الحافة العليا للشبكة لكي تتم مرور الكرة بين الشبكة والحبل.
- الكرة التي تمس الحبل أو الشبكة وتسقط في الملعب تعاد ولا تحتسب محاولة فاشلة ،
- يحسب لكل لاعب عشرة محاولات ناجحة.

كيفية تسجيل الدرجات :

- عند سقوط الكرة في المنطقة الأولى يحصل اللاعب على (2) درجة ، أما سقوطها في المنطقة الثانية فيحصل على (4) درجة والمنطقة الثالثة (5) درجات أما المنطقة الأخيرة فيحصل على (6) درجات .

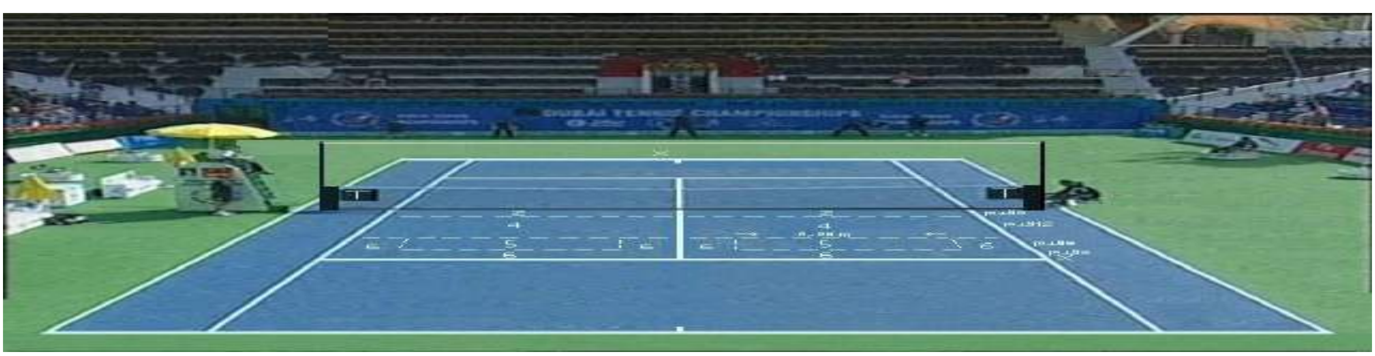

شكل (1) يوضح اختبار جونس لقياس دقة مهارة الارسال

1[1]) Jones ,S.K, A .Measure of Tennis Serving Ability, 1,os Angles1987, p62.(

3-4 التجربة الاستطلاعية : للوقوف على الأسس العلمية لاختبارات الرئيسية قام الباحثان بتجربة استطلاعية بتاريخ 2018/3/28/ على عدد من لاعبي المنتخب .الغرض منها الوقوف على :

1- لتدريب الباحثان على إجراء القياسات الجسمية

2-معرفة الصعوبات والمعوقات التي قد تواجه الباحثان

3- مدى تفهم عينة البحث لاختيار والقياس

4- لمعرفة الفترة الزمنية التي يستغرقها الاختيار والقياس

3-5 التجربة النهائية : بعد اكتمال الإجراءات المطلوبة وتوفر الشروط التي أوضحت إجراء القياسات الجسمية المختارة واختيار الارسال المستقيم قام الباحثان بتنفيذ القياسات الجسمية واختيار الارسال المستقيم في القاعة الداخلية الرياضية لكلية التربية الرياضية في خانقين بتاريخ 2018/4/1.

3-6- الأجهزة والأدوات المستخدمة :استخدم الباحثان عددا من الأجهزة والأدوات المستخدمة وهي

1- ميزان طبي لقياس الوزن لأقرب نصف كيلو غرام والطول

2- شريط قياس بطول 3م لقياس الأطوال

3- كرة التنس مع المضارب- 4- بلفومتر لقياس الأعراض

5- استمارة تسجيل القياسات الجسمية- 6 - استمارة تسجيل دقة الارسال

3-7- الوسائل الإحصائية المستخدمة : استخدم الباحثان برنامج الإحصائي SPSS للحصول على النتائج الخاصة بالبحث وهي الوسط الحسابي والانحراف المعياري ومعامل الارتباط البسيط .

4 - عرض وتحليل ومناقشة النتائج

4-1 عرض بيانات الوسط الحسابي والانحراف المعياري لمتغيرات عينة البحث

جدول (1)يوضح الأوساط ألحسابية والانحرافات المعيارية

ت	المتغيرات	وحدة القياس	س—	+-ع
1	طول الجسم	المتر وأجزائه	182.6	6.90
2	وزن الجسم	كغم وأجزائه	71.6	12.97
3	طول الذراع	سم	78.7	4.68
4	طول العضد	سم	35	3.50
5	طول الساعد	سم	29.8	6.79
6	طول الكف	سم	21.20	1.03
7	مدى الكف	سم	22.3	2.08
8	عرض الصدر	سم	29.28	2.37
9	عرض الكتف	سم	45.2	2.68
10	التهديف الثابت	عدد	22.25	3.84

نلاحظ من خلال الجدول رقم (1) والخاص بالقياسات الجسمية والارسال المستقيم للاعبي منتخب كلية التربية الرياضية في خانقين إذ تبين أن الأوساط الحسابية والانحرافات المعيارية لمتغيرات القياسات الجسمية (طول الجسم ،وزن الجسم ،طول الذراع ،طول العضد ،طول الساعد ،طول الكف ،مدى الكف ،عرض الصدر ،عرض الكتف) إذ نلاحظ إن الأوساط الحسابية والقياسات الجسمية المذكورة على التوالي (182.6 ،71.6 ،78.7 ،35 ، 29.8 ، 21.20، 22.25 ،45.2 ،29.28) اما بالنسبة إلى الانحرافات المعيارية فقد كانت على التوالي (6.90 ، 12.97، 4.68 ، 3.50 ، 6.79، 1.08، 2.08 ، 2.68، 2.37)

جدول (2)يوضح قيمة r المحتسبة لمتغيرات عينة البحث

ت	القياسات الجسمية	قيمة r المحتسبة
1	طول الجسم	0.443
2	وزن الجسم	0.202
3	طول الذراع	0.252
4	طول العضد	0.10
5	طول الساعد	0.432
6	طول الكف	0.032
7	مدى الكف	0.451
8	عرض الصدر	0.44
9	عرض الكتف	0.45

قيمة r الجدولية عند درجة الحرية (10) تساوي (0.576) عند مستوى الدلالة (0.05)

من خلال جدول (2) الخاص بالعلاقة الارتباطية بين القياسات الجسمية ودقة الرسال المستقيم يرى الباحثان بأن هناك ارتباط غير معنوي بين القياسات الجسمية المشمولة بالبحث وهي (طول الجسم ، وزن الجسم ، طول الذراع ، طول العضد ،طول الساعد ، طول الكف ، مدى الكف ، عرض الصدر، عرض الكتف) وبين الارسال المستقيم إذ نلاحظ ان قيم r المحتسبة للقياسات الجسمية هي اقل من قيمة r الجدولية عند مستوى المعنوية 0.05 وبدرجة حرية 10 (ن - 2)

ويعزو الباحثان عدم تأثير القياسات الجسمية التي سبق ذكرها في نجاح الارسال المستقيم من المحتمل ان تكون هناك علاقة ضعيفة بين القياسات الجسمية المذكورة الارسال المستقيم والسبب الرئيسي بذلك يعود إلى فاعلية التدريب على دقة الارسال المستقيم في الوحدات التدريبية والممارسة الكثيرة التي تؤدي إلى تثبيت مهارة الارسال المستقيم أكثر من تدخل القياسات الجسمية عليها .

5 -1 الاستنتاجات :

1- عدم وجود ارتباط معنوي بين القياسات الجسمية (طول الجسم ، وزن الجسم ، طول الذراع ، طول الساعد ، طول العضد ، طول الكف ، مدى الكف ، عرض الصدر ، عرض الكتف) ومهارة الارسال المستقيم للاعبي منتخب كلية التربية الرياضية في خانقين .

2-5 - التوصيات :

1- التأكيد في البرامج التدريبية للاعبين الذين لديهم ضعف في مهارة الارسال المستقيم

2-التأكيد على زيادة نسبة الارسال المستقيم في الوحدات التدريبية للاعبين بغرض تطويرها وتثبيتها

3- إجراء بحوث مشابهة للقياسات الجسمية التي لم يتناولها الباحثان في هذا البحث لتأكيد تأثيرها أو عدم تأثيرها في مهارة الارسال المستقيم

المصادر

1- إبراهيم ، مروان عبد المجيد (1999) : الاختبارات والقياس والتقويم في التربية الرياضية ، ط2، دار الفكر للطباعة والنشر والتوزيع ، القاهرة .

2- إبراهيم مروان عبد المجيد(2001) : تصميم وبناء اختبارات اللياقة البدنية باستخدام طرق التحليل العاملي ،ط1 ،مؤسسة الوراق للنشر ، عمان .

3- بسطويسي ، احمد بسطويسي (1999) : أسس ونظريات التدريب الراضي ، ط1 ، الفكر العربي، القاهرة

4- جواد ، علي سلوم (2004) : الاختبارات والقياس والإحصاء في المجال الرياضي ، جامعة القادسية .

5- حسانين محمد صبحي (1996) : القياس والتقويم في التربية الرياضية ، ج2 ، ط3 ، دار الفكر العربي ، القاهرة .

6- حسانين محمد صبحي(1987) : التقويم والقياس في التربية البدنية ج2 ، ط2 ، دار الفكر العربي، القاهرة

7- حمودة ، محمد خالد عبد القادر (1991) : تحديد بعض القياسات الانثروبومترية للاعبي الفريق العماني لكرة اليد ، المجلة العلمية للتربية البدنية والرياضية ، العدد التاسع ، : عمان

8- رضوان ، محمد نصر الدين(1997) :المرجع في القياسات الجسمية ، ط1 دار الفكر العربي، القاهرة .

9- الصميدعي ، لؤي غانم وآخرون (2010): الإحصاء والاختبار في المجال الرياضي ، ط1 ، اربيل .

10- كامل طه لويس سنة (1981) : علم النفس الرياضي ، دار الكتاب للطباعة والنشر ، الموصل .

11- محمد حسن أبو عبية (1964) : كرة السلة الحديثة ، مطبعة المصري ، القاهرة .

12- محمد حسن علاوي (1969): علم النفس في التدريب الرياضي، دار المعارف، مصر، القاهرة.

13- مصطفى محمد زيدان (1989) : كرة السلة للمدرس والمدرب ، دار الفكر العربي ، القاهرة .

14- الياسري ، محمد جاسم (2010) : القياس والتقويم في التربية البدنية ،ط1 ،جامعة بابل .

15- يوسف البازي ومهدي نجم (1975) : تكتيك في كرة السلة ، مطبعة واو فيست التحرير ، بغداد.

م /استبيان

السيد الخبير ......المحترم

يروم الباحثان إجراء البحث الموسوم (بعض القياسات الجسمية وعلاقتها بدقة الارسال المستقيم في لعبة التنس الارضي)لمنتخب كلية التربية الرياضية في خانقين ولكونكم من ذوي الخبرة والاختصاص وخدمة البحث العلمي يرجى إبداء رأيكم في تحديد أهم القياسات الجسمية الخاصة لمهارة الارسال المستقيم بالتنس الارضي

مع جزيل الشكر والتقدير ....

ملاحظة

يرجى وضع علامة (√) أمام الاختبار الذي تقترحونه

الاسم :

الدرجة العملية :

الاختصاص :

التاريخ :

الباحثان

ملحق (1)

استمارة اختيار القياسات الجسمية الخاصة بالبحث

ت	القياسات الجسمية	يصلح	لا يصلح	الملاحظات
1	الطول الكلي			
2	الوزن			
3	طول الذراع			
4	طول الساعد			
5	طول العضد			
6	طول الكتف			
7	مدى الكف			
8	محيط الصدر			
9	محيط الكتفين			
10	محيط البطن			
11	محيط الورك			
12	محيط العضد			
13	محيط العضد			
14	محيط الركبة			
15	محيط الفخد			
16	طول الطرف السفلي			
17	طول الفخد			
18	طول الساق			

أي قياس أخر تقترحونه

م /استبيان

السيد الخبير ......المحترم

يروم الباحثان إجراء البحث الموسوم (بعض القياسات الجسمية وعلاقتها بدقة الارسال المستقيم بالتنس الارضي) لمنتخب كلية التربية الرياضية في خانقين ولكونكم من ذوي الخبرة والاختصاص وخدمة البحث العلمي يرجى إبداء رأيكم في تحديد أهم الاختبارات الخاصة لمهارة الارسال المستقيم بالتنس الارضي

مع جزيل الشكر والتقدير ....

ملاحظة

يرجى وضع علامة (√) أمام الاختبار الذي تقترحونه

الاسم :

الدرجة العملية :

الاختصاص :

التاريخ :

الباحثان

ttp://jgu.garmian.edu.krd https://doi.org/10.24271/garmian.346

Padovan Numbers by the Permanents of a Certain Complex Pentadiagonal Matrix

Diyar O.Mustafa Zangana[1] Ahmet Öteleş[2]

[1]Siirt University, Faculty of Science, Department of Mathematics, TR-56100, Siirt, Turkey
diyar.math2@gmail.com
[2]Dicle University, Education Faculty, Department of Mathematics, TR-21280, Diyarbakir/Turkey
aoteles85@gmail.com

Abstract

In this paper, we consider a certain type of complex pentadiagonal matrices. Then we show that the permanents of this matrix generate Padovan numbers. Finally, we give a Maple procedure in order to verify our result.

***Keywords*:** Permanent, Pentadiagonal matrix, Padovan number.

1. Introduction

The famous integer sequences (e.g., Fibonacci, Lucas, Padovan) provide invaluable opportunities for exploration, and contribute handsomely to the beauty of mathematics, especially number theory [1, 2]. Among these sequences, Padovan numbers have achieved a kind of celebrity status. The Padovan sequence $\{P(n)\}$ is defined by the recurrence relation, for $n > 2$

$$P(n) = P(n-2) + P(n-3)$$

with $P(0) = P(1) = P(2) = 1$[3]. The number $P(n)$ is called n^{th} Padovan number. The Padovan numbers are

$$1, 1, 1, 2, 2, 3, 4, 5, 7, 9, 12, 16, 21, 28, 37, 49, \ldots$$

for $n = 0, 1, 2, \ldots$ This sequence is named as A000931 in [4].
The permanent of a $n \times n$ matrix $A = (a_{ij})$ is defined by

$$\mathrm{Per}(A) = \sum_{\sigma \in S_n} \prod_{i=1}^{n} a_{i\sigma}(i)$$

where the summation extends over all permutations σ of the symmetric group S_n. Thepermanent of a matrix is analogous to the determinant, where all of the signs used in theLaplace expansion of minors are positive.
Permanents have many applications in physics, chemistry, graph theory, electrical engineering, and so on [5, 6, 7, 8, 9]. One of the most important applications of permanents is the relationship between some special types of matrices and the well-known number sequences. There are many papers in relation to that applications. [10, 11, 12, 13, 14, 15, 16, 17, 18, 19, 20, 21, 22, 23, 24] are some of them.
In this paper, we consider a certain type of complex pentadiagonal matrices. Then we show that the permanents of this matrix generate Padovan numbers. Finally, we give a Maple procedure in order to verify our result.

2. Main Results

Let $A = [a_{ij}]$be an $m \times n$ real matrix with row vectors $a_1, a_2, \dots, a_m$. We say A iscontractible on column(resp. row) k if column (resp. row) kcontains exactly twonon-zero entries. Suppose A is contractibleon column k with $a_{ik} \neq 0 \neq a_{jk}$ and $i \neq j$. Then the $(m-1) \times (n-1)$matrix $A_{ij:k}$ obtained fromA by replacing row i with $a_{jk}\alpha_i + a_{ik}\alpha_j$ and deleting row j and column k is called the contraction of A on column k relative to rows i and j. If A is contractible on row $a_{ki} \neq 0 \neq a_{kj}$ and $i \neq j$, then the matrix $A_{k:ij} = \left[A_{ij:k}^{T}\right]^{T}$ is called the contraction of A on row k relative to columns i and j. We say that A can be contracted to a matrix B if either $B = A$ or there exist matrices $A_0, A_1, \dots, A_t$ $(t \geq 1)$ such that $A_0 = A$, $A_t = B$, and A_r is a contraction of A_{r-1} for $r = 1, \dots, t$ [6].

Brualdi and Gibson [6] proved the following result about the permanent of a matrix.
Lemma 1 LetA be a nonnegative integral matrix of order n for $n > 1$ and let B be a contraction of A. Then

perA = perB. (1)

Let $H_n = h_{ij}$ be an $n \times n$ pentadiagonal matrix as the following

$$A = \begin{pmatrix} 1 & i & -1 & 0 & \cdots & \cdots & 0 \\ -i & 0 & i & -1 & 0 & & \vdots \\ 0 & -i & 0 & i & \ddots & \ddots & \vdots \\ \vdots & 0 & \ddots & \ddots & \ddots & \ddots & 0 \\ \vdots & & \ddots & \ddots & \ddots & i & -1 \\ \vdots & & & 0 & -i & 0 & i \\ 0 & \cdots & \cdots & \cdots & 0 & -i & 0 \end{pmatrix}_{n\times n} . \qquad (2)$$

where $i = \sqrt{-1}$. If $n = 5$, then we obtain the permanent of H_5 by using Laplace
expansion as the following

$$\mathrm{Per}H_5 = \mathrm{Per} \begin{pmatrix} 1 & i & -1 & 0 & 0 \\ -i & 0 & i & -1 & 0 \\ 0 & -i & 0 & i & -1 \\ 0 & 0 & -i & 0 & i \\ 0 & 0 & 0 & -i & 0 \end{pmatrix}_{5\times 5}$$

$$= \mathrm{Per}\begin{pmatrix} 0 & i & -1 & 0 \\ -i & 0 & i & -1 \\ 0 & -i & 0 & i \\ 0 & 0 & -i & 0 \end{pmatrix} + (-1)\mathrm{Per}\begin{pmatrix} i & -1 & 0 & 0 \\ -i & 0 & i & -1 \\ 0 & -i & 0 & i \\ 0 & 0 & -i & 0 \end{pmatrix}$$

$$= (-i)\mathrm{Per}\begin{pmatrix} i & -1 & 0 \\ -i & 0 & i \\ 0 & -i & 0 \end{pmatrix} + \mathrm{Per}\begin{pmatrix} 0 & i & -1 \\ -i & 0 & i \\ 0 & -i & 0 \end{pmatrix} - \mathrm{Per}\begin{pmatrix} -1 & 0 & 0 \\ -i & 0 & i \\ 0 & -i & 0 \end{pmatrix}$$

$$= \mathrm{Per}\begin{pmatrix} 0 & i \\ -i & 0 \end{pmatrix} - \mathrm{Per}\begin{pmatrix} -1 & 0 \\ -i & 0 \end{pmatrix} + (-i)\mathrm{Per}\begin{pmatrix} i & -1 \\ -i & 0 \end{pmatrix} + \mathrm{Per}\begin{pmatrix} 0 & i \\ -i & 0 \end{pmatrix}$$

$$= 1 - 0 + 1 + 1 = 3 = P(5).$$

By the contraction method introduced by Brualdi in [6], we now present the following theorem that gives the relationship between the permanent of the pentadiagonal matrix H_n and the Padovan number P (n).

Theorem 2 Let H_n be the $n \times n$ pentadiagonal matrix given by (2). Then the permanent of the matrix is equal to the n^{th} Padovan number P (n).

Proof. Let H_n^k be the k^{th} contraction of $H_n, 1 \leq k \leq n-2.$ Since the definition of the matrix H_n; thematrix $H_n$can be contracted on column 1 so that

$$H_n^1 = \begin{pmatrix} 1 & 2i & -1 & 0 & \cdots & \cdots & 0 \\ -i & 0 & i & -1 & 0 & & \vdots \\ 0 & -i & 0 & i & \ddots & \ddots & \vdots \\ \vdots & 0 & \ddots & \ddots & \ddots & \ddots & 0 \\ \vdots & & \ddots & \ddots & \ddots & i & -1 \\ \vdots & & & 0 & -i & 0 & i \\ 0 & \cdots & \cdots & \cdots & 0 & -i & 0 \end{pmatrix}_{(n-1)\times(n-1)}$$

Since the matrix H_n^1 can be contracted on column 1

$$H_n^2 = \begin{pmatrix} 2 & 2i & -1 & 0 & \cdots & \cdots & 0 \\ -i & 0 & i & -1 & 0 & & \vdots \\ 0 & -i & 0 & i & \ddots & \ddots & \vdots \\ \vdots & 0 & \ddots & \ddots & \ddots & \ddots & 0 \\ \vdots & & \ddots & \ddots & \ddots & i & -1 \\ \vdots & & & 0 & -i & 0 & i \\ 0 & \cdots & \cdots & \cdots & 0 & -i & 0 \end{pmatrix}_{(n-2)\times(n-2)}$$

Furthermore, the matrix ${H_n}^2$ can be contracted on column 1 and
$P(3) = P(4) = 2, P(5) = 3$ so that

$$H_n^3 = \begin{pmatrix} 2 & 3i & -2 & 0 & \cdots & \cdots & 0 \\ -i & 0 & i & -1 & 0 & & \vdots \\ 0 & -i & 0 & i & \ddots & \ddots & \vdots \\ \vdots & 0 & \ddots & \ddots & \ddots & \ddots & 0 \\ \vdots & & \ddots & \ddots & \ddots & i & -1 \\ \vdots & & & 0 & -i & 0 & i \\ 0 & \cdots & \cdots & \cdots & 0 & -i & 0 \end{pmatrix}_{(n-3)\times(n-3)}$$

$$= \begin{pmatrix} P(4) & iP(5) & -P(3) & 0 & \cdots & \cdots & 0 \\ -i & 0 & i & -1 & 0 & & \vdots \\ 0 & -i & 0 & i & \ddots & \ddots & \vdots \\ \vdots & 0 & \ddots & \ddots & \ddots & \ddots & 0 \\ \vdots & & \ddots & \ddots & \ddots & i & -1 \\ \vdots & & & 0 & -i & 0 & i \\ 0 & \cdots & \cdots & \cdots & 0 & -i & 0 \end{pmatrix}_{(n-3)\times(n-3)}$$

Continuing this process, we have

$$H_n^k = \begin{pmatrix} P(k+1) & iP(k+2) & -P(k) & 0 & \cdots & \cdots & 0 \\ -i & 0 & i & -1 & 0 & & \vdots \\ 0 & -i & 0 & i & \ddots & \ddots & \vdots \\ \vdots & 0 & \ddots & \ddots & \ddots & \ddots & 0 \\ \vdots & & \ddots & \ddots & \ddots & i & -1 \\ \vdots & & & 0 & -i & 0 & i \\ 0 & \cdots & \cdots & \cdots & 0 & -i & 0 \end{pmatrix}_{(n-k)\times(n-k)}$$

for $3 \leq k \leq n-4$. Hence,

$$H_n^{n-3} = \begin{pmatrix} P(n-2) & iP(n-2) & -P(n-3) \\ -i & 0 & i \\ 0 & -i & 0 \end{pmatrix}_{3\times3}$$

which, by contraction of H_n^{n-3} on column 1, gives

$$H_n^{n-2} = \begin{pmatrix} P(n-1) & iP(n) \\ -i & 0 \end{pmatrix}_{2\times2}$$

By applying equation (1), we obtain $\mathrm{per}H_n = H_n^{n-2} = -i^2P(n) = P(n)$ which is desired

2.1. Maple Procedure

The following Maple procedure calculates the permanent of the pentadiagonal matrix H_n given by (2).

```
restart:
with(LinearAlgebra):
permanent:=proc(n)
```

```
local I,j,r,f,H;
f:=(i,j)->piecewise(i=1 and j=1,1,j-i=-1,-I,j-i=1,I,j-i=2,-1,0);
H:=Matrix(n,n,f):
for r from 0 to n-2 do
print(r,H):
for j from 2 to n-r do
H[1,j]:=H[2,1]*H[1,j]+H[1,1]*H[2,j]:
od:
H:=DeleteRow(DeleteColumn(Matrix(n-r,n-r,H),1),2):
od:
print(r,eval(H)):
end proc:with(LinearAlgebra):
permanent(n);
```

References

[1] T. Koshy, Fibonacci and Lucas Numbers with Applications, Wiley-Interscience, New York, 2001.

[2] T. Koshy, Fibonacci, Lucas, and Pell numbers, and Pascal's triangle, Mathematical Spectrum 43(3) (2011), 125-132.

[3] A. G. Shannon, P. G. Anderson, A. F. Horadam, Properties of Cordonnier, Perrin and Van der Laan numbers, International Journal of Mathematical Education in Science and Technology 37 (2006), 825-831.

[4] The OEIS Foundation Inc., The On-Line Encyclopedia of Integer Sequences, http://oeis.org, 2013.

[5] H. Minc, Permanents, Encyclopedia of mathematics and its applications, Addison-Wesley, New York, 1978.

[6] R. A. Brualdi, P. M. Gibson, Convex polyhedra of doubly stochastic matrices I: applications of the permanent function, J. Combin. Theory A 22 (1977), 194-230.

[7] R. A. Brualdi, D. Cvetkovic, A Combinatorial Approach to Matrix Theory and Its Applications, CRC Press, 2009.

[8] F. Harary, Determinants, permanents and bipartite graphs, Mathematics Magazine 42 (1969) 146-148.

[9] M. Marcus, H. Minc, Permanents, American Mathematical Monthly 72 (1965) 577-591.

[10] G. Y. Lee, S. G. Lee, and H. G. Shin, On the k-generalized Fibonacci matrix Q_k, Lin. Alg. Appl. 251 (1997) 73–88.

[11] G. Y. Lee, k-Lucas numbers and associated bipartite graphs, Lin. Alg. Appl. 320 (2000), 51–61.

[12] W. C. Shiu and Peter C. B. Lam, More on the generalized Fibonacci numbers and associated bipartite graphs, Int. Math. J. 3 (2003), 5–9.

[13] E. Kılıc¸ and D. Tascı, On families of bipartite graphs associated with sums of Fibonacci and Lucas numbers, Ars Combin. 89 (2008), 31–40.

[14] G. Y. Lee and S. G. Lee, A note on generalized Fibonacci numbers, Fibonacci Quart. 33 (1995), 273– 278.

[15] E. Kılıc¸ and D. Tascı, On the permanents of some tridiagonal matrices with applications to the Fibonacci and Lucas numbers, Rocky Mt. J. Math. 37 (2007), 1953–1969.

[16] M. Akbulak and A. Oteles¸, On the number of 1-factors of bipartite graphs, Math. Sci. Lett. 2 (2013), 1–7.

[17] A. Oteles¸, On the number of perfect matchings for some certain types of bipartite graphs, Filomat 31(2017), 4809–4818.

[18] K. Kaygisiz and A. Sahin, Determinants and permanents of Hessenberg matrices and generalized Lucas polynomials, Bull. Iranian Math. Soc. 39 (2013), 1065–1078.

[19] F. Yılmaz and D. Bozkurt, The adjacency matrix of one type of directed graph and the Jacobsthal numbers and their determinantal representation, J. Appl. Math. 2012 (2012), 1–14

[20] F. Yılmaz and D. Bozkurt, Some properties of Padovan sequence by matrix methods, Ars Combin. 104(2012), 149–160.

[21] C. M. da Fonseca, T. Sogabe, and F. Yılmaz, Lower k-Hessenberg matrices and k-Fibonacci, Fibonacci-p and Pell (p, i) number, Gen. Math. Notes 31 (2015), 10–17.

[22] E. Kılıc¸ and D. Tascı, On families of bipartite graphs associated with sums of generalized order-k Fibonacci and Lucas numbers, Ars Combin. 94 (2008), 13–23.

[23] E. Kılıc¸ and A. P. Stakhov, On the Fibonacci and Lucas p-numbers, their sums, families of bipartite graphs and permanents of certain matrices, Chaos Solitons Fractals 40 (2009), 10–21.

[24] P. Vasco, P. Catarino, H. Campos, A. P. Aires, and A. Borges, k-Pell, k-Pell-Lucas and modified k-Pell numbers: Some identities and norms of Hankel matrices, Int. J. Math. Anal. 9 (2015), 31–37.

ttp://jgu.garmian.edu.krd https://doi.org/10.24271/garmian.347

Phytogeographical Study of the Family Orobanchaceae in Kurdistan Region-Iraq

Sirwan Hassan Salih

Biology Department, College of Education, University of Garmian, Kalar, Kurdistan Region, Iraq

Email: herash1966@yahoo.com

Abstract

This study included a comprehensive survey of the north and northeast districts of Iraq, the ecology and geographical distribution of the Orobanchaceae species available in Iraqi Kurdistan regions in Duhok, Arbil and Sulaimani governorates were investigated, based on data collected from different sources, geographical distribution was made by the aid of prepared maps, ecological notes were pointed out regarding the different environmental types, species distribution of two genera (*Orobanche* L. *and Phelypaea* L**.**) of the family and two endemic species (*O. ovata* and *O. singarensis*) has been recorded, as well it was noted that the *O. aegyptiaca* Pers. is the most widely distributed specie (common species) and *Phelypaea coccinea* was the rare species.

Keywords: Phytogeography, Orobanchaceae, Kurdistan region-Iraq.

1. Introduction

Orobanchaceae (Broomrape family) widely distributed in warm and temperate area, about 90% of their species are old world natives and only about 10% of the species occur in the cold or hot regions (Thieret, 1971). It is obviously known that the plant spreading influenced by geographical and environmental conditions therefore the Orobanchaceae species show a high variation in their distribution in different environmental conditions. Ecological and geographical distribution of plants are clearly much relevance to plant taxonomy because each species or groups of plants are with a certain pattern of distribution which is one aspect of its definition. The aims of plant geography are to ascertain the essential features and recurrent patterns of the special distribution of plants and to discover their fundamental causes, which lie partly in their ecology. The data on geographical distribution of this study was obtained from some herbarial specimens that have been previously reported, literatures and personal field trip.

2. Materials and Methods:

The materials that were used as a data source are herbarial specimens(table 1), labels of major Iraqi herbaria (table 1), personal field trips in districts of MAM, MRO, MSU, FAR, FKI and FPF (figure 1,2), literatures and Iraqi plants lists that published by: Handle Mazzetti (1910); Zohary (1946); Blackelock (91949); Al-Rawi (1964); Khalaf (1980); Ridda and Daoud (1982); Faris (1983) and some Floras such as: Flora of Syria. Pal,. Sin. (Post, 1933); Flora Iranica (Parsa, 1949); Flora Lowland of Iraq (Rechinger, 1964); Flora Iranica (Rechinger, 1964); Flora of Turkey (Davis and et al, 1982). The altitudes were measured by altimeter while the taxonomic terminology were derived from Lawrence (991951); Guest, 1966; Al-Mussawi (1987); Al-Katib (1988). Geographical distribution was made by aid of prepared maps (figure 3, 4, 5) and it is focused on Iraqi Kurdistan regions (figure 2),

3. Results and Discussion:

3.1. Ecology and Geographical Distribution:

The results of this study showed that the species of two genera (*Orobanche* L. and *Phelypaea* L.) of the family Orobanchaceae in Iraq are distributed in Kurdistan region, three species of *Orobanche* are newly recorded for Iraq and species *Orobanche mutelii* is newly recorded for Kurdistan, so there are 12 species belongs to two genera distributed in Kurdistan region, species with large population as *O. aegyptiaca* due to it is grow on both wild and cultivated plants, while some species of *O. crenata*, *O. kurdica* and *O. ovata* are sparsely distributed, species *Phelypaea coccinea* and *O. arenaria* are rare in their distribution.

The Orobanchaceae species are obligatory parasite plants therefore the geographical distribution depended directly on the distribution of their hosts (wild and cultivated plants), *O. aegyptiaca* {figure 3, table 2} is the most widely distributed species extended in different environments and laces from Kifri (FKI), south of surveyed regions to Kany Massy near Zakho (MAM) north of included surveying regions, so the *O. aegyptiaca* was found in all districts which included in this investigation, it's altitude range 200-1700m; *O. anatolica* {figure 4, table 2} was dominated among examined species in Piramagrun and Azmer mountain (MSU), it's altitude range 900-1800m in rocky mountain; *O. arenaria* was newly recorded {figure 4, table 2} scarcely distributed in Piramagrun mountain (MSU), 1250-1550m altitude, it parasite on wild plants; *O. coelestis* (figure 5, table 2) spread in Piramagrun mountain (MSU) and Arbil (MRO), 750-1650 m alt., in rocky mountain; *O. crenata* (fig. 4, tab. 2) distributed in Duhok (MAM) and Piramagrun mountain (MSU), 900-1800m, parasites on wild plants; *O. kurdica* {figure 5, table 2} distribute with high density in Zakho and Duhok (MAM), Chuwarta and Piramagrun mountain (MSU), 900-1800m alt.; *O. minor* (new record)) (figure 4, table 2) scattered in Duhok (MAM) and Sartaky Bamou mountain (FPF), 1100-1750 m alt., it is only parasites on wild plants in rocky mountain; *O. mutelii* (newly recorded for Kurdistan) (figure 4, table 2) distributes in Kalar (FPF) in semi desert habitat, 200-450m, parasites on wild plants; *O. ovata* (endemic species) {figure 4, table 2} distributed in Piramagrun mountain (MSU) and Sere Hassan Beg (MRO), 1500-2000m, in rocky mountain, parasites on wild plants; *O. ramosa* (newly recorded) (figure 5, table 2) distributed in Zakho (MAM) and Erbil (MRO), 600-850 m, in hill, plateaus and Rocky Mountains, parasite on both wild and cultivated plants; *O. singarensis* (endemic species) (figure 5, table 2) distribute in Chuwarta and Piramagrun mountain (MSU) and Kalar (FPF) in addition to Sinjar mountain (FJS), 200-900m, it's habitats are plains and rocky mountains; *P. coccinea* (rare species) (figure 5, table 2)distribute only in a specific small area in Piramagrun mountain (MSU) 1500-2000m, parasite on wild plants, on the other hand the species *O. aegyptiaca*, *O. coelestis* and *O. mutelii* are distributes in another regions in mid and south of Iraq (according to the labels of herbarial specimens and of Iraqi plants lists) which are entirely different from their habitats with the habitats of Kurdistan in (climate, altitude, soil type and hosts). As well the results of (figure 6, 7) showed that the MSU district are the most districts where the species are spread (9 species) and the FKI is the less districts (1 species) and the most common species *O. aegyptiaca* are distributed in all six included districts and species of *P. coccinea*, *O. mutelii*, *O. crenata* and *O. anatolica* are less distributed species (1 district). The density of populations of studied species depended on densities of their hosts populations and somewhat on germination conditions and environments.

some of these species parasite on cultivated plants and others on wild plants while some species on both of them, likewise these species may be disappeared in their original places when their hosts are absent, consequently may cause to change the geographical distribution of these species from time to time,

Table (1) Herbaria which used their specimens during the study abbreviation follow Holmgren & Keuken 1989

BAG	Baghdad Iraq. College of Agriculture
BAH	Baghdad Iraq. National herbarium of Iraq
BUH	Baghdad, the university herbarium, college of Science, dept. of Biology
BUNH	Baghdad, Iraq. Natural history research center of Education University of Baghdad
BUE	Baghdad, Iraq. Dep. of biology, college of Education, University of Baghdad
SUH (ASUH)	Arbil, Iraq. College of Science, University of Salahaddin
ESUH	Erbil, Iraq. College of Education university of Salahaddin
MSUH	Mosul, Iraq. College of Science, University of Mosul

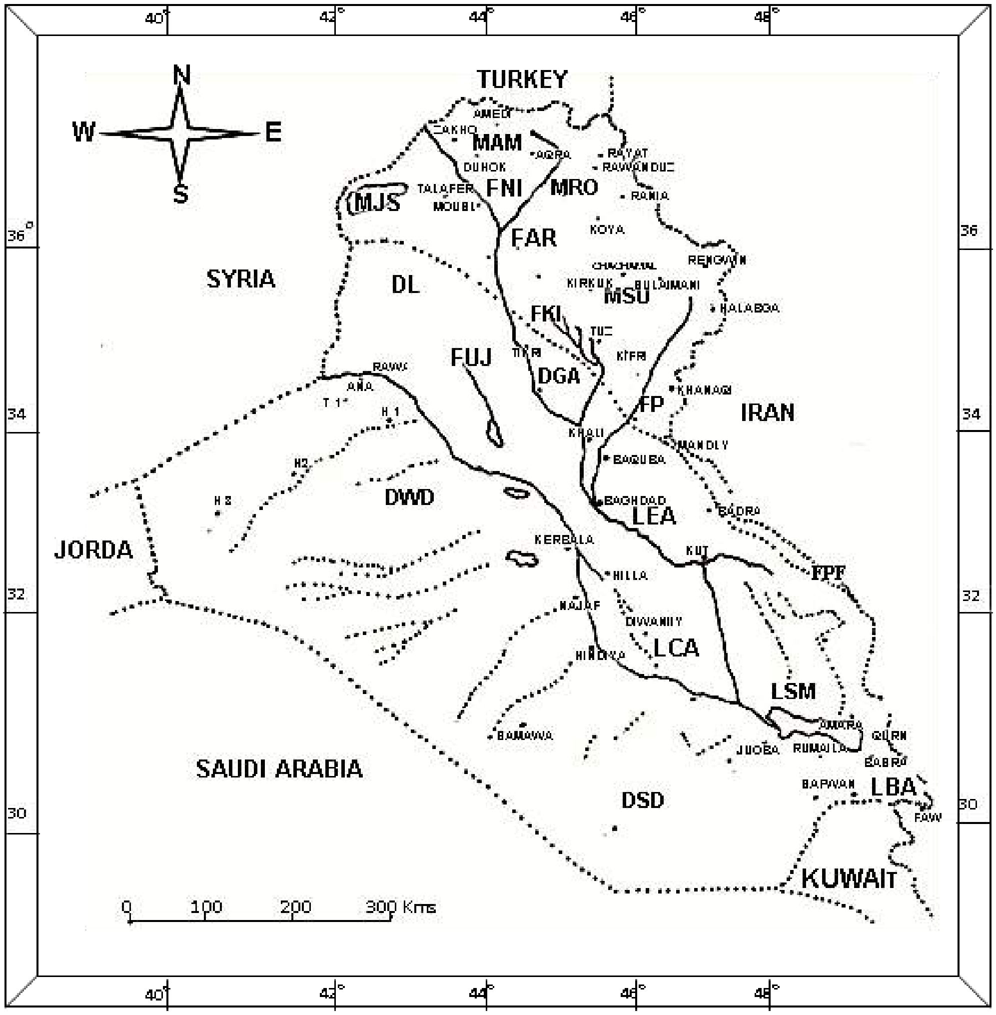

Figure (1) Physiographic regions and Districts map of Iraq

M - MOUNTAIN REGION

MAM - Amadiya District

MRO - Rowanduz District

MSU - Sulaimani District

MJS - Jabal Singar District

F - UPPER PLAINS AND FOOTHILLS REGION

FUJ- Upper Jaziera District

FNI- Nieneveh District

FAR- Arbil District

FKI- Kirkuk District

FPF- Persian District

D - LOWER PLATEAU REGION	L - LOWER MESOPOTAMIAN REGIO
DLJ - Lower Jaziera District	LEA- Eastern Alluvial Plain District
DGA- Ghurfa - Adhaim District	LCA- Central Alluvial Plain District
DWD - Western Desert District	LSM- Southern Marsh District
DSD- Southern Desert District	LBA- Basra Estuarine District

Physiographic regions and districts of Iraq.

(Physiographic is the abbreviation and details of Iraqi geographical districts)

Figure (2), surveyed regions map

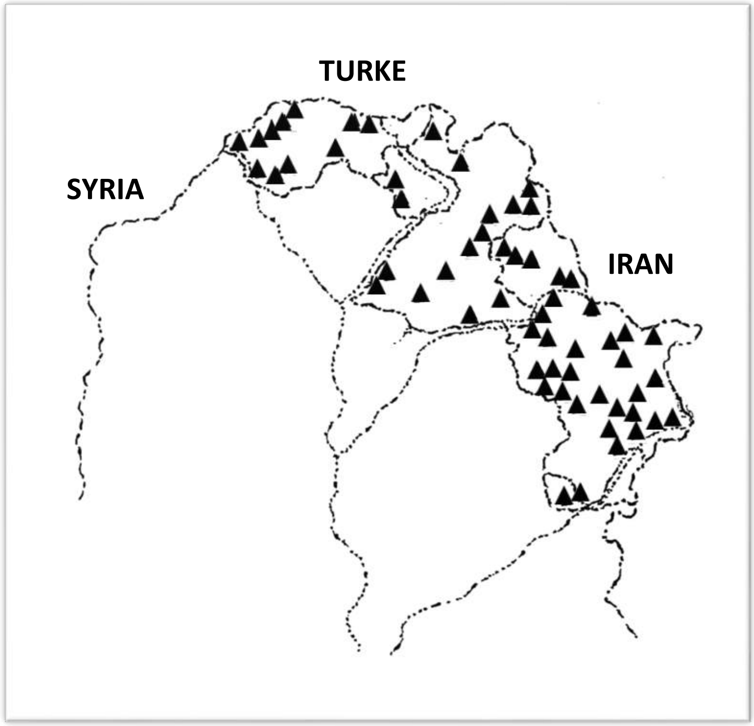

Figure (3) Distribution map of: *O. aegyptiaca*

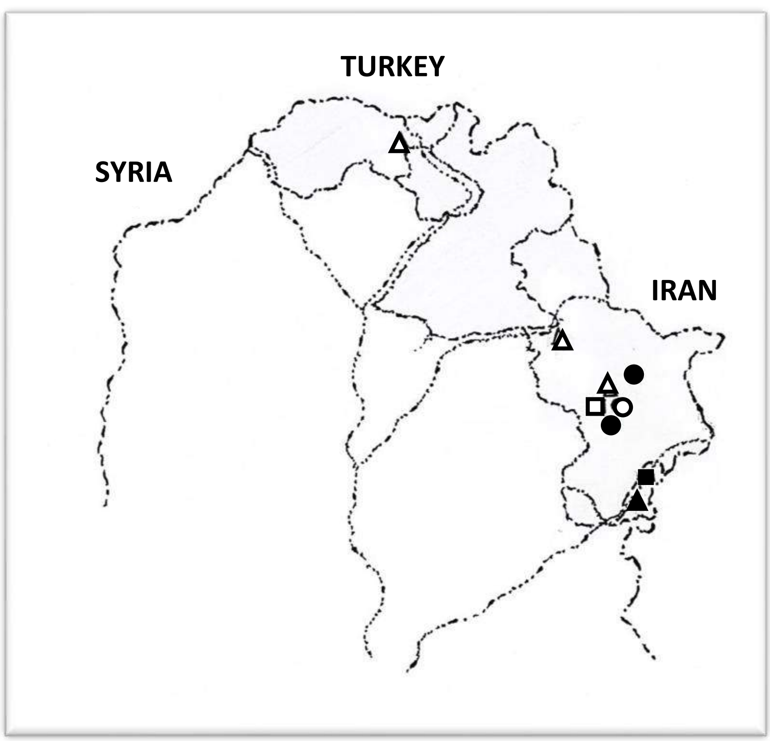

▲

Figure (4) Distribution map of:

□ *O. ovata* ▲ *O. mutelii* ○ *O. arenaria*
■ *O. minor* △ *O. crenata* ● *O. anatolica*

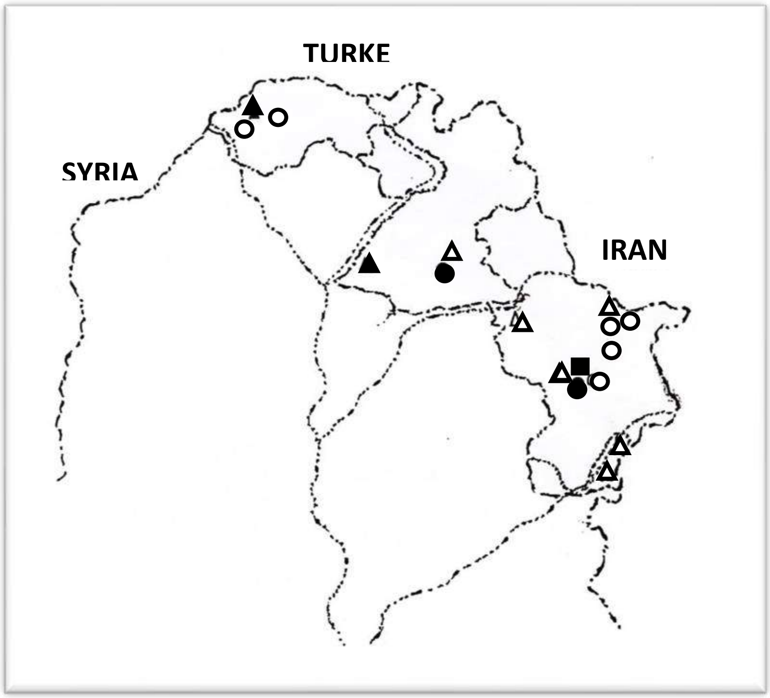

Figure (5) Distribution map of:

△ *O. singarensis* ■ *P. coccinea* ○ *O. kurdica*
▲ *O. ramosa* ● *O. coelestis*

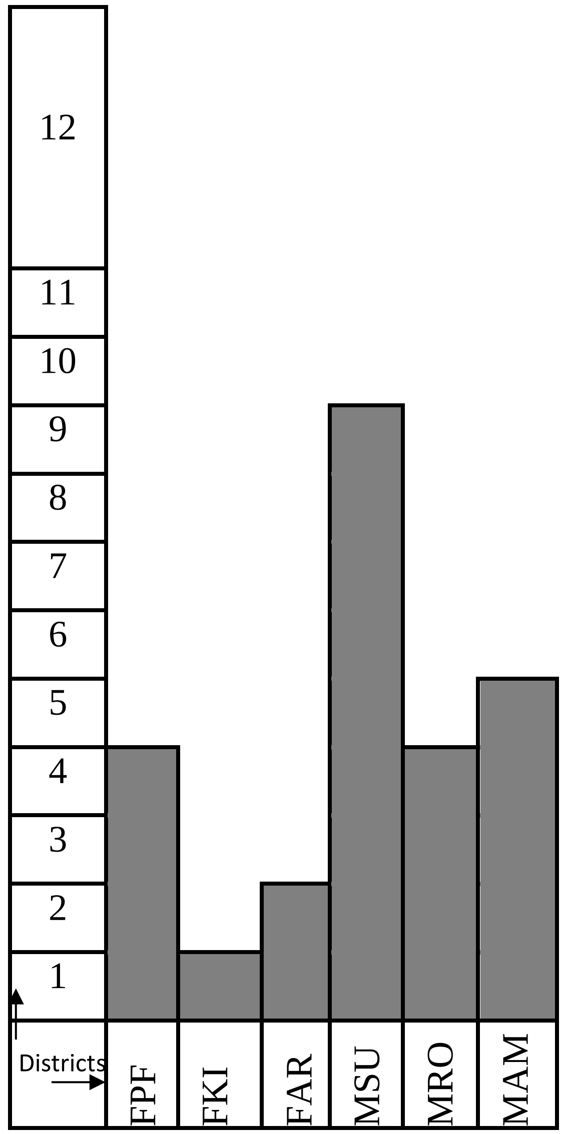

Figure (6) Number of species deployed in each district.

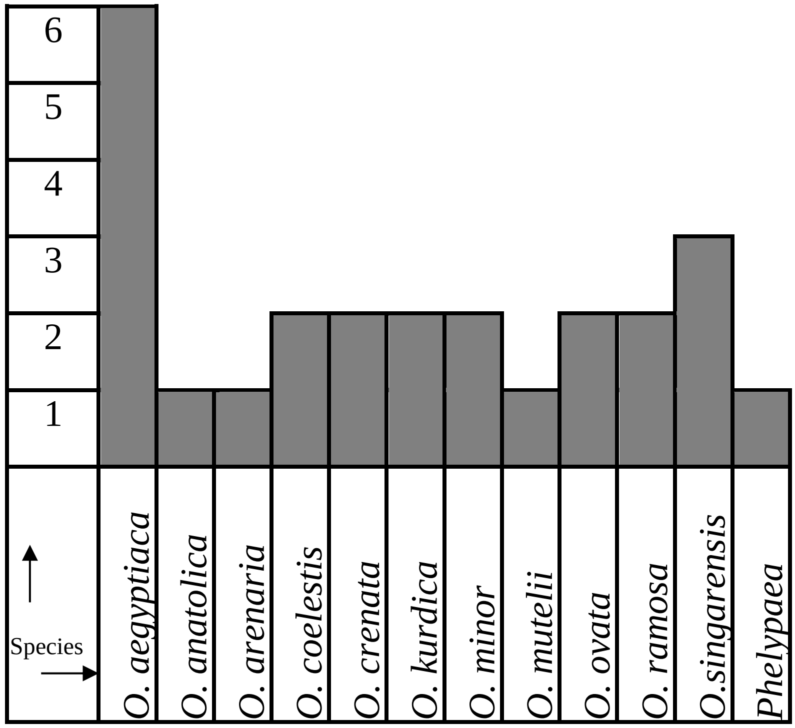

Figure (7) Districts occupied by studied species.

(Districts = FPF, FKI, FAR, MSU, MRO, MAM)

- Table (2) Geographical distribution, altitudes and host of examined

Spp.	Geographical districts							Hosts		Alt. (m)
	MAM	MRO	MSU	FNI	FAR	FKI	FPF	Wild plants	Cultivate plants	
O . aegyptiaca	❈	❈	❈	❈	❈	❈	❈	❈	❈	200 -1500
O . anatolica			❈					❈		1300 - 1750
O . arenaria			❈					❈		1500 - 1750
O . coelestis			❈					❈	❈	750 - 1750
O . crenata			❈					❈		1500 - 2000
O . kurdica	❈		❈					❈		900 - 1800
O . minor							❈	❈		1100 - 1400
O . mutelii							❈	❈		200 - 400
O . ovata			❈					❈		1500 - 2000
O . ramosa	❈				❈			❈	❈	600 - 850
O . singarensis							❈	❈		200 - 1500
P . coccinea			❈					❈		1600 - 2000

References

- Al-Katib, Y. M. (1988). Classification of seed Plants. University of Baghdad.
- Al-Mussawi, A. H. (1987), *Plant taxonomy*. Ministry of higher education and scientific research, Baghdad University.
- Al-Rawi, A. (1964). Wild Plants of Iraq with their distribution, the Ch. Bull. 14, Dir. Gem. Agriculture, Res., Proj. Ministry of Agriculture Government Press. P: 148.
- Blackelock, R. A. (1949). The Rustam Herbarium, Iraqi Systematic list (continued), part 4. Kew Bull. 3 pp: 441-444.
- Davis, P. H. ; Edmondson, J. R. and Mill, R. R. (1982). Flora of Turkey. The University Press. Edinburgh. vol. **7**. pp: 1-23.
- Faris, Y. S. (1983). The vascular Plants of Pirramagrun mountain. (MSc. thesis). Salahiddin University. College of science. p. 90.
- Guest, E. R. (1966). Flora of Iraq. Ministry of Agriculture Republic of Iraq. vol. 1.
- Handle Mazzetti, H. F. (1910). Die Vegetation' sVerhaltnisse von Mesopamien und Kurdistan. pp: 406-407.
- Khalaf, M. K. (1980). The vascular plants of Jabal Singar. Baghdad University. MSc. thesis. P: 125.
- Lawrence, G. H. M. (1951). Taxonomy of Vascular Planets. The Macmillan Company, Newyork. pp: 702-703.
- Parsa, A. (1949). Flora del, Iran. publication du Ministere del education Museum. D'Histoire Nuturelle de Teheran. voll. 4. pp: 486 -519.
- Post, G. E. (1933). Flora of Syria, Palestine and Sinai, American press. Beirut. vol. 2. pp: 310-316.
- Rechinger, K. H. (1964). Flora Lowland of Iraq. Weinheim Verlag von j. Cramer, Newyork, N. Y. Hafner publishing Co. pp: 551-554.
- Rechinger, K. H. (1964). Flora Iranica, Acadimische Druck –u- Verlag santalt Graz-Austria. no. 5. pp:1-24.

- Ridda, T. j. and Daoud, W. H., (1982). Geographical distribution of wild Vascular Plants of Iraq. National Herbarium of Iraq. Uni. pub. p: 90.
- Thieret, J. W. (1971).The genera of Orobanchaceae in the Southeastern United States. J. Arnold Arboritum, 52. pp: 404-413.
- Zohary, M. (1946), The flora of Iraq and its Phytogeographical Subdivision. Iraq Dep. Agriculture Bull. N. 31. Baghdad. pp: 135-136.

ttp://jgu.garmian.edu.krd https://doi.org/10.24271/garmian.348

Bioinformatic analysis reveals possible response of the *Arabidopsis* acetylated histone-binding protein (BRAT1) against abiotic stresses

Asaad M. Mahmood
Department of Biology, College of Education, University of Garmian, Kalar, Al- Sulaimaniyah, Kurdistan Region, Iraq
Email: asaad@garmian.edu.krd

Abstract
Transposable elements and other sequences of repetitive DNA including microsatellite are usually subject to both DNA methylation and transcriptional silencing. However, anti-silencing mechanisms which lead to promote transcription in such regions are not well investigated. A recent genetic screening in *Arabidopsis thaliana* identified an anti-silencing factor, named Bromodomain and ATPase domain-containing protein 1 (BRAT1). This protein is involved in DNA demethylation through a valuable association between histone acetylation and transcriptional anti-silencing at methylated genomic loci. This involvement can be conserved in eukaryotes. Although protein acts as an anti-silencing factor, there is no previous study identifies its contribution in gene regulation under unfavorable conditions. This study was analyzed several molecular patterns of the respective gene including protein-protein interactions, Nuclear Localization Signals (NLS), *Cis* regulatory elements (CREs) and intron-mediated enhancement (IMEter) using recent bioinformatic data bases. Results showed protein-protein interactions between the respective gene product and other proteins are involved against abiotic stresses, the protein of this gene is localized in nucleus. Results were also observed several CREs of non-coding regions representing their roles as stresses-responsive factors, according to IMEter analysis, this response is expected to valuably present in Intron **1,** suggesting experimental studies on mutant lines that contain insertions in their non-coding regions specifically intron 1of the underlying gene.

Keywords: Transposable elements, DNA methylation, Histone acetylation, BRAT1, Abiotic stresses

1. Introduction
DNA methylation is considered as an important chromatin modification which play roles in regulation of transposable element (TE) and transgene silencing, and to stabilize, imprint and regulate genome (1, 2), DNA methylation in *Arabidopsis thaliana*is enriched with TEs and other repetitive DNA sequences including microsatellites(2).The concentration of DNA methylation can be either diluted

passively during DNA replication or reduced markedly by active DNA demethylation modifiers(3, 4) including DNA glycosylase ROS1 (5), DML2 and DML3, and DME in DNA demethylation that they are subsequently involved to prevent transcriptional silencing (6).

A histone acetyltransferase named IDM1 is responsible to acetylate histone marks that are required for active DNA demethylation by ROS1 and then activating gene transcription (7, 8). However, the mechanisms that recognize acetylated histone marks which subsequently mediates DNA demethylation and anti-silencing are still unknown.

Bromodomain is regarded as an acetylated histone interaction module which is found in different types of nuclear proteins such as histone acetyltransferases, chromatin remodeling factors and transcriptional coactivators(9).

Previous studies have been determined bromodomain-containing proteins in *Arabidopsis*(10). A type of this protein including bromodomain protein BRAHMA (BRM) is involved in stress response(11). In *Arabidopsis*, another important member of a sub-group of bromodomain proteins (BET) functions as general transcription factors. Three of these transcription factors namely GTE4, GTE1/IMB1 and GTE6 are functionally found to involve in cell division, seed germination, and leaf development, respectively (12).

It is recently found that BRAT1 (Bromodomain and ATPase domain-containing protein 1) acts asan anti-silencing factor. They demonstrated that the bromodomain of BRAT1 is able to bind to acetylated histone and then influences levels of histone acetylation at methylated genomic regions; thereby they provided a potential link between each histone acetylation and anti-silencing factors and subsequently prevent transcriptional silencing(13, 14). However, there are no previous studies to confirm the contribution of the responsible gene (*At1g05910.1*) of bromodomain of BRAT1 against abiotic stresses. In order to understand the contribution of the respective gene in regulating gene expression under stress conditions, we analyzed the landscape of regulatory elements of this gene and determined its link with responsible genes that are involved against abiotic stress

2. Material and Methods

The present study was carried out during February to May, 2018. Here we used different bioinformatic software including String V9.1(15), Support Vector Machine-based localization predictor (AtSuP)(16), Database of Plant *cis*-acting Regulatory DNA elements(17)andIMEter (version 2.0)(14).

2.1. Protein-protein interactions

Protein–protein interaction networks using String V9.1 (http://string-db.org/) were investigated to study associations and integrations between the respective protein and other proteins are either involved in DNA methylation and demethylation or contributed in plant adaptation to unfavourable conditions.

2.2. Nuclear Localization Signal (NLS)

In order to predict the intracellular localisation of the proteinof respective gene (*AT1G05910.1* or *Brat1*) in *Arabidopsis*, protein sequences were analysed using Support Vector Machine-based localization predictor (AtSuP) programme which has seven possible categories, nucleus, mitochondrion, chloroplast, cytoplasm, plasma membrane, golgi apparatus and plasma membrane.

The software analysis included four options namely Amino acid composition-based, Dipeptide composition-based, N-Center-C terminal based and Best hybrid-based classifier (AA+PSSM+N-Center-C+PSI-BLAST).

2.3. Intronic*cis* element analysis

To identify *cis*regulatory elements (CREs) of *AT1G05910.1*, intronic regions of this gene were identifiedfrom TAIR (http://www.*Arabidopsis*.org/). The FASTA of this gene was obtained from NCBI (>NC_003070.9:1790216-1796715 *Arabidopsis thaliana* chromosome 1 sequence).To determine intronic *cis* regulatory elements, the sequence of each intron was filtered using the PLACE database (Database of Plant *cis*-acting Regulatory DNA elements; http://www.dna.affrc.go.jp/PLACE/). In addition, intron-mediated enhancement (IME) signals were obtained for each intron sequence using IMEter software (version 2.0) http://korflab.ucdavis.edu/cgi-bin/web-imeter2.pl.

3. Results and Discussion

3.1. Protein-protein interactions

To determine whether the activities of the respective gene product (protein) directly affect enzymes are involved in epigenetic regulation namely DNA methylation and demethylation, abiotic stress such as drought, dehydration, heat, cold and lights. Protein–protein interactions in association with physical and biological activities were investigated using String bioinformatics software.

The results presented in Figure 1, show strong protein links between the respective proteins and BRM, GTE6 and products of *AT3G15120* in *A. thaliana*. BRM intermediates valuable interactions between the respective protein with five important drought-responsive proteins including Transcription factor MYC2, MYB2(18), DREB2A, ERD1 and RD22(19). Moreover, through methyl transferase 1 (MET1), the respective gene product is also interacts with many epigenetic modifiers such as CMT3, DRM1, DRM2, ROS4, DML1 and DML2(18).

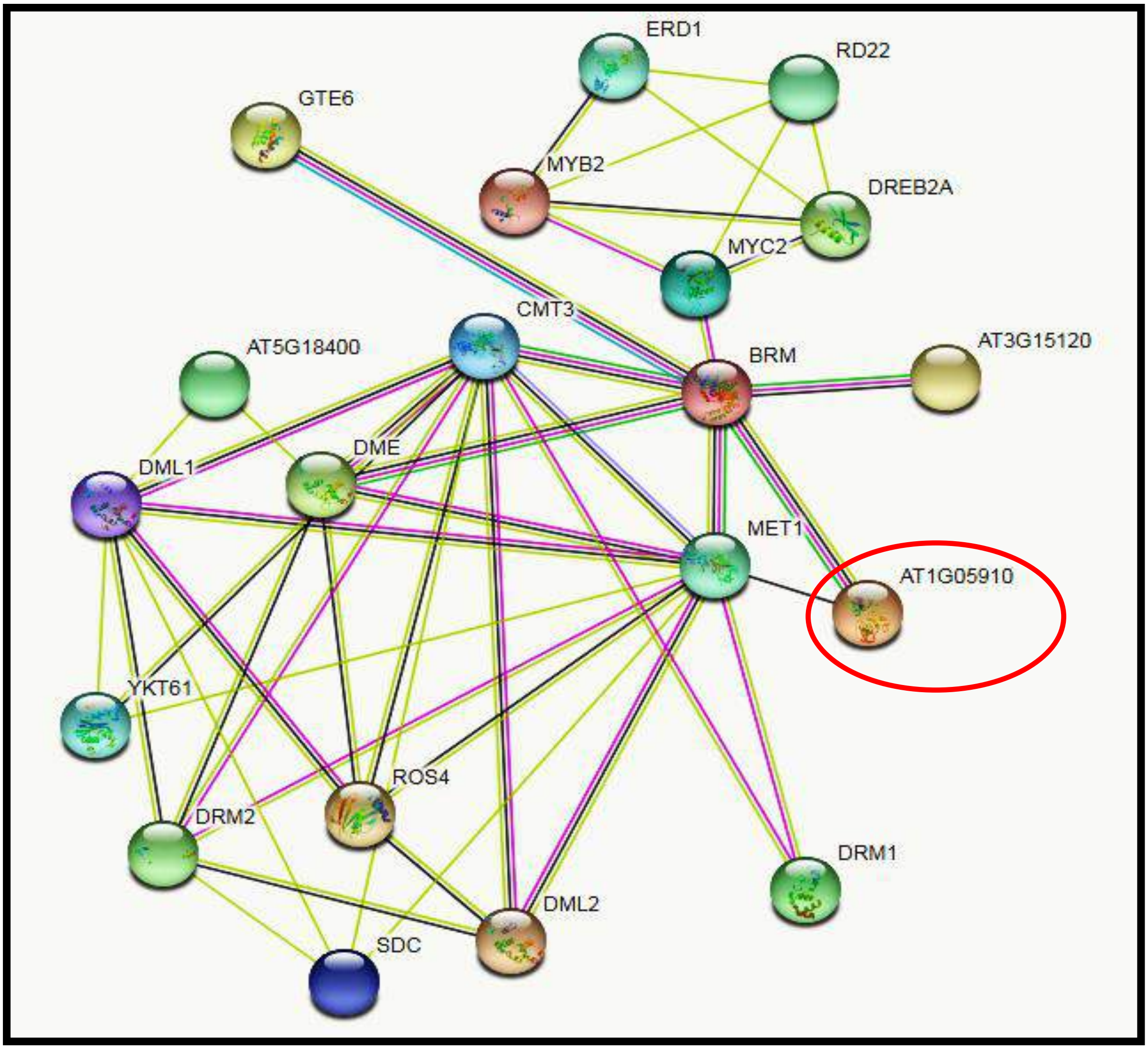

Figure 1. Protein-protein links between respective gene product (BRAT1) and other epigenetic modifiers and proteins that are involved in responding to abiotic stress in *A. thaliana* (http://string-db.org/).

In a relevant study, it is revealed that the BRAT1 mediates DNA demethylation (active removal of DNA methylation) at a small set of loci targeted through the involvement of the 5-methylcytosine DNA glycosylase ROS1.Moreover, the action of BRAT1 as an anti-silencing protein is largely independent of DNA demethylation. These researchers were also demonstrated that the bromodomain of BRAT1 is able to bind to acetylated histone, which might consequently act an anti-transcriptional silencing protein(13). Does this important involvement an anti-transcriptional silencing protein play roles in tolerations to abiotic stress? Previous studies have been demonstrated biological links between this protein and other epigenetic modifiers.

However, interactions between BRAT1 and other stress-responsive proteins haven't been documented yet.

Our results represent protein-protein interactions between the target proteins and BRM (is involved in stress response and phytohormone signalling, GTE6 (is involved in leaf development) and products of *AT3G15120* (contribute in histone acetylation) in *A. thaliana* (20-23). This result indicates active contribution of the respect gene product to regulate epigenetic modification, plant development and importantly stress conditions.

Furthermore, the Figure1 also identified important interactions of the studied protein with several important proteins including:- (I) Transcription factor MYC2, an enzyme is involved in response to oxidative stress and immunity in plant(24); (II) MYB2an enzyme is contributed to regulate the expression of dehydration-responsive genes(25),(III) DREB2A is another important protein that interacts with the respective protein through BRM, microarray and RNA gel blot analyses have been confirmed that the overexpression of transcriptional activation domain of DREB2Aled to significant drought stress tolerance in *Arabidopsis* plants (26),(IV) ERD1 that known to help the recovery of plants from drought stress and is involved in the biosynthesis of proline (27, 28), (IVI) RD22, an enzyme linked to the dehydration-induced by Abscisic acid (29). These findings opened a way for further investigations such as the contribution of regulatory region of introns of the respective gene against abiotic stresses.

3.2.Prediction of Nuclear Localization Signal (NLS)

To further investigate the action place of the respective gene product, we analyzed its active motifs and their localization in the cell. Prediction of nuclear localization signal showed similar patterns of amino acid residues (Table 1). The analysis predicted the presence of NLS to the nucleus for the protein encoded by the respective gene. Moreover, all methods including Amino Acid composition based SVM, Dipeptide composition (*sequence-order*) based, N-Center-C terminal (*3-parts*) based, PSI-BLAST (*similarity-search*) prediction and AA+NCC+PSI-BLAST+PSSM (*best hybrid*) based were shown the localization of the respective gene product in the nucleus.

Table 1. Prediction of subcellular localization of the protein of *AT1G05910.1* using BLAST

Method	Subcellular localization
Amino Acid composition based SVM	Nucleus
Dipeptide composition (*sequence-order*) based	Nucleus
N-Center-C terminal (*3-parts*) based	Nucleus
PSI-BLAST (*similarity-search*) prediction	Nucleus
AA+NCC+PSI-BLAST+PSSM (*best hybrid*) based	Nucleus

AtSubP= http://bioinfo3.noble.org/AtSubP/?dowhat=AtSubP

Results from this analysis showed similarities between methods used to predict the localization of the respective protein. These results demonstrated nucleus localization of the BRAT1, which is predicted to be useful in understanding the functional variety of proteins involved in histone acetylation and DNA demethylation and subsequently in regulating responses against stress conditions, including the exact role of the target protein and its regulatory signals. A relevant review was stated that a specific nuclear signal transduction regulates expression of specific gene sets, which consequently leads to an appropriate response to stress conditions(30). Interestingly, components of these pathways are subjected to post-translational modifications as well as epigenetic changes. Nuclear protein acetylation and/or deacetylation are important post-translational modifications that play major roles in the regulation of gene expression (31).

In light of this, in order to understand the precise localisation of this protein in response to unfavourable conditions, it would be important to experimentally study the subcellular localisation of BRAT1 protein, for example with techniques using green fluorescent protein (GFP) (32, 33). These techniques will be valuable to understand mechanisms that modulate gene expression under different environmental conditions. Due to its link to epigenetic modifiers and its localization in nucleus, a precise analysis to determine regulatory elements in the non-coding region of this gene can be of interest.

3.3. Landscape of regulatory elements of *AT1G05910.1*

Following obtaining interesting predictions in regards to protein-protein interactions of the respective gene product and showing active localization (nucleus). We further analyzed *Cis*-regulatory elements (CREs) of the target gene.

Identification of known motifs in a given gene provides possible insight into the functional characterization of that gene and predicts potential co-expressed genes. The analysis presented here, describes the distribution of important *cis* elements that are contributed effectively against abiotic stresses of respective gene (6592bp). The distribution and locations of important motifs within regions of this gene are given in **Error! Reference source not found.**.

---

1 AAAAAAAGAAAAAACGTTCGAAGAGGAAAAAAAAAAAAGAGGGAGAAGAG

(+) GT1CONSENSUS **[GRWAAW]**

(+) GT1GMSCAM4 **[GAAAAA]**

(-) ACGTATERD1 **[ACGT]**

(+) ACGTATERD1**[ACGT]**

201 TGTCAGTTGATTNTGTCTCCTCCAGTTCTTTGGCTAATGCAATCGGATAA

(-) MYB2CONSENSUSAT [YAACKG]

(+) MYBCORE**[CNGTTR]**
245 GGATA
(+) IBOXCORE **[GATAA]**
251 ACAGTCGTTTTAGCAGTTATTTGCAAGGATTTGNTTTATATTTCTCAACA
(-) MYB2AT **[TAACTG]**
651 ATAGGCTTAGGAGGAGGCCCAAATTGCATGGTCGCTCATACTTGTACTAC
(-) SITEIIATCYTC **[TGGGCY]**
801 GAGGGCATCAAATGCCGCGGTAAGCATTACATGTTTCTTCCTATGATATT
(-) CGCGBOXAT **[**VCGCGB**]**
(+) CGCGBOXAT **[**VCGCGB**]**
1051 CCGTTTTTTTTTTGNTCTCATTAAACCAGAATGTTTATACATTTGCTAAT
(+) MYB1AT **[WAACCA]**
1101 GACGTACAGCCAATTGCATCTGATCTCCGGCGTTCNCACGAGGAAGAGAA

(+) CCAATBOX1 **[CCAAT]**
1951 GCACCTTGGCTATTTGGGGGTTTGGACACGTATGGGTNCAAGTTCATTGG
(-) ZDNAFORMINGATCAB1 **[ATACGTGT]**
2301 CGAGCATTAGCATGTGCTGCTTCAAAAGCTGGACAGAAAGTTNAGCTTTT
(-) MYCATRD2 **[**CACATG**]**
(+) MYCATERD1**[CATGTG]**
2651 GAGTTTAATTTTTCCTTACCAGGTTGCGAAGCACGAGCCGAAATATTNGG
(+) LTRE1HVBLT49 [CCGAAA]
2851 TTATACCAGTGATGATAAATACGCCATAGATGTTGGGTTGGTTAATGTTG
(+) GT1CORE **[GGTTAA]**
3801 TTTTGTTATCCCATAAAAGCTGGTAGGGCACTTNTCTTTGAAAGTCGGTC
(-) DRE2COREZMRAB17**[ACCGAC]**

Figure 2. *AT1G05910.1* analysis. Motifs with similar coloured fonts represent similar motifs related to adverse environmental conditions. (+) = Forward strand and (-) = Reverse strand.

In addition, intron sequences are also important in transcriptional regulation. In regards to the investigated elements, different motifs which regulate the transcription of genes are involved in controlling plants against unfavorable conditions were found for intron (10 introns) of the target gene. To identify the effective location of BRAT1 as an anti-silencing factor, all intronic regions of this gene were analyzed to demonstrate the distribution CREs in all introns and to identify the most effective (by sensing or signaling) fragment against abiotic stresses. The location, sequence length (bps) and *Cis* regulatory elements for each intron of the respective are given in Table.

Table 2: Intronic location, length and number of CREs in the introns of *AT1G05910.1*

Introns	Location	bps	Number of CREs
Intron 1	132-538	406	65
Intron 2	809-1094	285	57
Intron 3	1197-1302	105	17
Intron 4	3127-3207	80	11
Intron 5	3397-3543	146	22
Intron 6	3681-4194	513	87
Intron 7	4438-4855	417	61
Intron 8	5043-5312	269	21
Intron 9	5379-5490	111	14
Intron 10	5741-5881	140	20

This table shows that the two longest introns are introns 6 and 7containing 513 and 417 base pairs respectively. However, the two shortest introns are identified to be introns 4 and 5 possessing 80 and 105 base pairs respectively. The highest numbers of CREs (87 and 65) are respectively found in introns 6 and 1. In contrast, both introns 4 and 9 are given the lowest of CREs occupying only 11 and 14 elements respectively.

To further understand the richest intron with CREs, these elements are shown in percentage rates (Figure 3).

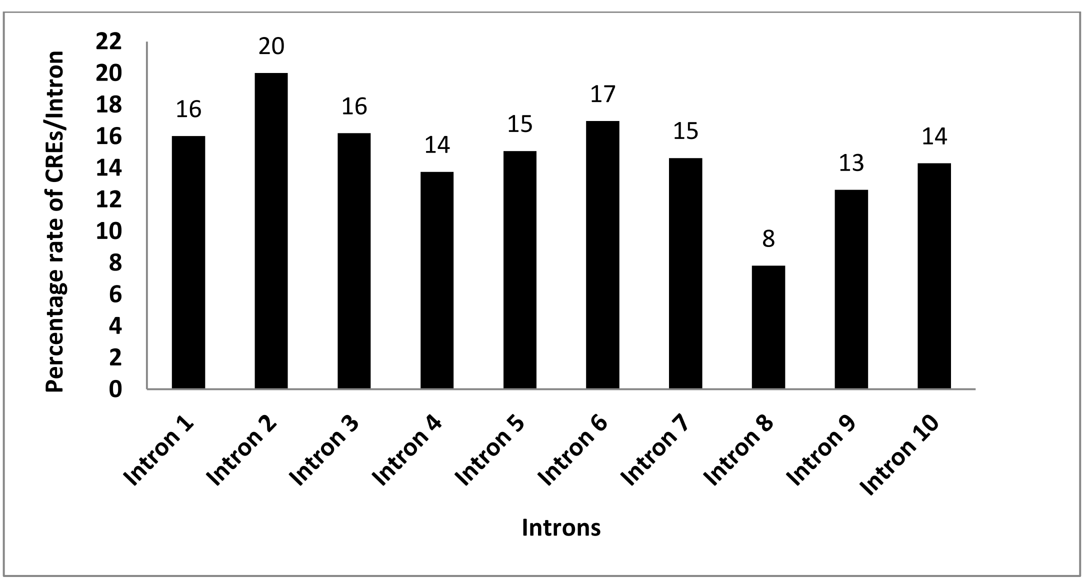

Figure 3. Percentage rate of *cis* regulatory elements in intronic regions of *Brat1*.

The highest percentage of CREs are counted in intron 2 (20%) which follows by intron 6 (17%), 1 and 2 (16%). In order to determine which intron is likely enhances gene expression; we calculated the intron-mediated enhancement (IMEter) for each intron. The higher the IMEter the score, the more likely the intron is expected to enhance expression(34). Our results show that the intron 1 and 10 are given the highest IMEter score (20.8 and 8.0 respectively), demonstrating most likely gene expression enhancer. Whereas, the smallest score of IMEter (1.2) was shown by intron 9 (Figure 4).

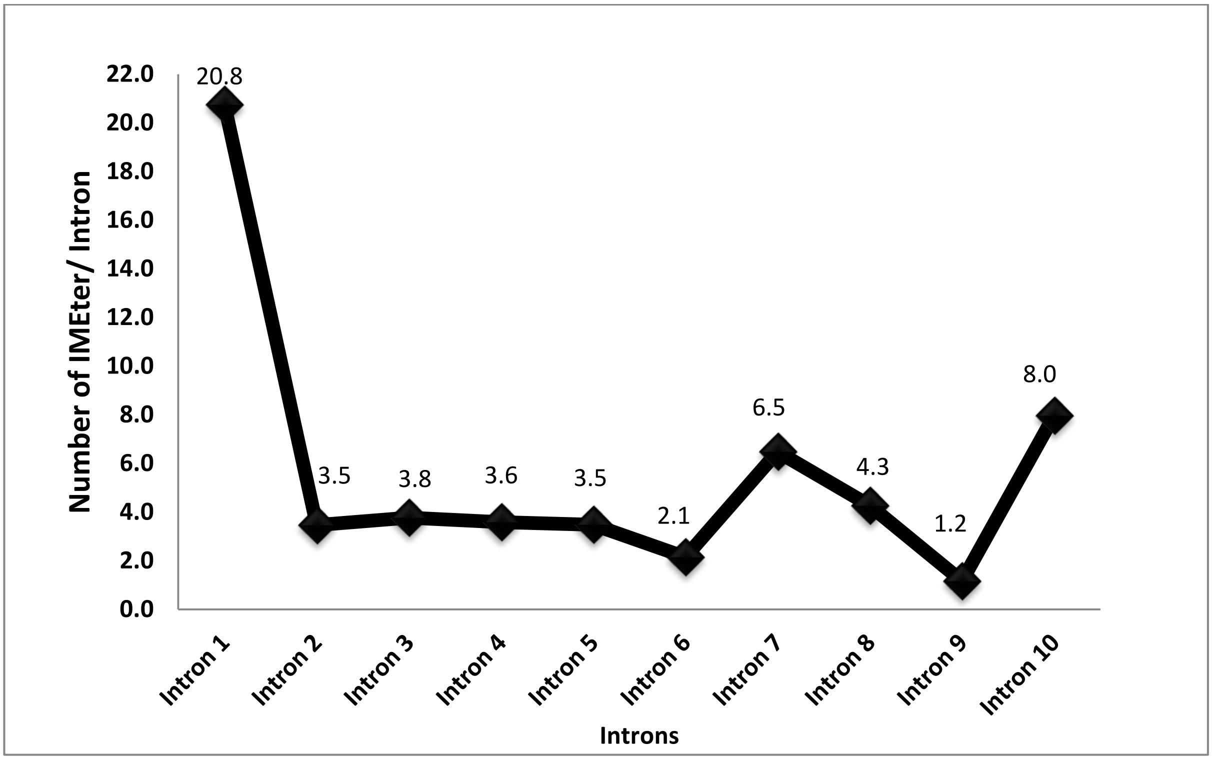

Figure 4. Distribution of IMEter v2.0 scores across each intron of *Brat1*.
Introns with an (IMEter) v2.0 score above 20: introns that can strongly enhance gene expression
Introns with an (IMEter) v2.0 score under 10: introns that less likely enhance gene expression.

CREs such as enhancers and promoters are regions/sequences of non-coding DNA that regulate gene expression. Mutations that affect the function of these regions/sequences may lead to phenotypic diversity within and between species(35, 36). Motifs that are common to the promoters of several genes may represent a key signature for a family of co-regulated genes with such motifs usually being involved with a variety of complex interactions with transcription factors (37). Additionally, single motifs may bind different transcription factors thereby bringing genes under multiple regulatory controls.

A recent study was found active contribution of *de novo* mutations in regulatory elements of non-coding region (introns) to the neuro-developmental disorders, This set of genetically heterogeneous of disorders might play roles to combine functional and evolutionary evidences, which is important to identify regulatory causes of genetic disorders such as fetal brain diseases(38).In the current study, we determined regulatory region of introns of the respective gene in order to understand its possible roles against abiotic stresses as well as evolutionary patterns.

CREs analysis shows the presence of (GT1CONSENSUS, GT1GMSCAM4), these elements are light and salinity- responsive factors (39-41). In addition, CCAATBOX1 is involved cooperatively with heat shock elements (HSEs) to increase adaptations to heat shock (42, 43).ZDNAFORMINGATCAB1 is also involved in light-dependent developmental expression of the gene(44). LTRE1HVBLT49 is a cold-responsive element(45, 46), which we found in the intronic regions of the respective gene sequence

Within this sequence, ACGTATERD1 factor containing (ACGT) was found, this sequence is required for etiolation-induced expression of early responsive to dehydration (erd1) which is actively involved in the upregulation of gene expression under water stress conditions (47).

All elements including MYB2CONSENSUSAT, MYBCORE, MYB2AT, MYCATRD2, MYCATERD1 and DRE2COREZMRAB17 that they belong to MYBs were determined in the non-coding regions specifically introns of the target gene. Previous studies recognized that MYB site was found in the promoters of the dehydration-responsive gene (rd22) Arabidopsis. Furthermore, binding site for all animal MYB and Arabidopsis MYB proteins including ATMYB1 and ATMYB2 are involved in regulation of genes that are responsive to water stress (48-53).

These results indicate the presence of several elements that are valuably involved in gene regulations under abiotic stresses such as light, salinity and drought. In order to investigate the distributions of regulatory elements within intronic regions of the target gene, the highest percentage rate of such elements were found in intron 2 followed by intron 6 and 1 respectively.

This finding followed by further investigation including IMEter, this analysis shows the positive effect of introns on gene expression in which introns with higher IMEter score represents higher potential on gene expression(14). Results showed that intron 1 possesses higher score in comparison with other introns; this means the most effective non-coding region of the respective gene is intron 1. Moreover, any mutation such as insertion within this sequence can be much valuable than other regions.

In conclusion, presumably, this gene is involved in epigenetic regulations and specifically establishing a link between histone acetylation and DNA demethylation leading anti-silencing transcriptions. Protein-protein interaction demonstrated vital links between the respective gene and others that are stresses-responsive. The presence of several *Cis* regulatory elements of stresses-responsive factors in the non-coding regions of *Brat1* might confirm this link. Due to its localization in nucleus, this gene might effectively involve in regulating histone acetylation and subsequently adaptation to unfavourable conditions. In order to experientially confirm this involvement, it is recommended to use mutant lines containing insertions in their first intron because it has the highest IMEter and it is expected to play much effective role in the regulation of post-transcriptional mechanisms.

References

1. Hindorff LA, Sethupathy P, Junkins HA, Ramos EM, Mehta JP, Collins FS, et al. Potential etiologic and functional implications of genome-wide association loci for human diseases and traits. Proceedings of the National Academy of Sciences. 2009;106(23):9362-7.
2. Maurano MT, Humbert R, Rynes E, Thurman RE, Haugen E, Wang H, et al. Systematic localization of common disease-associated variation in regulatory DNA. Science. 2012:1222794.
3. Hill RE, Lettice LA. Alterations to the remote control of Shh gene expression cause congenital abnormalities. Philosophical Transactions of the Royal Society B: Biological Sciences. 2013;368(1620):20120357.
4. Naville M, Ishibashi M, Ferg M, Bengani H, Rinkwitz S, Krecsmarik M, et al. Long-range evolutionary constraints reveal cis-regulatory interactions on the human X chromosome. Nature communications. 2015;6:6904.
5. Köhler S, Vasilevsky N, Engelstad M, Foster E, McMurry J, Aymé S, et al. The human phenotype ontology in 2017. 2017.
6. Wright CF, Fitzgerald TW, Jones WD, Clayton S, McRae JF, Van Kogelenberg M, et al. Genetic diagnosis of developmental disorders in the DDD study: a scalable analysis of genome-wide research data. The Lancet. 2015;385(9975):1305-14.
7. McRae JF, Clayton S, Fitzgerald TW, Kaplanis J, Prigmore E, Rajan D, et al. Prevalence and architecture of de novo mutations in developmental disorders. Nature. 2017;542(7642):433.
8. Lek M, Karczewski KJ, Minikel EV, Samocha KE, Banks E, Fennell T, et al. Analysis of protein-coding genetic variation in 60,706 humans. Nature. 2016;536(7616):285.
9. Koren A, Handsaker RE, Kamitaki N, Karlić R, Ghosh S, Polak P, et al. Genetic variation in human DNA replication timing. Cell. 2014;159(5):1015-26.
10. Kong A, Thorleifsson G, Gudbjartsson DF, Masson G, Sigurdsson A, Jonasdottir A, et al. Fine-scale recombination rate differences between sexes, populations and individuals. Nature. 2010;467(7319):1099.

11. Gao T, He B, Liu S, Zhu H, Tan K, Qian J. EnhancerAtlas: a resource for enhancer annotation and analysis in 105 human cell/tissue types. Bioinformatics. 2016;32(23):3543-51.
12. Shooshtari P, Huang H, Cotsapas C. Integrative genetic and epigenetic analysis uncovers regulatory mechanisms of autoimmune disease. The American Journal of Human Genetics. 2017;101(1):75-86.
13. Zhang C-J, Hou X-M, Tan L-M, Shao C-R, Huang H-W, Li Y-Q, et al. The Arabidopsis acetylated histone-binding protein BRAT1 forms a complex with BRP1 and prevents transcriptional silencing. Nature communications. 2016;7:11715.
14. Rose AB, Elfersi T, Parra G, Korf I. Promoter-proximal introns in Arabidopsis thaliana are enriched in dispersed signals that elevate gene expression. The Plant Cell. 2008;20(3):543-51.
15. Bao W, He F, Gao J, Meng F, Zou H, Luo B. Alpha-1-antitrypsin: a novel predictor for long-term recovery of chronic disorder of consciousness. Expert review of molecular diagnostics. 2018;18(3):307-13.
16. Kaundal R, Saini R, Zhao PX. Combining machine learning and homology-based approaches to accurately predict subcellular localization in Arabidopsis thaliana. Plant physiology. 2010:pp. 110.156851.
17. Higo K, Ugawa Y, Iwamoto M, Korenaga T. Plant cis-acting regulatory DNA elements (PLACE) database: 1999. Nucleic acids research. 1999;27(1):297-300.
18. Grzybkowska D, Morończyk J, Wójcikowska B, Gaj MD. Azacitidine (5-AzaC)-treatment and mutations in DNA methylase genes affect embryogenic response and expression of the genes that are involved in somatic embryogenesis in Arabidopsis. Plant Growth Regulation. 2018;85(2):243-56.
19. Lu X, Zhang X, Duan H, Lian C, Liu C, Yin W, et al. Three stress-responsive NAC transcription factors from Populus euphratica differentially regulate salt and drought tolerance in transgenic plants. Physiologia plantarum. 2018;162(1):73-97.
20. Efroni I, Han S-K, Kim HJ, Wu M-F, Steiner E, Birnbaum KD, et al. Regulation of leaf maturation by chromatin-mediated modulation of cytokinin responses. Developmental cell. 2013;24(4):438-45.
21. Han S-K, Sang Y, Rodrigues A, Wu M-F, Rodriguez PL, Wagner D. The SWI2/SNF2 chromatin remodeling ATPase BRAHMA represses abscisic acid responses in the absence of the stress stimulus in Arabidopsis. The Plant Cell. 2012:tpc. 112.105114.
22. Wu M-F, Sang Y, Bezhani S, Yamaguchi N, Han S-K, Li Z, et al. SWI2/SNF2 chromatin remodeling ATPases overcome polycomb repression and control floral organ identity with the LEAFY and SEPALLATA3 transcription factors. Proceedings of the National Academy of Sciences. 2012;109(9):3576-81.

23. Wang J, Tadeo X, Hou H, Tu PG, Thompson J, Yates JR, et al. Epe1 recruits BET family bromodomain protein Bdf2 to establish heterochromatin boundaries. Genes & development. 2013;27(17):1886-902.
24. Cui H, Qiu J, Zhou Y, Bhandari DD, Zhao C, Bautor J, et al. Antagonism of transcription factor MYC2 by EDS1/PAD4 complexes bolsters salicylic acid defense in Arabidopsis effector-triggered immunity. Molecular Plant. 2018.
25. Gaponenko A, Shulga O, Mishutkina Y, Tsarkova E, Timoshenko A, Spechenkova N. Perspectives of Use of Transcription Factors for Improving Resistance of Wheat Productive Varieties to Abiotic Stresses by Transgenic Technologies. Russian Journal of Genetics. 2018;54(1):27-35.
26. Reis RR, da Cunha BADB, Martins PK, Martins MTB, Alekcevetch JC, Chalfun-Júnior A, et al. Induced over-expression of AtDREB2A CA improves drought tolerance in sugarcane. Plant science. 2014;221:59-68.
27. Cecchini NM, Monteoliva MI, Alvarez ME. Proline dehydrogenase contributes to pathogen defense in Arabidopsis. Plant Physiology. 2011;155(4):1947-59.
28. Borges AA, Jiménez-Arias D, Expósito-Rodríguez M, Sandalio LM, Pérez JA. Priming crops against biotic and abiotic stresses: MSB as a tool for studying mechanisms. Frontiers in plant science. 2014;5:642.
29. Yamaguchi-Shinozaki K, Shinozaki K. The plant hormone abscisic acid mediates the drought-induced expression but not the seed-specific expression of rd22, a gene responsive to dehydration stress in Arabidopsis thaliana. Molecular and General Genetics MGG. 1993;238(1-2):17-25.
30. Grandperret V, NICOLAS-FRANCÈS V, Wendehenne D, Bourque S. Type-II histone deacetylases: elusive plant nuclear signal transducers. Plant, cell & environment. 2014;37(6):1259-69.
31. Chen ZJ, Tian L. Roles of dynamic and reversible histone acetylation in plant development and polyploidy. Biochimica et Biophysica Acta (BBA)-Gene Structure and Expression. 2007;1769(5-6):295-307.
32. Bakhoum SF, Ngo B, Laughney AM, Cavallo J-A, Murphy CJ, Ly P, et al. Chromosomal instability drives metastasis through a cytosolic DNA response. Nature. 2018.
33. Etchegaray J-P, Chavez L, Huang Y, Ross KN, Choi J, Martinez-Pastor B, et al. The histone deacetylase SIRT6 controls embryonic stem cell fate via TET-mediated production of 5-hydroxymethylcytosine. Nature cell biology. 2015;17(5):545.
34. Gallegos JE, Rose AB. Intron-mediated enhancement is not limited to introns. bioRxiv. 2018:269852.

35. Wittkopp PJ, Kalay G. Cis-regulatory elements: molecular mechanisms and evolutionary processes underlying divergence. Nature Reviews Genetics. 2012;13(1):59.
36. Zhao B, Cao JF, Hu GJ, Chen ZW, Wang LY, Shangguan XX, et al. Core cis-element variation confers subgenome-biased expression of a transcription factor that functions in cotton fiber elongation. New Phytologist. 2018;218(3):1061-75.
37. Wang H, Caruso LV, Downie AB, Perry SE. The embryo MADS domain protein AGAMOUS-Like 15 directly regulates expression of a gene encoding an enzyme involved in gibberellin metabolism. The Plant Cell. 2004;16(5):1206-19.
38. Short PJ, McRae JF, Gallone G, Sifrim A, Won H, Geschwind DH, et al. De novo mutations in regulatory elements in neurodevelopmental disorders. Nature. 2018;555(7698):611.
39. Zhou D-X. Regulatory mechanism of plant gene transcription by GT-elements and GT-factors. Trends in plant science. 1999;4(6):210-4.
40. Park HC, Kim ML, Kang YH, Jeon JM, Yoo JH, Kim MC, et al. Pathogen-and NaCl-induced expression of the SCaM-4 promoter is mediated in part by a GT-1 box that interacts with a GT-1-like transcription factor. Plant physiology. 2004;135(4):2150-61.
41. Li T, Sun J, Li C, Lu Z, Xia J. Cloning and expression analysis of the FvNCED3 gene and its promoter from ash (Fraxinus velutina). Journal of Forestry Research.1-12.
42. Wenkel S, Turck F, Singer K, Gissot L, Le Gourrierec J, Samach A, et al. CONSTANS and the CCAAT box binding complex share a functionally important domain and interact to regulate flowering of Arabidopsis. The Plant Cell. 2006;18(11):2971-84.
43. Srivastava R, Rai KM, Srivastava R. Plant Biosynthetic Engineering Through Transcription Regulation: An Insight into Molecular Mechanisms During Environmental Stress. Biosynthetic Technology and Environmental Challenges: Springer; 2018. p. 51-72.
44. Yadav V, Mallappa C, Gangappa SN, Bhatia S, Chattopadhyay S. A basic helix-loop-helix transcription factor in Arabidopsis, MYC2, acts as a repressor of blue light–mediated photomorphogenic growth. The Plant Cell. 2005;17(7):1953-66.
45. Dunn MA, White AJ, Vural S, Hughes MA. Identification of promoter elements in a low-temperature-responsive gene (blt4. 9) from barley (Hordeum vulgare L.). Plant molecular biology. 1998;38(4):551-64.
46. Zhang C, Jia H, Wu W, Wang X, Fang J, Wang C. Functional conservation analysis and expression modes of grape anthocyanin synthesis genes responsive to low temperature stress. Gene. 2015;574(1):168-77.

47. Simpson SD, Nakashima K, Narusaka Y, Seki M, Shinozaki K, Yamaguchi-Shinozaki K. Two different novel cis-acting elements of erd1, a clpA homologous Arabidopsis gene function in induction by dehydration stress and dark-induced senescence. The Plant Journal. 2003;33(2):259-70.
48. Solano R, Nieto C, Avila J, Canas L, Diaz I, Paz-Ares J. Dual DNA binding specificity of a petal epidermis-specific MYB transcription factor (MYB. Ph3) from Petunia hybrida. The EMBO Journal. 1995;14(8):1773-84.
49. Abe H, Urao T, Ito T, Seki M, Shinozaki K, Yamaguchi-Shinozaki K. Arabidopsis AtMYC2 (bHLH) and AtMYB2 (MYB) function as transcriptional activators in abscisic acid signaling. The Plant Cell. 2003;15(1):63-78.
50. Urao T, Yamaguchi-Shinozaki K, Urao S, Shinozaki K. An Arabidopsis myb homolog is induced by dehydration stress and its gene product binds to the conserved MYB recognition sequence. The Plant Cell. 1993;5(11):1529-39.
51. Busk PK, Pagès M. Regulation of abscisic acid-induced transcription. Plant molecular biology. 1998;37(3):425-35.
52. Dubouzet JG, Sakuma Y, Ito Y, Kasuga M, Dubouzet EG, Miura S, et al. OsDREB genes in rice, Oryza sativa L., encode transcription activators that function in drought-, high-salt-and cold-responsive gene expression. The Plant Journal. 2003;33(4):751-63.
53. Tran L-SP, Nakashima K, Sakuma Y, Simpson SD, Fujita Y, Maruyama K, et al. Isolation and functional analysis of Arabidopsis stress-inducible NAC transcription factors that bind to a drought-responsive cis-element in the early responsive to dehydration stress 1 promoter. The Plant Cell. 2004;16(9):2481-98.